Dissertation zur Erlangung des Doktorgrades
der Fakultät für Chemie und Pharmazie
der Ludwig-Maximilians-Universität München

Development of new mGAT4 inhibitors by variation of the amino acid subunit and lipophilic domain of (*S*)-SNAP-5114

Michael Christopher Böck

aus

Gräfelfing, Deutschland

2020

Erklärung

Diese Dissertation wurde im Sinne von § 7 der Promotionsordnung vom 28. November 2011 von Herrn Prof. Dr. Klaus T. Wanner betreut.

Eidesstattliche Versicherung

Diese Dissertation wurde eigenständig und ohne unerlaubte Hilfe erarbeitet.

München, den 29.01.2020 Michael Böck

Dissertation eingereicht am	14.02.2020
1. Gutachter	Prof. Dr. Klaus T. Wanner
2. Gutachter Prof.	Prof. Dr. Franz F. Paintner
Mündliche Prüfung am	05.03.2020

Die vorliegende Arbeit entstand in der Zeit von April 2014 bis Januar 2020 am Department Pharmazie – Zentrum für Pharmaforschung – der Ludwig-Maximilians-Universität München auf Anregung und unter Leitung von Herrn Prof. Dr. Klaus T. Wanner.

Für die hervorragende und äußerst engagierte Betreuung und Förderung meiner Arbeit sowie die ausgezeichneten Forschungsbedingungen möchte ich mich bei Herrn Prof. Dr. Klaus T. Wanner sehr herzlich bedanken.

Herrn Prof. Dr. Franz Paintner danke ich sehr herzlich für die Übernahme des Korreferats.

Danksagung

Für die schöne gemeinsame Zeit, die angenehme Arbeitsatmosphäre und die kollegiale Zusammenarbeit möchte ich mich bei allen aktuellen und ehemaligen Mitarbeitern des Arbeitskreises bedanken.

Besonderer Dank gilt hierbei meinen ehemaligen Laborpartnern Simone Huber und Sebastian Rappenglück für die unvergessliche Zeit im Labor C1.053. Janina Andreß danke ich für die interessanten Gespräche auf dem Weg zum Mittagessen, und für das Auf-dem-Laufenden-halten über die Geschehnisse im Arbeitskreis während meiner Zeit in der Abgeschiedenheit des Schreibraums.

Ganz besonders danken möchte ich auch Dr. Jörg Pabel für die zahlreichen guten Tipps und Ratschläge – sowohl in Bezug auf die Promotion, als auch im privaten Bereich, und hier insbesondere während der 3.-Semester-Abschlussfeier 2014. Teamkapitän Dr. Lars Allmendinger danke ich herzlich für die Organisation der Laufgruppe, und die damit verbundene Motivation zur sportlichen Ertüchtigung.

Jürgen Gabriel, Thomas Ackermann und Heinrich Rudy danke ich für die überaus erfolgreiche DPhG-Konferenz, Maren Jung für die gemeinsame Zeit im Schreibraum, und Krisztian Toth für die humorvolle Begleitung des Laborgeschehehs.

Außerdem möchte ich mich bedanken bei Sonja Sichler, Patrick Neiens, Tobias Hauke, Mark Währa, Valentin Nitsche, Tamara Bernauer, Gerd Bauschke, Davia Prischich, Giulia di Bergamo, Niklas Winter, Elisabeth Zoller, Herrn Li, Adrian Müller-Deku, Elena Longhi, Alex Sailer, Ines Trübenbach, Janin Germer, Ludwig Angermeier und Hannah Kipka.

Dr. Georg Höfner, Silke Duensing-Kropp, Miriam Sandner und Tanja Franz danke ich für die biologische Testung der von mir synthetisierten Substanzen. Für die Präsentationen zum Molecular Modeling und die Erläuterungen zum Struktur-basierten Moleküldesign bin ich Herrn Dr. Thomas Wein sehr dankbar.

Herzlicher Dank geht auch an Anne Kärtner für die unermüdliche Versorgung mit Labormaterialien, und an Katharina Heimberger für die Unterstützung bei zahlreichen organisatorischen Aufgaben.

Den Mitarbeitern der analytischen Abteilung, Dr. Lars Allmendinger, Claudia Glas, Ursula Groß und Keum-Ja Pankau, gebührt mein Dank für die eifrige Messung von über anderthalbtausend (!) NMR-Proben.

Ganz besonderer Dank gebührt meiner Familie und Linda für die großartige Unterstützung während der gesamten Promotionszeit.

This cumulative thesis is based on the following original publications and manuscripts:

First publication:

Janina C. Andreß, Michael C. Böck, Georg Höfner, Klaus T. Wanner

Submitted to *Medicinal Chemistry Research*, 23.12.2019.

"Synthesis and biological evaluation of α- and β-hydroxy substituted amino acid derivatives as potential mGAT4 inhibitors"

Second publication:

Michael C. Böck, Georg Höfner, Klaus T. Wanner

Submitted to *ChemMedChem*, 20.12.2019.

"Synthesis and Biological Evaluation of N-Substituted Nipecotic Acids as (*S*)-SNAP-5114 Analogues with Modified Lipophilic Domains"

Manuscript of the third publication:

Michael C. Böck, Georg Höfner, Klaus T. Wanner

"Synthesis and Biological Evaluation of N-Substituted Nipecotic Acids as (*S*)-SNAP-5114 Analogues Containing Sterically Demanding Aliphatic Moieties in the Lipophilic Domain"

Meinen Eltern

Table of contents

1. Introduction

1.1 GABAergic neurotransmission

The neuronal signal transduction in the mammalian central nervous system (CNS) is regulated by the complex interaction of various excitatory and inhibitory neurotransmitters. GABA (γ-aminobutyric acid, **1**) constitutes the main inhibitory neurotransmitter, with estimates assuming that at least 40% of inhibitory synaptic processing in the mammalian brain is mediated by GABA.[1,2]

In the CNS GABA for neurotransmission is synthesized from L-glutamate (**2**) by the enzyme glutamate decarboxylase GAD65,[3] and subsequently transported through specific vesicular neurotransmitter transporters (VGAT) into synaptic vesicles for storage.[4,5] In case of an arriving action potential, the accompanying influx of calcium ions causes GABA to be released via exocytosis from the storage vesicles into the synaptic cleft, where it unfolds its effect by interaction with pre- and postsynaptic GABA receptors.

Located almost exclusively on post-synaptic neurons, $GABA_A$ receptors are ligand controlled chloride channels, which upon activation effectuate an influx of chloride ions causing hyperpolarization and thus conveying a fast reduction of the excitability of the neuron. By contrast, $GABA_B$ receptors are $G_{i/o}$-protein coupled receptors (GPCRs) found on pre- and postsynaptic neurons as well as on the surrounding glia cells.[4,6,7] Activation of post-synaptic $GABA_B$ receptors triggers a *second messenger cascade* which results in an increased potassium efflux, hence contributing to the hyperpolarization and, as a consequence thereof, to the deactivation of the neuron. Pre-synaptic $GABA_B$ receptors on the other hand play a central role in the regulation of the GABAergic signaling by upon activation reducing the calcium current responsible for GABA exocytosis, hence providing a crucial negative feedback mechanism.

GABAergic signaling is mainly terminated by the uptake of the molecule from the synaptic cleft into the surrounding neurons and glia cells, respectively. This process is mediated by specific, high-affinity transport proteins termed GABA transporters (GATs). The GABA uptake predominantly takes place into presynaptic neurons,

where the neurotransmitter is either transported back into the storage vesicles, or subjected to catabolism by the mitochondrial bound enzyme GABA transaminase (GABA-T) forming succinic semialdehyde (SSA, **3**).[8,9,10] Besides, a lesser amount of GABA is also transported from the synaptic cleft into the glia cells surrounding the GABAergic axon, where it is likewise catabolized by GABA-T.[11]

Figure 1. *Structure of GABA, L-glutamate and succinic semialdehyde.*

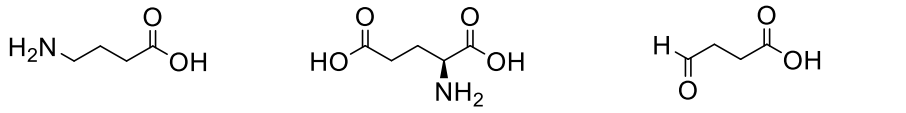

GABA (**1**) L-Glutamate (**2**) Succinic semialdehyde (**3**)

Figure 2. *GABA neurotransmission pathways.*

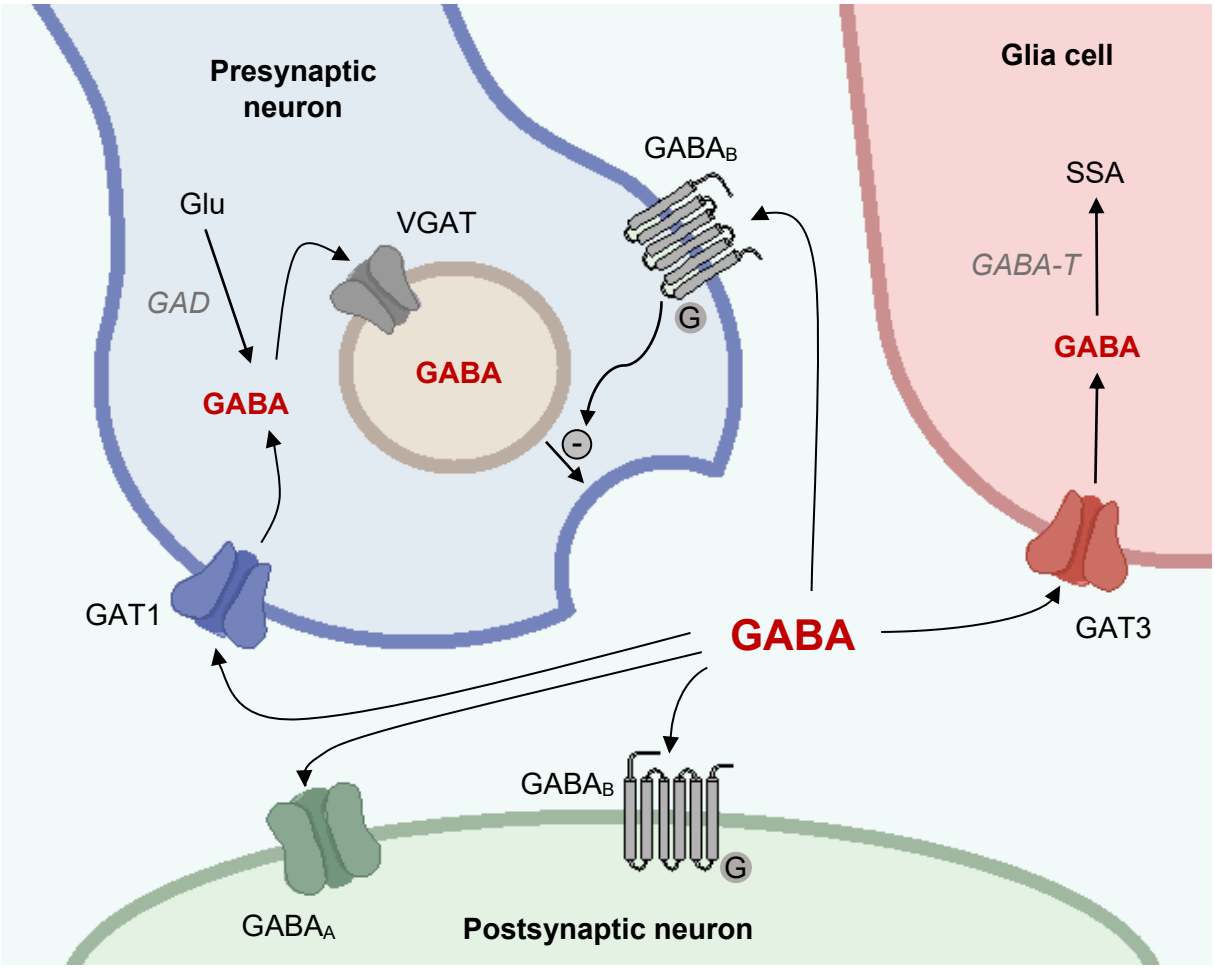

1.2 GABA related diseases and treatment

Deficient GABAergic neurotransmission results in a pathological attenuation of the inhibitory activity in the CNS, which is associated with a variety of severe neurological disorders including neuropathic pain,[12,13] Huntington´s disease,[14,15] anxiety disorders,[16,17] depression,[16,17,18] Alzheimer´s disease[19,20], and epilepsy[14,21,22,23]. As a consequence of the high prevalence and clinical importance of these GABA related diseases – epilepsy alone affects more than 50 million people worldwide according to the latest data from the World Health Organization (WHO)[24] – intensive efforts in medical chemistry have aimed at the modulation of the GABAeric system by pharmacological agents.

One possibility to redress insufficient GABAergic signaling exists in the direct stimulation of GABA receptors with appropriate ligands. For example, the muscle relaxant Baclofen (Lioresal®, **4**) acts as agonist of the metabotropic $GABA_B$ receptor.[6,25] Benzodiazepines, such as the lead substance Diazepam (Valium®, **5**), constitute allosteric modulators of the ionotropic $GABA_A$ receptor. Upon binding to a specific allosteric binding site a conformational change of the receptor is set in motion, which increases the opening frequency of the chloride channel. [26,27] A similar modulation mechanism which affects the opening duration of the $GABA_A$ receptor is shown by the anesthetic Propofol (Diprivan®, **6**) and by barbiturates such as Phenobarbital (Luminal®, **7**).[28,29,30] In addition, Propofol might also activate $GABA_A$ receptors directly at high doses, thus behaving as $GABA_A$ receptor agonist.[31,32]

Another strategy for improving the GABAergic status aims at enhancing the concentration of GABA by inhibition of its degradation. Vigabatrin (**8**) accomplishes this task by irreversible inhibition of the GABA transaminase (GABA-T). Furthermore, inhibition of the GABA transporters (GATs) by GABA reuptake inhibitors allows to enhance GABAergic signaling by impeding the removal of GABA from the synaptic cleft, hence resulting in a prolonged dwell time of GABA at the site of action. As yet, Tiagabine (Gabatril®, **9**, see table 2) is the only drug with this mechanism of action that has been approved for clinical use by the U.S. Food and Drug Administration (FDA) and the European Medicines Agency (EMA), respectively. As selective inhibitor of the GAT1 subtype (for a detailed discussion of the GAT subtypes and

their nomenclature see chapter 1.2.2), it has seen clinical use for the add-on treatment of partial-onset seizures.[33,34] Unfortunately, its application is accompanied by a number of severe adverse effects, including dizziness, somnolence, headache, memory loss, diarrhea, tremor, and depression,[35,36] which seem to be closely linked to the function of mGAT1. Hence, other GAT subtypes have come into focus as potential drug targets.[37,38,39]

Figure 3. *Drugs targeting the GABAergic system.*

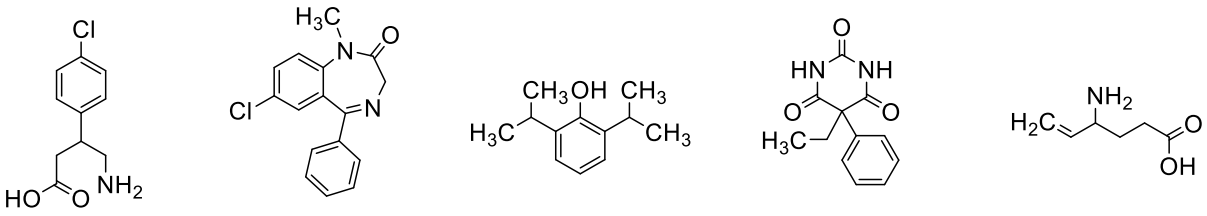

Baclofen (**4**) Diazepam (**5**) Propofol (**6**) Phenobarbital (**7**) Vigabatrin (**8**)

1.3 GABA transporters as pharmacological targets

1.3.1 Structure and transport mechanism of GATs

The GABA transporters (GATs) belong to the solute carrier 6 (SLC6) gene family,[40] which share the common feature of using the co-transport of sodium ions as a driving force to translocate their substrate against the chemical gradient existing across the cell membrane, with the necessary sodium ion gradient being sustained by the Na^+/K^+-ATPase.[40,41] As a consequence of this underlying transport mechanism, SLC6 transporters are also termed *neurotransmitter-sodium symporters* (NSS). The precise stoichiometry, including the symport of chloride ions or the antiport of potassium ions,[42] can vary between different transporters within the SLC6 family. In case of GABA transporters (GATs) a co-transport of two sodium ions and one chloride ion for each GABA molecule was assumed. However, more recent evidence suggests a 3 Na^+ : 1 Cl^- : 1 GABA stoichiometry.[43]

The first step towards the general understanding of the structure and function of the SLC6 transporters was taken with the isolation of rGAT-1 from rat brain by Radian et al.,[44] which led to the sequencing and finally to the successful cloning of the transporter by Guastella et al.[45] Further important progress was made with the successful X-ray structure analysis of the leucine transporter $LeuT_{Aa}$ from the bacterium *Aquifex aeolicus* following its crystallization in the presence of the substrate leucine and two sodium ions (Yamashita et al., 2005).[46] Despite the overall sequence of $LeuT_{Aa}$ being only 20-25% identical to that of the eukaryontic SLC6-transporters, parts of the amino acid sequence, especially in proximity to the substrate binding site, are highly conserved, hence conveying crucial insights with regard to the functioning of eukaryotic SLC6-transporters.[47,48] Recently, the soundness of $LeuT_{Aa}$ as homology model was retroactively confirmed by the first successful X-ray structure analyses of eukaryotic SLC6 transporters, including the human serotonin transporter (hSERT) and the dopamine transporter from the fly *Drosophila melanogaster* (dDAT).[49,50]

Being assumed ever since the primary structure of rGAT1 has been elucidated, the work of Yamashita et al. finally demonstrated that the transporters of the SLC6 gene family consist of 12 transmembrane helices, which are connected by loops that protrude into the intra- and extracellular space, respectively, with the amino- and carboxy-terminus being both located at the intracellular side. Four of the transmembrane helices (TM 1, TM3, TM6 and TM8) form an inner ring that holds the central substrate binding site S1 as well as the binding site for the sodium ions in its centre halfway across the cell membrane. Arranged around the inner ring exists an outer ring, comprising the transmembrane helices TM2, TM4, TM5, TM7, TM9 and TM10. At the binding site, the α-helical structure of TM1 and TM6 is interrupted, resulting in short, unwound segments that allow interactions between the substrate and the exposed side chains of the amino acids forming the S1 pocket.

In the substrate-bound state, the S1 site of $LeuT_{Aa}$ is shielded towards the extracellular space by a network of interactions between the side chains of the highly conserved amino acids Tyr108 (TM3), Phe253 (TM6), Arg30 (TM1), and Asp404 (TM10). At this, the aromatic side chains of Tyr108 (TM3) and Phe253 (TM6) form a barrier across the top of the binding pocket, which is augmented by an overlying

network of salt bridges between the guanidine group of Arg30 (TM1), a pair of water molecules, and the carboxylate group of Asp404 (TM10). A second gate separating the S1 site towards the intracellular space is constituted by a complex interaction network between the amino acids of TM1, TM6 and TM8.[37,46,55]

Figure 4. *Structure of the $LeuT_{Aa}$ transporter.[46] The positions of leucine and the two sodium ions are depicted as a yellow triangle and blue circles, respectively.*

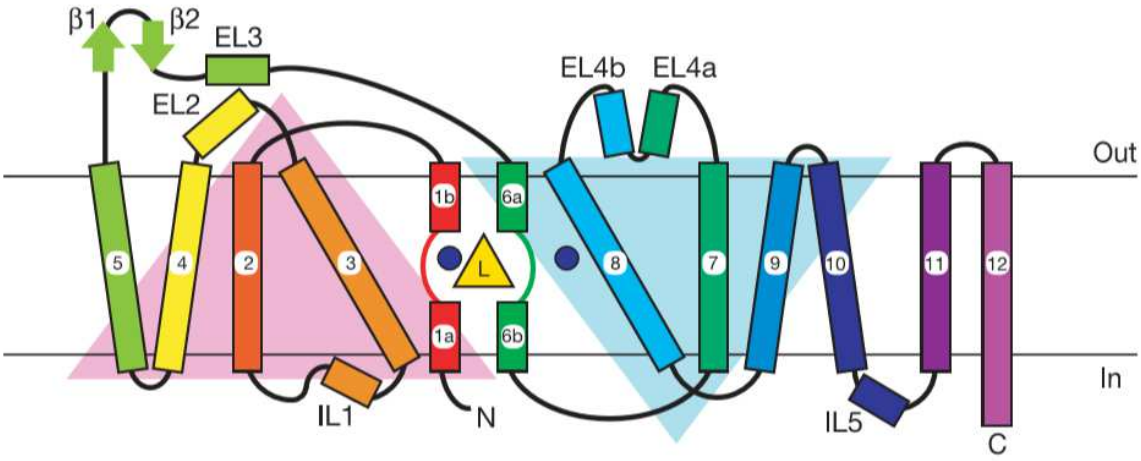

According to the *alternate access model* proposed by Yamashita et al., the transport mechanism relies on the alternate opening and closing of these two gates towards the intra- and extracellular space, respectively, hence allowing the specific and directed transport of the substrate into the cell. During this process the transporter passes through several distinct states, which are each induced by conformational changes mediated by the binding of the substrate and co-substrate: In the *outward facing state* the extracellular gate stands open, allowing the substrate to access the binding site through the funnel-like vestibule from the extracellular space. The substrate binding triggers a conformational change to the *substrate occluded state*, at which both gates are closed and the substrate is trapped at the binding site. Subsequently, another conformational change transforms the transporter into the *inward facing state*, hence opening the intracellular gate and allowing the substrate to pass into the cytoplasma (figure 5).[46,51]

Figure 5. *Postulated transport mechanism of the SLC6 transporters according to Yamashita et al.*[46]

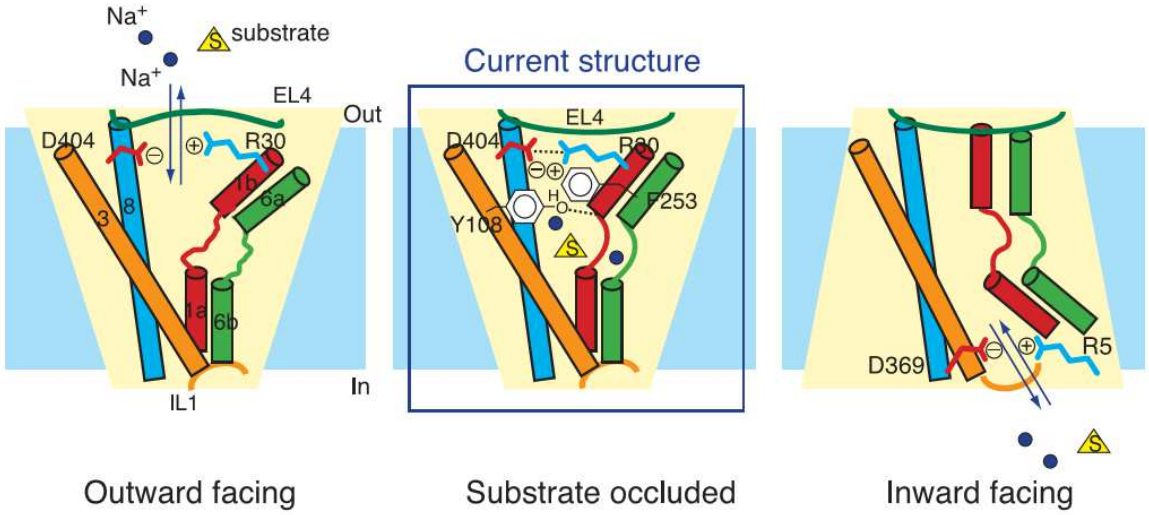

At the bottom of the extracellular vestibule, separated from the S1 binding site by the extracellular gate, exists a second substrate binding site termed S2.[37] Evidence suggests the occupation of S2 by a substrate molecule setting in motion the conformational changes that cause the release of the substrate from the S1 pocket into the cell.[52,53,54] The recent crystallisation of the human serotonin transporter (hSERT) in complex with the antidepressants (*S*)-Citalopram or Paroxetine as well as the crystallisation of LeuT in presence of desipramine have given rise to the theory that S2 also constitutes a binding site for non-competitive inhibitors, which upon binding prevent conformational changes of transporter, hence blocking the substrate transport.[48,55] Detergents such as octylglucosides might likewise inhibit the transporter by binding to S2.[56]

1.3.2 GAT subtypes

There are four GAT subtypes, the nomenclature of which depends on the species the transporters originate from (table 1). When cloned from murine brain cells, the four GAT subtypes are termed mGAT1-4.[57,58] For transporters from cell lines that are derived from other species, including human or rat, a deviant nomenclature is used which denotes the transporters as h/rGAT-1 (≙ mGAT1), h/rBGT-1 (≙ mGAT2),

h/rGAT-2 (≙ mGAT3) and h/rGAT-3 (≙ mGAT4), respectively.[39] Furthermore, a simplified version of the latter nomenclature was introduced following a proposal from the Human Genome Organization (HUGO), which omits the prescriptor designating the species and the hyphen, hence labeling the GAT subtypes as GAT1, BGT1, GAT2 and GAT3. In this dissertation the nomenclature referring to mouse cells will be consistently applied since the biological test system used in our research group is predominantly based on murine cell lines. Exceptions will only be made when a GAT subtype from a particular species is to be emphasized.

Table 1. *Different nomenclatures of the GAT transporters.*

Species	GAT subtypes			
mouse	mGAT1	mGAT2	mGAT3	mGAT4
human	hGAT-1	hBGT-1	hGAT-2	hGAT-3
rat	rGAT-1	rBGT-1	rGAT-2	rGAT-3
HUGO	GAT1	BGT1	GAT2	GAT3

mGAT1, the dominant GAT subtype in the mammalian CNS, is primarily found on pre-synaptic neuronal membranes where it mediates the neuronal GABA uptake.[41,59] However, in some brain regions, such as the thalamus, mGAT1 is found on astrocytes.[60] GAT4, which constitutes the second most abundant GAT subtype after mGAT1, is almost exclusively expressed on astrocytes, where it conducts the glial GABA uptake.[62] mGAT1 and mGAT4 also differ with regard to the regions of the CNS where they are most prevalent. While mGAT1 is widely distributed throughout the entire CNS,[38] its highest densities are found in neocortex, brainstem, spinal cord, cerebellum, basal ganglia, and hippocampus.[61,62] mGAT4 on the other hand is particularly expressed in olfactory bulb, brainstem, and diencephalon.[38] By contrast, mGAT2 and mGAT3 are found in the CNS in very low densities and specific brain structures only and hence are believed not to play any significant role in the termination of the GABAergic neurotransmission in the CNS.[62,63]

Outside the CNS, mGAT1 and mGAT4 have only been found in the retina, whereas mGAT2 and mGAT3 have been shown to be present in the periphery, mainly in

kidney and liver.[63,64] Despite the precise physiological function of mGAT2 and mGAT3 in these organs still being a subject of debate, recent findings suggest that their main role might entail the regulation of metabolic processes as these GAT subtypes transport in addition to GABA also other substrates such as betaine (mGAT2) and taurine (mGAT3).[63,65]

1.3.3 GAT inhibitors

Considering the clinical prominence and severity of disorders resulting from pathophysiologically impaired GABAergic signaling, it is not surprising that there have been comprehensive efforts in medicinal chemistry to influence the GABAergic system by inhibition of the GABA uptake.

Among the earliest compounds identified to inhibit the GABA uptake was muscimol (**10**), an alkaloid isolated from the fly agaric mushroom (*Amanita muscaria*). **10** constitutes a GABA analogue which possesses an isoxazol-3-ol unit as bioisosteric substitute for the carboxylic acid function present in the parent molecule. However, in addition to showing some inhibitory effects on the GABA uptake, **10** is also an agonist at both the $GABA_A$ and the $GABA_B$ receptor as well as a substrate for GABA transaminase.[66] Rigidisation of the molecule by integrating the amino side chain of **10** into a ring, subsequent to the elongation of the distance between the amino nitrogen atom and the isoxazol-3-ol partial structure, led to the first selective, but still only mildly potent GABA uptake inhibitor THPO (**11**, table 2, entry 1).[67]

Important progress was made with the discovery of the conformationally restricted amino acids guvacine (**12**, table 1, entry 1) and nipecotic acid [(*R*)-**13**, table 2, entry 3, and (*S*)-**13**, table 2, entry 4], which formally result from the replacement of the isoxazol-3-ol partial structure present in **11** with a bioisosteric carboxylic acid function.[68] Despite lacking subtype selectivity and being hardly able to cross the *blood brain barrier* (BBB) due to being predominantly present in the zwitterionic state under physiological conditions, **12**, (*R*)-**13** and (*S*)-**13** served as lead structures for the development of more potent and selective GABA uptake inhibitors.

***Table 2**. Inhibitory potencies (pIC_{50}) of GAT inhibitors*

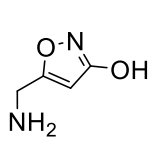

Muscimol (**10**)

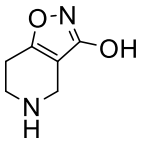

THPO (**11**)

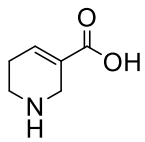

Guvacine (**12**)

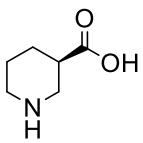

(*R*)-Nipecotic acid [(*R*)-**13**]

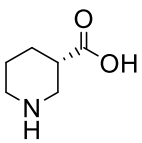

(*S*)-Nipecotic acid [(*S*)-**13**]

Entry	Compound	GABA uptake inhibition (pIC_{50} ± SEM)[a]			
		mGAT1	mGAT2	mGAT3	mGAT4
1	THPO (**11**)[b]	3.0	2.5	<2.5	<2.5
2	Guvacine (**12**)[c]	4.87 ± 0.06	3.31 ± 0.03	4.59 ± 0.05	4.59 ± 0.05
3	(*R*)-Nipecotic acid [(*R*)-**13**][c]	5.19 ± 0.03	3.40 ± 0.05	4.76 ± 0.05	4.95 ± 0.05
4	(*S*)-Nipecotic acid [(*S*)-**13**][c]	4.24 ± 0.05	3.13 ± 0.14	3.83 ± 0.04	3.63 ± 0.06

(a) Results of the [^{3}H]GABA Uptake Assays are given as pIC_{50} ± SEM. (b) Reference literature[69]. (c) For consistency the values determined in our research group are listed.

The pharmacologically most important modification of the cyclic amino acids **12**, (*R*)-**13** and (*S*)-**13** was the introduction of lipophilic residues, usually at the amino nitrogen atom. This did not only improve the pharmacokinetic properties such as *blood brain barrier* (BBB) penetration, which is crucial for the intended therapeutic application, but also significantly increased inhibitory potency and subtype selectivity.

For instance, compounds comprising a diaryl or biaryl unit, which is connected to the amino nitrogen atom of **12** or (*R*)-**13** via a flexible linker, proved to be highly potent and selective inhibitors of the mGAT1 subtype. As a result of this modification, the pIC_{50} values at mGAT1 increased by approximately two log units as compared to unsubsituted (*R*)-nipecotic acid [(*R*)-**13**, table 2, entry 3], which constitutes the more potent enantiomer, whereas the inhibitory activity at mGAT3 and mGAT4 decreased distinctly, resulting in vastly improved subtype selectivity in favor of mGAT1. A considerable number of compounds with this general structure have been synthesized and characterized for their inhibitory potential, including Tiagabine (Gabatril®, **9**), NO-711 (**14**, table 3, entry 2), SKF-89976A (**15**, table 3, entry 3) and **16** (table 3, entry 4).[70,71,72]

***Table 3**. Inhibitory potencies (pIC_{50}) of mGAT1 inhibitors*

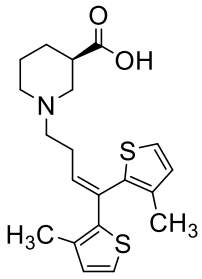

Tiagabine (**9**)

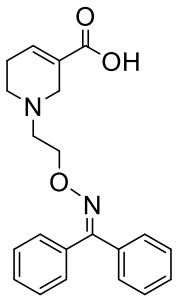

NO-711 (**14**)

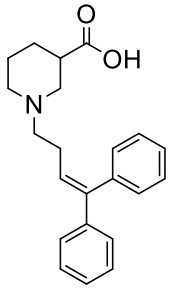

SKF-89976A (**15**)

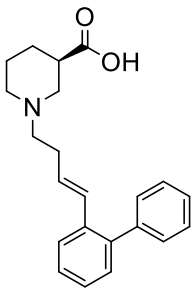

16

Entry	Compound	GABA uptake inhibition (pIC_{50} ± SEM)[a]			
		mGAT1	mGAT2	mGAT3	mGAT4
1	Tiagabine (**9**)	6.88 ± 0.12	50%	64%	73%
2	NO-711 (**14**)	6.83 ± 0.06	3.20 ± 0.09	3.62 ± 0.04	3.07 ± 0.05
3	SKF-89976A (**15**)	6.16 ± 0.05	3.43 ± 0.07	3.71 ± 0.04	3.56 ± 0.06
4	**16**	6.79 ± 0.16	3.87	3.49 ± 0.11	3.54

(a) Results of the [^{3}H]GABA Uptake Assays are given as pIC_{50} ± SEM. Percent values represent remaining [^{3}H]GABA uptake in presence of 100µM test compound.

In a similar fashion, the introduction of a triaryl moiety at the amino nitrogen atom of (*S*)-**13** via an ethylenoxy linker furnished inhibitors of the mGAT4 subtype. Developed by Dhar et al. in 1994 (*S*)-SNAP-5114 (**17**, table 4, entry 1) is considered the lead substance of this class.[73] Conspicuously, the (*S*)-isomer exhibits higher inhibitory potency than the respective (*R*)-isomer, which is contrary to what is observed in case of unsubstituted nipecotic acid [compare (*R*)-**13**, table 2, entry 3, and (*S*)-**13**, table 2, entry 4] and mGAT1 inhibitors such as tiagabine (**9**, table 3, entry 1).

Unfortunately, **17** is associated with a number of detriments. Despite its pIC_{50} value of 5.71 ± 0.07 (table 4, entry 1) numbering amongst the highest of any mGAT4 inhibitors developed so far, it is still considered somewhat unsatisfactory. Furthermore, the compound exerts relatively high inhibitory activity at mGAT3 as well (pIC_{50} = 5.29 ± 0.04), hence constituting a mixed mGAT3/4 subtype inhibitor rather than a pure mGAT4 selective inhibitor. **17** is also characterized by a distinct lack of chemical stability resulting from a tritylether function, which is prone to decomposition

under acidic conditions, being present in its lipophilic domain. The latter issue was successfully addressed by the development of DDPM-1457 (**18**, table 4, entry 2), which avoids the labile tritylether function in the linker in favour of an unsaturated all carbon spacer. Furthermore, minor modifications of the trityl moiety, such as the introduction of a methyl group in the ortho position of one of the three aromatic groups, led to compounds with somewhat improved subtype selectivity (DDPM-859, **19**, table 4, entry 3).[74]

Interestingly, other unsubstituted amino acids apart from nipecotic acid [(*R*)-**13**, (*S*)-**13**] also show considerable inhibitory activity at some GAT subtypes. This includes the substrate GABA itself (**1**, table 4, entry 4), which constitutes a potent inhibitor of all GAT subtypes, the respective pIC_{50} values ranging from 4.56 ± 0.06 (mGAT2) to 5.18 ± 0.13 (mGAT4). But also other acyclic amino acids such as β-alanine (**20**, table 4, entry 5), *rac*-isoserine (**21**, table 4, entry 6), *rac*-2,3-diaminopropionic acid (**22** table 4, entry 7) and (*Z*)-4-aminobut-2-enoic acid (**23**, table 4, entry 8) display inhibitory potencies at mGAT3-4 that lie in the same order of magnitude as those of (*R*)-**13**, while exerting distinctly less inhibitory activity at mGAT1-2.[75] This led to the idea of combining the established lipophilic domain and linker of **17** with amino acid units other than nipecotic acid. Among the resulting compounds, **24** (table 4, entry 9), comprising a 2-hydroxy-2-pyrrolidine-2-yl-acetic acid unit that can be regarded as a rigidized derivative of isoserine **21**, stands out for displaying improved subtype selectivity in favor of mGAT4. This comes, however, at the detriment of a moderate reduction of the inhibitory potency displayed at mGAT4 as compared to the parent molecule **17**.[76]

More recently, high-throughput screening experiments by Damgard et al. have helped to identify a new class of non-competitive hGAT3 (≙ mGAT4) inhibitors derived from isatin. The most potent compound from this class, 5-(thiophen-2-yl)indoline-2,3-dione (**25**, table 4, entry 10), is not only characterized by a pIC_{50} value > 5.0 at mGAT4, but shows also distinct selectivity in favor of this subtype.[77]

***Table 4**. Inhibitory potencies (pIC_{50}) of mGAT4 inhibitors*

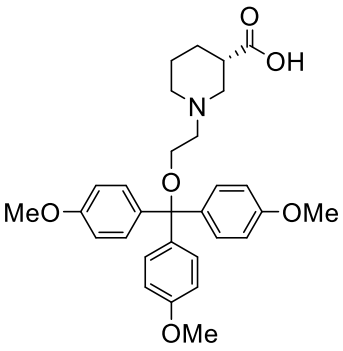

(*S*)-SNAP-5114 (**17**)

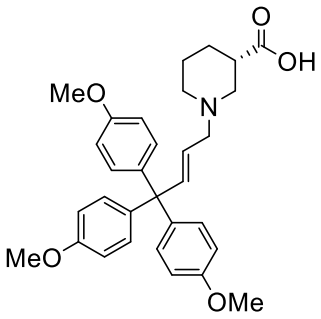

DDPM-1457 (**18**)

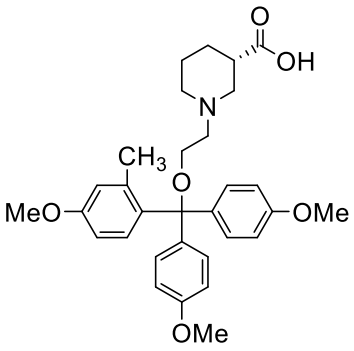

DDPM-859 (**19**)

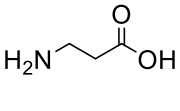

ß-Alanine (**20**)

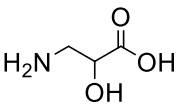

rac-Isoserine (**21**)

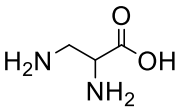

rac-2,3-Diamino-propionic acid (**22**)

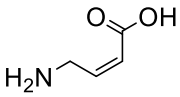

(Z)-4-Aminobut-2-enoic acid (**23**)

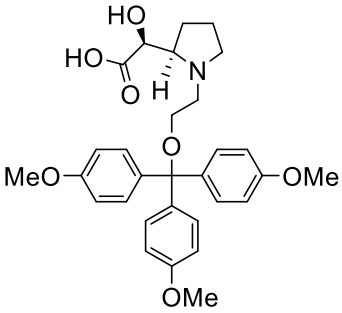

24

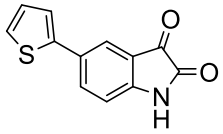

5-(Thiophen-2-yl)indoline-2,3-dione (**25**)

Entry	Compound	GABA uptake inhibition (pIC_{50} ± SEM)[a]			
		mGAT1	mGAT2	mGAT3	mGAT4
1	(*S*)-SNAP-5114 (**17**)[b]	4.07 ± 0.09	56%	5.29 ± 0.04	5.71 ± 0.07
2	DDPM-1457 (**18**)[b]	4.40 ± 0.05	4.42 ± 0.11	5.47 ± 0.02	5.87 ± 0.08
3	DDPM-859 (**19**)[b]	4.19 ± 0.07	4.12 ± 0.08	4.85 ± 0.04	5.78 ± 0.03
4	GABA (**1**)[c]	5.14 ± 0.09	4.56 ± 0.06	4.94 ± 0.09	5.18 ± 0.13

5	β-Alanine (**20**)[c]	2.59 ± 0.03	3.48 ± 0.11	4.66 ± 0.06	4.46 ± 0.13
6	*rac*-Isoserine (**21**)[c]	2.33 ± 0.05	3.39 ± 0.11	4.87 ± 0.05	4.78 ± 0.14
7	*rac*-2,3-Diaminopropionic acid (**22**)[c]	3.11 ± 0.02	3.50 ± 0.12	4.66 ± 0.08	5.05 ± 0.02
8	(*Z*)-4-Aminobut-2-enoic acid (**23**)[c]	2.99 ± 0.04	3.67 ± 0.08	4.95 ± 0.04	5.04 ± 0.06
9	**24**[d]	80 %	64 %	70 %	5.18 ± 0.05
10	5-(Thiophen-2-yl)indoline-2,3-dione (**25**)	- 4.53[c]	3.21 ± 0.19[e] 52 %[c]	3.74 ± 0.14[e] 44 %[c]	5.20 ± 0.05[e] 4.61 [c]

(a) Results of the [^{3}H]GABA Uptake Assays are given as pIC_{50} ± SEM. Percent values represent remaining [^{3}H]GABA uptake in presence of 100µM test compound. (b) Reference literature[78]. (c) For consistency the values determined in our research group are listed. (d) Reference literature[76]. (e) Reference literature[77]. The pIC_{50} values refer to the four human GAT subtypes hGAT1, hBGT1, hGAT2 and hGAT3, respectively.

Whereas many mGAT4 inhibitors, including the lead substance (*S*)-SNAP-5114 (**17**, table 4, entry 1), exhibit considerable biological activity at mGAT3 as well and can thus, strictly speaking, be considered mixed mGAT3/4 subtype inhibitors, there are few pure mGAT3 selective inhibitors known to this date. To some extent, 3-imidazol-2-ylpropionic acid (**26**, table 5, entry 1) can be regarded as such as it is about one log unit more active at mGAT3 than at mGAT2 and mGAT4. However, being characterized by a pIC_{50} value of 4.54 ± 0.15, the actual inhibitory potency exerted at the targeted GAT subtype is comparatively low.

Likewise, there is only a small number of relatively low-potency mGAT2 inhibitors available so far, with the exception of a class of recently developed, bicyclic GABA-analogues. The lead compound **27** (table 5, entry 2) is characterized by a pIC_{50} value of 6.23 ± 0.32 at mGAT2 and hence approximately two log units more active at this transporter subtype than at mGAT1 and mGAT3-4.[79] However, it remains unclear whether the compounds of this class can serve as a starting point for the development of higher-molecular inhibitors with better pharmacokinetic properties.

Conspicuously, NNC05-2090 (**29**, table 5, entry 5), an example of an mGAT2 inhibitor featuring a lipophilic domain, does not comprise a carboxylic acid function in its molecule. This sets the compound apart from inhibitors of the other GAT subtypes, implying that in case of mGAT2 the overall structure of the molecule might play a more decisive role than specific interactions between the carboxylic acid group and

the target. Similarly, substitution of the nipecotic acid substructure present in the prototypical mGAT1 inhibitor tiagabine [(*R*)-**9**, table 3, entry 1] with a (*S*)-N-methyl-exo-THPO unit results in a compound with significantly attenuated inhibitory activity at mGAT1, the respective pIC_{50} value decreasing ~3 log units from 6.88 ± 0.12 to 3.92 [(*S*)-EF1502, (*S*)-**28**, table 5, entry 3]. At the same time, the inhibitory potency displayed at mGAT2 is moderately increased to a pIC_{50} value of 4.47, furnishing compound which is about half a log unit more active at mGAT2 than at the other transporter subtypes.

The corresponding (*R*)-enantiomer [(*R*)-**28**, table 5, entry 4] however, while exerting comparable inhibitory activity at mGAT2, remains a relatively potent mGAT1 inhibitor (pIC_{50} = 5.40), highlighting the significance of stereochemistry when it comes to inhibitory potency and subtype selectivity of GAT inhibitors.

***Table 5**. Inhibitory potencies (pIC_{50}) of mGAT2 and mGAT3 inhibitors*

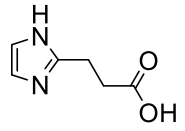

3-Imidazol-2-yl-propionic acid (**26**)

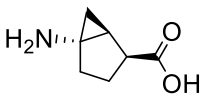

(1*S*,2*S*,5*R*)-5-aminobicyclo-[3.1.0]-hexane-2-carboxylic acid (**27**)

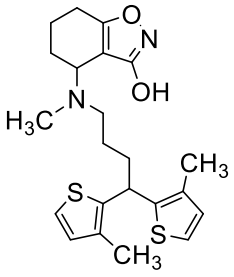

EF1502 [(*R*/*S*)-**28**]

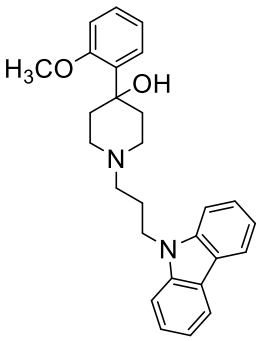

NNC05-2090 (**29**)

Entry	Compound	GABA uptake inhibition (pIC_{50} ± SEM)[a]			
		mGAT1	mGAT2	mGAT3	mGAT4
1	3-imidazol-2-ylpropionic acid (**26**)	63%	3.28 ± 0.12	4.54 ± 0.15	3.51 ± 0.03
2	**27**[b]	<4.00	6.23 ± 0.32	<4.00	4.12 ± 0.24
3	(*R*)-EF1502 [(*R*)-**28**][c]	5.40	4.66	<3.82	<3.82
4	(*S*)-EF1502 [(*S*)-**28**][c]	3.92	4.47	<3.82	<3.82
5	NNC05-2090 (**29**)[d]	4.72	5.85	4.39	4.82

(a) Results of the [^{3}H]GABA Uptake Assays are given as pIC_{50} ± SEM. Percent values represent remaining [^{3}H]GABA uptake in presence of 100µM test compound. (b) Reference literature[79]. (c) Reference literature[80]. (d) Reference literature[81].

In conclusion, despite many advances in recent years, there still exists a lack of sufficiently potent and selective inhibitors of the GABA transporter subtypes mGAT2-4. This is particularly true for mGAT4, the second most abundant GAT subtype in the mammalian CNS after mGAT1. Despite constituting a potentially highly interesting pharmacological target for the treatment of a wide variety of neuronal diseases, the precise physiological significance of mGAT4 is not yet fully clarified due to the unavailability of appropriate pharmacological tools. Hence, the situation requires the development of potent and selective mGAT4 inhibitors.

2. Aims and scope

As the currently available mGAT4 inhibitors can be regarded not really satisfying with regard to inhibitory potency and subtype selectivity, there exists a strong demand for the development of more efficient inhibitors. For this to be achieved, a deeper understanding of the structure activity relationship (SAR) of mGAT4 inhibitors is required. The objective of this dissertation aimed at broadening the knowledge in this respect and, as a consequence thereof, at identifying mGAT4 inhibitors with higher potency and subtype selectivity. To this end, a series of analogues of the lead compound (*S*)-SNAP-5114 (**17**) should be synthesized and examined for the inhibitory effects exhibited at the four GAT subtypes.

First, possible variations of the amino acid partial structure of (*S*)-SNAP-5114 (**17**) should be investigated. As demonstrated by a previous study from Stefan et al.[76] substitution of the nipecotic acid unit with other cyclic amino acids can lead to mGAT4 inhibitors that show moderately high potency at mGAT4 while at the same time exhibiting a favorable selectivity pattern. In particular, **24** (table 4, entry 9), featuring a 2-hydroxy-2-(pyrrolidin-2-yl)acetic acid unit while retaining the linker and lipophilic domain of **17**, is characterized by considerably increased subtype selectivity in favour of mGAT4 as compared to the parent compound, even though this is accompanied by a slight reduction of the inhibitory potency displayed at the targeted subtype.

Based on these findings, we aimed at the development of further cyclic hydroxyl-substituted amino acids as potential alternatives to the nipecotic acid subunit present in most mGAT4 inhibitors. In that context, an approach of fragment based design should be taken, i.e. the amino acids themselves should be synthesized and evaluated for their inhibitory potential rather than larger inhibitor molecules comprising these amino acids as subunits.

According to molecular modelling studies by Wein et al.[78] regarding mGAT1, unsubstituted amino acids such as nipecotic acid adapt a binding pose at the target whereby the amino nitrogen atom is aligned towards the intracellular space. However, if lipophilic moieties are introduced at the nitrogen atom, as is the case with inhibitors such as Tiagabine (**9**, table 3, entry 1), the binding pose is altered so that

the nitrogen atom faces towards the extracellular space, with the lipophilic domain extending into the extracellular vestibule (figure 6). Even comparatively small substituents at the nitrogen atom, such as a butyl moiety, seem to be sufficient to effect the described alteration of the binding pose.

Figure 6. *Postulated binding poses of nipecotic acid (**13**, left) and Tiagabine (**9**, right) at mGAT1.*

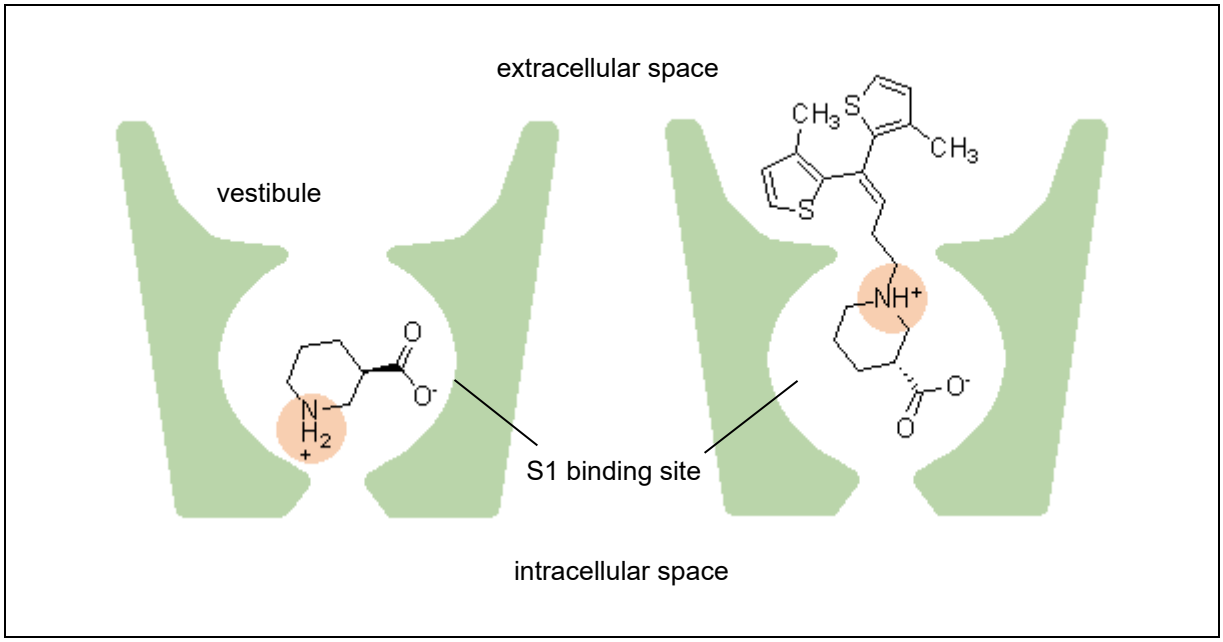

Despite no reliable *in silico* model being available for GAT subtypes other than mGAT1 it seems highly likely due to the structural homology of the GABA transporter subtypes that these findings are also true for mGAT2-4. Hence, N-butylated amino acids were of particular interest for our project as their biological test results would allow to draw direct conclusions about the suitability of the amino acid structure as subunit in (*S*)-SNAP-5114 (**17**) analogues, therefore dispensing the need for the introduction of more complex lipophilic domains. Our attention in this regard was focused on the N-butyl derivatives of α- and β-hydroxy-substituted amino acids featuring an azetidine, pyrrolidine and piperidine heterocycle, respectively (scheme 1).

Scheme 1. *Overview over the hydroxy-substituted amino acids that were synthesized and evaluated as potential alternatives to the nipecotic acid subunit (highlighted in green) present in (S)-SNAP-5114 (**17**). In order to warrant according binding modes, n-butyl moieties (highlighted in blue) were introduced at the amino nitrogen atom of the test compounds.*

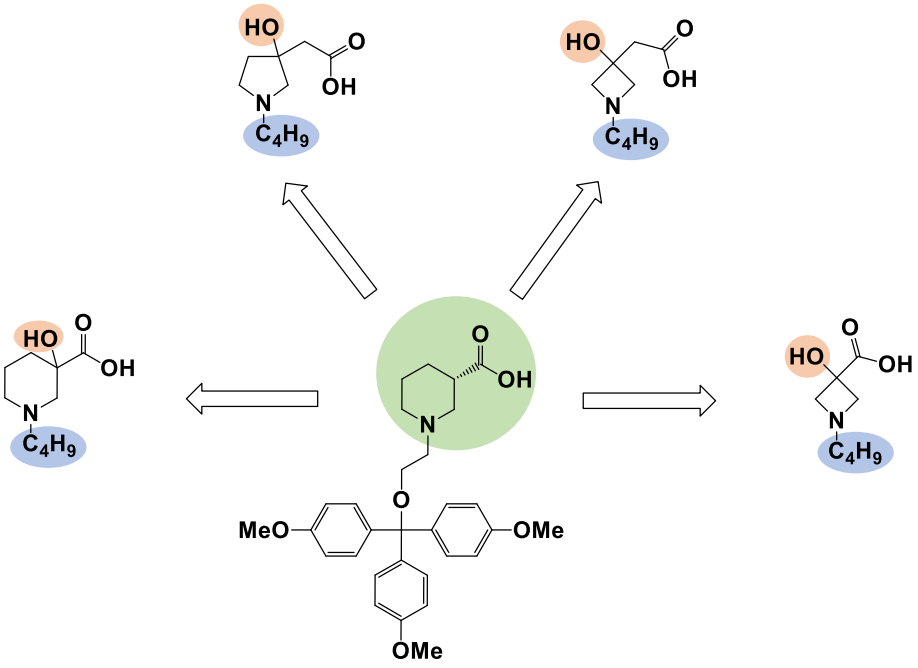

(*S*)-SNAP-5114 (**17**)

The main part of this dissertation aimed at the development of (*S*)-SNAP-5114 (**17**) analogues with modified lipophilic domains. In this context, we were interested in compounds comprising polar moieties therein, e.g. a carboxylic acid, carbaldehyde, carboxamide, sulfonamide, alcohol, or nitrile function, an acetyl or methoxymethylene group, or an amino acid substructure. The introduction of these polar groups into the lipophilic domain might cause increased polar interactions between the inhibitor and the binding site, hence possibly enhancing the potency and/or the subtype selectivity of the resulting compound.

Hence, analogues of (*S*)-SNAP-5114 (**17**) should be synthesized that feature those polar moieties in place of one of the methoxy groups present in the lipophilic domain

of the parent compound (scheme 2, a). Besides, it should be examined how the formal replacement of an entire aromatic moiety with a polar group, thus diverting from the established triaryl pattern, influences the biological activity of the resulting compounds (scheme 2, b). Moreover, the question should be addressed how compounds that have two or all three of the aromatic methoxy groups in the lipophilic domain replaced by other groups (scheme 2, c) compare to inhibitors with only one such alteration.

Scheme 2. *Overview of the structure modifications of the (S)-SNAP-5114* (**17**) *aiming at the introduction of polar groups (highlighted in red) into the lipophilic domain.*

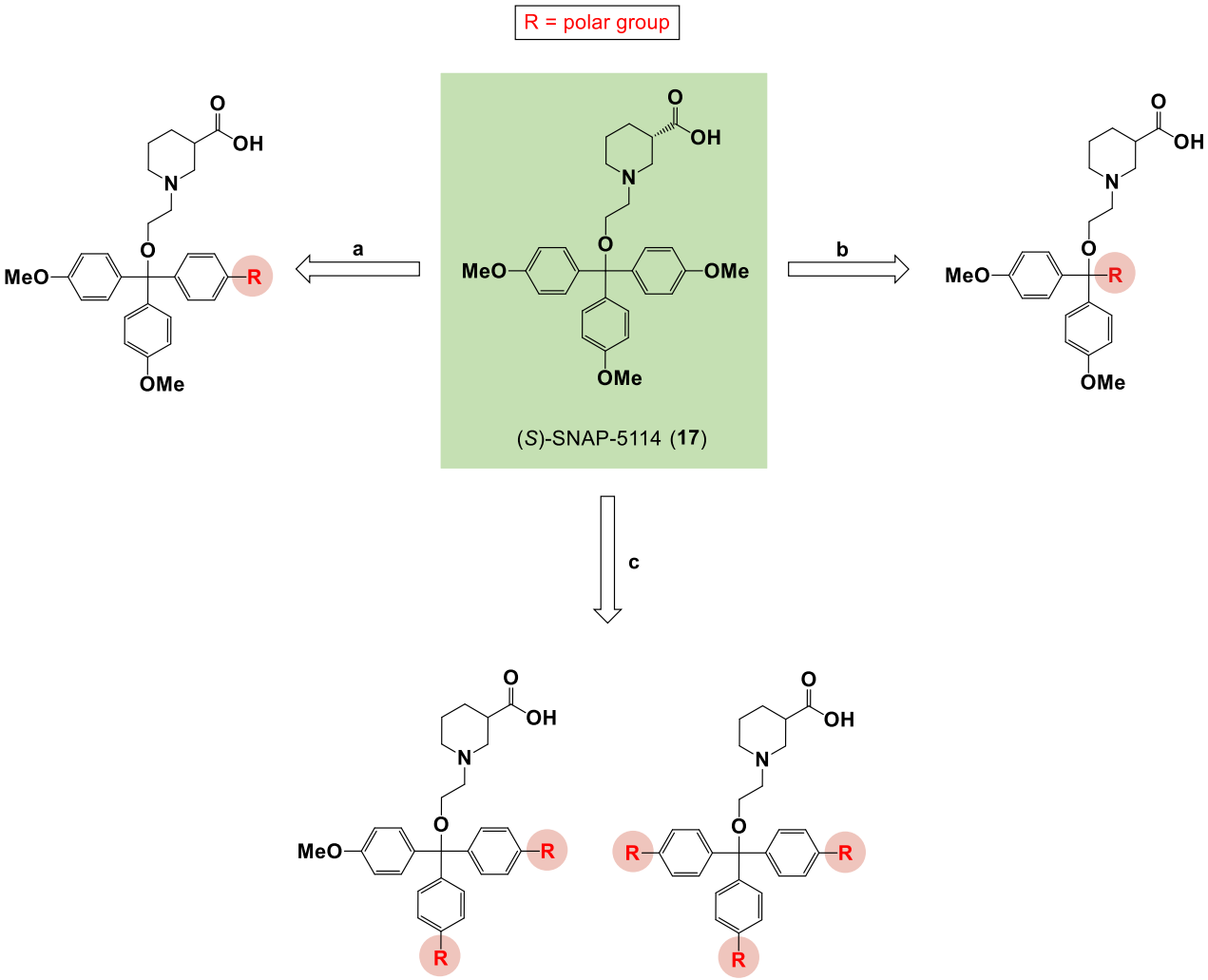

During an earlier study conducted in our group,[74] an (*S*)-SNAP-5114 (**17**) analogue was developed which differs from the parent compound by comprising an additional methyl group in the *ortho*-position of one of the three aryl groups (**19**, table 4, entry 3). Interestingly, this modification was well tolerated by mGAT4, the pIC_{50} value of **19** being very similar to that of the parent molecule (**19**: 5.78 ± 0.03, **17**: 5.71 ± 0.07) while at the same time exhibiting somewhat improved subtype selectivity in favour of mGAT4. This finding led to the idea of increasing the space requirements of the lipophilic domain even further by the introduction of sterically demanding, aliphatic groups, e.g. a *tert*-butyl, 1-methylcyclohex-1-yl or adamantyl moiety.

In the simplest case, the sterically demanding group should formally substitute one of the three aromatic moieties featured by the parent compound **17** (scheme 3, a). However, modifications of the lipophilic domain following this pattern are accompanied by a distinct increase of the overall size and possibly even of the molecular weight of the molecule, which may be considered unfavourable under pharmacokinetic aspects. Hence, it should also be examined whether mGAT4 tolerates downsized lipophilic domains comprising only one aromatic moiety in addition to the sterically demanding group, the second aromatic moiety being replaced by a hydrogen atom (scheme 3, b). Finally, N-substituted nipecotic acid derivatives should be synthesized that deviate even more extensively from the parent compound by having the sterically demanding group, such as an adamantane partial structure, integrating the quaternary carbon atom of the former trityl function (scheme 3, c). As a side project, it should also be studied how the replacement of the carboxylic acid function by a carboxamide group affects the inhibitory potency and subtype selectivity of the resulting compounds.

Scheme 3. *Overview of the structure modifications of the (S)-SNAP-5114* (**17**) *aiming at the introduction of sterically demanding, aliphatic moieties (highlighted in blue) into the lipophilic domain.*

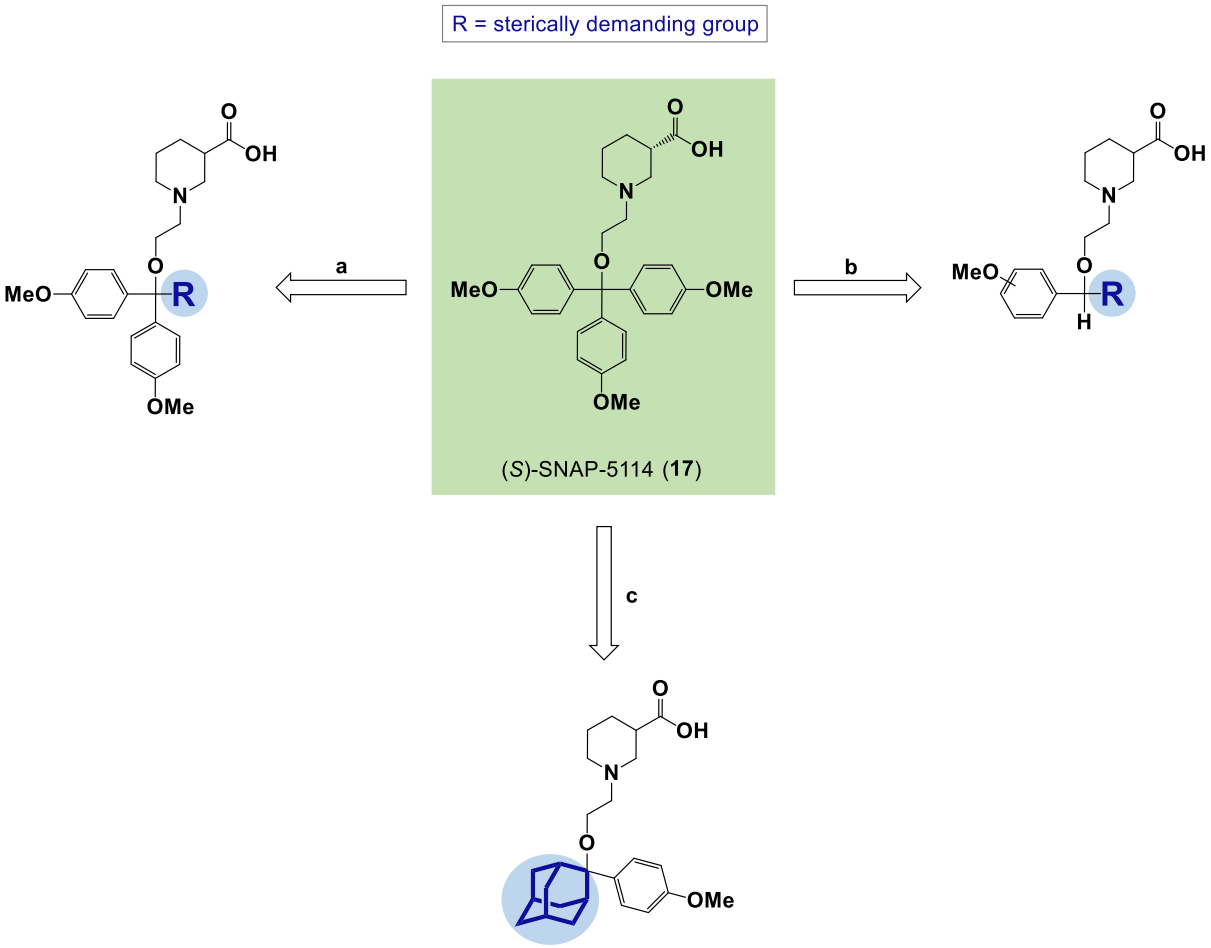

Since the stereochemistry of the nipecotic acid partial structure plays a crucial role for the biological activity of derived mGAT4 inhibitors, all target compounds should be first synthesized in racemic form as this provides information on both enantiomers. In case of racemic compounds exhibiting similar or higher inhibitory potency at mGAT4 than the benchmark inhibitor **17**, the pure (*R*)- and (*S*)-isomers should additionally be synthesized and biologically evaluated.

The results of this study would allow to draw important conclusions about the structure activity relationship (SAR) of mGAT4 inhibitors with regard to polarity, size, and number of matching substituents in the lipophilic domain, and hence provide an

essential extension of the data for future developments of more potent mGAT4-inhibitors.

3. Summary of manuscripts and published results

3.1. First publication: "Synthesis and biological evaluation of α- and β-hydroxy substituted amino acid derivatives as potential mGAT4 inhibitors"

Typically, mGAT4 inhibitors such as the lead compound (*S*)-SNAP-5114 (**17**) share the common scaffold of a nipecotic acid unit, which has its amino nitrogen atom connected to a lipophilic domain via a flexible linker. Aiming at the development of mGAT4 inhibitors with increased inhibitory potency and/or subtype selectivity, various cyclic and acyclic hydroxy-substituted amino acids were explored as potential alternatives to the nipecotic acid unit present in most mGAT4 inhibitors. At this, an approach of fragment based design was chosen using the N-butyl derivatives of the concerning amino acids in order to estimate their suitability as subunits in larger inhibitor molecules.

Furthermore, derivatives of hydroxy-substituted amino acids were synthesized that have the linker and lipophilic domain of the lead compound (*S*)-SNAP-5114 (**17**) introduced at the OH function rather than at the amino nitrogen atom. This molecular structure might enable the amino acid unit to adopt a more favorable binding pose as compared to N-substituted derivatives, while still facilitating interactions between the lipophilic domain and the target.

Synthesis of the cyclic N-butyl amino acids proceeded from the appropriate cyclic benzyl- or benzhydryl-protected 3-aminoketones comprising an azetidine, pyrrolidine and piperidine skeleton, respectively. Reaction of these compounds with trimethylsilylcyanide and hydrolysis of the obtained TMS-protected cyanohydrines furnished α-hydroxycarboxamides. Similary, reaction of the 3-aminoketones with lithium 1-ethoxyethen-1-olate at low temperatures led to the corresponding β-hydroxyesters. The subsequent deprotection and N-butylation of the amino nitrogen atom, followed by hydrolysis of the carboxamide function and the ester group, respectively, gave the desired cyclic hydroxy-substituted N-butyl amino acids. The open-chained analogues were available in a one-step synthesis by N-alkylation of hydroxy-substituted amino acids with 1-bromobutane.

In order to construct the amino acid derivatives that have a 4,4´,4´´-trimethoxytrityl oxyl ethyl [(4-MeO-C_6H_4)$_3$$COCH_2CH_2$] residue attached to the alcohol function, the free, hydroxy-substituted amino acids were first protected at the amino nitrogen atom and at the carboxyl group as phthalimide and ester, respectively. Treatment with 2-iodoethoxy-TBDPS in the presence of Ag_2CO_3 and subsequent removal of the TBDPS protecting group with HF-pyridine facilitated the hydroxylethylation of the OH function. Finally, reaction with 4,4´,4´´-trimethoxytrityl chloride, followed by the deprotection of the amino nitrogen atom and the carboxylic acid function, gave the desired O-derivatized amino acids.

The biological evaluation of the synthesized compounds showed the cyclic N-butyl amino acids have only minor or negligible inhibitory activity at mGAT4. However, some of the acyclic N-butyl amino acids were found to exhibit promising inhibitory potency at the targeted transporter subtype. In particular, 4-(butylamino)-3-hydroxybutanoic acid (pIC_{50} = 3.42 ± 0.12) and N-butyl isoserine (pIC_{50} = 3.26 ± 0.10) are characterized by pIC_{50} values on par with the reference compound N-butylnipecotic acid (pIC_{50} = 3.32 ± 0.04), while exhibiting a different selectivity pattern regarding the transporter subtypes mGAT1-3. Hence, an amino acid unit derived from 4-amino-3-hydroxybutanoic acid or isoserine might be a suitable alternative to the nipecotic acid partial structure present in most mGAT4 inhibitors.

On the other hand, the O-substituted amino acid derivatives synthesized for this study were found to display relatively poor inhibitory potency as compared to the corresponding unsubstituted hydroxyamino acids. This finding demonstrates that introducing the lipophilic domain and spacer at the hydroxy function is not beneficial in terms of inhibitory activity, and thus probably not a path worth pursuing in future developments.

Declaration of contributions: Synthesis of the cyclic N-butyl amino acids and their precursor molecules was done by myself, including the evaluation of the analytical data. The open-chained amino acid derivatives and their precursors were synthesized by Janina Andreß from our group, who also evaluated the analytical data of these compounds. The biological testing was carried out by the technical assistants of the group under the supervision of Dr. Georg Höfner.

3.2. Second publication: "Synthesis and Biological Evaluation of N-Substituted Nipecotic Acids as (*S*)-SNAP-5114 Analogues with Modified Lipophilic Domains"

The GABA transporter subtype mGAT4 constitutes a potentially highly interesting pharmacological target for the treatment of various neurological diseases, including epilepsy, anxiety disorders, neuropathic pain and depression. However, the currently available inhibitors of mGAT4 can be regarded as insufficient in terms of inhibitory potency and subtype selectivity. This situation requires the development of more efficient agents and, as a prerequisite, the deepening of the general understanding of the structure activity relationships (SAR) with regard to mGAT4 inhibitors.

In order to expand the knowledge hereof, analogues of the lead substance (*S*)-SNAP-5114 (**17**) were synthesized that differ from the parent compound by having one or more of the aromatic methoxy groups in the lipophilic domain substituted by polar moieties such as a carboxy, hydroxymethylene, carboxamide, carbaldehyde or sulfonamide function, or an acetyl or methoxymethylene group. Likewise, the introduction of amino acid partial structures into the lipophilic domain was of interest. These modifications might enable increased interactions between the inhibitor and polar regions at the binding site, which in turn might result in improved binding affinity, inhibitory potency, and subtype selectivity. In addition, we also aimed to explore how the substitution of an entire aromatic residue in the lipophilic domain with a small, polar moiety, hence deviating from the established triaryl pattern, affects the inhibitory activity and subtype selectivity of the resulting compounds.

For the construction of the test compounds a series of tertiary alcohols comprising the desired moieties, or appropriate precursors thereof, was synthesized as building blocks for the construction of what should become the lipophilic domain. This was accomplished by reaction of Grignard or organolithium reagents with appropriate electrophiles such as acid chlorides, esters and ketones, respectively. Conversion of the thus obtained tertiary alcohols into the corresponding chlorides by treatment with acetyl chloride in presence of a catalytic amount of DMF, followed by alcoholysis with *rac*-ethyl N-(2-hydroxyethyl)nipecotinate, furnished the racemic N-substituted nipecotic acid esters. These were either hydrolized at this stage to give the desired

N-substituted nipecotic acids, or functional group interconversions in the lipophilic domain were performed beforehand, including the introduction of various amino acid partial structures via reductive amination. After final hydrolysis of the ester functions, the obtained racemic N-substituted nipecotic acids were evaluated for their inhibitory potency at all four mGAT subtypes.

As demonstrated by the results of the biological evaluation, there exists no direct correlation between the polarity or size of the newly introduced group, and the inhibitory potency exhibited by the resulting compound. However, analogues of (*S*)-SNAP-5114 (**17**) which are characterized by clog *D* values similar to that of the parent compound (i.e. 2.0 – 2.4), while comprising a hydrogen bridge accepting moiety in the lipophilic domain, were found to exert the highest inhibitory potencies. Being the most potent of the racemic compounds synthesized for this study, the (*S*)-SNAP-5114 (**17**) analogue that has one of the methoxy groups in the lipophilic domain substituted by a carbaldehyde function was also synthesized in form of the enantiopure (*R*)- and (*S*)-isomers. With its pIC_{50} value amounting to 5.89 ± 0.07, the (*S*)-enantiomer was found to be a nominally more potent mGAT4 inhibitor than (*S*)-SNAP-5114 (**17**), while the subtype selectivity in favour of mGAT4 is comparable to that of the parent compound. On the other hand, (*S*)-SNAP-5114 (**17**) analogues having one of the aromatic moieties in the lipophilic domain replaced by a small, non-aromatic polar group are characterized by negligible potency at mGAT4, hence stressing the importance of the triaryl structure in the lipophilic domain for the inhibitory activity of mGAT4 inhibitors.

The findings of this study convey important aspects about the structure activity relationships (SAR) of (*S*)-SNAP-5114 (**17**) analogues with regard to size, polarity, and electronic effects of the substituents in the lipophilic domain, and are thus expected to harness future research aiming at the development of more potent mGAT4 inhibitors.

Declaration of contributions: Synthesis of the N-substituted nipecotic acid derivatives and all precursor molecules was done by myself, including the evaluation of the analytical data of all compounds. The biological testing was carried out by the technical assistants of the group under the supervision of Dr. Georg Höfner.

3.3. Manuscript of the third publication: "Synthesis and Biological Evaluation of N-Substituted Nipecotic Acids as (*S*)-SNAP-5114 Analogues Containing Sterically Demanding Aliphatic Moieties in the Lipophilic Domain"

In pursuit of finding more potent and subtype selective inhibitors for mGAT4 a variety of N-substituted nipecotic acids derived from the lead compound (*S*)-SNAP-5114 (**17**) was synthesized and biologically evaluated. The structural modifications of (*S*)-SNAP-5114 (**17**) included the formal substitution of one of the aromatic residues present in the parent compound by a sterically demanding aliphatic moiety, such as a *tert*-butyl, 1-methylcyclopentan-1-yl, 1-methylcyclohexan-1-yl, or adamantan-1-yl group. Furthermore, analogues of (*S*)-SNAP-5114 (**17**) were synthesized which comprise in the lipophilic domain only one aromatic residue besides the sterically demanding group, the second aromatic residue being replaced by a hydrogen atom. Finally, compounds were studied that have the sterically demanding group integrating the quaternary carbon atom of the $COCH_2CH_2$ linker, hence resulting in a lipophilic domain with significantly reduced space requirements.

The key step in the reaction sequence leading to the desired test compounds involved the construction of the ether function which links the lipophilic domain to the short carbon chain leading to the nipecotic acid unit. To this end, tertiary alcohols featuring the required sterically hindered moieties were first converted into the corresponding chlorides using acetyl chloride in presence of a catalytic amount of DMF. Subsequently, the ether function was established by alcoholysis with *rac*-ethyl 1-(2-hydroxyethyl)nipecotate, hence furnishing the desired racemic N-substituted nipecotic acids in form of their ester precursors.

A different synthetic approach was required for the etherification of secondary alcohols. Reaction of these compounds with 2-chloroethanol under solvent-free conditions in presence of the Lewis-acid catalyst indium(III)-chloride led to the corresponding β-chloroethyl ethers. In the ensuing step, the nipecotic acid unit was introduced into the molecules by reaction with *rac*-ethyl nipecotate, hence furnishing the ester derivatives of the desired test compounds as ~1:1 mixtures of racemic diastereomers.

After final hydrolysis of the ester functions, the obtained N-substituted nipecotic acids were evaluated for their inhibitory potential at all four mGAT subtypes. Interestingly, the data from the biological evaluation revealed a tight correlation between the size of the sterically demanding group that was present in the lipophilic domain, and the inhibitory activity of the resulting compounds.

In case of (*S*)-SNAP-5114 (**17**) analogues that feature lipophilic domains derived from tertiary alcohols, i.e. comprising two aromatic residues in addition to the sterically demanding group, the inhibitory potency exerted at mGAT4 increases with the size of this group from *tert*-butyl to 1-methylcyclopent-1-yl to 1-methylcyclohexyl-1-yl to adamant-1-yl. Being the most potent of the racemic test compounds with this structural motif, the adamant-1-yl derivative was additionally synthesized in form of its enantiopure (*R*)- and (*S*)-isomers. Hereby, the (*S*)-enantiomer was found to exert a pIC_{50} value of 6.13 ± 0.10, hence surpassing the inhibitory potency of the benchmark inhibitor (*S*)-SNAP-5114 (**17**, pIC_{50} = 5.71 ± 0.07) by nominally ~0.4 log units. This renders the compound among the most active mGAT4 inhibitors known so far, even though its subtype selectivity in favor of mGAT4 is somewhat less pronounced as compared to (*S*)-SNAP-5114 (**17**). Similarly, the enantiopure (*S*)-SNAP-5114 (**17**) analogue having a 1-methylcyclohexyl-1-yl moiety in the lipophilic domain is characterized by considerable inhibitory potency, with the pIC_{50} amounting to 5.94 ± 0.04.

Furthermore, we examined N-substituted nipecotic acid derivatives with lipophilic domains derived from secondary alcohols, which were obtained and biologically evaluated as mixtures of racemic diastereomers (~1:1). The inhibitory potency of these compounds was also found to be strongly dependent on the size of the sterically demanding moiety. In this context, the (*S*)-SNAP-5114 (**17**) analogue comprising in the lipophilic domain an adamant-1-yl group next to a single aromatic residue was found to exhibit a pIC_{50} value of 5.49 ± 0.01 at mGAT4. By contrast, compounds featuring smaller or larger sterically demanding moieties, such as a 1-methylcyclohexyl-1-yl or 3,5-dimethyladamantyl group, respectively, are characterized by distinctly less inhibitory potency at the targeted transporter subtype. Considering the extent to which these compounds differ from the prototypic mGAT4

inhibitor (*S*)-SNAP-5114 (**17**), they may be regarded as a new class of inhibitors with potentially beneficial characteristics, including reduced molecular weight and presumptively also increased chemical stability. Thus, compounds of this type may represent a promising basis for future developments of mGAT4 inhibitors.

As opposed to this, (*S*)-SNAP-5114 (**17**) analogues featuring an even more downscaled lipophilic domain by having an adamant-2-yl moiety as sterically demanding group integrating the quaternary carbon atom of the $COCH_2CH_2$ linker, are characterized by comparatively weak inhibitory potency at mGAT4. This finding is likely attributable to an insufficient filling of the binding cavity.

Notably, the introduction of polar moieties into the sterically demanding group, such as a methoxy group or an ether function, led to a sharp decline in biological activity as compared to the corresponding all-carbon analogues, hence highlighting the necessity for the sterically demanding, aliphatic group to be apolar irrespective of the fact that it replaces a relatively polar 4-methoxyphenyl residue.

As a side project analogues of (*S*)-SNAP-5114 (**17**) were synthesized which have the carboxylic acid function substituted by a carboxamide moiety. This modification should facilitate insights into whether the carboxylic acid function can be replaced by other polar groups that are not mostly ionized under physiological conditions, which would result in compounds with improved pharmacokinetic characteristics. Synthesis of the carboxamide derivatives was accomplished by aminolysis of the ester precursors of the N-substituted nipecotic acids with ammonia in presence of sodium cyanide as catalyst. Interestingly, in case of carboxamides derived from N-substituted nipecotic acids with high inhibitory potency this structure variation was accompanied by a distinct loss of activity of more than one log unit. However, carboxamides derived from relatively weak inhibitors were found to be on par with the corresponding free amino acids in terms of inhibitory potency. This finding suggests that the binding mode of weak inhibitors relies predominantly on unspecific ligand-target interactions that are hardly affected by the exchange of the carboxylate by a carboxamide function.

Declaration of contributions: Synthesis of the N-substituted nipecotic acid derivatives and all precursor molecules was done by myself, including the evaluation of the analytical data of all compounds. The biological testing was carried out by the technical assistants of the group under the supervision of Dr. Georg Höfner.

4. Summary of the thesis

Diseases related to deficient GABAergic neurotransmission, such as epilepsy, depression, Alzheimer´s disease and anxiety disorders, represent a major world health issue, hence requiring effective and tolerable medication. In this context, the GABA transporter subtype mGAT4 has come into focus as potentially promising pharmacological target, however, the currently available inhibitors of mGAT4 can be regarded as not really satisfying in terms of subtype selectivity and inhibitory potency. This necessitates the expansion of the current state of knowledge regarding the structure activity relationships (SAR) of mGAT4 inhibitors as a prerequisite for the development of more efficient drugs. To further that cause, this study aimed at the synthesis and biological evaluation of a variety of structurally modified analogues of the lead compound (*S*)-SNAP-5114 (**17**).

The (*S*)-SNAP-5114 (**17**) molecule comprises a nipecotic acid unit which is connected at the amino nitrogen atom to a 4,4´,4´´-trimethoxytrityl moiety via a CH_2CH_2O linker. First, it should be explored whether a positive effect with regard to inhibitory potency and/or subtype selectivity can be achieved by substituting the nipecotic acid substructure with other amino acid units. As is the case with the nipecotic acid unit to be replaced, these should also incorporate the amino nitrogen atom into a heterocycle, e.g. an azetidine, pyrroline or piperidine ring, and thus be structurally relatively rigid. In this context, α- and β-hydroxy-substituted amino acids were of particular interest as the OH function might facilitate additional interactions with the binding site. Taking an approach of fragment based design, we focused specifically on the N-butyl derivatives of the concerning amino acids in order to estimate their suitability as subunits in larger inhibitor molecules, hence avoiding the need for the introduction of more complex lipophilic domains.

Synthesis of the α-hydroxy-substituted N-butylamino acids commenced from cyclic, benzyl- or benzhydryl-protected 3-aminoketones, which were reacted with trimethylsilyl cyanide to give the respective TMS-protected cyanohydrines. Hydrolysis of these compounds using concentrated H_2SO_4 furnished the corresponding α-hydroxycarboxamides. After deprotection and N-butylation of the amino nitrogen

atom, which was achieved in a single reaction step by exposing the compounds to hydrogen in presence of palladium catalyst and N-butyraldehyde, the α-hydroxycarboxamide function was hydrolyzed with $Ba(OH)_2$ to give the desired α-hydroxycarboxylic acids.

The β-hydroxy-substituted N-butylamino acids were constructed following a similar reaction sequence. First, the carbonyl group of the benzyl- or benzhydryl-protected 3-aminoketones was transformed into a β-hydroxyester function by reaction with lithium 1-ethoxyethen-1-olate, which was generated at low temperatures from ethyl acetate and LiHMDS. Subsequently, the amino nitrogen atom was deprotected and N-butylated applying the same reaction conditions as described above. Finally, hydrolysis of the ester function led to the free β-hydroxy-substituted N-butylamino acids.

Unfortunately, the inhibitory activity exerted by test compounds at mGAT4 was found to be almost negligible as compared to the reference compound N-butylnipecotic acid. Likewise, only minor inhibitory activity is displayed at the other GAT subtypes, with the exception of 1-butyl-3-hydroxyazetidine-3-carboxylic acid (pIC_{50} = 3.17) and 2-(1-butyl-3-hydroxypyrrolidin-3-yl)acetic acid (pIC_{50} = 3.38 ± 0.08) showing moderate inhibitory potency at mGAT2.

Therefore, we decided to retain nipecotic acid as amino acid subunit and devoted our efforts to modifying the lipophilic domain of (*S*)-SNAP-5114 (**17**). At this, two different strategies were followed. On the one hand, polar groups should be introduced into the lipophilic domain, which might result in enhanced polar interactions between the inhibitor and the target, hence possibly increasing the inhibitory potency and/or subtype selectivity as compared to the parent compound. Based on these contemplations, (*S*)-SNAP-5114 (**17**) analogues should synthesized and biologically evaluated that differ from the parent compound by having one or more of the methoxy moieties present in the lipophilic domain, or an entire aryl residue, substituted by a polar group. As such, a carboxyl, alcohol, carboxamide, carbaldehyde or sulfonamide function seemed well-suited, but also an acetyl or methoxymethylene group, or various amino acid partial structures.

On the other hand, previous work in our group has shown that increasing the sterical demands of the lipophilic domain, e.g. by introducing a methyl group into the *ortho*-position of one of the aromatic residues, is not only well tolerated by mGAT4 but also accompanied by a slight increase in subtype selectivity [DDPM-859 (**19**)]. Hence, it seemed reasonable to increase the space requirements of the lipophilic domain even further by introducing bulky aliphatic groups. The structural modifications of (*S*)-SNAP-5114 (**17**) aiming at this should include the formal substitution of one of the aromatic residues present in the parent compound by a *tert*-butyl, 1-methylcyclopent-1-yl, 1-methylcyclohex-1-yl or adamant-1-yl moiety.

Furthermore, analogues of (*S*)-SNAP-5114 (**17**) should be synthesized which comprise in the lipophilic domain only one aromatic residue besides the sterically demanding group, the second aromatic residue being replaced by a hydrogen atom. Compounds with this structural motif would benefit from reduced molecular weight and presumably also increased chemical stability, while still having different sterical requirements as compared to mGAT4 inhibitors featuring the common triaryl moiety. Likewise, compounds were of interest that have the sterically demanding group integrating the quaternary carbon atom of the $COCH_2CH_2$ linker, or that feature polar substructures within the sterically demanding group, e.g. an ether bridge or a methoxy group, in analogy to the 4-methoxyphenyl moiety it replaces.

Considering that the stereochemistry of the nipecotic acid unit plays a significant role in the biological activity of mGAT4 inhibitors, we opted to synthesize the target compounds as racemates since this provides information on both enantiomers. Racemic compounds exhibiting similar or higher inhibitory potency at mGAT4 as compared to the benchmark inhibitor (*S*)-SNAP-5114 (**17**) were additionally synthesized in form of their (*R*)- and (*S*)-isomers by using enantiopure nipecotic acid derivatives as starting material.

The reaction sequence leading to the desired test compounds commenced with the synthesis of secondary and tertiary alcohols as building blocks for the construction of what should become the lipophilic domain. The secondary alcohols were accessible by reaction of Grignard reagents with one equivalent of an acid chloride, hence furnishing ketones which were subsequently reduced to the corresponding secondary alcohols using $NaBH_4$. Similarly, the tertiary alcohols were synthesized by reaction of

Grignard or organolithium reagents with appropriate electrophiles such as acid chlorides, ketones and esters.

Next, it was necessary to construct the ether function which links the lipophilic domain to the short carbon spacer comprising the nipecotic acid unit. To this end, the secondary alcohols were converted into the corresponding β-chloroethyl ethers by treatment with 2-chloroethanol in presence of the Lewis acid catalyst indium(III)-chloride. The nipecotic acid unit was then introduced by reaction with ethyl nipecotate, hence furnishing the ester derivatives of the desired N-substituted nipecotic acids. Hydrolysis of the ester function with $Ba(OH)_2$, followed by workup with CO_2, led to the desired (*S*)-SNAP-5114 (**17**) analogues, which were obtained and biologically evaluated as mixture of diastereomers (~1:1).

In order to realize the etherification of the tertiary alcohols, the compounds were first transformed into the corresponding chlorides using acetyl chloride in presence of a catalytic amount of DMF. Subsequent alcoholysis with ethyl 1-(2-hydroxyethyl)nipecotate furnished the N-substituted nipecotic acids in form of their ester derivatives. In case of the (*S*)-SNAP-5114 (**17**) analogue which differs from the parent compound by having one of the methoxy groups substituted by a carbaldehyde function, various amino acid partial structures were introduced into the lipophilic domain at this stage using a reductive amination procedure. Finally, hydrolysis of the ester function by applying the reaction conditions described above furnished the desired N-substituted nipecotic acids.

The test compounds were evaluated for their inhibitory potency at all four mGAT subtypes and, in selected cases, also at hGAT3, the human analogue of mGAT4. With regard to (*S*)-SNAP-5114 (**17**) analogues that have one of the methoxy groups in the lipophilic domain substituted by a polar moiety, the data imply no clear correlation between the polarity and size of the compound and the inhibitory potency exerted at mGAT4. Nevertheless, all test compounds with this structural motif that are characterized by a $pIC_{50} \geq 5.0$ contain a functional group which can act as hydrogen bond acceptor, but not as donor, and that is of similar size as the methoxy moiety it replaces. This applies to the racemic compounds which comprise in the lipophilic domain a nitrile ($pIC_{50} = 5.07 \pm 0.12$), carbaldehyde ($pIC_{50} = 5.77 \pm 0.04$), acetyl ($pIC_{50} = 5.43 \pm 0.04$) or methoxymethylene group ($pIC_{50} = 5.42 \pm 0.10$).

Furthermore, the clog *D* values calculated for these compounds lie in the area of 2.0 – 2.4, which coincides with the value of the parent compound (clog *D* = 2.32).

As the test substance featuring an aldehyde function in the lipophilic domain was found to be the most potent of the compounds of this type, it was also synthesized in form of its enantiopure (*R*)- and (*S*)-isomers. As is the case with the parent compound, the (*S*)-enantiomer exerts a distinctly higher inhibitory potency at the targeted transporter subtype than the (*R*)-enantiomer. Being characterized by a pIC_{50} value of 5.89 ± 0.07, it constitutes a nominally more potent mGAT4 inhibitor than (*S*)-SNAP-5114 (**17**, pIC_{50} = 5.71 ± 0.07) while displaying almost identical subtype selectivity.

Additionally, we also studied how the substitution of several methoxy groups in the lipophilic domain affects the inhibitory potency of the resulting compounds using the example of the methoxymethylene group. Whereas the introduction of one methoxymethylene group at the expense of a methoxy group is associated with only a minor decrease of the pIC_{50} value from 5.71 ± 0.07 to 5.42 ± 0.10, the loss of activity became increasingly more distinct with the substitution of further methoxy moieties. These findings suggest mGAT4 being able to tolerate a single inappropriate substituent reasonably well as long as the other two methoxy moieties in the lipophilic domain remain available for interactions with the target. However, if these are also substituted, the inhibitory potency of the resulting compounds decreases significantly, i.e. to pIC_{50} values < 4.0.

Interestingly, deviations from the triaryl pattern in the lipophilic domain resulting from the formal substitution of one of the aryl residues of (*S*)-SNAP-5114 (**17**) with a small polar group were associated with an almost complete loss of inhibitory activity, which implies that mGAT4 does not tolerate decreasing the size and steric demand of the lipophilic domain to such an extent.

As outlined above, we also examined (*S*)-SNAP-5114 (**17**) analogues comprising sterically demanding, aliphatic groups in the lipophilic domain. The structural modifications of the lead compound (*S*)-SNAP-5114 (**17**) that were implemented in that context included the formal substitution of one aryl residue in the lipophilic domain by a sterically demanding, aliphatic group. Interestingly, the inhibitory

potency of the resulting compounds was found to be strongly dependent on the size of the sterically demanding moiety. In this context, the compound featuring a *tert*-butyl group in the lipophilic domain is characterized by a comparatively low pIC_{50} of 4.37, whereas its analogue comprising a larger 1-methylcyclopentan-1-yl moiety exhibits a distinctly higher pIC_{50} value of 5.16 ± 0.04. Further expansion of the cyclopentyl ring by a methylene group, resulting in a 1-methylcyclohexan-1-yl moiety, leads to a compound with a pIC_{50} value of 5.70 ± 0.10. Interestingly, the (*S*)-SNAP-5114 (**17**) analogue comprising an even bulkier adamantan-1-yl moiety in the lipophilic domain exhibits very similar inhibitory activity, with the pIC_{50} value amounting to 5.77 ± 0.09, despite the difference of both moieties with regard to rigidness and size.

Exhibiting the highest inhibitory potencies, the (*S*)-SNAP-5114 (**17**) analogues featuring in the lipophilic domain a 1-methylcyclohexan-1-yl group and an adamantan-1-yl group, respectively, were additionally synthesized and biologically evaluated in form of their enantiopure (*R*)- and (*S*)-isomers. Analogous to the parent compound, the (*S*)-enantiomers exhibit more pronounced activity than the (*R*)-enantiomers, with the respective pIC_{50} values amounting to 5.76 ± 0.09 in case of the 1-methylcyclohexan-1-yl derivate and 6.13 ± 0.10 in case of the adamantan-1-yl derivate. Hence, the (*S*)-enantiomer of the 1-methylcyclohexan-1-yl derivate is on par with the lead compound (*S*)-SNAP-5114 (**17**, pIC_{50} = 5.71 ± 0.07) in terms of inhibitory potency, whereas its analogue comprising an adamantan-1-yl moiety in the lipophilic domain exceeds both compounds by a notable margin of nominally ~0.4 log units, which makes it one of the most potent mGAT4 inhibitors developed so far. Unfortunately, the compound does not exhibit good subtype selectivity in favor of mGAT4 as it is also a potent inhibitor of mGAT3 (pIC_{50} = 5.62 ± 0.02), whereas the inhibitory potency displayed at mGAT1 (pIC_{50} = 4.93 ± 0.13) and mGAT2 (pIC_{50} = 5.06 ± 0.06) is lower in comparison, but still considerable.

Apparently, the size of the sterically demanding moiety is also a crucial factor in case of (*S*)-SNAP-5114 (**17**) analogues that have one of the aryl residues in the lipophilic domain substituted by a sterically demanding group, and another one by a hydrogen atom. While the pIC_{50} value of the compound featuring a comparatively small 1-methylcyclohexan-1-yl group amounts to 4.88 ± 0.08, a considerable increase in

inhibitory potency is observed if this position is occupied by an adamantan-1-yl residue (pIC_{50} = 5.49 ± 0.01). However, further enlargement of the substituent by introducing two methyl groups into the 3- and 5-position of the adamantane scaffold leads to a compound with reduced inhibitory activity (pIC_{50} = 5.17 ± 0.09). This finding implies that there exists an optimal size for the sterically demanding group, which has been exceeded in this case.

In that context, we also examined a (*S*)-SNAP-5114 (**17**) analogue that has an adamantan-2-yl moiety as sterically demanding group integrating the quaternary carbon atom of the $COCH_2CH_2$ linker, hence resulting in a lipophilic domain with even lesser space requirements. The compound is characterized by a relatively weak inhibitory activity at mGAT4 (pIC_{50} = 3.64 ± 0.08), which is likely attributable to an insufficient filling of the binding cavity.

Furthermore, it is noteworthy that the introduction of polar moieties into the sterically demanding group causes a distinct decline of the inhibitory potency exerted by the resulting compound. For instance, the (*S*)-SNAP-5114 (**17**) analogue that has one of the aryl residues of the lipophilic domain substituted by a 1-methylcyclohex-1-yl group is characterized by a relatively high pIC_{50} value of 5.70 ± 0.10. If this group is modified by formally replacing a methylene moiety in the cyclohexane ring by an ether oxygen atom, resulting in a 4-methyltetrahydro-2H-pyran-4-yl moiety, the pIC_{50} value decreases to 4.76 ± 0.09, which amounts to a potency loss of a full log unit as compared to its carba analogue. Likewise, the introduction of a methoxy group into the 4-position of the 1-methylcyclohexan-1-yl scaffold is accompanied by a similarly striking reduction of inhibitory activity (pIC_{50} = 4.70).

The ester derivatives of the N-substituted nipecotic acids, which were obtained as intermediates during the synthesis, were also evaluated for their inhibitory potential at mGAT4. In case of all (*S*)-SNAP-5114 (**17**) analogues with a pIC_{50} value ≥ 5.0 that comprise a triarylmethyl or alkyl diarylmethyl structure, the ester derivatives exhibit distinctly lower inhibitory potencies than the corresponding free acids, hence implying that the carboxyl function is essential for mGAT4 inhibitors with this structural motif. This notion is further supported by the observation that substituting the carboxylic acid function in *rac*-SNAP-5114 by an carboxamide group is accompanied by a distinct loss of inhibitory activity of more than one log unit.

By contrast, the ester precursors of (*S*)-SNAP-5114 (**17**) analogues that comprise in the lipophilic domain only one aromatic residue besides an sterically demanding group, exhibit high inhibitory potencies themselves, which in many cases exceed those of the corresponding acids. Hence, it seems likely that a different binding mode is involved, which does not depend on the presence of a carboxylic acid function.

In conclusion, the results of this study reveal important information about the structure-activity-relationship of mGAT4 inhibitors with regard to size, polarity, and electronic effects of the substituents in the lipophilic domain. These new insights are expected to be greatly beneficial for future developments of more potent inhibitors.

Furthermore, several mGAT4 inhibitors with potencies comparable to or higher than that of the lead compound (*S*)-SNAP-5114 (**17**) were developed. In this context, we also identified a promising new structural motif for mGAT4 inhibitors, i.e. (*S*)-SNAP-5114 (**17**) analogues that comprise a sterically demanding, aliphatic moiety in the lipophilic domain as opposed to the established triaryl structure. At this, compounds with lipophilic domains comprising only one aromatic residue in addition to the sterically demanding group, the other one being substituted by a hydrogen atom, are characterized by beneficial properties, including reduced molecular weight and probably also enhanced chemical stability. Therefore, compounds of this type may represent a promising starting point for further research projects.

5. List of abbreviations

BBB	blood-brain-barrier
CNS	central nervous system
dDAT	dopamine transporter from *Drosophila melanogaster*
DMF	dimethylformamide
EL	extracellular loop
FDA	U.S. Food and Drug Administration
GABA	γ-aminobutyric acid
GABA-T	GABA transaminase
GAD	glutamate decarboxylase
GATs	GABA transporters
GPCRs	$G_{i/o}$-protein coupled receptors
hGAT	human GABA transporter
hSERT	human serotonin transporter
HUGO	Human Genome Organization
IC_{50}	half maximal inhibitory concentration
IL	intracellular loop
K_i	inhibition constant
$LeuT_{Aa}$	leucine transporter from *Aquifex aeolicus*
LiHMDS	lithium hexamethyldisilazide
mGAT	murine GABA transporter
NSS	neurotransmitter-sodium symporters
SAR	structure-activity relationship
SEM	standard error of mean
SLC6	solute carrier 6
SSA	succinic semialdehyde
THPO	4,5,6,7-tetrahydroisoxazolo[4,5-c]pyridin-3-ol
TM	transmembrane helices
VGAT	vesicular neurotransmitter transporters

6. Literature

[1] B.S. Meldrum, A.G. Chapman, *Epilepsia* **1999**, *40*, 9, 2-6.

[2] N.G. Bowery, T.G. Smart, *Br. J. Pharmacol.* **2006**, *147*, 109-119.

[3] D.L. Martin, K. Rimvall, *J. Neurochem.* **1993**, *60*, 395-407.

[4] A.R. Kriegstein, D.F. Owens, *Nat. Rev. Neurosci.* **2002**, *3*, 715-727.

[5] S.L. McIntire, R.J. Reimer, K. Schuske, R.H. Edwards, E.M. Jorgensen, *Nature* **1997**, *389*, 870-876.

[6] A.C. Foster, J.A. Kemp, *Curr Opin Pharmacol.* **2006**, *6*, 7-17.

[7] F.C. Roth, A. Dragun, *Neural Plast.* **2012**, 805-830.

[8] N.H. Chen, M.E. Reith, M.W. Quick, *Pflug Arch Eur J Phy.* **2004**, 447, 519-531.

[9] V. Eulenburg, J. Gomeza, *Brain Res Rev.* **2010**, *63*, 103-112.

[10] X.T. Jin, J.F. Pare, Y. Smith, *Eur J Neurosci.* **2011**, *33*, 1504-1518.

[11] J.M. Kuhar, Life Sci. **1973**, *13*, 1623.

[12] M.A. Daemen, G. Hoogland, J.M. Cijntje, G.H. Spincemaille, *Neuroscience Letters* **2008**, *444*, 112-115.

[13] A.A. Todorov, C.B. Kolchev, A.B. Todorov, *Clin. J. Pain* **2005**, *21*, 358-361.

[14] S.R. Kleppner, A.J. Tobin**,** *Expert Opinion on Therapeutic Targets* **2001**, *5*, 219-239.

[15] D. Zadori, A. Geisz, E. Vamos, L. Vecsei, P. Klivenyi, *Pharmacol. Biochem. Behav.* **2009**, *94*, 148-153.

[16] P. Nuss, *Neuropsychiatric Disease and Treatment* **2015**, *11*, 165–175.

[17] A.V. Kalueff, D. J. Nutt, *Depression and Anxiety* **2007**, *24*, 495–517.

[18] J.H. Krystal, G. Sanacora, H. Blumberg, A. Anand, D.S. Charney, G. Marek, C.N. Epperson, A. Goddard, G.F. Mason, *Mol. Psychiatry* **2002**, *7*, 71-80.

[19] K.L. Lanctot, N. Herrmann, P. Mazzotta, L.R. Khan, N. Ingber, *Canadian Journal of Psychiatry* **2004**, *49*, 439-453.

[20] T. Aoyagi, T. Wada, M. Nagai, F. Kojima, S. Harada, T. Takeuchi, H. Takahashi, T. Tsumita, *Chem. Pharm. Bull.* **1990**, *38*, 1748-1749.

[21] D.M. Treiman**,** *Epilepsia* **2001**, *42*, 8-12.

[22] H.E. Scharfman, *Curr Neurol Neurosci Rep* **2007**, 7, 348-354.

[23] H.F. Bradford, *Prog. Neurobiol.* **1995**, 47, 477-511.

[24] Fact Sheet Epilepsy www.who.int/news-room/fact-sheets/detail/epilepsy (accessed July 19, 2019).

[25] L.P. Carter, W. Koek, C.P. France, *Pharmacol. Ther.* **2008**, *121*, 100–114.

[26] K.E. McCarson, S.J. Enna, *Neurochem Res.* **2014**, *39*, 1948-1963.

[27] D.J. Nutt, A.L. Malizia, *Brit J Psychiat.* **2018**, *179*, 390-396.

[28] G. M. Yip, Z. W. Chen, C. J. Edge, E.H. Smith, R. Dickinson, E. Hohenester, R.R. Townsend, K. Fuchs, W. Sieghart, A.S. Evers, N.P, Franks, *Nat. Chem. Biol.* **2013**, *11*, 715–20.

[29] W. Löscher, M.A. Rogawski, *Epilepsia* **2012**, *53*, 12–25.

[30] D.C. Chiara, S. Jayakar, X. Zhou, X. Zhang, P.Y. Savechenkov, K.S. Bruzik, K.W. Miller, J.B. Cohen *Journal of Biological Chemistry* **2003**, 288 (*27*), 19343–19357.

[31] G. Trapani, A. Latrofa, M. Franco, C. Altomare, E. Sanna, M. Usala, G. Biggio, G. Liso, *Journal of Medicinal Chemistry* **1998**, *11*, 1846-1854.

[32] M.D. Krasowski, A. Jenkins, P. Flood, A.Y. Kung, A.J. Hopfinger, N.L. Harrison, *J. Pharmacol. Exp. Ther.* **2001**, *297*, 338–51.

[33] S.M. LaRoche, S.L. Helmers, *JAMA* **2004**, *291*, 605-614.

[34] P. Genton, R. Guerrini, E. Perucca, *Epilepsia* **2001**, *42*, 42-45.

[35] I.E. Leppik, L. Gram, R. Deaton, K.W. Sommerville, *Epilepsy Research* **1999**, *33*, 235–246.

[36] J.P. Leach, M.J. Brodie, *Lancet* **1998**, *351*, 203-207.

[37] A.S. Kristensen, J. Andersen, T.N. Jørgensen, L. Sørensen, J. Eriksen, C.J. Loland, K. Strømgaard, U. Gether, *Pharmacological Reviews* **2011**, *63*, 3, 585-640.

[38] K.K. Madsen, H.S. White, A. Schousboe, *Pharmacology & Therapeutics* **2010**, *125*, 394-401.

[39] K.K. Madsen, R.P. Clausen, O.M. Larsson, P. Krogsgaard-Larsen, A. Schousboe, H.S. White, *Journal of Neurochemistry* **2009**, *109*, 139-144.

[40] S. Bröer, U. Gether, *British Journal of Pharmacology* **2012**, *167*, 2, 256-278.

[41] L.A. Borden, *Neurochemistry International* **1996**, *29*, 4, 335-356.

[42] G. Rudnick, *J. Memr. Biol.* **2006**, *213*, 101-110.

[43] S. L. Willford, C. M. Anderson, S. R. Spencer, S. Eskandari, *J Membrane Biol* **2015**, *248*, 795–810.

[44] R. Radian, B.I. Kanner, *J. Biol. Chem.* **1985**, *260*, 11859-11865.

[45] J. Guastella, N. Nelson, H. Nelson, L. Czyzyk, S. Keynan, M.C. Miedel, N. Davidson, H.A. Lester, B.I. Kanner, *Science* **1990**, *249*, 1303-1306.

[46] A. Yamashita, S.K. Singh, T. Kawate, Y. Jin, E. Gouaux, *Nature* **2005**, *437*, 215-223.

[47] T. Beuming, L. Shi, J.A. Javitch, H. Weinstein, *Mol. Pharmacol.* **2006**, *70*, 1630-1642.

[48] A. Penmatsa, E. Gouaux, *J. Physiol.* **2014**, *592*, 863-869.

[49] J.A. Coleman, E.M. Green, E. Gouaux, *Nature* **2016**, *532*, 334-339.

[50] A. Penmatsa, K.H. Wang, E. Gouaux, *Nature*, **2013**, *503*, 85-90.

[51] H. Krishnamurthy, E. Gouaux, *Nature* **2012**, *481*, 469-474.

[52] L. Shi, M. Quick, Y. Zhao, H. Weinstein, J.A. Javitch, *Molecular Cell* **2008**, *30*, 667–677.

[53] Y Zhau, D.S. Terry, L. Shi, M. Quick, H. Weinstein, S.C: Blanchard, J.A. Javitch, *Nature* **2011**, *474*, 109-113.

[54] J. Zhen, M.E. Reith, *J Neurochem* **2016**, 138, *5*, 694-699

[55] Z. Zhou, J. Zhen, N.K. Karpowich, R.M. Goetz, C.J. Law, M.E. Reith, D.N. Wang, *Science* **2007**, *317*, 1390-1393.

[56] M. Quick, A.M. Winther, L. Shi, P. Nissen, H. Weinstein, J.A. Javitch, *P Natl Acad Sci USA*, **2009**, *106*, 5563-5569.

[57] N. O. Dalby, *Eur. J. Pharmacol.* **2003**, 479, 127-137.

[58] B. Christiansen, A. K. Meinild, A. A. Jensen, H. Bräuner-Osbore, *Journal of Biological Chemistry* **2007**, *282*, 19331-19341.

[59] F. Conti, M. Melone, S. DeBiasi, A. Minelli, N.C. Brecha, A. Ducati, *J Comp Neurol* **1998**, *396*, 51-63.

[60] A. Minelli, S. DeBiasi, N.C. Brecha, L.V: Zuccarello, F. Conti, *J Neurosci.* **1996**, *16*, 6255-6264.

[61] M.M. Durkin, K.E. Smith, L.A. Borden, R.L. Weinshank, T.A. Branchek, E.L. Gustafson, *Brain Res Mol Brain Res* **1995**, *33*, 7-21.

[62] Y. Zhou, N.C. Danbolt, *Front Endocrinol* **2013**, *4*, 165.

[63] S.A. Kempson SA, Y. Zhou Y, N.C. Danbolt, *Frontiers in Physiology* **2014**, *5*, 159.

[64] Y. Zhou, S. Holmseth, R. Hua, A. C. Lehre, A. M. Olofsson, I. Poblete-Naredo, S. A. Kempson, N. C. Danbolt, *American Journal of Physiology – Renal Physiology* **2012**, *302*, 313-328.

[65] Y. Zhou, S. Holmseth, C. Guo, B. Hassel, G. Höfner, H.S. Huitfeldt, K.T. Wanner, N.C. Danbolt, *J. Biol. Chem.* **2012**, *287*, 35733-35746.

[66] S. Høg, J.R. Greenwood, K.B. Madsen, O.M. Larsson, B. Frølund, A. Schusboe, P. Krogsgaard-Larsen, R.P. Clausen, *Current Topics in Medicinal Chemistry* **2006**, *6*, 1861-1882.

[67] H.S. White, A. Sarup, T. Bolvig, A. Kristensen, G. Petersen, N. Nelson, D. Pickering, O.M. Larsson, B. Frølund, P. Krogsgaard-Larsen, A. Schousboe, *J. Pharmacol. Exp. Ther.* **2002**, *302*, 636-644.

[68] P. Krogsgaard-Larsen, *J Med Chem* **1981**, *24*, 1377-1383.

[69] H.S. White, A. Sarup, T. Bolvig, A. Kristensen, G. Petersen, N. Nelson, D. Pickering, O.M. Larsson, B. Frølund, P. Krogsgaard-Larsen, A. Schousboe, *J. Pharmacol. Exp. Ther.* **2002**, *302*, 636-644.

[70] F.E. Ali, W.E. Bondinell, P.A. Dandridge, J.S. Frazee, E. Garvey, G.R. Girard, C. Kaiser, T.W. Ku, J.J. Lafferty, G.I. Moosammy, et al. *J Med Chem.* **1985**, 28, 653-660.

[71] P.D. Suzdak, K. Frederiksen, K.E. Andersen, P.O. Huusfeldt, L.J. Knutsen, E.B. Nielsen, *Eur J Pharmacol.* **1992**, *224*, 189-198.

[72] C. Braestrup, E.B. Nielsen, U. Sonnewald, L.J.S. Knutsen, K.E. Andersen, J.A. Jansen, K. Frederiksen, P.H. Andersen, A. Mortensen, P.D. Suzdak, *J Neurochem.* **1990**, *54*, 639-647.

[73] T.G.M. Dhar, L.A. Borden, S. Tyagarajan, K.E. Smith, T.A. Branchek, R.L. Weinshank, C. Gluchowski, *Journal of Medicinal Chemistry* **1994**, *37*, 2334-2342.

[74] J. Pabel, M. Faust, C. Prehn, B. Woerlein, L. Allmendinger, G. Höfner, K.T. Wanner, *ChemMedChem* **2012**, *7*, 1245-1255.

[75] A. Kragler, G. Höfner, K.T. Wanner, *European Journal of Pharmacology* **2008**, *43*, 2404-2411.

[76] T. Steffan, T. Renukappa-Gutke, G. Höfner, K.T. Wanner, *Bioorg. Med. Chem.* **2015**, *23*, 1284-1306.

[77] M. Damgaard, R.P. Clausen, *ACS Chem. Neurosci.* **2015**, *6*, 1591−1599.

[78] T. Wein, M. Petrera, L. Allmendinger, G. Höfner, J. Pabel, K.T. Wanner *ChemMedChem*. **2016**, *11*, 509-518.

[79] T. Kobayashi, A. Suemasa, A. Igawa, S. Ide, H. Fukuda, H. Abe, M. Arisawa, M. Minami, S. Shuto, *ACS Med. Chem. Lett.* **2014**, *5*, 889-893.

[80] B. Kragholm, T. Kvist, K.K. Madsen, L. Jørgensen, S.B. Vogensen, A. Schusboe, P.R. Clausen, A.A. Jensen, H. *Bräuner-Osborne, Biochem. Pharmacol.* **2013**, *86*, 512-528.

[81] C. Thomsen, P.O. Sørensen, J. Egebjerg, *J. Br. Pharmacol.* **1997**, *120*, 983-985.

7. Publications and manuscripts

7.1 First publication:

Janina C. Andreß, Michael C. Böck, Georg Höfner, Klaus T. Wanner

Submitted to *Medicinal Chemistry Research* 23.12.2019.

"Synthesis and biological evaluation of α- and β-hydroxy substituted amino acid derivatives as potential mGAT4 inhibitors"

7.2 Second publication:

Michael C. Böck, Georg Höfner, Klaus T. Wanner

Submitted to *ChemMedChem* 20.12.2019.

"Synthesis and Biological Evaluation of N-Substituted Nipecotic Acids as (*S*)-SNAP-5114 Analogues with Modified Lipophilic Domains"

7.3 Manuscript of the third publication:

Michael C. Böck, Georg Höfner, Klaus T. Wanner

"Synthesis and Biological Evaluation of N-Substituted Nipecotic Acids as (*S*)-SNAP-5114 Analogues Containing Sterically Demanding Aliphatic Moieties in the Lipophilic Domain"

Synthesis and biological evaluation of α- and β-hydroxy substituted amino acid derivatives as potential mGAT4 inhibitors

Janina C. Andreß, Michael C. Böck, Georg Höfner, Klaus T. Wanner
Department of Pharmacy – Center for Drug Research
Ludwig-Maximilians-Universität München
Butenandtstraße 5-13, 81377 Munich, Germany

✉ Klaus T. Wanner
klaus.wanner@cup.uni-muenchen.de

Abstract

In this study, we report the synthesis and biological evaluation of a variety of α- and β-hydroxy substituted amino acid derivatives as potential amino acid subunits in mGAT4 inhibitors. In order to ensure that the test compounds adopt a binding pose similar to that presumed for related larger GAT inhibitors, lipophilic residues were introduced either at the amino nitrogen atom or at the alcohol function. Among the tested compounds we identified 4-(butylamino)-3-hydroxybutanoic acid (pIC_{50} = 3.42 ± 0.12) and N-butylisoserine (pIC_{50} = 3.26 ± 0.10) to exert inhibitory potencies at mGAT4 comparable to the N-butyl derivative of nipecotic acid, which was used as a reference since nipecotic acid constitutes the amino acid partial structure of many important GAT inhibitors such as Tiagabine and (*S*)-SNAP-5114.

Keywords

Neurochemistry, GABA transporters, GABA uptake inhibitors, mGAT4, amino acids.

1. Introduction

Gamma-aminobutyric acid (GABA) is the most abundant inhibitory neurotransmitter in the mammalian central nervous system (CNS) (Bowery and Smart, 2006), with up to 40% of synapses estimated to be GABAergic(Meldrum and Chapman, 1999). Deficient GABAergic neurotransmission is assumed to play a decisive role in the pathogenesis of several severe neurological diseases, including Alzheimer`s disease(Lanctôt et al., 2004), depression (Kalueff and Nutt, 2007), epilepsy (Treimann 2001), and neuropathic pain (Daemen et al., 2008). A

promising therapeutical approach for the treatment of these diseases exists in the inhibition of the transport molecules responsible for the removal of GABA from the synaptic cleft, resulting in the prolongation of the effect exerted by the available GABA (Krogsgaard-Larsen et al., 1991). Belonging to the SLC6 transporter gene family, these membrane-bound proteins termed GABA transporters (GATs) use the co-transport of sodium ions for the translocation of the substrate against the chemical gradient (Kristensen et al., 2011). The nomenclature of the four GAT subtypes depends on the species the transporters are cloned from. When originating from mouse brain cells, the GAT subtypes are termed mGAT1-4. For all other species, including humans, an alternate nomenclature is used which has also been adopted by the Human Genome Organisation (HUGO), denoting the transporters GAT1 (= mGAT1), BGT1 (= mGAT2), GAT2 (= mGAT3) and GAT3 (= mGAT4) (Madsen et al., 2009). Hereafter the nomenclature referring to the murine transporters will be applied as the biological test system used in our group is based on these. mGAT1 and mGAT4 are the most abundant GATs in the mammalian CNS, with the former being predominantly located on presynaptic neuronal membranes mediating the neuronal GABA uptake, whereas mGAT4, which is mainly expressed on glia cells, is responsible for the glial GABA uptake (Minelli et al., 1996; Jin et al., 2011). The other two GAT subtypes, mGAT2 and mGAT3, are primarily located in the periphery, with the highest densities being found in liver and kidneys, and hence are thought to not play any significant role in the termination of GABAergic signaling in the CNS (Zhou et al., 2012).

The first parent compound selectively targeting GATs was THPO (**1**, table 1, entry 1) (White et al., 2002), which is derived from muscimol, an alkaloid isolated from fly agaric (*Amanita muscaria*) that can be considered an bioisostere of GABA(Corvey et al., 1994). Replacement of the isoxazol-3-ol partial structure of THPO with a carboxylic acid function led to the more potent GAT inhibitors guvacine (**2**, table 1, entry 2) and nipecotic acid [(*R*)-**3**,*(S)*-**3** table 1, entry 3-4] (Krogsgaard-Larsen et al., 2000). However, these cyclic GABA analogues still lacked inhibitory potency and subtype selectivity (table 1, entry 1-4). Moreover, due to being present in the zwitterionic state under physiological conditions, guvacine (**2**) and nipecotic acid [(*R*)-**3**,(*S*)-**3**] are hardly able to cross the *blood brain barrier* (BBB), which strongly limits any potential therapeutic application (Seth et al., 2018).

When bulky, lipophilic residues were introduced at the nitrogen atom, this led to compounds with not only increased lipophilicity and hence improved BBB penetration, but

also with significantly higher inhibitory potency. In this context, compounds possessing a diaryl methyl or a biaryl unit as lipophilic domain which is connected to the nipecotic acid partial structure via a flexible linker of 3-5 atoms proved to be highly potent and selective mGAT1 inhibitors, with the respective pIC_{50} values rising from ~5 to almost 7 as compared to unsubsituted (*R*)-nipecotic acid. Among these compounds, Tiagabine (Gabatril®, **4**, table 1, entry 5) stands out for being the only GAT inhibitor that has been approved for clinical use (Nielsen et al., 1991).

In a similar way the introduction of a lipophilic residue consisting of a triarylmethyl group, which is linked to the nipecotic acid subunit via a spacer of three atoms, furnishes mGAT4 selective inhibitors, with (*S*)-SNAP-5114 constituting the prototypic representative of this group (**5**, table 1, entry 6) (Dhar et al., 1994). Remarkably, the (*S*)-isomer **5** exhibits higher inhibitory potency than the respective (*R*)-isomer, running contrary to what is observed for the unsubstituted nipecotic acid [(*R*)-**3**, (*S*)-**3**] as well as for mGAT1 inhibitors such as Tiagabine (**4**).

Table 1. *GAT inhibitors.*

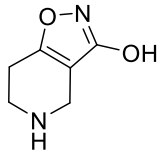

THPO (**1**)

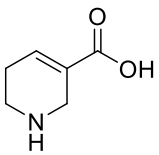

guvacine (**2**)

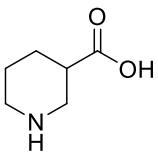

nipecotic acid [(*R*/*S*)-**3**]

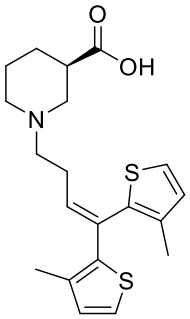

Tiagabine (**4**)

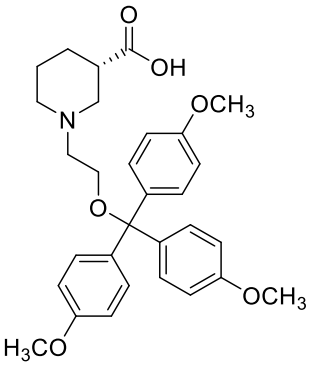

(*S*)-SNAP-5114 (**5**)

		GABA uptake inhibition (pIC_{50} ± SEM)[a]			
entry	**compound**	**mGAT1**	**mGAT2**	**mGAT3**	**mGAT4**
1	**1**	3.0	2.5	<2.5	<2.5
2	**2**	4.87 ± 0.06	3.31 ± 0.03	4.59 ± 0.05	4.59 ± 0.05
3	(*R*)-**3**	5.19 ± 0.03	3.39 ± 0.05	4.76 ± 0.05	4.95 ± 0.05
4	(*S*)-**3**	4.24 ± 0.05	3.13 ± 0.14	3.83 ± 0.04	3.63 ± 0.06
5	**4**	6.88 ± 0.12	50 %[b]	64 %[b]	73 %[b]
6	**5**	4.07 ± 0.09	62 %[b]	5.29 ± 0.04	5.71 ± 0.20

[a] Results of the [^{3}H]GABA uptake assays are given as pIC_{50} ± SEM. [b] Percentages represent remaining [^{3}H]GABA uptake in presence of 100 µM test compound.

Interestingly, small amino acids including β-alanine (**6**, table 2, entry 1), isoserine (**7a**, table 2, entry 2), 2,3-diaminopropionic acid (**8**, table 2, entry 3) and (*Z*)-4-aminobut-2-enoic acid (**9**, table 2, entry 4) also show moderate biological activity at mGAT3 and mGAT4 that is comparable to that exerted by (*R*)-nipecotic acid [(*R*)-**3**, table 1, entry 3], while being distinctly less potent inhibitors of mGAT1 (Kragler et al., 2005). Thus, substitution of the nipecotic acid partial structure in the lead compound (*S*)-SNAP-5114 (**5**) with a (*S*)-2-hydroxy-2-[(*R*)-pyrrolidin-2-yl]acetic acid unit, which can be understood as rigidized derivative of *rac*-isoserine (**7a**), led to compound **10**, which displays significantly improved subtype selectivity in favor of mGAT4. However, this structure variation is also accompanied by a moderate decrease of inhibitory potency (pIC_{50} = 5.18 ± 0.05, table 2, entry 5) as compared to the parent compound **5** (pIC_{50} = 5.71 ± 0.20, table 1, entry 6) (Steffan et al., 2015).

Table 2. *GAT inhibitors.*

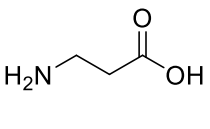

ß-alanine (**6**)

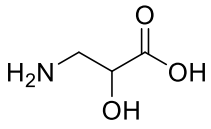

isoserine (**7a**)

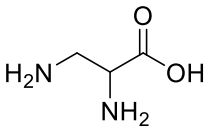

2,3-diamino-propionic acid (**8**)

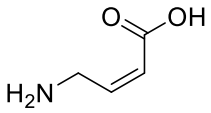

(*Z*)-4-aminobut-2-enoic acid (**9**)

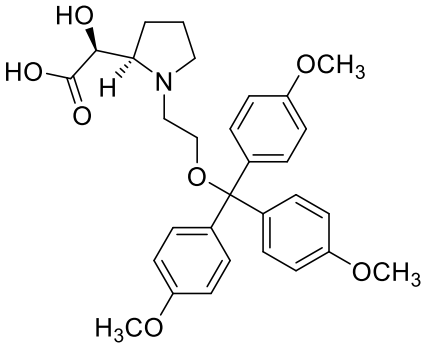

10

		GABA uptake inhibition (pIC_{50} ± SEM)[a]			
entry	**compound**	**mGAT1**	**mGAT2**	**mGAT3**	**mGAT4**
1	**6**	2.59 ± 0.03	3.48 ± 0.11	4.66 ± 0.06	4.46 ± 0.13
2	**7a**	2.33 ± 0.05	3.39 ± 0.11	4.87 ± 0.05	4.78 ± 0.14
3	**8**	3.11 ± 0.02	3.50 ± 0.12	4.66 ± 0.08	5.05 ± 0.02
4	**9**	2.99 ± 0.04	3.67 ± 0.08	4.95 ± 0.04	5.04 ± 0.06
5	**10**	80 %[b]	64 %[b]	70 %[b]	5.18 ± 0.05

[a] For consistency the values determined in our research group are listed. [b] Remaining [^{3}H]GABA uptake at 100 µM compound concentration.

For the development of mGAT4 inhibitors with increased subtype selectivity, this study hence aims to identify further cyclic and acyclic 2- and 3-hydroxy amino acids as possible alternatives to the nipecotic acid partial structure present in the scaffold of important mGAT4 inhibitors such as **5**. Proceeding from the basic structure of isoserine **7a**, it was intended to implement several structural modifications, including elongation of the carbon chain by insertion of methylene groups at various positions, and the rigidization of the molecule by integrating the amino acid backbone into larger heterocycles. Accordingly, a set of compounds featuring both variations and thus deviating from the original isoserine (**7a**) structure should be synthesized and biologically evaluated (scheme 1).

Despite the stereochemistry of amino acids such as nipecotic acid [(*R*)-**3**, (*S*)-**3**] being known to represent an important factor when it comes to the biological activity of mGAT4 inhibitors, we opted for the synthesis of the target compounds in racemic form as this provides information about the biological activity of both enantiomers.

Scheme 1. *Planned structure variations of isoserine (**7a**).*

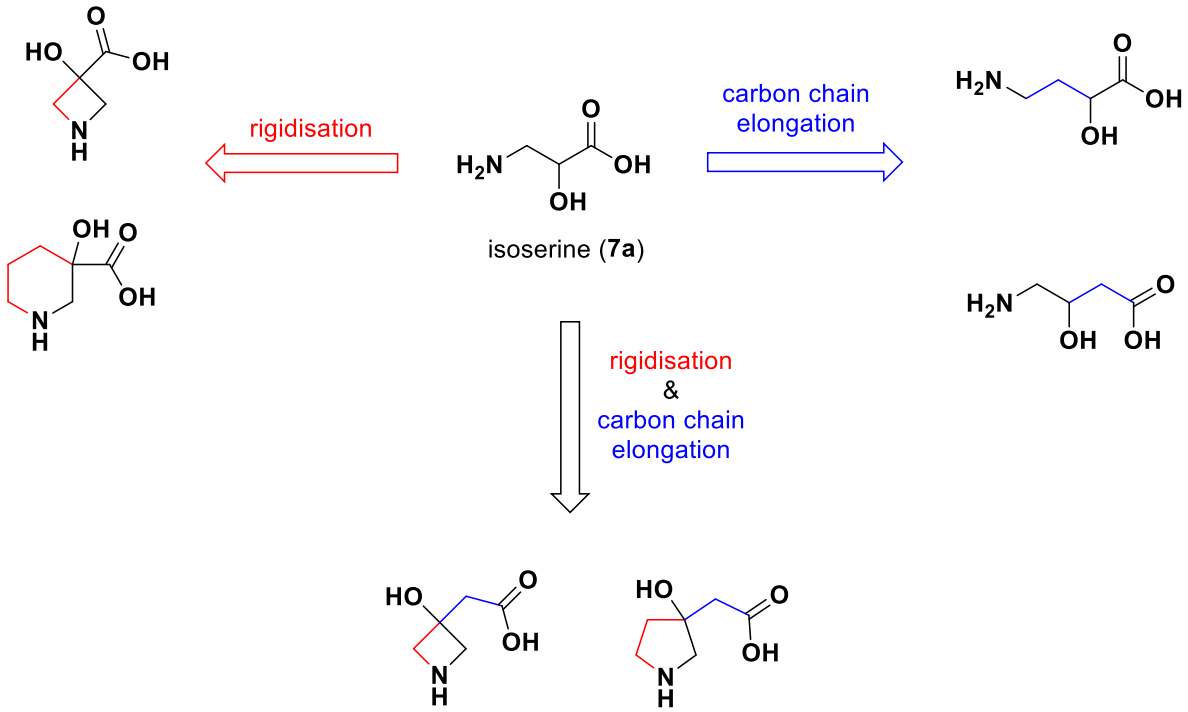

According to the results of molecular modelling experiments performed by us for mGAT1, small inhibitors such as nipecotic acid adapt a binding pose at which the amino nitrogen atom is facing towards the intracellular space. However, if bulky, lipophilic moieties are introduced at the nitrogen atom, as it is the case with Tiagabine (**4**, table 1, entry 5), the binding pose is altered in a way that the nitrogen atom is orientated towards the extracellular site, with the lipophilic side chain looming into the extracellular vestibule, although the position of the carboxylic acid function remains largely unchanged (Scheme 2) (Wein et al.; 2016). For this change in binding mode also the presence of small N-substituents e.g. N-butyl residues are sufficient. Also no reliable *in silico* models exists so far for the other GAT subtypes, it seems highly likely that these findings also apply to mGAT2-4.

Thus, in order to ensure that the orientation of the parent compounds in the binding pocket corresponds to the orientation they would have as part of larger molecules comprising a lipophilic domain, all parent compounds included in this study were also evaluated as N-butyl derivatives for their inhibitory potential.

Scheme 2. *Postulated binding poses of nipecotic acid (**3**, a) and Tiagabine (**4**, b) at mGAT1.*

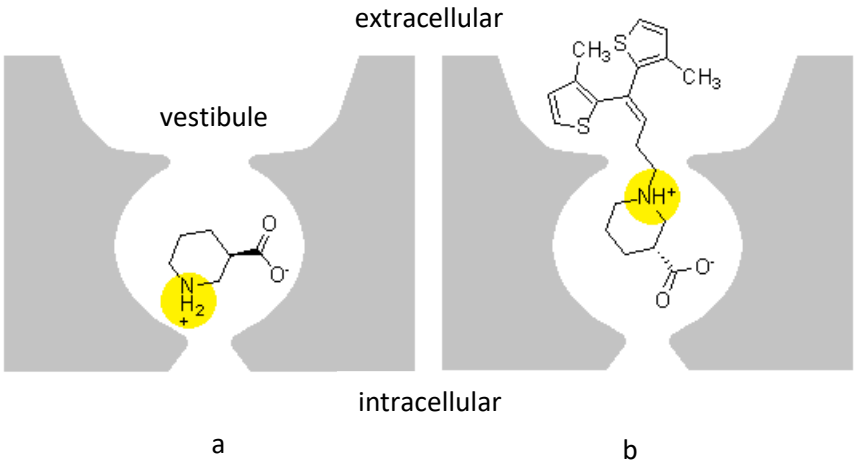

Additionally, unsubstituted α- and β-hydroxy amino acids exhibiting higher biological activity than their corresponding N-butyl derivatives should in addition be substituted at the alcohol function. In detail, the alcohol function should be provided with a 4,4´,4´´-trimethoxytrityloxyethyl residue [(4-MeO-C_6H_4)$_3$$COCH_2CH_2$], which is a characteristic structural motif of mGAT4 inhibitors such as **5** and **10**. According to the model pointed out above, this might allow the amino acid substructure to stay in the position with the nitrogen atom facing towards the intracellular space, which would evidently be more favourable than the antagonal orientation found in the N-substituted amino acids. At the same time, the newly introduced lipophilic domain might be accommodated in the vestibule, which is known to contribute in general significantly to inhibitory potency and selectivity of GAT inhibitors (compare table 1, entries 3 and 4 with 6).

2. Materials and Methods

Chemistry

Moisture-sensitive reactions were carried out in oven-dried glassware under inert gas atmosphere. Commercially available starting materials were used without further purification. Tetrahydrofuran (THF) was freshly distilled from sodium benzophenone ketyl. All other solvents were distilled prior to use. Microwave reactions were carried out with Biotage Initiator™. Flash column chromatography was performed on Merck silica gel 60 (mesh 0.040 - 0.063 mm) as stationary phase; thin-layer chromatography (TLC) was carried out on Merck silica gel 60 F_{254} sheets. Preparative MPLC was performed using a Buechi instrument (C-605 binary pump system, C-630 UV detector at 254 nm and C-660 fraction collector) and a Sepacore B-685 (26V230 mm) glass column equipped with YMC Gel Triart Prep C18-S (12 nm, 5–20 µm). ^{1}H and ^{13}C NMR spectra were, unless stated otherwise, recorded at rt with JNMR-GX (JEOL 400 or 500 MHz) or Bruker BioSpin Avance III HD (400 or 500 MHz) and integrated with the NMR software MestReNova. IR samples were measured as KBr pellets or film with Perkin-Elmer FT-IR 1600. HRMS data were obtained with JMS-GCmate II (EI, Jeol) or Thermo Finnigan LTQ FT Ultra (ESI, Thermo Finnigan).

General procedure for the synthesis of the β-hydroxyamino acid esters (**GP1**): A solution of lithium-HMDS in MTBE (0.97 M) was cooled to -78°C and anhydrous ethyl acetate (EtOAc, 1.0 eq) was added dropwise. After complete addition the mixture was stirred for 25 minutes and a solution of ketone (1.0 eq) in dry THF was added. The reaction mixture was allowed to slowly warm up to -10°C, quenched with brine, diluted with H_2O and extracted thrice with CH_2Cl_2. The combined CH_2Cl_2 phases were dried over sodium sulfate (Na_2SO_4) and concentrated in vacuum to yield the crude product.

General procedure for the deprotection and N-butylation of the amino acid amides and amino acid esters (**GP2**): A mixture of the benzyl or benzhydryl protected amino acid derivative, palladium on charcoal (10% Pd, 0.1 eq) and butyraldehyde (2.5 eq) in EtOH was stirred vigorously under 15 bar hydrogen pressure for 16 h, filtered over Cealite® and reduced in vacuum.

General procedure for the hydrolysis of the amides and esters (**GP3**): A mixture of carboxamide or ester and barium hydroxide octahydrate (2.0 - 2.4 eq) was stirred under reflux conditions (carboxamides) or at rt (esters) in EtOH/H_2O 1:1 for the appropriate time. Carbon dioxide was passed through until no further precipitate formed. The suspension was filtered over a cotton wool pad and a syringe filter (Perfect-Flow®, WICOM Germany GmbH, PTFE, 0.2 µM) and reduced in vacuum. The residue was solved in distilled water (2.0 ml) and lyophilized.

General procedure for the N-butylation of the acyclic amino acids (**GP4**): The amino acid (1.0 eq) and KOH (2.0 eq) were suspended in EtOH and H_2O was added until the reaction mixture became homogeneous. 1-Bromobutane (0.9 eq) was added dropwise. After stirring at rt for 16h the reaction mixture was reduced in vacuum. The crude compound was purified by MPLC (eluent: MeOH/H_2O 1:9).

General procedure for the protection of the acyclic amino acids I (**GP5a**): A solid, well-grounded mixture of the amino acid (1.0 eq) and phtalic anhydride (1.0 eq) was heated to 140°C, resulting in a colourless melting. After 30 min, the reaction mixture was cooled to rt and re-dissolved in EtOAc (300 ml). The solution was washed with 1M sodium hydrogen sulfate solution (100 ml), water (3 x 100 ml), and brine (100 ml). The organic layer was dried over Na_2SO_4, filtered, and concentrated in vacuum. The resulting residue was solved in anhydrous MeOH (250 ml) and 2M HCl in Et_2O (250ml) was added. The mixture was stirred at rt until TLC indicated complete consumption of the educt and reduced in vacuum. The crude compound was purified by flash column chromatography on silica (eluent: CH_2Cl_2/EtOAc 9:1).

General procedure for the protection of the acyclic amino acids II (**GP5b**): A solid, well-grounded mixture of the amino acid (1.0 eq) and phtalic anhydride (1.0 eq) was heated to 140°C, resulting in a colourless melting. After 30 min, the reaction mixture was cooled to rt, solved in anhydrous MeOH (250 ml) and 2M HCl in Et_2O (250 ml) was added. The mixture was stirred at rt until TLC indicated complete consumption of the educt and reduced in vacuum. The crude compound was purified by flash column chromatography on silica (eluent: CH_2Cl_2/EtOAc 9:1).

General procedure for the formation of the ether function (**GP6**): *tert*-Butyl(2-iodethoxy) diphenylsilane (1.4 eq) and silver carbonate (4.0 eq) were added to a suspension of the amino acid derivative (1.0 eq) in toluene (10.0 ml). The reaction mixture was stirred in a pressure tube at 120°C until TLC indicated complete consumption of the amino acid derivative, cooled to rt, filtered through a paper filter and reduced in vacuum. The residue was purified by flash column chromatography on silica (eluent: pentane/Et_2O 7:3).

General procedure for cleavage of the TBDPS protecting group (**GP7**): The TBDPS-protected compound (1.0 eq) was solved in THF/pyridine 9:1 (v/v) in a polypropylene tube. A 70% solution of HF in pyridine (5.0 eq) was added dropwise at 0°C. The suspension was stirred at rt and the progress of the reaction was monitored by TLC. After complete consumption of the educt phosphate buffer (pH = 6.0, 1.0 M, 100 ml) was added and the mixture was extracted with ethyl acetate (100 ml). The organic phase was washed with water (100 ml) and brine (100 ml), dried over $MgSO_4$ and reduced in vacuum. The crude product was purified by flash column chromatography on silica (eluent: CH_2Cl_2/EtOAc 65:35).

*General Procedure for the coupling of the alcohol with 4,4`,4``-trimethoxytrithyl chloride* (**GP8**): The alcohol (1.0 eq) was solved in pyridine. Dimethylformamide (DMF, 1 drope) and 4,4`,4``-trimethoxytrithyl chloride (1.8 eq.) were added. The mixture was stirred at 55°C for 16 h and reduced in vacuum. The crude product was purified by flash chromatography on silica (eluent Et_2O/pentane: 6:4).

General procedure for the deprotection of the acyclic amino acid derivatives I (**GP9a**): 12 M NaOH (2.0 eq) was added to a solution of the protected compound (1.0 eq) in MeOH (15.0 ml). After stirring for 16 h at rt, 1,2-diaminoethane (7.0 eq) was added and the mixture was heated in a microwave for 16h at 140 °C. Finally, the reaction mixture was reduced in vacuum and purified by MPLC (eluent: MeOH/H_2O 7:3).

General procedure for the deprotection of the acyclic amino acid derivatives II (**GP9b**): 12 M NaOH (2.0 eq) was added to a solution of the protected compound (1.0 eq) in MeOH (15.0 ml). After stirring for 16 h at rt, the mixture was freeze-dried. 1,2-Diaminoethane (7.0 eq)

was added and the mixture was heated in a microwave for 16h at 140 °C. Finally, the reaction mixture was reduced in vacuum and purified by MPLC (eluent: MeOH/H_2O 7:3).

3-(Butylamino)-2-hydroxypropanoic acid (**7b**): GP4 was followed using **7a** (90 mg, 0.86 mmol), EtOH (1.0 ml), KOH (114 mg, 1.72 mmol), 1-bromobutane (106 mg, 0.774 mmol). The desired compound was obtained as amorphous white solid (110 mg, 79 %). ^{1}H NMR (400 MHz, MeOD) δ = 4.07 (dd, *J* = 8.1, 4.7 Hz, 1H, COOHC*H*), 3.24 (dd, *J* = 12.5, 4.7 Hz, 1H, COOHCHCH_2), 3.06 (dd, J = 12.5, 8.1 Hz, COOHCHC*H*2), 3.04 – 2.99 (m, 2H, $CH_3CH_2CH_2CH_2$), 1.74 – 1.57 (m, 2H, $CH_3CH_2CH_2$), 1.43 (m, 2H, $CH_3CH_2CH_2$), 0.99 (t, *J* = 7.4 Hz, 3H, $CH_3CH_2CH_2$) ppm; ^{13}C NMR (101 MHz, MeOD) δ = 177.22 (COOH), 68.88 (COOH*C*H), 52.22 (COOHCH*C*H_2), 48.64 (N*C*$H_2CH_2CH_2CH_3$), 29.21 ($NCH_2CH_2CH_2CH_3$), 20.82 ($NCH_2CH_2CH_2CH_3$), 13.88 ($NCH_2CH_2CH_2CH_3$) ppm; IR (KBr): ṽ= 3397, 1463, 1390, 1135, 1110, 770, cm^{-1}; HRESIMS *m/z* (pos): 162.1123 $C_7H_{16}NO_3$ (calcd. 162.1130).

Methyl 3-(1,3-dioxoisoindolin-2-yl)-2-hydroxypropanoate (**7c**): GP5b was followed using 3-amino-2-hydroxypropionic acid **7a** (1.10 g, 10.5 mmol,), phthalic anhydride (1.56 g, 10.5 mmol) in MeOH (80.0 ml) and 2M HCl in Et_2O (80.0 ml). The desired compound was obtained as amorphous white solid (2,00 g, 76 %). ^{1}H NMR (400 MHz, $CDCl_3$) δ = 7.90 – 7.83 (m, 2H, $NCOC_{ar}CH_{ar}CH_{ar}$), 7.78 – 7.69 (m, 2H, $NCOC_{ar}CH_{ar}CH_{ar}$), 4.50 (td, *J* = 6.5, 5.1 Hz, 1H, NCH_2CH), 4.08 (dd, *J* = 14.1, 5.1 Hz, 1H, N*C*H_2), 4.02 (dd, *J* = 14.1, 6.4 Hz, 1H, N*C*H_2), 3.82 (s, 3H, O*C*H_3), 3.07 (d, *J* = 6.8 Hz, 1H, O*H*) ppm; ^{13}C NMR (101 MHz, $CDCl_3$) δ = 173.16 (*C*OOCH_3), 168.37 (N*C*O), 134.33 ($NCOC_{ar}CH_{ar}CH_{ar}$), 132.03 ($NCOC_{ar}CH_{ar}CH_{ar}$), 123.66 ($NCOC_{ar}CH_{ar}CH_{ar}$), 68.66 (NCH_2CH), 53.18 (O*C*H_3), 41.23(N*C*H_2) ppm; IR (HBr): ṽ = 3497, 1747, 1700, 1464, 1440, 1396, 1310, 1231, 1095, 983, 883, 722 cm^{-1}; HRESIMS: *m/z* (pos): 272.0529 $C_{12}H_{11}NO_5Na$ (calcd. 272.0535).

Methyl 3-{2-[(tert-butyldiphenylsilyl)oxy]ethoxy}-3-{-(1,3-dioxoisoindolin-2-yl})propanoate (**7d**): GP6 was followed using **7c** (4.3 mmol, 1072 mg), *tert*-butyl(2-iodoethoxy)diphenylsilane (6.02 mmol, 2374 mg), Ag_2CO_3 (17.2 mmol, 4743 mg), toluene (15.0 ml), 4d. The desired compound was obtained as yellow oil (1882 mg, 82 %). ^{1}H NMR (500 MHz, CD_2Cl_2) δ = 7.85 – 7.78 (m, 2H, $NCOC_{ar}CH_{ar}CH_{ar}$), 7.76 – 7.68 (m, 2H, $NCOC_{ar}CH_{ar}CH_{ar}$), 7.66 – 7.57 (m, 4H$_r$C*H*$_{ar}$), 7.47 – 7.33 (m, 6H, C*H*$_{ar}$), 4.38 (dd, *J* = 6.8, 6.0 Hz, 1H, NCH_2CH), 4.02 (dd, J = 14.0, 6.8 Hz,1H, N*C*H_2), 3.98 (dd, J = 14.0, 6.0 Hz, 1H, N*C*H_2), 3.78 –

3.68 (m, 6H, CHOCH_2CH_2Si, OCH_3), 3.58 – 3.49 (m, 1H, CHOCH_2CH$_2$Si), 0.94 (s, 9H, CCH_3) ppm; ^{13}C NMR (126 MHz, CD_2Cl_2) δ = 171.33 (*C*OOCH$_3$), 168.37 (N*C*O), 136.09 (C$_{ar}$), 134.60 (C$_{ar}$), 134.03 (C$_{ar}$), 132.52 (C$_{ar}$), 130.16 (C$_{ar}$), 128.20 (C$_{ar}$), 123.80 (C$_{ar}$), 76.72 (NCH$_2$*C*H), 72.42 (O*C*H$_2$CH$_2$Si), 63.89 (OCH$_2$*C*H$_2$Si), 52.68 (O*C*H$_3$), 39.89 (N*C*H$_2$CH), 26.98 (SiC*C*H$_3$), 19.44 (Si*C*) ppm; IR (Film): ṽ=2930, 1755, 1700, 1427, 1395, 1208, 1111, 703 cm^{-1}; HRESIMS *m/z* (pos): 554.1970 $C_{30}H_{33}NO_6SiNa$ (calcd. 554.1975).

Methyl 3-(1,3-dioxoisoindolin-2-yl)-3-(2-hydroxyethoxy)propanoate (**7e**): GP7 was followed using **7d** (737 mg, 1.35 mmol,) THF/pyridine 9:1 (10.0 ml), HF-pyridine (1.93 g, 6.75 mmol). The desired compound was obtained as a yellow oil (350 mg, 84 %). ^{1}H NMR (400 MHz, CD_2Cl_2) δ = 7.89 – 7.82 (m, 2H, NCOC$_{ar}$C*H*$_{ar}$CH$_{ar}$), 7.81 – 7.72 (m, 2H, NCOC$_{ar}$CH$_{ar}$C*H*$_{ar}$), 4.25 (dd, *J* = 6.5, 5.5 Hz, 1H, NCH$_2$C*H*), 4.00 (dd, *J* = 14.0, 6.5 Hz, 1H, NC*H*$_2$), 4.05 (dd, *J* = 14.0, 5.5 Hz, 1H, NC*H*$_2$), 3.75 (s, 3H, OC*H*$_3$), 3.70 – 3.54 (m, 4H, OC*H*$_2$C*H*$_2$OH) ppm; ^{13}C NMR (101 MHz, CD_2Cl_2) δ = 171.55 *C*OOCH$_3$), 168.60 (N*C*O), 134.76 (NCOC$_{ar}$CH$_{ar}$*C*H$_{ar}$), 132.45 (NCO*C*$_{ar}$CH$_{ar}$), 123.86 (NCOC$_{ar}$*C*H$_{ar}$), 76.92 (NCH$_2$*C*H), 73.35 (O*C*H$_2$CH$_2$OH), 61.98 (OCH$_2$*C*H$_2$OH), 52.94 (O*C*H$_3$), 40.02 (N*C*H$_2$) ppm; IR (Film): ṽ=3474, 1774, 1770, 1429, 1396, 1213, 1029, 720 cm^{-1}; HRESIMS *m/z* (pos): 294.0973 $C_{14}H_{16}NO_6$ (calcd. 294.0978).

Methyl 3-{1,3-dioxoisoindolin-2-yl}-2-{2-[tris(4-methoxyphenyl)methoxy]ethoxy}propanoat (**7f**): GP8 was followed using **7e** (367 mg, 1.25 mmol), DMF (1 drop), pyridine (4.0 ml), 4,4`,4``-trimethoxytrithyl chloride (856 mg, 2.25 mmol). The desired compound was obtained as yellow oil (705 mg, 90 %). ^{1}H NMR (500 MHz, CD_2Cl_2) δ = 7.87 – 7.76 (m, 2H, NCOC$_{ar}$C*H*$_{ar}$CH$_{ar}$), 7.76 – 7.67 (m, 2H, NCOC$_{ar}$CH$_{ar}$C*H*$_{ar}$), 7.26 – 7.17 (m, 6H, C$_{ar}$C*H*$_{ar}$CH$_{ar}$C$_{ar}$OCH$_3$), 6.81 – 6.68 (m, 6H, C$_{ar}$CH$_{ar}$C*H*$_{ar}$C$_{ar}$OCH$_3$), 4.38 (dd, *J* = 7.3, 5.5 Hz, 1H, NCH$_2$C*H*), 4.06 (dd, *J* = 14.0, 7.4 Hz, 1H, NC*H*$_2$), 4.00 (dd, *J* = 14.1, 5.5 Hz, 1H, NC*H*$_2$), 3.77 (s, 9H, C$_{ar}$OC*H*$_3$), 3.74 (s, 3H, COOC*H*$_3$), 3.73 (ddd, J = 10.5, 5.4, 3.5 Hz, 1H, OC*H*$_2$CH$_2$OCC$_{ar}$) ,3.52 (ddd, *J* = 10.4, 6.9, 3.5 Hz, 1H, OC*H*$_2$CH$_2$OCC$_{ar}$), 3.16 (ddd, *J* = 10.4, 6.9, 3.5 Hz, 1H, OCH$_2$C*H*$_2$OCC$_{ar}$), 3.06 (ddd, *J* = 10.3, 5.3, 3.5 Hz, 1H, OCH$_2$C*H*$_2$OCC$_{ar}$) ppm; ^{13}C NMR (126 MHz, CD_2Cl_2) δ = 171.33 (*C*OOCH$_3$), 168.37(N*C*O), 158.92 (CC$_{ar}$CH$_{ar}$CH$_{ar}$*C*$_{ar}$OCH$_3$), 137.21 (C*C*$_{ar}$CH$_{ar}$), 134.59 (NCOC$_{ar}$CH$_{ar}$*C*H$_{ar}$), 132.51 (NCO*C*$_{ar}$), 130.19 (CH$_3$OC$_{ar}$CH$_{ar}$*C*H$_{ar}$), 123.80 (NCOC$_{ar}$CH$_{ar}$*C*H$_{ar}$), 113.51 (CC$_{ar}$*C*H$_{ar}$*C*H$_{ar}$C$_{ar}$OCH$_3$), 86.15 (OCH$_2$CH$_2$O*C*C$_{ar}$), 76.81 (NCH$_2$*C*H), 70.88 (O*C*H$_2$CH$_2$OCC$_{ar}$), 63.48 (OCH$_2$*C*H$_2$OCC$_{ar}$), 55.73 (C$_{ar}$O*C*H$_3$), 52.72 (COO*C*H$_3$), 39.95

(N*C*H$_2$CH) ppm; IR (Film): ṽ=1776, 1607, 1506, 1464, 1395, 1249, 1176, 1034, 827 cm^{-1}; HRESIMS *m/z* (pos): 648.2210 $C_{36}H_{35}NO_9Na$ (calcd. 648.2210).

3-Amino-2-{2-[tris(4-methoxyphenyl)methoxy]ethoxy}propanoic acid (**7g**): GP9a was followed using **7f** (192 mg, 0.300 mmol), MeOH (3.0 ml), 12M NaOH (0.05 ml), 1,2-diaminoethane (126 mg, 2.10 mmol). The desired compound was obtained as amorphous white solid (123 mg, 83%). ^{1}H NMR (500 MHz, 0.1 M NaOD/MeOD) δ = 7.46 – 7.14 (m, 6H, CH$_3$OC$_{ar}$CH$_{ar}$C*H*$_{ar}$), 7.05 – 6.65 (m, 6H, CH$_3$OC$_{ar}$C*H*$_{ar}$CH$_{ar}$), 3.85 (ddd, J = 10.6, 5.2, 4.4 HZ, 1H, OC*H*$_2$CH$_2$OCC$_{ar}$), 3.81 (dd, *J* = 6.4, 3.8 Hz, 1H, NCH$_2$C*H*), 3.77 (s, 9H, OC*H*$_3$), 3.52 (ddd, *J* = 10.9, 6.7, 4.1 Hz, 1H, OC*H*$_2$CH$_2$OCC$_{ar}$), 3.31 (m. 1H, OCH$_2$C*H*$_2$OCC$_{ar}$), 3.24 (ddd, *J* = 10.0, 5.4, 4.1 Hz, 1H, OCH$_2$C*H*$_2$OCC$_{ar}$), 2.93 (dd, *J* = 13.4, 3.8 Hz, 1H, NC*H*$_2$), 2.85 (dd, *J* = 13.4, 6.4 Hz, 1H, NC*H*$_2$) ppm; ^{13}C NMR (126 MHz, 1M NaOD/MeOD) δ = 180.82 (COOH), 179.19 (CH$_3$O*C*$_{ar}$CH$_{ar}$CH$_{ar}$C$_{ar}$), 159.93 (CH$_3$OC$_{ar}$CH$_{ar}$CH$_{ar}$*C*$_{ar}$), 138.00 (CH$_3$OC$_{ar}$*C*H$_{ar}$CH$_{ar}$C$_{ar}$), 130.96 (CH$_3$OC$_{ar}$CH$_{ar}$*C*H$_{ar}$C$_{ar}$), 87.32 (OCH$_2$CH$_2$O*C*C$_{ar}$), 84.33 (NCH$_2$*C*H), 70.53 (O*C*H$_2$CH$_2$OCC$_{ar}$), 64.40 (OCH$_2$*C*H$_2$OCC$_{ar}$), 55.87 (O*C*H$_3$), 45.20 (N*C*H$_2$CH) ppm; IR (HBR): ṽ=3375, 1608, 1508, 1420, 1303, 1176, 1034 cm^{-1}; HRESIMS *m/*z (neg): 480.2030 $C_{27}H_{30}NO_7$ (calcd. 480.2028).

1-Butyl-3-hydroxyazetidine-3-carboxamide (**11c**): GP2 was followed using 1-benzhydryl-3-hydroxyazetidine-3-carboxamide **11b** (350 mg, 1.20 mmol), palladium on charcoal (10% Pd, 131 mg, 0.120 mmol) and butyraldehyde (0.28 ml, 3.1 mmol) in EtOH (2.0 ml). The crude product was purified by flash column chromatography on silica (eluent: EtOAc/MeOH 95 : 5 + 3 % triethylamine) to afford the desired compound as amorphous white solid (177 mg, 83 %). ^{1}H NMR (400 MHz, MeOD): δ (ppm) = 3.65 – 3.55 (m, 2H, NC*H*$_2$COH), 3.27 – 3.22 (m, 2H, NC*H*$_2$COH), 2.57 – 2.48 (m, 2H, CH$_3$CH$_2$CH$_2$C*H*$_2$N), 1.41 – 1.28 (m, 4H, CH$_3$C*H*$_2$CH$_2$CH$_2$N + CH$_3$CH$_2$C*H*$_2$CH$_2$N), 0.96 - 0.87 (m, 3H, C*H*$_3$CH$_2$CH$_2$CH$_2$N); ^{13}C NMR (101 MHz, MeOD): δ (ppm) = 14.38 (*C*H$_3$CH$_2$CH$_2$CH$_2$N), 21.54 (CH$_3$*C*H$_2$CH$_2$CH$_2$N), 30.58 (CH$_3$CH$_2$*C*H$_2$CH$_2$N), 59.82 (CH$_3$CH$_2$CH$_2$*C*H$_2$N), 65.59 (N*C*H$_2$COH), 72.15 (NCH$_2$*C*OH), 178.42 (*C*ONH$_2$); IR (KBr): ṽ = 3467, 2930, 2361, 1694, 1383, 1252, 1164, 899, 765, 669 cm^{-1}; HRESIMS *m/z* (pos): 173.1288 $C_8H_{17}N_2O_2$ (calcd. 173.1285).

1-Butyl-3-hydroxyazetidine-3-carboxylic acid (**11d**)**:** GP3 was followed using 1-butyl-3-hydroxyazetidine-3-carboxamide **11c** (88 mg, 0.51 mmol) and barium hydroxide octahydrate (380 mg, 1.20 mmol) in EtOH/H$_2$O 1:1 (10.0 ml), 24h, reflux. The desired compound was

obtained as amorphous white solid (84 mg, 95 %). ^{1}H NMR (400 MHz, D_2O + NaOD): δ (ppm) = 3.58 (d, *J* = 9.2 Hz, 2H, NC*H*$_2$COH), 3.21 (d, *J* = 9.1 Hz, 2H, NC*H*$_2$COH), 2.54 – 2.48 (m, 2H, $CH_3CH_2CH_2CH_2N$), 1.36 – 1.20 (m, 4H, $CH_3CH_2CH_2CH_2N$ + $CH_3CH_2CH_2CH_2N$), 0.89 – 0.82 (m, 3H, $CH_3CH_2CH_2CH_2N$); ^{13}C NMR (101 MHz, D_2O + NaOD): δ (ppm) = 180.47 (*C*OO), 72.59 (NCH_2COH), 64.70 (NCH_2COH), 58.84 ($CH_3CH_2CH_2CH_2N$), 29.36 ($CH_3CH_2CH_2CH_2N$), 20.54 ($CH_3CH_2CH_2CH_2N$), 13.39 ($CH_3CH_2CH_2CH_2N$); IR (KBr): ṽ = 3467, 2930, 2361, 1694, 1383, 1252, 1164, 899, 765, 669 cm^{-1}; HRESIMS *m/z* (pos): 173.1129 $C_8H_{16}NO_3$ (calcd. 174.1125).

Ethyl 2-(1-benzhydryl-3-hydroxyazetidin-3-yl)acetate (**11e**): GP1 was followed using LiHMDS in methyl *tert*-butyl ether (2.0 ml, 1.9 mmol), EtOAc (0.19 ml, 1.9 mmol) and 1-benzhydrylazetidin-3-one **11a** (424 mg, 1.70 mmol) in THF (2.0 ml). The crude product was purified by flash column chromatography on silica (eluent: pentane/Et_2O 3:1 + 2 % diethylmethylamine) to afford the desired compound as amorphous white solid (448 mg, 80 %).^{1}H NMR (500 MHz, $CDCl_3$): δ (ppm) = 7.47 – 7.11 (m, 10H, CH_{ar}), 4.39 (s, 1H, $NCHC_{ar}$), 4.17 (q, *J* = 7.1 Hz, 2H, COOC*H*$_2$CH$_3$), 3.79 (s, 1H, OH), 3.34 – 3.17 (m, 2H, NC*H*$_2$COH), 3.09 – 2.98 (m, 2H, NC*H*$_2$COH), 2.91 (s, 2H, CH_2COO), 1.28 (t, *J* = 7.2 Hz, 3H, $COOCH_2CH_3$); ^{13}C NMR (101 MHz, $CDCl_3$): δ (ppm) = 172.91 (*C*OOCH$_2$CH$_3$), 142.28 (NCH*C*CHCHCH), 128.54 (NCHCCH*C*HCH), 127.59 (NCHC*C*HCHCH), 127.25 (NCHCCHCH*C*H), 77.94 ($NCHC_{ar}$), 67.62 (NCH_2COH), 65.21 (NCH_2COH), 61.10 ($COOCH_2CH_3$), 42.96 (CH_2COO), 14.31 ($COOCH_2CH_3$); IR (KBr): ṽ = 3404, 2952, 1718, 1451, 1304, 1231, 1080, 902, 749, 706 cm^{-1}; HREIMS *m/z* (pos): 325.1662 $C_{20}H_{23}NO_3$ (calcd. 325.1672).

Ethyl 2-(1-butyl-3-hydroxyazetidin-3-yl)acetate (**11f**): GP2 was followed using **11e** (263 mg, 0.810 mmol), palladium on charcoal (10% Pd, 84 mg, 0.081 mmol) and butyraldehyde (0.18 ml, 2.0 mmol) in EtOH (5.0 ml). The crude product was purified by flash column chromatography on silica gel (eluent: Et_2O + 3 % triethylamine) to afford the desired compound as colourless oil (195 mg, 87 %). ^{1}H NMR (500 MHz, $CDCl_3$): δ (ppm) = 4.19 (q, 2H, *J* = 7.2 Hz, COOC*H*$_2$CH$_3$), 3.92 (br s, 1H, OH), 3.43 - 3.25 (m, 2H, NC*H*$_2$COH), 3.14 - 2.96 (m, 2H, NC*H*$_2$COH), 2.86 (s, 2H, CH_2COO), 2.52 - 2.40 (m, 2H, NC*H*$_2$CH$_2$CH$_2$CH$_3$), 1.37 - 1.23 (m, 7H, NCH$_2$C*H*$_2$CH$_2$CH$_3$ + NCH$_2$CH$_2$C*H*$_2$CH$_3$ + COOCH$_2$C*H*$_3$), 0.98 - 0.71 (m, 3H, NCH$_2$CH$_2$CH$_2$C*H*$_3$); ^{13}C NMR (126 MHz, $CDCl_3$): δ (ppm) = 172.97 (*C*OOCH$_2$CH$_3$), 68.30 (COH), 66.25 (NCH_2COH), 61.03 ($COOCH_2CH_3$), 59.70 ($NCH_2CH_2CH_2CH_3$), 42.81 (CH_2COO), 30.13 ($NCH_2CH_2CH_2CH_3$),

20.63 ($NCH_2CH_2\mathit{C}H_2CH_3$), 14.32 ($COOCH_2\mathit{C}H_3$), 14.20 ($NCH_2CH_2CH_2\mathit{C}H_3$); IR (film): ṽ = 3456, 2958, 2933, 1737, 1465, 1370, 1190, 1031, 948, 879 cm^{-1}; HRESIMS *m/z* (pos): 216.1589 $C_{11}H_{22}NO_3$ (calcd. 216.1594).

2-(1-Butyl-3-hydroxyazetidin-3-yl)acetic acid (**11g**): GP3 was followed using **11f** (34 mg, 0.16 mmol) and barium hydroxide octahydrate (201 mg, 0.630 mmol) in EtOH/H_2O 1:1 (6.0 ml), 19h, rt. The desired compound was obtained as amorphous white solid (26 mg, 87 %). ^{1}H NMR (400 MHz, D_2O + NaOD): δ (ppm) = 3.39 – 3.33 (m, 2H, $NC\mathit{H}_2COH$), 3.09 – 3.02 (m, 2H, $NC\mathit{H}_2COH$), 2.61 (s, 2H, $CC\mathit{H}_2COO$), 2.54 – 2.45 (m, 2H, $CH_3CH_2CH_2C\mathit{H}_2N$), 1.40 – 1.27 (m, 4H, $CH_3C\mathit{H}_2CH_2CH_2N$ + $CH_3CH_2C\mathit{H}_2CH_2N$), 0.96 – 0.87 (m, 3H, $C\mathit{H}_3CH_2CH_2CH_2N$); ^{13}C NMR (101 MHz, D_2O + NaOD): δ (ppm) = 180.44 (*C*OO), 69.06 ($NCH_2\mathit{C}OH$), 66.11 ($N\mathit{C}H_2COH$), 59.60 ($CH_3CH_2CH_2\mathit{C}H_2N$), 46.06 ($\mathit{C}H_2COO$), 29.77 ($CH_3CH_2\mathit{C}H_2CH_2N$), 20.90 ($CH_3\mathit{C}H_2CH_2CH_2N$), 14.29 ($\mathit{C}H_3CH_2CH_2CH_2N$); IR (film): ṽ = 3427, 2930, 2360, 2342, 1583, 1569, 1420, 1108, 912, 686 cm^{-1}; HREIMS *m/z* (pos): 187.1193 $C_9H_{17}NO_3$ (calcd. 187.1203).

Ethyl 2-(1-benzyl-3-hydroxypyrrolidin-3-yl)acetate (**12e**): GP1 was followed using LiHMDS in MTBE (2.1 ml, 2.0 mmol), EtOAc (0.20 ml, 2.0 mmol) and 1-benzylpyrrolidin-3-one **12a** (371 mg, 2.10 mmol) in THF (1.0 ml). The crude product was purified by flash column chromatography on silica (eluent: pentane/EtOAc 6:4 + 2 % diethylmethylamine) to afford the desired compound as pale yellow oil (499 mg, 93 %). ^{1}H NMR (500 MHz, $CDCl_3$): δ (ppm) = 7.26 (m, 5H, CH_{ar}), 4.17 (q, *J* = 7.1 Hz, 2H, $COOC\mathit{H}_2CH_3$), 3.64 (s, 2H, $C_{ar}CH_2N$), 3.58 (br s, 1H, OH), 2.80 - 2.74 (m, 1H, $NC\mathit{H}_2CH_2$), 2.71 - 2.54 (m, 5H, $NC\mathit{H}_2CH_2$ + $NC\mathit{H}_2COH$ + $NC\mathit{H}_2COH$ + CH_2COO), 2.01 - 1.94 (m, 1H, $NCH_2C\mathit{H}_2$), 1.93 - 1.85 (m, 1H, $NCH_2C\mathit{H}_2$), 1.26 (t, *J* = 7.1 Hz, 3H, $COOCH_2C\mathit{H}_3$); ^{13}C NMR (126 MHz, $CDCl_3$): δ (ppm) = 172.82 ($\mathit{C}OOCH_2CH_3$), 138.96 ($NCH_2\mathit{C}CHCHCH$), 128.86 ($NCH_2C\mathit{C}HCHCH$), 128.38 ($NCH_2CCH\mathit{C}HCH$), 127.11 ($NCH_2CCHCH\mathit{C}H$), 66.56 ($N\mathit{C}H_2COH$), 60.89 ($COO\mathit{C}H_2CH_3$), 60.26 ($N\mathit{C}H_2C_{ar}$), 52.87 ($N\mathit{C}H_2CH_2$), 44.53 ($\mathit{C}H_2COO$), 39.44 ($NCH_2\mathit{C}H_2$), 14.32 ($COOCH_2\mathit{C}H_3$); IR (film): ṽ = 3512, 2978, 2796, 1732, 1372, 1189, 1029, 911, 740, 699 cm^{-1}; HREIMS *m/z* (pos): 263.1525 $C_{15}H_{21}NO_3$ (calcd. 263.1516).

Ethyl 2-(1-butyl-3-hydroxypyrrolidin-3-yl)acetate (**12f**): GP2 was followed using **12e** (290 mg, 1.10 mmol), palladium on charcoal (10% Pd, 117 mg, 0.110 mmol) and butyraldehyde (0.30 ml, 3.3 mmol) in EtOH (3.5 ml). The crude product was purified by flash column

chromatography on silica gel (eluent: pentane/Et_2O 7:3 + 3 % diethylmethylamine) to afford the desired compound as colourless oil (195 mg, 77 %).^{1}H NMR (400 MHz, $CDCl_3$): δ (ppm) = 4.18 (q, *J* = 7.2 Hz, 2H, COOC*H*$_2$CH$_3$), 3.54 (br s, 1H, OH), 2.81 - 2.61 (m, 4H, CH_2COO + NC*H*$_2$CH$_2$COH + NC*H*$_2$COH), 2.57 - 2.38 (m, 4H, NC*H*$_2$CH$_2$COH + NC*H*$_2$COH + NC*H*$_2$CH$_2$CH$_2$CH$_3$), 2.01 - 1.92 (m, 1H, NCH$_2$C*H*$_2$COH), 1.86 (m, 1H, NCH$_2$C*H*$_2$COH), 1.51 - 1.40 (m, 2H, NCH$_2$C*H*$_2$CH$_2$CH$_3$), 1.38 - 1.25 (m, 5H, COOCH$_2$C*H*$_3$ + NCH$_2$CH$_2$C*H*$_2$CH$_3$), 0.91 (t, *J* = 7.3 Hz, 3H, NCH$_2$CH$_2$CH$_2$C*H*$_3$); ^{13}C NMR (126 MHz, $CDCl_3$): δ (ppm) = 172.84 (*C*OOCH$_2$CH$_3$), 77.56 (COH), 66.96 (N*C*H$_2$COH), 60.88 (COO*C*H$_2$CH$_3$), 56.16 (N*C*H$_2$CH$_2$CH$_2$CH$_3$), 53.14 (N*C*H$_2$CH$_2$COH), 44.56 (*C*H$_2$COO), 39.41 (NCH$_2$*C*H$_2$COH), 30.93 (NCH$_2$*C*H$_2$CH$_2$CH$_3$), 20.88 (NCH$_2$CH$_2$*C*H$_2$CH$_3$), 14.32 (COOCH$_2$*C*H$_3$), 14.19 (NCH$_2$CH$_2$CH$_2$*C*H$_3$); IR (film): ṽ = 3442, 2958, 2797, 1735, 1465, 1370, 1190, 1031, 946, 904 cm^{-1}; HREIMS *m/z* (pos): 229.1673 $C_{12}H_{23}NO_3$ (calcd. 229.1672).

2-(1-Butyl-3-hydroxypyrrolidin-3-yl)acetic acid (**12g**)**:** GP3 was followed using **12f** (181 mg, 0.790 mmol) and barium hydroxide octahydrate (500 mg, 1.58 mmol) in EtOH/H_2O 1:1 (8.0 ml), 6h, rt. The desired compound was obtained as amorphous off-white solid (153 mg, 96 %). ^{1}H NMR (400 MHz, D_2O + NaOD): δ (ppm) = 3.90 - 3.66 (m, 2H, NC*H*$_2$COH + NC*H*$_2$CH$_2$COH), 3.46 - 3.14 (m, 4H, NC*H*$_2$COH + NC*H*$_2$CH$_2$COH + NC*H*$_2$CH$_2$CH$_2$CH$_3$), 2.80 - 2.59 (m, 2H, C*H*$_2$COO), 2.36 - 2.03 (m, 2H, NCH$_2$C*H*$_2$COH + NCH$_2$C*H*$_2$COH), 1.78 - 1.62 (m, 2H, NCH$_2$C*H*$_2$CH$_2$CH$_3$), 1.39 (h, *J* = 7.4 Hz, 2H, NCH$_2$CH$_2$C*H*$_2$CH$_3$), 0.93 (t, *J* = 7.4 Hz, 3H, NCH$_2$CH$_2$CH$_2$C*H*$_3$); ^{13}C NMR (101 MHz, D_2O + NaOD): δ (ppm) = 180.19 (*C*OOCH$_2$CH$_3$), 78.13 (*C*OH), 65.66 (N*C*H$_2$COH), 55.88 (N*C*H$_2$CH$_2$CH$_2$CH$_3$), 52.70 (N*C*H$_2$CH$_2$COH), 47.08 (*C*H$_2$COO), 38.47 (NCH$_2$*C*H$_2$COH), 29.72 (NCH$_2$*C*H$_2$CH$_2$CH$_3$), 20.33 (NCH$_2$CH$_2$*C*H$_2$CH$_3$), 13.39 (NCH$_2$CH$_2$CH$_2$*C*H$_3$); IR (KBr): ṽ = 3426, 2965, 2876, 2360, 1589, 1395, 1094, 1014, 741, 669 cm^{-1}; HRESIMS *m/z* (pos): 202.1439 $C_{10}H_{20}NO_3$ (calcd. 202.1438).

1-Benzyl-3-hydroxypiperidine-3-carboxamide (**13b**): 1-Benzylpiperidin-3-one hydrochloride **13a** (571 mg, 2.50 mmol) was solved in dry CH_2Cl_2 (4.0 ml). Freshly distilled triethylamine (0.85 ml, 6.1 mmol) was added and the brownish suspension was placed in an ultrasound bath for 15 minutes. After addition of trimethylsilyl cyanide (0.80 ml, 6.3 mmol) the reaction mixture was stirred for 48 h, diluted with CH_2Cl_2 (10.0 ml), filtered through a paper filter and reduced in vacuum. The oily residue was solved in CH2Cl2 (7.0 ml) and cooled to 0°C. Concentrated sulfuric acid (0.70 ml, 13 mmol) was added and the biphasic mixture was

stirred for 2h at rt, after which the mixture was cooled to 0°C, diluted with H_2O (5.0 ml) and alkalized with 25% ammonium hydroxide solution. Potassium sodium tartrate (0.50 g) was added and the mixture was extracted five times with CH_2Cl_2 (20.0 ml). The combined organic phases were dried over $MgSO_4$ and reduced in vacuum. The crude product was purified by flash column chromatography on silica (eluent: ethyl acetate + 3 % triethylamine) to afford the desired compound as amorphous off-white solid (567 mg, 96 %). ^{1}H NMR (400 MHz, 1,1,2,2-tetrachloroethane-d2, 80°C): δ (ppm) = 7.61 (br s, 1H, NH_2), 7.44 – 7.29 (m, 5H, CH_{ar}), 5.46 (br s, 1H, NH_2), 3.92 (br s, 1H, O*H*), 3.64 (s, 2H, NCH_2C_{ar}), 2.74 (dd, *J* = 11.3, 1.0 Hz, 1H, $NCH_{ax}H_{eq}COH$), 2.63 – 2.46 (m, 3H, $NCH_{ax}H_{eq}COH$ + $NCH_{ax}H_{eq}CH_2CH_2$ + $NCH_{ax}H_{eq}CH_2CH_2$), 1.96 (dddd, *J* = 13.0, 7.8, 5.1, 1.0 Hz, 1H, $NCH_2CH_2CH_{ax}H_{eq}$), 1.89 – 1.57 (m, 3H, $NCH_2CH_2CH_{ax}H_{eq}$ + $NCH_2CH_{ax}H_{eq}CH_2$ + $NCH_2CH_{ax}H_{eq}CH_2$); ^{13}C NMR (101 MHz, 1,1,2,2-tetrachloroethane-d2, 80°C): δ (ppm) = 176.79 (CNH_2), 137.18 ($NCH_2CCHCHCH$), 128.88 ($NCH_2CCHCHCH$), 128.29 ($NCH_2CCHCHCH$), 127.28 ($NCH_2CCHCHCH$), 71.85 (NCH_2COH), 62.56 (NCH_2C_{ar}), 60.29 (NCH_2COH), 52.67 ($NCH_2CH_2CH_2$), 33.59 ($NCH_2CH_2CH_2$), 21.49 ($NCH_2CH_2CH_2$); IR (KBr): ṽ = 3457, 3409, 2790, 1663, 1274, 1206, 1020, 924, 735, 665 cm^{-1}; HREIMS *m/z* (pos): 234.1361 $C_{13}H_{18}N_2O_2$ (calcd. 234.1363).

1-Butyl-3-hydroxypiperidine-3-carboxamide (**13c**): GP2 was followed using 1-benzyl-3-hydroxypiperidine-3-carboxamide **13b** (300 mg, 1.30 mmol), palladium on charcoal (10% Pd, 138 mg, 0.130 mmol) and butyraldehyde (0.29 ml, 3.20 mmol) in EtOH (3.5 ml). The crude product was purified by flash column chromatography on silica (eluent: EtOAc + 3 % triethylamine) to afford the desired compound as amorphous white solid (238 mg, 93 %). ^{1}H NMR (400 MHz, 1,1,2,2-tetrachloroethane-d2, 80°C): δ (ppm) = 7.65 (br s, 1H, NH_2), 5.35 (br s, 1H, NH_2), 3.96 (br s, 1H, OH), 2.63 (d, *J* = 11.4 Hz, 1H, $NCH_{ax}H_{eq}COH$), 2.48 – 2.28 (m, 5H, $CH_3CH_2CH_2CH_2N$ + $NCH_{ax}H_{eq}COH$ + $NCH_{ax}H_{eq}CH_2CH_2OH$ + $NCH_{ax}H_{eq}CH_2CH_2OH$), 1.86 – 1.78 (m, 1H, $NCH_2CH_2CH_{ax}H_{eq}COH$), 1.76 – 1.57 (m, 2H, $NCH_2CH_{ax}H_{eq}CH_2COH$ + $NCH_2CH_{ax}H_{eq}CH_2COH$), 1.54 – 1.37 (m, 3H, $CH_3CH_2CH_2CH_2N$ + $NCH_2CH_2CH_{ax}H_{eq}COH$), 1.34 – 1.20 (m, 2H, $CH_3CH_2CH_2CH_2N$), 0.88 (t, *J* = 7.3 Hz, 3H, $CH_3CH_2CH_2CH_2N$); ^{13}C NMR (101 MHz, 1,1,2,2-tetrachloroethane-d2, 80°C): δ (ppm) = 177.36 (CNH_2), 72.13 (NCH_2COH), 61.04 (NCH_2COH), 58.07 ($CH_3CH_2CH_2CH_2N$), 53.08 ($NCH_2CH_2CH_2COH$), 34.15 ($NCH_2CH_2CH_2COH$), 28.96 ($NCH_2CH_2CH_2OH$), 21.35 ($CH_3CH_2CH_2CH_2N$), 14.05 ($CH_3CH_2CH_2CH_2N$); IR (KBr): ṽ = 3462,

2955, 2805, 1682, 1454, 1399, 1137, 1019, 917, 659 cm^{-1}; HREIMS *m/z* (pos): 200.1519 $C_{10}H_{20}N_2O_2$ (calcd. 200.1525).

1-Butyl-3-hydroxypiperidine-3-carboxylic acid (**13d**)**:** GP3 was followed using 1-butyl-3-hydroxypiperidine-3-carboxamide **13c** (80 mg, 0.40 mmol) and barium hydroxide octahydrate (254 mg, 0.801 mmol) in EtOH/H_2O 1:1 (10.0 ml), 5h, reflux. The desired compound was obtained as colorless semi-solid (76 mg, 94 %). ^{1}H NMR (400 MHz, D_2O + NaOD): δ (ppm) = 2.49 (br d, *J* = 10.8 Hz, 1H, $NCH_{ax}\mathit{H}_{eq}CH_2CH_2COH$), 2.38 (d, *J* = 12.0 Hz, 1H, $NCH_{ax}\mathit{H}_{eq}COH$), 2.06 – 1.90 (m, 3H, $CH_3CH_2CH_2C\mathit{H}_2N$ + $NC\mathit{H}_{ax}H_{eq}COH$), 1.72 – 1.61 (m, 1H, $NC\mathit{H}_{ax}H_{eq}CH_2CH_2COH$), 1.47 – 1.20 (m, 4H, $NCH_2CH_2C\mathit{H}_{ax}H_{eq}COH$ + $NCH_2CH_2CH_{ax}\mathit{H}_{eq}COH$ + $NCH_2C\mathit{H}_{ax}H_{eq}CH_2COH$ + $NCH_2CH_{ax}\mathit{H}_{eq}CH_2COH$), 1.15 – 1.03 (m, 2H, $CH_3CH_2C\mathit{H}_2CH_2N$), 0.92 (h, *J* = 7.3 Hz, 2H, $CH_3C\mathit{H}_2CH_2CH_2N$), 0.54 (t, *J* = 7.3 Hz, 3H, $C\mathit{H}_3CH_2CH_2CH_2N$); ^{13}C NMR (101 MHz, D_2O + NaOD): δ (ppm) = 182.05 (*C*OO), 74.27 ($NCH_2\mathit{C}OH$), 59.59 ($N\mathit{C}H_2COH$), 57.89 ($CH_3CH_2CH_2\mathit{C}H_2N$), 52.75 ($N\mathit{C}H_2CH_2CH_2COH$), 32.18 ($NCH_2CH_2\mathit{C}H_2COH$), 27.22 ($CH_3CH_2\mathit{C}H_2CH_2N$), 20.27 ($NCH_2CH_2\mathit{C}H_2COH$), 20.18 ($CH_3\mathit{C}H_2CH_2CH_2N$), 13.28 ($\mathit{C}H_3CH_2CH_2CH_2N$); IR (KBr): ṽ = 3414, 2961, 2874, 1609, 1388, 1179, 1120, 1016, 949, 719 cm^{-1}; HREIMS *m/z* (pos): 201.1365 $C_{10}H_{19}NO_3$ (calcd. 201.1359).

4-(Butylamino)-2-hydroxybutanoic acid (**14b**): GP4 was followed using **14a** (134 mg, 1,12 mmol), EtOH (2.4 ml), KOH (56,1 mg, 2.25 mmol), 1-bromobutane (139 mg, 1.01 mmol). The desired compound was obtained as amorphous white solid (155 mg, 79 %). ^{1}H NMR (500 MHz, MeOD) δ = 4.00 (t, *J* = 5.7 Hz, 1H,$C\mathit{H}$OH), 3.16 – 3.09 (m, 2H, $OHCCH_2C\mathit{H}_2N$), 2.97 (m, 2H, $NC\mathit{H}_2CH_2CH_2CH_3$), 2.05 (dtd, *J* = 14.2, 7.1, 5.5 Hz, 1H, $OHCHC\mathit{H}_2$), 1.95 (dq, *J* = 14.5, 6.2 Hz, 1H, $OHCHC\mathit{H}_2$), 1.65 (m, 2H, $CH_3CH_2C\mathit{H}_2$), 1.43 (m, 2H, $CH_3C\mathit{H}_2CH_2$), 0.99 (t, *J* = 7.4 Hz, 3H, $C\mathit{H}_3CH_2CH_2$ ppm); ^{13}C NMR (126 MHz, MeOD) δ = 179.99 (*C*OOH), 72.01 (COOH*C*H), 49.84 ($N\mathit{C}H_2CH_2CH_2CH_3$), 46.78 ($OHCHCH_2\mathit{C}H_2$), 31.74 ($OHCH\mathit{C}H_2CH_2$), 29.40 ($NCH_2\mathit{C}H_2CH_2CH_3$), 20.78 ($NCH_2CH_2\mathit{C}H_2CH_3$), 13.88 ($NCH_2CH_2CH_2\mathit{C}H_3$) ppm; IR (KBr): ṽ= 3411, 1651, 1359, 1335, 1103, 820 cm^{-1}; HRESIMS *m/z* (pos): 176.1281 $C_8H_{18}NO_3$ (calcd. 176.1287).

Methyl 2-{2-[(tert-butyldiphenylsilyl)oxy]ethoxy}-4-(1,3-dioxoisoindolin-2-yl)butanoate (**14d**): GP6 was followed using **14c** (369 mg, 1.20 mmol), *tert*-butyl(2-iodoethoxy)diphenylsilane (805 mg, 1.70 mmol), Ag_2CO_3 (1.32 g, 4.80 mmol), toluene (2.0 ml), 4d. The desired

compound was obtained as yellow oil (500 mg, 76 %). ^{1}H NMR (500 MHz, CD_2Cl_2) δ = 7.83 – 7.77 (m, 2H, $NCOC_{ar}CH_{ar}CH_{ar}$), 7.73 – 7.66 (m, 6H, CH_{ar}), 7.47 – 7.36 (m, 6H, CH_{ar}), 4.02 (dd, *J* = 8.8, 3.8 Hz, 1H, NCH_2CH_2CH), 3.86 – 3.70 (m, 5H, NCH_2, $SiOCH_2CH_2$), 3.68 (s, 3H, $COOCH_3$), 3.54 (ddd, *J* = 9.7, 6.2, 4.2 Hz, 1H, $SiOCH_2CH_2$), 2.11 (dtd, *J* = 14.4, 7.3, 3.8 Hz, 1H, NCH_2CH_2), 2.08 – 2.00 (m, 1H, NCH_2CH_2), 1.04 (s, 9H, CCH_3) ppm; ^{13}C NMR (126 MHz, CD_2Cl_2) δ = 172.93 ($COOCH_3$), 168.65 (NCO), 136.15 (C_{ar}), 134.46 (C_{ar}), 134.24 (C_{ar}), 132.74 (C_{ar}), 130.17 (C_{ar}), 128.21 (C_{ar}), 123.56 (C_{ar}), 77.76 (NCH_2CH_2CH), 72.39 ($SiOCH_2CH_2$), 63.92 ($SiOCH_2CH_2$), 52.33 ($COOCH_3$), 35.10 (NCH_2), 32.20 (NCH_2CH_2), 27.11 (CCH_3), 19.57 (CCH_3) ppm; IR (Film): ṽ = 2932, 1770, 1468, 1396, 1112, 823, 738, 703 cm^{-1}; HRESIMS *m/z* (pos): 568.2125 $C_{31}H_{35}NO_6SiNa$ (calcd. 568.2126).

Methyl 4-(1,3-dioxoisoindolin-2-yl)-2-(2-hydroxyethoxy)butanoate (**14e**): GP7 was followed using **14d** (442 mg, 0.810 mmol), THF/pyridine 9:1 (10.0 ml), HF-pyridine (116 mg, 4.05 mmol). The desired compound was obtained as yellow oil (190 mg, 76 %). ^{1}H NMR (500 MHz, $CDCl_3$) δ = 7.93 – 7.80 (m, 2H, $C_{ar}CH_{ar}CH_{ar}$), 7.80 – 7.66 (m, 2H, $C_{ar}CH_{ar}CH_{ar}$), 3.99 (ddd, *J* = 13.9, 8.8, 5.0 Hz, 1H, NCH_2), 3.92 (dd, *J* = 9.9, 3.2 Hz, 1H, NCH_2CH_2CH), 3.81 (dt, *J* = 14.0, 5.5 Hz, 1H, NCH_2), 3.76 – 3.67 (m, 6H, OCH_3, $CHOCH_2CH_2OH$), 3.63 – 3.56 (m, 1H, $CHOCH_2CH_2OH$), 2.94 (t, *J* = 5.7 Hz, 1H, OH), 2.19 (dddd, *J* = 14.3, 8.7, 5.5, 3.2 Hz, 1H, NCH_2CH_2), 2.08 (ddt, *J* = 14.9, 9.78, 5.25, 5.25 Hz, 1H, NCH_2CH_2) ppm; ^{13}C NMR (126 MHz, $CDCl_3$) δ = 173.03 ($COOCH_3$), 168.61 (NCO), 134.28 ($C_{ar}CH_{ar}CH_{ar}$), 132.16 ($C_{ar}CH_{ar}CH_{ar}$), 123.51 ($C_{ar}CH_{ar}CH_{ar}$), 76.69 (NCH_2CH_2CH), 72.73 ($CHOCH_2CH_2OH$), 61.95 ($CHOCH_2CH_2OH$), 52.34 (OCH_3), 34.45 (NCH_2CH_2), 31.95 (NCH_2CH_2) ppm; IR (Film): ṽ=3464, 1771, 1760, 1700, 1438, 1398, 1148, 721 cm^{-1}; HRESIMS *m/z* (pos): 330.0946 $C_{15}H_{17}NO_6Na$ (calcd. 330.0948).

Methyl 4-{1, 3-dioxoisoindolin-2-yl}-2-{2-[tris(4-methoxyphenyl)methoxy]ethoxy}butanoate (**14f**): GP8 was followed using **14e** (461 mg, 1.50 mmol), DMF (1 drop), pyridine (4.0 ml), 4,4`,4``-trimethoxytrithyl chloride (1.03 g, 2.70 mmol). The desired compound was obtained as a yellow oil (789 mg, 82 %). ^{1}H NMR (400 MHz, $CDCl_3$) δ = 7.75-7.80 (m, 2H, $NCOC_{ar}CH_{ar}CH_{ar}$), 7.73 – 7.64 (m, 2H, $NCOC_{ar}CH_{ar}CH_{ar}$), 7.37 – 7.28 (m, 6H, $CH_3OC_{ar}CH_{ar}CH_{ar}$), 6.86 – 6.77 (m, 6H, $CH_3OC_{ar}CH_{ar}CH_{ar}$), 4.04 (dd, *J* = 7.6, 5.0 Hz, 1H, NCH_2CH_2CH), 3.88 (t, *J* = 6.9 Hz, 2H, NCH_2), 3.79 (s, 10H, $C_{ar}OCH_3$, $CHOCH_2CH_2$), 3.72 (s, 3H, $COOCH_3$), 3.59 (ddd, *J* = 10.3, 6.2, 4.4 Hz, 1H, $CHOCH_2CH_2$), 3.22 (ddd, *J* = 10.3, 6.2, 4.3 Hz, 1H, $CHOCH_2CH_2$), 3.14

(ddd, *J* = 10.2, 5.8, 4.4 Hz, 1H, $CHOCH_2CH_2$), 2.30 – 1.88 (m, 2H, NCH_2CH_2) ppm; ^{13}C NMR (101 MHz, *CDCl₃*) δ = 172.66 66 ($COOCH_3$), 168.28 (NCO), 158.41 ($CH_3OC_{ar}CH_{ar}CH_{ar}C$), 136.92 ($CH_3OC_{ar}CH_{ar}CH_{ar}C$), 133.98 ($NCOC_{ar}CH_{ar}CH_{ar}$), 132.27 ($NCOC_{ar}CH_{ar}CH_{ar}$), 129.92 ($CH_3OC_{ar}CH_{ar}CH_{ar}C$), 123.32 ($NCOC_{ar}CH_{ar}CH_{ar}$), 113.18 ($CH_3OC_{ar}CH_{ar}CH_{ar}C$), 85.77 ($OCC_{ar}$), 77.58 ($NCH_2CH_2CH$), 70.46 ($CHOCH_2CH_2$), 63.15 ($CHOCH_2CH_2$), 55.34 ($C_{ar}OCH_3$), 52.13 ($COOCH_3$), 34.90 ($NCH_2CH_2$), 31.90 ($NCH_2CH_2$) ppm; IR (Film): ṽ = 1748, 1700, 1607, 1508, 1398, 1249, 1176, 1034 cm^{-1}; HRESIMS *m/z* (pos): 678.2091 $C_{37}H_{37}NO_9$ (calcd. 678.210).

4-Amino-2-{2-[tris(4-methoxyphenyl)methoxy]ethoxy}butanoic acid (**14g**): GP9a was followed using **14f** (192 mg, 0.300 mmol), MeOH (3.0 ml), 12 M NaOH (0.05 ml), 1,2-diaminoethane (126 mg, 2.10 mmol). The desired compound was obtained as amorphous white solid (102 mg, 69%). ^1H NMR (400 MHz, 0.1 M NaOD/MeOD) δ = 7.48 – 7.04 (m, 6H, $CH_3OC_{ar}CH_{ar}CH_{ar}$), 6.99 – 6.66 (m, 6H, $CH_3OC_{ar}CH_{ar}CH_{ar}$), 3.87 (dd, *J* = 8.1, 4.4 Hz, 1H, NCH_2CH_2CH), 3.77 (s, 10H, $CHOCH_2CH_2OC$, OCH_3), 3.45 (ddd, *J* = 10.9, 7.2, 3.9 Hz, 1H, $CHOCH_2CH_2OC$), 3.27 (m, 1H, $CHOCH_2CH_2OC$), 3.19 (m, 1H, $CHOCH_2CH_2OC$), 2.85 – 2.68 (m, 2H, NCH_2CH_2), 1.96 – 1.74 (m, 2H, NCH_2CH_2) ppm; ^{13}C NMR (101 MHz,0.1 M NaOD/ MeOD) δ = 180.86 (*C*OOH), 159.93 ($CC_{ar}CH_{ar}CH_{ar}COCH_3$), 138.08 ($CC_{ar}CH_{ar}CH_{ar}COCH_3$), 130.99 ($CC_{ar}CH_{ar}CH_{ar}COCH_3$), 114.06 ($CC_{ar}CH_{ar}CH_{ar}COCH_3$), 87.20 ($CC_{ar}CH_{ar}CH_{ar}COCH_3$), 82.05 ($NCH_2CH_2CH$), 70.40 ($CHOCH_2CH_2C$), 64.40 ($CHOCH_2CH_2C$), 55.80 ($OCH_3$), 40.08 ($NCH_2CH_2$), 37.45 ($NCH_2CH_2$) ppm; IR (KBr): ṽ= 1606, 1505, 1463, 1249, 1175, 1034, 828, 735 cm^{-1}; HRESIMS *m/z* (neg): 494.2185 $C_{28}H_{32}NO_7$ (calcd. 494.2184).

4-(Butylamino)-3-hydroxybutanoic acid (**15b**): GP4 was followed using **15a** (238 mg, 2.00 mmol), EtOH (2.4 ml), KOH (264 mg, 4.00 mmol), 1-bromobutane (249 mg, 1.80 mmol). The desired compound was obtained as amorphous white solid (263 mg, 75 %). ^1H NMR (500 MHz, MeOD) δ = 4.11 (dtd, *J* = 8.1, 6.2, 3.9 Hz, 1H, NCH_2CHCH_2), 3.09 (dd, *J* = 12.5, 3.8 Hz, 1H, NCH_2CHCH_2), 3.02 – 2.93 (m, 3H, NCH_2CHCH_2, $NCH_2CH_2CH_2CH_3$), 2.46 (dd, *J* = 15.6, 6.2 Hz, 1H, $COOHCH_2$), 2.42 (dd, *J* = 15.6, 6.2 Hz, 1H, $COOHCH_2$), 1.75 – 1.54 (m, 2H, $NCH_2CH_2CH_2CH_3$), 1.43 (m, 2H, $NCH_2CH_2CH_2CH_3$), 0.99 (t, *J* = 7.4 Hz, 3H, $NCH_2CH_2CH_2CH_3$) ppm; ^{13}C NMR (126 MHz, MeOD) δ = 178.65 (*C*OOH), 65.91(OH*C*H), 53.90 ($OHCHCH_2N$) 49.17 ($NCH_2CH_2CH_2CH_3$), 43.92 ($COOHCH_2$), 29.40 ($NCH_2CH_2CH_2CH_3$), 20.89 ($NCH_2CH_2CH_2CH_3$), 13.91 ($NCH_2CH_2CH_2CH_3$)

ppm; IR (KBr): ṽ= 3223, 1629, 1564, 1359, 1251, 1074 cm^{-1}; HRESIMS *m/z* (pos): 176.1280 $C_8H_{18}NO_3$ (calcd. 176.1287).

Methyl 4-(1,3-dioxoisoindolin-2-yl)-3-hydroxybutanoate (**15c**): GP5a was followed using 4-amino-3-hydroxybutanoic acid **15a** (1.25 g, 10.3 mmol), phthalic anhydride (1.56 g, 10.3 mmol), MeOH (80.0 ml) and 2M HCl in Et_2O (80.0 ml). The desired compound was obtained as amorphous white solid (2.00 g, 74 %). ^{1}H NMR (500 MHz, $CDCL_3$) δ = 7.83 – 7.91 (m, 2H, $NCOC_{ar}CH_{ar}CH_{ar}$), 7.80 – 7.70 (m, 2H, $NCOC_{ar}CH_{ar}CH_{ar}$), 4.37 (ddq, J = 8.56, 7.11, 4.53, 4.49 Hz, 1H, NCH_2CHCH_2), 3.89 (dd, *J* = 14.1, 7.1 Hz, 1H, NCH_2CHCH_2), 3.79 (dd, *J* = 14.1, 4.5 Hz, 1H, NCH_2CHCH_2), 3.72 (s, 3H, OCH_3), 3.20 (d, *J* = 5.1 Hz, 1H, O*H*), 2.61 (dd, *J* = 16.5, 4.0 Hz, 1H, NCH_2CHCH_2), 2.53 (dd, *J* = 16.5, 8.3 Hz, 1H, NCH_2CHCH_2) ppm; ^{13}C NMR (126 MHz, $CDCl_3$) δ = 172.36 ($COOCH_3$), 168.74 (N*C*O), 134.32 ($NCOC_{ar}CH_{ar}CH_{ar}$), 132.06 ($NCOC_{ar}CH_{ar}CH_{ar}$), 123.63 ($NCOC_{ar}CH_{ar}CH_{ar}$), 66.78 (NCH_2CHCH_2), 52.10 (OCH_3), 43.04 (NCH_2CHCH_2), 38.95 (NCH_2CHCH_2) ppm; IR (KBr): ṽ = 3450, 1773, 1700, 1610, 1395, 1206, 1024, 717 cm^{-1}; HRESIMS *m/z* (pos): 286.0687 $C_{13}H_{13}NO_5Na$ (calcd. 286.0691).

Methyl 3-{2-[(tert-butyldiphenylsilyl)oxy]ethoxy}-4-{-(1,3-dioxoisoindolin-2-yl})butanoate (**15d**): GP6 was followed using **15c** (369 mg, 1.20 mmol), *tert*-butyl(2-iodoethoxy)diphenylsilane (662 mg, 1.68 mmol), Ag_2CO_3 (1.32 g, 4.80 mmol), toluene (15 ml), 4d. The desired compound was obtained as a yellow oil (537 mg, 82.0%). ^{1}H NMR (500 MHz, $CDCl_3$) δ = 7.83-7.77 (m, 2H, $NCOC_{ar}CH_{ar}CH_{ar}$), 7.73 – 7.68 (m, 2H, $NCOC_{ar}CH_{ar}CH_{ar}$), 7.67 – 7.62 (m, 4H, CH_{ar}), 7.43 – 7.32 (m, 6H, CH_{ar}), 4.14 (dq, *J* = 7.4, 5.5 Hz, 1H, NCH_2CHCH_2), 3.90 – 3.84 (m, 2H, NCH_2CHCH_2), 3.78 (dt, J = 9.7, 4.9 Hz, 1H, OCH_2CH_2Si), 3.75 – 3.71 (m, 2H, OCH_2CH_2Si), 3.66 (dt, *J* = 9.6, 4.5 Hz, 1H, OCH_2CH_2Si), 3.61 (s, 3H, OCH_3), 2.60 (dd, *J* = 16.1, 7.5 Hz, 1H, NCH_2CHCH_2), 2.55 (dd, *J* = 16.1, 5.5 Hz, 1H, NCH_2CHCH_2), 1.00 (s, 9H ppm, $SiCCH_3$)ppm; ^{13}C NMR (126 MHz, $CDCl_3$) δ = 171.50 ($COOCH_3$), 168.42 (N*C*O), 135.73 (C_{ar}), 134.13(C_{ar}), 133.77(C_{ar}), 132.12(C_{ar}), 129.68 (C_{ar}), 127.73 (C_{ar}), 123.48 (C_{ar}), 74.50 (NCH_2CHCH_2), 71.45 ($OCH_2CH2OSi$, 63.46 (OCH_2CH_2Si), 51.82 (OCH_3), 40.30 (NCH_2CHCH_2), 38.61(NCH_2CHCH_2), 26.88 ($SiCCH_3$), 19.26 (Si*C*) ppm; IR (Film): ṽ=2932, 1774, 1770, 1469, 1428, 1396, 1361, 1281, 1192, 1112, 823, 738 cm^{-1}; HRESIMS *m/z* (pos): 568.2132 $C_{31}H_{35}NO_6SiNa$ (calcd. 568.2131).

Methyl 4-(1,3-dioxoisoindolin-2-yl)-3-(2-hydroxyethoxy)butanoate (**15e**): GP7 was followed using **15d** (442 mg, 0.81 mmol), THF/pyridine 9:1 (10.0 ml), HF-pyridine (116 mg, 4.05 mmol). The desired compound was obtained as yellow oil (206 mg, 83 %). ^{1}H NMR (500 MHz, CD_2Cl_2) δ = 7.92 – 7.80 (m, 2H, $NCOC_{ar}CH_{ar}CH_{ar}$), 7.80 – 7.71 (m, 2H, $NCOC_{ar}CH_{ar}CH_{ar}$), 4.10 (dq, *J* = 9.0, 4.5 Hz, 1H, NCH_2CHCH_2), 3.87 (dd, *J* = 14.3, 4.9 Hz, 1H, NCH_2CHCH_2), 3.80 (dd, *J* = 14.3, 4.5 Hz, 1H, NCH_2CHCH_2), 3.73 (ddd, *J* = 10.3, 5.9, 3.1 Hz, 1H, OCH_2CH_2OH), 3,66 (s, 3H, OCH_3), 3.65 (ddd, J = 10.3, 5.9, 2.8 Hz, 1H, OCH_2CH_2OH), 3.60 (ddd, *J* = 12.3, 6.1, 2.8 Hz, 1H, OCH_2CH_2OH), 3.56 (ddd, J = 12.2, 6.0, 3.0, 1H, OCH_2CH_2OH), 2.76 (t, *J* = 6.3 Hz, 1H, O*H*), 2.59 (dd, *J* = 16.4, 4.3 Hz, 1H, NCH_2CHCH_2), 2.52 (dd, *J* = 16.4, 8.7 Hz, 1H, NCH_2CHCH_2) ppm; ^{13}C NMR (126 MHz, CD_2Cl_2) δ = 172.31 ($COOCH_3$, 169.10 (NCO), 134.74 ($NCOCarCHarCH_{rar}$), 132.51 ($NCOC_{ar}CH_{ar}CH_{ar}$), 123.82 ($NCOC_{ar}CH_{ar}CH_{ar}$), 75.27 (NCH_2CHCH_2), 72.58 (OCH_2CH_2OH), 62.27 (OCH_2CH_2OH), 52.29 (OCH_3), 40.86 (NCH_2CHCH_2), 38.60 (NCH_2CHCH_2) ppm; IR (Film): ṽ=3472, 2951, 1773, 1770, 1467, 1397, 112, 725 cm^{-1}; HRESIMS *m/z* (pos): 330.0949 $C_{15}H_{17}NO_6Na$ (calcd. 330.0954).

Methyl 4-{1,3-dioxoisoindolin-2-yl}-3-{2-[tris(4-methoxyphenyl)methoxy]ethoxy}butanoate (**15f**): GP8 was followed using **15e** (338 mg, 1.10 mmol), DMF (1 drop), pyridine (4.0 ml), 4,4`,4``-trimethoxytrithyl chloride (753 mg, 1.98 mmol). The desired compound was obtained as yellow oil (520 mg, 74 %). ^{1}H NMR (400 MHz, CD_2Cl_2) δ = 7.89 – 7.76 (m, 2H, $NCOC_{ar}CH_{ar}CH_{ar}$), 7.76 – 7.65 (m, 2H, $NCOC_{ar}CH_{ar}CH_{ar}$), 7.32 – 7.18 (m, 6H, $CH_3OC_{ar}CH_{ar}CH_{ar}$), 6.86 – 6.72 (m, 6H, $CH_3OC_{ar}CH_{ar}CH_{ar}$), 4.13 (dq, *J* = 7.2, 5.6 Hz, 1H, NCH_2CHH_2), 3.89 (dd, *J* = 14.1, 5.5 Hz, 1H, NCH_2CHCH_2), 3.81 (dd, *J* = 14.0, 5.7 Hz, 1H, NCH_2CHH_2), 3.77 (s, 9H, $C_{ar}OCH_3$), 3.76 (ddd, J = 10.2, 5.6, 4.4 Hz, 1H, $OCH_2CH_2OCC_{ar}$), 3.64 (ddd, J = 10.2, 5.6, 4.5 Hz, 1H, $OCH_2CH_2OCC_{ar}$), 3.59 (s, 3H, $COOCH_3$), 3.10 (ddd, J = 12.2, 5.6, 4.3 Hz, 1H, $OCH_2CH_2OCC_{ar}$), 3.07 (ddd, J = 12.2, 5.6, 4.2 Hz, 1H, $OCH_2CH_2OCC_{ar}$), 2.62 (dd, J = 16.0, 7.1 Hz, 1H, NCH_2CHCH_2), 2.56 (dd, J = 16.0, 5.4 Hz, 1H, NCH_2CHCH_2) ppm; ^{13}C NMR (101 MHz, CD_2Cl_2) δ = 171.78 ($COOCH_3$), 168.78 (NCO), 158.94 (CH_3OC_{ar}), 137.38 ($CC_{ar}CH_{ar}$), 134.56 ($NCOC_{ar}CH_{ar}CH_{ar}$), 132.59 ($NCOC_{ar}$), 130.25 ($CH_3OC_{ar}CH_{ar}CH_{ar}$), 123.72 ($NCOC_{ar}CH_{ar}CH_{ar}$), 113.49 ($CH_3OC_{ar}CH_{ar}CH_{ar}$), 86.09 ($CC_{ar}CH_{ar}CH_{ar}$), 75.13 ($NCH_2CHCH_2$), 70.33 ($OCH_2CH_2OCC_{ar}$), 63.72 ($OCH_2CH_2OCC_{ar}$), 55.73 ($C_{ar}OCH_3$), 52.14 ($COOCH_3$), 40.97 ($NCH_2CHCH_2$), 38.89 ($NCH_2CHCH_2$) ppm; IR (Film): ṽ=1773, 1607, 1507, 1396, 1249, 1175, 1033, 828 cm^{-1}; HRESIMS *m/z* (pos): 662.2365 $C_{37}H_{37}NO_9Na$ (calcd. 662.2366).

4-Amino-3-{2-[tris(4-methoxyphenyl)methoxy]ethoxy}butanoic acid (**15g**): GP9b was followed using **15f** (141 mg, 0.220 mmol), MeOH (3.0 ml), 12M NaOH (0.05 ml), 1,2-diaminoethane (92,6 mg, 1.54 mmol). The desired compound was obtained as amorphous white solid (75 mg, 69 %). ^{1}H NMR (400 MHz, 0.1 M NaOD/MeOD) δ = 7.36 – 7.21 (m, 6H, $CH_3OC_{ar}CH_{ar}CH_{ar}$), 6.90 – 6.69 (m, 6H, $CH_3OC_{ar}CH_{ar}CH_{ar}$), 3.82-3.72 (m, 11H, CH_2CHCH_2, OCH_3, $CHOCH_2CH_2OC$), 3.63 (ddd, *J* = 10.35, 6.16, 3.94 Hz, 1H, $CHOCH_2CH_2OC$), 3.28 – 3.09 (m, 2H, $CHOCH_2CH_2OC$), 2.81 (dd, *J* = 13.4, 3.5 Hz, 1H, NCH_2CHCH_2), 2.64 (dd, *J* = 13.4, 7.2 Hz, 1H, NCH_2CHCH_2), 2.51 (dd, *J* = 14.2, 6.1 Hz, 1H, NCH_2CHCH_2), 2.25 (dd, *J* = 14.2, 7.3 Hz, 1H, NCH_2CHCH_2) ppm; ^{13}C NMR (101 MHz, 0.1 M NaOD/ MeOD) δ = 180.20 (*C*OOH), 159.81 ($CC_{ar}CH_{ar}CH_{ar}COCH_3$), 138.03 ($CC_{ar}CH_{ar}CH_{ar}COCH_3$), 130.93 ($CC_{ar}CH_{ar}CH_{ar}COCH_3$), 114.07 ($CC_{ar}CH_{ar}CH_{ar}COCH_3$), 87.11 ($CC_{ar}CH_{ar}CH_{ar}COCH_3$), 80.75 ($NCH_2CHCH_2$), 70.09 ($CHOCH_2CH_2C$), 64.62 ($CHOCH_2CH_2C$), 55.95 (, OCH_3), 46.18 (NCH_2CH), 42.21 (NCH_2CHCH_2) ppm; IR (KBr): ṽ= 3375, 1606, 1505, 1463, 1249, 1175, 1034, 828, 735 cm^{-1}; HRESIMS *m/z* (neg): 494.2196 $C_{28}H_{33}NO_7$ (calcd. 494.2184).

Biological evaluation

[^{3}H]GABA uptake assays: The [^{3}H]GABA uptake assays were performed in a 96-well plate format with intact HEK293 cells expressing mGAT1, mGAT2, mGAT3 and mGAT4, respectively.

MS Binding Assays: The MS Binding Assays were performed with mGAT1 membrane preparations obtained from a stable HEK293 cell line and NO711 as unlabeled marker in competitive binding experiments.

3. Results and Discussion

3.1 Synthesis

Synthesis of the cyclic N-butylamino acid derivatives

For the synthesis of the cyclic N-butylhydroxyamino acids **11d**, **11g**, **12g** and **13d** we intended to start from the benzyl- or benzhydryl-protected cyclic aminoketones **11a**, **12a** and **13a**, respectively. Reaction of **11a** and **13a** with tetramethylsilyl cyanide followed by acidic hydrolysis of the thus to be formed TMS-protected cyanohydrines should furnish the

corresponding α-hydroxycarboxamides **11b** and **13b**. Likewise, reaction of the cyclic aminoketones **11a** and **12a** with lithium 1-ethoxyethen-1-olate should lead to the β-hydroxyesters **11e** and **12e**. Deprotection of the amino nitrogen atom of **11b**, **11e**, **12e** and **13b**, followed by introduction of a n-butyl rest via reductive amination and hydrolysis of the carboxamide and ester function, respectively, should finally furnish the desired free amino acids **11d**, **11g**, **12g** and **13d**.

Synthesis of the cyclic α-hydroxycarboxamide **11b** was performed according to literature (Lamb 2008). The same reaction sequence was applied for the synthesis of its ring-expanded analogue **13b**. Hence, the N-benzylpyrrolid-3-one **13a** was reacted with trimethylsilyl cyanide to give the respective TMS-protected cyanohydrine. Due to the lability of the TMS ether function, the TMS-protected cyanohydrine was not purified and characterized, but used for the next reaction step, the hydrolysis with concentrated sulfuric acid. This gave the corresponding α-hydroxycarboxmide **13b** in an excellent yield of 96 % over both reaction steps. The β-hydroxyesters **11e** and **12e** were obtained in good yields of 80-93 % from the cyclic-aminoketones **11a** and **12a** by reaction with lithium 1-ethoxyethen-1-olate, which was generated from ethyl acetate and LiHMDS at low temperature (scheme 3).

Next, the carboxamide and ester derivatives **11b**, **11e**, **12e** and **13b** were subjected to deprotection of the nitrogen atom and subsequent n-butylation, accomplished in a single reaction step by exposing the compounds to hydrogen (10 bar) in presence of palladium on cabon and 2.0 - 2.4 equivalents of n-butyraldehyde. This furnished the respective N-butyl derivatives **11c**, **11f**, **12f** and **13c** in yields of 77 – 93 %. Finally, after basic hydrolysis and workup (barium hydroxide, carbon dioxide workup), the free amino acids **11d**, **11g**, **12g** and **13d** were hence obtained in yields of 87 – 96 % (scheme 3).

Scheme 3. *Synthesis of the cyclic hydroxyamino acids* ***11d, 11g, 12d*** *and* ***13d****.*

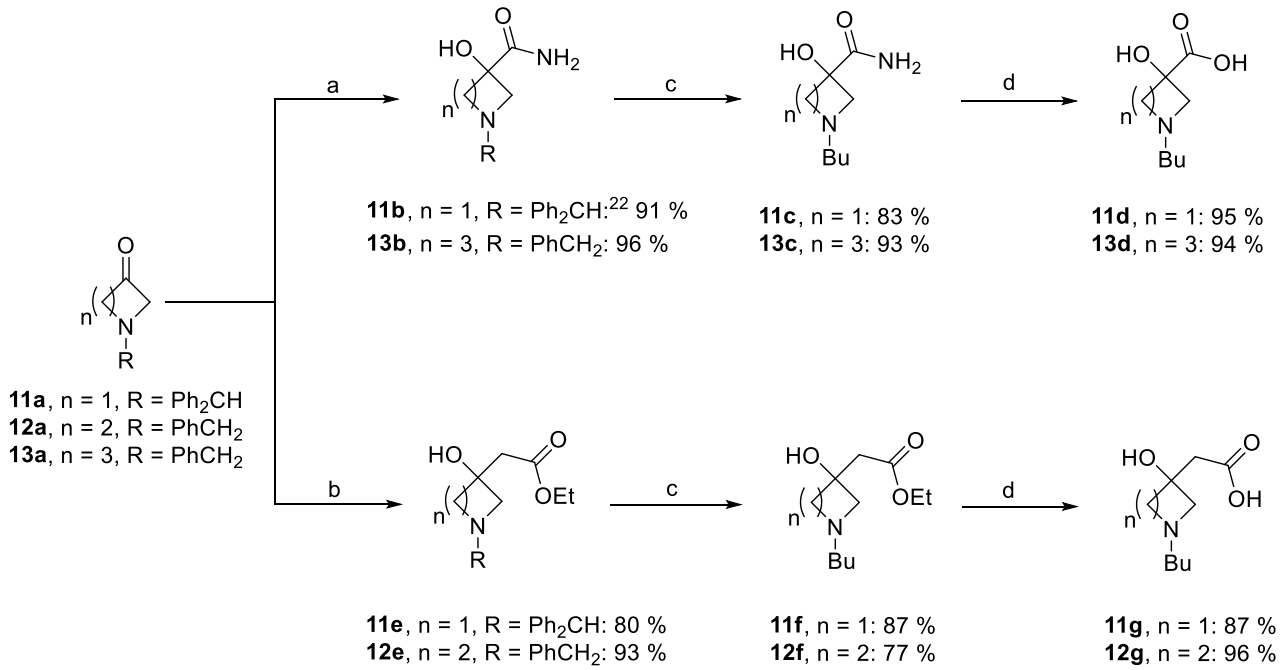

Reagents and conditions: (a) 1. Trimethylsilyl cyanide (2.5 eq), dichloromethane, rt, 48h; 2. sulfuric acid (5.2 eq), dichloromethane, 0°C - rt, 2h. (b) 1. LiHMDS (1.0 eq), ethylacetate (1.0 eq), methyl *tert*-butyl ether, -78°C, 25min, 2. **11a**/**12a**, THF, -78°C to -10°C. (c) H_2 (10 bar), n-butyraldehyde (2.5 eq), 10% palladium on charcoal (0.1 eq), rt, 16h; (d) barium hydroxide octahydrate (2.0 – 2.4 eq), ethanol/water 1:1, rt or reflux.

Synthesis of the acyclic N-butyl amino acid derivatives

For the synthesis of the N-butyl derivatives **7b**, **14b** and **15b** from the cyclic hydroxyamino acids **7a**, **14a** and **15a**, a specialised procedure developed for the monobutylation of β-alanine (Santimukul and Perez, 2011) was followed. When according to this procedure **7a**, **14a** and **15a** were treated with n-bromobutane in a mixture of methanol and water under reflux the desired test compounds **7b**, **14b** and **15b** were obtained in yields of 75-79% (scheme 4).

Scheme 4. *N-Butylation of the acyclic hydroxyamino acids* ***7a, 14a*** *and* ***15a****, furnishing* ***7b, 14b*** *and* ***15b****.*

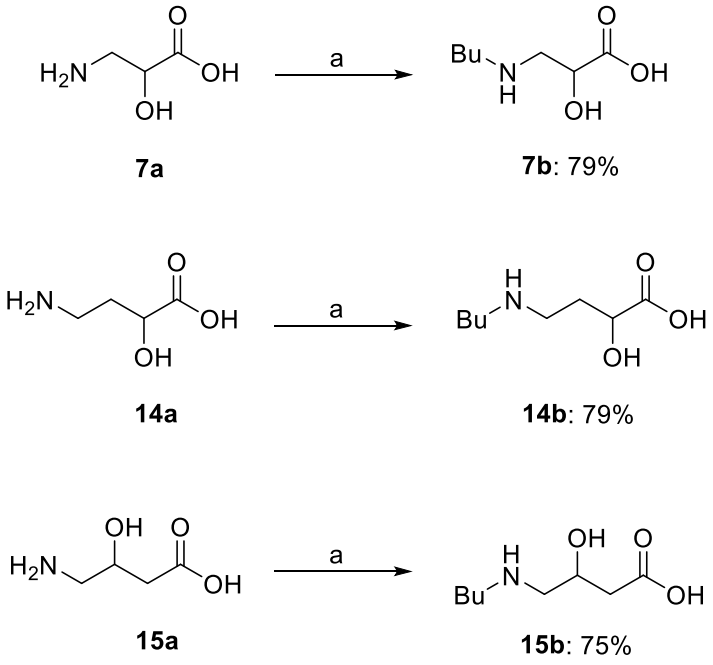

Reagents and conditions: (a) bromobutane (0.9 eq), potassium hydroxide (2.0 eq), methanol/water, reflux.

Synthesis of O-alkylated hydroxy amino acid derivatives

Since the unsubstituted hydroxyamino acids **7a**, **14a** and **15a** had been found to exhibit higher inhibitory potencies at all GAT subtypes than the corresponding N-butyl derivatives **7b**, **14b** and **15b** (see chapter 3 "biological evaluation, table 3), also the respective amino acid derivatives with an tris(4-methoxyphenyl)methyloxyethyl attached to the hydroxy function of the parent compounds should be included in this study.

As starting compounds for this synthesis of the target compounds **7g**, **14g** and **15g**, the derivatives **7c**, **14c** and **15c** seemed well suited, as they should allow a selective functionalization of the OH group as the carboxylic acid and the amino moieties in **7g**, **14g** and **15g** are protected in form of ester and phthalimidic moieties, respectively. The preparation of **14c** has been described in literature (Farkas et al., 2009), the synthesis of **7c** and **15c** should be accomplished in an analogous manner. Based on these starting materials, **7c**, **14c** and **15c**, in the next steps first a 2-hydroxyethyl residue should be attached to the free OH function to serve as linker to the lipophilic domain of the target compound. The

trityl based lipophilic moiety should be introduced only after that, as the reaction conditions required for the formation of the first ether function were thought to cause side reactions if the terminal trityl moiety were already present. Deprotection of the carboxylic acid and the amino group in **7f**, **14f** and **15f** should finally lead to the target compounds **7g**, **14g** and **15g**.

The synthesis of **14c** was accomplished according to literature(Farkas et al., 2009) by first reacting **14a** with phthalic anhydride to protect the terminal amino group as phthalimide moiety, followed by etherification of the carboxyl group to give the corresponding carboxylic acid ester, the overall product being **14c**. Applying the same procedure to **7a** and **15a**, the analogous compounds **7c** and **15c** could be obtained in yields of 73% (**7c**) and 72% (**15c**).

Scheme 5. *Synthesis of the protected amino acid derivatives **7c**, **14c** and **15c**.*

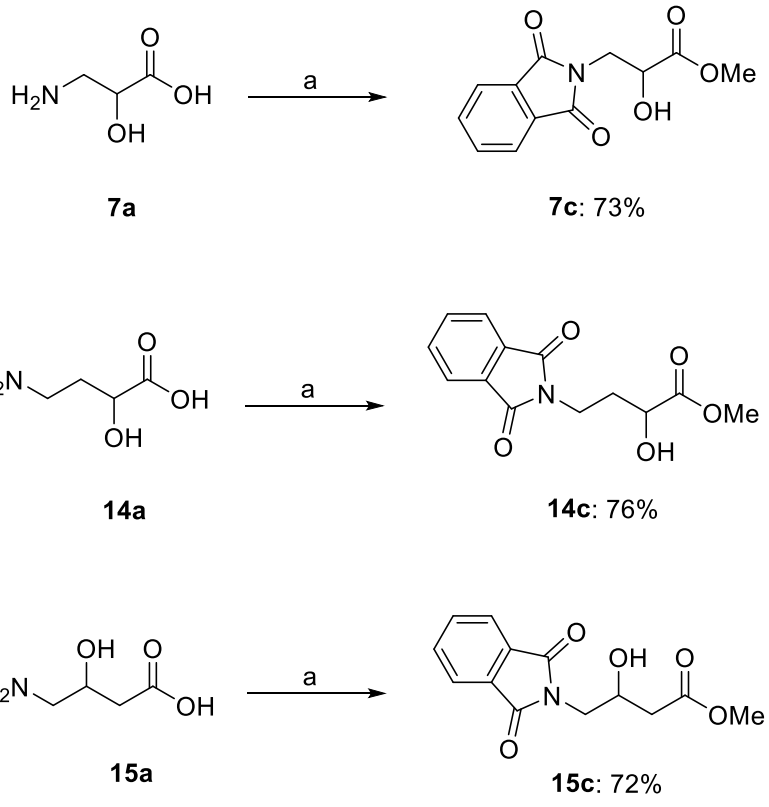

Reagents and conditions: (a) 1. Phthalic anhydride (1.0 eq), 140°C, 30 min; 2. MeOH, HCl, rt, 16h.

The required hydroxylethylation of the OH function could be realized by treatment of **7c**, **14c** and **15c** with 2-iodoethoxy-TBDPS in the presence of Ag_2CO_3 furnishing the corresponding ethers **7d**, **14d** and **15d** in good yields of 76 - 82%. Removal of the TBDPS protecting group by treatment with HF-pyridine yielded in the free alcohols **7e**, **14e** and **15e** (76 - 84%), which upon reaction with 4,4´,4´´-trimethoxytrityl chloride, gave the trityl derivatives **7f**, **14f** and **15f** (74 - 90%, scheme 6).

The final deprotection of the amino and the carboxylic acid function of **7f**, **14f** and **15f** in order to obtain the free amino acids **7g**, **14g** and **15g** was first attempted in a two-step reaction sequence. Hydrazinolysis of the phthalimide moiety should liberate the terminal amino group, and subsequently hydrolysis of the methyl ester function under alkaline conditions (NaOH) the carboxylic acid moiety . Unfortunately, when the primary amine was formed in the first reaction step, it immediately reacted with the methyl ester function leading to the formation of the corresponding lactame, which could not be cleaved again without destruction of the molecule. Hence, the sequence of the deprotection was altered applying first NaOH to hydrolyse the methyl ester function. Thereby, also the phthaloyl group protecting the amino function was partially cleaved leading to the corresponding phthalamide moieties. Still,the free amino acids **7g**, **14g** and **15g** could be obtained by subjecting the thus obtained crude reaction product without prior isolation to heating with 1,2-diaminoethane. This furnished the desired target compounds **7g**, **14g** and **15g** in yields of 69-83% over both reaction steps (scheme 6).

Scheme 6. *Synthesis of acyclic amino acid derivatives comprising a 4,4´,4´´-trimethoxytrityl moiety, which is linked to the 2- or 3-position of the carbon chain via an OCH_2CH_2O spacer (**7g**, **14g** and **15g**).*

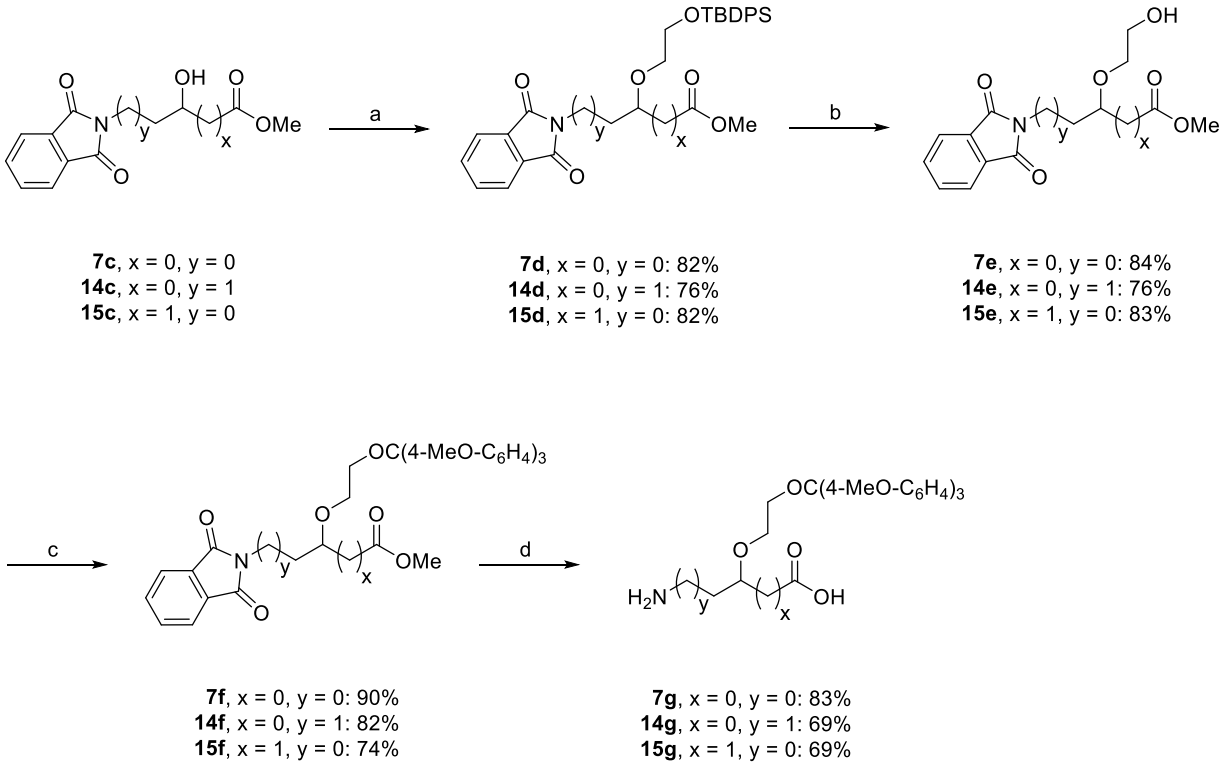

7c, x = 0, y = 0
14c, x = 0, y = 1
15c, x = 1, y = 0

7d, x = 0, y = 0: 82%
14d, x = 0, y = 1: 76%
15d, x = 1, y = 0: 82%

7e, x = 0, y = 0: 84%
14e, x = 0, y = 1: 76%
15e, x = 1, y = 0: 83%

7f, x = 0, y = 0: 90%
14f, x = 0, y = 1: 82%
15f, x = 1, y = 0: 74%

7g, x = 0, y = 0: 83%
14g, x = 0, y = 1: 69%
15g, x = 1, y = 0: 69%

Reagents and conditions: (a) Ag_2CO_3 (4.0 eq), 2-iodoethoxy-TBDPS (1.4 eq), toluene, reflux; (b) HF-Pyridine (5.0 eq), tetrahydrofurane, 0°C-rt; (c) 4,4´,4´´-trimethoxytrityl chloride (1.8 eq.), pyridine/DMF, rt; (d) 1. 1M NaOH (2.0 eq), MeOH, rt; 2. ethylenediamine (7.0 eq), 140 °C.

3.2 Biological evaluation

The amino acids **7a**, **7b**, **7g**, **11d**, **11g**, **12g**, **13d**, **14a**, **14b**, **14g**, **15a**, **15b**, **15g**, as well as the carboxamide and ester derivatives **11c**, **11f**, **12f** and **13c** were tested for their inhibitory potencies on the four GABA transporter subtypes mGAT1-4 in a [^{3}H]GABA uptake assay previously developed by our group (Kragler et al., 2008) The tests were performed in a standardized manner in triplicates using HEK293 cell lines, each expressing one of the four GAT subtypes. Additionally, binding affinities towards mGAT1 were examined employing a standardized MS Binding Assay with NO711 as native MS marker (Zepperitz et al., 2008). The results are summarized in table 3. Inhibitory potencies and binding affinities of the tested compounds are represented as pIC_{50} and pK_i, respectively. Each test compound was characterized in three independent experiments performed in triplicates and the standard error of mean (SEM) is given. If the determination of the pIC_{50} value proved not feasible due

to low inhibitory potency, as percentage of the remaining [^{3}H]GABA uptake at 100 µM concentration of the test compound. Correspondingly, the percentage of remaining MS marker is given in cases when the tested compound caused only a minor reduction of the MS marker binding.

As can be seen from the data in table 3, the unsubstituted α- and β-hydroxyamino acids **7a**, **14a** and **15a**, which served as the starting material for the synthesis of the N-butyl derivatives **7b**, **14b** and **15b**, exhibit considerable inhibitory activities at most of the GAT subtypes, with the pIC_{50} values ranging from 4.06 ± 0.08 (**15a**, mGAT1, table 3, entry 16) to 4.99 ± 0.08 (**14a**, mGAT1, table 3, entry 13). Only for **7a** at mGAT1 (pIC_{50} = 2.33 ± 0.05, table 3, entry 2) and at mGAT2 (pIC_{50} = 3.38 ± 0.11, table 3, entry 2) and **14a** (pIC_{50} = 3.25 ± 0.02, table 3, entry 13) at mGAT2 distinctly lower pIC_{50} values were found.

As compared to the unsubstituted α- and β-hydroxyamino acids **7a**, **14a** and **15a** the N-butyl derivatives **7b**, **14b** and **15b** are characterized by lower inhibitory activity throughout, which might indicate that the binding pose in which the amino nitrogen atom is oriented towards the cytosol, as postulated by molecular modelling experiments performed by Wein et al. (Wein et al., 2016) is energetically disfavoured. As reported in table 3, entry 3, N-butyl isoserine (**7b**) shows a pIC_{50} value of 3.26 ± 0.10 at mGAT4, which is on par with the value reported for racemic N-butylnipecotic acid **16** (pIC_{50} = 3.32 ± 0.04, table 3, entry 1), which can be considered as a reasonable reference point since nipecotic acid constitutes the amino acid partial structure of many important GAT inhibitors including tiagabin (**4**, table 1, entry 5) and (*S*)-SNAP-5114 (**5**, table 1, entry 6). Interestingly, **7b** exerts a somewhat higher inhibitory potency at mGAT3 (pIC_{50} = 3.54 ± 0.04) than at mGAT4, whereas the activity at mGAT1-2 can be considered negligible ([^{3}H]GABA at 100µM = 101% and 95%, respectively). This selectivity pattern deviates significantly from that of the reference compound **16**, which exerts its highest inhibitory potency at mGAT1 (pIC_{50} = 4.11 ± 0.08) while being less active at mGAT2 (pIC_{50} = 3.23) and mGAT3 ([^{3}H]GABA at 100µM = 81%).

For the homologue of **7b**, compound **14b**, formally derived from **7b** by inserting a methylene group at the end of the carboxyl acid carbon chain, the potency at mGAT4 has decreased distinctly, i.e. to a value below the identification threshold ([^{3}H]GABA at 100µM = 107%, table 3, entry 14). The biological activity at mGAT3 on the other hand is only slightly reduced from 3.54 ± 0.04 for **7b** to 3.21 ± 0.08 for **14b**. The effects exerted at mGAT1 and mGAT2 are

slightly higher as compared to **7b**, with the remaining [^{3}H]GABA uptake for **14b** amounting to 79% (mGAT1) and 59% (mGAT2), respectively.

By contrast, if the elongation of the carbon chain is performed by inserting a methylene group between the carbon carrying the OH function and the carboxylic acid group (**15b**, table 3, entry 17), the pIC_{50} value at mGAT4 increases nominally from 3.26 ± 0.10 for **7b** to 3.42 ± 0.12 for **15b**, while the effect exerted at mGAT3 remains unaltered (**15b**: pIC_{50} = 3.59 ± 0.07, **7b**: pIC_{50} = 3.54 ± 0.04). As is the case with N-butylisoserine (**7b**), **15b** exhibits no determinable inhibition at mGAT1 ([^{3}H]GABA at 100µM = 100%), whereas a slight effect at mGAT2 is found ([^{3}H]GABA at 100µM = 76%).

Unexpectedly, rigidization of the N-butylisoserine (**7b**) molecule by linking the C-2 atom with the nitrogen atom via a methylene bridge, resulting in azetidine heterocycle **11d**, leads to a compound which exerts its highest inhibitory potency at mGAT2 (pIC_{50} = 3.38 ± 0.08, table 3, entry 6). At the same time the effects of **11d** at the other GATs are minor, the [^{3}H]GABA uptake amounting to 72% (mGAT3), 85% (mGAT4) and 89% (mGAT1). Formal enlargement of the azetidine ring present in **11d** to a piperidine ring causes the inhibitory potency at mGAT2 to completely vanish (**13d**, [^{3}H]GABA at 100µM = 104 %, table 3, entry 12). In addition, the activity exerted at the other GAT subtypes is extremely low, the values for the remaining [^{3}H]GABA uptake at 100µM being 96% (mGAT1), 85% (mGAT3) and 91% (mGAT4), respectively. As compared to its desoxy analogoue N-butylnipecotic acid (**16**, table 3, entry 1), this constitutes a distinct decline of inhibitory potency at all GATs, hence demonstrating that the introduction of a hydroxy group into the 3-position of the nipecotic acid scaffold is associated with a strong reduction of biological activity.

11c and **13c**, the carboxamide derivatives of the cyclic N-butyl-α-hydroxyamino acids **11d** and **13d**, were also tested for their inhibitory potential at all GAT subtypes. **11c**, comprising an azetidine heterocyle, is characterized by marginal or non-detectable inhibitory potencies (table 3, entry 5), the values of the remaining [^{3}H]GABA uptake at 100µM test compound concentration ranging from 83% (mGAT1) to nominally 105% (mGAT2). Likewise, **13c** (table 3, entry 11), which features a piperidine ring, reduces the [^{3}H]GABA uptake to 84% (mGAT2), 79% (mGAT3) and 90% (mGAT4), whereas it appears to be completely inactive at mGAT1 at 100µM, the [^{3}H]GABA uptake amounting nominally to 109%.

Exhibiting pIC_{50} values of 3.59 ± 0.07 at mGAT3 and 3.42 ± 0.12 at mGAT4, **15b** showed the highest inhibitory activity of the tested open-chain N-butylhydroxyamino acids (table 3, entry 17). Hence, analogues of **15b** that have the structure of the molecule rigidized by integrating the amino nitrogen atom and parts of the carbon chain into an azetidine (**11g**) and pyrrolidine ring (**12g**), respectively, seem of interest. However, **11g** was found to exert only minor inhibitory potency at mGAT1-3, with the values for the remaining [^{3}H]GABA uptake at 100µM lying between 78% (mGAT2) and 80% (mGAT3) and the inhibitory potency at mGAT4 being negligible ([^{3}H]GABA uptake at 100µM = 99%, table 3, entry 8). By contrast, the open chain analogue **15b** exerted reasonable inhibitory potencies at mGAT3 (pIC_{50} = 3.59 ± 0.07, table 3, entry 17) and at mGAT4 (pIC_{50} = 3.42 ± 0.12).

Linking the C-3 atom and the amino nitrogen atom of **15b** via a C_2-bridge, resulting in a pyrrolidine substructure, is likewise accompanied by a complete loss of inhibitory potency at mGAT3-4, the values for the remaining [^{3}H]GABA uptake being nominally 103% and 105%, respectively (**12g**, table 3, entry 10). However, the compound exerts some activity at mGAT2 (pIC_{50} = 3.17). For mGAT1, a value of 94% remaining GABA uptake at 100µM was determined, which is consistent with the parent compound **15b** not showing any effect at this subtype (**15b**, remaining [^{3}H]GABA uptake = 100%, table 3, entry 17).

11f and **12f**, the ester derivatives of the cyclic amino acids **11g** and **12g**, were also tested for their inhibitory potency at mGAT1-4. As shown in table 3, entry 7, the azetidine derivative **11f** exhibits some activity at mGAT1 (remaining [^{3}H]GABA uptake = 66%), whereas the effect at mGAT2-4 is less pronounced (91%, 82% and 88%, respectively). **12f** (table 3, entry 9), which is the ester derivative of **12g**, is characterized by minor or negligible inhibitory activity at all GAT subtypes, the values of the remaining [^{3}H]GABA uptake being 104% (mGAT1), 96% (mGAT2), 86% (mGAT3) and 71% (mGAT4), respectively.

Since both the cyclic and acyclic N-butyl derivatives of **7a**, **14a** and **15a** were found to exhibit distinctly lower inhibitory potencies than the parent compounds consistently, derivatives of **7a**, **14a** and **15a** were synthesized which have the alcohol function linked to a C_2 spacer bearing a 4,4´,4´´-trimethoxytrityloxy moiety. In theory, this would allow the amino acid subunit to keep the more favorable orientation towards the intracellular space, while at the same time enabling interactions between the lipophilic domain and the extracellular vestibule, which are thought to significantly increase inhibitory potency and selectivity in

case of nipecotic acid derivatives such as (*S*)-SNAP-5114 (**5**, table 1, entry 6). Unfortunately, the introduction of the lipophilic domain into the scaffold of **7a**, **14a** and **15a** caused a reduction of inhibitory potency. For the derivatives resulting from this modification (**7g**, **14g** and **15g**) the values for the [^{3}H]GABA uptake at 100µM test compound concentration remained at > 50% at all transporter subtypes, equating to pIC_{50} values < 4.0. Moreover, **7g** and **15g** were found to display only negligible subtype selectivity. In particular, **7g** reduced the [^{3}H]GABA uptake to 63% (mGAT1), 57% (mGAT2), 63% (mGAT3) and 60% (mGAT4), respectively (table 3, entry 4). Likewise, the remaining [^{3}H]GABA uptake in presence of 100µM **15g** ranged from 54% (mGAT3) to 67% (mGAT1 and mGAT2). For mGAT4, a pIC_{50} value just short below 4.0 was determined (pIC_{50} = 3.95, table 3, entry 18). **14g** (table 3, entry 15) was found to reduce the [^{3}H]GABA uptake to 78% (mGAT1), 66% (mGAT2), 94% (mGAT3) and 73% (mGAT4), respectively.

For all test substances the binding affinities at mGAT1 were found to be very low as compared to the reference compound **16** (pK_i = 3.36 ± 0.02, table 3, entry 1), the only exception being **14a** (pK_i = 3.61 ± 0.05, table 3, entry 11).

Table 3. *Results of the biological evaluation.*

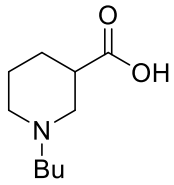

16

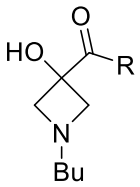

11c, R = NH_2
11d, R = OH

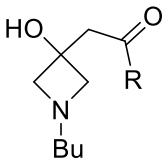

11f, R = OEt
11g, R = OH

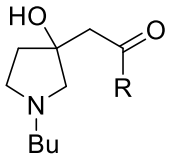

12f, R = OEt
12g, R = OH

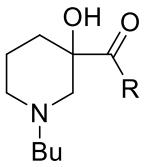

13c, R = NH_2
13d, R = OH

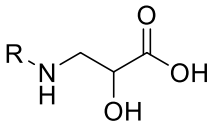

7a, R = H
7b, R = Bu

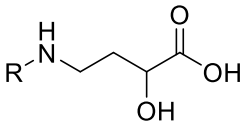

14a, R = H
14b, R = Bu

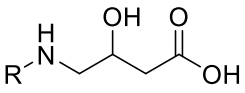

15a, R = H
15b, R = Bu

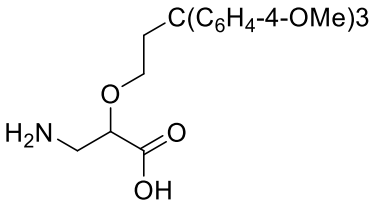

7g

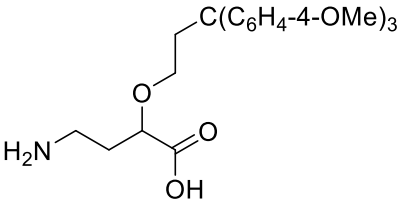

14g

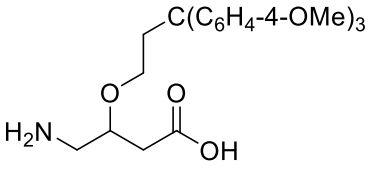

15g

entry	compound	binding affinity (pK_i ± SEM)[a]	GABA uptake inhibition (pIC_{50} ± SEM)[b]			
			mGAT1	mGAT2	mGAT3	mGAT4
1	**16**	3.36 ± 0.02	4.11 ± 0.08	3.23	81%	3.32 ± 0.04
2	**7a**	2.43 ± 0.03	2.33 ± 0.05	3.38 ± 0.11	4.87 ± 0.05	4.78 ± 0.14
3	**7b**	86 %	101 %	92 %	3.54 ± 0.04	3.26 ± 0.10
4	**7g**	85 %	63 %	57 %	63 %	60 %
5	**11c**	101 %	83 %	105 %	92 %	96 %
6	**11d**	97 %	89 %	3.38 ± 0.08	72 %	85 %
7	**11f**	106 %	66 %	91 %	82 %	88 %
8	**11g**	93 %	79 %	78 %	80 %	99 %

Table 3 *(continued).*

entry	compound	binding affinity (pK_i ± SEM)[a]	GABA uptake inhibition (pIC_{50} ± SEM)[b]			
			mGAT1	mGAT2	mGAT3	mGAT4
9	**12f**	88 %	104 %	96 %	86 %	71 %
10	**12g**	93 %	94 %	3.17	103 %	105 %
11	**13c**	103 %	109 %	84 %	79 %	90 %
12	**13d**	97 %	96 %	104 %	85 %	91 %
13	**14a**	3.61 ± 0.05	4.99 ± 0.08	3.25 ± 0.02	4.73 ± 0.10	4.64 ± 0.03
14	**14b**	107 %	79 %	59 %	3.21 ± 0.08	107 %
15	**14g**	61 %	78 %	66 %	94 %	73 %
16	**15a**	2.31	4.06 ± 0.08	4.19 ± 0.01	4.41 ± 0.09	4.37 ± 0.14
17	**15b**	94 %	100 %	76 %	3.59 ± 0.07	3.42 ± 0.12
18	**15g**	74 %	67 %	67 %	54 %	3.95

(a) Results of the MS Binding Assays are given as pK_i ± SEM. Percent values represent remaining specific NO711 binding in presence of 100 µM test compound. (b) Results of the [^{3}H]GABA uptake assays are given as pIC_{50} ± SEM. Percent values represent remaining [^{3}H]GABA uptake in presence of 100 µM test compound.

4. Conclusion

A series of cyclic and acyclic hydroxyamino acid derivatives was synthesized and biologically evaluated for their potential as amino acid subunits in GAT inhibitors. According to molecular modelling experiments performed by Wein et al. (Wein et al., 2016), unsubstituted amino acids assume a binding pose at mGAT1 which is characterized by the amino nitrogen atom being orientated towards the cytosol. However, if a lipophilic rest is introduced at the nitrogen atom, as is the case with GAT inhibitors such as Tiagabine (**4**) or, this binding pose is altered, with the nitrogen atom facing towards the extracellular space which is thought to be also true for mGAT4 inhibitors like (*S*)-SNAP-5114 (**5**). As a butyl moiety is known to be sufficient to effect this change of the binding pose for mGAT1 ligands, the N-butyl derivatives of the respective amino acids were of particular interest.

Whereas the cyclic and hence more rigid N-butylhydroxyamino acids displayed only weak inhibitory potency at mGAT3 and mGAT4, moderate activity was observed in case of some acyclic compounds tested for this study. In particular, 4-(butylamino)-3-hydroxybutanoic acid

(pIC_{50} = 3.42 ± 0.12) and N-butyl isoserine (pIC_{50} = 3.26 ± 0.10) were found to be equal to N-butylnipecotic acid (pIC_{50} = 3.32) in terms of inhibitory potency at mGAT4, while being distinctly stronger mGAT3 inhibitors with the pIC_{50} values amounting to 3.59 ± 0.07 and 3.54 ± 0.04, respectively,*N*-butylnipecotic acid: [^{3}H]GABA uptake at 100 µM = 81%. At the same time, both compounds exert no identifiable inhibitory effect at mGAT1 under the test conditions ([^{3}H]GABA uptake at 100 µM = 100% and 101%, respectively), hence deviating strongly from the reference compound *N*-butylnipecotic acid, which constitutes a potent inhibitor of this GAT subtype (mGAT1: pIC_{50} = 4.11 ± 0.08). 4-(Butylamino)-3-hydroxybutanoic acid and N-butyl isoserine might thus be suitable alternatives to the nipecotic acid subunit in mGAT3/4 inhibitors. Furthermore, we identified 1-butyl-3-hydroxyazetidine-3-carboxylic acid and, even more so, 2-(1-butyl-3-hydroxypyrrolidin-3-yl)acetic acid to be selective and moderately potent inhibitors of mGAT2.

Interestingly, the unsubstituted hydroxyamino acids isoserine, 4-amino-3-hydroxybutanoic acid and 4-amino-2-hydroxybutanoic acid displayed even as racemates distinctly higher inhibitory potencies at mGAT3 and mGAT4 than (*S*)-nipecotic acid. Also, the pIC_{50} values of the unsubstituted hydroxyamino acids are in most cases more than one log unit higher at all GAT subtypes than the values of the respective N-butyl analogues, indicating that, as postulated, the binding pose of the nitrogen atom facing towards the intracellular space is more favourable than the reversed binding pose adapted by the N-butyl derivatives. Therefore, each of the hydroxyamino acids was derivatized by linking the alcohol function to a C_2 spacer bearing a 4,4´,4´´-trimethoxytrityloxy moiety, which is a common structural motif of mGAT4 inhibitors such as (S)-SNAP-5114. In theory, this would allow the amino acid subunit to adapt the more favourable binding pose, while at the same time enabling interactions between the target and the lipophilic domain. Unfortunately, the resulting compounds displayed poor inhibitory potency and selectivity as compared to the unsubstituted hydroxyamino acids and, even more so, as compared to (*S*)-SNAP-5114.

Conflict of interest

None of the authors have conflict of interest related to the information described in this paper.

References

Bowery NG, Smart TG (2006) GABA and glycine as neurotransmitters: a brief history. Br J Pharmacol 147:S109-S119

Corey JL, Guastella J, Davidson N, Lester HA (1994) GABA uptake and release by a mammalian cell line stably expressing a cloned rat brain GABA transporter. Molecular Membrane Biology 11:23-30

Daemen MA, Hoogland G, Cijntje JM, Spincemaille GH (2008) Upregulation of the GABA transporter GAT-1 in the spinal cord contributes to pain behaviour in experimental neuropathy. Neurosci Lett 444:112-115

Dhar TGM, Borden LA, Tyagarajan S, Smith KE, Branchek TA, Weinshank RL, Gluchowski C (1994) Design, synthesis and evaluation of substituted triarylnipecotic acid derivatives as GABA uptake inhibitors: identification of a ligand with moderate affinity and selectivity for the cloned human GABA transporter GAT-3. J Med Chem 37:2334-2342

Farkas M, Li B, Dose C, Dervan P (2009) DNA sequence selectivity of hairpin polyamide turn units. Bioorg Med Chem Lett 19:3919-3923

Jin XT, Galvan A, Wichmann T, Smith Y (2011) Localization and function of GABA transporters GAT-1 and GAT-3 in the basal ganglia. Front Syst Neurosci 5:63

Kalueff AV, Nutt DJ (2007) Role of GABA in anxiety and depression. Depress Anxiety 24:495-517

Kragler A, Höfner G, Wanner KT (2005) Novel parent structures for inhibitors of the murine GABA transporters mGAT3 and mGAT4. Eur J Pharmacol 519:43-47

Kragler A, Höfner G, Wanner KT (2008) Synthesis of Aminomehtylphenol Derivatives as Inhibitors of the Murine GABA Transporters mGAT1-mGAT4. Eur J Med Chem 43:2404-2411

Kristensen AS, Andersen J, Jørgensen TN, Sørensen L, Eriksen J, Loland CJ, Strømgaard K, Gether U (2011) SLC6 neurotransmitter transporters: structure, function, and regulation. Pharmacol Rev 63:585-640

Krogsgaard-Larsen P, Falch E, Larsson OM, Schousboe A (1991) GABA uptake inhibitors: kinetics and molecular pharmacology. Adv Biosciences 82:197-200

Krogsgaard-Larsen P, Frolund, B, Frydenvang K (2000) GABA uptake inhibitors: design, molecular pharmacology and therapeutic aspects. Current Pharmaceutical Design 6:1193-1209

Lamb P (2008) Methods of using combinations of MEK and JAK-2 inhibitors. PCT Int. Appl. 2008124085

Madsen KK, Clausen RP, Larsson OM, Krogsgaard-Larsen P, Schousboe A, White HS (2009) Synaptic and extrasynaptic GABA transporters as targets for anti-epileptic drugs. J Neurochem 109:139-144

Meldrum BS, Chapman AG (1999) Basic mechanisms of gabitril (tiagabine) and future potential developments. Epilepsia 40:S2-S6

Minelli A, DeBiasi S, Brecha NC, Zuccarello LV, Conti F (1996) GAT-3, a high-affinity GABA plasma membrane transporter, is localized to astrocytic processes, and it is not confined to the vicinity of GABAergic synapses in the cerebral cortex. J Neurosci 16:6255

Nielsen EB, Suzdak PD, Andersen KE, Knutsen LJ, Sonnewald U, Braestrup C (1991) Characterization of tiagabine (NO-328), a new potent and selective GABA uptake inhibitor. Eur J Pharmacol 196:257-266

Santimukul S, Perez JM (2011) Selective *N*-Alkylation of β-Alanine Facilitates the Synthesis of a Poly(amino acid)-Based Theranostic Nanoagent. Biomacromolecules 12:3917-3927

Seth A, Sharma PA, Tripathi A, Choubey PK, Srivastava P, Tripathi PN, Shrivastava SK (2018) Design, Synthesis, Evaluation and Computational Studies of Nipecotic Acid-Acetonaphthone Hybrids as Potential Antiepileptic Agents. Medicinal Chemistry 14:409-426

Steffan T, Renukappa-Gutke T, Höfner G, Wanner KT (2015) Design, synthesis and SAR studies of GABA uptake inhibitors derived from 2-substituted pyrrolidine-2-yl-acetic acids. Bioorg Med Chem 23:1284-1306

Treiman DM (2001). GABAergic mechanisms in epilepsy. Epilepsia 42:8-12

Wein T, Petrera M, Allmendinger L, Höfner G, Pabel J, Wanner KT (2016). Different Binding Modes of Small and Large Binders of GAT1. Chem. Med. Chem. 11:509-518

White HS, Sarup A, Bolvig T, Kristensen A, Petersen G, Nelson N, Pickering D, Larsson OM, Frølund B, Krogsgaard-Larsen P, Schousboe A (2002) Correlation between anticonvulsant activity and inhibitory action on glial gamma-aminobutyric acid uptake of the highly selective mouse gamma-aminobutyric acid transporter 1 inhibitor 3-hydroxy-4-amino-4,5,6,7-tetrahydro-1,2-benzisoxazole and its N-alkylated analogues. J Pharmacol Exp Ther 302:636-644

Zepperitz C, Höfner G, Wanner KT (2006) MS-Binding assays: kinetic, saturation and competitive experiments based on quantitation of bound marker – exemplified by the GABA transporter mGAT1. ChemMedChem 1:208-217.

Zhou Y, Holmseth S, Hua R, Lehre AC, Olofsson AM, Poblete-Naredo I, Kempson SA, Danbolt NC (2012) The betaine-GABA transporter (BGT1, slc6a12) is predominantly expressed in the liver and at lower levels in the kidneys and at the brain surface. Am. J. Physiol. Renal. Physiol. 302:F316-F328

Supplementary Material

Synthesis and biological evaluation of α- and β-hydroxy substituted amino acid derivatives as potential mGAT4 inhibitors

Janina C. Andreß, Michael C. Böck, Georg Höfner, Klaus T. Wanner

✉ Klaus T. Wanner
Klaus.wanner@cup.uni-muenchen.de

Ludwig-Maximilians-Universität München, Department of Pharmacy – Center for Drug Research, Butenandtstraße 5-13, 81377 Munich, Germany, Tel.: +49-89-2180-77249; fax: +49-89-2180-77247;

3-(Butylamino)-2-hydroxypropanoic acid (7b)

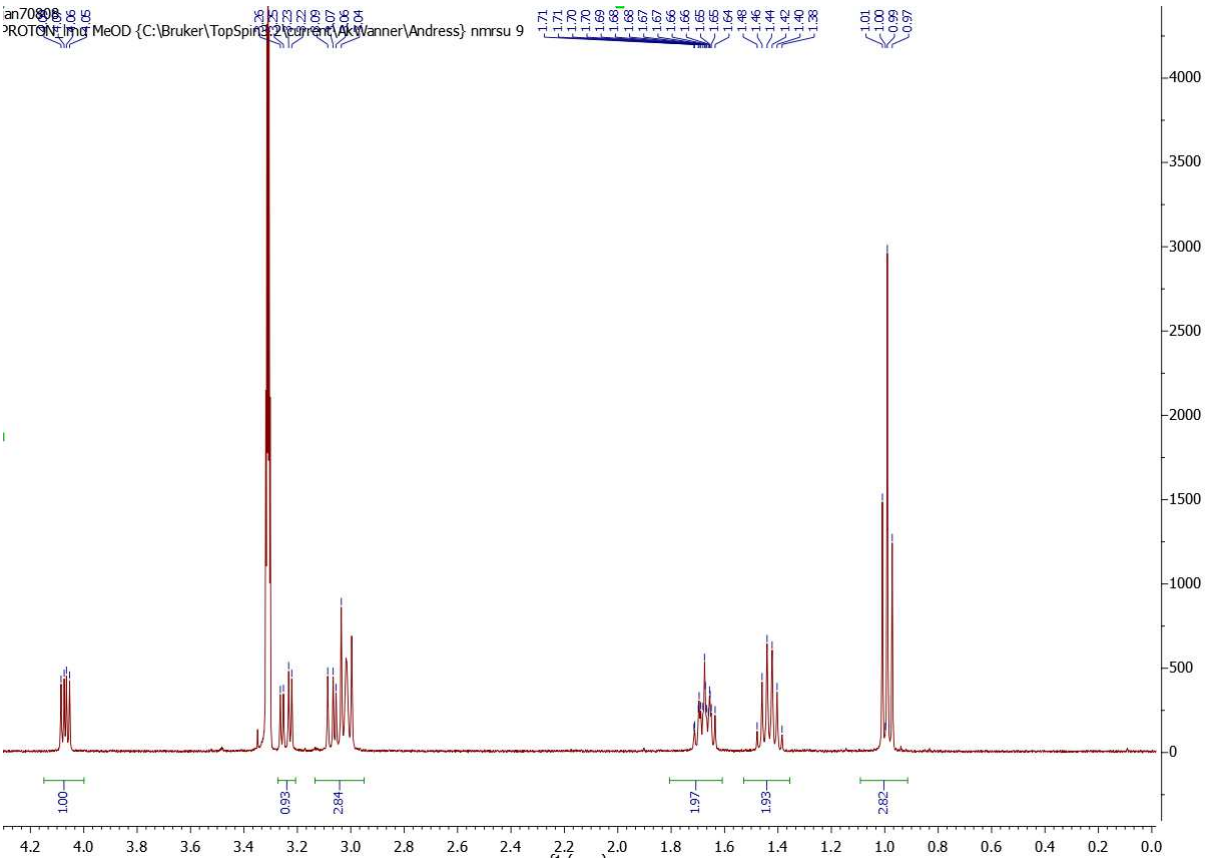

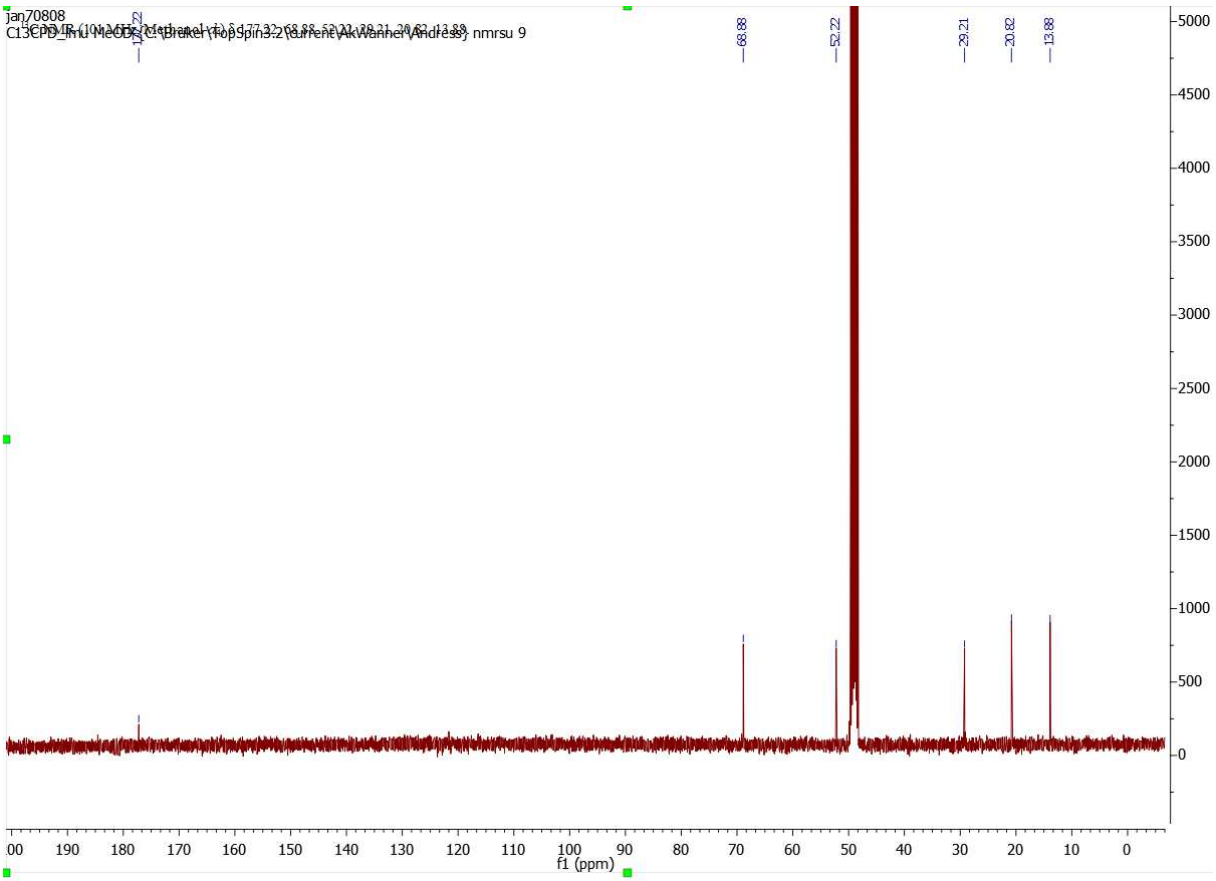

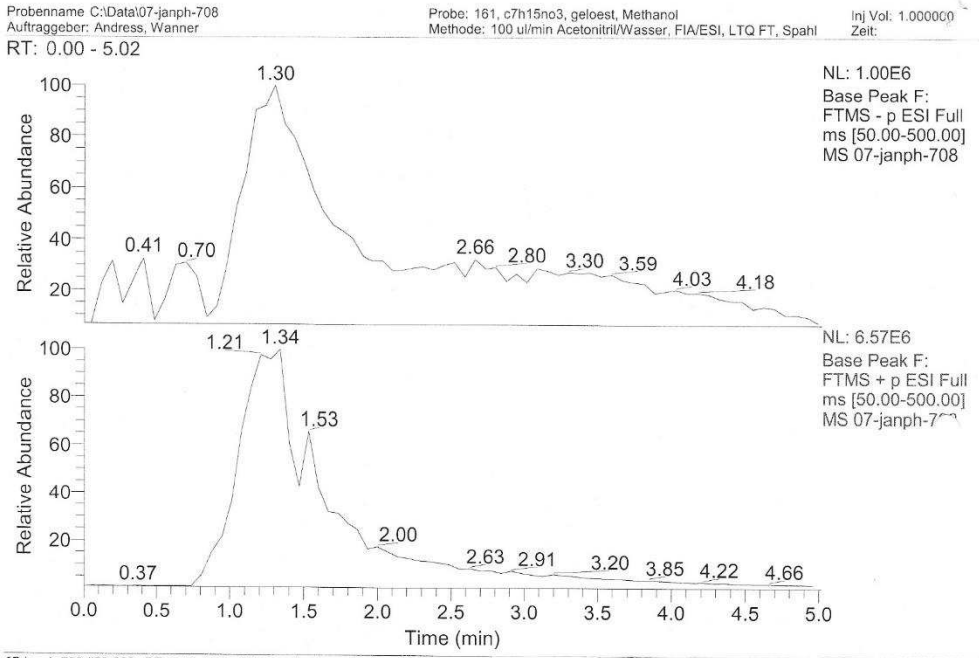
Probenname C:\Data\07-janph-708
Auftraggeber: Andress, Wanner
Probe: 161, c7h15no3, geloest, Methanol
Methode: 100 ul/min Acetonitril/Wasser, FIA/ESI, LTQ FT, Spahl
Inj Vol: 1.000000
Zeit:
RT: 0.00 - 5.02
NL: 1.00E6
Base Peak F:
FTMS - p ESI Full
ms [50.00-500.00]
MS 07-janph-708
Relative Abundance
1.30
0.41
0.70
2.66
2.80
3.30
3.59
4.03
4.18
NL: 6.57E6
Base Peak F:
FTMS + p ESI Full
ms [50.00-500.00]
MS 07-janph-7
1.21
1.34
1.53
2.00
0.37
2.63
2.91
3.20
3.85
4.22
4.66
Time (min)

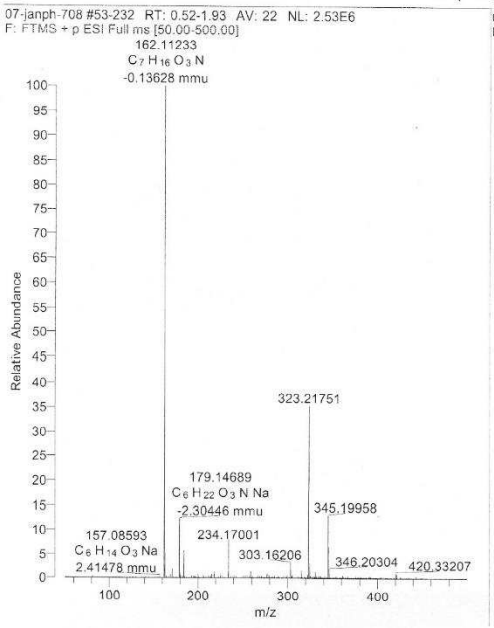
07-janph-708 #53-232 RT: 0.52-1.93 AV: 22 NL: 2.53E6
F: FTMS + p ESI Full ms [50.00-500.00]
162.11233
C7 H16 O3 N
-0.13628 mmu
323.21751
179.14689
C6 H22 O3 N Na
-2.30446 mmu
345.19958
157.08593
C6 H14 O3 Na
2.41478 mmu
234.17001
303.16206
346.20304
420.33207
Relative Abundance
m/z

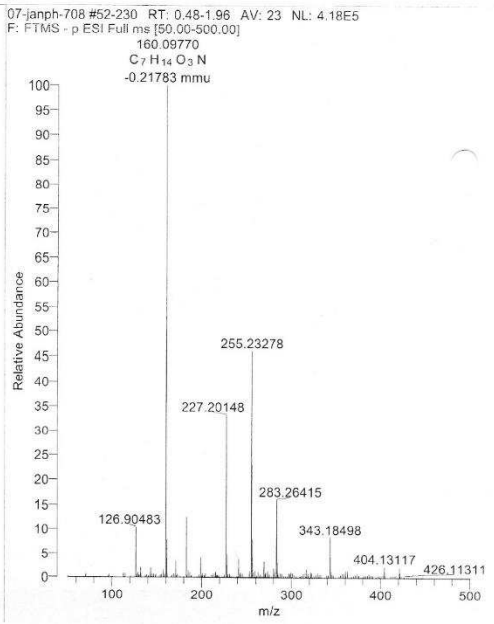
07-janph-708 #52-230 RT: 0.48-1.96 AV: 23 NL: 4.18E5
F: FTMS - p ESI Full ms [50.00-500.00]
160.09770
C7 H14 O3 N
-0.21783 mmu
255.23278
227.20148
283.26415
126.90483
343.18498
404.13117
426.11311
Relative Abundance
m/z

Methyl 3-(1,3-dioxoisoindolin-2-yl)-2-hydroxypropanoate (7c)

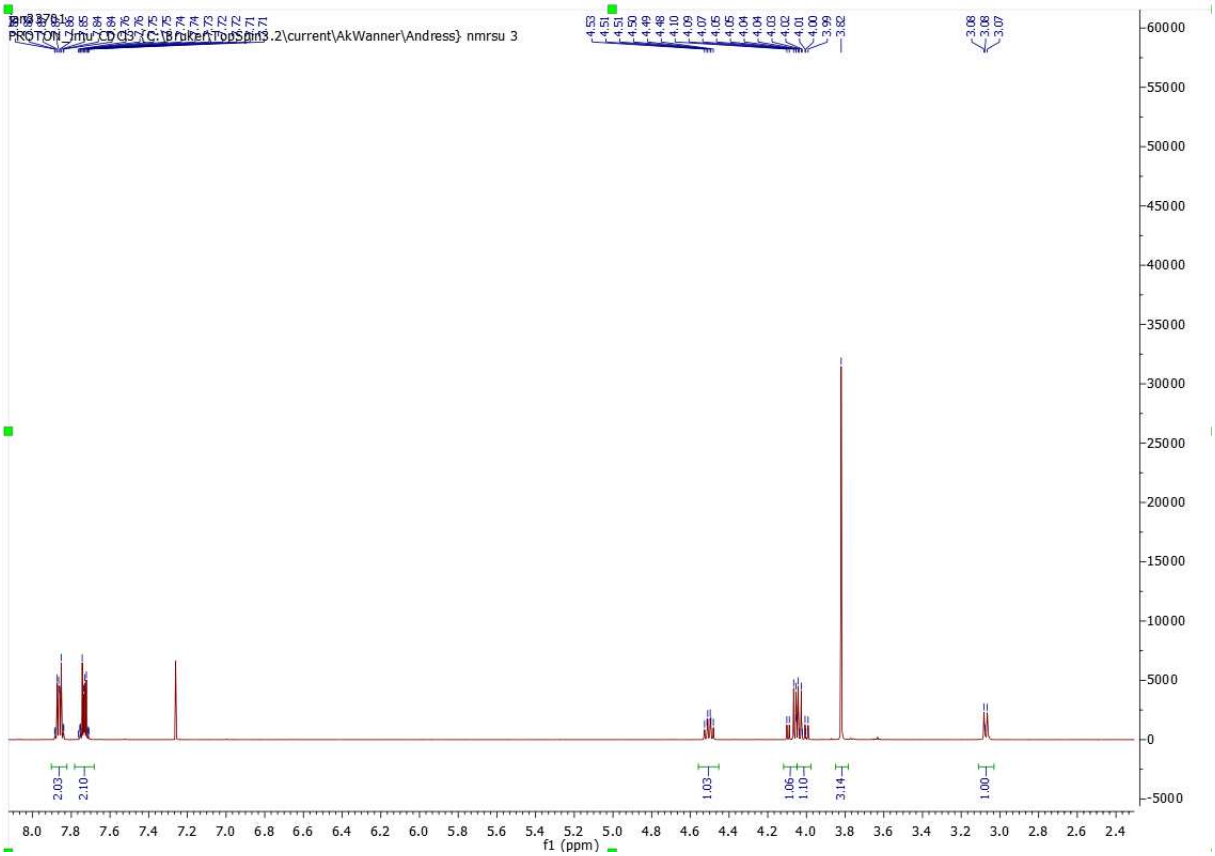

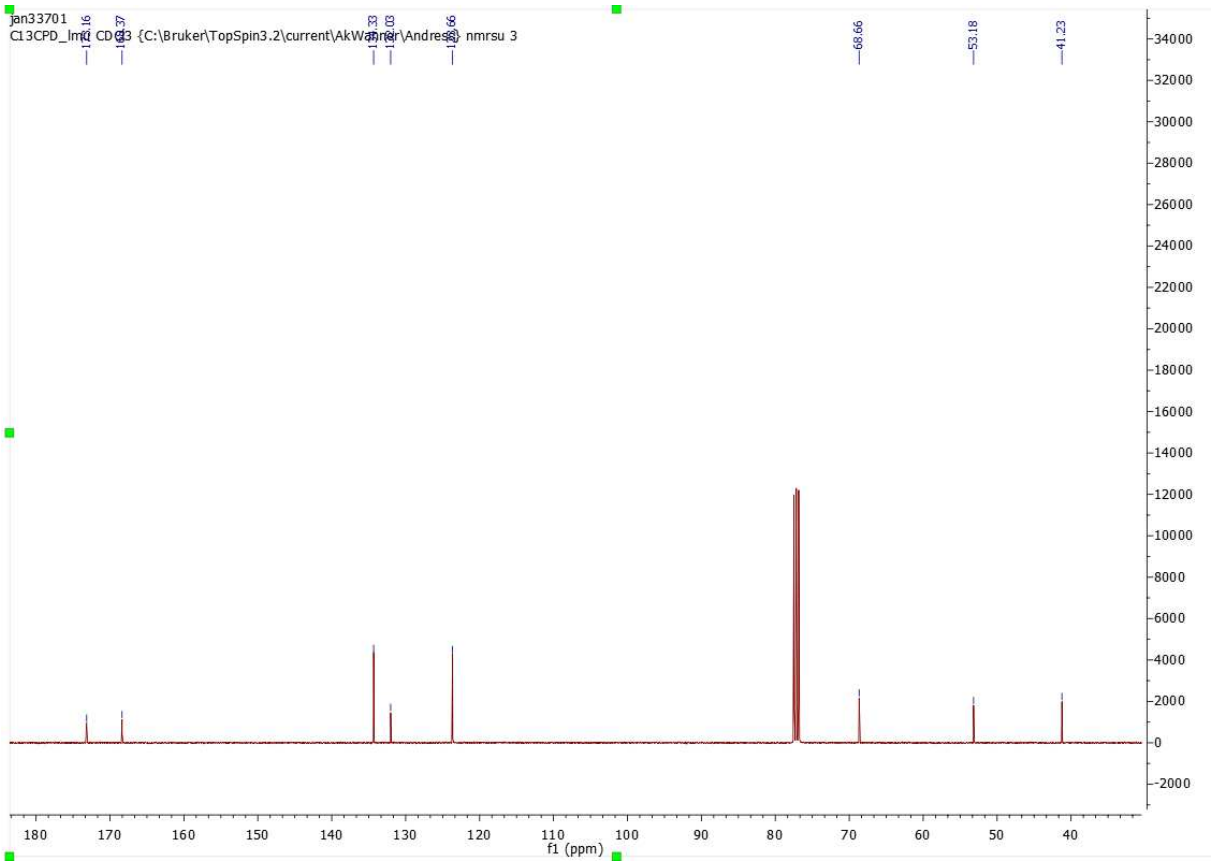

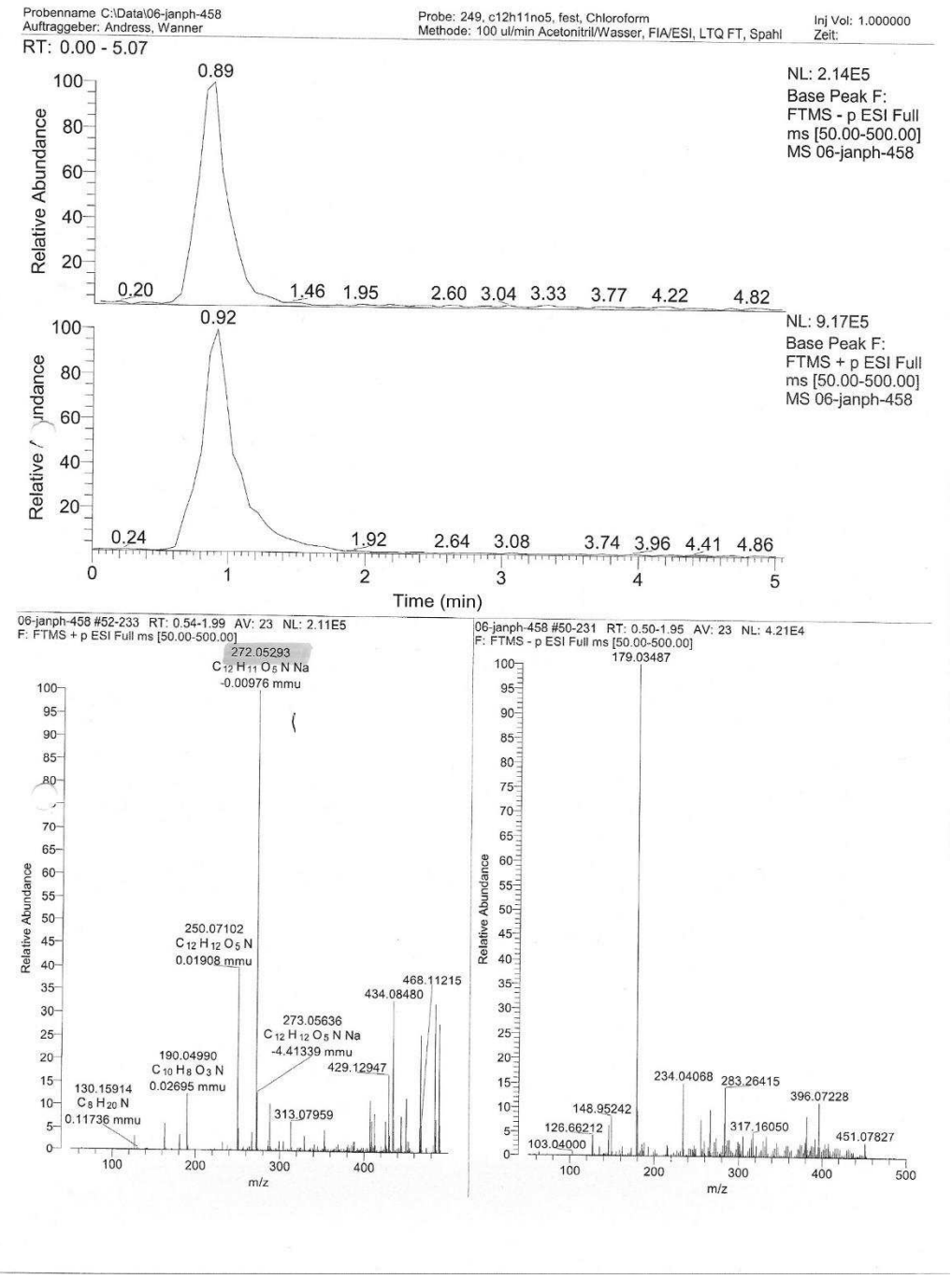
Probenname C:\Data\06-janph-458
Auftraggeber: Andress, Wanner
Probe: 249, c12h11no5, fest, Chloroform
Methode: 100 ul/min Acetonitril/Wasser, FIA/ESI, LTQ FT, Spahl
Inj Vol: 1.000000
Zeit:
RT: 0.00 - 5.07
NL: 2.14E5
Base Peak F:
FTMS - p ESI Full
ms [50.00-500.00]
MS 06-janph-458
NL: 9.17E5
Base Peak F:
FTMS + p ESI Full
ms [50.00-500.00]
MS 06-janph-458
Relative Abundance
Time (min)
06-janph-458 #52-233 RT: 0.54-1.99 AV: 23 NL: 2.11E5
F: FTMS + p ESI Full ms [50.00-500.00]
272.05293
C12 H11 O5 N Na
-0.00976 mmu
250.07102
C12 H12 O5 N
0.01908 mmu
273.05636
C12 H12 O5 N Na
-4.41339 mmu
190.04990
C10 H8 O3 N
0.02695 mmu
130.15914
C8 H20 N
0.11736 mmu
468.11215
434.08480
429.12947
313.07959
m/z
06-janph-458 #50-231 RT: 0.50-1.95 AV: 23 NL: 4.21E4
F: FTMS - p ESI Full ms [50.00-500.00]
179.03487
234.04068
283.26415
396.07228
148.95242
126.66212
317.16050
451.07827
103.04000
m/z

Methyl 3-{2-[(tert-butyldiphenylsilyl)oxy]ethoxy}-3-{-(1,3-dioxoisoindolin-2-yl})propanoate (7d)

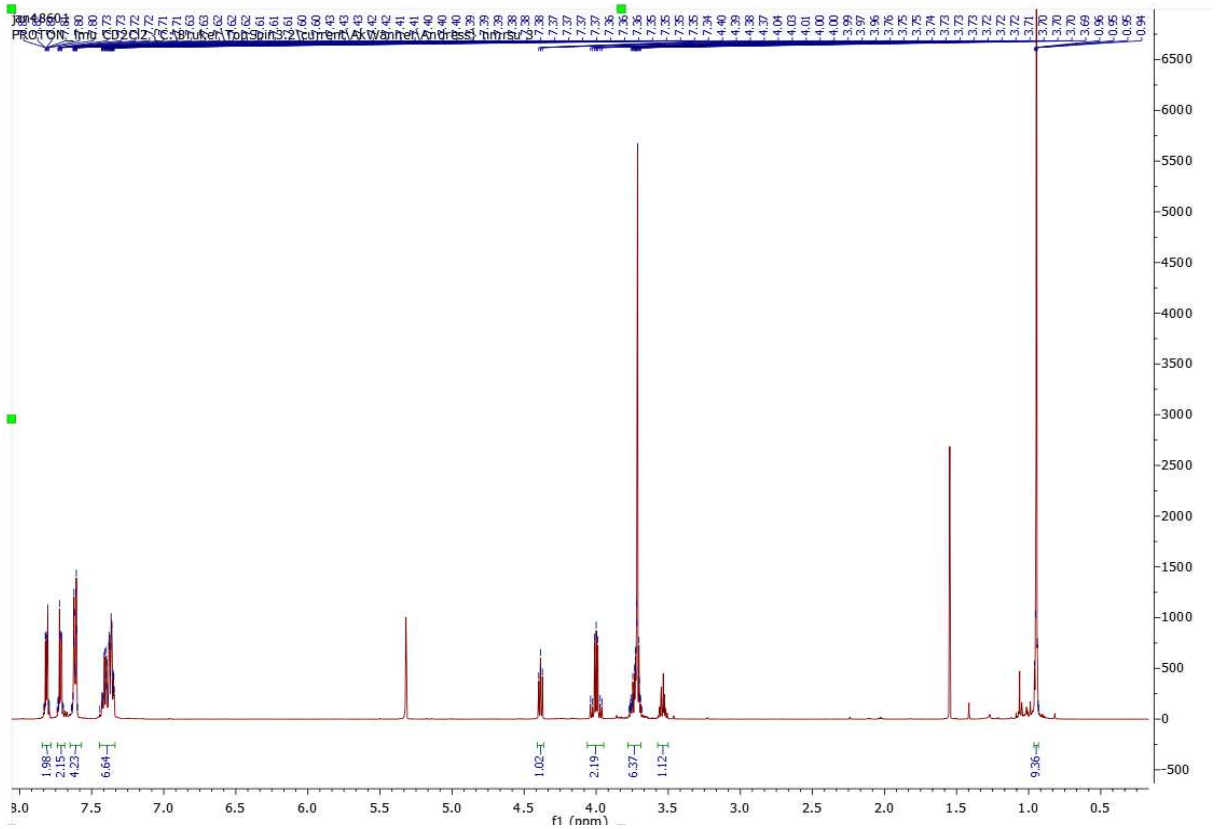

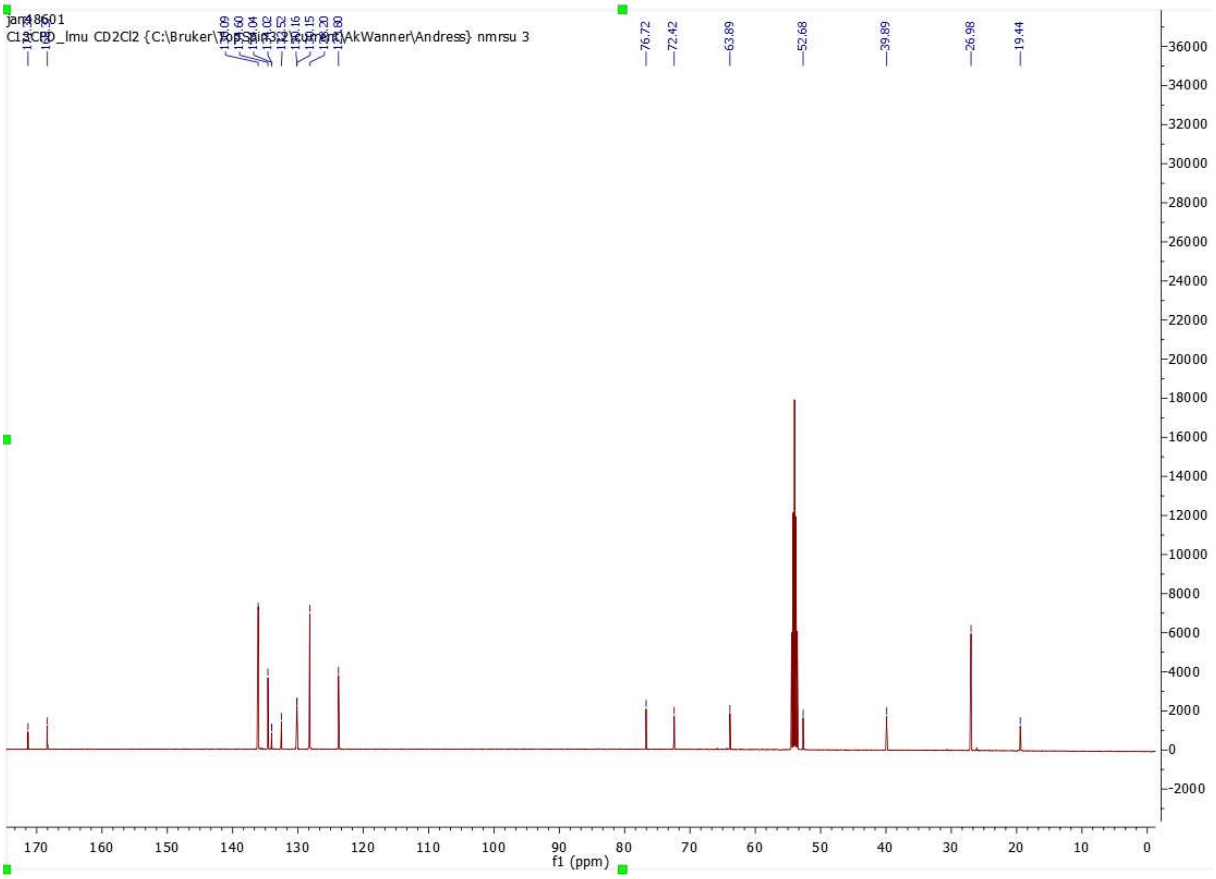

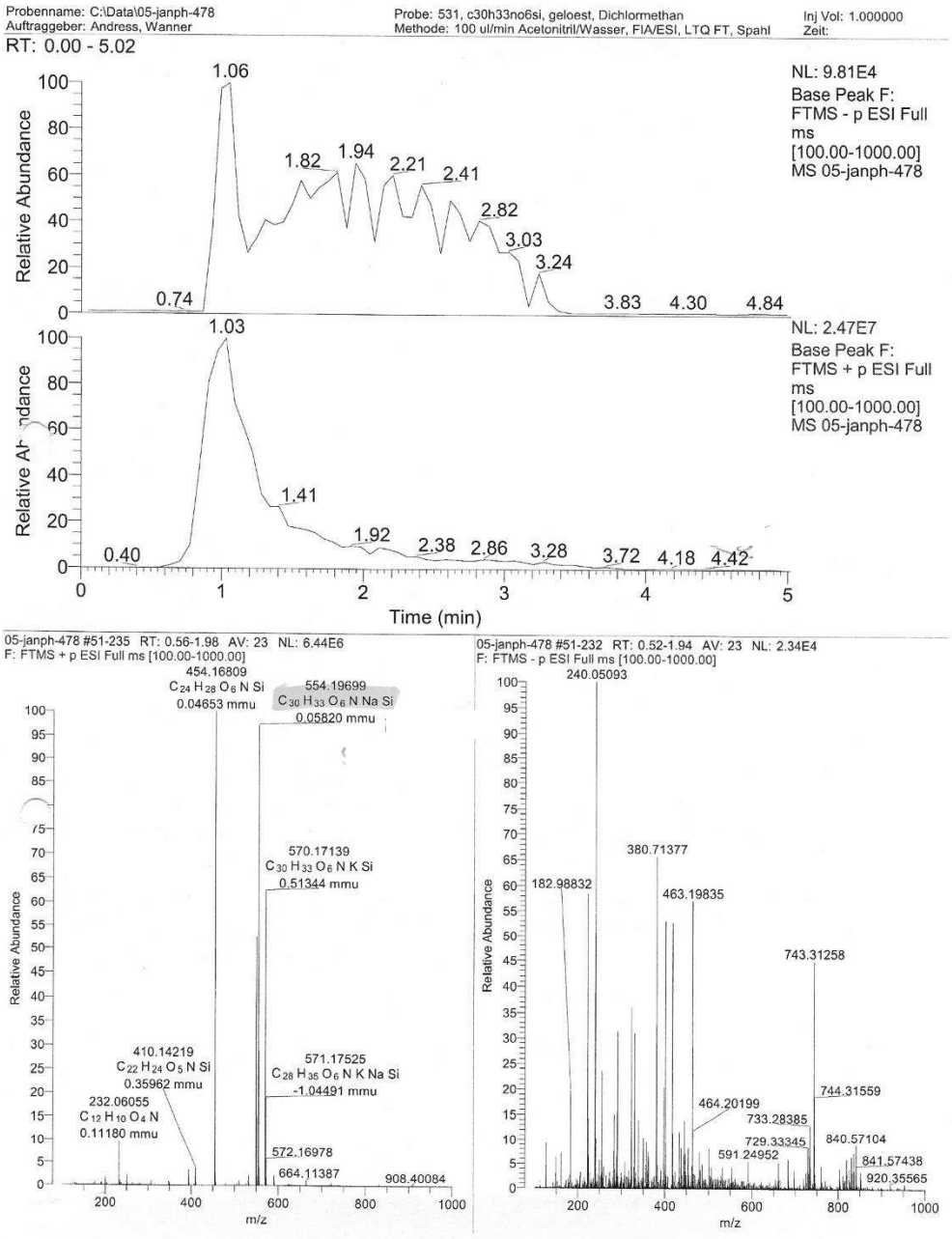
Probenname: C:\Data\05-janph-478
Auftraggeber: Andress, Wanner
Probe: 531, c30h33no6si, geloest, Dichlormethan
Methode: 100 ul/min Acetonitril/Wasser, FIA/ESI, LTQ FT, Spahl
Inj Vol: 1.000000
Zeit:
RT: 0.00 - 5.02
NL: 9.81E4
Base Peak F:
FTMS - p ESI Full
ms
[100.00-1000.00]
MS 05-janph-478
Relative Abundance
1.06
1.82
1.94
2.21
2.41
2.82
3.03
3.24
0.74
3.83
4.30
4.84
NL: 2.47E7
Base Peak F:
FTMS + p ESI Full
ms
[100.00-1000.00]
MS 05-janph-478
1.03
1.41
1.92
2.38
2.86
3.28
3.72
4.18
4.42
0.40
Time (min)
05-janph-478 #51-235 RT: 0.56-1.98 AV: 23 NL: 6.44E6
F: FTMS + p ESI Full ms [100.00-1000.00]
454.16809
C24 H28 O6 N Si
0.04653 mmu
554.19699
C30 H33 O6 N Na Si
0.05820 mmu
570.17139
C30 H33 O6 N K Si
0.51344 mmu
410.14219
C22 H24 O5 N Si
0.35962 mmu
232.06055
C12 H10 O4 N
0.11180 mmu
571.17525
C28 H35 O6 N K Si
-1.04491 mmu
572.16978
664.11387
908.40084
m/z
05-janph-478 #51-232 RT: 0.52-1.94 AV: 23 NL: 2.34E4
F: FTMS - p ESI Full ms [100.00-1000.00]
240.05093
380.71377
182.98832
463.19835
743.31258
744.31559
464.20199
733.28385
729.33345
840.57104
591.24952
841.57438
920.35565
m/z

Methyl 3-(1,3-dioxoisoindolin-2-yl)-3-(2-hydroxyethoxy)propanoate (7e):

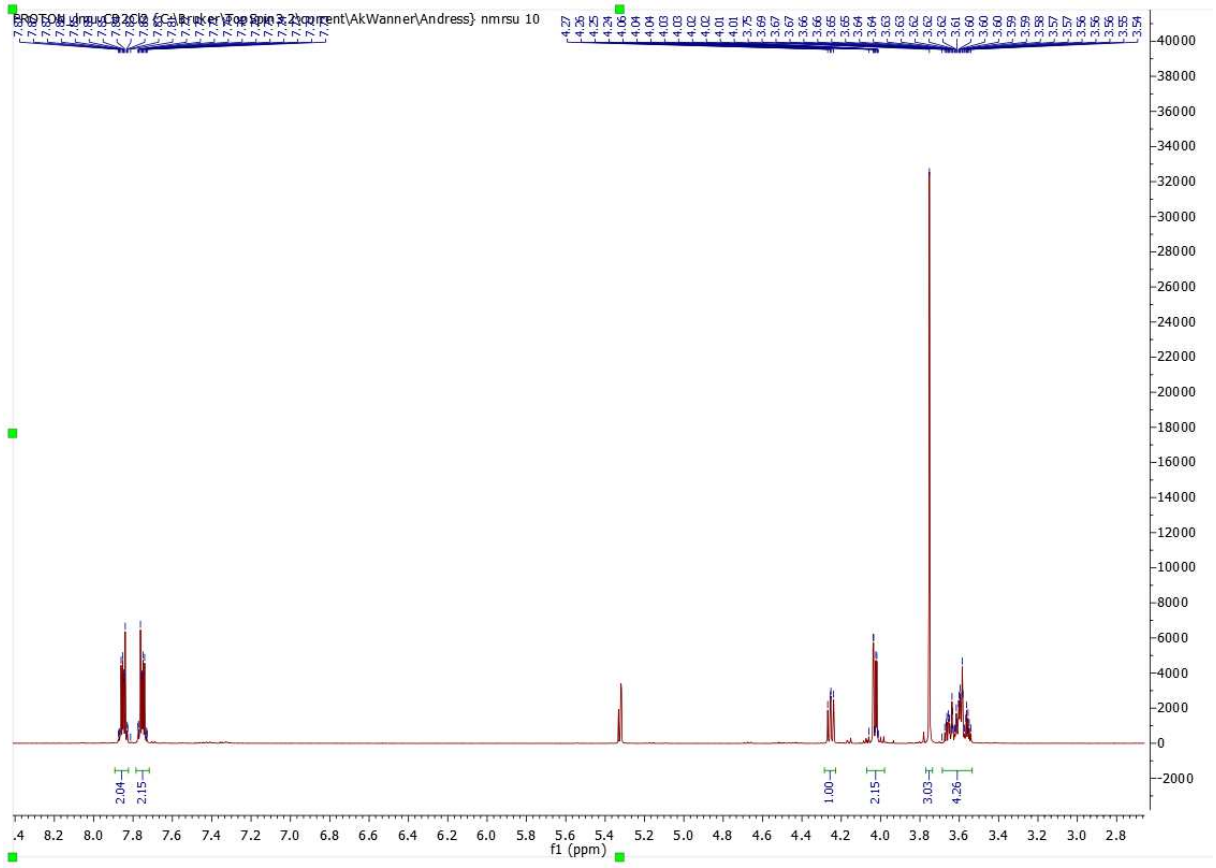

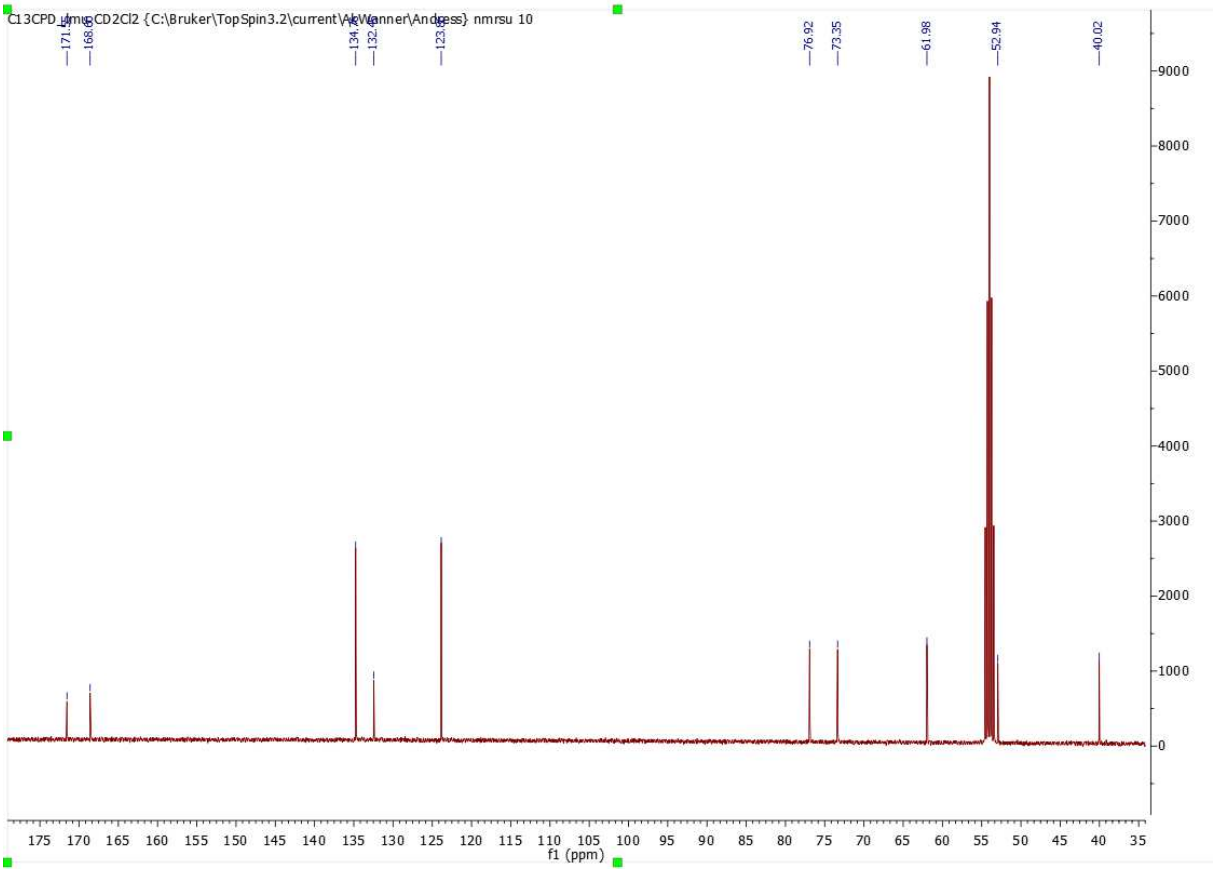

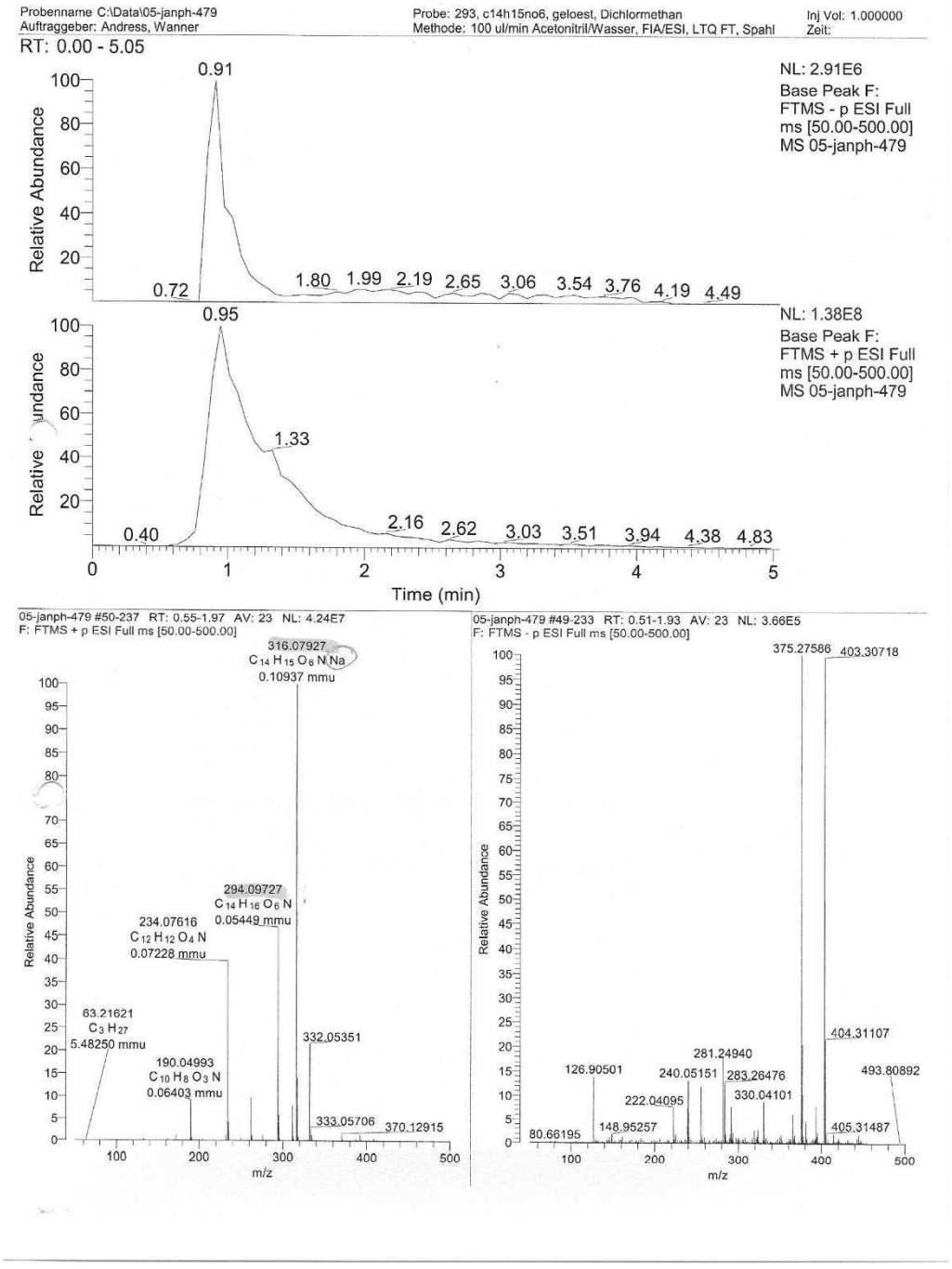
Probenname C:\Data\05-janph-479
Auftraggeber: Andress, Wanner
Probe: 293, c14h15no6, geloest, Dichlormethan
Methode: 100 ul/min Acetonitril/Wasser, FIA/ESI, LTQ FT, Spahl
Inj Vol: 1.000000
Zeit:
RT: 0.00 - 5.05
NL: 2.91E6
Base Peak F:
FTMS - p ESI Full
ms [50.00-500.00]
MS 05-janph-479
Relative Abundance
0.91
0.72
1.80 1.99 2.19 2.65 3.06 3.54 3.76 4.19 4.49
NL: 1.38E8
Base Peak F:
FTMS + p ESI Full
ms [50.00-500.00]
MS 05-janph-479
0.95
1.33
0.40
2.16 2.62 3.03 3.51 3.94 4.38 4.83
Time (min)
05-janph-479 #50-237 RT: 0.55-1.97 AV: 23 NL: 4.24E7
F: FTMS + p ESI Full ms [50.00-500.00]
316.07927
C14 H15 O6 N Na
0.10937 mmu
294.09727
C14 H16 O6 N
0.05449 mmu
234.07616
C12 H12 O4 N
0.07228 mmu
63.21621
C3 H27
5.48250 mmu
190.04993
C10 H8 O3 N
0.06403 mmu
332.05351
333.05706
370.12915
m/z
05-janph-479 #49-233 RT: 0.51-1.93 AV: 23 NL: 3.66E5
F: FTMS - p ESI Full ms [50.00-500.00]
375.27586
403.30718
404.31107
281.24940
126.90501
240.05151
283.26476
493.80892
330.04101
222.04095
148.95257
80.66195
405.31487
m/z

Methyl 3-{1,3-dioxoisoindolin-2-yl}-2-{2-[tris(4-methoxyphenyl)methoxy]ethoxy}propanoat (7f)

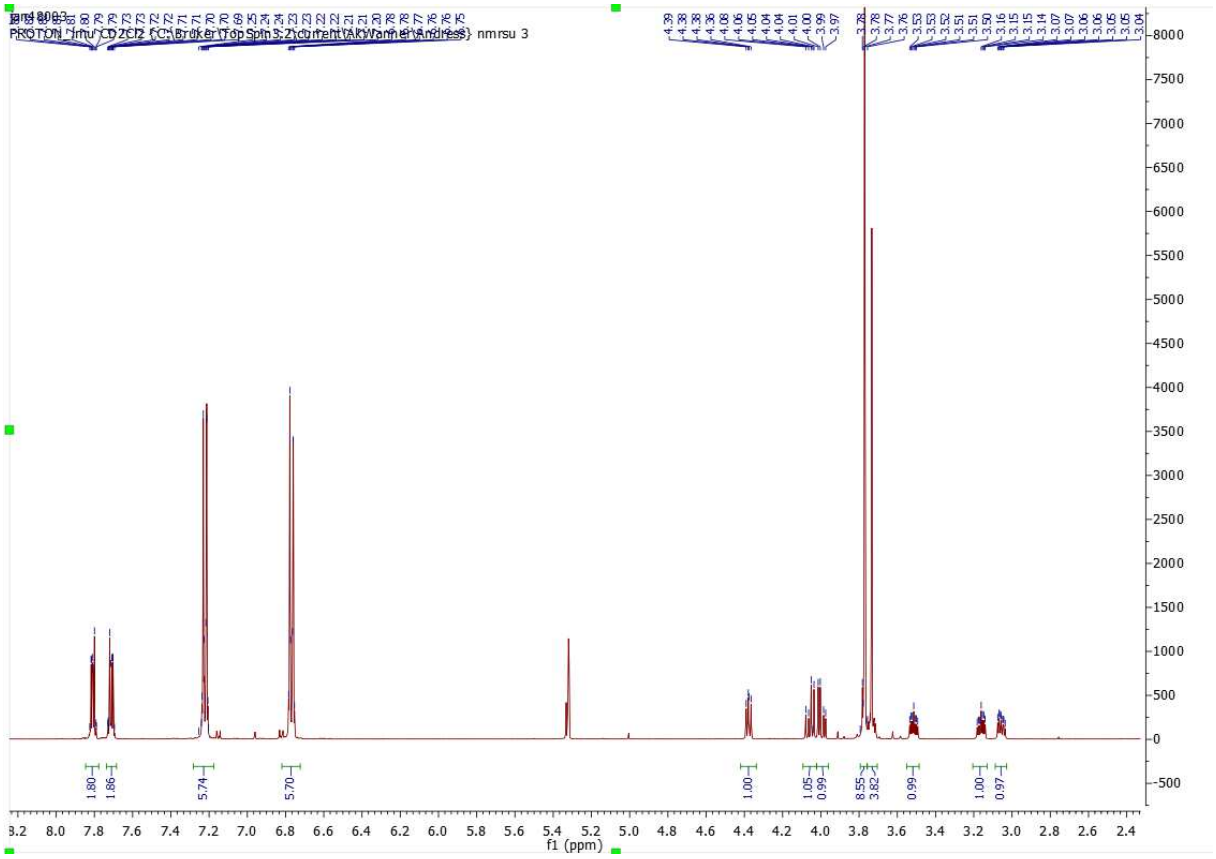

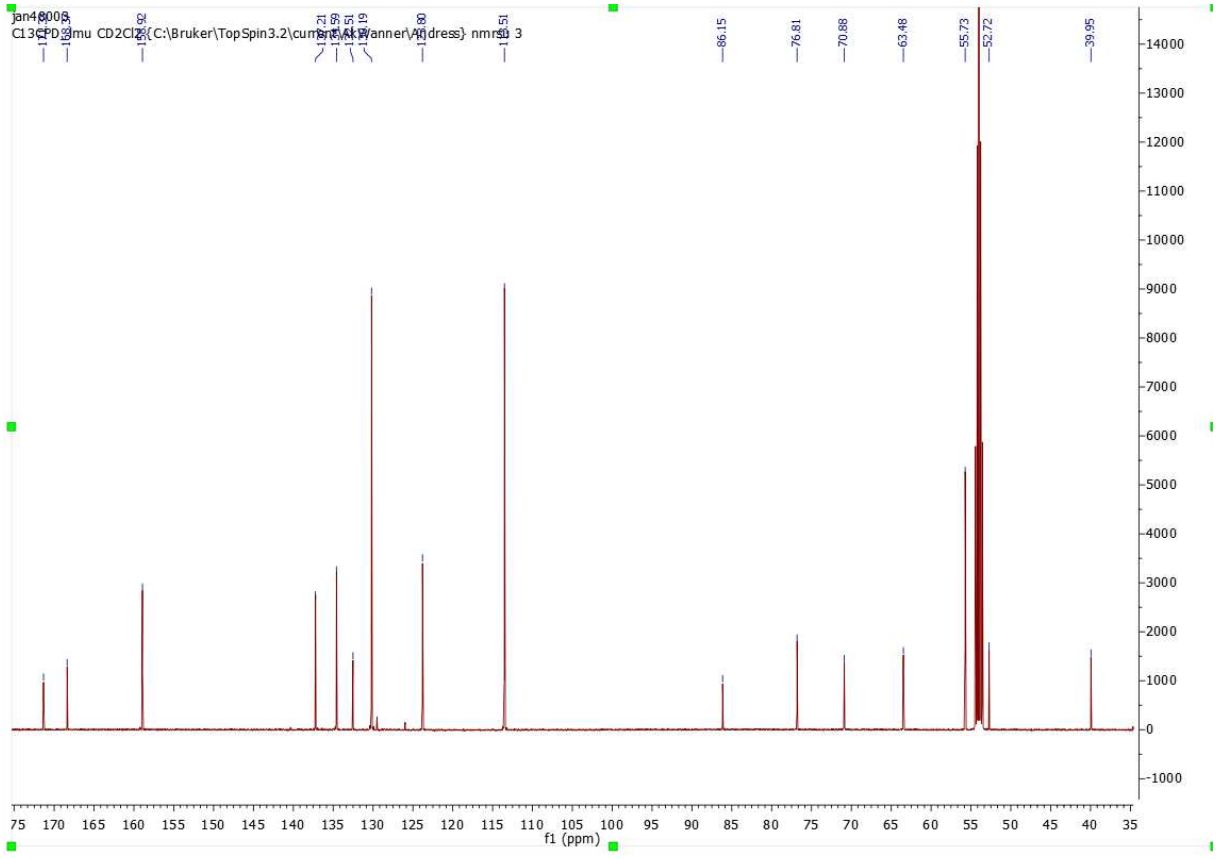

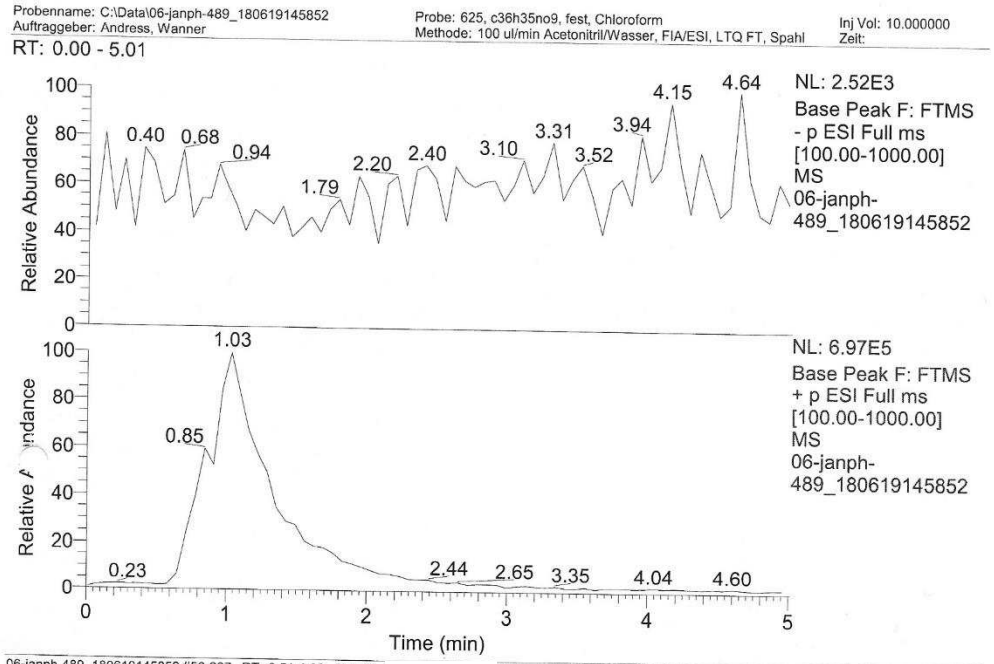
Probenname: C:\Data\06-janph-489_180619145852
Auftraggeber: Andress, Wanner
Probe: 625, c36h35no9, fest, Chloroform
Methode: 100 ul/min Acetonitril/Wasser, FIA/ESI, LTQ FT, Spahl
Inj Vol: 10.000000
Zeit:
RT: 0.00 - 5.01
Relative Abundance
NL: 2.52E3
Base Peak F: FTMS - p ESI Full ms [100.00-1000.00] MS 06-janph-489_180619145852
NL: 6.97E5
Base Peak F: FTMS + p ESI Full ms [100.00-1000.00] MS 06-janph-489_180619145852
Time (min)

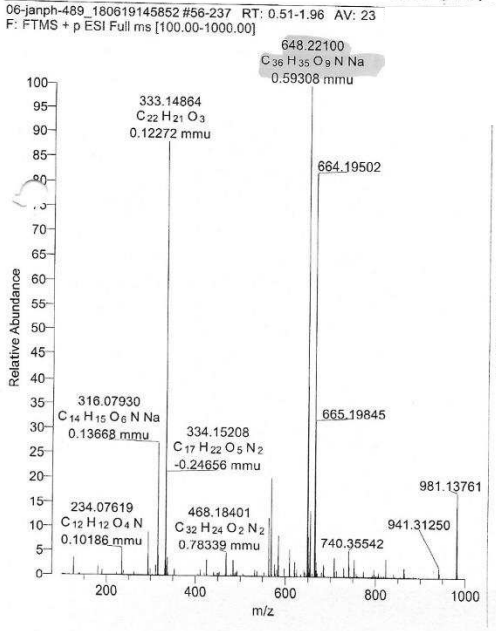
06-janph-489_180619145852 #56-237 RT: 0.51-1.96 AV: 23
F: FTMS + p ESI Full ms [100.00-1000.00]
Relative Abundance
m/z

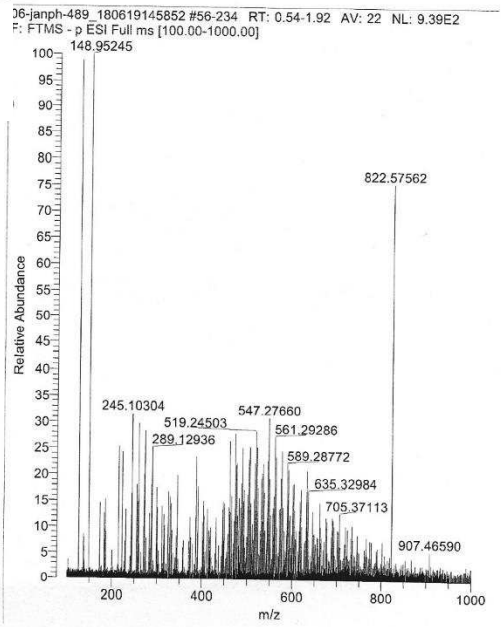
06-janph-489_180619145852 #56-234 RT: 0.54-1.92 AV: 22 NL: 9.39E2
F: FTMS - p ESI Full ms [100.00-1000.00]
Relative Abundance
m/z

3-Amino-2-{2-[tris(4-methoxyphenyl)methoxy]ethoxy}propanoic acid (7g)

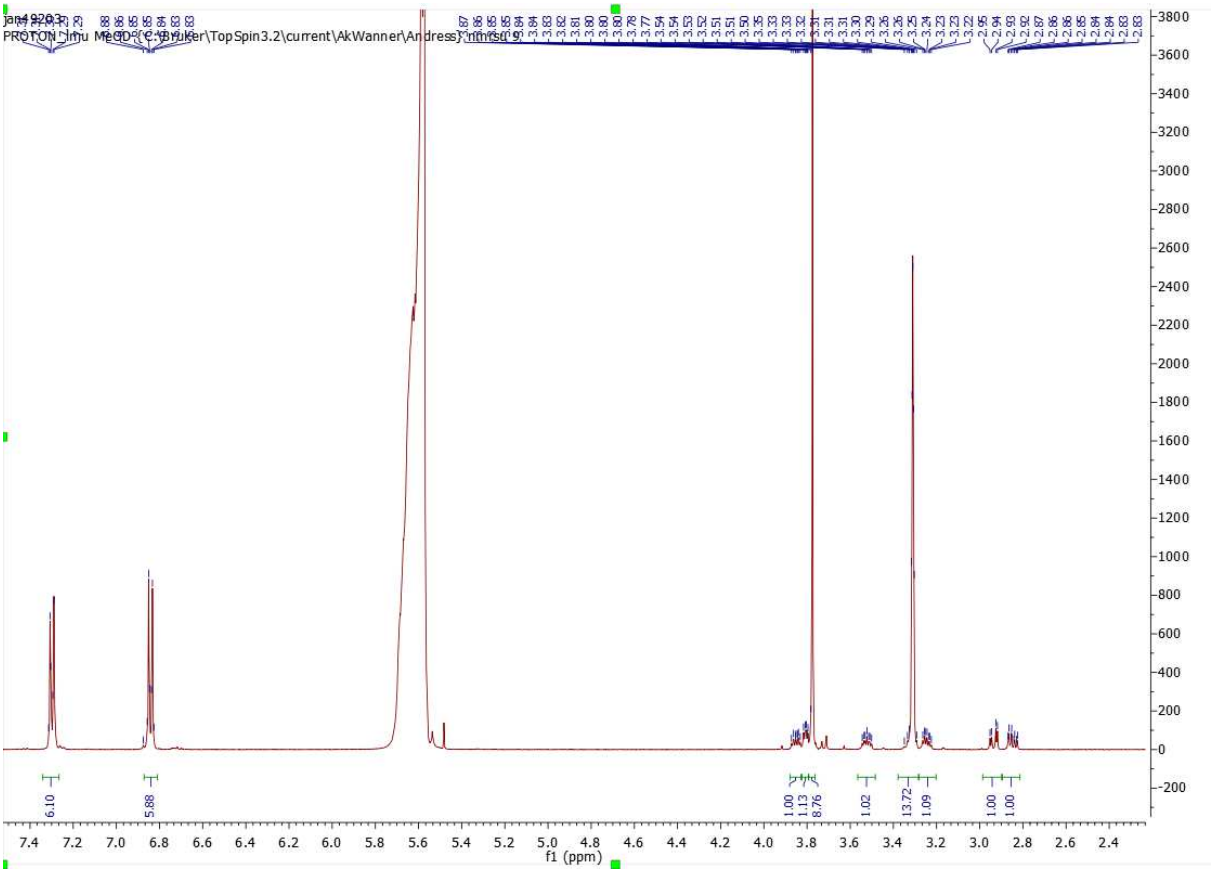

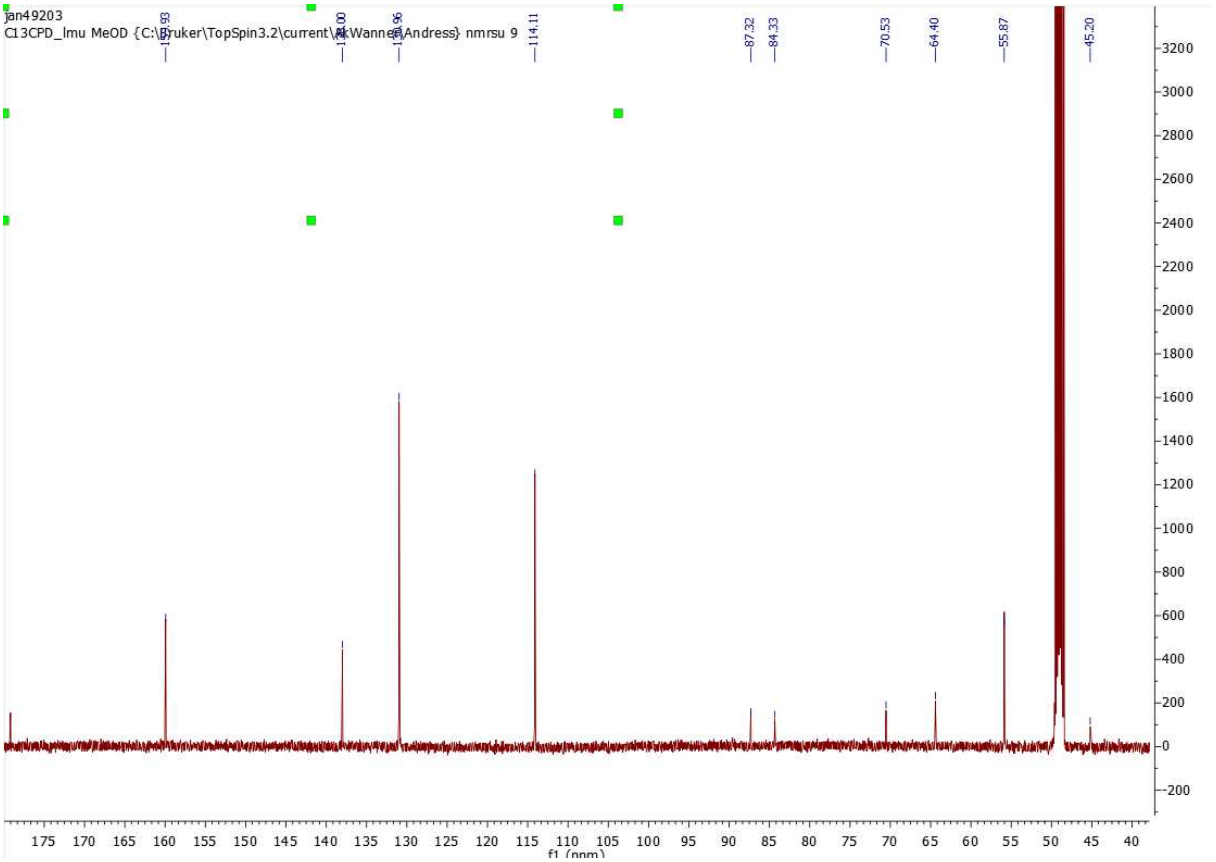

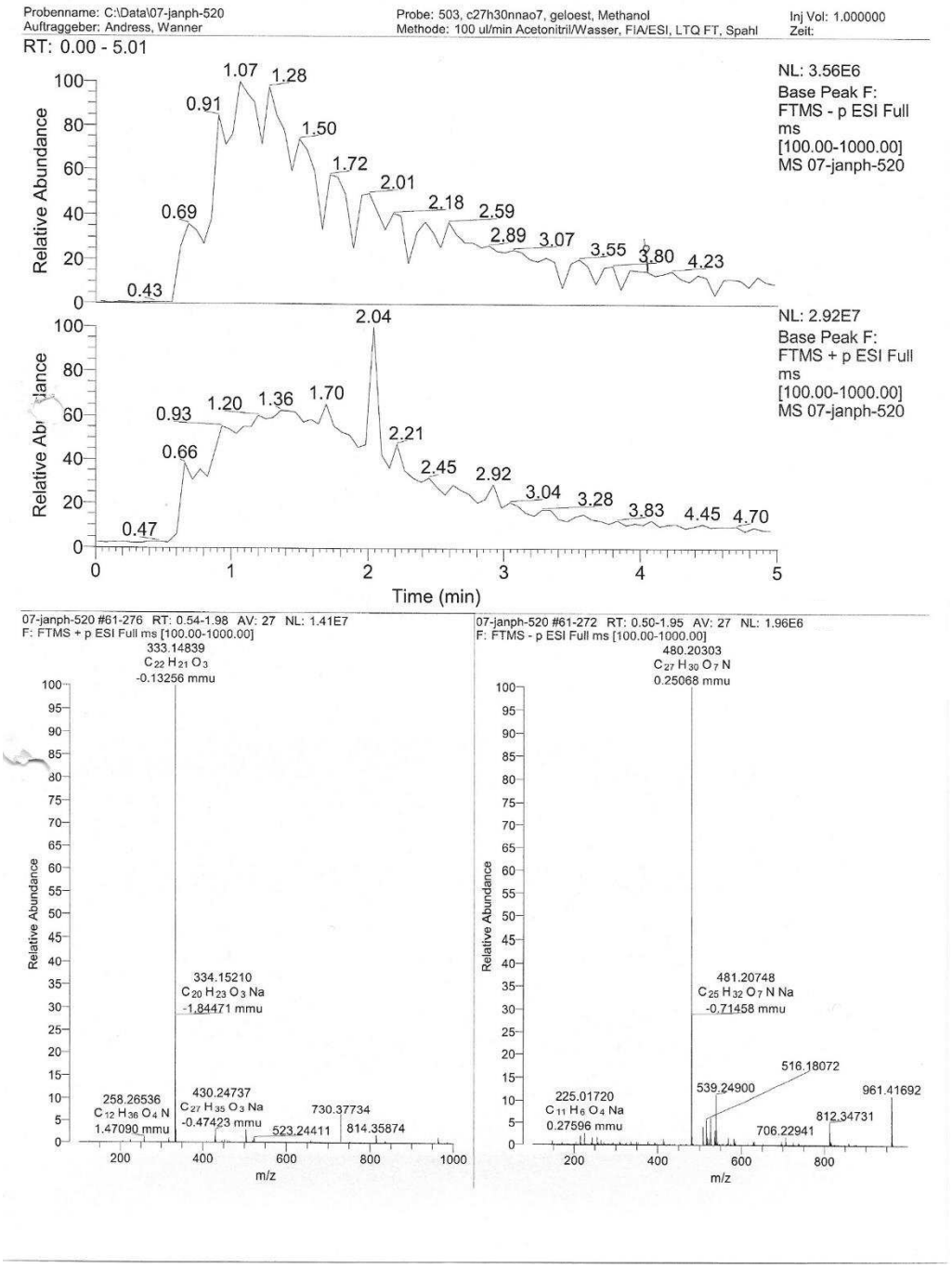
Probenname: C:\Data\07-janph-520
Auftraggeber: Andress, Wanner
Probe: 503, c27h30nnao7, geloest, Methanol
Methode: 100 ul/min Acetonitril/Wasser, FIA/ESI, LTQ FT, Spahl
Inj Vol: 1.000000
Zeit:
RT: 0.00 - 5.01
NL: 3.56E6
Base Peak F: FTMS - p ESI Full ms [100.00-1000.00] MS 07-janph-520
NL: 2.92E7
Base Peak F: FTMS + p ESI Full ms [100.00-1000.00] MS 07-janph-520
Relative Abundance
Time (min)
07-janph-520 #61-276 RT: 0.54-1.98 AV: 27 NL: 1.41E7
F: FTMS + p ESI Full ms [100.00-1000.00]
333.14839
C22 H21 O3
-0.13256 mmu
334.15210
C20 H23 O3 Na
-1.84471 mmu
258.26536
C12 H36 O4 N
1.47090 mmu
430.24737
C27 H35 O3 Na
-0.47423 mmu
730.37734
523.24411
814.35874
m/z
07-janph-520 #61-272 RT: 0.50-1.95 AV: 27 NL: 1.96E6
F: FTMS - p ESI Full ms [100.00-1000.00]
480.20303
C27 H30 O7 N
0.25068 mmu
481.20748
C25 H32 O7 N Na
-0.71458 mmu
225.01720
C11 H6 O4 Na
0.27596 mmu
516.18072
539.24900
961.41692
812.34731
706.22941
m/z

1-Butyl-3-hydroxyazetidine-3-carboxamide (11c)

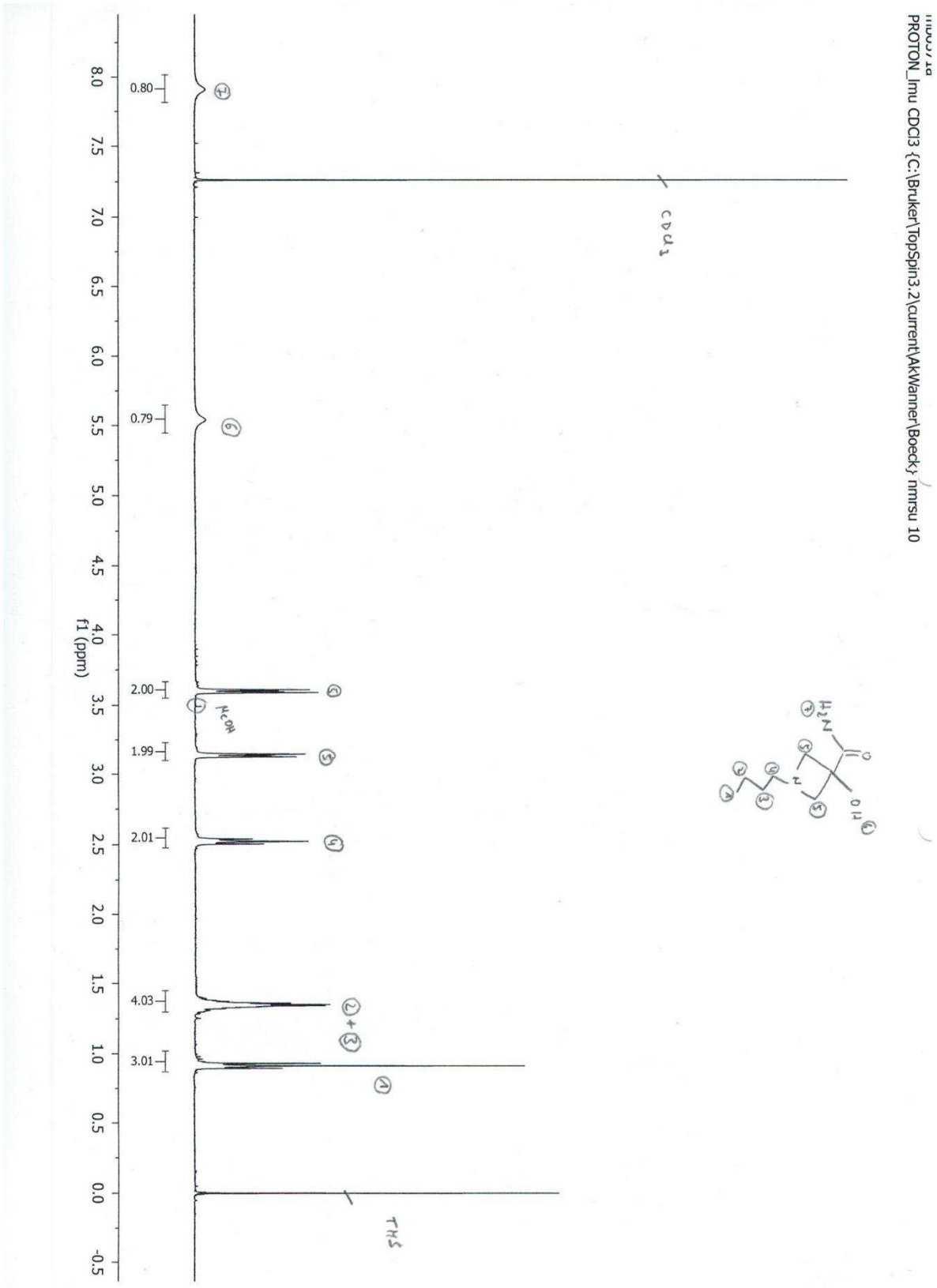

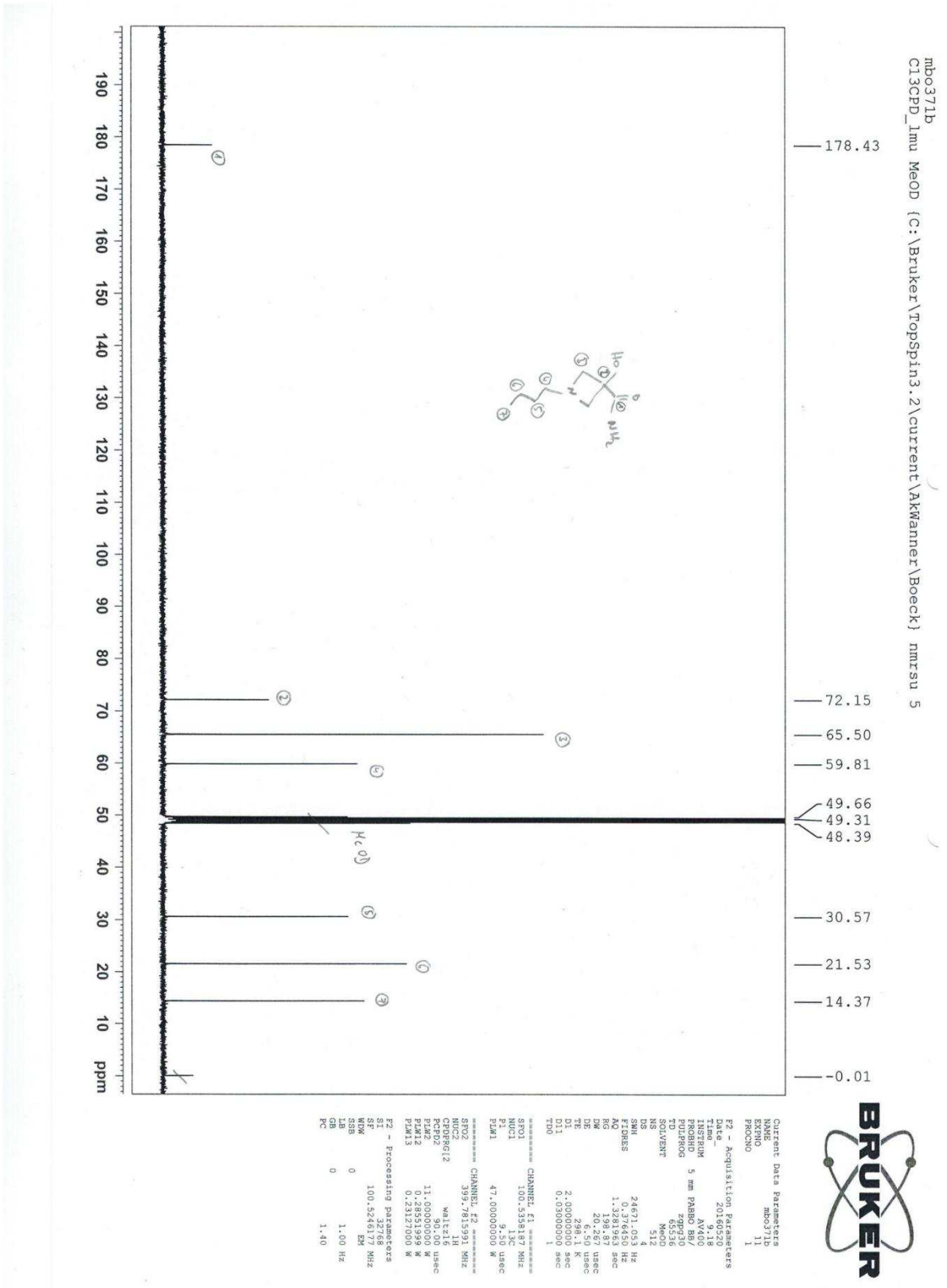
mbo371b
C13CPD_1mu MeOD {C:\Bruker\TopSpin3.2\current\AkWanner\Boeck} nmrsu 5
178.43
72.15
65.50
59.81
49.66
49.31
48.39
30.57
21.53
14.37
-0.01
ppm
Current Data Parameters
NAME mbo371b
EXPNO 11
PROCNO 1
F2 - Acquisition Parameters
Date_ 20160720
Time 9.18
INSTRUM AV400
PROBHD 5 mm PABBO BB/
PULPROG zgpg30
TD 65536
SOLVENT MeOD
NS 512
DS 4
SWH 24671.053 Hz
FIDRES 0.376450 Hz
AQ 1.3281963 sec
RG 198.87
DW 20.267 usec
DE 6.00 usec
TE 298.1 K
D1 2.00000000 sec
D11 0.03000000 sec
TD0 1
======== CHANNEL f1 ========
SFO1 100.5358187 MHz
NUC1 13C
P1 9.50 usec
PLW1 47.00000000 W
======== CHANNEL f2 ========
SFO2 399.7815991 MHz
NUC2 1H
CPDPRG[2 waltz16
PCPD2 90.00 usec
PLW2 11.00000000 W
PLW12 0.28551999 W
PLW13 0.23127000 W
F2 - Processing parameters
SI 32768
SF 100.5246177 MHz
WDW EM
SSB 0
LB 1.00 Hz
GB 0
PC 1.40

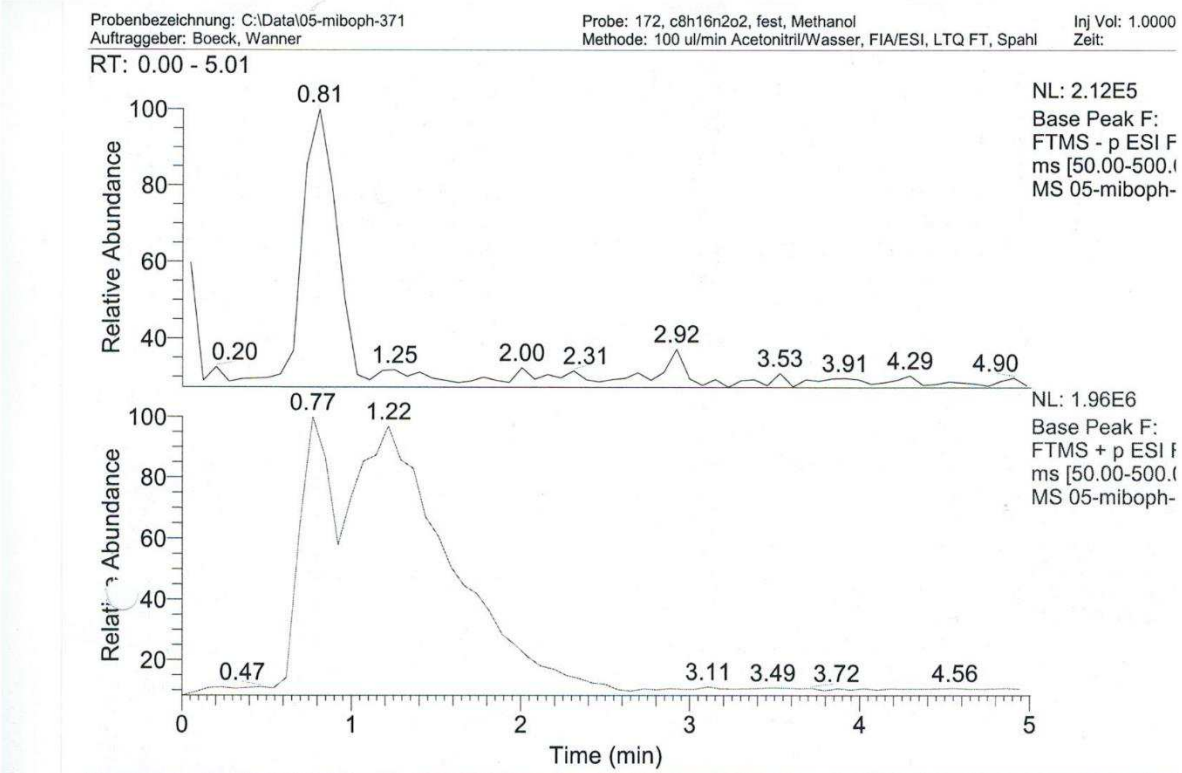
Probenbezeichnung: C:\Data\05-miboph-371
Auftraggeber: Boeck, Wanner
Probe: 172, c8h16n2o2, fest, Methanol
Methode: 100 ul/min Acetonitril/Wasser, FIA/ESI, LTQ FT, Spahl
Inj Vol: 1.0000
Zeit:
RT: 0.00 - 5.01
NL: 2.12E5
Base Peak F:
FTMS - p ESI F
ms [50.00-500.
MS 05-miboph-
NL: 1.96E6
Base Peak F:
FTMS + p ESI F
ms [50.00-500.
MS 05-miboph-
Relative Abundance
Time (min)
0.81
0.20
1.25
2.00
2.31
2.92
3.53
3.91
4.29
4.90
0.77
1.22
0.47
3.11
3.49
3.72
4.56

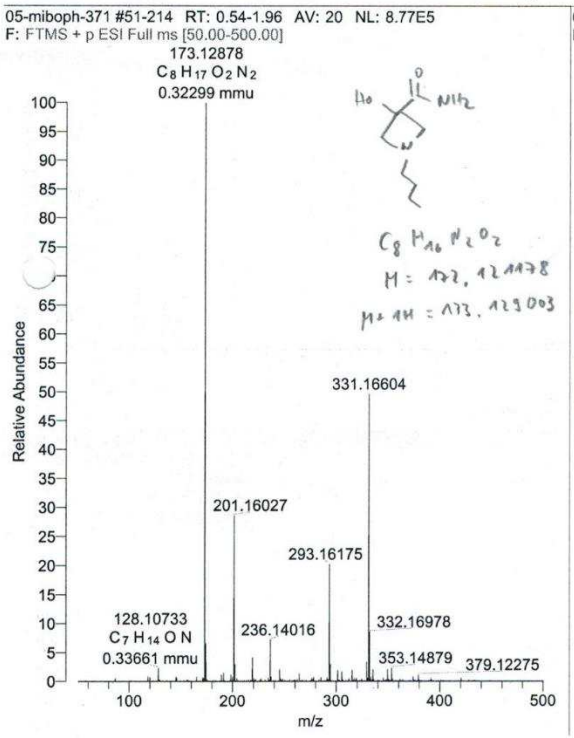
05-miboph-371 #51-214 RT: 0.54-1.96 AV: 20 NL: 8.77E5
F: FTMS + p ESI Full ms [50.00-500.00]
173.12878
C8 H17 O2 N2
0.32299 mmu
331.16604
201.16027
293.16175
128.10733
C7 H14 O N
0.33661 mmu
236.14016
332.16978
353.14879
379.12275
Relative Abundance
m/z

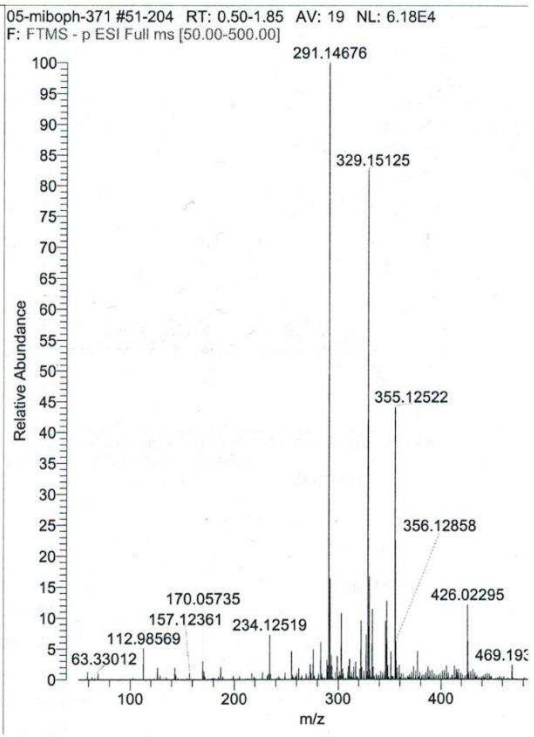
05-miboph-371 #51-204 RT: 0.50-1.85 AV: 19 NL: 6.18E4
F: FTMS - p ESI Full ms [50.00-500.00]
291.14676
329.15125
355.12522
356.12858
426.02295
170.05735
157.12361
234.12519
112.98569
63.33012
Relative Abundance
m/z

1-Butyl-3-hydroxypiperidine-3-carboxylic acid (11d)

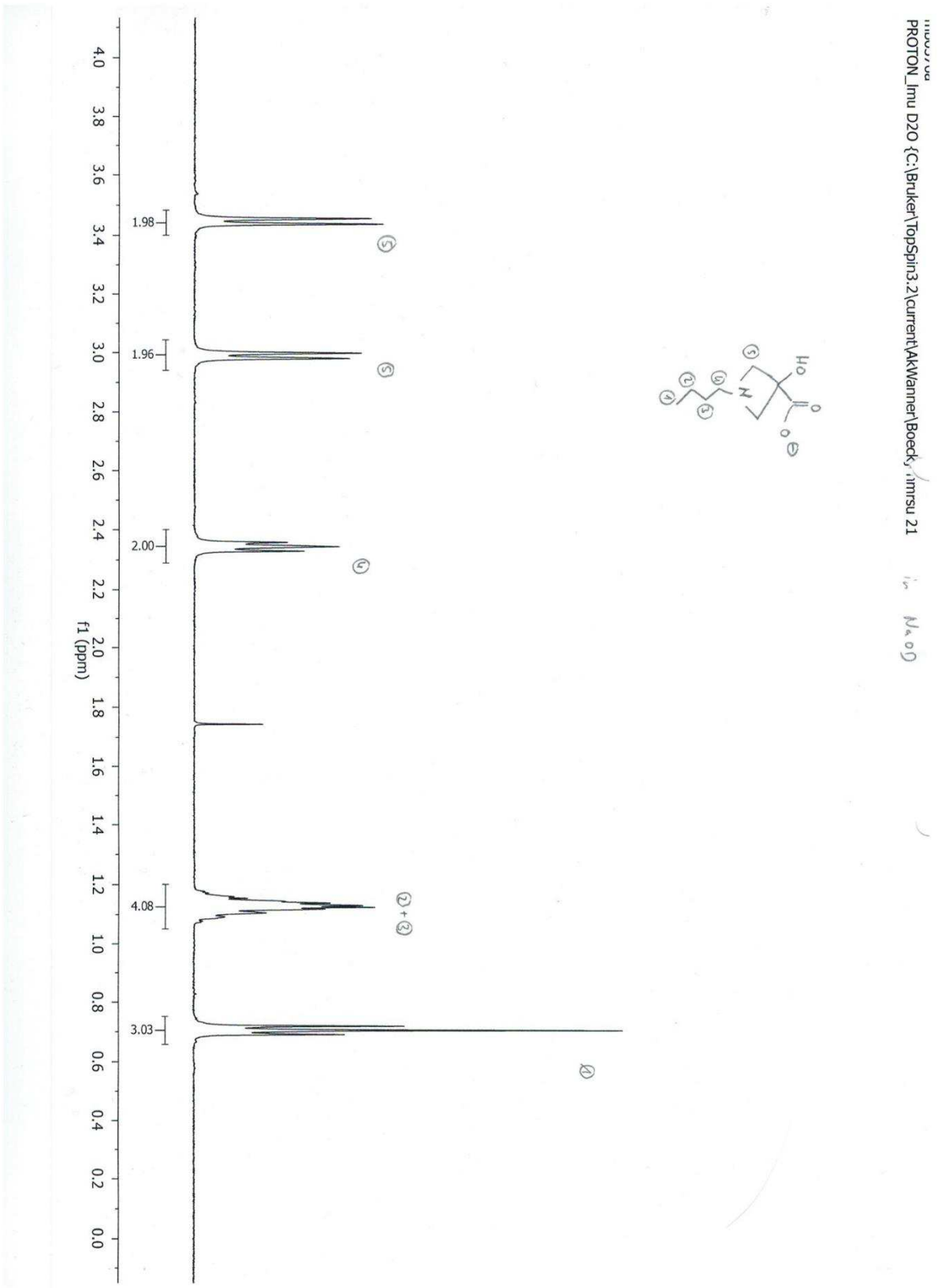

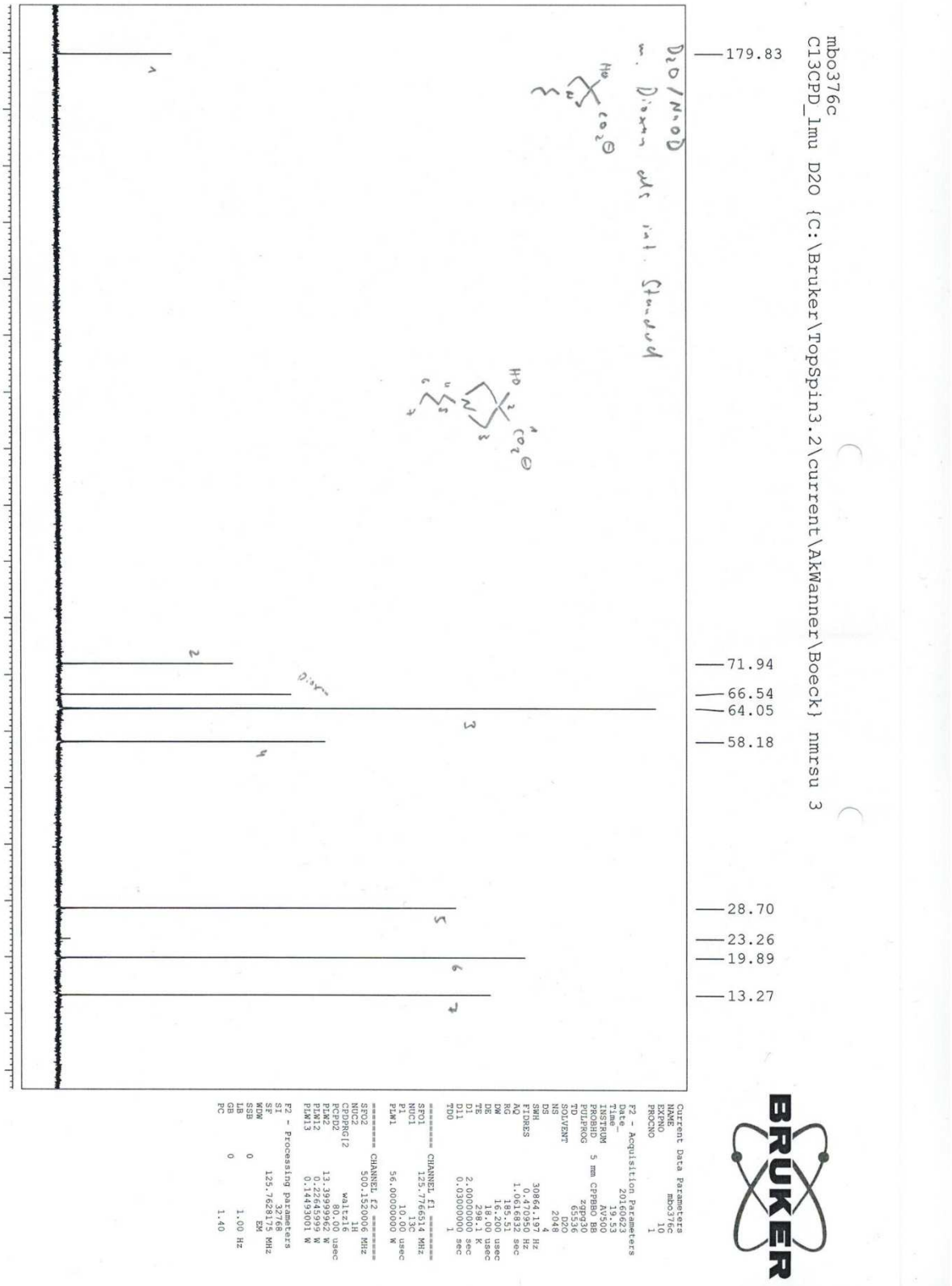
mbo376c
C13CPD_1mu D20 {C:\Bruker\TopSpin3.2\current\AkWanner\Boeck} nmrsu 3
179.83
71.94
66.54
64.05
58.18
28.70
23.26
19.89
13.27
D2O / NaOD
Current Data Parameters
NAME mbo376c
EXPNO 10
PROCNO 1
F2 - Acquisition Parameters
Date_ 20160623
Time 19.53
INSTRUM spect
PROBHD 5 mm CPPBBO BB
PULPROG zgpg30
TD 65536
SOLVENT D2O
NS 2048
DS 16
SWH 30864.197 Hz
FIDRES 0.470950 Hz
AQ 1.0616832 sec
RG 185.51
DW 16.200 usec
DE 18.00 usec
TE 298.0 K
D1 2.00000001 sec
D11 0.03000000 sec
TD0 1
======== CHANNEL f1 ========
SFO1 125.7765314 MHz
NUC1 13C
P1 10.00 usec
PLW1 56.00000000 W
======== CHANNEL f2 ========
SFO2 500.1520006 MHz
NUC2 1H
CPDPRG[2 waltz16
PCPD2 80.00 usec
PLW2 13.39999962 W
PLW12 0.22645999 W
PLW13 0.14493001 W
F2 - Processing parameters
SI 32768
SF 125.7628175 MHz
WDW EM
SSB 0
LB 1.00 Hz
GB 0
PC 1.40

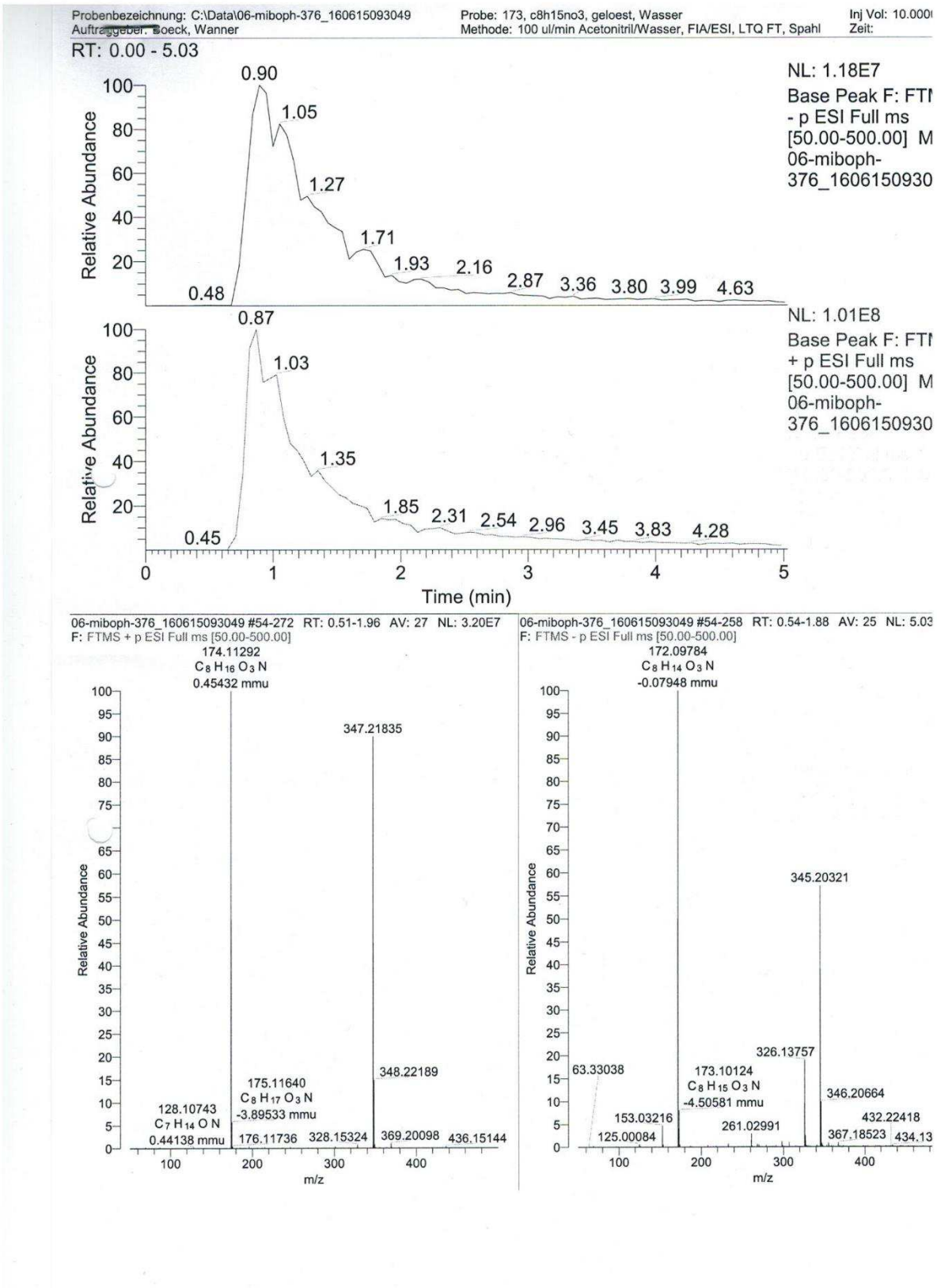
Probenbezeichnung: C:\Data\06-miboph-376_160615093049
Auftraggeber: Boeck, Wanner
Probe: 173, c8h15no3, geloest, Wasser
Methode: 100 ul/min Acetonitril/Wasser, FIA/ESI, LTQ FT, Spahl
Inj Vol: 10.000
Zeit:
RT: 0.00 - 5.03
NL: 1.18E7
Base Peak F: FTI
- p ESI Full ms
[50.00-500.00] M
06-miboph-
376_1606150930
Relative Abundance
0.90
1.05
1.27
1.71
1.93
2.16
2.87
3.36
3.80
3.99
4.63
0.48
NL: 1.01E8
Base Peak F: FTI
+ p ESI Full ms
[50.00-500.00] M
06-miboph-
376_1606150930
0.87
1.03
1.35
1.85
2.31
2.54
2.96
3.45
3.83
4.28
0.45
Time (min)
06-miboph-376_160615093049 #54-272 RT: 0.51-1.96 AV: 27 NL: 3.20E7
F: FTMS + p ESI Full ms [50.00-500.00]
174.11292
C8 H16 O3 N
0.45432 mmu
347.21835
348.22189
175.11640
C8 H17 O3 N
-3.89533 mmu
128.10743
C7 H14 O N
0.44138 mmu
176.11736
328.15324
369.20098
436.15144
m/z
06-miboph-376_160615093049 #54-258 RT: 0.54-1.88 AV: 25 NL: 5.03
F: FTMS - p ESI Full ms [50.00-500.00]
172.09784
C8 H14 O3 N
-0.07948 mmu
345.20321
326.13757
63.33038
173.10124
C8 H15 O3 N
-4.50581 mmu
346.20664
153.03216
261.02991
432.22418
125.00084
367.18523
434.13
m/z

Ethyl 2-(1-benzhydryl-3-hydroxyazetidin-3-yl)acetate (11e)

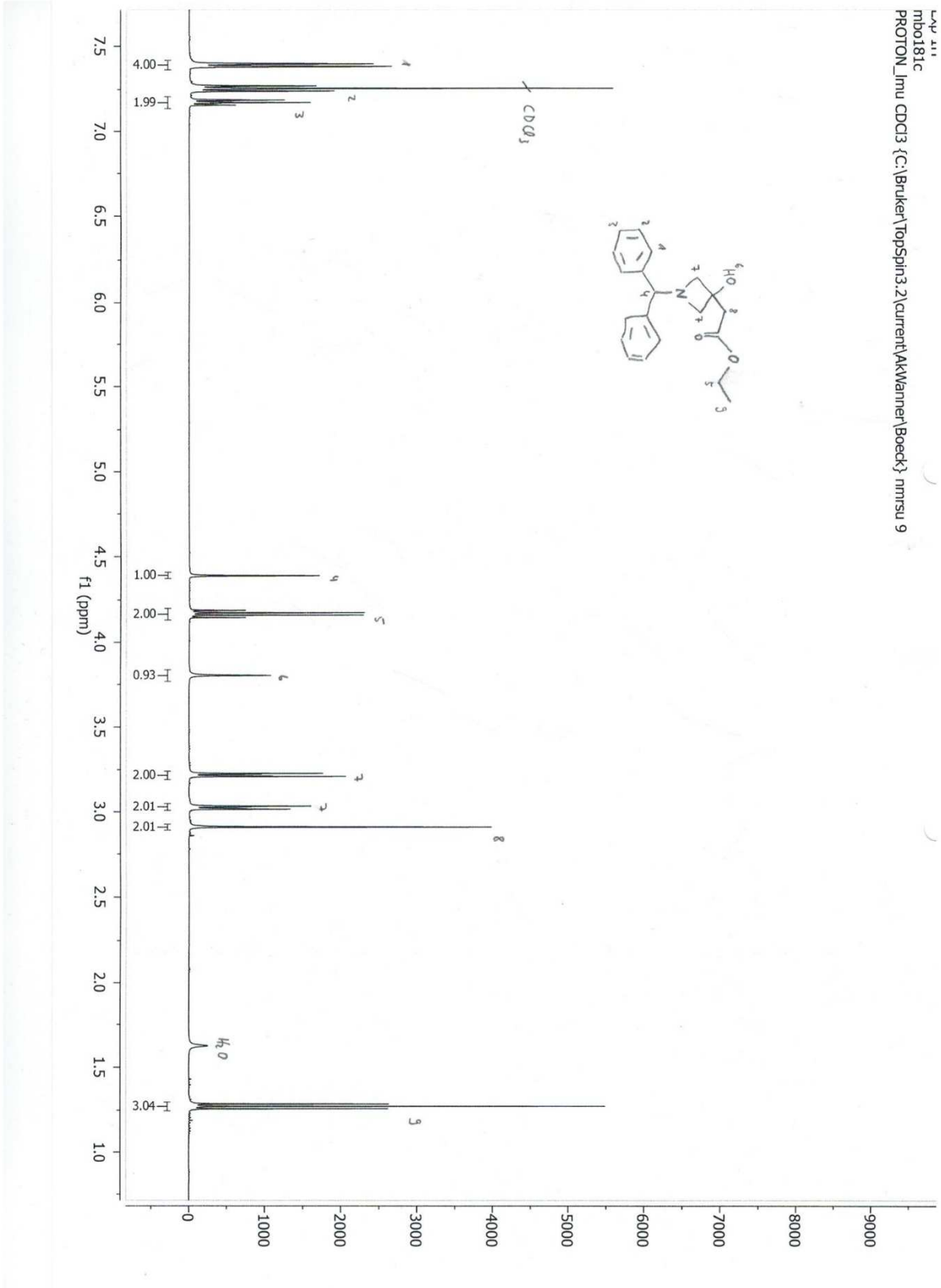

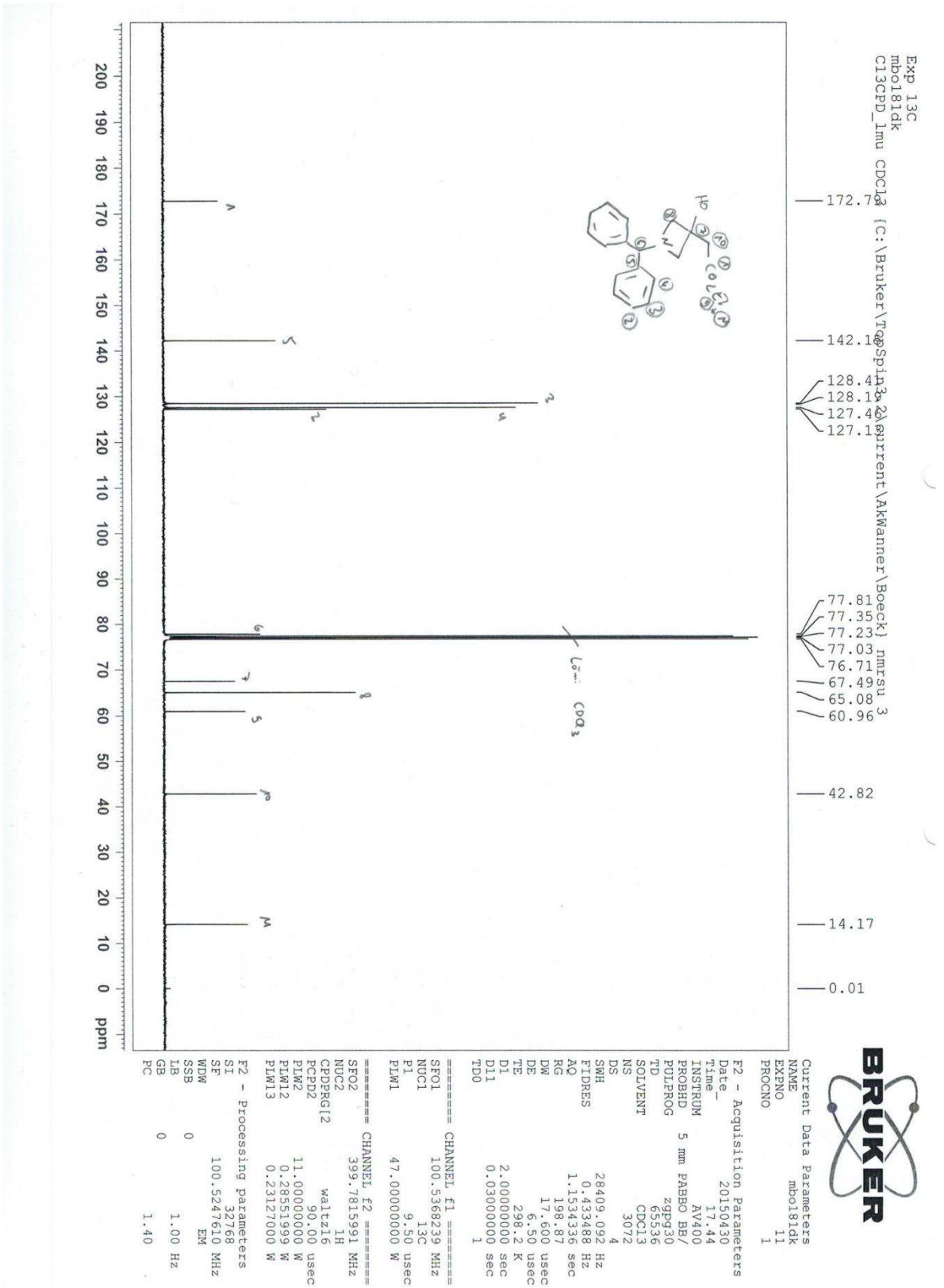
Exp 13C
mbo181dk
C13CPD_lmu CDCl3 {C:\Bruker\TopSpin3.2\current\AkWanner\Boeck} nmrsu 3
172.78
142.18
128.43
128.13
127.42
127.13
77.81
77.35
77.23
77.03
76.71
67.49
65.08
60.96
42.82
14.17
0.01
CDCl3
A
S
2
4
6
7
8
5
9
M
200 190 180 170 160 150 140 130 120 110 100 90 80 70 60 50 40 30 20 10 0 ppm
Current Data Parameters
NAME mbo181dk
EXPNO 11
PROCNO 1
F2 - Acquisition Parameters
Date_ 20150430
Time_ 17.44
INSTRUM AV400
PROBHD 5 mm PABBO BB/
PULPROG zgpg30
TD 65536
SOLVENT CDCl3
NS 3072
DS 4
SWH 28409.092 Hz
FIDRES 0.433488 Hz
AQ 1.1534336 sec
RG 198.87
DW 17.600 usec
DE 6.50 usec
TE 298.2 K
D1 2.00000000 sec
D11 0.03000000 sec
TD0 1
======== CHANNEL f1 ========
SFO1 100.5368239 MHz
NUC1 13C
P1 9.50 usec
PLW1 47.00000000 W
======== CHANNEL f2 ========
SFO2 399.7815991 MHz
NUC2 1H
CPDPRG[2 waltz16
PCPD2 90.00 usec
PLW2 11.00000000 W
PLW12 0.28551999 W
PLW13 0.23127000 W
F2 - Processing parameters
SI 32768
SF 100.5247610 MHz
WDW EM
SSB 0
LB 1.00 Hz
GB 0
PC 1.40

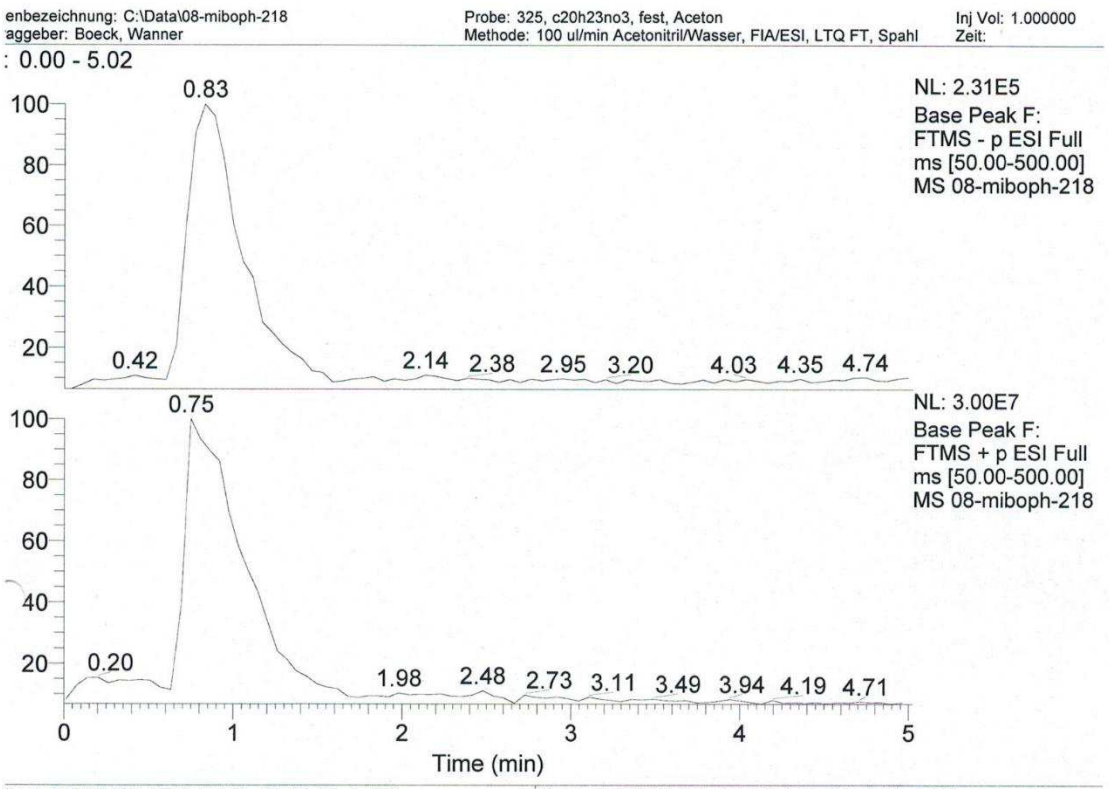
enbezeichnung: C:\Data\08-miboph-218
aggeber: Boeck, Wanner
Probe: 325, c20h23no3, fest, Aceton
Methode: 100 ul/min Acetonitril/Wasser, FIA/ESI, LTQ FT, Spahl
Inj Vol: 1.000000
Zeit:
: 0.00 - 5.02
NL: 2.31E5
Base Peak F:
FTMS - p ESI Full
ms [50.00-500.00]
MS 08-miboph-218
0.83
0.42
2.14 2.38 2.95 3.20 4.03 4.35 4.74
NL: 3.00E7
Base Peak F:
FTMS + p ESI Full
ms [50.00-500.00]
MS 08-miboph-218
0.75
0.20
1.98 2.48 2.73 3.11 3.49 3.94 4.19 4.71
Time (min)

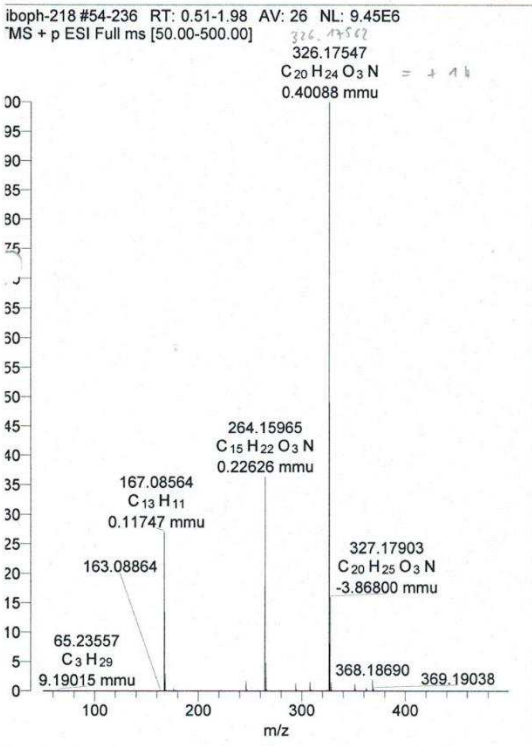
iboph-218 #54-236 RT: 0.51-1.98 AV: 26 NL: 9.45E6
MS + p ESI Full ms [50.00-500.00]
326.17547
C20 H24 O3 N
0.40088 mmu
264.15965
C15 H22 O3 N
0.22626 mmu
167.08564
C13 H11
0.11747 mmu
163.08864
327.17903
C20 H25 O3 N
-3.86800 mmu
65.23557
C3 H29
9.19015 mmu
368.18690
369.19038
m/z

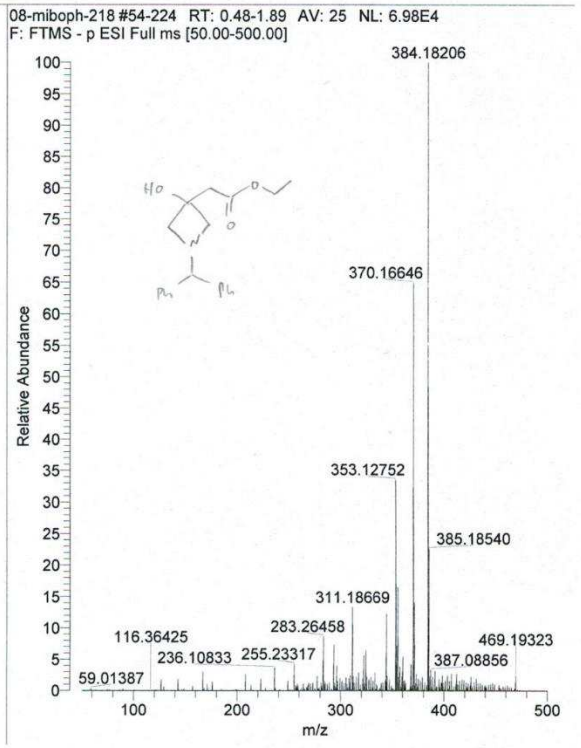
08-miboph-218 #54-224 RT: 0.48-1.89 AV: 25 NL: 6.98E4
F: FTMS - p ESI Full ms [50.00-500.00]
384.18206
370.16646
353.12752
385.18540
311.18669
283.26458
116.36425
236.10833
255.23317
469.19323
387.08856
59.01387
Relative Abundance
m/z

Ethyl 2-(1-butyl-3-hydroxyazetidin-3-yl)acetate (11f)

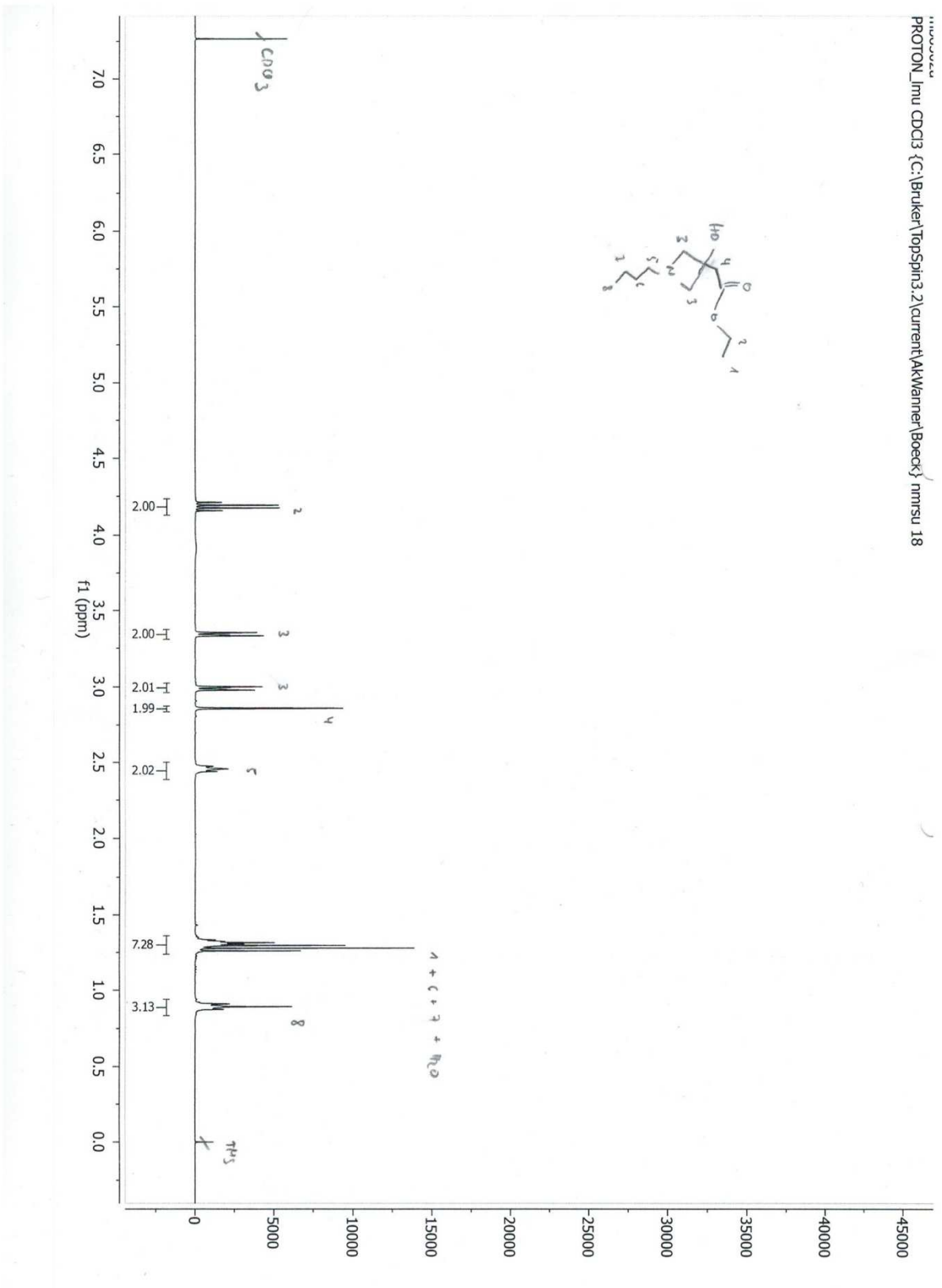

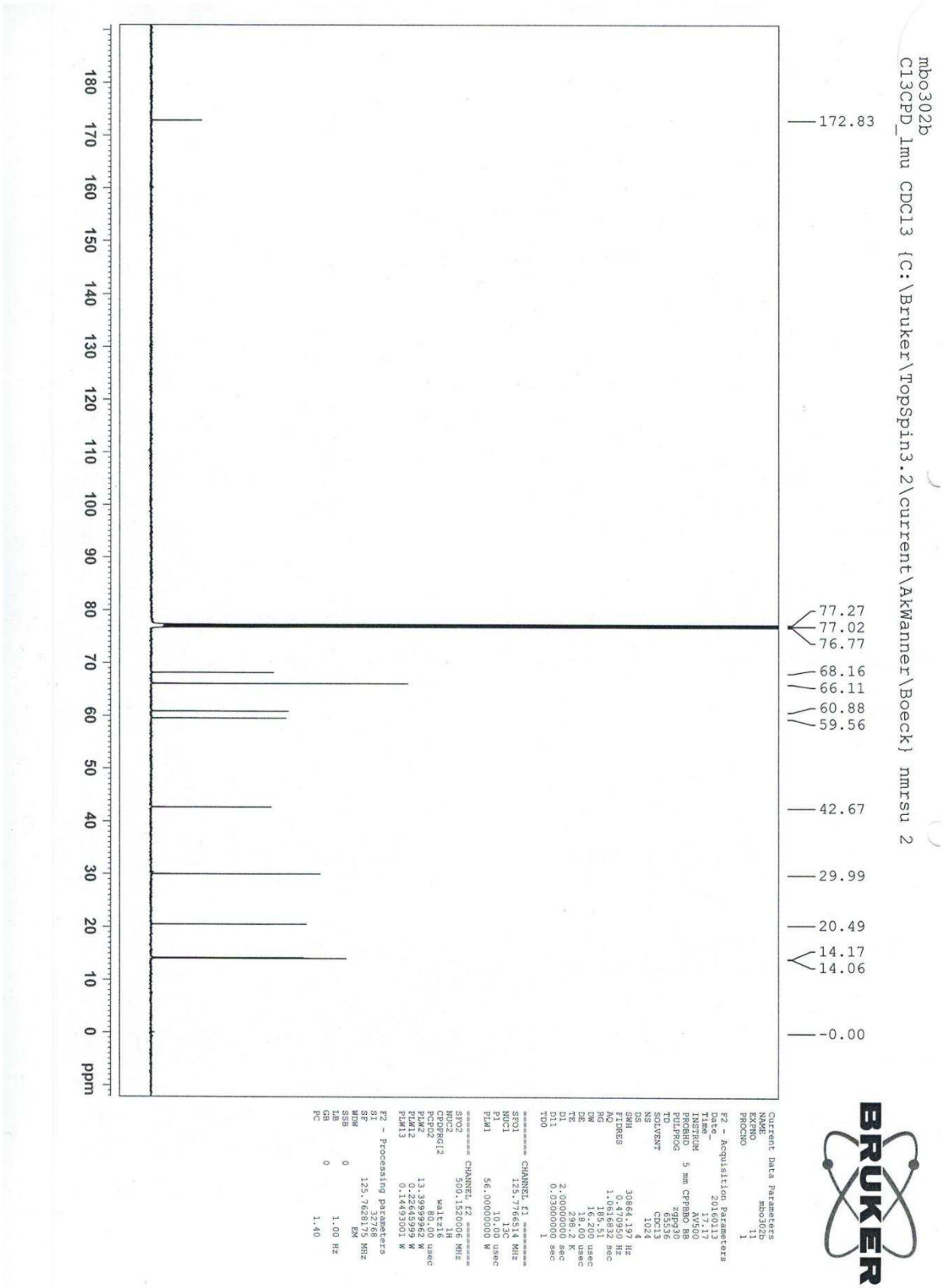
mbo302b
C13CPD_lmu CDCl3 {C:\Bruker\TopSpin3.2\current\AkWanner\Boeck} nmrsu 2
172.83
77.27
77.02
76.77
68.16
66.11
60.88
59.56
42.67
29.99
20.49
14.17
14.06
-0.00
180 170 160 150 140 130 120 110 100 90 80 70 60 50 40 30 20 10 0 ppm
Current Data Parameters
NAME mbo302b
EXPNO 11
PROCNO 1
F2 - Acquisition Parameters
Date_ 20160113
Time_ 17.17
INSTRUM AVS00
PROBHD 5 mm CPFBBO BB
PULPROG zgpg30
TD 65536
SOLVENT CDCl3
NS 1024
DS 4
SWH 30864.197 Hz
FIDRES 0.470950 Hz
AQ 1.0616832 sec
RG 16.5
DW 16.200 usec
DE 18.00 usec
TE 298.2 K
D1 2.00000000 sec
D11 0.03000000 sec
TD0 1
======== CHANNEL f1 ========
SFO1 125.7766514 MHz
NUC1 13C
P1 10.00 usec
PLW1 56.00000000 W
======== CHANNEL f2 ========
SFO2 500.1520006 MHz
NUC2 1H
CPDPRG2 waltz16
PCPD2 100.00 usec
PLW2 13.38999100 W
PLW12 0.22645999 W
PLW13 0.14493001 W
F2 - Processing parameters
SI 32768
SF 125.7628173 MHz
WDW EM
SSB 0
LB 1.00 Hz
GB 0
PC 1.40
BRUKER

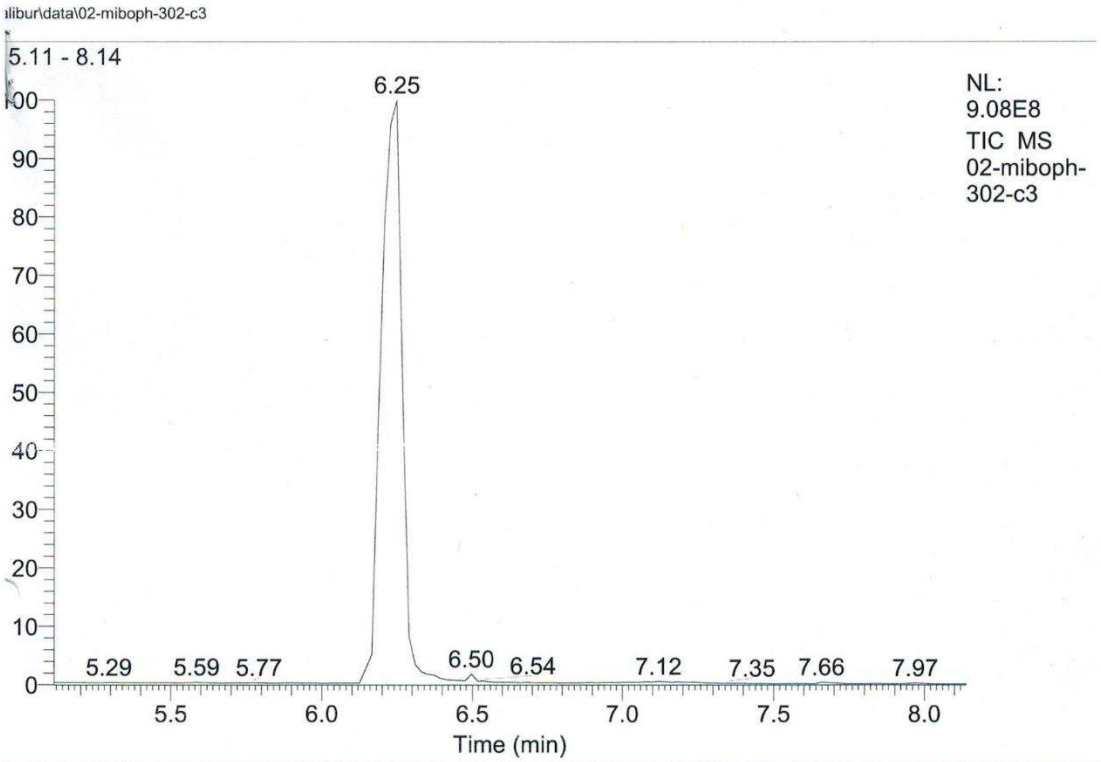

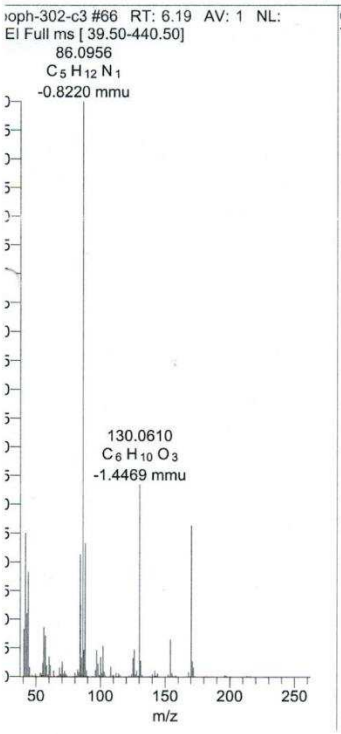

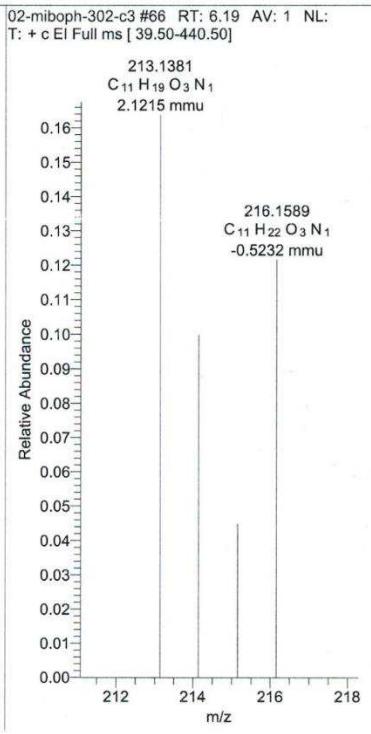

02-miboph-302-c3#66 RT: 6.19
T: + c EI Full ms [39.50-440.50]
m/z= 37.50-262.26

m/z	Intensity	Relative	Flags
40.4761	2112687.0	2.22	
40.4922	7910372.0	8.31	
41.6811	2685138.0	2.82	
41.7073	23805184.0	25.01	
42.7888	6440697.0	6.77	
42.8144	10520064.0	11.05	
43.8888	17382656.0	18.26	
55.0257	2219598.0	2.33	
55.0615	2270441.0	2.39	
56.0332	8214950.0	8.63	
56.0571	3573215.0	3.75	
57.0402	2140959.0	2.25	
57.0656	6785070.0	7.13	
57.0754	6381896.0	6.70	
58.0474	1865959.0	1.96	
60.0254	3312589.0	3.48	
61.0330	1848141.0	1.94	
70.0653	2540570.0	2.67	
84.0197	20289280.0	21.31	
84.0794	12029440.0	12.64	
85.0262	3098529.0	3.25	
86.0600	2600322.0	2.73	
86.0956	95193600.0	100.00	
87.0989	4390256.0	4.61	
88.0513	22135808.0	23.25	
97.0286	4376476.0	4.60	
98.0972	2128367.0	2.24	
100.1127	3216012.0	3.38	
102.0314	5065341.0	5.32	
125.0597	3083442.0	3.24	
126.0553	4498355.0	4.73	
130.0610	31821568.0	33.43	
131.0672	2645581.0	2.78	
154.0859	6122457.0	6.43	
170.1178	25043712.0	26.31	
171.1219	2569792.0	2.70	

2/6 9/12

2-(1-Butyl-3-hydroxyazetidin-3-yl)acetic acid (11g)

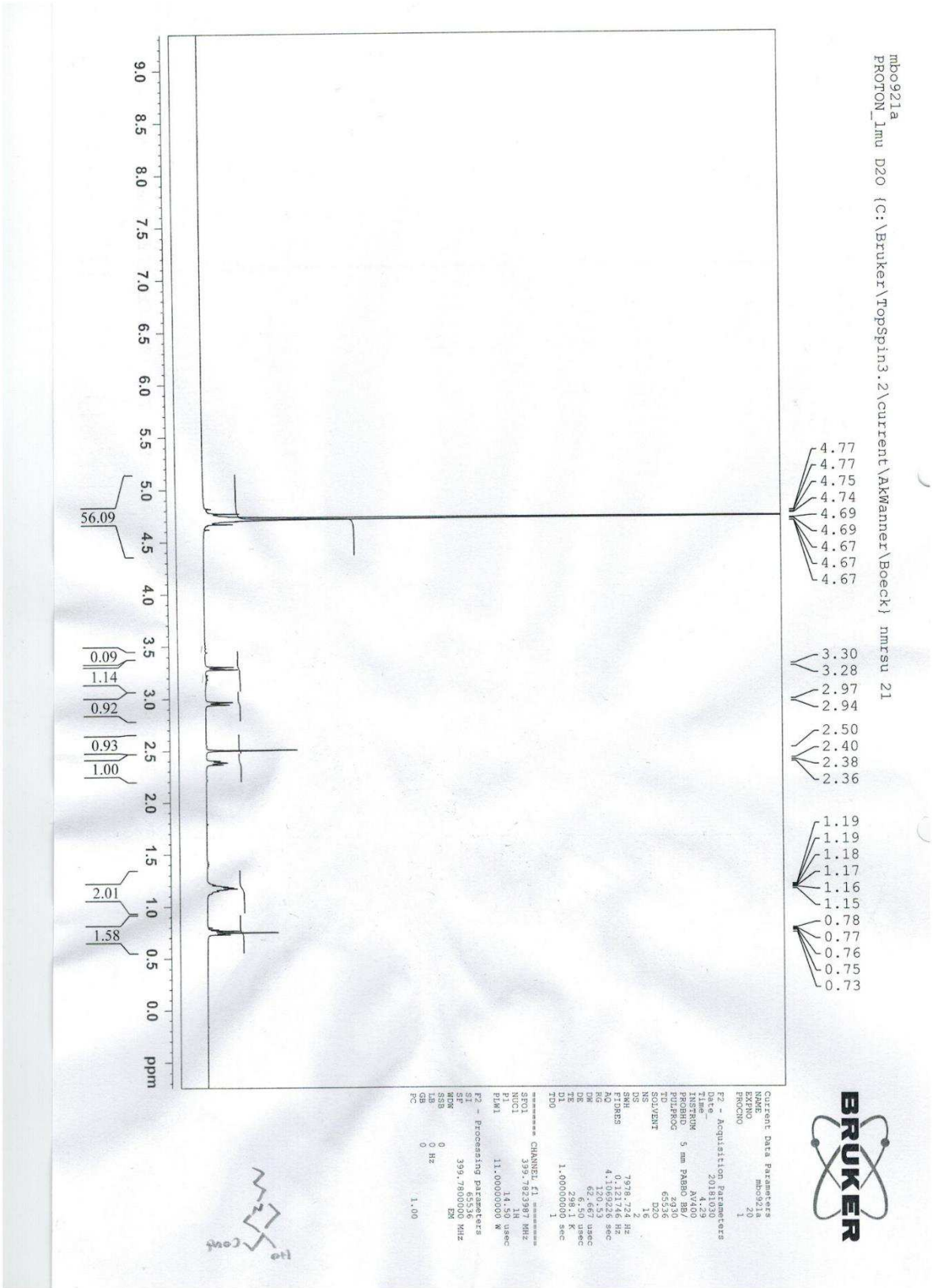

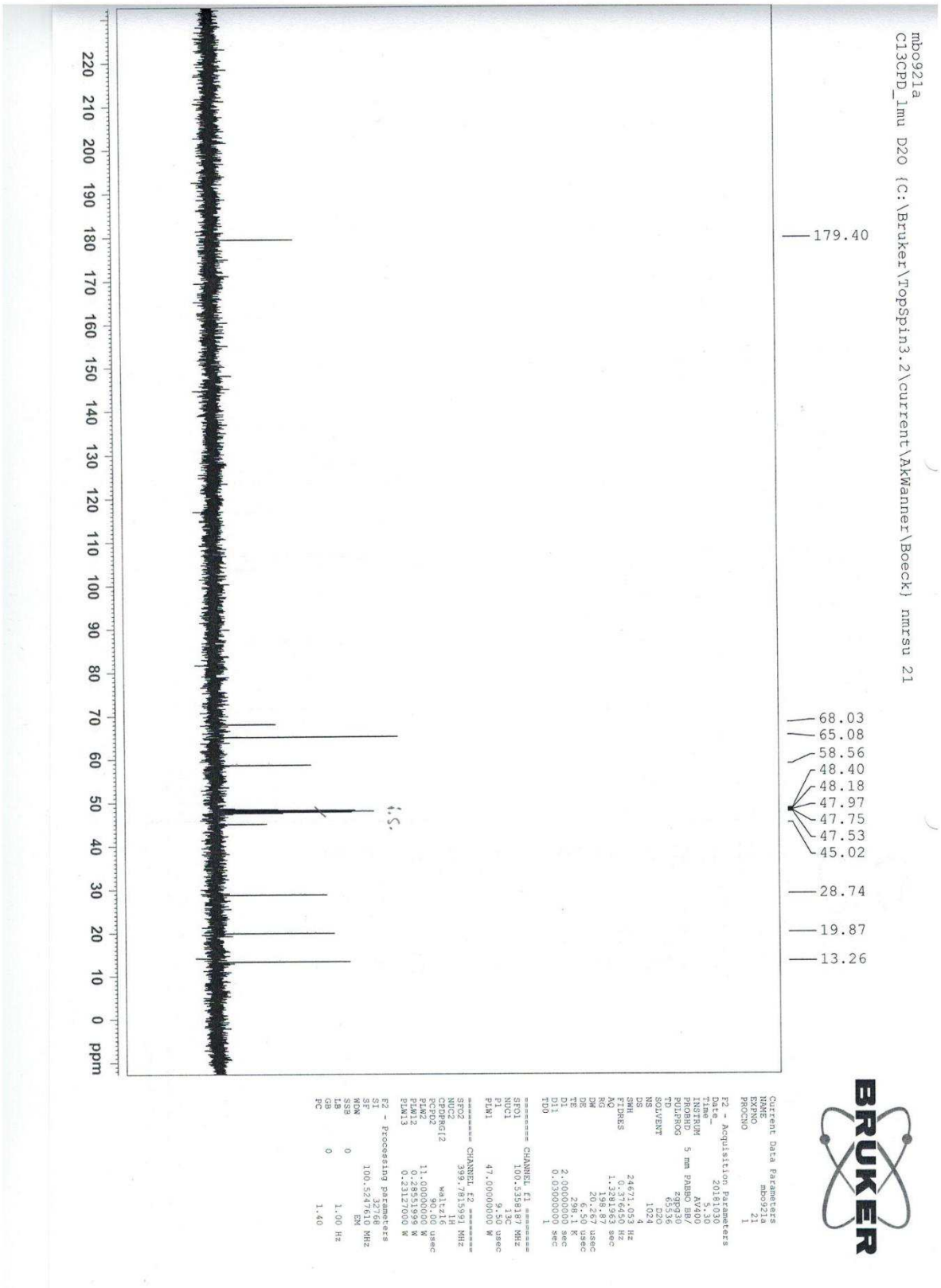
mbo921a
C13CPD_1mu D2O {C:\Bruker\TopSpin3.2\current\AkWanner\Boeck} nmrsu 21
179.40
68.03
65.08
58.56
48.40
48.18
47.97
47.75
47.53
45.02
28.74
19.87
13.26
220 210 200 190 180 170 160 150 140 130 120 110 100 90 80 70 60 50 40 30 20 10 0 ppm
Current Data Parameters
NAME mbo921a
EXPNO 2
PROCNO 1
F2 - Acquisition Parameters
Date_ 20181030
Time 5.30
INSTRUM AV400
PROBHD 5 mm PABBO BB/
PULPROG zgpg30
TD 65536
SOLVENT D2O
NS 1024
DS 4
SWH 24671.053 Hz
FIDRES 0.376450 Hz
AQ 1.3281963 sec
RG 198.87
DW 20.267 usec
DE 6.50 usec
TE 298.1 K
D1 2.00000000 sec
D11 0.03000000 sec
TD0 1
======== CHANNEL f1 ========
SFO1 100.5358187 MHz
NUC1 13C
P1 9.50 usec
PLW1 47.00000000 W
======== CHANNEL f2 ========
SFO2 399.7815991 MHz
NUC2 1H
CPDPRG2 waltz16
PCPD2 90.00 usec
PLW2 11.00000000 W
PLW12 0.28551999 W
PLW13 0.23127000 W
F2 - Processing parameters
SI 32768
SF 100.5247610 MHz
WDW EM
SSB 0
LB 1.00 Hz
GB 0
PC 1.40

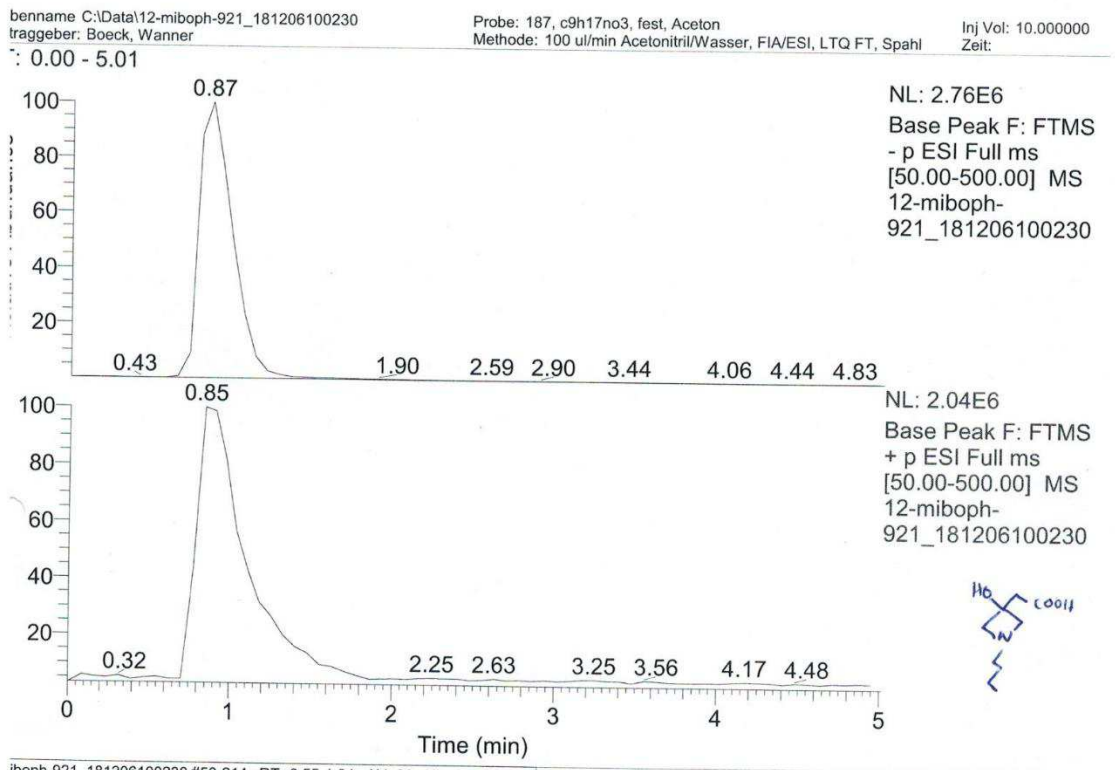
benname C:\Data\12-miboph-921_181206100230
traggeber: Boeck, Wanner
Probe: 187, c9h17no3, fest, Aceton
Methode: 100 ul/min Acetonitril/Wasser, FIA/ESI, LTQ FT, Spahl
Inj Vol: 10.000000
Zeit:
: 0.00 - 5.01
NL: 2.76E6
Base Peak F: FTMS - p ESI Full ms [50.00-500.00] MS 12-miboph-921_181206100230
0.87
0.43
1.90
2.59
2.90
3.44
4.06
4.44
4.83
NL: 2.04E6
Base Peak F: FTMS + p ESI Full ms [50.00-500.00] MS 12-miboph-921_181206100230
0.85
0.32
2.25
2.63
3.25
3.56
4.17
4.48
Time (min)

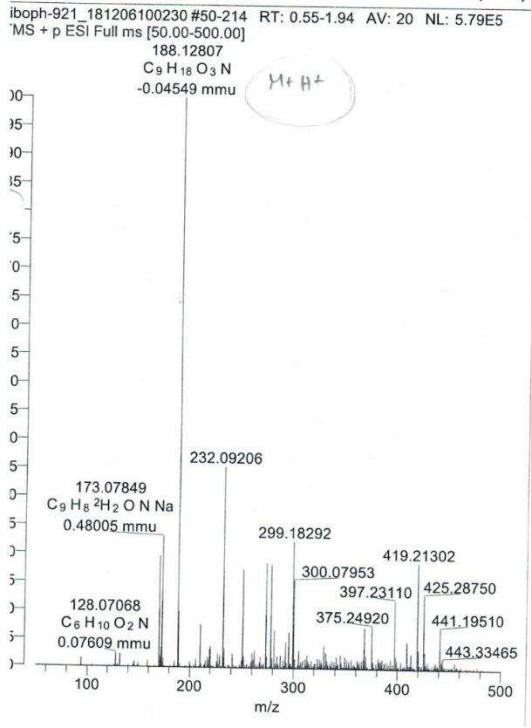
iboph-921_181206100230 #50-214 RT: 0.55-1.94 AV: 20 NL: 5.79E5
MS + p ESI Full ms [50.00-500.00]
188.12807
C9 H18 O3 N
-0.04549 mmu
M+H+
232.09206
173.07849
C9 H8 2H2 O N Na
0.48005 mmu
299.18292
419.21302
300.07953
397.23110
425.28750
128.07068
C6 H10 O2 N
0.07609 mmu
375.24920
441.19510
443.33465
m/z

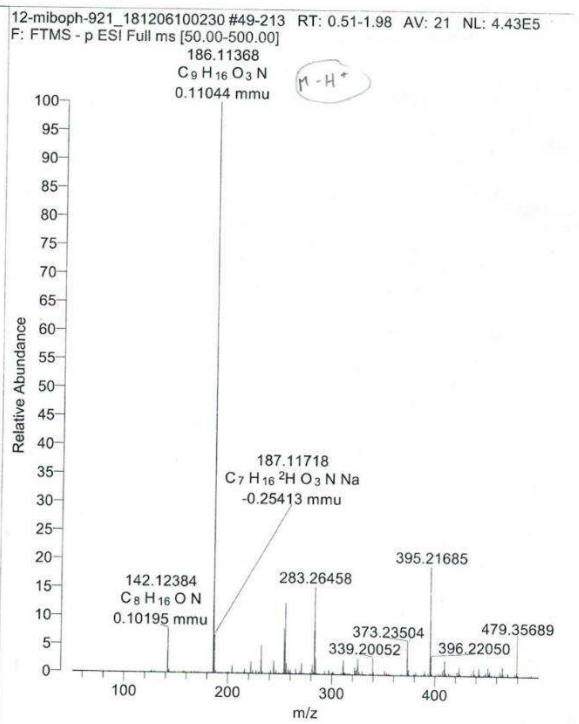
12-miboph-921_181206100230 #49-213 RT: 0.51-1.98 AV: 21 NL: 4.43E5
F: FTMS - p ESI Full ms [50.00-500.00]
186.11368
C9 H16 O3 N
0.11044 mmu
M-H+
Relative Abundance
187.11718
C7 H16 2H O3 N Na
-0.25413 mmu
142.12384
C8 H16 O N
0.10195 mmu
283.26458
395.21685
373.23504
339.20052
396.22050
479.35689
m/z

Ethyl 2-(1-benzyl-3-hydroxypyrrolidin-3-yl)acetate (12e)

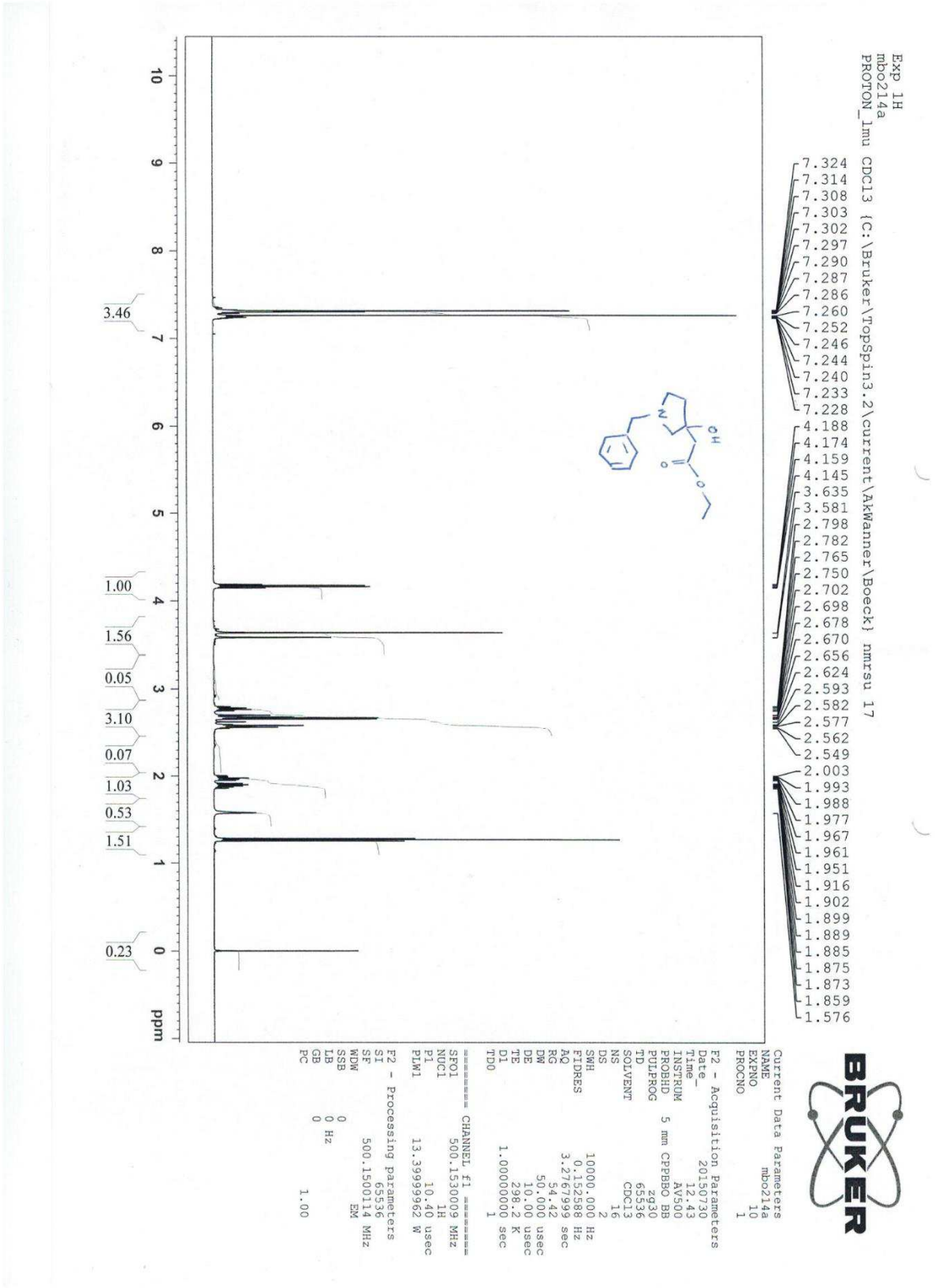

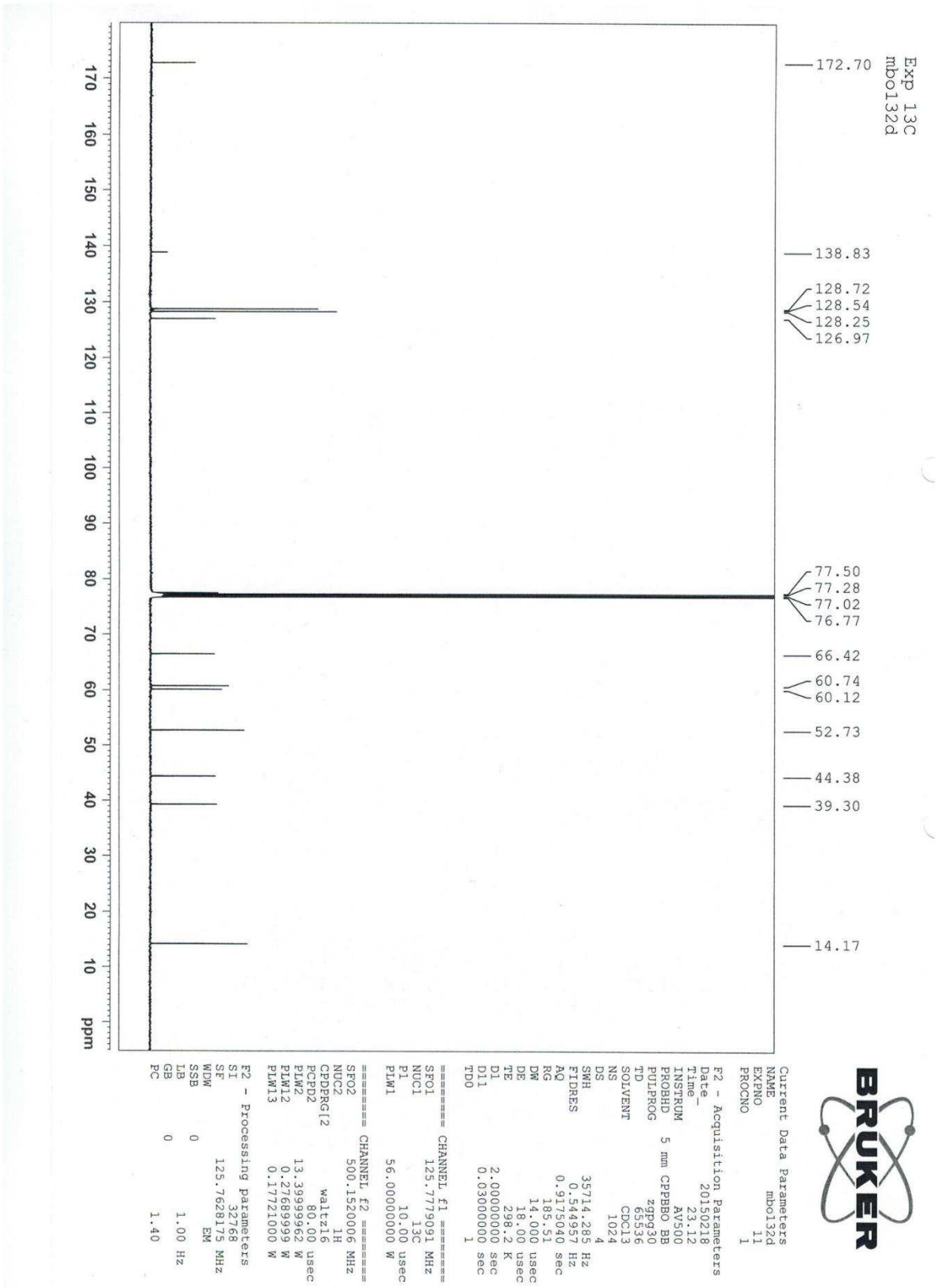
Exp 13C
mbo132d
172.70
138.83
128.72
128.54
128.25
126.97
77.50
77.28
77.02
76.77
66.42
60.74
60.12
52.73
44.38
39.30
14.17
170 160 150 140 130 120 110 100 90 80 70 60 50 40 30 20 10 ppm
Current Data Parameters
NAME mbo132d
EXPNO 11
PROCNO 1
F2 - Acquisition Parameters
Date_ 20150218
Time 23.12
INSTRUM AV500
PROBHD 5 mm CPPBBO BB
PULPROG zgpg30
TD 65536
SOLVENT CDCl3
NS 1024
DS 4
SWH 35714.285 Hz
FIDRES 0.544957 Hz
AQ 0.9175040 sec
RG 185.51
DW 14.000 usec
DE 18.00 usec
TE 298.2 K
D1 2.00000000 sec
D11 0.03000000 sec
TD0 1
======== CHANNEL f1 ========
SFO1 125.7779091 MHz
NUC1 13C
P1 10.00 usec
PLW1 56.00000000 W
======== CHANNEL f2 ========
SFO2 500.1520006 MHz
NUC2 1H
CPDPRG[2 waltz16
PCPD2 80.00 usec
PLW2 13.39999962 W
PLW12 0.27689999 W
PLW13 0.17721000 W
F2 - Processing parameters
SI 32768
SF 125.7628175 MHz
WDW EM
SSB 0
LB 1.00 Hz
GB 0
PC 1.40

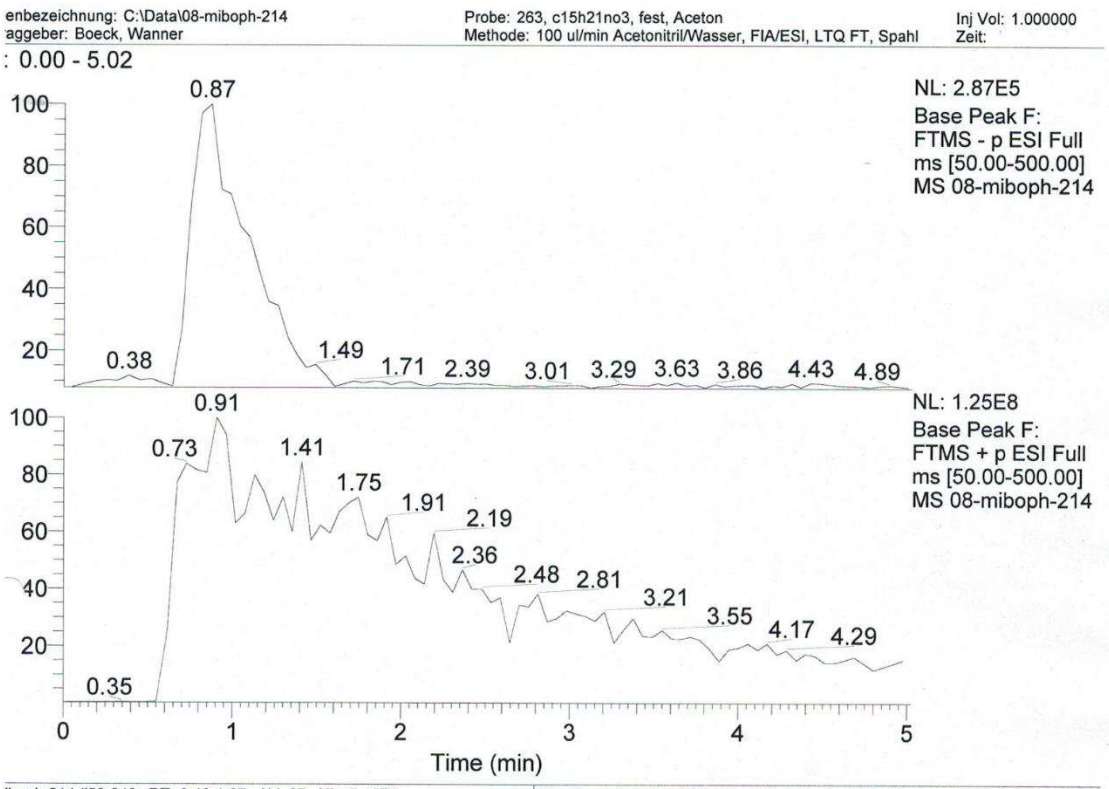
enbezeichnung: C:\Data\08-miboph-214
aggeber: Boeck, Wanner
Probe: 263, c15h21no3, fest, Aceton
Methode: 100 ul/min Acetonitril/Wasser, FIA/ESI, LTQ FT, Spahl
Inj Vol: 1.000000
Zeit:
: 0.00 - 5.02
NL: 2.87E5
Base Peak F:
FTMS - p ESI Full
ms [50.00-500.00]
MS 08-miboph-214
0.87
0.38
1.49
1.71
2.39
3.01
3.29
3.63
3.86
4.43
4.89
NL: 1.25E8
Base Peak F:
FTMS + p ESI Full
ms [50.00-500.00]
MS 08-miboph-214
0.91
0.73
1.41
1.75
1.91
2.19
2.36
2.48
2.81
3.21
3.55
4.17
4.29
0.35
Time (min)

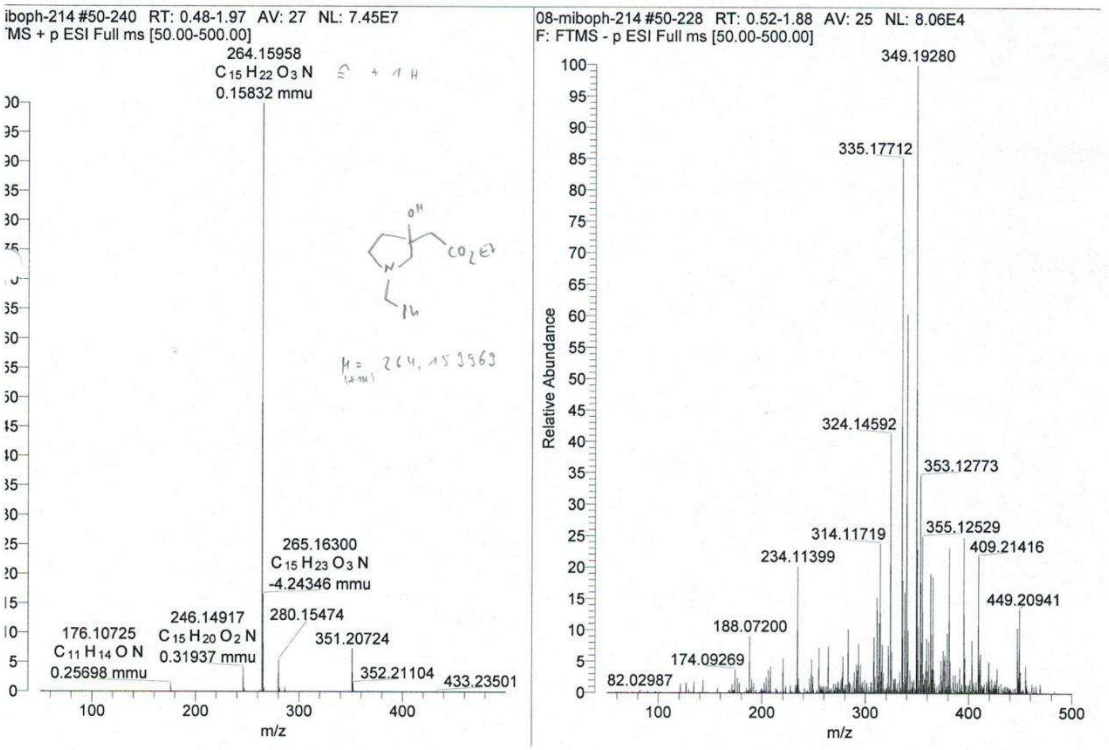
iboph-214 #50-240 RT: 0.48-1.97 AV: 27 NL: 7.45E7
MS + p ESI Full ms [50.00-500.00]
264.15958
C15 H22 O3 N
0.15832 mmu
265.16300
C15 H23 O3 N
-4.24346 mmu
246.14917
C15 H20 O2 N
0.31937 mmu
280.15474
351.20724
352.21104
433.23501
176.10725
C11 H14 O N
0.25698 mmu
m/z
08-miboph-214 #50-228 RT: 0.52-1.88 AV: 25 NL: 8.06E4
F: FTMS - p ESI Full ms [50.00-500.00]
349.19280
335.17712
324.14592
353.12773
355.12529
314.11719
409.21416
234.11399
449.20941
188.07200
174.09269
82.02987
Relative Abundance
m/z

Ethyl 2-(1-butyl-3-hydroxypyrrolidin-3-yl)acetate (12f)

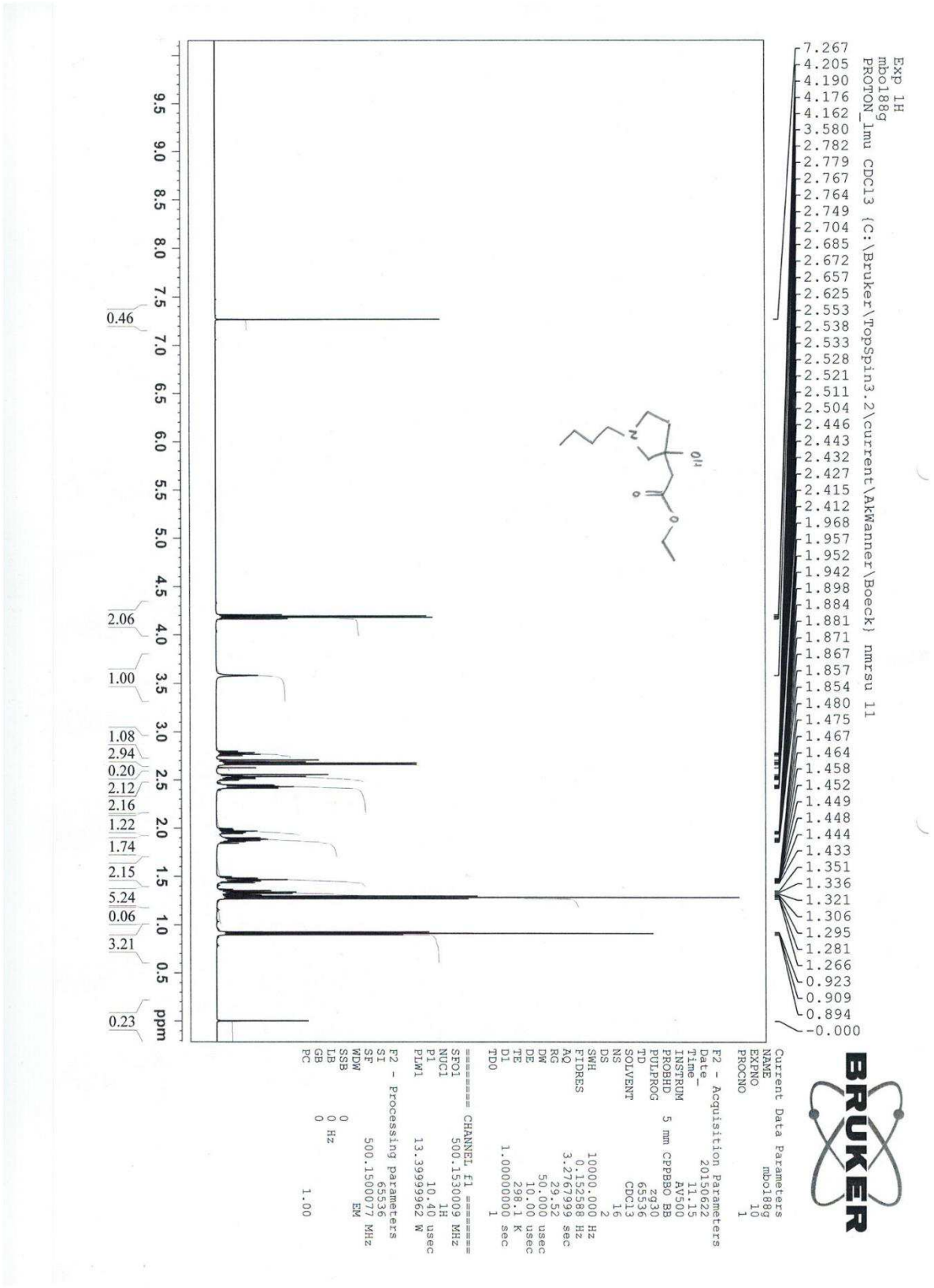

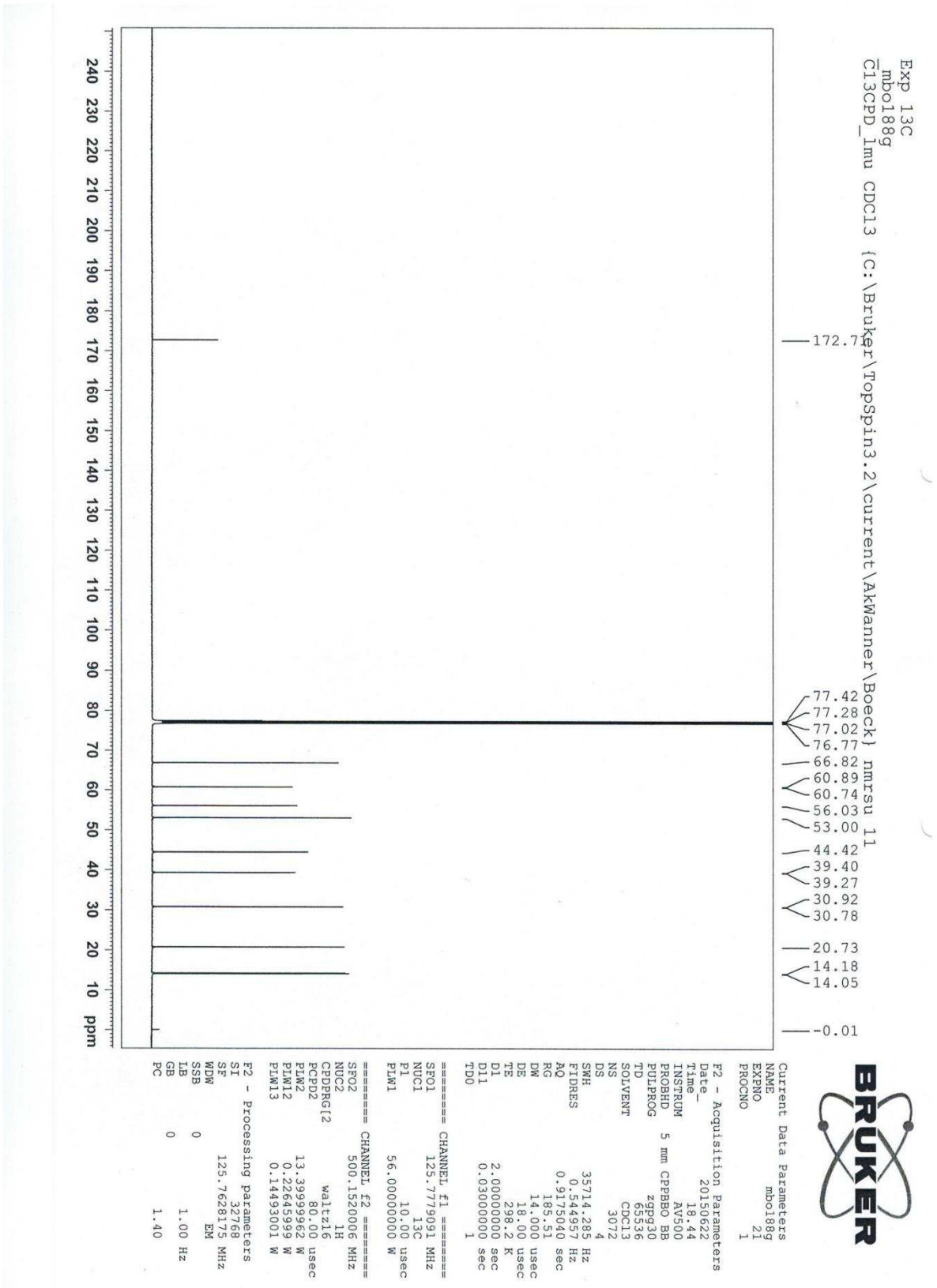
Exp 13C
_mbo188g
C13CPD_lmu CDC13 {C:\Bruker\TopSpin3.2\current\AkWanner\Boeck} nmrsu 11
172.78
77.42
77.28
77.02
76.77
66.82
60.89
60.74
56.03
53.00
44.42
39.40
39.27
30.92
30.78
20.73
14.18
14.05
-0.01
240 230 220 210 200 190 180 170 160 150 140 130 120 110 100 90 80 70 60 50 40 30 20 10 ppm
BRUKER
Current Data Parameters
NAME mbo188g
EXPNO 21
PROCNO 1
F2 - Acquisition Parameters
Date_ 20150622
Time_ 18.44
INSTRUM AV500
PROBHD 5 mm CPPBBO BB
PULPROG zgpg30
TD 65536
SOLVENT CDC13
NS 3072
DS 4
SWH 35714.285 Hz
FIDRES 0.544957 Hz
AQ 0.9175040 sec
RG 185.51
DW 14.000 usec
DE 18.00 usec
TE 298.2 K
D1 2.00000000 sec
D11 0.03000000 sec
TD0 1
======== CHANNEL f1 ========
SFO1 125.7779091 MHz
NUC1 13C
PL1 10.00 usec
PLW1 56.00000000 W
======== CHANNEL f2 ========
SFO2 500.1520006 MHz
NUC2 1H
CPDPRG[2 waltz16
PCPD2 80.00 usec
PLW2 13.39999962 W
PLW12 0.22645999 W
PLW13 0.14493001 W
F2 - Processing parameters
SI 32768
SF 125.7628175 MHz
WDW EM
SSB 0
LB 1.00 Hz
GB 0
PC 1.40

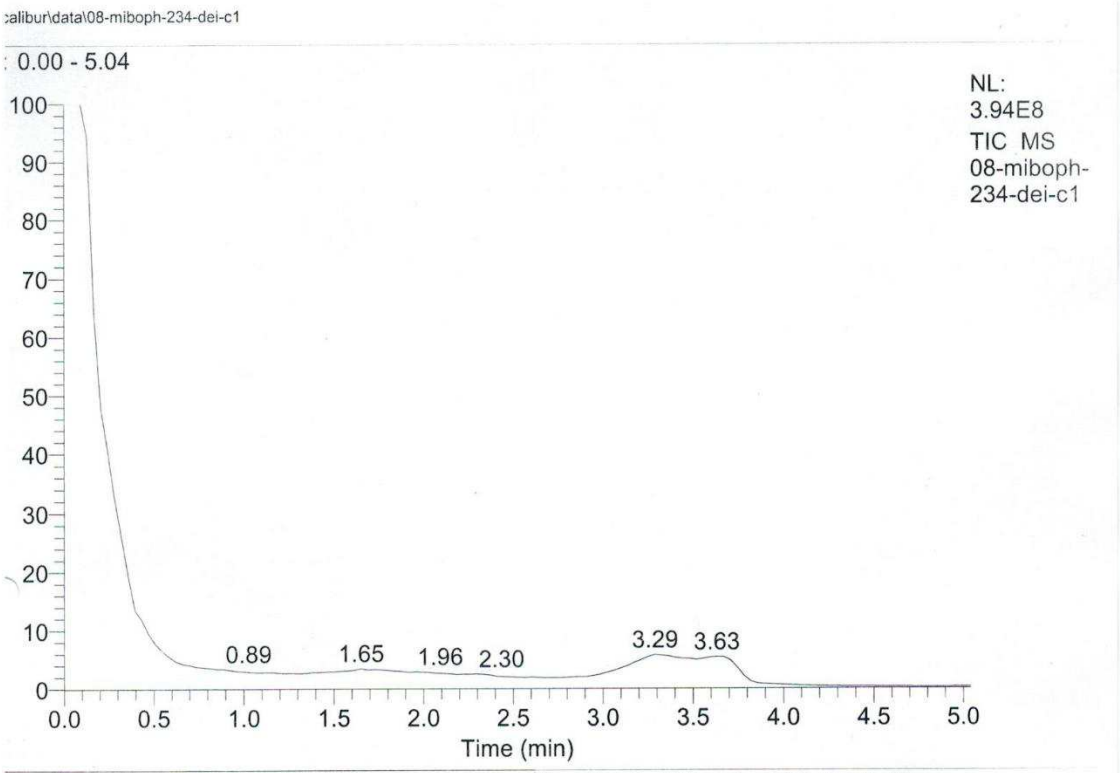

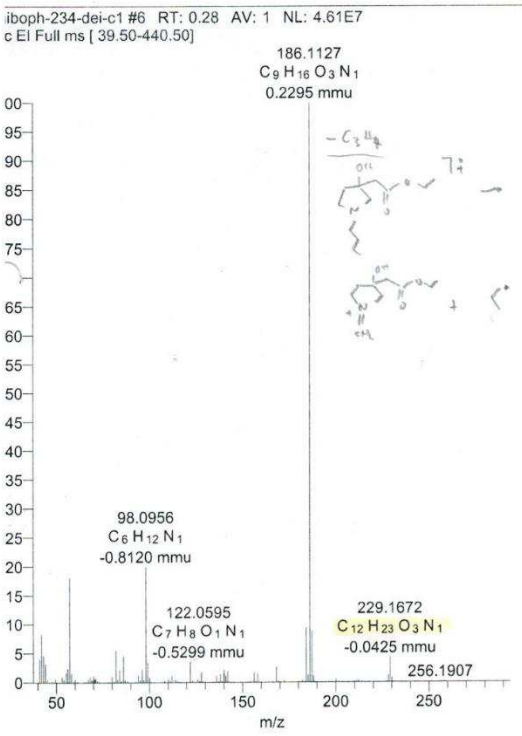

08-miboph-234-dei-c1#6 RT: 0.28
T: + c EI Full ms [39.50-440.50]
m/z= 37.50-293.66

m/z	Intensity	Relative	Flags
41.0405	1893836.0	4.11	
42.0417	3805892.0	8.26	
43.0252	975696.0	2.12	
43.0487	2094046.0	4.55	
44.0559	1459448.0	3.17	
55.0518	766164.0	1.66	
56.0468	1079508.0	2.34	
57.0543	8315450.0	18.05	
82.0644	2555340.0	5.55	
84.0802	976684.0	2.12	
86.0958	2070035.0	4.49	
96.0800	1075483.0	2.33	
98.0594	2087125.0	4.53	
98.0956	9180416.0	19.93	
99.1028	1550548.0	3.37	
122.0595	1595816.0	3.46	
128.0697	765316.0	1.66	
140.0701	990244.0	2.15	
140.1060	855075.0	1.86	
142.1222	874567.0	1.90	
156.1015	776333.0	1.69	
168.1008	1196315.0	2.60	
184.1329	4358570.0	9.46	
186.1127	46060288.0	100.00	
187.1169	4051088.0	8.80	
229.1672	1942494.0	4.22	

2-(1-Butyl-3-hydroxypyrrolidin-3-yl)acetic acid (12g)

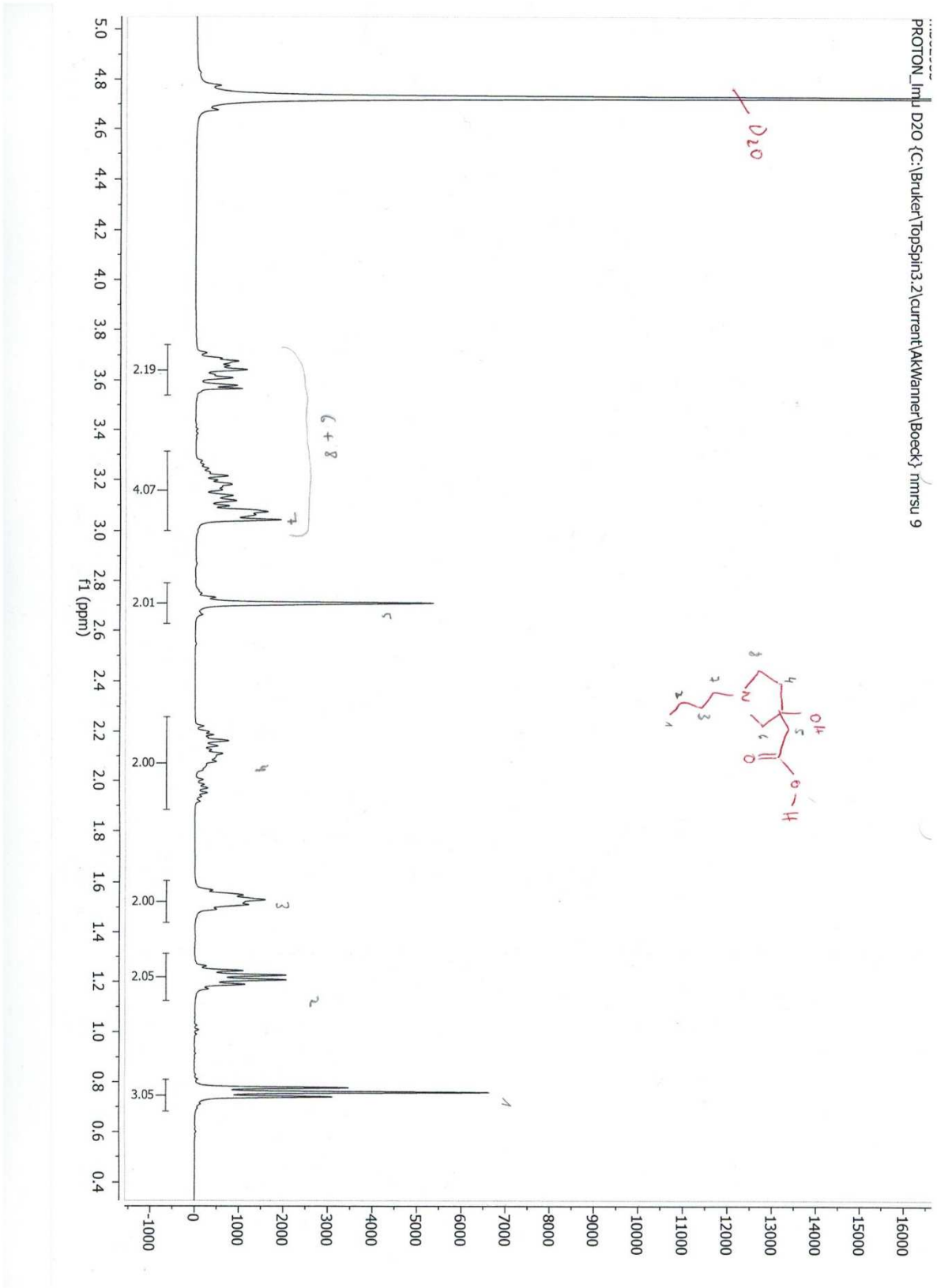

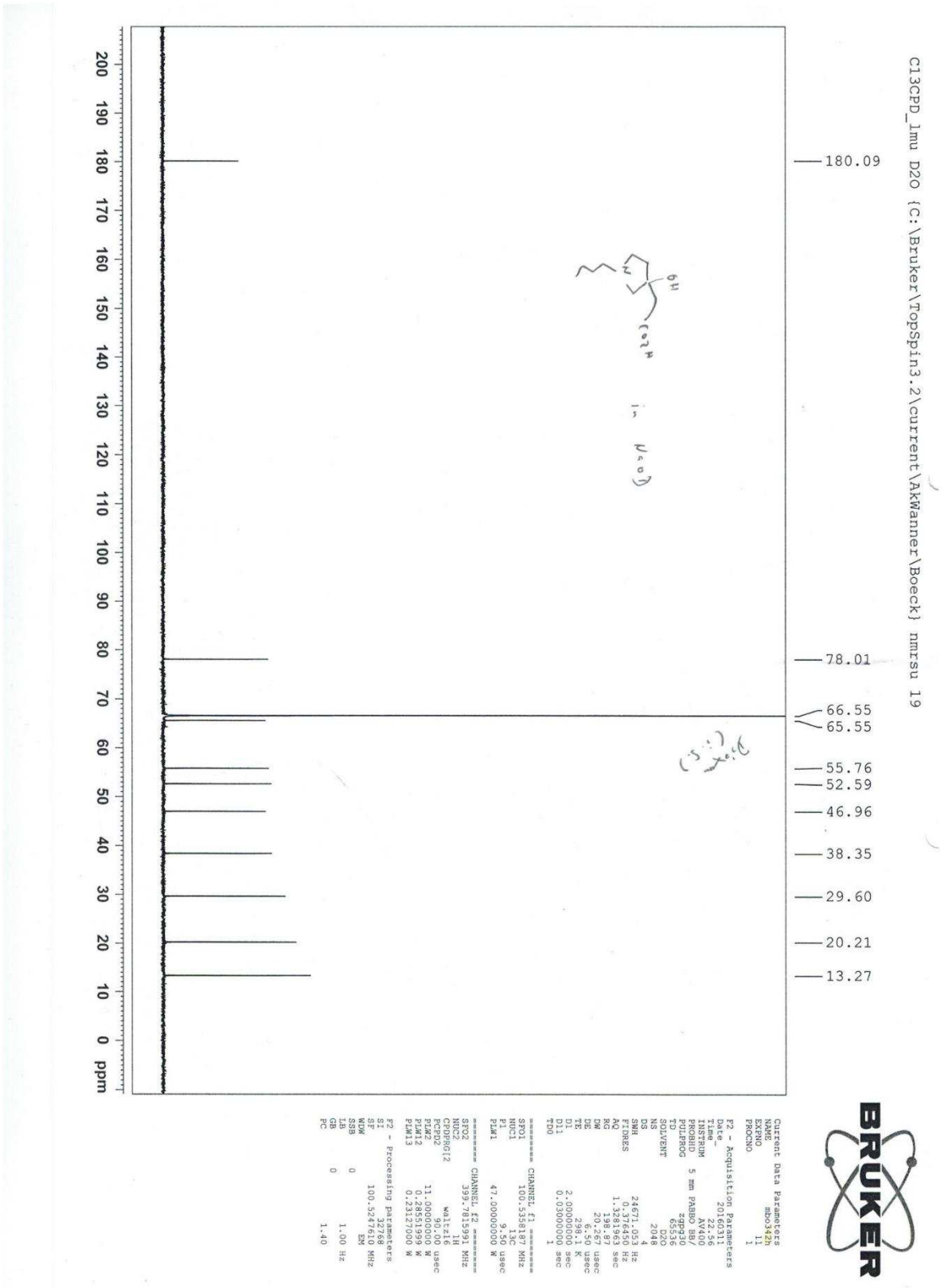
C13CPD_lmu D2O {C:\Bruker\TopSpin3.2\current\AkWanner\Boeck} nmrsu 19
180.09
78.01
66.55
65.55
55.76
52.59
46.96
38.35
29.60
20.21
13.27
200 190 180 170 160 150 140 130 120 110 100 90 80 70 60 50 40 30 20 10 0 ppm
BRUKER

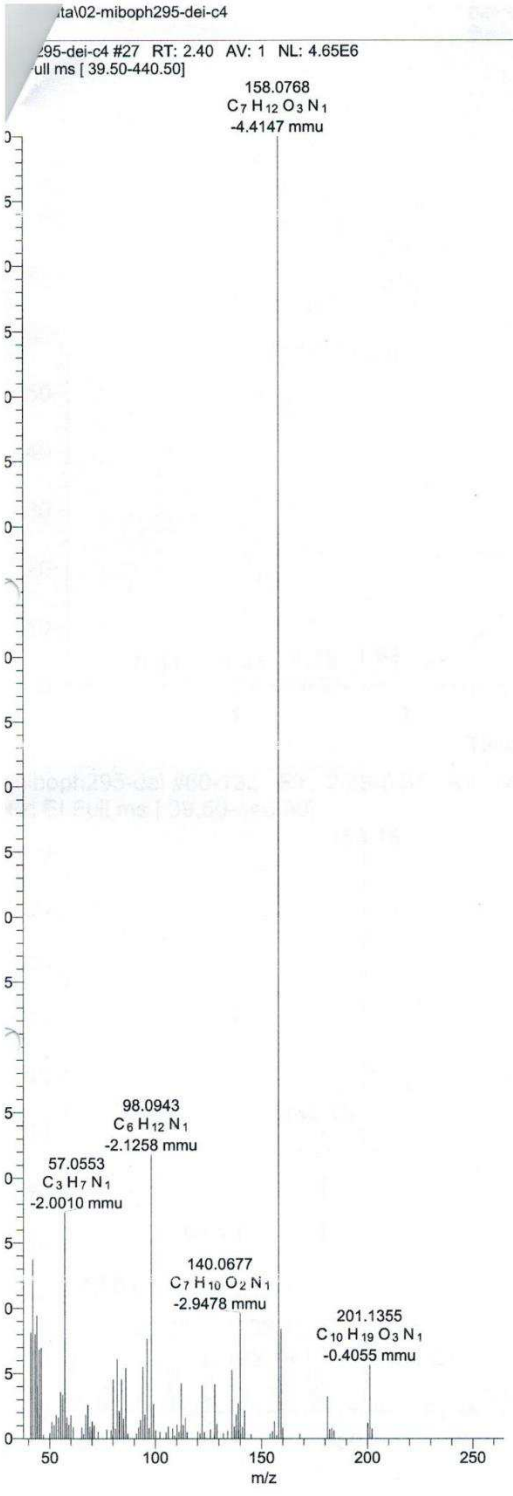

02-miboph295-dei-c4#27 RT: 2.40
T: + c EI Full ms [39.50-440.50]
m/z= 37.50-442.50

m/z	Intensity	Relative	Flags
41.0427	377069.0	8.12	
42.0427	637140.0	13.71	
43.0260	371249.0	7.99	
43.0497	174845.0	3.76	
43.9952	438063.0	9.43	
44.0550	187495.0	4.04	
45.0009	317085.0	6.83	
46.0081	323499.0	6.96	
55.0513	166233.0	3.58	
57.0553	805690.0	17.34	
80.0486	209648.0	4.51	
82.0647	282520.0	6.08	
84.0815	211073.0	4.54	
86.0961	250449.0	5.39	
94.0641	255081.0	5.49	
96.0787	356283.0	7.67	
98.0584	301644.0	6.49	
98.0943	1012131.0	21.79	
112.0756	196166.0	4.22	
122.0577	189217.0	4.07	
128.0677	192840.0	4.15	
136.1106	243500.0	5.24	
140.0677	445547.0	9.59	
158.0768	4645698.0	100.00	
159.0827	391086.0	8.42	
201.1355	261555.0	5.63	

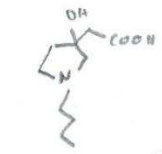

$C_{10}H_{19}NO_3$

1-Benzyl-3-hydroxypiperidine-3-carboxamide (13b)

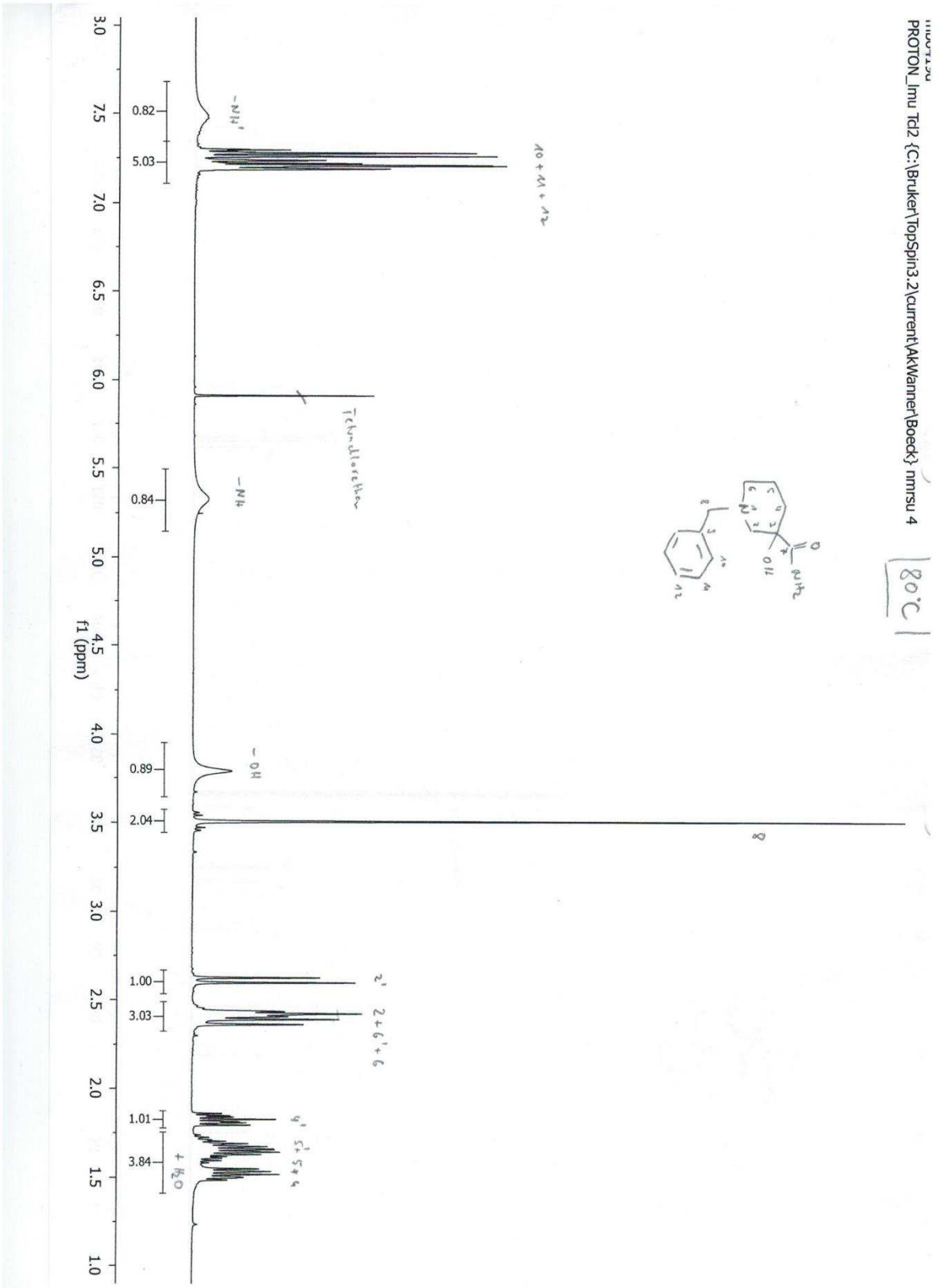

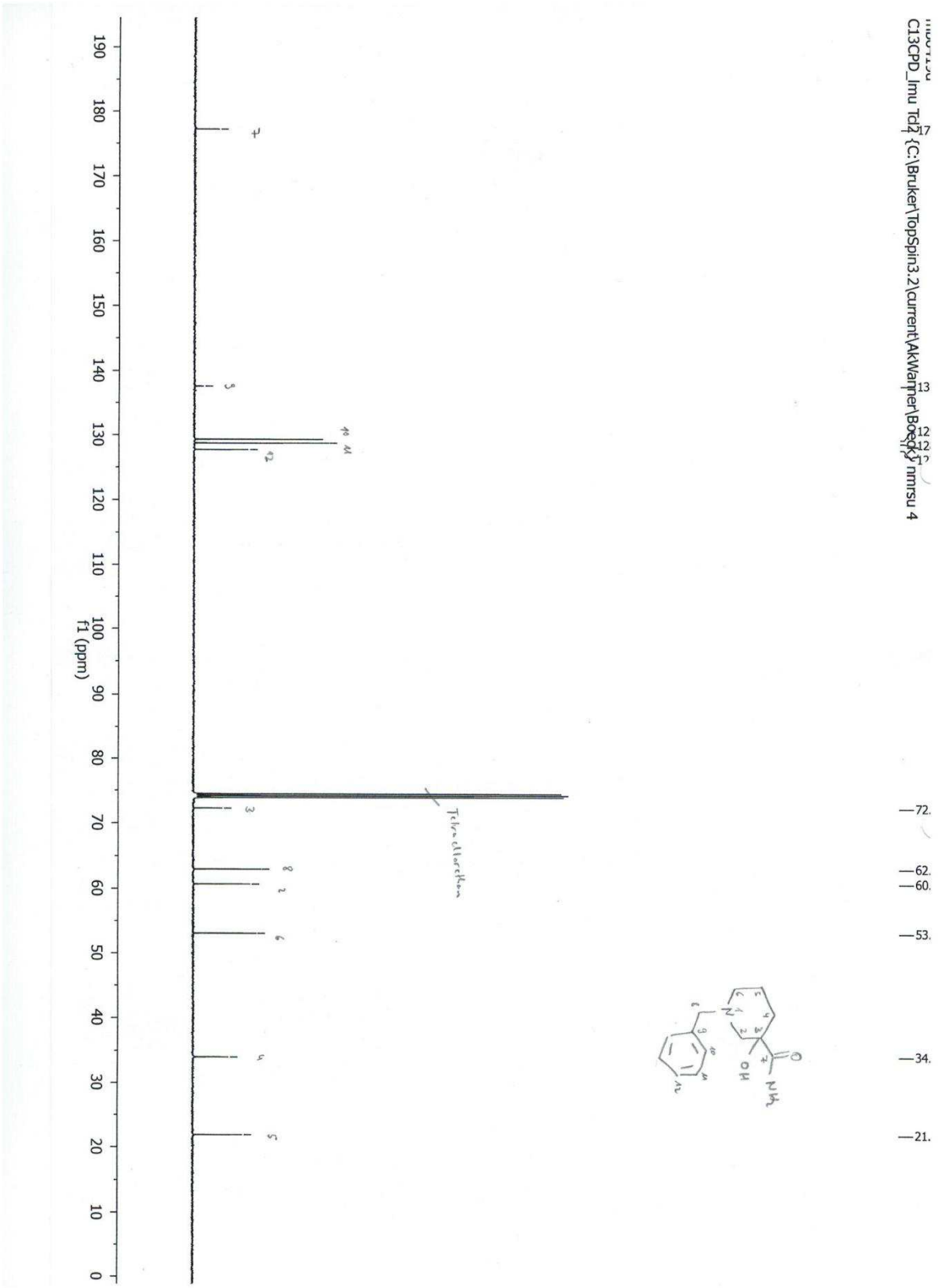
C13CPD_lmu Td4 {C:\Bruker\TopSpin3.2\current\AkWarmer\Boeck\ nmrsu 4
f1 (ppm)
Tetrachlorethen
—72.
—62.
—60.
—53.
—34.
—21.

File: 7887H
Sample: MBO 419
Instrument: JEOL GCmate
Inlet: Direct Probe

Date Run: 08-10-2016
Ionization mode: EI+

Time Run: 13:23:08
Run By: NMR
Printed by: NMR

Scan: 41
Base: m/z 216; 5.4%FS TIC: 2234576

R.T.: 1:01
#Ions: 174

Selected Isotopes : $H_{0-18}C_{0-13}N_{0-2}O_{0-2}$

Error Limit : 1000 mmu

Measured Mass	*% Base*	*Formula*	*Calculated Mass*	*Error*
234.1361	21.0%	$C_{13}H_{18}N_2O_2$	234.1368	-0.7

Scan: 41
Base: m/z 216; 5.4%FS TIC: 1909992

R.T.: 1:01
#Ions: 174

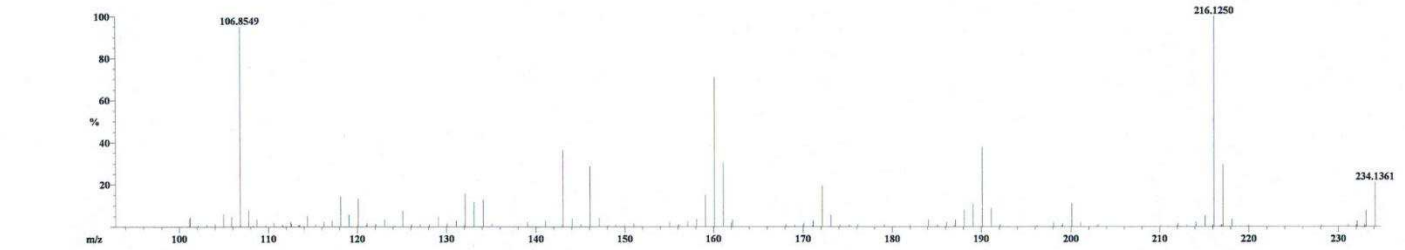

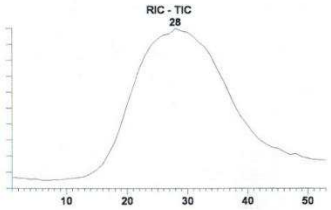

1-Butyl-3-hydroxypiperidine-3-carboxamide (13c)

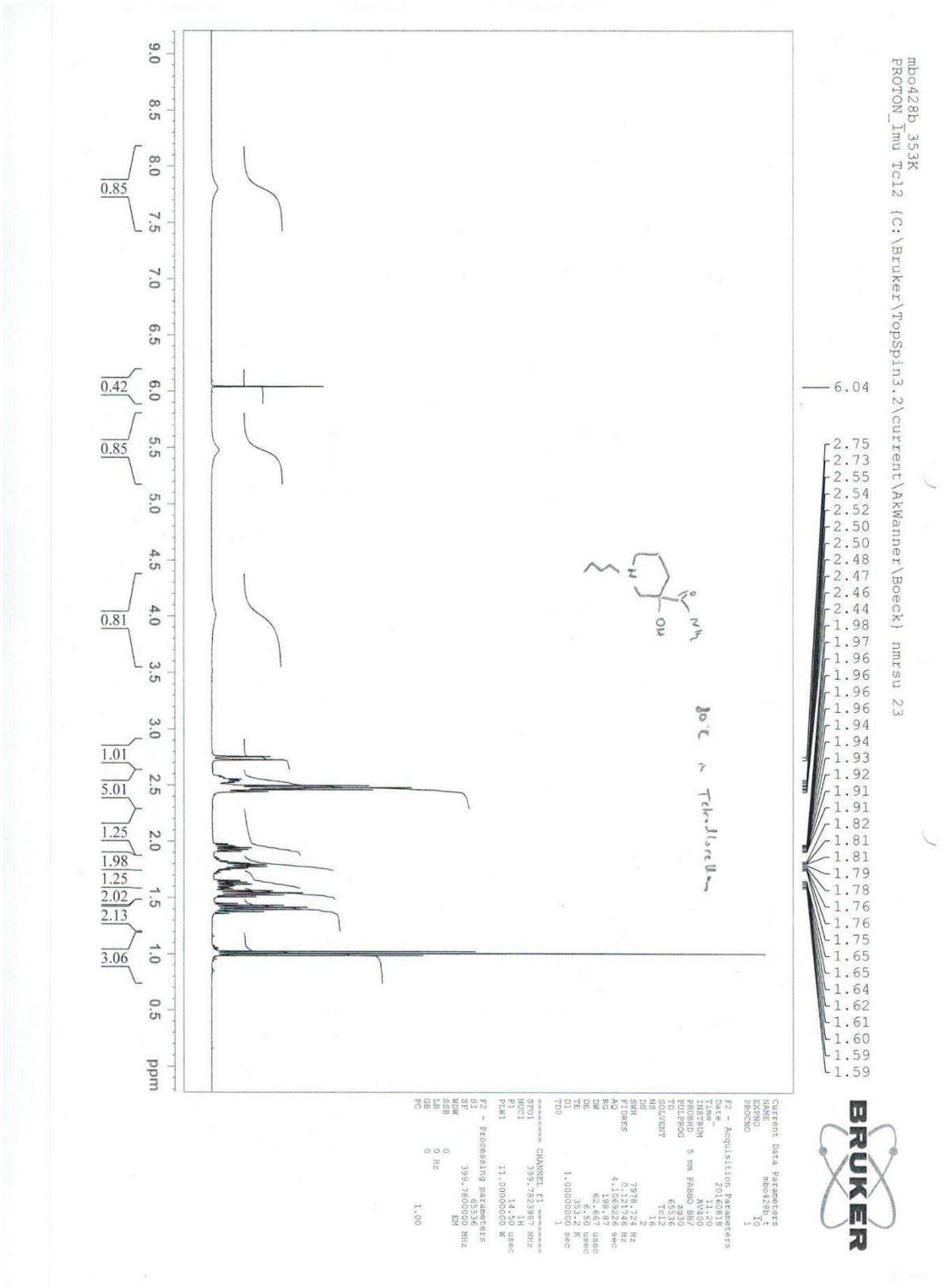

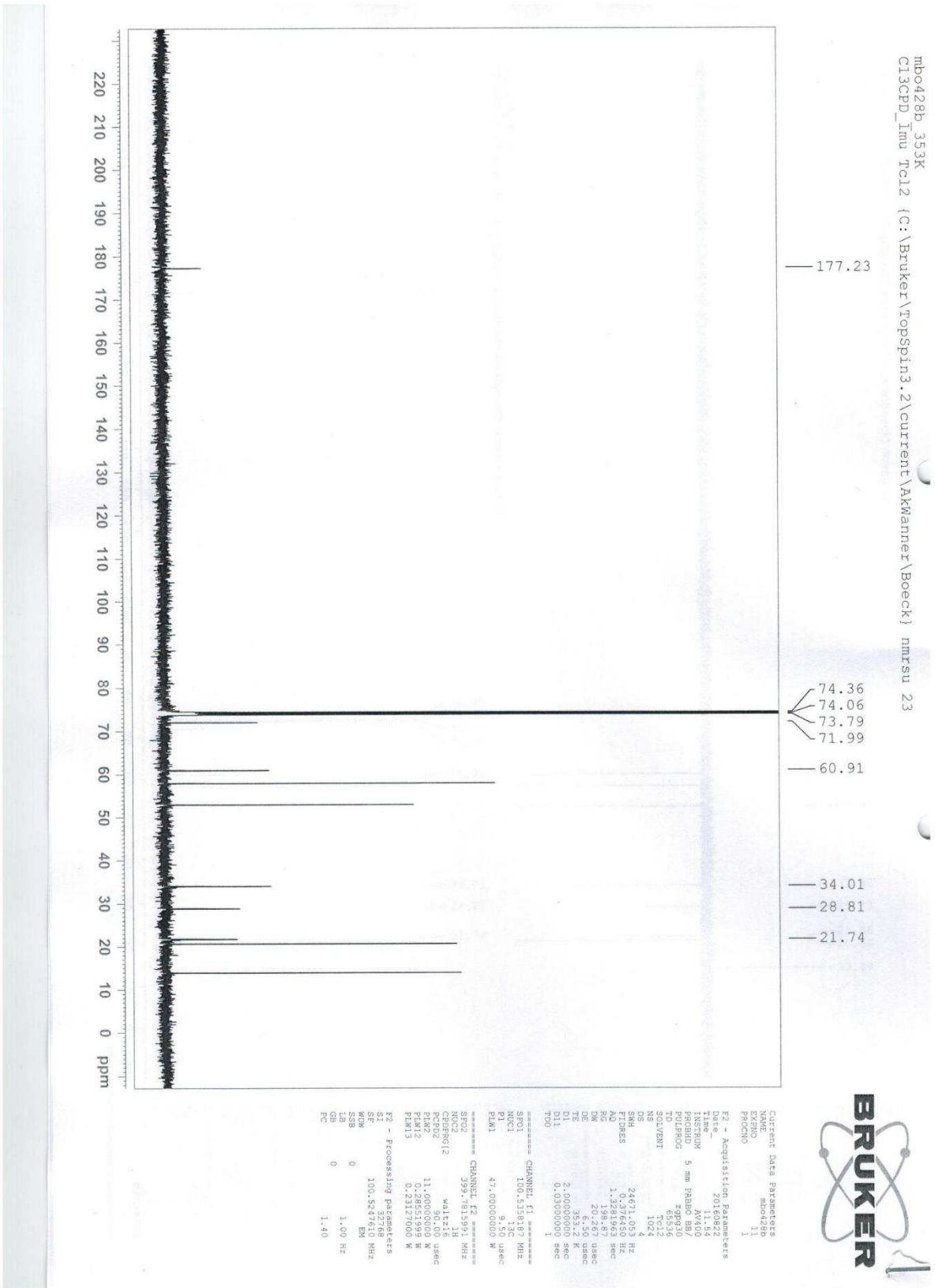
mbo428b 353K
C13CPD_Imu Tc12 {C:\Bruker\TopSpin3.2\current\AkWanner\Boeck} nmrsu 23
177.23
74.36
74.06
73.79
71.99
60.91
34.01
28.81
21.74
220 210 200 190 180 170 160 150 140 130 120 110 100 90 80 70 60 50 40 30 20 10 0 ppm
Current Data Parameters
NAME mbo428b
EXPNO 11
PROCNO 1
F2 - Acquisition Parameters
Date_ 20160822
Time 11.54
INSTRUM AV600
PROBHD 5 mm PABBO BB/
PULPROG zgpg30
TD 65536
SOLVENT DMSO
NS 1024
DS 4
SWH 24671.053 Hz
FIDRES 0.376450 Hz
AQ 1.3281983 sec
RG 203.67
DW 20.267 usec
DE 6.50 usec
TE 353.2 K
D1 2.00000000 sec
D11 0.03000000 sec
TD0 1
======== CHANNEL f1 ========
SFO1 100.5358187 MHz
NUC1 13C
P1 9.50 usec
PL1 47.00000000 W
======== CHANNEL f2 ========
SFO2 399.7815991 MHz
NUC2 1H
CPDPRG2 waltz16
PCPD2 80.00 usec
PL2 11.00000000 W
PL12 0.28551999 W
PL13 0.23127000 W
F2 - Processing parameters
SI 32768
SF 100.5247676 MHz
WDW EM
SSB 0
LB 1.00 Hz
GB 0
PC 1.40
BRUKER

File: 7893H
Sample: MBO428
Instrument: JEOL GCmate
Inlet: Direct Probe

Date Run: 08-18-2016
Ionization mode: EI+

Time Run: 12:23:51
Run By: NMR
Printed by: NMR

Scan: 14
Base: m/z 157; 3.3%FS TIC: 653944

R.T.: 0:20

#Ions: 96

Selected Isotopes : $H_{0-20}C_{0-10}N_{0-2}O_{0-2}$

Error Limit : 1000 mmu

Measured Mass	*% Base*	*Formula*	*Calculated Mass*	*Error*
200.1549	11.6%	$C_{10}H_{20}N_2O_2$	200.1525	2.4

Scan: 14
Base: m/z 157; 3.3%FS TIC: 653944

R.T.: 0:20

#Ions: 96

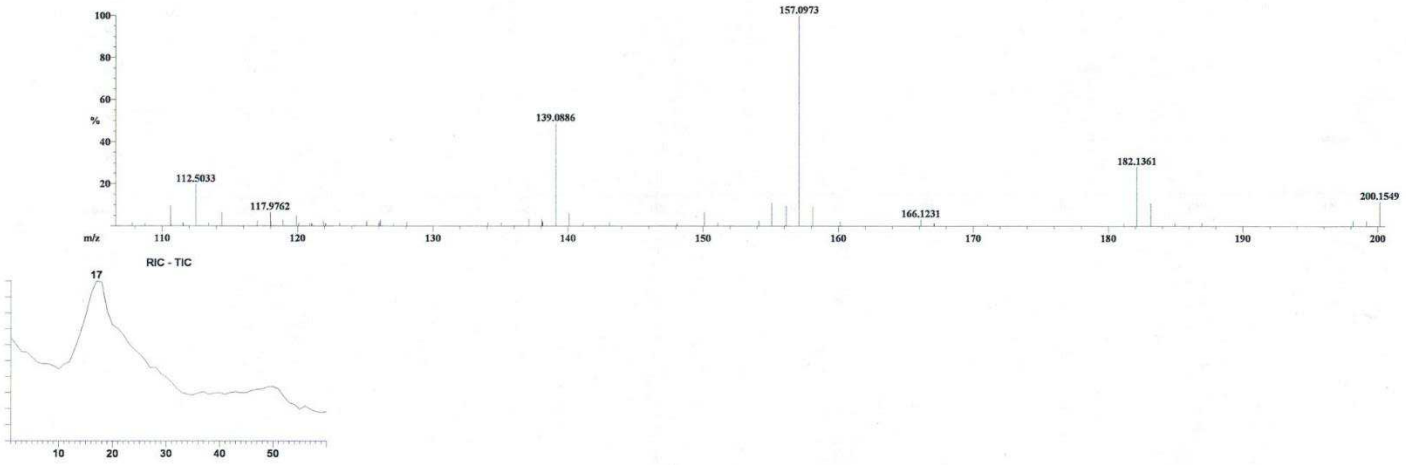

1-Butyl-3-hydroxypiperidine-3-carboxylic acid (13d)

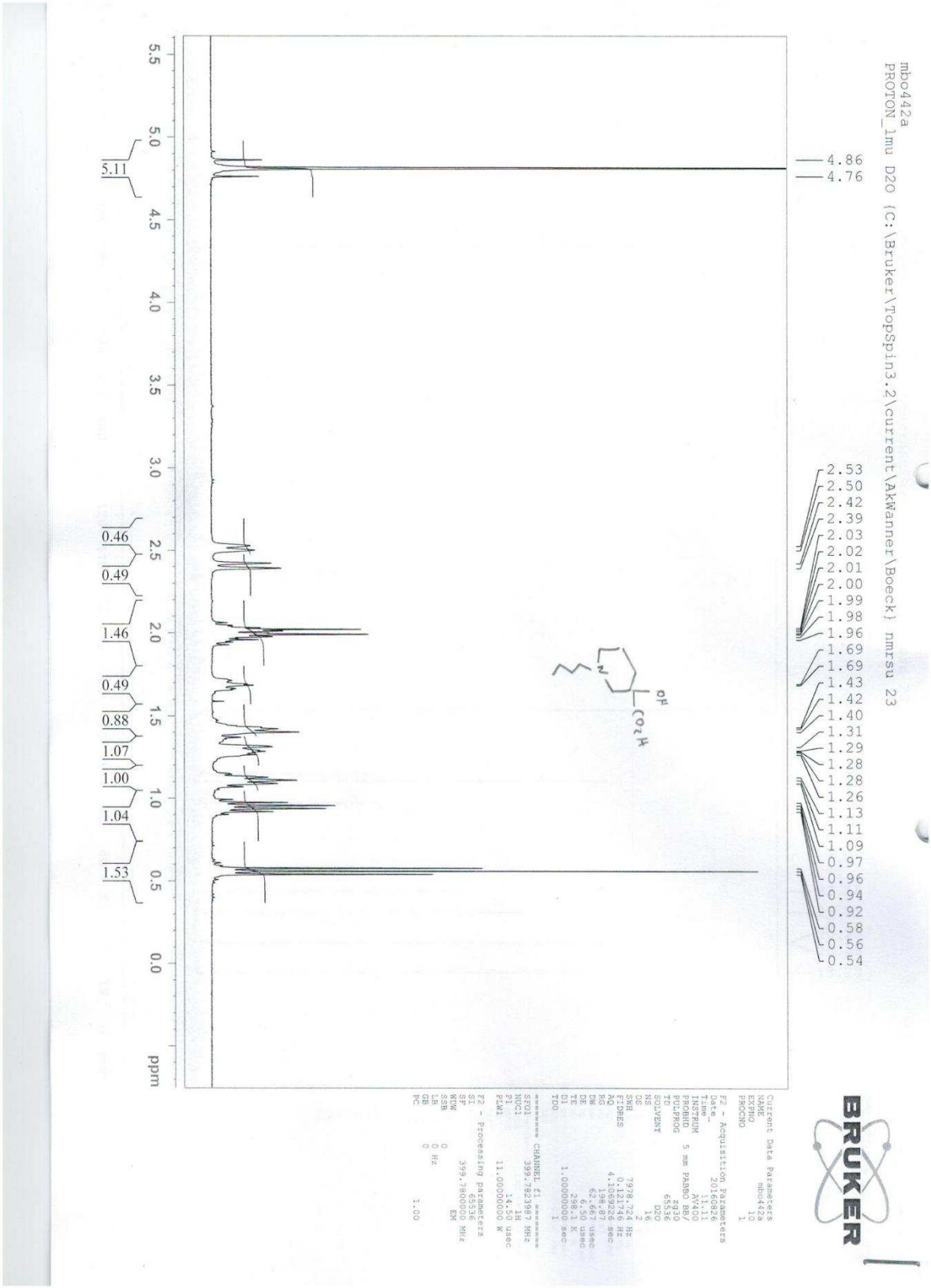

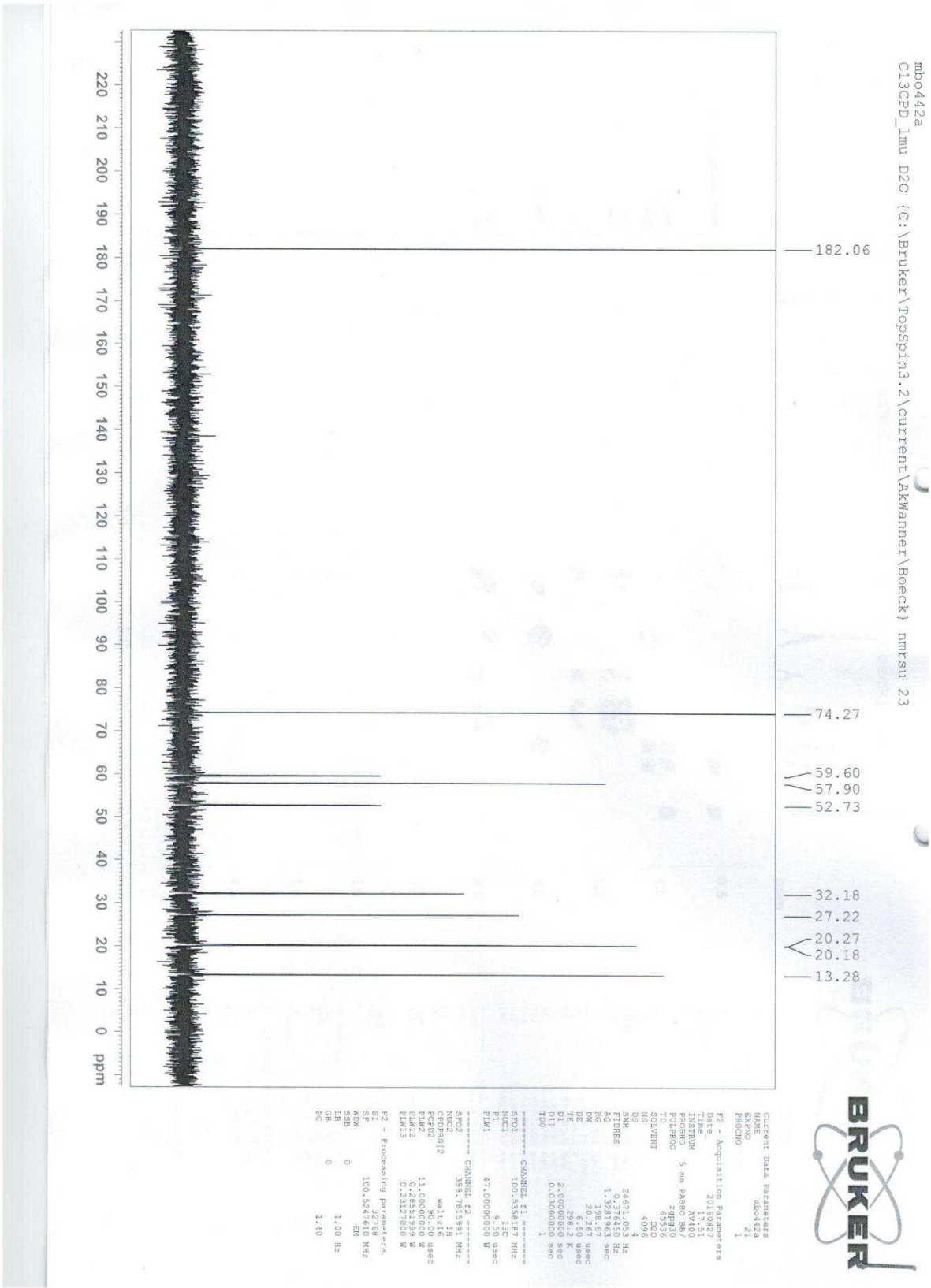
mbo442a
C13CPD_lmu D2O {C:\Bruker\TopSpin3.2\current\AkWanner\Boeck} nmrsu 23
182.06
74.27
59.60
57.90
52.73
32.18
27.22
20.27
20.18
13.28
220 210 200 190 180 170 160 150 140 130 120 110 100 90 80 70 60 50 40 30 20 10 0 ppm
Current Data Parameters
NAME mbo442a
EXPNO 21
PROCNO 1
F2 - Acquisition Parameters
Date_ 20160827
Time 17.15 h
INSTRUM av400
PROBHD 5 mm PABBO BB/
PULPROG zgpg30
TD 65536
SOLVENT D2O
NS 4096
DS 16
SWH 24671.053 Hz
FIDRES 0.376450 Hz
AQ 1.3281963 sec
RG 198.87
DW 20.267 usec
DE 6.50 usec
TE 298.0 K
D1 2.00000000 sec
D11 0.03000000 sec
TD0 1
======== CHANNEL f1 ========
SFO1 100.5358187 MHz
NUC1 13C
P1 9.50 usec
PLW1 47.00000000 W
======== CHANNEL f2 ========
SFO2 399.7819931 MHz
NUC2 1H
CPDPRG2 waltz16
PCPD2 90.00 usec
PLW2 11.00000000 W
PLW12 0.28551999 W
PLW13 0.23127000 W
F2 - Processing parameters
SI 32768
SF 100.5247610 MHz
WDW EM
SSB 0
LB 1.00 Hz
GB 0
PC 1.40
BRUKER

File: 7916H
Sample: MBO 442
Instrument: JEOL GCmate
Inlet: Direct Probe

Date Run: 08-29-2016

Ionization mode: EI+

Time Run: 14:25:36
Run By: NMR
Printed by: NMR

Scan: 37
Base: m/z 158; 89.8%FS TIC: 7089216

R.T.: 0:55

#Ions: 243

Selected Isotopes : $H_{0-19}C_{0-10}N_{0-1}O_{0-3}$

Error Limit : 1000 mmu

Measured Mass	*% Base*	*Formula*	*Calculated Mass*	*Error*
201.1393	2.9%	$C_{10}H_{19}NO_3$	201.1365	2.8

Scan: 37
Base: m/z 158; 89.8%FS TIC: 7089216

R.T.: 0:55

#Ions: 243

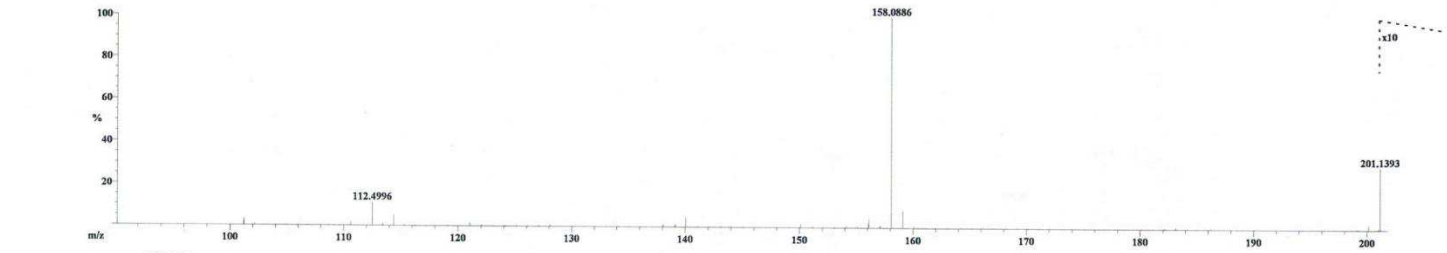

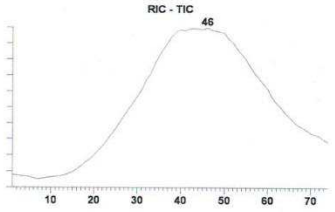

4-(Butylamino)-2-hydroxybutanoic acid (14b)

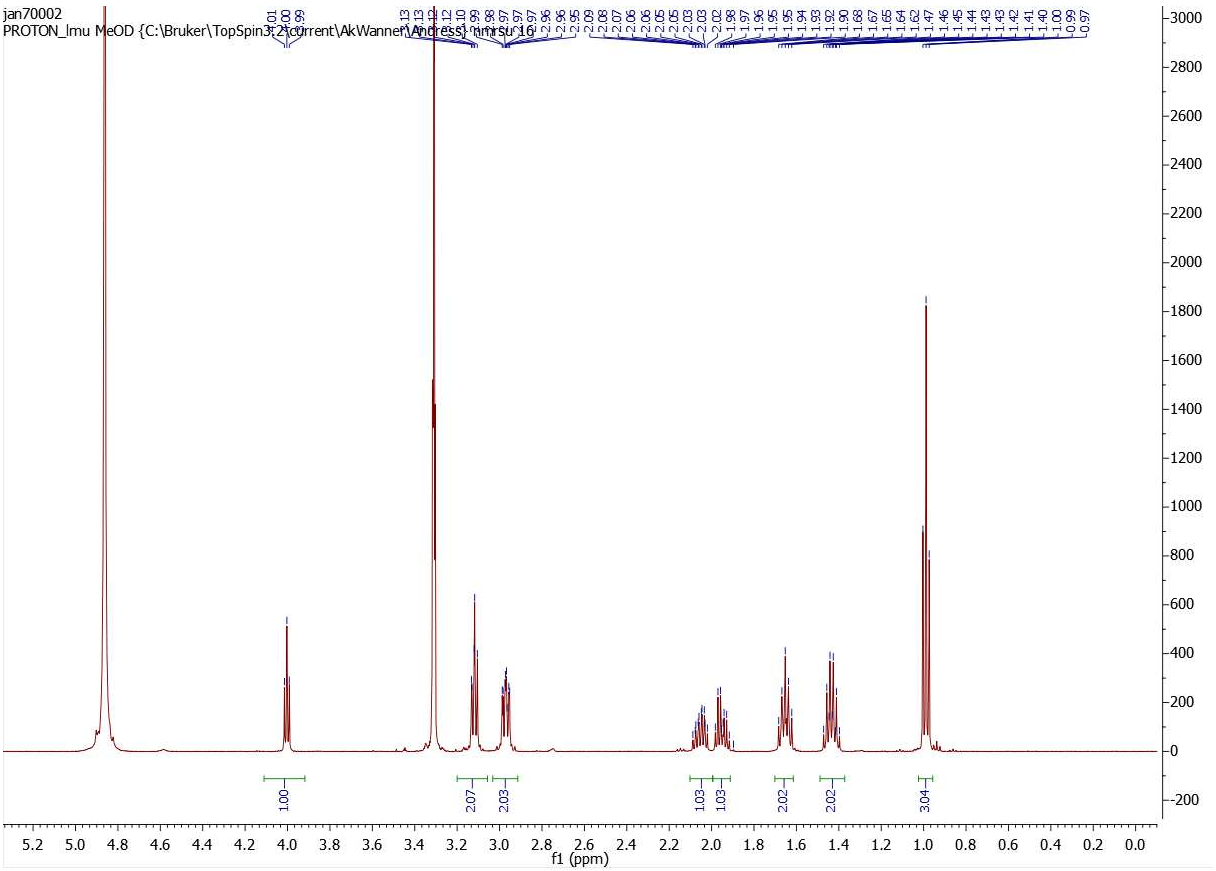

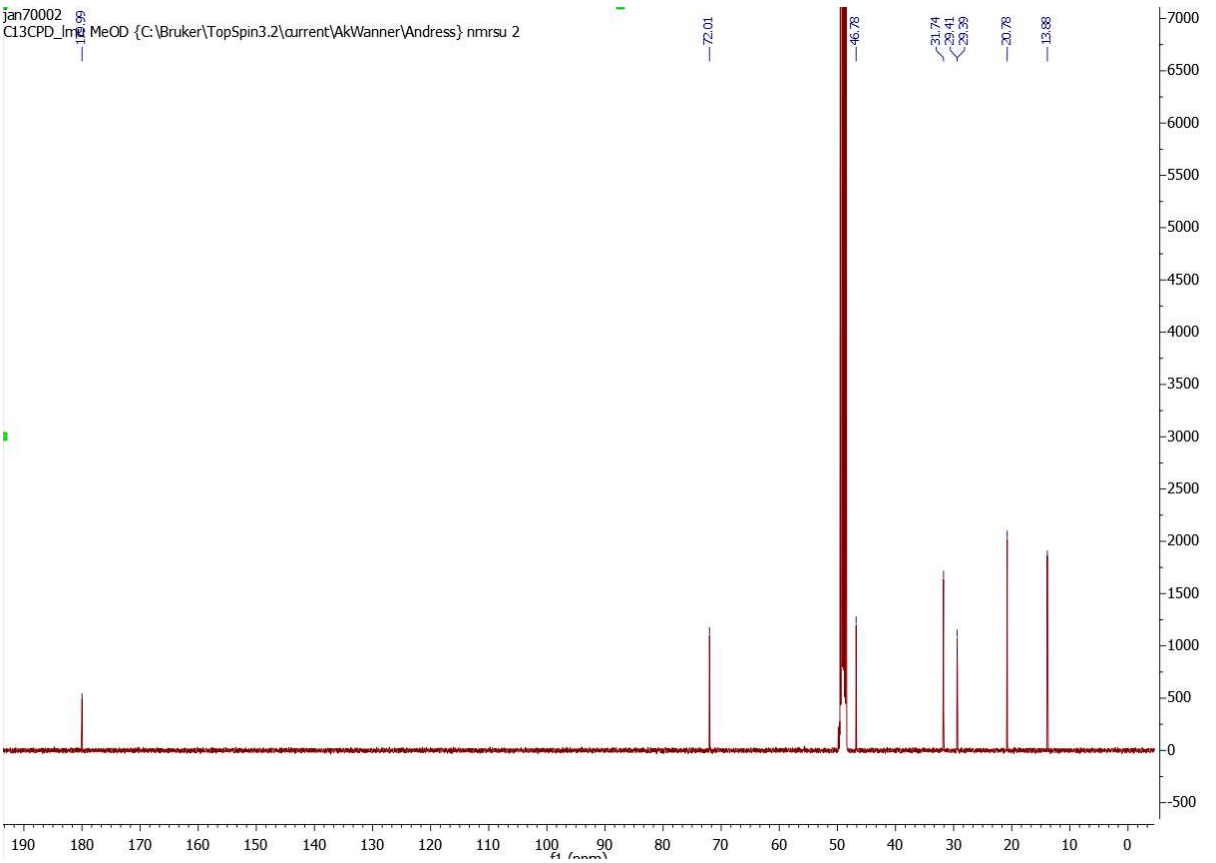

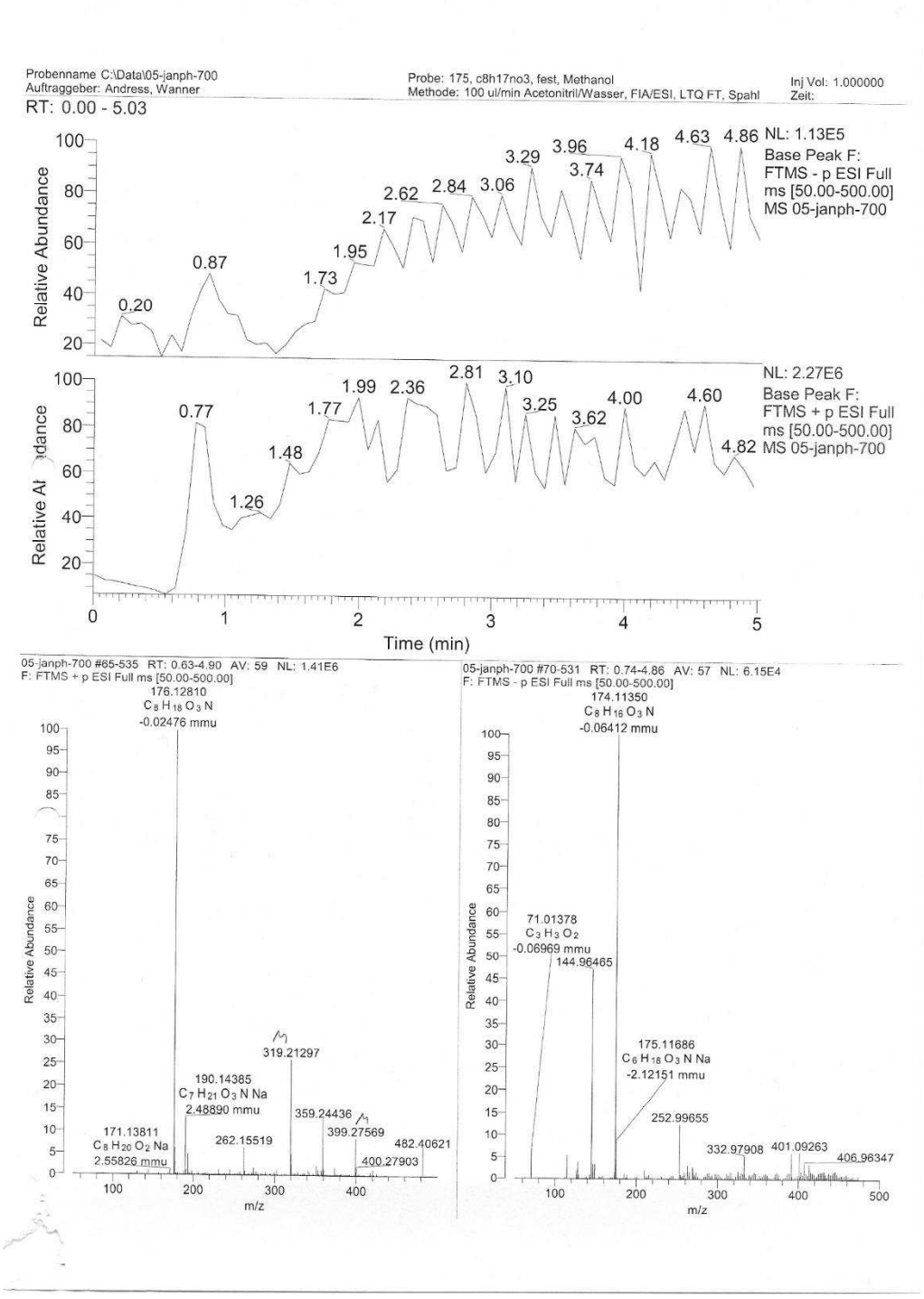
Probenname C:\Data\05-janph-700
Auftraggeber: Andress, Wanner
Probe: 175, c8h17no3, fest, Methanol
Methode: 100 ul/min Acetonitril/Wasser, FIA/ESI, LTQ FT, Spahl
Inj Vol: 1.000000
Zeit:
RT: 0.00 - 5.03
Relative Abundance
NL: 1.13E5
Base Peak F:
FTMS - p ESI Full
ms [50.00-500.00]
MS 05-janph-700
NL: 2.27E6
Base Peak F:
FTMS + p ESI Full
ms [50.00-500.00]
MS 05-janph-700
Time (min)
05-janph-700 #65-535 RT: 0.63-4.90 AV: 59 NL: 1.41E6
F: FTMS + p ESI Full ms [50.00-500.00]
176.12810
C8 H18 O3 N
-0.02476 mmu
319.21297
190.14385
C7 H21 O3 N Na
2.48890 mmu
359.24436
399.27569
171.13811
C8 H20 O2 Na
2.55826 mmu
262.15519
482.40621
400.27903
m/z
05-janph-700 #70-531 RT: 0.74-4.86 AV: 57 NL: 6.15E4
F: FTMS - p ESI Full ms [50.00-500.00]
174.11350
C8 H16 O3 N
-0.06412 mmu
71.01378
C3 H3 O2
-0.06969 mmu
144.96465
175.11686
C6 H18 O3 N Na
-2.12151 mmu
252.99655
332.97908
401.09263
406.96347
m/z

Methyl 2-{2-[(tert-butyldiphenylsilyl)oxy]ethoxy}-4-(1,3-dioxoisoindolin-2-yl)butanoate (14d)

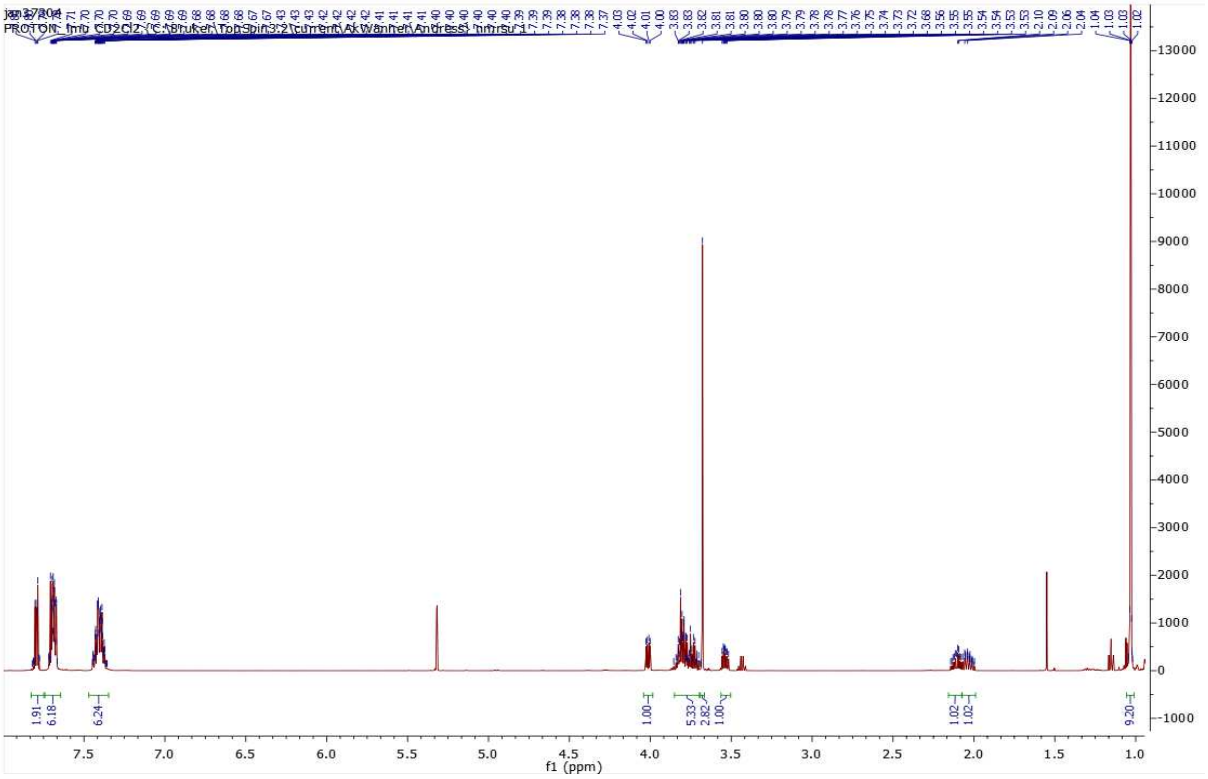

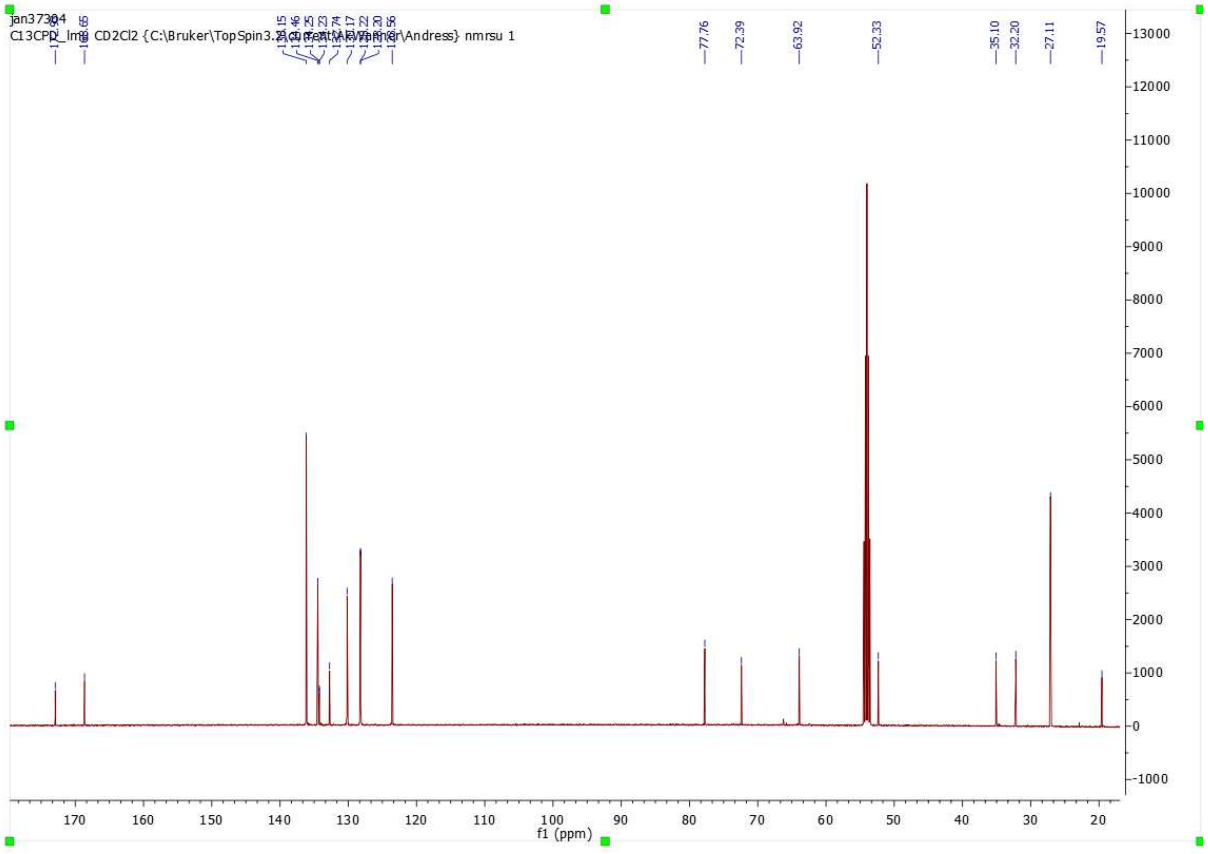

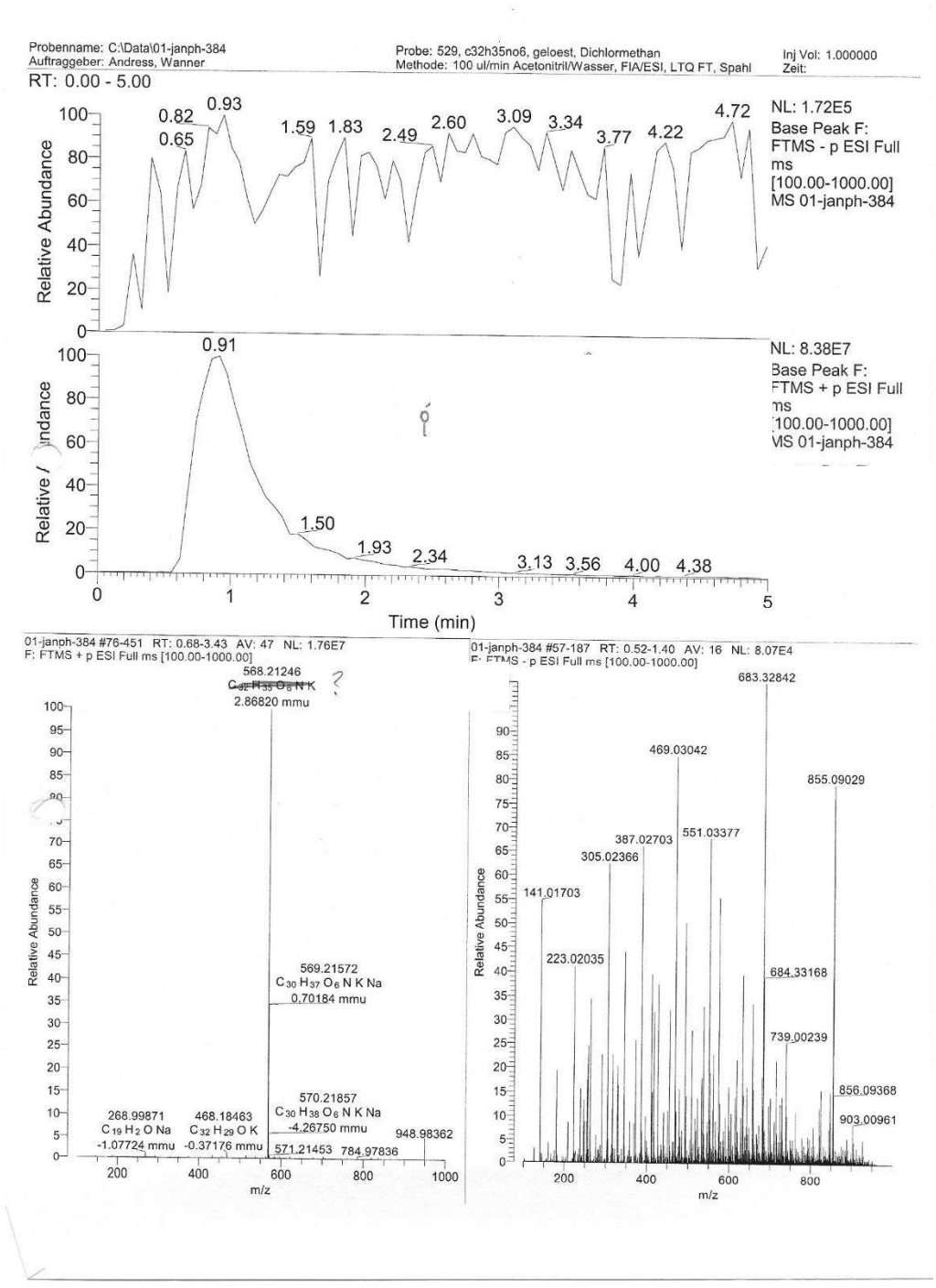
Probenname: C:\Data\01-janph-384
Auftraggeber: Andress, Wanner
Probe: 529, c32h35no6, geloest, Dichlormethan
Methode: 100 ul/min Acetonitril/Wasser, FIA/ESI, LTQ FT, Spahl
Inj Vol: 1.000000
Zeit:
RT: 0.00 - 5.00
Relative Abundance
NL: 1.72E5
Base Peak F:
FTMS - p ESI Full
ms
[100.00-1000.00]
MS 01-janph-384
NL: 8.38E7
Base Peak F:
FTMS + p ESI Full
ms
[100.00-1000.00]
MS 01-janph-384
Time (min)
01-janph-384 #76-451 RT: 0.68-3.43 AV: 47 NL: 1.76E7
F: FTMS + p ESI Full ms [100.00-1000.00]
568.21246
2.86820 mmu
569.21572
C30 H37 O6 N K Na
0.70184 mmu
570.21857
C30 H38 O6 N K Na
-4.26750 mmu
268.99871
C19 H2 O Na
-1.07724 mmu
468.18463
C32 H29 O K
-0.37176 mmu
571.21453
784.97836
948.98362
m/z
01-janph-384 #57-187 RT: 0.52-1.40 AV: 16 NL: 8.07E4
683.32842
469.03042
855.09029
387.02703
551.03377
305.02366
141.01703
223.02035
684.33168
739.00239
856.09368
903.00961
m/z

Methyl 4-(1,3-dioxoisoindolin-2-yl)-2-(2-hydroxyethoxy)butanoate (14e)

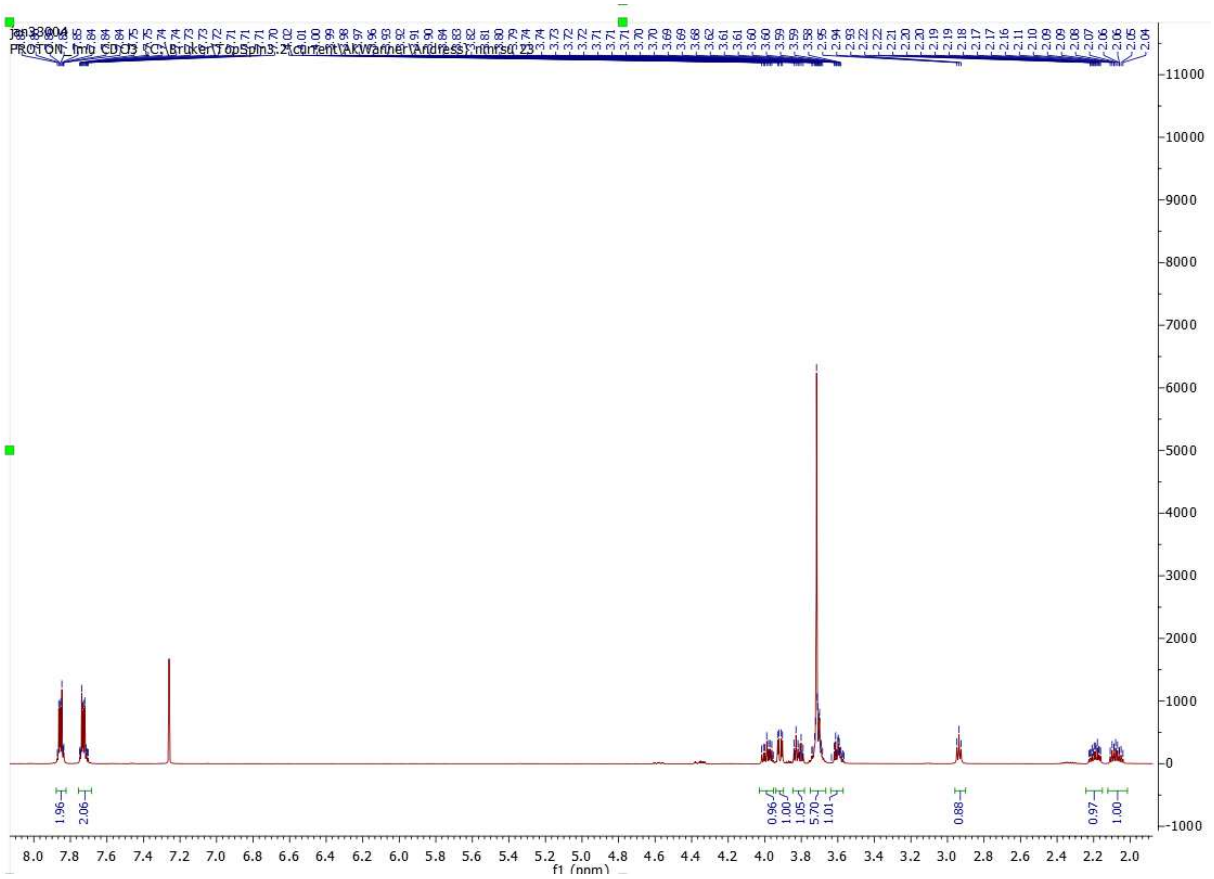

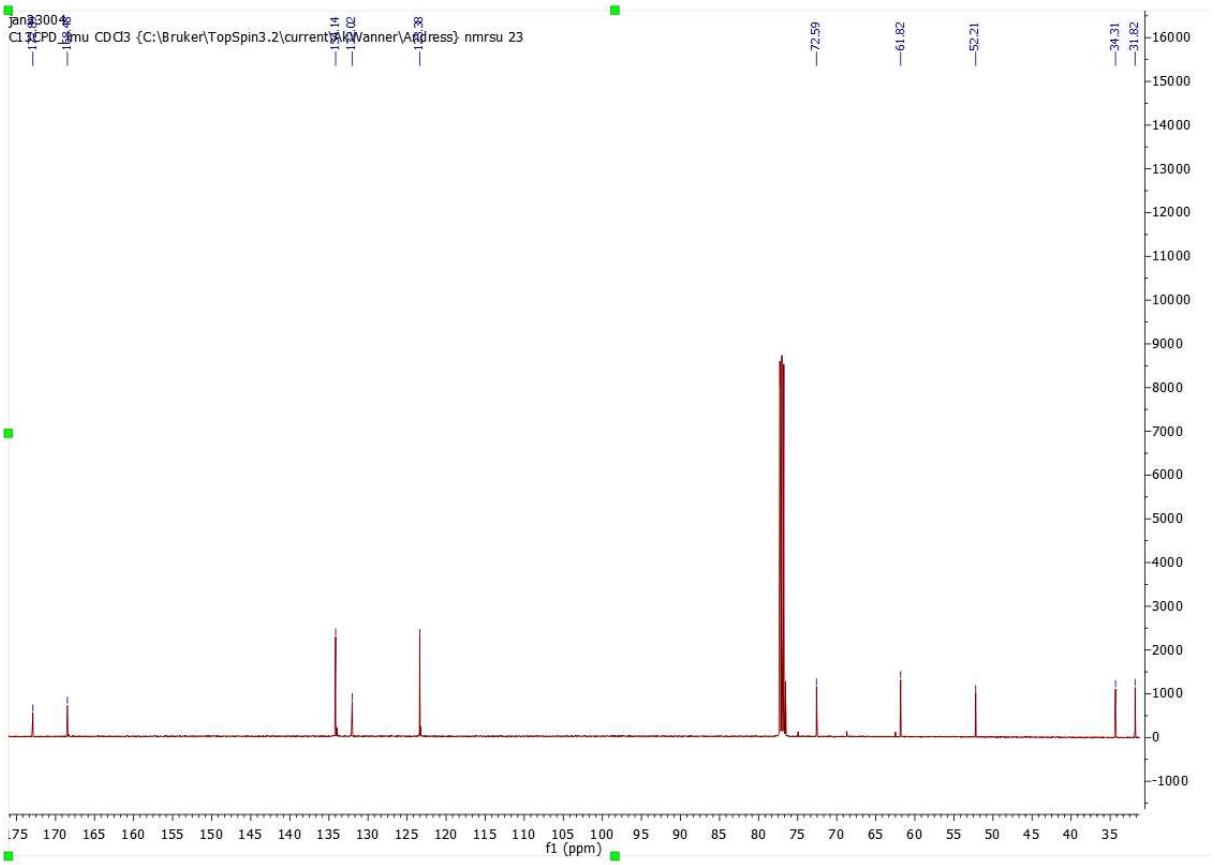

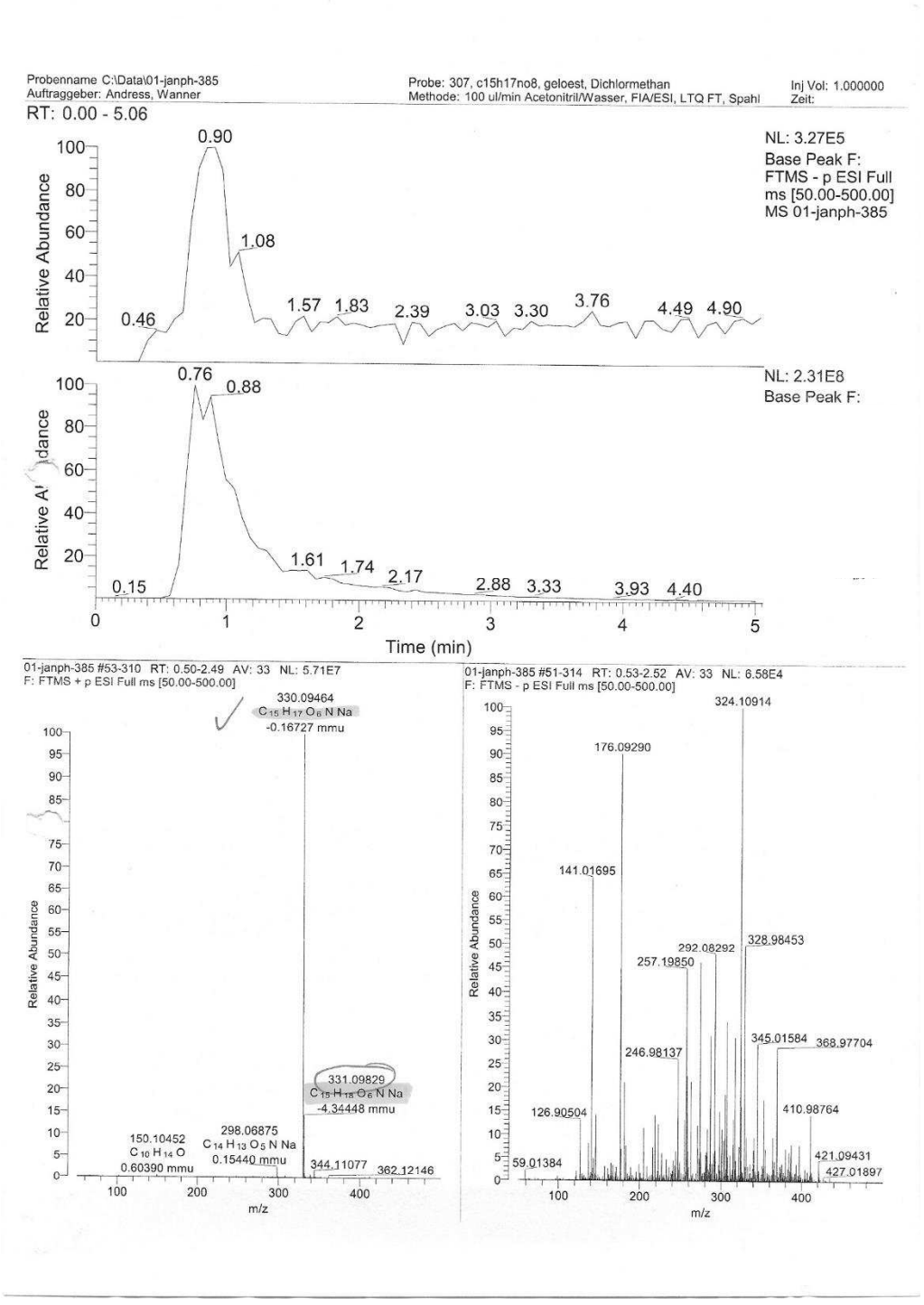
Probenname C:\Data\01-janph-385
Auftraggeber: Andress, Wanner
Probe: 307, c15h17no8, geloest, Dichlormethan
Methode: 100 ul/min Acetonitril/Wasser, FIA/ESI, LTQ FT, Spahl
Inj Vol: 1.000000
Zeit:
RT: 0.00 - 5.06
NL: 3.27E5
Base Peak F:
FTMS - p ESI Full
ms [50.00-500.00]
MS 01-janph-385
Relative Abundance
0.90
1.08
0.46
1.57
1.83
2.39
3.03
3.30
3.76
4.49
4.90
NL: 2.31E8
Base Peak F:
0.76
0.88
0.15
1.61
1.74
2.17
2.88
3.33
3.93
4.40
Time (min)
01-janph-385 #53-310 RT: 0.50-2.49 AV: 33 NL: 5.71E7
F: FTMS + p ESI Full ms [50.00-500.00]
330.09464
C15 H17 O6 N Na
-0.16727 mmu
331.09829
C15 H18 O6 N Na
-4.34448 mmu
150.10452
C10 H14 O
0.60390 mmu
298.06875
C14 H13 O5 N Na
0.15440 mmu
344.11077
362.12146
m/z
01-janph-385 #51-314 RT: 0.53-2.52 AV: 33 NL: 6.58E4
F: FTMS - p ESI Full ms [50.00-500.00]
324.10914
176.09290
141.01695
328.98453
292.08292
257.19850
345.01584
368.97704
246.98137
126.90504
410.98764
59.01384
421.09431
427.01897
m/z

Methyl 4-{1, 3-dioxoisoindolin-2-yl}-2-{2-[tris(4-methoxyphenyl)methoxy]ethoxy}butanoate (14f)

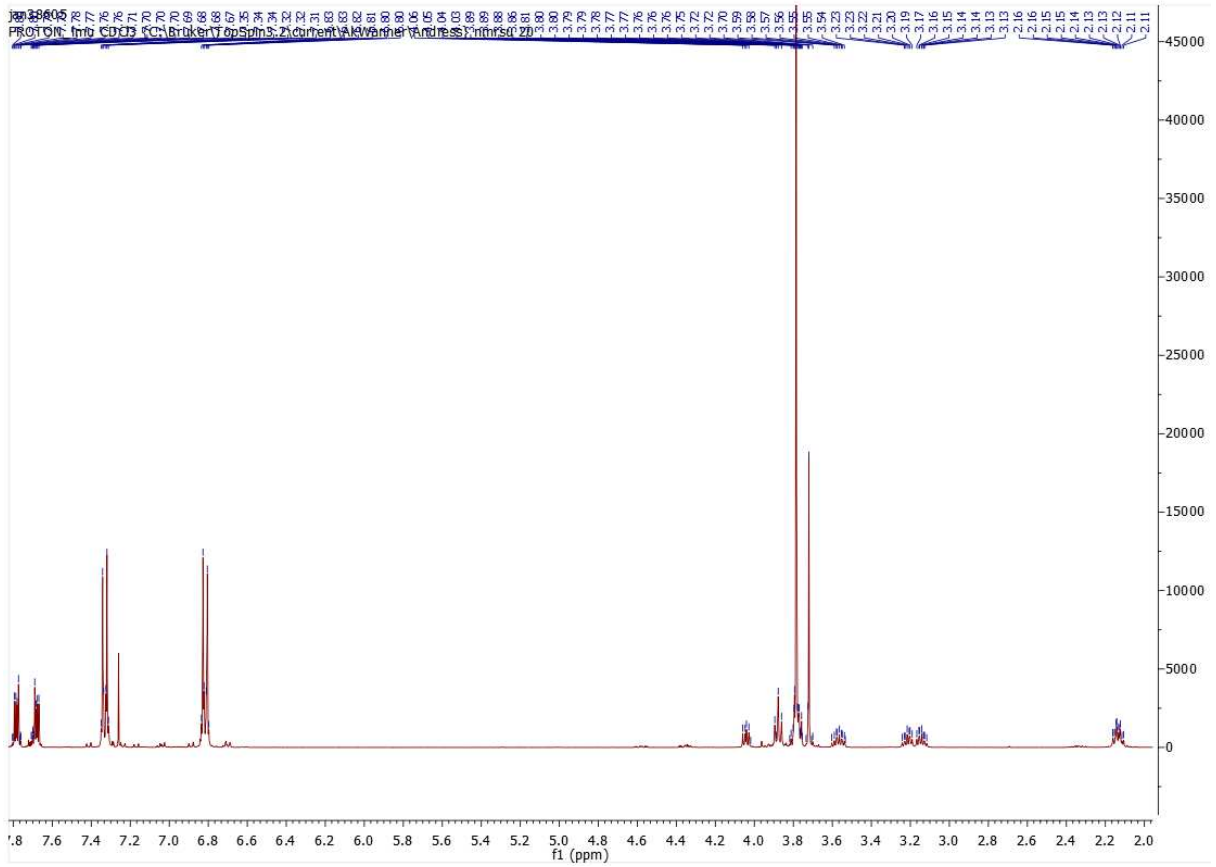

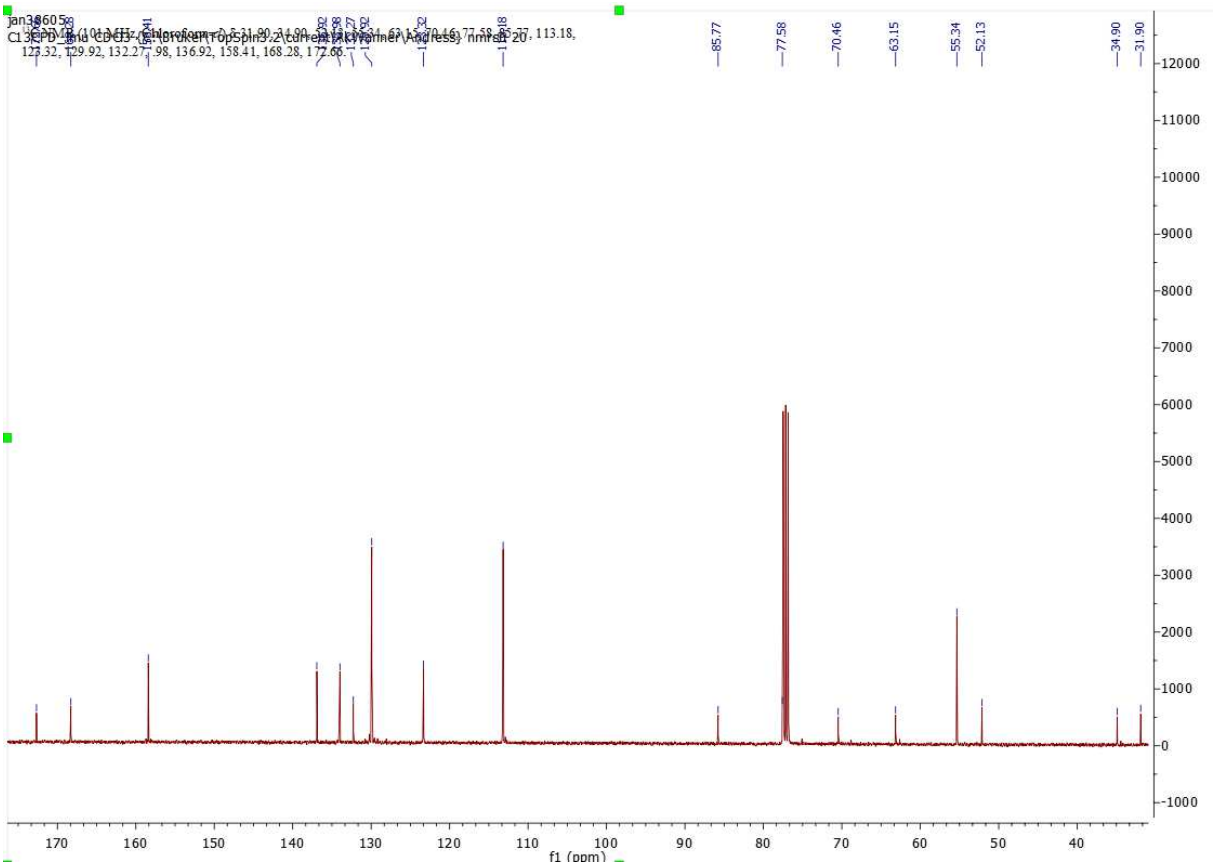

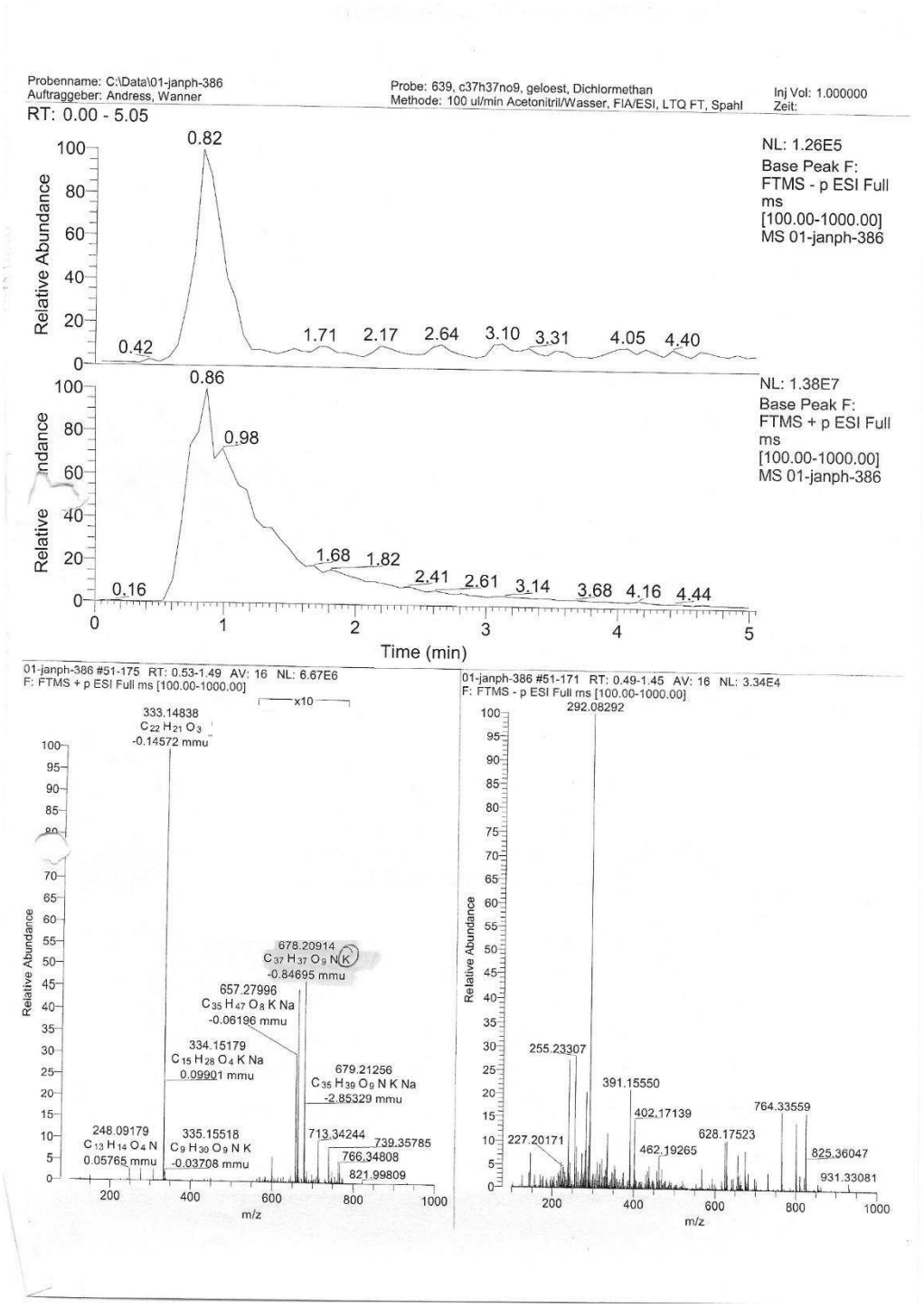
Probenname: C:\Data\01-janph-386
Auftraggeber: Andress, Wanner
Probe: 639, c37h37no9, geloest, Dichlormethan
Methode: 100 ul/min Acetonitril/Wasser, FIA/ESI, LTQ FT, Spahl
Inj Vol: 1.000000
Zeit:
RT: 0.00 - 5.05
NL: 1.26E5
Base Peak F:
FTMS - p ESI Full
ms
[100.00-1000.00]
MS 01-janph-386
Relative Abundance
0.82
0.42
1.71
2.17
2.64
3.10
3.31
4.05
4.40
NL: 1.38E7
Base Peak F:
FTMS + p ESI Full
ms
[100.00-1000.00]
MS 01-janph-386
0.86
0.98
0.16
1.68
1.82
2.41
2.61
3.14
3.68
4.16
4.44
Time (min)
01-janph-386 #51-175 RT: 0.53-1.49 AV: 16 NL: 6.67E6
F: FTMS + p ESI Full ms [100.00-1000.00]
x10
333.14838
C22 H21 O3
-0.14572 mmu
678.20914
C37 H37 O9 N K
-0.84695 mmu
657.27996
C35 H47 O8 K Na
-0.06196 mmu
334.15179
C15 H28 O4 K Na
0.09901 mmu
679.21256
C35 H39 O9 N K Na
-2.85329 mmu
248.09179
C13 H14 O4 N
0.05765 mmu
335.15518
C9 H30 O9 N K
-0.03708 mmu
713.34244
739.35785
766.34808
821.99809
m/z
01-janph-386 #51-171 RT: 0.49-1.45 AV: 16 NL: 3.34E4
F: FTMS - p ESI Full ms [100.00-1000.00]
292.08292
255.23307
391.15550
402.17139
764.33559
628.17523
227.20171
462.19265
825.36047
931.33081
m/z

4-Amino-2-{2-[tris(4-methoxyphenyl)methoxy]ethoxy}butanoic acid (14g)

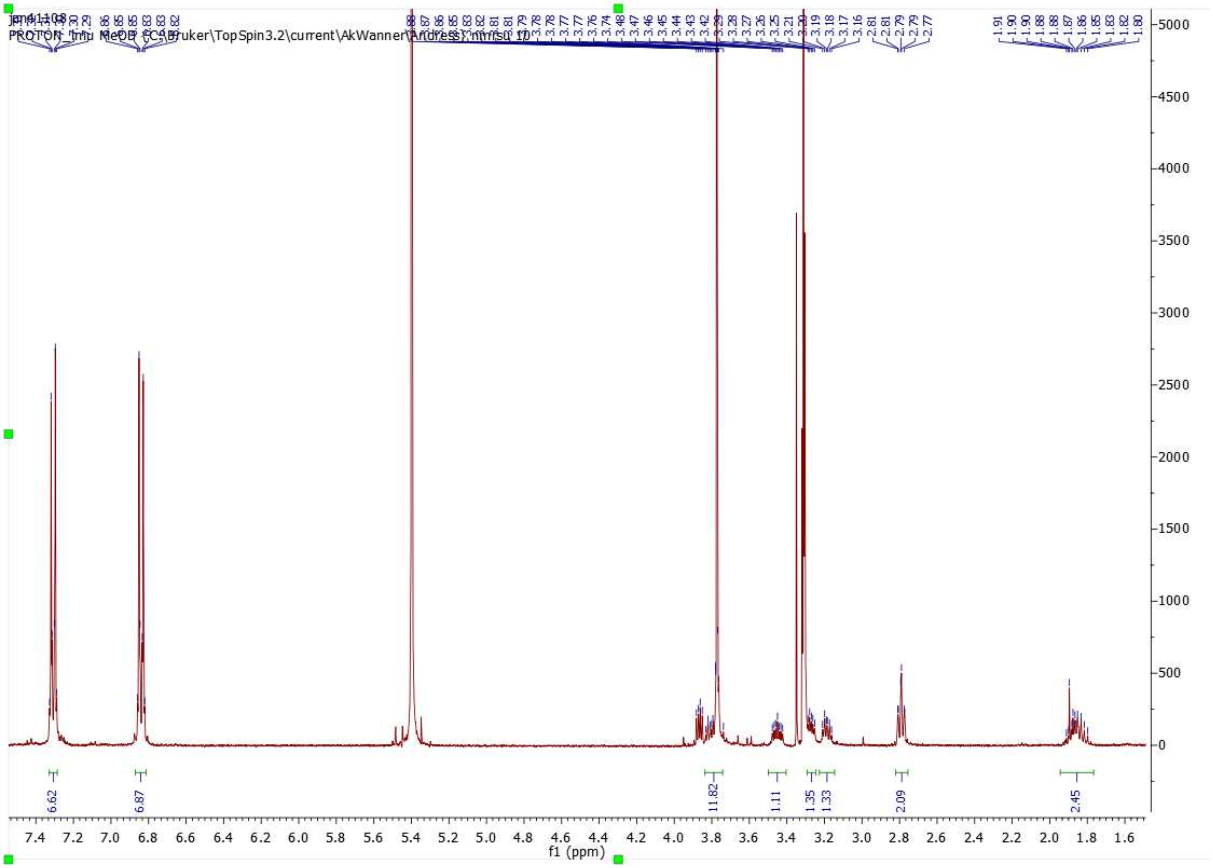

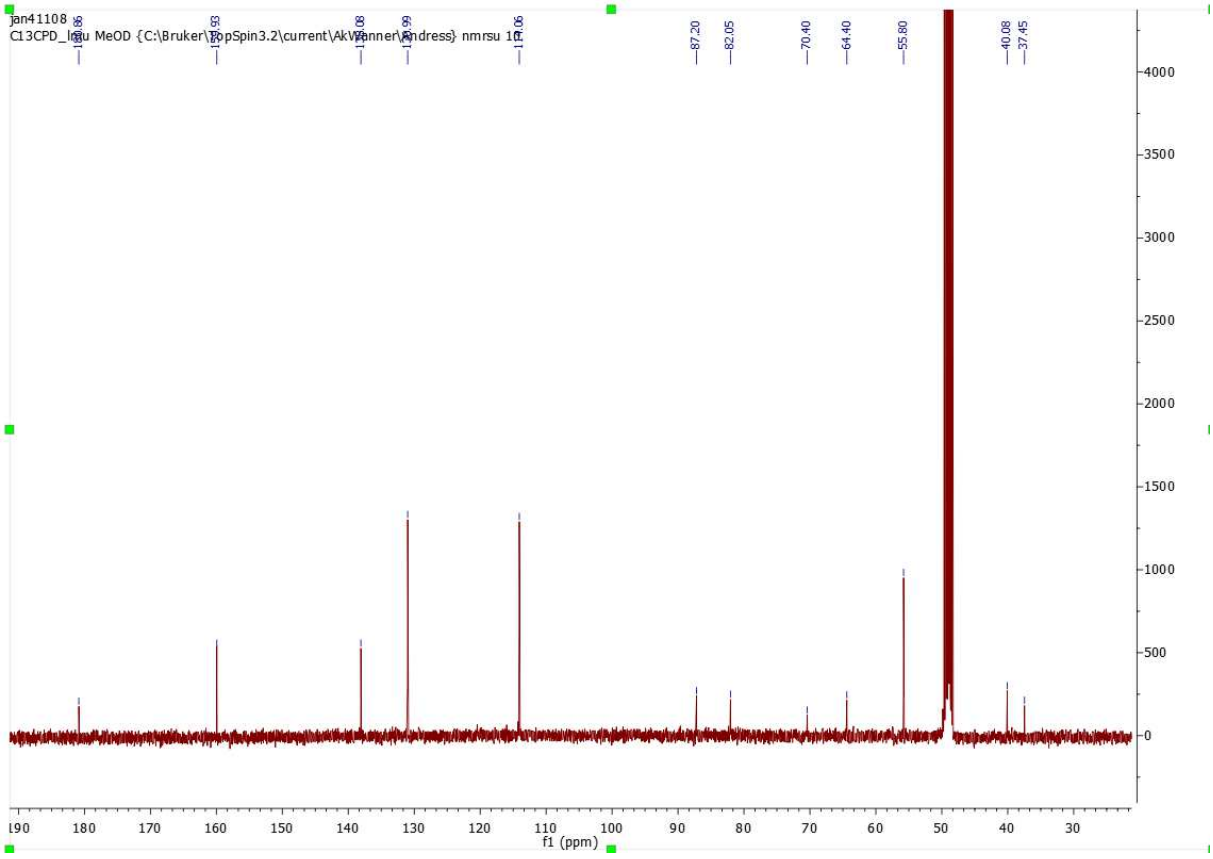

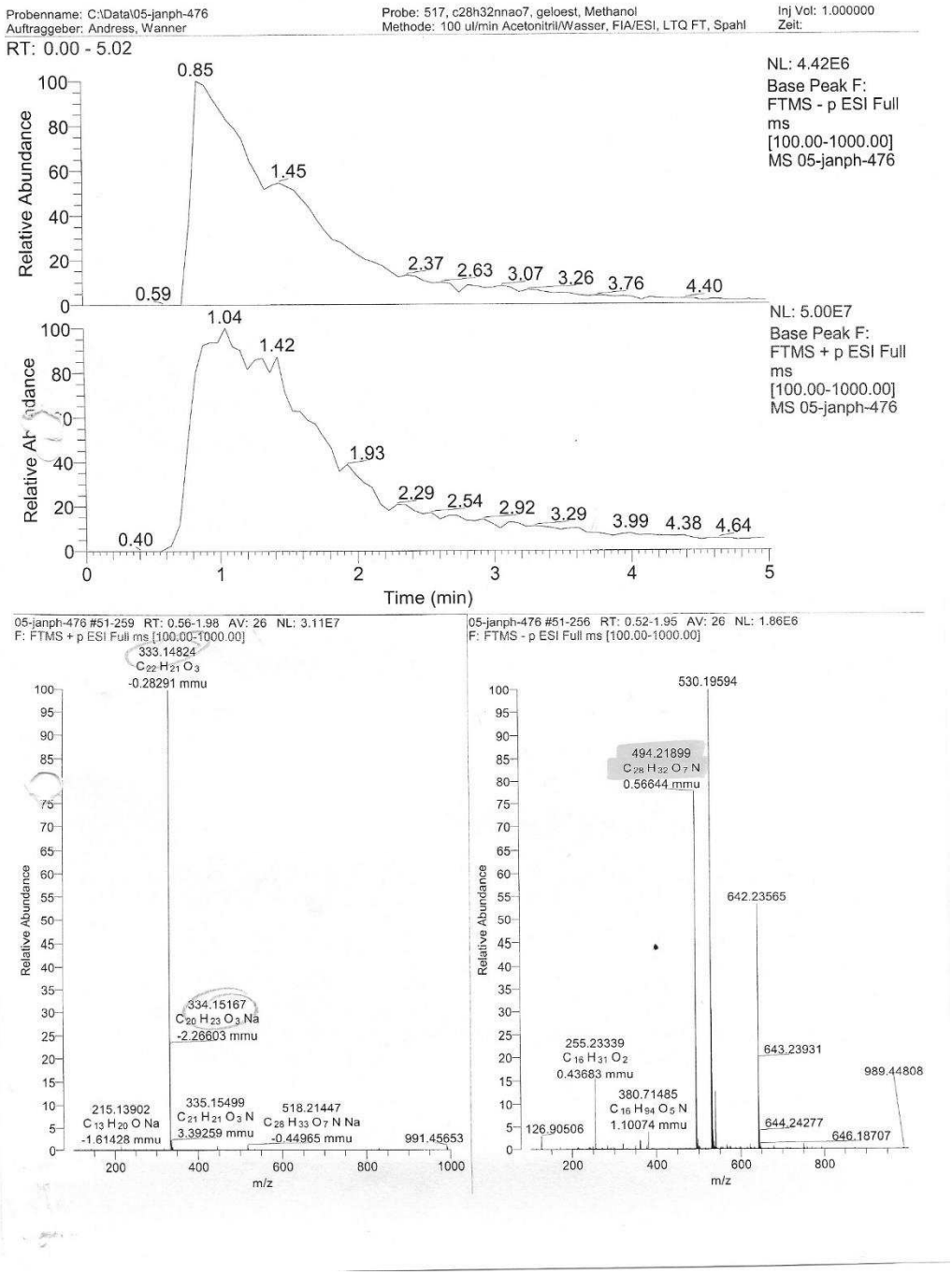
Probenname: C:\Data\05-janph-476
Auftraggeber: Andress, Wanner
Probe: 517, c28h32nnao7, geloest, Methanol
Methode: 100 ul/min Acetonitril/Wasser, FIA/ESI, LTQ FT, Spahl
Inj Vol: 1.000000
Zeit:
RT: 0.00 - 5.02
NL: 4.42E6
Base Peak F:
FTMS - p ESI Full
ms
[100.00-1000.00]
MS 05-janph-476
Relative Abundance
0.85
1.45
0.59
2.37
2.63
3.07
3.26
3.76
4.40
NL: 5.00E7
Base Peak F:
FTMS + p ESI Full
ms
[100.00-1000.00]
MS 05-janph-476
1.04
1.42
1.93
0.40
2.29
2.54
2.92
3.29
3.99
4.38
4.64
Time (min)
05-janph-476 #51-259 RT: 0.56-1.98 AV: 26 NL: 3.11E7
F: FTMS + p ESI Full ms [100.00-1000.00]
333.14824
C22 H21 O3
-0.28291 mmu
334.15167
C20 H23 O3 Na
-2.26603 mmu
215.13902
C13 H20 O Na
-1.61428 mmu
335.15499
C21 H21 O3 N
3.39259 mmu
518.21447
C28 H33 O7 N Na
-0.44965 mmu
991.45653
m/z
05-janph-476 #51-256 RT: 0.52-1.95 AV: 26 NL: 1.86E6
F: FTMS - p ESI Full ms [100.00-1000.00]
530.19594
494.21899
C28 H32 O7 N
0.56644 mmu
642.23565
643.23931
989.44808
255.23339
C16 H31 O2
0.43683 mmu
380.71485
C16 H94 O5 N
1.10074 mmu
644.24277
126.90506
646.18707
m/z

4-(Butylamino)-3-hydroxybutanoic acid (15b)

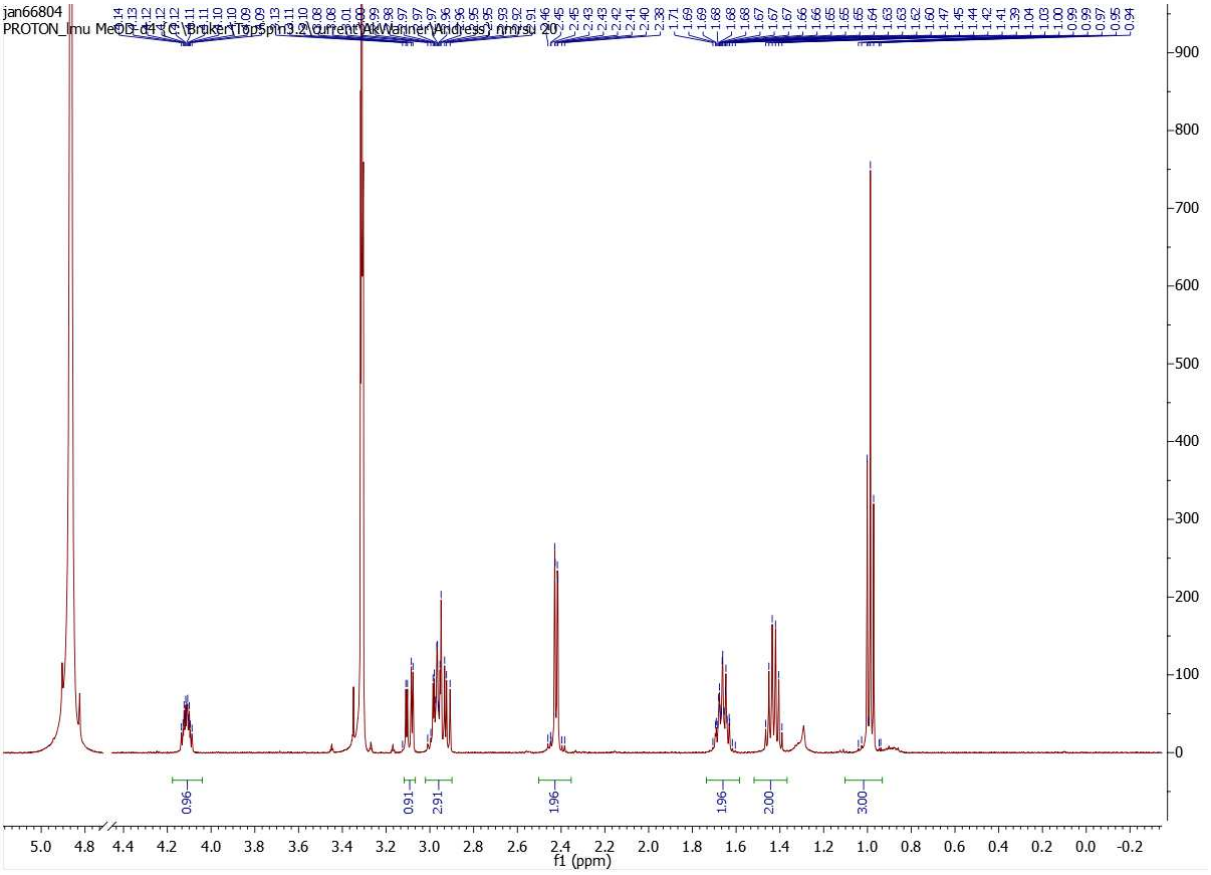

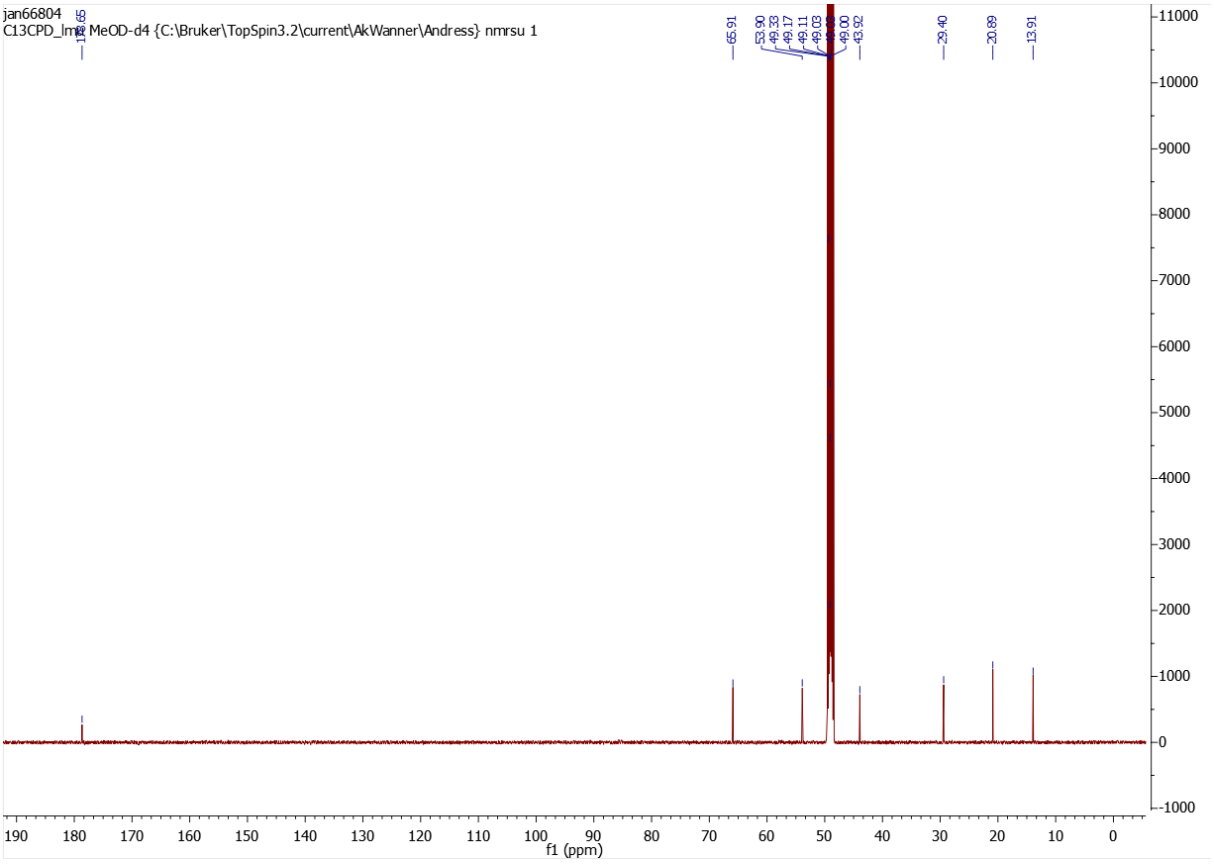

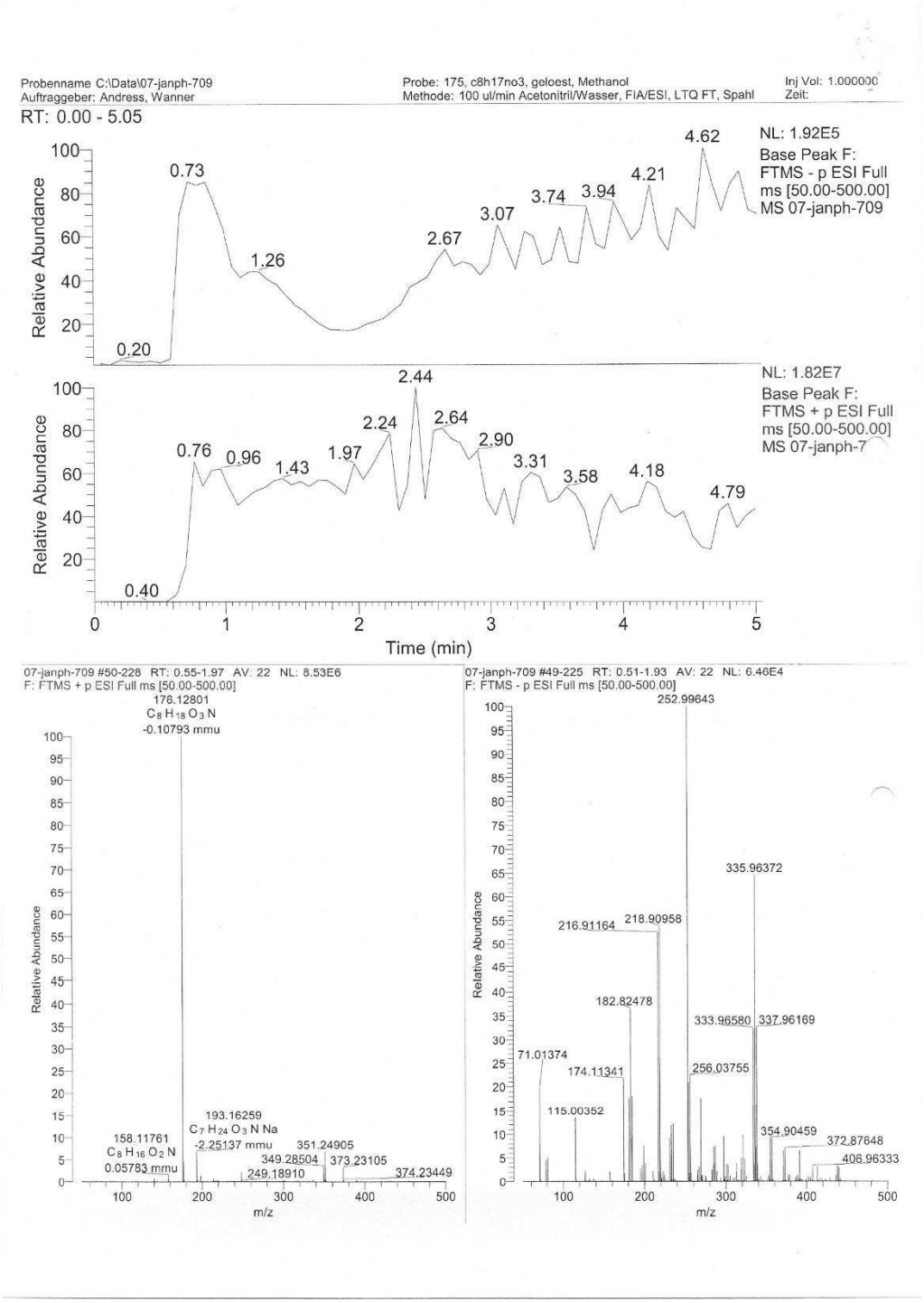
Probenname C:\Data\07-janph-709
Auftraggeber: Andress, Wanner
Probe: 175, c8h17no3, geloest, Methanol
Methode: 100 ul/min Acetonitril/Wasser, FIA/ESI, LTQ FT, Spahl
Inj Vol: 1.000000
Zeit:
RT: 0.00 - 5.05
NL: 1.92E5
Base Peak F:
FTMS - p ESI Full
ms [50.00-500.00]
MS 07-janph-709
NL: 1.82E7
Base Peak F:
FTMS + p ESI Full
ms [50.00-500.00]
MS 07-janph-7
Relative Abundance
Time (min)
07-janph-709 #50-228 RT: 0.55-1.97 AV: 22 NL: 8.53E6
F: FTMS + p ESI Full ms [50.00-500.00]
176.12801
C8 H18 O3 N
-0.10793 mmu
158.11761
C8 H16 O2 N
0.05783 mmu
193.16259
C7 H24 O3 N Na
-2.25137 mmu
m/z
07-janph-709 #49-225 RT: 0.51-1.93 AV: 22 NL: 6.46E4
F: FTMS - p ESI Full ms [50.00-500.00]
252.99643
335.96372
216.91164
218.90958
182.82478
333.96580
337.96169
71.01374
174.11341
256.03755
115.00352
354.90459
372.87648
406.96333

Methyl 4-(1,3-dioxoisoindolin-2-yl)-3-hydroxybutanoate (15c)

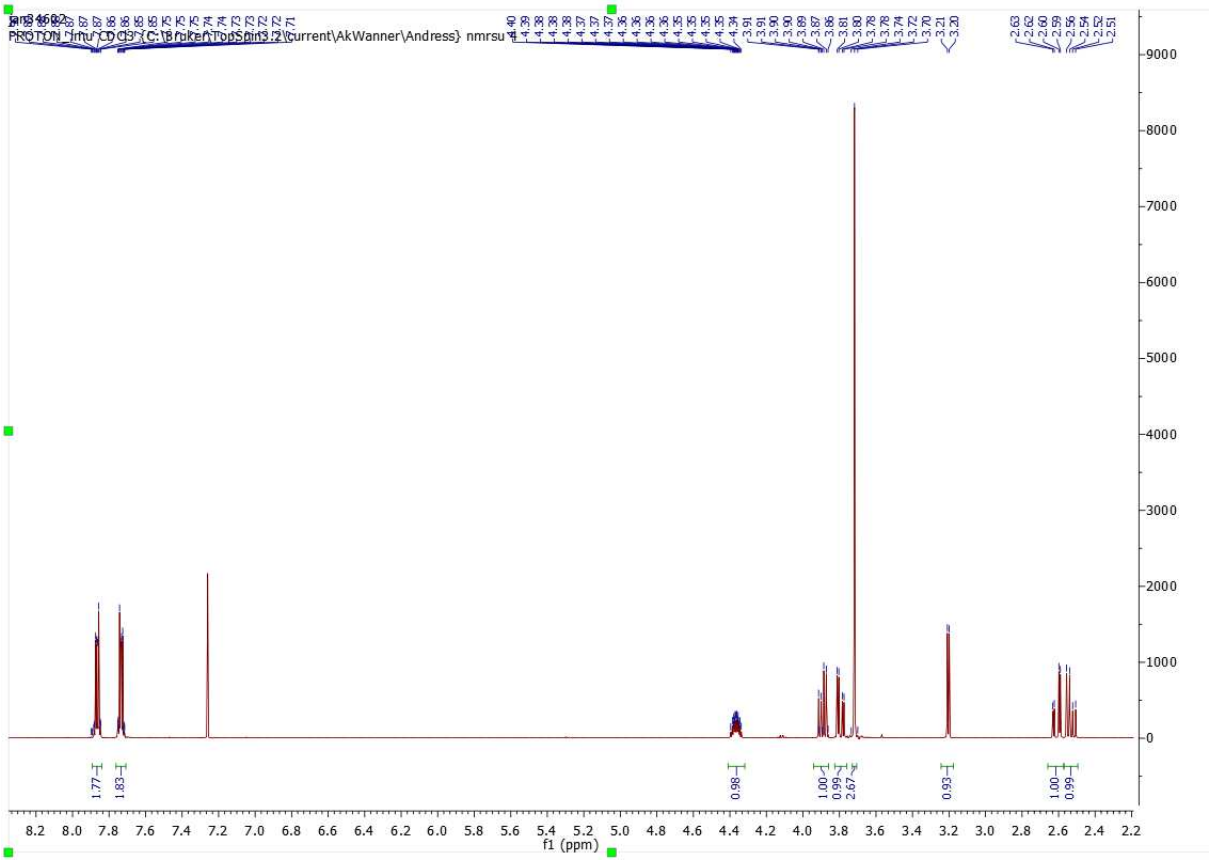

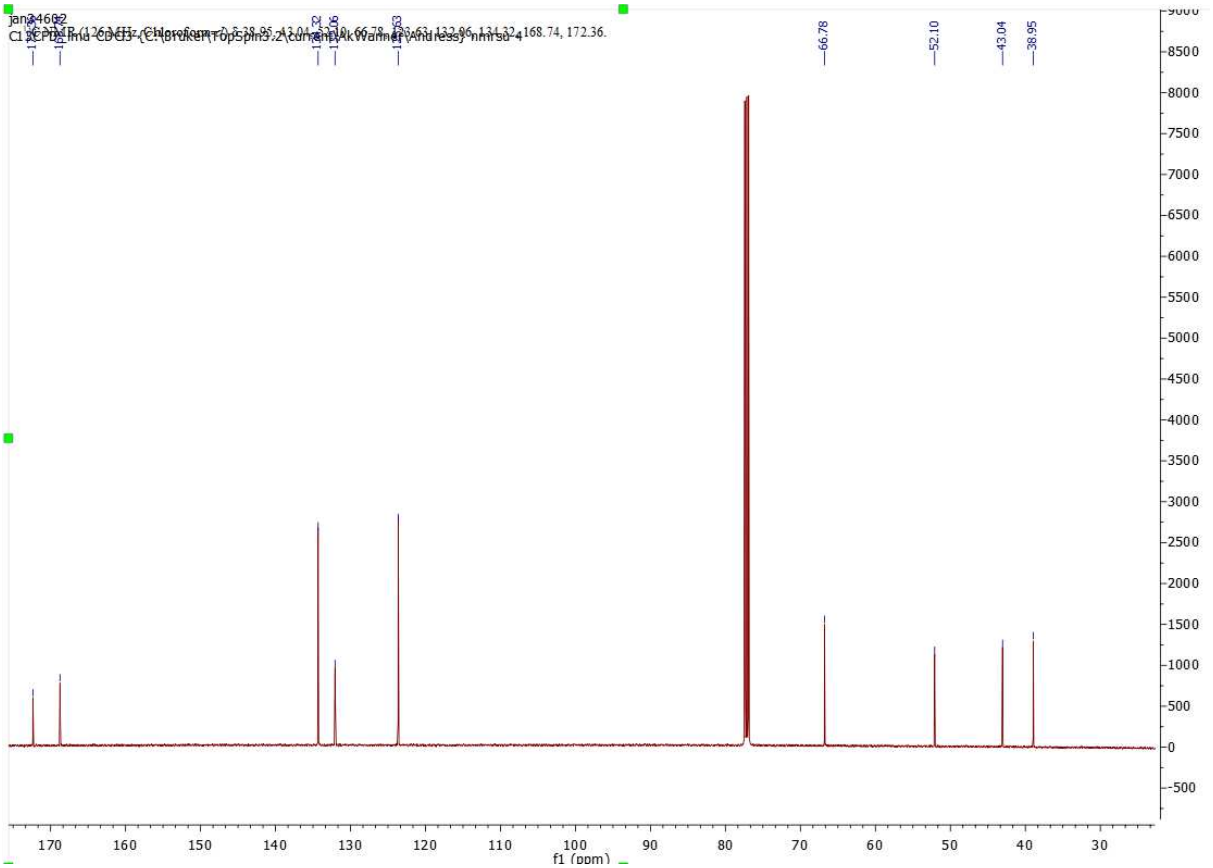

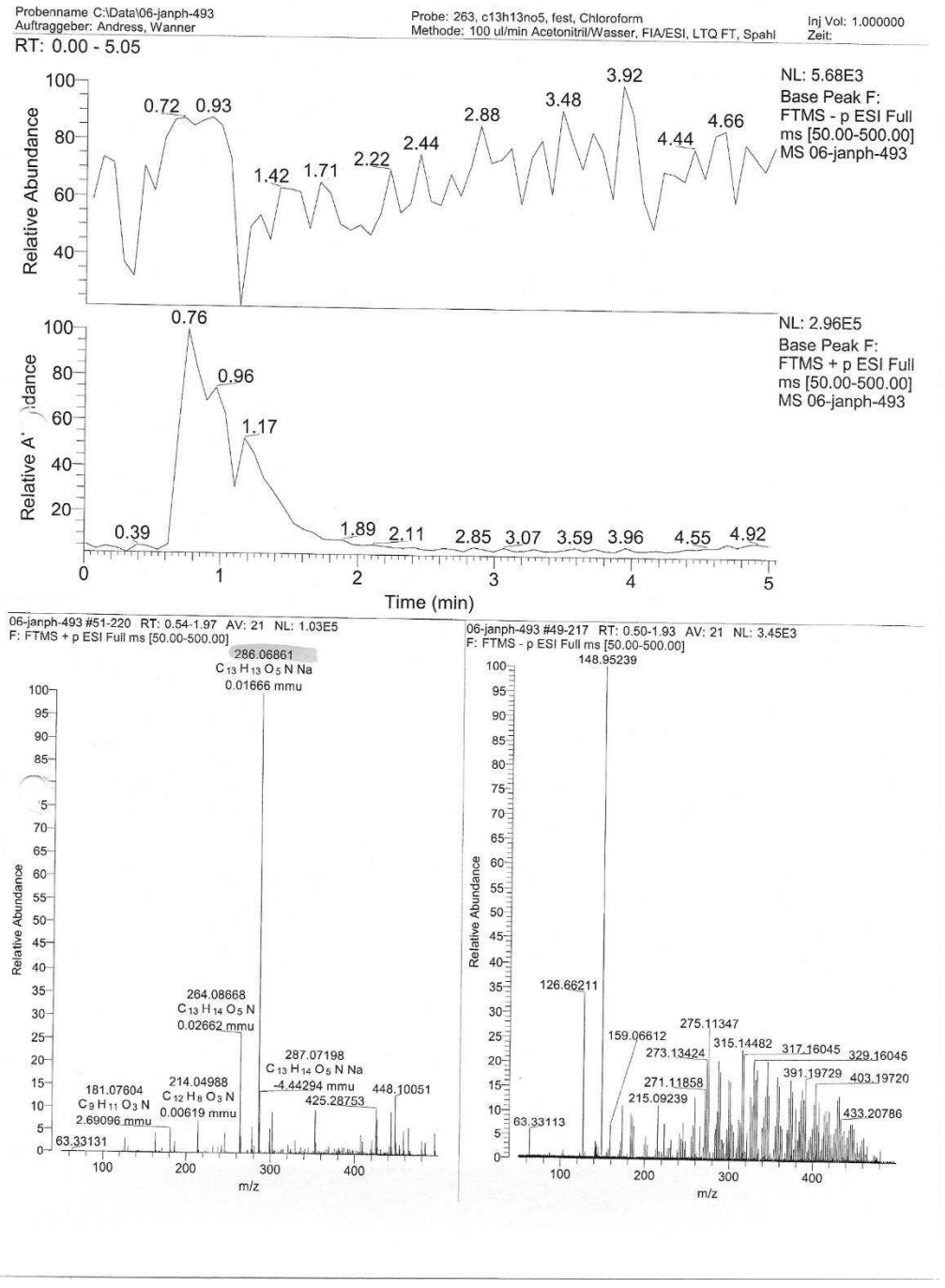
Probenname C:\Data\06-janph-493
Auftraggeber: Andress, Wanner
Probe: 263, c13h13no5, fest, Chloroform
Methode: 100 ul/min Acetonitril/Wasser, FIA/ESI, LTQ FT, Spahl
Inj Vol: 1.000000
Zeit:
RT: 0.00 - 5.05
Relative Abundance
NL: 5.68E3
Base Peak F:
FTMS - p ESI Full
ms [50.00-500.00]
MS 06-janph-493
NL: 2.96E5
Base Peak F:
FTMS + p ESI Full
ms [50.00-500.00]
MS 06-janph-493
Time (min)
06-janph-493 #51-220 RT: 0.54-1.97 AV: 21 NL: 1.03E5
F: FTMS + p ESI Full ms [50.00-500.00]
286.06861
C13 H13 O5 N Na
0.01666 mmu
264.08668
C13 H14 O5 N
0.02662 mmu
287.07198
C13 H14 O5 N Na
-4.44294 mmu
181.07604
C9 H11 O3 N
2.69096 mmu
214.04988
C12 H8 O3 N
0.00619 mmu
425.28753
448.10051
63.33131
m/z
06-janph-493 #49-217 RT: 0.50-1.93 AV: 21 NL: 3.45E3
F: FTMS - p ESI Full ms [50.00-500.00]
148.95239
126.66211
159.06612
275.11347
273.13424
315.14482
317.16045
329.16045
391.19729
403.19720
271.11858
215.09239
433.20786
63.33113
m/z

Methyl 3-{2-[(tert-butyldiphenylsilyl)oxy]ethoxy}-4-{-(1,3-dioxoisoindolin-2-yl}butanoate (15d)

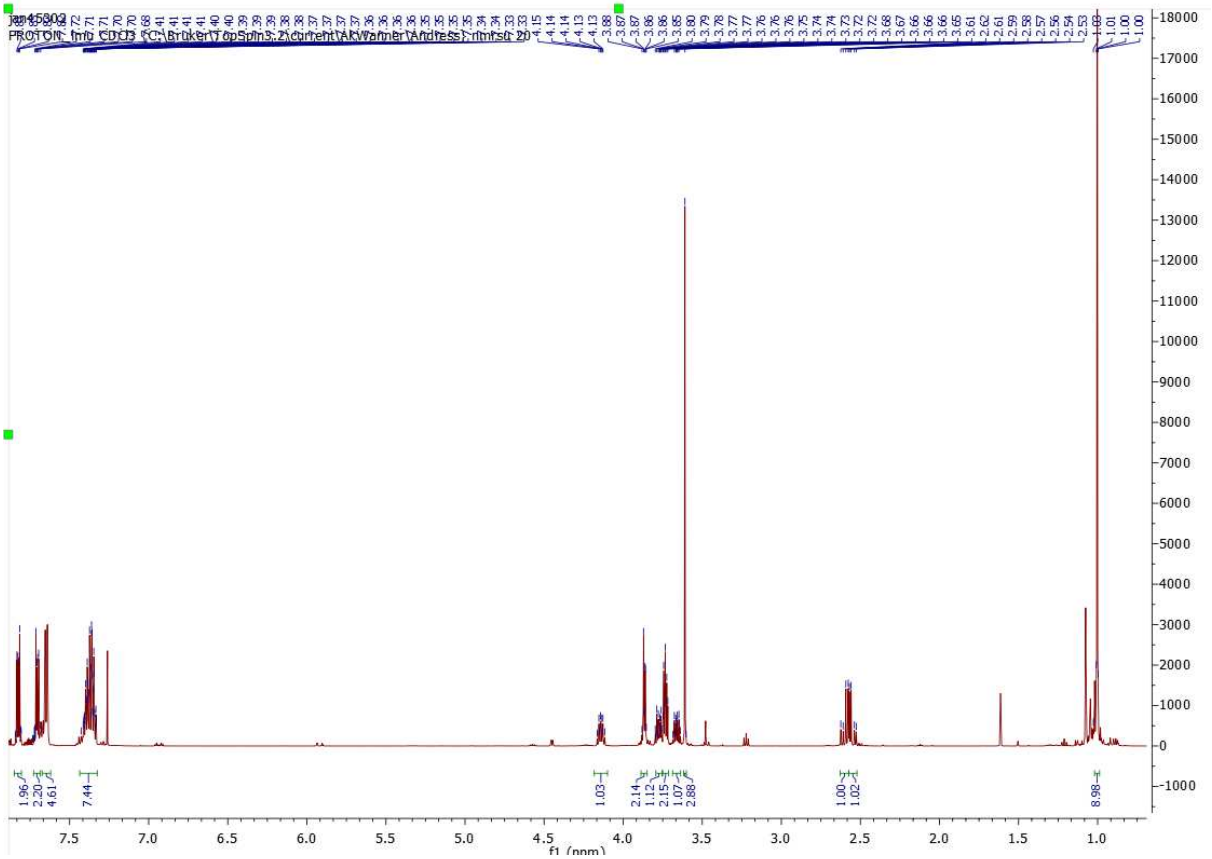

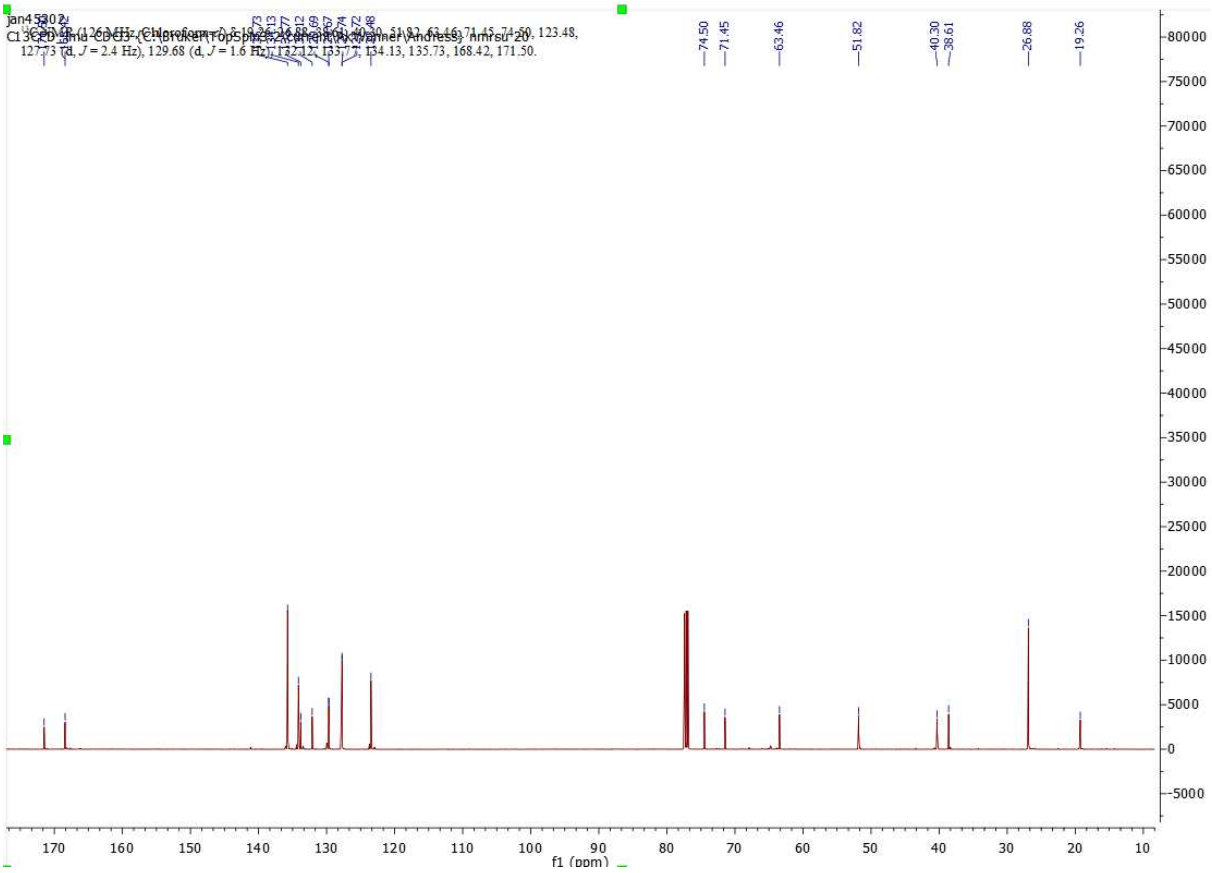

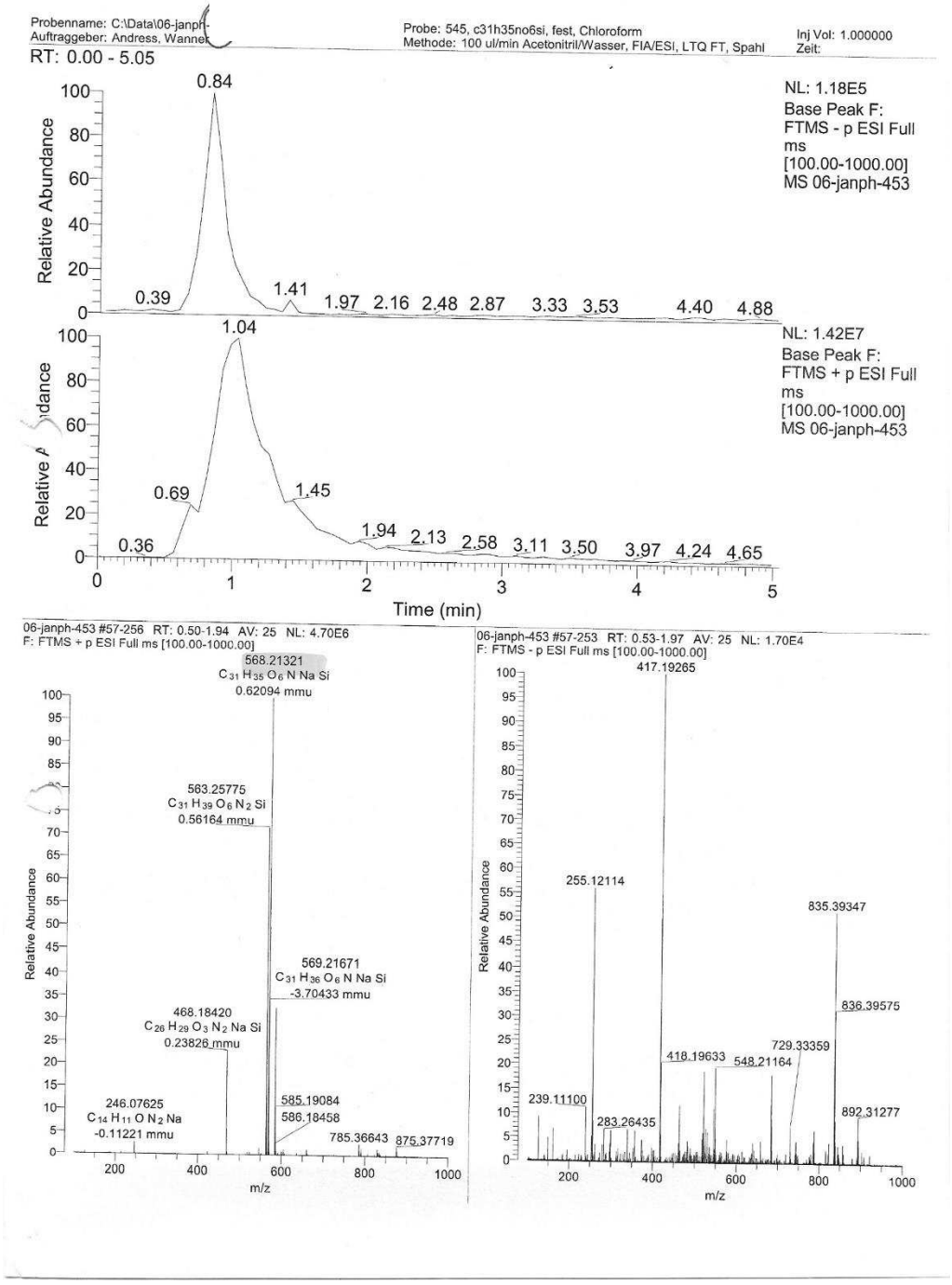
Probenname: C:\Data\06-janph-
Auftraggeber: Andress, Wannet
Probe: 545, c31h35no6si, fest, Chloroform
Methode: 100 ul/min Acetonitril/Wasser, FIA/ESI, LTQ FT, Spahl
Inj Vol: 1.000000
Zeit:
RT: 0.00 - 5.05
NL: 1.18E5
Base Peak F:
FTMS - p ESI Full
ms
[100.00-1000.00]
MS 06-janph-453
Relative Abundance
0.84
0.39
1.41
1.97
2.16
2.48
2.87
3.33
3.53
4.40
4.88
NL: 1.42E7
Base Peak F:
FTMS + p ESI Full
ms
[100.00-1000.00]
MS 06-janph-453
1.04
0.69
1.45
0.36
1.94
2.13
2.58
3.11
3.50
3.97
4.24
4.65
Time (min)
06-janph-453 #57-256 RT: 0.50-1.94 AV: 25 NL: 4.70E6
F: FTMS + p ESI Full ms [100.00-1000.00]
568.21321
C31 H35 O6 N Na Si
0.62094 mmu
563.25775
C31 H39 O6 N2 Si
0.56164 mmu
569.21671
C31 H36 O6 N Na Si
-3.70433 mmu
468.18420
C26 H29 O3 N2 Na Si
0.23826 mmu
246.07625
C14 H11 O N2 Na
-0.11221 mmu
585.19084
586.18458
785.36643
875.37719
m/z
06-janph-453 #57-253 RT: 0.53-1.97 AV: 25 NL: 1.70E4
F: FTMS - p ESI Full ms [100.00-1000.00]
417.19265
255.12114
835.39347
836.39575
729.33359
418.19633
548.21164
239.11100
283.26435
892.31277
m/z

Methyl 4-(1,3-dioxoisoindolin-2-yl)-3-(2-hydroxyethoxy)butanoate (15e)

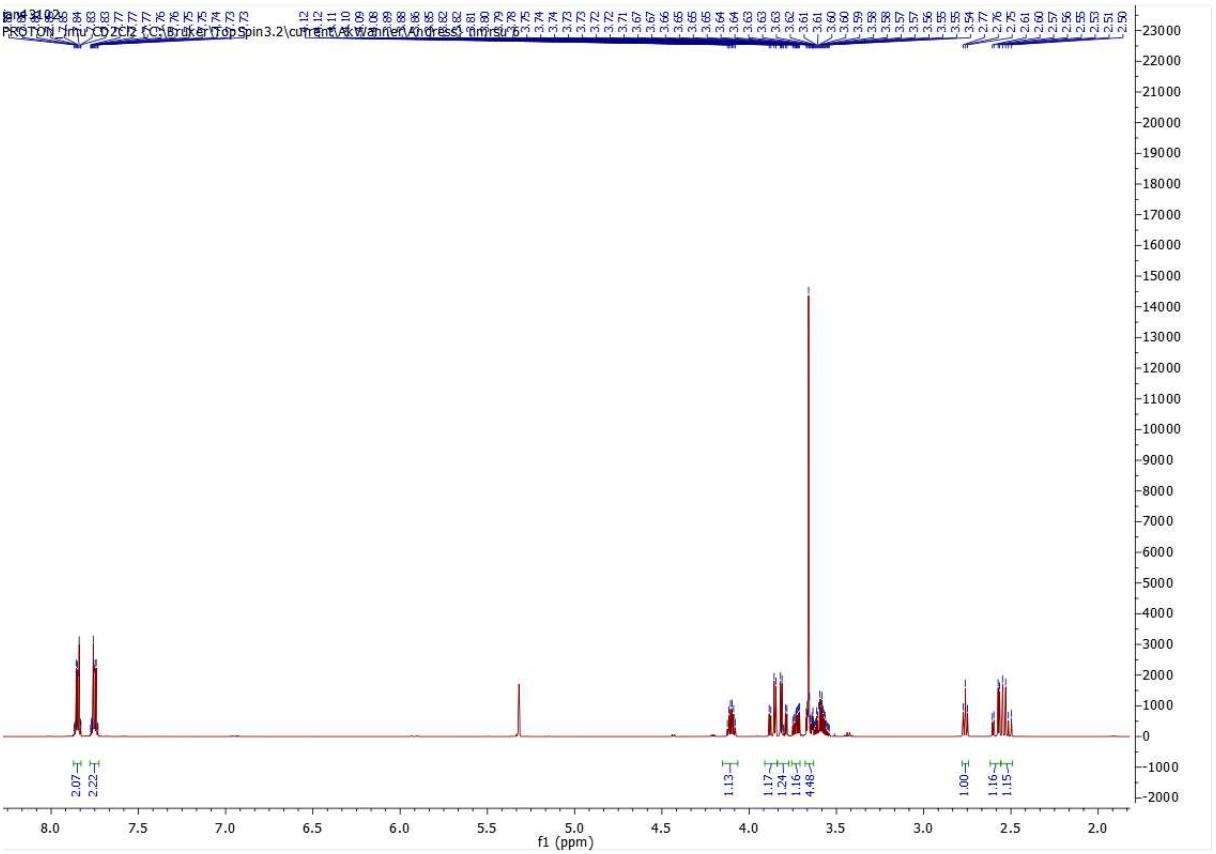

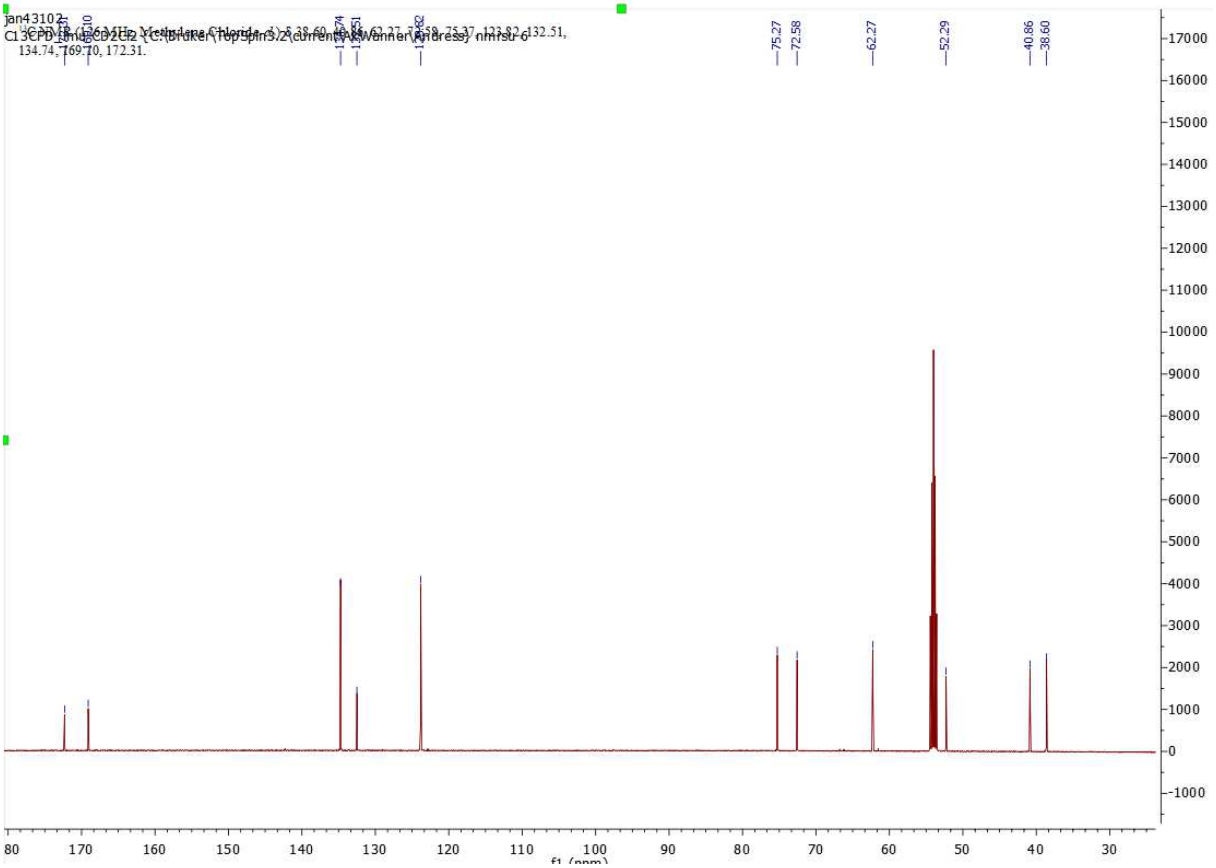

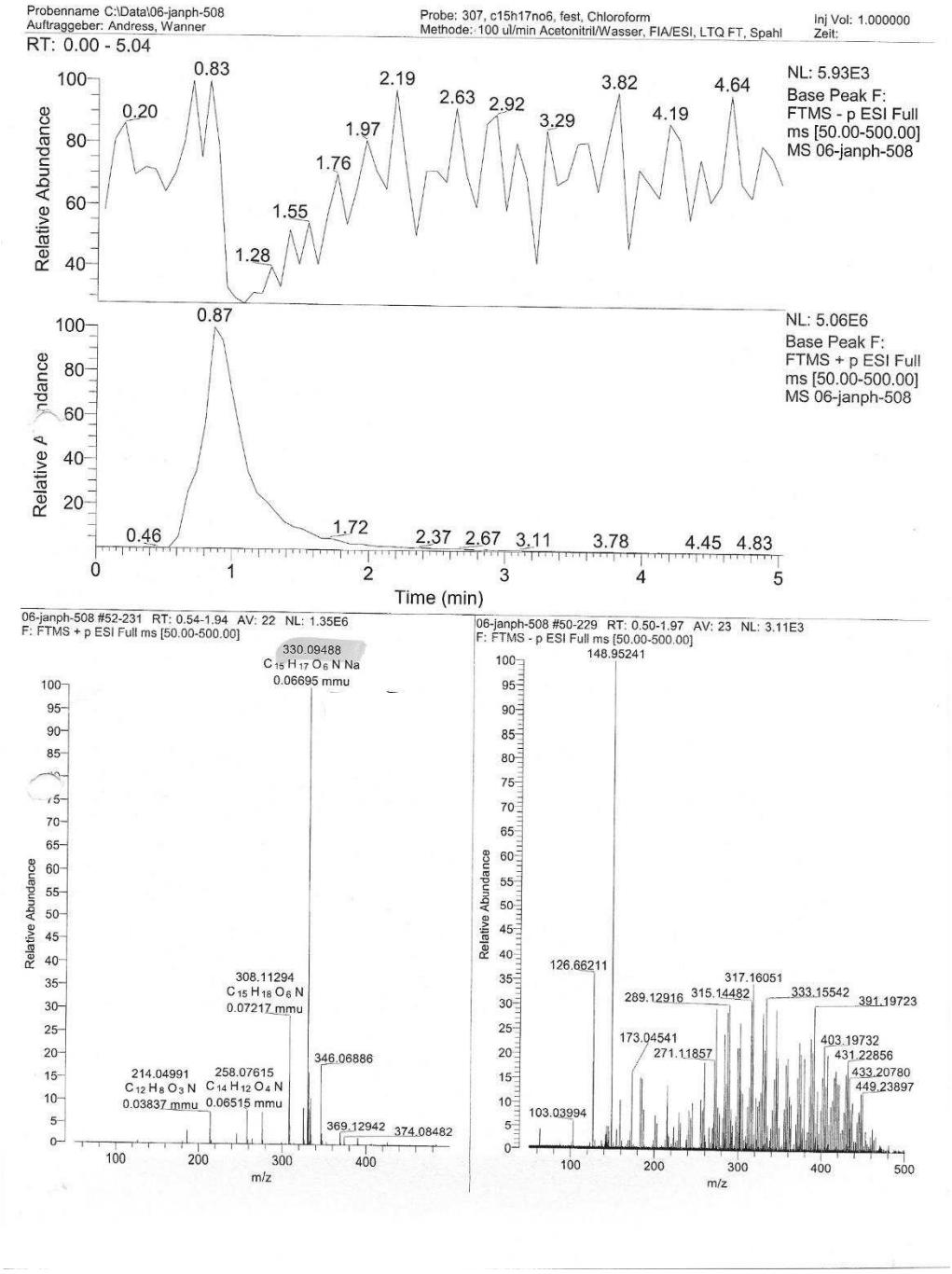
Probenname C:\Data\06-janph-508
Auftraggeber: Andress, Wanner
Probe: 307, c15h17no6, fest, Chloroform
Methode: 100 ul/min Acetonitril/Wasser, FIA/ESI, LTQ FT, Spahl
Inj Vol: 1.000000
Zeit:
RT: 0.00 - 5.04
NL: 5.93E3
Base Peak F:
FTMS - p ESI Full
ms [50.00-500.00]
MS 06-janph-508
NL: 5.06E6
Base Peak F:
FTMS + p ESI Full
ms [50.00-500.00]
MS 06-janph-508
Relative Abundance
Time (min)
06-janph-508 #52-231 RT: 0.54-1.94 AV: 22 NL: 1.35E6
F: FTMS + p ESI Full ms [50.00-500.00]
330.09488
C15 H17 O6 N Na
0.06695 mmu
308.11294
C15 H18 O6 N
0.07217 mmu
346.06886
214.04991
C12 H8 O3 N
0.03837 mmu
258.07615
C14 H12 O4 N
0.06515 mmu
369.12942
374.08482
m/z
06-janph-508 #50-229 RT: 0.50-1.97 AV: 23 NL: 3.11E3
F: FTMS - p ESI Full ms [50.00-500.00]
148.95241
126.66211
317.16051
289.12916
315.14482
333.15542
391.19723
173.04541
271.11857
403.19732
431.22856
433.20780
449.23897
103.03994
m/z

Methyl 4-{1,3-dioxoisoindolin-2-yl}-3-{2-[tris(4-methoxyphenyl)methoxy]ethoxy}butanoate (15f)

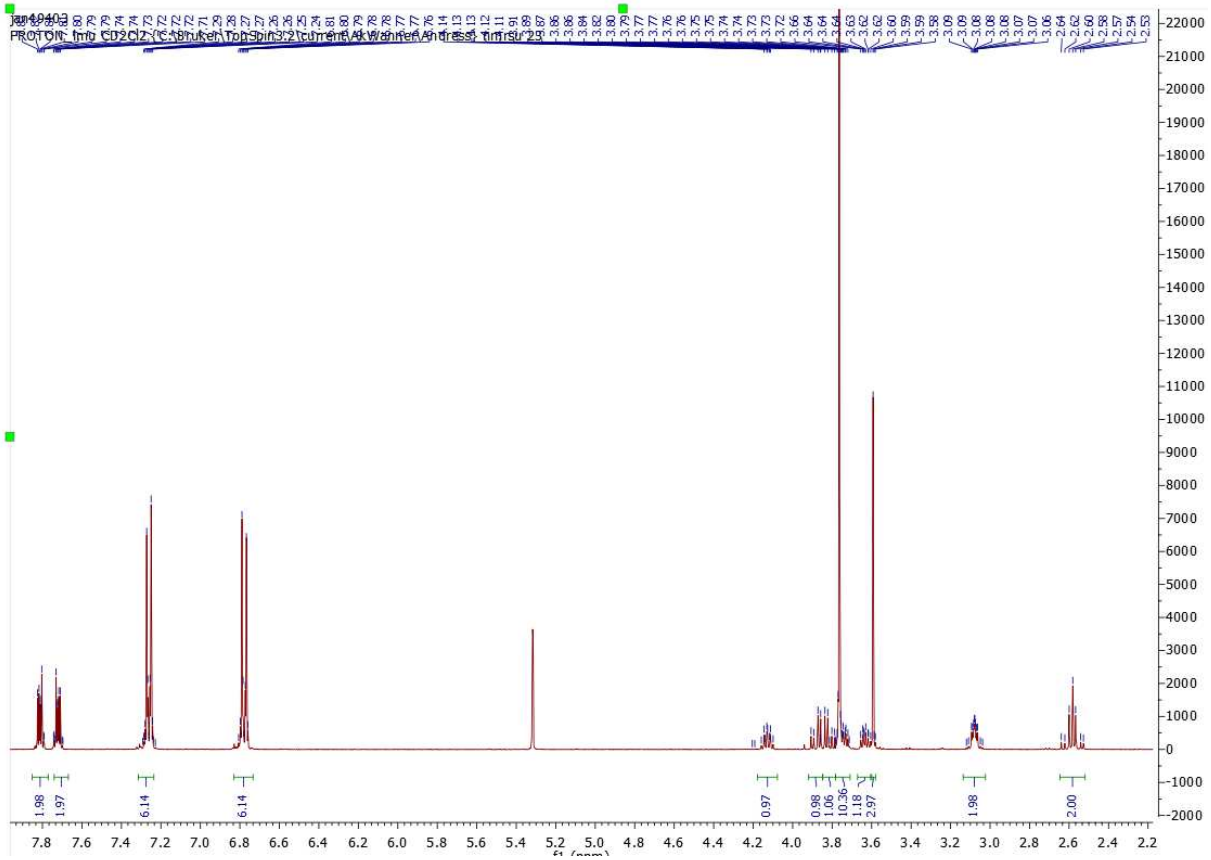

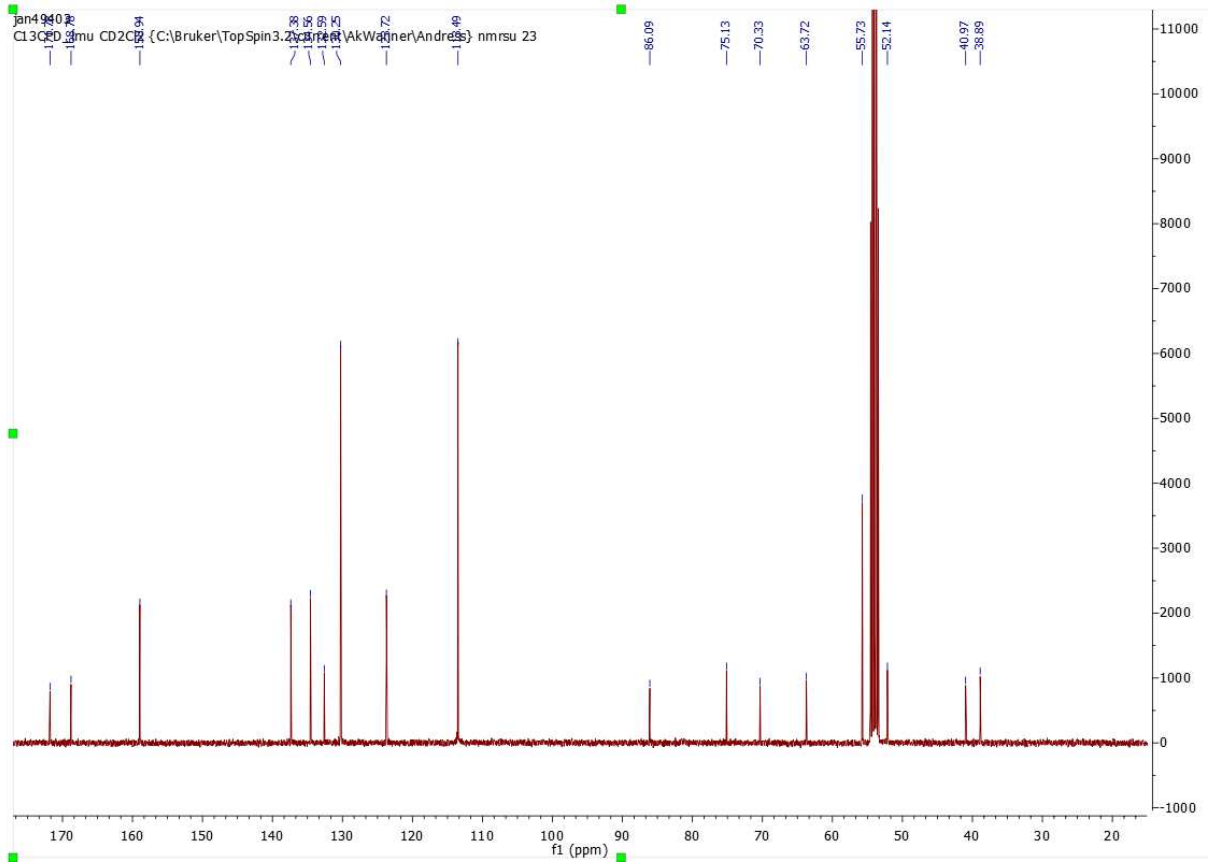

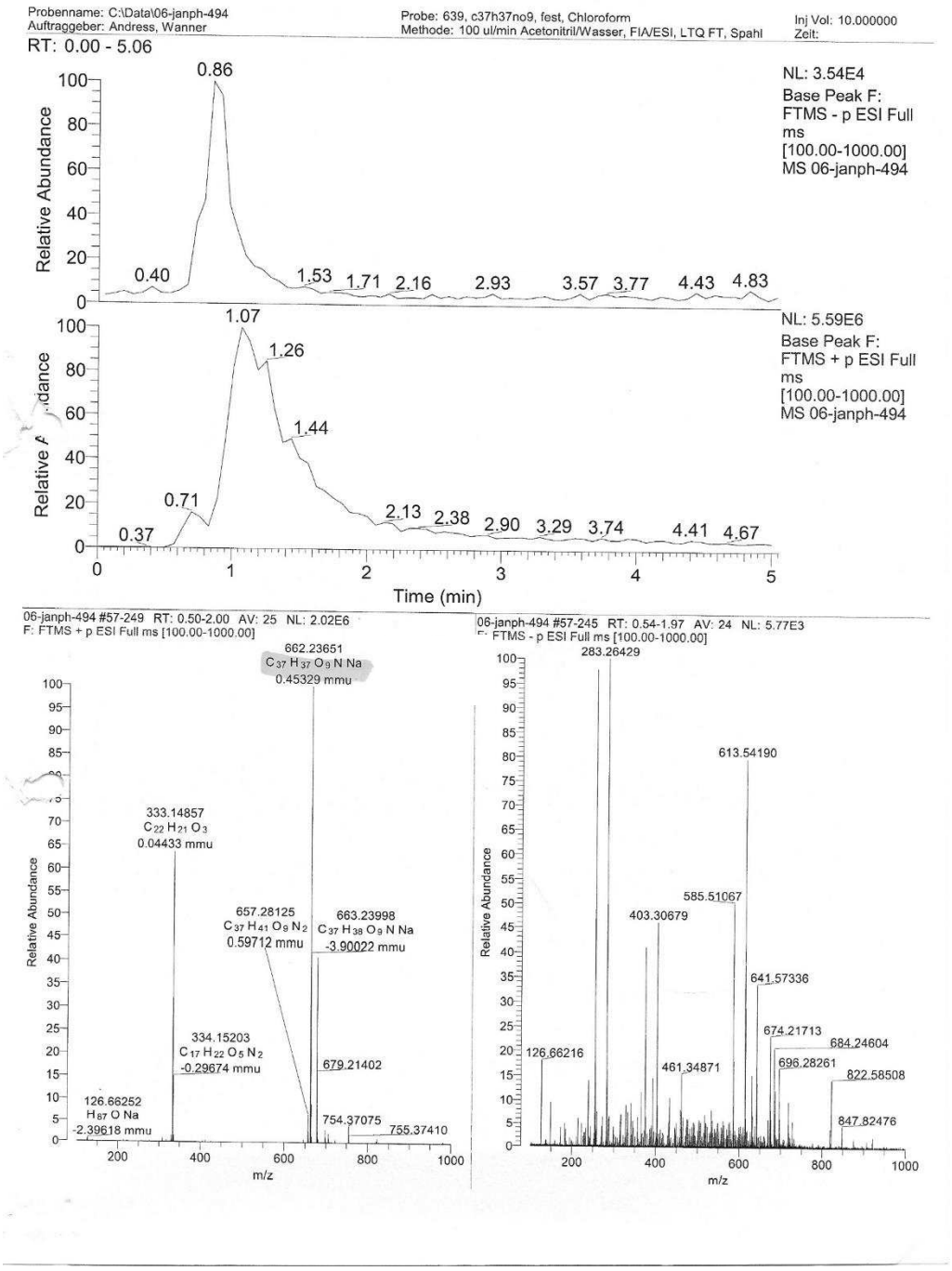
Probenname: C:\Data\06-janph-494
Auftraggeber: Andress, Wanner
Probe: 639, c37h37no9, fest, Chloroform
Methode: 100 ul/min Acetonitril/Wasser, FIA/ESI, LTQ FT, Spahl
Inj Vol: 10.000000
Zeit:
RT: 0.00 - 5.06
NL: 3.54E4
Base Peak F: FTMS - p ESI Full ms [100.00-1000.00] MS 06-janph-494
NL: 5.59E6
Base Peak F: FTMS + p ESI Full ms [100.00-1000.00] MS 06-janph-494
Relative Abundance
Time (min)
06-janph-494 #57-249 RT: 0.50-2.00 AV: 25 NL: 2.02E6
F: FTMS + p ESI Full ms [100.00-1000.00]
662.23651
C37 H37 O9 N Na
0.45329 mmu
333.14857
C22 H21 O3
0.04433 mmu
657.28125
C37 H41 O9 N2
0.59712 mmu
663.23998
C37 H38 O9 N Na
-3.90022 mmu
334.15203
C17 H22 O5 N2
-0.29674 mmu
679.21402
126.66252
H87 O Na
-2.39618 mmu
754.37075
755.37410
m/z
06-janph-494 #57-245 RT: 0.54-1.97 AV: 24 NL: 5.77E3
F: FTMS - p ESI Full ms [100.00-1000.00]
283.26429
613.54190
585.51067
403.30679
641.57336
674.21713
684.24604
696.28261
822.58508
847.82476
126.66216
461.34871
m/z

4-Amino-3-{2-[tris(4-methoxyphenyl)methoxy]ethoxy}butanoic acid (15g)

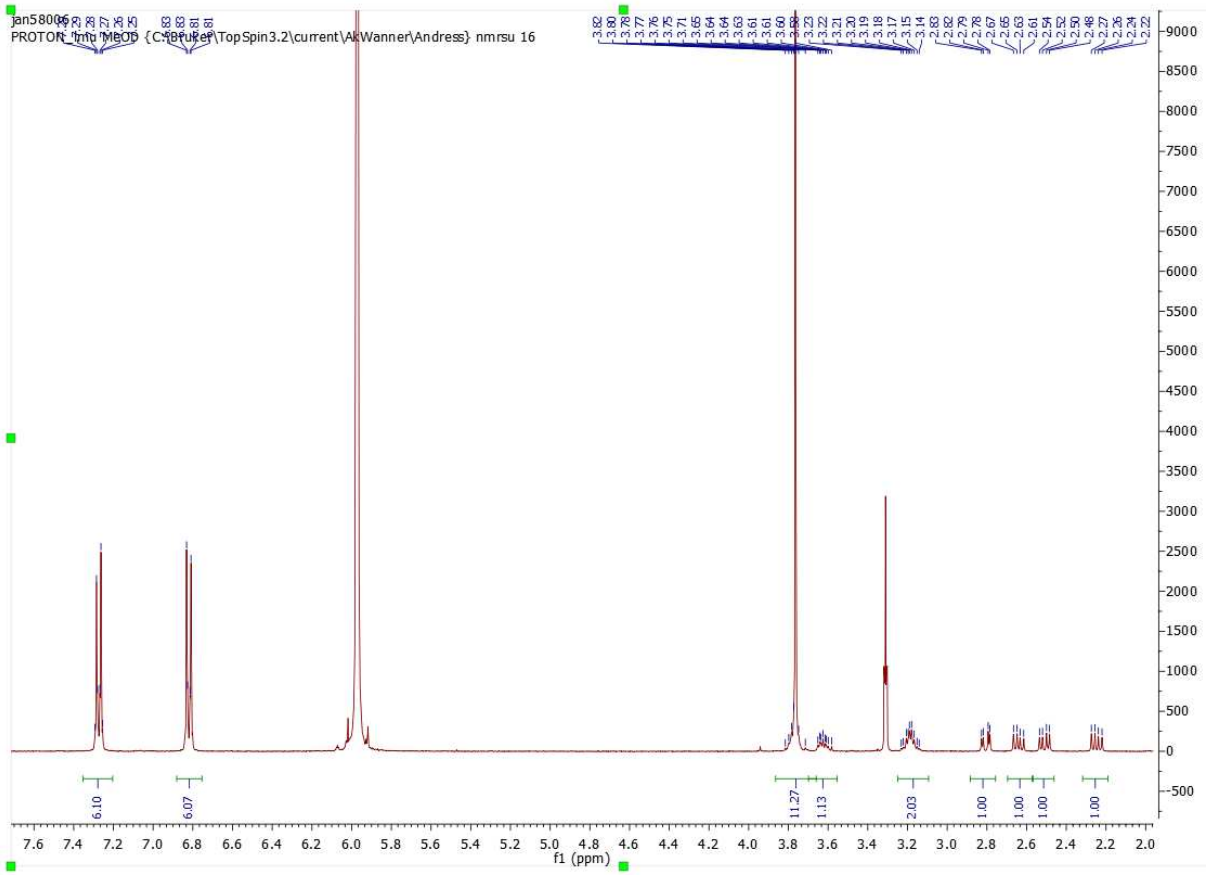

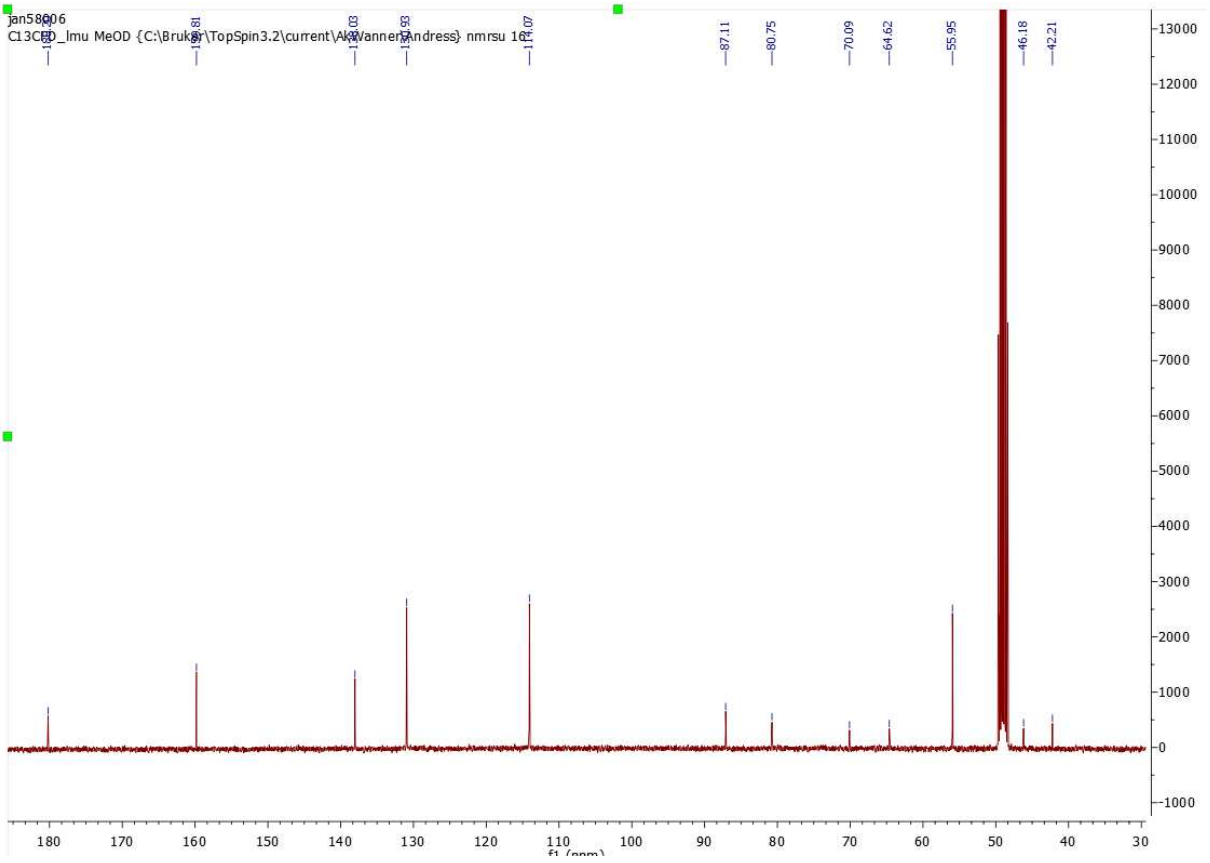

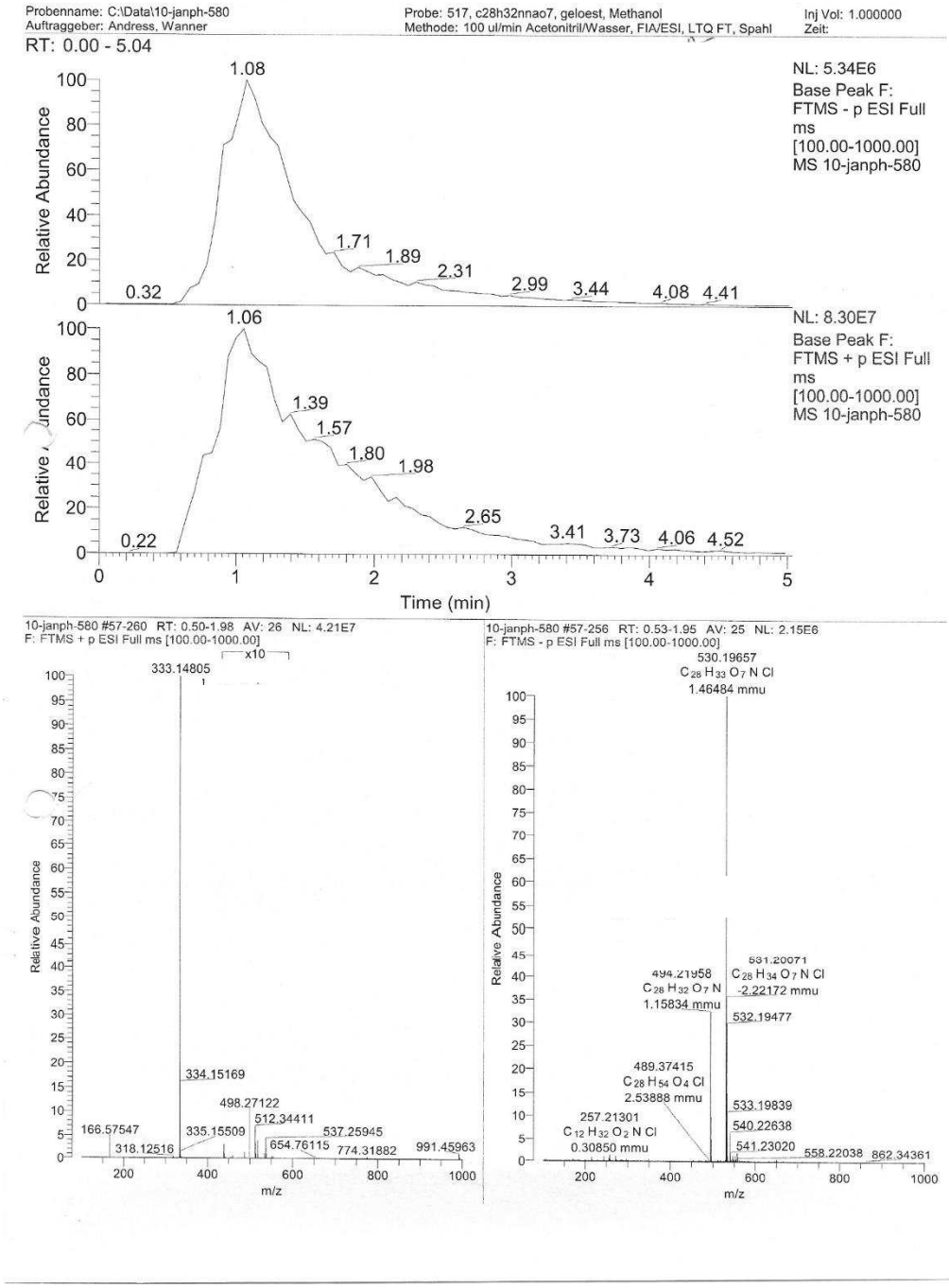
Probenname: C:\Data\10-janph-580
Auftraggeber: Andress, Wanner
Probe: 517, c28h32nnao7, geloest, Methanol
Methode: 100 ul/min Acetonitril/Wasser, FIA/ESI, LTQ FT, Spahl
Inj Vol: 1.000000
Zeit:
RT: 0.00 - 5.04
NL: 5.34E6
Base Peak F:
FTMS - p ESI Full
ms
[100.00-1000.00]
MS 10-janph-580
Relative Abundance
1.08
1.71
1.89
2.31
2.99
3.44
4.08
4.41
0.32
NL: 8.30E7
Base Peak F:
FTMS + p ESI Full
ms
[100.00-1000.00]
MS 10-janph-580
1.06
1.39
1.57
1.80
1.98
2.65
3.41
3.73
4.06
4.52
0.22
Time (min)
10-janph-580 #57-260 RT: 0.50-1.98 AV: 26 NL: 4.21E7
F: FTMS + p ESI Full ms [100.00-1000.00]
x10
333.14805
334.15169
498.27122
512.34411
166.57547
318.12516
335.15509
537.25945
654.76115
774.31882
991.45963
m/z
10-janph-580 #57-256 RT: 0.53-1.95 AV: 25 NL: 2.15E6
F: FTMS - p ESI Full ms [100.00-1000.00]
530.19657
C28 H33 O7 N Cl
1.46484 mmu
494.21958
C28 H32 O7 N
1.15834 mmu
531.20071
C28 H34 O7 N Cl
-2.22172 mmu
532.19477
489.37415
C28 H54 O4 Cl
2.53888 mmu
257.21301
C12 H32 O2 N Cl
0.30850 mmu
533.19839
540.22638
541.23020
558.22038
862.34361
m/z

Synthesis and Biological Evaluation of N-Substituted Nipecotic Acids as (*S*)-SNAP-5114 Analogues with Modified Lipophilic Domains

Michael C. Böck, Georg Höfner, Klaus T. Wanner
Department of Pharmacy – Center for Drug Research
Ludwig-Maximilians-Universität München
Butenandtstraße 5-13, 81377 Munich, Germany

Abstract

Potential mGAT4 inhibitors derived from the lead substance (*S*)-SNAP-5114 have been synthesized and characterized for their inhibitory potency. Variations from the parent compound included the substitution of one of its aromatic 4-methoxy and 4-methoxyphenyl groups, respectively, with a more polar moiety, including a carboxylic acid, alcohol, nitrile, carboxamide, sulfonamide, aldehyde or ketone function, or amino acid partial structures. Furthermore, it was investigated how the substitution of more than one of the aromatic 4-methoxy groups affects the potency and selectivity of the resulting compounds. Among the synthesized test substances (*S*)-1-{2-[(4-formylphenyl)bis(4-methoxyphenyl)methoxy]ethyl}-piperidine-3-carboxylic acid, that features a carbaldehyde function in place of one of the aromatic 4-methoxy moieties of (*S*)-SNAP-5114, was found to have a pIC_{50} value of 5.89 ± 0.07, hence constituting a slightly more potent mGAT4 inhibitor than the parent substance while showing comparable subtype selectivity.

Introduction

The neuronal signal transduction in the mammalian central nervous system (CNS) is regulated by a complex equilibrium of various excitatory and inhibitory neurotransmitters. γ-Aminobutyric acid (GABA) is the most abundant of the latter,[1]with approximately 40% of synapses estimated to be GABAergic.[2] Pathologically deficient GABA release into the synaptic cleft results in attenuation of the inhibitory component, which is associated with a variety of severe neurological disorders including epilepsy,[3,4] neuropathic pain,[5] anxiety disorders,[6] depression,[6,7] and Alzheimer´s disease.[8] A promising approach to the treatment of these disorders is the application of drugs that inhibit the GABA reuptake[8,9,10,11] into the presynaptic neurons and the surrounding glial cells, respectively, thereby enhancing the GABA concentration in the synaptic cleft and thus prolonging the effect of the released GABA. The specific and high affinity membrane based[12] transport proteins accomplishing the GABA reuptake (GATs) are thus an important therapeutical target. Belonging to the solute carrier 6 (SLC6) family,[13] they consist of 12 transmembrane helices, four of which (TM 1, TM3, TM6 and TM8) form the inner ring that in its center halfway across the cell membrane holds the central substrate binding site S1. Separated from the S1 binding site by the extracellular gate a second substrate binding site exists at the bottom of the extracellular vestibule, termed S2,[12] the occupation of which is assumed to trigger the conformational changes necessary for the release of the substrate from the S1 pocket into the cell.[14] Four GAT subtypes have been identified, termed GAT1, GAT2, GAT3, and BGT1 in accordance with the nomenclature proposed by the Gene Nomenclature Committee of the Human Genome Organisation (HUGO),[15] or, when cloned from mouse brain, mGAT1 (≙ GAT1), mGAT2 (≙ BGT1), mGAT3 (≙ GAT2) and mGAT4 (≙GAT3).[16,17] Since the biological test system developed in our group is based on GABA transporters cloned from mouse cells, in this paper the corresponding nomenclature will be used.

The predominant GABA transporter in the mammalian CNS, mGAT1, is located primarily in pre-synaptic neuronal membranes,[18]with its highest densities found in neocortex, spinal cord, brainstem, cerebellum, basal ganglia, and hippocampus.[2,19] As the occurrence of mGAT2 and mGAT3 in the CNS is restricted to low densities in specific brain structures, these

subtypes play only a marginal role in the termination of the cerebral GABAergic neurotransmission.[20,21] mGAT4 is the second most abundant GABA transporter after mGAT1 and found particularly in olfactory bulb, brainstem, and diencephalon,[22] where it is most commonly expressed on glia cells.[18] The selective targeting of mGAT4 may therefore provide the possibility of treating neurological disorders associated with these brain regions with minimal impairment of the GABA reuptake in other parts of the CNS. Compared to mGAT1-selective inhibitors such as Tiagabine (Gabatril®) (**1**, table 1, entry 1), adverse effects, including dizziness, somnolence, headache, memory loss, and tremor,[23] could hence be possibly reduced, resulting in more tolerable medication and better patient compliance.

(*S*)-SNAP-5114 (*S*)-**2** (table 1, entry 3) can be considered the benchmark mGAT4 inhibitor. Since its publication,[24] it has been the prototype for the development of further mGAT4 inhibitors with the goal of increasing potency, subtype selectivity, and chemical stability. The structural modifications implemented in the (*S*)-SNAP-5114 scaffold so far include variations of the spacer between the nipecotic acid partial structure and the trityl rest, as it is for example the case with DDPM-1457 **3** (table 1, entry 4),[25] resulting in compounds with enhanced stability due to the labile trityl ether function being avoided. Variations of the substitution pattern of the trityl structure, e.g. by introduction of an additional methyl group in the 2-position of one of the three aryl residues (**4**, table 1, entry 5), was found to lead to compounds with slightly improved subtype selectivity. Unfortunately, the moderate potency inherent to the parent compound (*S*)-**2**, which is characterized by a pIC_{50} value of 5.71 ± 0.07 (table 1, entry 3), remains largely unaffected by these structural modifications. This underlines the necessity of further research in order to advance the general understanding of the structure activity relationship (SAR) of mGAT4 inhibitors.

***Table 1**. Binding affinities (pK_i) and inhibitory potencies (pIC_{50}) of reference compounds **1-5** from the literature*

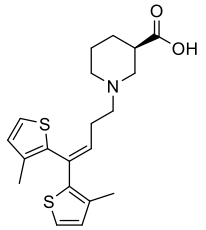

Tiagagbine [(*R*)-**1**]

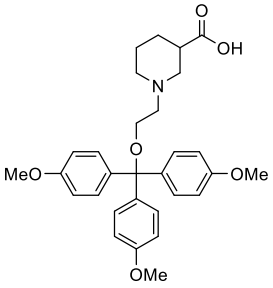

rac-SNAP-5114 [*rac*-**2**]

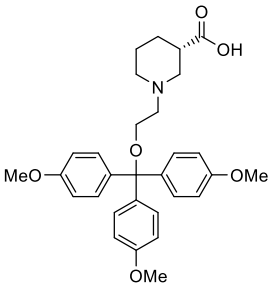

(*S*)-SNAP-5114 [(*S*)-**2**]

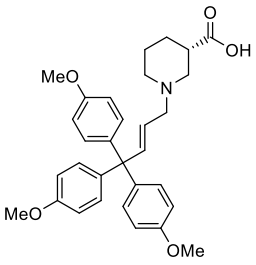

DDPM-1457 [(*S*)-**3**]

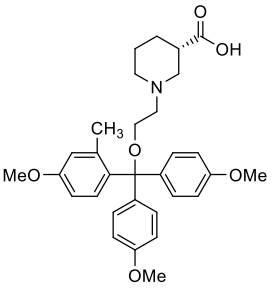

DDPM-859 [(*S*)-**4**]

Entry	Compound	pK_i[a]	pIC_{50}[b]			
		mGAT1	mGAT1	mGAT2	mGAT3	mGAT4
1	Tiagabine [(*R*)-**1**][d]	7.43 ± 0.11	6.88 ± 0.12	50%	64%	73%
2	*rac*-SNAP-5114[c] [*rac*-**2**]	-	4.08	-	4.96	5.64 ± 0.05
3	(*S*)-SNAP-5114[c] [(*S*)-**2**]	4.56[e] ± 0.02	4.07 ± 0.09	56%	5.29 ± 0.04	5.71 ± 0.07
4	DDPM-1457[d] [(*S*)-**3**]	4.33 ± 0.06	4.40 ± 0.05	4.42 ± 0.11	5.47 ± 0.02	5.87 ± 0.08
5	DDPM-859[d] [(*S*)-**4**]	-	4.19 ± 0.07	4.12 ± 0.08	4.85 ± 0.04	5.78 ± 0.03

(a) Results of the MS Binding Assays are given as pKi ± SEM. (b) Results of the [^{3}H]GABA uptake assays are given as pIC_{50} ± SEM. Percent values represent remaining [^{3}H]GABA uptake in presence of 100 µM compound. (c) Reference literature[25]. (d) Reference literature[26].

To this end, the present study aims at the synthesis of (*S*)-SNAP-5114 [(*S*)-**2**] analogues that feature a more polar moiety in place of one of the methoxy groups present in the trityl rest of the parent compound (*S*)-**2** (Scheme 1, a). As such polar moieties carboxylic acid, alcohol aldehyde, nitrile, carboxamide, sulfonamide, aldehyde or ketone functions were taken into consideration, as well as amino acid partial structures. These modifications might result in

increased polar interactions of the inhibitor with the target, thus possibly affecting its potency and subtype selectivity. In that context, we also aimed to clarify how a wider variation of the original (*S*)-SNAP-5114 [(*S*)-**2**] structure, comprising the replacement of one entire 4-methoxyphenyl moiety of the trityl residue by a polar group (Scheme 1, d), would influence the biological activity. A further question addressed with this study is how the inhibitory potency of (*S*)-SNAP-5114 [(*S*)-**2**] analogues that have two (Scheme 1, b) or all three (Scheme 1, c) 4-methoxy groups in the trityl moiety of (*S*)-**2** substituted with other residues compare to inhibitors with only one such alteration. The findings would allow to draw conclusions about the SAR of mGAT4 inhibitors with regard to polarity, size, and number of matching substituents in the aromatic domain, and therefore point out important aspects to consider in future development of more potent mGAT4-inhibitors.

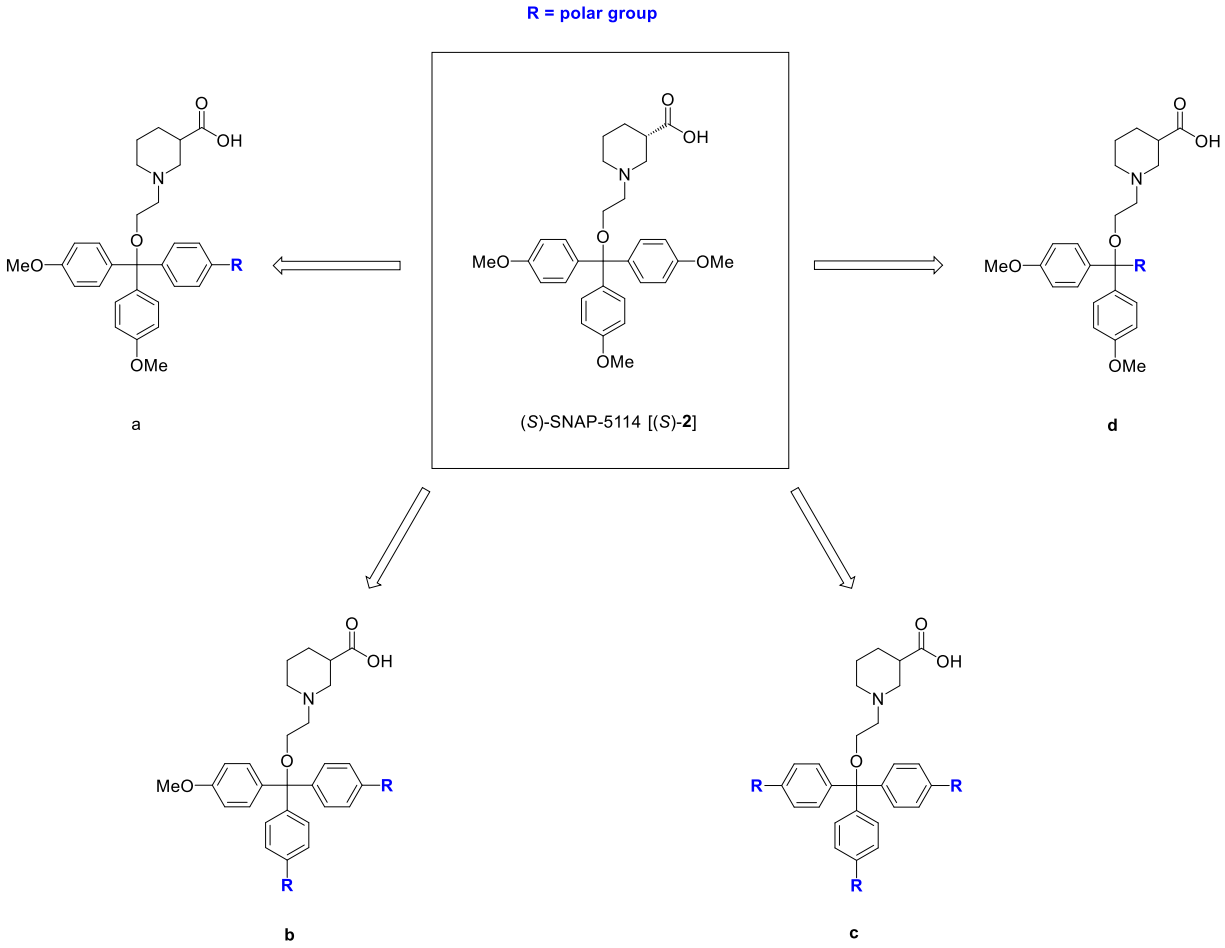

***Scheme 1**. Overview of the structural modifications of (S)-SNAP-5114 conducted in this study*

Results and Discussion

Chemistry

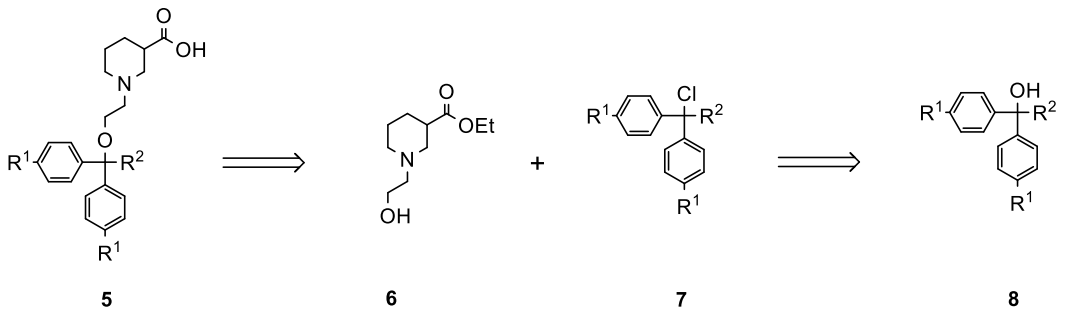

***Scheme 2**. Retrosynthetic analysis for the preparation of (S)-SNAP-5114 analogues*

Synthesis of the desired (*S*)-SNAP-5114 [(*S*)-**2**] analogues was performed according to the reaction sequence shown in scheme 2 that had been described by Schirrmacher et al.[27] for the preparation of [^{18}F] labelled (*S*)-SNAP-5114 analogues. According to this plan, the respective tertiary alcohols **8** exhibiting the desired polar function attached to the aryl moieties, or suitable precursors thereof, are transformed into the corresponding trityl chlorides, which can e.g. be accomplished by reaction with acetyl chloride. Subsequent treatment of the prepared trityl chlorides **7** with N-(2-hydroxyethyl)nipecotinate **6**, which may be prepared according to literature,[28] will furnish the fully assembled target compounds in form of their carboxylic acid esters and finally the free nipecotic acids **5** upon hydrolysis of the carboxylic acid ester function. Although the stereochemistry of the nipecotic acid partial structure is known to play a decisive role in the biological activity of mGAT4 inhibitors,[24], we opted for the synthesis of racemic compounds for economic reasons. However, for those racemic compounds showing equal or higher activity than (*S*)-SNAP-5114 in the biological testing, additionally the (*R*)- and (*S*)-isomers should be synthesized and evaluated for their biological activity. To achieve the synthesis of these enantiopure compounds following the depicted synthetic pathway (scheme 2), only *rac*-**6** has to be replaced by its (*R*)- and (*S*)-isomer, respectively.

Synthesis of the tertiary alcohols **8a-k**

Initially for the construction of the target compounds **5a-i** in which one or more of the three methoxy substituents of (*S*)-SNAP-5114 [(*S*)-**2**] are replaced by an alternative polar moiety (compound type a-c in Scheme 1), the corresponding tertiary alcohols **8a**-**i** had to be synthesized (table 2, entry 1-9, table 3, entry 9). This was accomplished by transforming aryl halides **9a-h** into the corresponding Grignard or organolithium reagents, which were subsequently reacted with the appropriate electrophiles, i.e. with 4,4´-dimethoxybenzophenone (**10a**, table 2, entry 1-6), 4-cyanobenzoyl chloride (**10b**, table 2, entry 7), methyl 4-methoxybenzoate (**10c**, table 2, entry 8), and dimethyl carbonate (**10d**, table 2, entry 9). This led to the differently substituted trityl alcohols **8a-i** in acceptable to good yields of 53% – 99%, most of which exhibit two of the three 4-methoxyphenyl units present in (*S*)-SNAP-5114 [(*S*)-**2**] together with a third aryl moiety with a different structure (table 2, entry 1-7). Trityl alcohol **8j** (table 3, entry 9), featuring an amide group and two methoxy groups, respectively, in the 4-position of the three aromatic moieties, was obtained in a yield of 96% by hydratisation of the nitrile function of **8g** (table 2, entry 7), which was accomplished by the treatment with potassium *tert*-butoxide in *tert*-butanol, following a general procedure from literature.[29] 4,4´-Dimethoxybenzilic acid methyl ester **8k** (table 3, entry 10) as precursor for the preparation of compounds of type d (Scheme 1) was synthesized by benzilic acid rearrangement of 4,4'-dimethoxybenzil,[30] followed by esterification with methyl iodide in analogy to a method published for benzilic acid.[31]

Table 2. *Synthesis of the trityl alcohols* ***2a-i.***

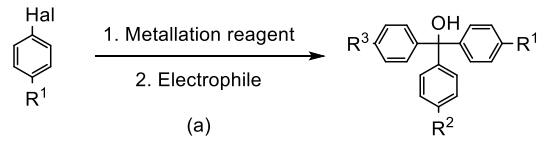

9a-i **8a-i**

Entry	Aryl halide	Metallation reagent	Electrophile	Product	R^1	R^2	R^3	Yield (%)
1	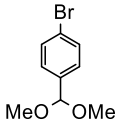 **9a**	*t*-BuLi	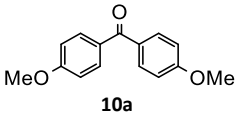 **10a**	**8a**	-CH(OMe)$_2$	-OMe	-OMe	99
2	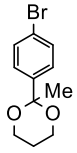 **9b**	"	"	**8b**		"	"	87
3	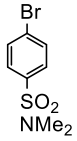 **9c**[b]	"	"	**8c**	-SO_2NMe_2	"	"	53
4	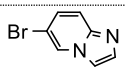 **9d**	*n*-BuLi	"	**8d**	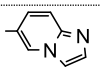	"	"	56
5	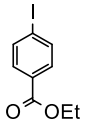 **9e**	*i*-PrMgCl	"	**8e**	-COOEt	"	"	77
6	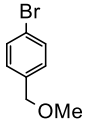 **9f**	Mg	"	**8f**	-CH_2OMe	"	"	92

***Table 2** (continued).*

Entry	Aryl halide	Metallation reagent	Electrophile	Product	R^1	R^2	R^3	Yield (%)
7	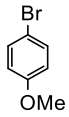 **9g**	"	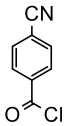 **10b**	**8g**	-CN	"	"	94
8	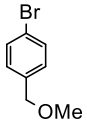 **9h**	"	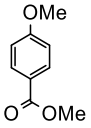 **10c**	**8h**	$-CH_2OMe$	$-CH_2OMe$	"	70
9	**"**	"	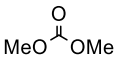 **10d**	**8i**	"	"	$-CH_2OMe$	85

Reagents and conditions: (a) entry 1-3: t-BuLi (2.0 eq), THF, -78°C, 2h, 4,4´-dimethoxybenzophenone (1.0 eq), THF, -78°C-rt; entry 5: iPrMgCl (1.0 eq), THF, -20°C, 1.5h, 4,4´-dimethoxybenzophenone (1.0 eq), THF, -20°C-rt; entry 6: n-BuLi (1.0 eq), diethyl ether, -78°C, 0.5h, 4,4´-dimethoxybenzophenone (0.83 eq), diethyl ether, -78°C-rt; entry 7: magnesium (1.0 eq), THF, rt, 4-cyanobenzoylchloride, THF, 0°C-rt; entry 8: magnesium (1.0 eq), THF, rt, methyl 4-methoxybenzoate (0.89 eq), THF, reflux; entry 9: magnesium (1.0 eq), THF, rt, dimethyl carbonate (0.33 eq), THF, reflux. (b) Synthesized by N-alkylation of 4-bromobenzenesulfonamide with dimethyl sulfate (2.0 eq) in presence of potassium carbonate (4.0 eq) and tetrabutylammonium tetrafluoroborate (10 mol%) under reflux conditions.

Construction of target compounds **5a**-**l** from N-(2-hydroxyethyl)nipecotic acid ethyl ester **6** and tertiary alcohols **8a-l**

The synthesis of the target compounds **5a**-**k** should be achieved by etherification of the hydroxy function of N-(2-hydroxyethyl)nipecotic acid ethyl ester **6** with the tertiary alcohols **8a-k** that had been prepared for this purpose. To this end, in the first step alcohols **8a-k** were transformed into the corresponding tertiary chlorides **7a-k** by reaction with acetyl chloride in the presence of a catalytic amount of dimethyl formamide (table 3, step a). Under these conditions, also the acetal function of **8a** was completely transformed in an aldehyde group as wanted. Therefore, the reaction mixture obtained after treatment of **8a** with acetylchloride, resulting in **7a** with the deprotected aldehyde function, could be directly used for the next step, the etherification reaction with N-(2-hydroxyethyl)nipecotic acid

ethyl ester (**6**). In contrast, the more stable acetal function of **8b** was only partially transformed into the ketone under the conditions for the halide formation. Hence, **8b** was first transformed into ketone **11** by refluxing in aqueous acid (93% yield), which was subsequently converted in chloride **7b**. Due to their high reactivity and susceptibility to hydrolysis upon exposure to moisture, the tertiary chlorides were directly used without prior purification or characterization for the next step, the alcoholysis with racemic 1-(2-hydroxyethyl)nipecotic acid ethyl ester (**6**) (table 3, step b). The desired products **12a-k** with the newly created trityl ether function were thus obtained in yields from 42% to 88% over both reaction steps (based on **8a-k** as starting material).

For the synthesis of an analogue of *rac*-SNAP-5114 [(*S*)-**2**] that features a hydroxyl function in place of one of the 4-methoxyphenyl groups, we decided to use a propyl instead of the ethoxy linker to warrant chemical stability of the product. The synthesis was accomplished by reacting anisyl lithium with ethyl 4-chlorobutanoate to give the required alcohol **8l** with an ω-chloropropyl residue, which upon reaction with ethyl nipecotinate led to the desired N-substituted nipecotic acid ester **12l** in 66% yield (table 3, step c).

In order to obtain the free nipecotic acid derivatives **5a-l**, compounds **12a-l** were treated with barium hydroxide octahydrate in methanol/water 4:1 for the hydrolysis of the ester function, followed by workup with carbon dioxide (table 3, step d). Thereupon, the target compounds **5a-l** could be isolated in yields from 61% to 97%.

Table 3. *Synthesis of the N-substituted nipecotic acid ethyl esters* ***12a-k*** *and their hydrolysis to the free nipecotic acid derivatives* ***5b-k****.*

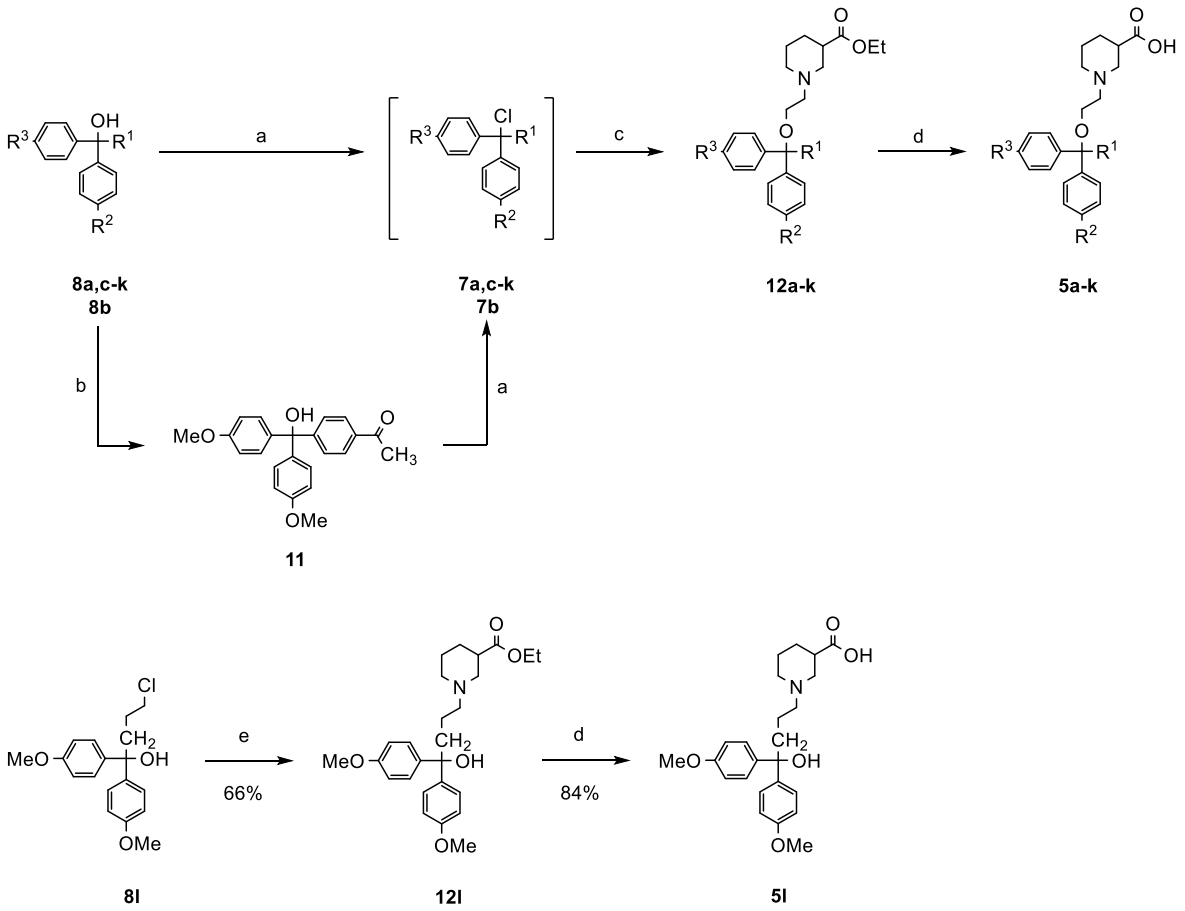

Entry	Starting material	R^1	R^2	R^3	Product of step a+b	R^1	Yield[e] (%)	Product of step d	R^1	Yield (%)
1	**8a**	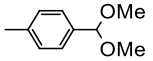	-OMe	-OMe	**12a**	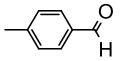	70	**5a**	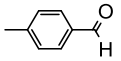	89
2	**8b**	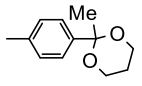	"	"	**12b**	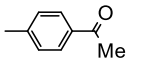	50	**5b**	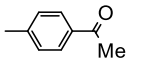	86
3	**8c**	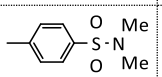	"	"	**12c**	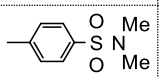	64	**5c**	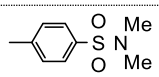	88
4	**8d**	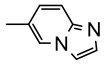	"	"	**12d**	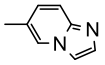	48	**5d**	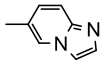	80
5	**8e**	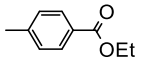	"	"	**12e**	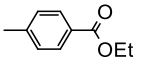	54	**5e**	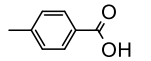	61
6	**8f**	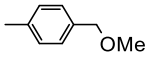	"	"	**12f**	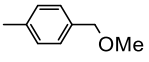	44	**5f**	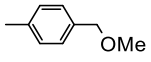	81
7	**8g**	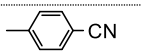	"	"	**12g**	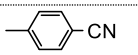	85	**5g**	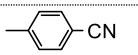	86

Table 3 *(continued).*

Entry	Starting material	R^1	R^2	R^3	Product of step a+b	R^1	Yield[e] (%)	Product of step d	R^1	Yield (%)
8	**8h**	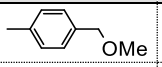	$-CH_2OMe$	"	**12h**	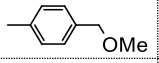	46	**5h**	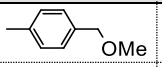	94
9	**8i**	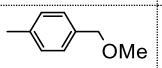	"	$-CH_2OMe$	**12i**	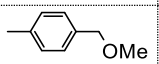	42	**5i**	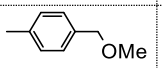	90
10	**8j**	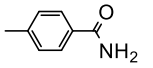	-OMe	-OMe	**12j**	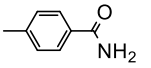	49	**5j**	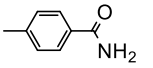	87
11	**8k**	-COOMe	"	"	**12k**	-COOMe	88	**5k**	-COOH	97

*Reagents and conditions: (a) acetyl chloride, dimethyl formamide (cat.), rt; b) HCl, THF/H_2O, reflux; c) 1-(2-hydroxyethyl)nipecotic acid ethyl ester (**6**) (1.1 eq), potassium carbonate (2.5 eq), acetontrile, rt; (d) barium hydroxide octahydrate (2-4 eq), methanol/water 4:1; carbon dioxide; (e) ethyl nipecotinate (1.1 eq), potassium carbonate (2.5 eq), potassium iodide (0.1 eq), acetonitrile, microwave, 80°C.*

Synthesis of target compounds **5m**-**t** with amino acid derived residues substituting one of the three methoxy groups in (*S*)-SNAP-5114 [(*S*)-**2**]

Next, we aimed at the synthesis *rac*-SNAP-5114 analogues that feature a hydroxy methyl moiety or an amino acid subunit as a polar group replacing one of the three methoxy residues in the lipophilic domain of (*S*)-SNAP-5114 [(*S*)-**2**]. As starting material for the synthesis compound **12a,** a nipecotic acid derivative with one of the three methoxy groups of the trityl moiety having been replaced by a formyl residue was used. Reduction of the aldehyde function in **12a** was accomplished by treatment with sodium borohydride in methanol, providing the corresponding alcohol **12m** in a yield of 89% (table 4, entry 1). Reductive amination of the aldehyde function in **12a** was performed employing a set of amino acids and amino acid ester hydrochlorides (table 4, entry 2-8). Upon application of a slightly modified standard method[32] employing sodium acetoxyborohydride in dichloromethane as reductant (instead of dichloroethane) to **12a** and the respective amino acid ester hydrochlorides led to the glycine methyl ester **12n**, β-alanine ethyl ester **12o**, 1-aminocyclopropane-1-carboxylic acid ethyl ester **12p**, and 2-amino-2-methylpropanoic acid ethyl ester derivatives **12q** (table 4, entry 2-5) in yields of 42 to 64%. The γ-aminobutyric acid ethyl ester derivative of **12a** could not be obtained by this procedure since the product underwent partial γ-lactamization during workup, resulting in a mixture of the desired compound and the corresponding γ-butyrolactame. Attempts to reopen the lactame

function under basic conditions (barium hydroxide or sodium hydroxide at rt or reflux) (table 3, entry 6) led to a completion of the formation of lactame **5r**, or to cleavage of the ether function when lithium hydroxide was used under reflux conditions. Hence, the reductive amination of **12a** was attempted with the free γ-aminobutyric acid (GABA). Applying the established reaction conditions did not lead to the desired product **12s**, which is likely to be due to the very low solubility of GABA in dichloromethane. However, when dichloromethane was replaced by methanol and sodium triacetoxyborohydride by sodium cyanoborohydride, **12s** (table 4, entry 7) was formed in a yield of 40%. The same method could also be successfully applied to the synthesis of p-aminobenzoic acid derivative **12t** (table 4, entry 8). The free nipecotic acids **5m-q** and **5s-t** became finally available upon subjecting compounds **12m-q** and **12s-t** to alkaline hydrolysis using the procedure as already described above [$Ba(OH)_2 \cdot 8H_2O$, CO_2 workup] for the transformation of compounds **12a-l** into **5a-l** (table 4, step b), the yields of this transformation amounting to 65-96%.

Table 4. *synthesis of the target compounds* ***5m-t*** *with amino acid derived residues substituting one of the three methoxy groups in (S)-SNAP-5114*.

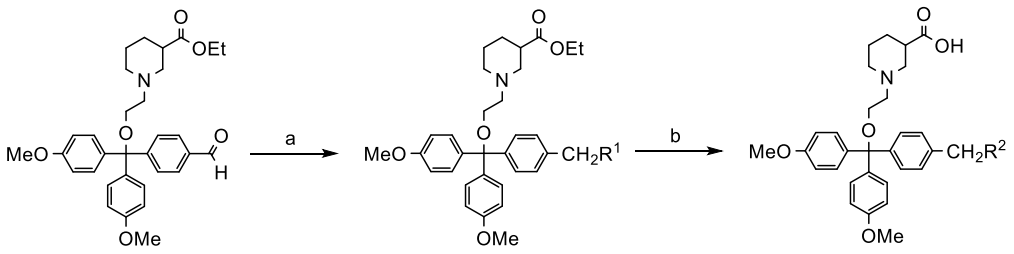

12a **12m-q 12s-t** **5m-q 5s-t**

Entry	Product of step a	R^1	Yield (%)	Product of step b	R^2	Yield (%)
1	**12m**	-OH	89	**5m**	-OH	69
2	**12n**	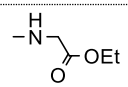	57	**5n**	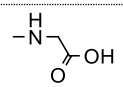	65
3	**12o**	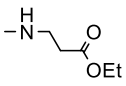	42	**5o**	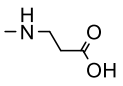	74
4	**12p**	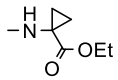	59	**5p**	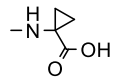	82
5	**12q**	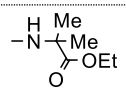	64	**5q**	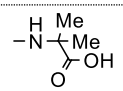	92

Table 4 *(continued).*

Entry	Product of step a	R^1	Yield (%)	Product of step b	R^2	Yield (%)
6				**5r**	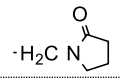	47[c]
7	**12s**	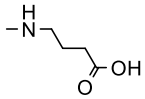	40	**5s**	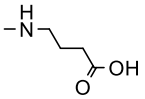	84
8	**12t**	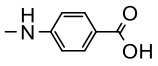	25	**5t**	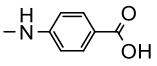	96

Reagents and conditions: (a) entry 1: sodium borohydride (2.5 eq), methanol, rt; entry 2-5: sodium triacetoxyborohydride (1.4 eq), amino acid ethylester hydrochloride (2.0 eq), dichloromethane, rt; entry 7-8: sodium cyanoborohydride (1.4 eq), free amino acid (2.0 eq), methanol, rt. (b) barium hydroxide octahydrate (2-4 eq), methanol/water 4:1; carbon dioxide. (c) yield over two steps.

Biological evaluation

The N-substituted nipecotic acids **5a-t**, and their ester precursors **12a-q** and **12s-t** were tested for their inhibitory potencies on the four GABA transporter subtypes mGAT1-4 in a [^{3}H]GABA uptake assay that was previously developed by our group.[33] The tests were performed in a standardized manner using HEK293 cell lines, each expressing one of the four tested GABA transporter subtypes. Furthermore, binding affinities towards mGAT1 were examined employing a standardized MS Binding Assay with NO711 as native MS marker.[34] For compounds that in prelimary experiments did not reduce [^{3}H]GABA uptake beyond 50% at a test concentration of 100 µM, which equals a pIC_{50} of ≤ 4.0, only the percent values of the remaining [^{3}H]GABA uptake are listed. Correspondingly, the percentage of remaining marker is given in cases when the tested compound did not cause a reduction of the MS marker binding beyond 50%, equating to a pK_i of ≤ 4.0. When [^{3}H]GABA uptake or NO711 binding was reduced below 50%, at a concentration of 100 µM, inhibitory potencies (pIC_{50} values) and binding affinities (pK_i values) were determined in full scale [^{3}H]GABA uptake and MS Binding Assays, respectively, measurements being performed as triplicates. For compounds with pIC_{50} ([^{3}H]GABA uptake assay) or pK_i (MS Binding Assays) values close to or above 5.0, these experiments were repeated twice and SEM have been calculated. The results are summarized in table 5.

As outlined above, the structure of the prototypic mGAT4 inhibitor *rac*-SNAP-5114 (*rac*-**2**) was modified by formally replacing one of the three aromatic methoxy moieties in its lipophilic domain with a variety of different functional groups. For the purpose of estimating the effect that these modifications exert on the polarity of the resulting molecule, the log *D* values of the compounds under physiological conditions (pH = 7.4, electrolyte concentration = 0.154 mmol/l) were calculated (clog *D*: calculated log *D*) using MarvinSketch.[35]

Replacement of one of the methoxy substituents in the *rac*-SNAP-5114 (*rac*-**2**) molecule by the larger methoxymethylene group leads to **5f**, which at mGAT4 exhibits a pIC_{50} value of 5.42 ± 0.10 (table 5, entry 14). This constitutes only a minor decrease in inhibitory potency at the transporter compared to the parent compound *rac*-**2** (pIC_{50} = 5.64 ± 0.05, table 1, entry 2), suggesting that a slight increase in the space requirements of the substituent is tolerated relatively well by mGAT4. If a nitrile function is introduced in place of a methoxy moiety, the loss of potency at mGAT4 is more pronounced, amounting to a pIC_{50} value 5.07 ± 0.12 (**5g**, table 5, entry 16). Since the nitrile function is also a hydrogen bridge acceptor and conveys very similar polarity compared to the methoxy moiety it replaces (clog *D* of **5g** 2.33, clog D of *rac*-**2** 2.32), this finding is likely attributable to the linear shape of the nitril function not being ideal for interaction with the target. For *rac*-**5a**, featuring an aldehyde function in one of the aromatic 4-positions of *rac*-SNAP-5114 (*rac*-**2**), a pIC_{50} of 5.77 ± 0.04 was determined (table 5, entry 2), which places the potency of compound *rac*-**5a** nominally above that of *rac*-SNAP-5114 (*rac*-**2**) despite the oxygen atom being placed one bond further away from the aromatic moiety. **5b**, which has one of the methoxy groups of *rac*-**2** replaced by the larger, but similar polar acetyl moiety (**5b**: clog *D* = 2.00), exhibits only a slightly decreased inhibitory potency compared to the parent compound, with its pIC_{50} value amounting to 5.43 ± 0.04 (table 5, entry 6). On the other hand, the introduction of a hydroxymethylene group, leading to the distinctly more polar compound **5m** (clog *D* = 1.71), is accompanied by a reduction of the pIC_{50} value from 5.64 ± 0.05 for *rac*-SNAP-5114 to 4.90, which equates to a potency loss of ~0.75 log units (table 5, entry 28). Interestingly, an equivalent pIC_{50} of 4.86 was determined for **5e** (table 5, entry 12), which has one of the three aromatic 4-positions of *rac*-**2** occupied by a carboxylic acid moiety. This finding is astonishing as the carboxyl group is significantly more polar than the corresponding alcohol moiety present in **5m**, with the respective clog *D* value amouting to -1.40 under physiological conditions.

By contrast, the inhibitory potency of **5j**, featuring a carboxamide moiety in this position, is strongly reduced (pIC_{50} < 4.0, remaining [^{3}H]GABA at 100 µM = 65.2 %, table 5, entry 22), irrespective of the fact that this group is of similar size as the carboxylic acid found in **5e** while conveying a less pronounced increase in polarity (clog *D* = 1.32). Apparently, no correlation between polarity and inhibitory potency seems to exist. **5c**, which features a N,N-dimethylsulfonamide group (clog *D* = 1.98) in place of one of the methoxy groups of *rac*-**2**, is characterized by an even lower activity; the compound causes a [^{3}H]GABA uptake reduction to 82.0 % at 100 µM, denoting a pIC_{50} of well below 4.0 (table 5, entry 8).

Of the compounds obtained from **12a** by reductive amination and subsequent hydrolysis, **5n**, featuring a glycine partial structure that is connected to the 4-position of one of the aromatic moieties by a methylene spacer, reduces the [^{3}H]GABA uptake to 72.2 % at 100 µM test compound concentration (table 5, entry 30); its analogue derived from β-alanine, **5o**, causes a slightly more pronounced reduction to 56.3% (table 5, entry 32). In this context, it is noticeable that the potency of the free nipecotic acid derivatives **5n** and **5o** is even lower than that of the corresponding esters **12n** [pIC_{50} (mGAT4) = 4.18, Table 5, entry 29] and **12o** [pIC_{50} (mGAT4) = 4.66, Table 5, entry 31]. By contrast, compounds that contain bulky, sterically hindered amino acid partial structures in the same position, such as 1-aminocyclopropane-1-carboxylic acid (**5p**) and 2-amino-2-methylpropanoic acid (**5q**), are characterized by a pIC_{50} of 4.88 (table 5, entry 34) and 4.34 (table 5, entry 36), respectively. Since these substances retain comparatively more of the inhibitory activity at mGAT4 of the parent compound, increased space requirements do evidently not contribute to the decline in potency in this case. Compound **5s**, which formally results from elongation of the amino acid chain of **5o** by one methylene group, hence exhibiting a γ-aminobutyric acid subunit, shows slightly higher inhibitory potency with a pIC_{50} value of 4.13 compared to its shorter chain analogues (compare table 5, entry 39 to entry 30 and 32). Compound **5t**, whose 4-aminobenzoic acid partial structure resembles to some extent a more rigid homologue of the γ-aminobutyric acid moiety present in **5s**, is characterized by equal inhibitory potency (remaining [^{3}H]GABA at 100µM = 50.0%, table 5, entry 41). Surprisingly, **5r**, featuring a lactame structure derived from the γ-aminobutyric acid substructures present in **5s**, exhibits a similar activity at mGAT4 (pIC_{50} = 4.19, table 5, entry 37), despite not posessing an ionized

functional group in the aromatic domain and thus having a distinctly higher clog *D* value of 1.87 compared to the value of -0.44 calculated for **5s**.

In conclusion, the data imply no clear correlation between the polarity and size of the compound and the inhibitory potency exerted at mGAT4. Still the fact remains conspicuous that all test compounds with a free carboxylic acid function of the nipecotic acid residue possessing a $pIC_{50} \geq 5.0$ contain a functional group that can act as hydrogen bond acceptor, but not as donor, and that is of similar size as the 4-methoxy moiety in the lipophilic domain it replaces. Furthermore, the clog *D* values calculated for these compounds consistently lie in the range of 2.0 – 2.4, as is the case with the parent compound *rac*-**2** (clog *D* = 2.32) and the most potent inhibitor synthesized within the scope of this study, **5a** (clog *D* = 2.15). This might turn out to be beneficial with regard to potential therapeutical applications, since compounds with log *D* values between 2 and 5,[36] or even better with values closer to 2,[37] are thought to possess the highest propensity for blood-brain barrier (BBB) penetration.

Since **5a** turned out to be the most potent mGAT4 inhibitor of all racemic compounds tested for this study, its enantiopure isomers (*S*)-**5a** and (*R*)-**5a** were synthesized and evaluated for their biological activities as well. As is the case with the lead substance SNAP-5114, the (*S*)-enantiomer of **5a** was found to exhibit a more pronounced inhibitory potency at mGAT4 than the (*R*)-enantiomer, with the respective pIC_{50} values amounting to 5.89 ± 0.07 for (*S*)-**5a** (table 5, entry 3) and 4.86 ± 0.03 for (*R*)-**5a** (table 5, entry 4). Hence, (*S*)-**5a** constitutes nominally a more potent mGAT4 inhibitor than the benchmark compound (*S*)-**2** (pIC_{50} = 5.71 ± 0.07, table 1, entry 3).

Next, we aimed to elucidate whether the biological activity of **5a** is solely attributable to competitive inhibition at the target, or whether a reaction of the aldehyde function with [^{3}H]GABA serving as substrate in the [^{3}H]GABA uptake assay might have affected the outcome of the biological study. Reaction of [^{3}H]GABA with the aldehyde function of the test compounds **5a**, (*S*)-**5a** and (*R*)-**5a** might lead to depletion of the substrate of the uptake assay, thus falsifying the outcome of the assay. Alternatively a thus formed intermediate might be a potent inhibitor by itself. To this end the uptake experiment was repeated using an assay recently developed by our group,[38] which has GABA replaced by the chemically inert imidazolacetic acid. Since **5a** and its enantiopure isomers (*R*)-**5a** and (*S*)-**5a** display

similar inhibitory activity when tested under these conditions as compared to the assay based on [^{3}H]GABA, it appears reasonable to assume that possible reactions of the aldehyde function of **5a** with the substrate does not or at least not crucially contribute to the biological effects oberserved for this compound.

Of the *rac*-SNAP-5114 (*rac*-**2**) analogues that have an entire 4-methoxyphenyl residue replaced by a polar moiety, **5d**, possessing an imidazo[1,2-α]pyridine subunit instead of the aforementioned 4-methoxyphenyl rest, displays a pIC_{50} of 4.58 (table 5, entry 10). As compared to the potency of *rac*-**2a** at mGAT4 (pIC_{50} = 5.64 ± 0.05) this equates to a distinct, but still moderate reduction of inhibitory potency of about one log unit. However, the introduction of a small, polar functional group in place of one of the 4-methoxyphenyl residues is associated with a drastic loss of activity at mGAT4. For example, the compound featuring a carboxylic acid function in this position, **5k**, is devoid of almost any inhibitory activity at mGAT4, reducing the [^{3}H]GABA uptake to only 96.5 % at 100 µM (table 5, entry 24). By comparison, **5e**, which also features a carboxyl group, albeit located on one of the aromats of the lipophilic domain of *rac*-**2** supplanting a 4-methoxy group, conserves significantly more of the inhibitory potency of the parent compound [pIC_{50}(mGAT4) = 4.86, Table 5, entry 12]. The same phenomenon is observed for **5l**, that formally results from the replacement of one of the 4-methoxyphenyl groups of *rac*-**2** with a hydroxy moiety, in combination with a simultaneous exchange of the ether oxygen of the spacer by a methylene group to warrant chemical stability. The compound reduces the [^{3}H]GABA uptake to 92.0% at 100 µM (table 5, entry 26). Compound **5m** on the other hand, which also contains a hydroxy function, but retains triaryl pattern of the parent compound by substituting one of the three methoxy groups with a hydroxymethylene moiety, still possesses a pIC_{50} of 4.90 (table 5, entry 28). These results suggest that decreasing size and steric demand of the lipophilic domain is accompanied by a pronounced decline in biological activity at mGAT4. The three aromatic moieties on the quaternary carbon atom can therefore be regarded as essential for high inhibitory potency at mGAT4 of these compounds, and variations, e.g. in order to alter the polarity of a compound, should only be implemented by modification of the substituents, but not by replacement of one of these aromatic moieties in favour of a smaller functional group.

Next, we aimed to study how the number of aryl moieties in the lipophilic domain, which are modified with regard to their substitutents, affects the inhibitory potency. To that end, an array of *rac*-SNAP-5514 analogues was synthesized that had one, two, or all three of the methoxy groups replaced by methoxymethylene moieties. While the introduction of one methoxymethylene group caused only a minor decrease in inhibitory potency to a pIC_{50} of 5.42 (**5f**, table 5, entry 14) as compared to the reference compound *rac*-**2** (pIC_{50} = 5.64 ± 0.05, table 1, entry 2), the loss of activity became increasingly more pronounced with each further methoxymethylene group (**5h**, mGAT4: pIC_{50} = 4.77, table 5, entry 18; **5i**, mGAT4: remaining [^{3}H]GABA at 100µM = 76.1%, table 5, entry 20). These findings support the notion that the biological system can tolerate an inapt substituent on one of the aryl groups relatively well as long as the other two 4-methoxy moieties of the lipophilic domain remain unchanged and thus are still available for interactions with the target. However, substitution of further methoxy moieties will result in an exceeding decline of inhibitory potency at mGAT4.

Also the nipecotic acid ester derivatives **12** that have been synthesized in this study were evaluated for their inhibitory potencies at all four GAT subtypes. With regard to mGAT4 inhibition, most nipecotic acid esters **12** display distinctly lower potencies at this transporter subtype than their nipecotic acid analogues **5**, signifying the importance of the free nipecotic acid partial structure for mGAT4 inhibition. Only in case of the nipecotic acids **5j** – **5l** which exert very low inhibitory potencies at mGAT4 (pIC_{50} < 4.0), the inhibitory potencies of the free acids were lower than that of the corresponding esters **12j** – **12l**, the differences being, however, marginal. However, carboxylic acid ester **12k** cannot be directly compared to nipecotic acid **5k**, as the latter possesses a carboxy function instead of a methoxy carbonyl moiety attached to one of the aryl residues of the lipophilic domain.

Regarding the effects at other GAT subtypes, inhibition of mGAT1 is the pharmacologically most relevant due to its high abundance in the mammalian CNS. Of the compounds presented in this study, none of the carboxylic acid analogues of *rac*-SNAP-5114 **5** show a reasonable inhibitory potency at mGAT1, i.e. pIC_{50} values ≥ 4, which is also true for the ester analogues **12** with two exceptions. Thus, for **12d**, that has one of the three 4-methoxyphenyl groups (of *rac*-**2**) substituted by an imidazo[1,2-a]pyridine-7-yl moiety, and **12o**, featuring a

β-alanine ethyl ester partial structure which is linked to one of the three aromatic residues in the 4-position by a methylene spacer, pIC_{50} values of 4.39 and 4.59 were found (**12d,** table 5, entry 9, and **12o**, table 5, entry 31). All other compounds lie below that mark, i.e. a pIC_{50} = 4.0, and can thus be regarded as less potent mGAT1 inhibitors than *rac*-**2**, which has a pIC_{50} of 4.08 (**2**, table 1, entry 2). Hence, contrary to what applies to the potency at mGAT4, transforming the ester function of **12** into a free acid moiety exerts little to no influence on inhibitory potency at mGAT1, the latter usually amounting to pIC_{50} values of below 4.0 for both compound classes.

The compounds synthesized and tested for this study were generally found to be weak binders at mGAT1, which correlates well with the uniformly low inhibitory potencies at this GABA transporter subtype. In that context, only the *rac*-SNAP-5114 analogues possessing a formyl [(**5a**), (*R*)-**5a**], acetyl (**5b**), or nitrile function (**5g**) in the lipophilic domain or in which a 4-methoxyphenyl residue has been replaced by an imidazo[1,2-a]pyridine-7-yl moiety (**5d**) or an hydroxy function (**5l**) differ by displaying moderate pK_i values > 4.0. In detail, the values determined for these compounds were 4.50 ± 0.06 (**5a**, table 5, entry 2), 4.91 ± 0.09 [(*R*)-**5a**, table 5, entry 4], 4.51 ± 0.03 (**5b**, table 5, entry 6), 4.40 ± 0.01 (**5g**, table 5, entry 16), 4.03 (**5d**, table 5, entry 10) and 4.49 (**5l**, table 5, entry 26), respectively.

Furthermore, none of the free nipecotic acids **5** reduced [^{3}H]GABA below 50% at a concentration of 100 µM when tested at mGAT2, which corresponds to pIC_{50} values < 4.0, except for **5t** (pIC_{50} = 4.18, table 5, entry 41). Nevertheless, some of the ester precursors **12** exceeded this mark, the most potent among these being the imidazo[1,2-a]pyridine derivative **12d** with a pIC_{50} of 4.88 (table 5, entry 9). Likewise, the ester derivatives of the compounds that feature in the lipophilic domain a formyl (**12a**, table 5, entry 1, pIC_{50} = 4.57), a methoxymethyl (**12h**, table 5, entry 17, pIC_{50} = 4.30) or an amino acid residue (**12n**, table 5, entry 29, pIC_{50} = 4.29; **12o**, table 5, entry 31, pIC_{50} = 4.72) display pIC_{50} values ≥ 4.00 at this transporter subtype.

Serving as lead structure of this study, *rac*-SNAP-5114 (*rac*-**2**) possesses a comparatively high pIC_{50} value at mGAT3 of 4.96 (table 1, entry 2); as a consequence, its desired mGAT4 selectivity is quite poor with regard to this GAT subtype. The modifications of the *rac*-**2**

structure that were undertaken for the purpose of this study resulted in compounds with lower activity at mGAT3, **5a** being the only exception (pIC_{50} = 4.98 ± 0.08, table 5, entry 2). This is of particular importance for those compounds that show relatively high inhibitory potency at mGAT4 and are thus of interest as pharmacological tools. In case of **5b** and **5f**, which comprise an acetyl group and a methoxymethylene group in the lipophilic domain, the inhibitory potency at mGAT4 is moderately reduced to pIC_{50} values of 5.43 ± 0.04 (**5b,** table 5, entry 6) and 5.42 ± 0.10 (**5f,** table 5, entry 14), respectively. However, the potency loss at mGAT3 caused by these structural modifications is slightly more pronounced, with a pIC_{50} value of 4.24 ± 0.02 determined for **5b** (table 5, entry 6) and 4.51 ± 0.04 for **5f** (table 5, entry 14). Accordingly, these compounds display considerably higher mGAT4 selectivity than *rac*-**2**, albeit at the cost of some inhibitory potency.

As compared to the enantiopure benchmark inhibitor (*S*)-**2** (table 1, entry 3), the most potent compound synthesized for this study, (*S*)-**5a**, displays almost identical subtype selectivity (table 5, entry 3). In particular, the pIC_{50} values amount to 5.16 ± 0.05 at mGAT3 [(*S*)-**2**: 5.29 ± 0.04] and 4.14 ± 0.00 at mGAT1 [(*S*)-**2**: 4.07 ± 0.09]. At mGAT2 both compounds exert only weak inhibitory effects, reducing the [^{3}H]GABA uptake to 72.6% [(*S*)-**5a**] and 56% [(*S*)-**2**], respectively. Hence, (*S*)-**5a** can be considered a viable alternative to (*S*)-**2** as a pharmacological tool.

***Table 5**. Binding affinities (pK_i) and inhibitory potencies (pIC_{50}) of the N-substituted nipecotic acids **6a,c-u** and nipecotic acid ethyl esters **12a,c-r,t-u**.*

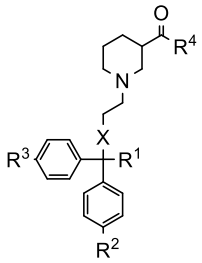

Entry	Compound	R^1	R^2	R^3	R^4	X	pK_i[a]	pIC_{50}[b]			
								mGAT1	mGAT2	mGAT3	mGAT4
1	**12a**	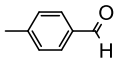	OMe	OMe	OEt	O	85.4 %	55.5%	4.57	4.90	55.9%
2	**5a**				OH		4.41 ± 0.11	4.17 ± 0.08	66.3 %	4.98 ± 0.08	5.77 ± 0.04
3	**(*S*)-5a**						77.4 %	4.14 ± 0.00	72.6 %	5.16 ± 0.05	5.89 ± 0.07
4	**(*R*)-5a**						4.91 ± 0.09	4.45 ± 0.08	50.1 %	4.47 ± 0.05	4.86 ± 0.03
5	**12b**	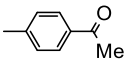			OEt		84.6 %	72.9 %	66.4 %	55.2 %	84.2 %
6	**5b**				OH		4.51 ± 0.03	64.6 %	64.2 %	4.24 ± 0.02	5.43 ± 0.04
7	**12c**	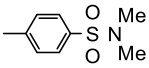			OEt		93.8 %	75.7 %	73.2 %	95.9 %	94.3 %
8	**5c**				OH		62.1 %	67.9 %	78.0 %	77.1 %	82.0 %
9	**12d**	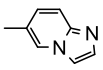			OEt		77.2 %	4.39	4.88	4.71	4.24
10	**5d**				OH		4.03	84.9 %	72.9 %	81.8 %	4.58
11	**12e**	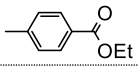			OEt		74.8 %	84.6 %	87.3 %	79.0 %	76.1%
12	**5e**	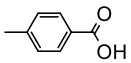			OH		71.4 %	96.5 %	85.2 %	4.24	4.86
13	**12f**	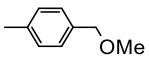			OEt		55.3 %	66.6 %	58.8 %	56.9 %	50.8 %
14	**5f**				OH		89.4 %	67.1 %	72.7 %	4.51 ± 0.08	5.42 ± 0.10
15	**12g**	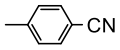			OEt		97.6 %	76.6 %	80.7 %	63.6 %	71.9 %
16	**5g**				OH		4.40 ± 0.10	74.8 %	82.9 %	4.31 ± 0.12	5.07 ± 0.12
17	**12h**	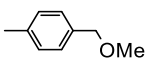	CH_2OMe		OEt		72.9 %	64.9 %	4.30	50.6 %	4.05
18	**5h**				OH		74.1 %	70.5 %	55.2 %	52.2 %	4.77
19	**12i**			CH_2OMe	OEt		87.5 %	70.3 %	65.0 %	4.02	51.4 %
20	**5i**				OH		92.7 %	90.7 %	72.6 %	68.3 %	76.1 %
21	**12j**	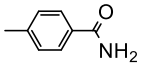	OMe	OMe	OEt		89.3 %	57.8 %	56.1 %	4.10	60.0 %
22	**5j**				OH		87.0 %	79.6 %	96.1 %	82.1 %	65.2 %
23	**12k**	-COOMe			OEt		90.8 %	89.1 %	92.6 %	64.1 %	78.2 %
24	**5k**	-COOH			OH		96.9 %	100 %	101 %	94.0 %	96.5 %

***Table 5** (continued).*

Entry	Compound	R^1	R^2	R^3	R^4	X	pK_i[a]	pIC_{50}[b]			
								mGAT1	mGAT2	mGAT3	mGAT4
25	**12l**	-OH	OMe	OMe	OEt	CH_2	104.0%	79.3 %	70.4 %	65.0 %	73.8 %
26	**5l**				OH		4.49	69.5 %	62.5 %	80.7 %	92.0 %
27	**12m**	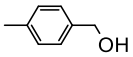			OEt	O	75.3 %	50.4 %	49.3 %	4.45	4.23
28	**5m**				OH		55.0 %	78.1 %	91.6 %	58.7 %	4.90
29	**12n**	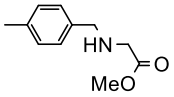			OEt		91.7 %	51.8 %	4.29	4.47	4.18
30	**5n**	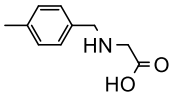			OH		86.2 %	81.8 %	96.1 %	90.9 %	72.2 %
31	**12o**	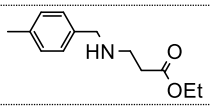			OEt		72.4 %	4.59	4.72	4.63	4.66
32	**5o**	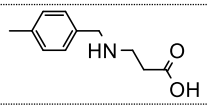			OH		82.3 %	94.4 %	69.5 %	89.1 %	56.3 %
33	**12p**	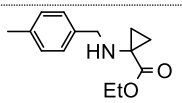			OEt		95.8 %	75.5 %	103 %	58.8%	66.1 %
34	**5p**	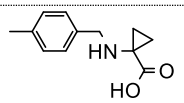			OH		58.8 %	78.2 %	76.0 %	69.1 %	4.88
35	**12q**	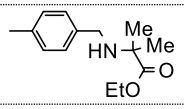			OEt		90.9 %	66.9 %	67.4 %	49.3 %	57.4 %
36	**5q**	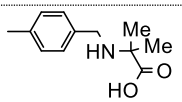			OH		77.0 %	80.7 %	77.0 %	61.1 %	4.34
37	**5r**	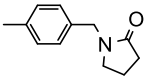					97.0 %	76.0 %	79.7 %	64.2 %	4.19
38	**12s**	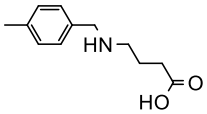			OEt		84.9 %	52.4 %	76.7 %	59.3 %	67.6 %
39	**5s**				OH		86.5 %	48.5 %	51.5 %	4.33	4.13
40	**12t**	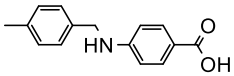			OEt		101.6%	52.3 %	73.5 %	49.7 %	63.9 %
41	**5t**				OH		54.1 %	99,5 %	4,18	96,0 %	50,0 %

(a) Results of the MS Binding Assays are given as pK_i ± SEM. For compounds with low pK_i values only one measurement was performed, therefore no SEM can be reported. Percent values represent remaining specific NO711 binding in presence of 100 µM compound. (b) Results of the [^{3}H]GABA uptake assays are given as pIC_{50} ± SEM. For compounds with low pIC_{50} values only one measurement was performed, therefore no SEM can be reported. Percent values represent remaining [^{3}H]GABA uptake in presence of 100 µM compound.

Conclusion

In order to gain insight into the structure activity relationship of mGAT4 inhibitors, analogues of *rac*-SNAP-5114 were synthesized that differ from the parent compound by having one or more of the 4-methoxy groups attached to the lipophilic domain, or a complete 4-methoxyphenyl group, replaced by a moiety with higher polarity. These modifications might increase interactions between the inhibitor and polar regions of binding site, and hence improve binding affinity, inhibitory potency, and selectivity.

The test compounds were accessible through conversion of tertiary alcohols featuring the respective functional groups or appropriate precursors into the corresponding chlorides, followed by etherification with ethyl N-(2-hydroxyethyl)nipecotinate. The obtained N-substituted nipecotic acid esters were either directly hydrolized at this stage, or functional group interconversions were performed beforehand, including the introduction of various amino acid partial structures via reductive amination.

The biological evaluation of the obtained N-substituted nipecotic acids revealed no direct correlation between the polarity of the newly introduced group and the biological activity of the resulting compound. However, compounds with clog *D* values of 2.0 – 2.4 consistently exert the highest inhibitory potencies. In this context, we found (*S*)-1-{2-[(4-formylphenyl)bis(4-methoxyphenyl)methoxy]ethyl}piperidine-3-carboxylic acid [(*S*)-**5a**], that has one of the three methoxy groups of the parent substance substituted by a formyl moiety, to be the most potent test compound synthesized in this study. Being characterized by a pIC_{50} value of 5.89 ± 0.07 at mGAT4, it even exhibits slightly higher inhibitory potency than the benchmark substance (*S*)-SNAP-5114, while showing comparable subtype selectivity. Furthermore, the racemic SNAP-5114 analogues comprising in the lipophilic domain an acetyl and an methoxymethylene substituent, respectively, were found to be slightly less potent mGAT4 inhibitors than the parent compound, but somewhat more subtype selective, especially at mGAT3.

Also, it has been demonstrated that *rac*-SNAP-5114 analogues that have one of the aromatic moieties in the lipophilic domain replaced by a small, non-aromatic moiety show a distinct

deprivation of inhibitory potency. This finding indicates the essentiality of the triaryl structure in the lipophilic domain for the biological activity of mGAT4 inhibitors. Finally, we determined how the substitution of several methoxy groups in the lipophilic domain of *rac*-SNAP-5114 impacts the inhibitory potency of the resulting compounds using the example of the methoxymethylene group. As the results of the biological evaluation suggest, mGAT4 can tolerate one inapt substituent reasonably well. However, the replacement of additional methoxy groups will result in an exceeding decline of inhibitory potency.

These findings are expected to be beneficial for future developments of more potent mGAT4 inhibitors since they reveal essential structure activity relationships with regard to size, polarity, and electronic effects of the substituents in the lipophilic domain.

Experimental Section

Chemistry

Moisture-sensitive reactions were carried out in oven-dried glassware under inert gas atmosphere. Commercially available starting materials were used without further purification. Dry acetonitrile (MeCN) was purchased from VWR (HiPerSolv Chromanonorm, water content > 30ppm) and tetrahydrofuran (THF) was freshly distilled from sodium benzophenone ketyl. All other solvents were distilled prior to use. Microwave reactions were carried out with CEM Discover® SP Microwave Synthesizer (model no. 909 155). Flash column chromatography was performed on Merck silica gel 60 (mesh 0.040 - 0.063 mm) as stationary phase; thin-layer chromatography (TLC) was carried out on Merck silica gel 60 F_{254} sheets. ^{1}H and ^{13}C NMR spectra were, unless stated otherwise, recorded at room temperature with JNMR-GX (JEOL 400 or 500 MHz) or Bruker BioSpin Avance III HD (400 or 500 MHz) and integrated with the NMR software MestReNova. IR samples were measured as KBr pellets or film with Perkin-Elmer FT-IR 1600. HRMS data were obtained with JMS-GCmate II (EI, Jeol) or Thermo Finnigan LTQ FT Ultra (ESI, Thermo Finnigan).

General procedure for the synthesis of trityl alcohols by Grignard reaction (**GP1**): Magnesium turnings were scraped with a glass rod and suspended in dry THF. The appropriate aryl

halide or a solution thereof in THF was added portion wise. After completion of the Grignard reagent formation a solution of the electrophile in THF was added dropwise to the solution. The mixture was stirred for the prescribed time and temperature, quenched with saturated ammonium chloride (NH_4Cl) solution, diluted with water and extracted thrice with dichloromethane (CH_2Cl_2). The combined organic phases were dried over magnesium sulfate ($MgSO_4$), filtered and reduced in vacuum.

General procedure for the synthesis of trityl alcohols by lithiation of an aryl halide and subsequent reaction with 4,4´-dimethoxybenzophenone (**GP2**): *tert*-Butyllithium solution (1.7M in pentane, 2.0 eq.) was added dropwise to a solution of the aryl halide (1.0 eq.) in THF at -78°C. After 2h a solution of 4,4´-dimethoxybenzophenone (1.0 eq) in THF was added. The mixture was allowed to slowly warm up to room temperature overnight, quenched with water and extracted thrice with CH_2Cl_2. The combined organic phases were dried over $MgSO_4$, filtered and reduced in vacuum.

General procedure for the etherification of tertiary alcohols (**GP3**): The tertiary alcohol (1.0 eq) was charged with a catalytic amount of DMF. Acetyl chloride was added and the reaction mixture was stirred at room temperature for 24 hours, reduced in vacuum and dried under high vacuum. The oily or solid residue was solved in dry MeCN. Racemic, (*R*)- or (*S*)-ethyl 1-(hydroxyalkyl)nipecotinate (1.1 eq) and oven-dried potassium carbonate (K_2CO_3, 2.5 eq) were added. After stirring 16 hours at room temperature, the mixture was filtered and reduced in vacuum.

General procedure for the hydrolysis of the ethyl ester function (**GP4**): The ester (1.0 eq) was dissolved in MeOH. Bidest. water and barium hydroxide octahydrate (2.0-4.0 eq) were added and the mixture was stirred at room temperature until TLC indicated complete consumption of the ester. Carbon dioxide was passed through the solution until no further precipitate formed. The suspension was diluted with MeOH (1:1), filtered through a paper filter and reduced in vacuum. If necessary, the crude acid was purified by flash column chromatography. The solid residue was solved in MeOH (1.0 ml), filtered through a syringe filter (Perfect-Flow®, WICOM Germany GmbH, PTFE, 0.2µM), diluted with bidest. water (4.0 ml) and lyophilized.

General procedure for reductive amination I (**GP5**): The appropriate amino acid ester hydrochloride (2.0 eq) and sodium triacetoxyborohydride (1.4 eq) were added to a solution of aldehyde **3a** (1.0 eq) in CH_2Cl_2. The reaction mixture was stirred at room temperature until TLC indicated complete consumption of the aldehyde, quenched with saturated sodium carbonate (Na_2CO_3) solution and extracted thrice with CH_2Cl_2. The combined organic phases were dried over $MgSO_4$, filtered and reduced in vacuum.

General procedure for reductive amination II (**GP6**): The appropriate amino acid (2.0 eq) and sodium cyanoborohydride (1.4 eq) were added to a solution of aldehyde **3a** (1.0 eq) in MeOH. The reaction mixture was stirred at room temperature until TLC indicated complete consumption of the aldehyde and reduced in vacuum.

***rac*-1-{2-[(4-Formylphenyl)bis(4-methoxyphenyl)methoxy]ethyl}piperidine-3-carboxylic acid (5a):** GP4 was followed using **12a** (101 mg, 0.190 mmol), barium hydroxide octahydrate (241 mg, 0.764 mmol), MeOH/H_2O 4:1 (5.0 ml). The crude compound was purified by flash column chromatography on silica (eluent MeOH). Amorphous colourless solid (85 mg, 89 %).

(*S*)-1-{2-[(4-Formylphenyl)bis(4-methoxyphenyl)methoxy]ethyl}piperidine-3-carboxylic acid [(*S*)-5a]: GP4 was followed using (*S*)-**12a** (38 mg, 0.071 mmol), barium hydroxide octahydrate (90 mg, 0.28 mmol), MeOH/H_2O 4:1 (5.0 ml). The crude compound was purified by flash column chromatography on silica (eluent MeOH). Amorphous colourless solid (34 mg, 93 %).

(*R*-1-{2-[(4-Formylphenyl)bis(4-methoxyphenyl)methoxy]ethyl}piperidine-3-carboxylic acid [(*R*)-5a]: GP4 was followed using (*R*)-**12a** (37 mg, 0.070 mmol), barium hydroxide octahydrate (89 mg, 0.28 mmol), MeOH/H_2O 4:1 (5.0 ml). The crude compound was purified by flash column chromatography on silica (eluent MeOH). Amorphous colourless solid (32.5 mg, 92 %).

***rac*-1-{2-[(4-Acetylphenyl)bis(4-methoxyphenyl)methoxy]ethyl}piperidine-3-carboxylic acid (5b):** GP4 was followed using **12b** (87 mg, 0.16 mmol), barium hydroxide octahydrate (197 mg, 0.62 mmol), MeOH/H_2O 4:1 (3.5 ml). The crude compound was purified by flash column chromatography on silica (eluent MeOH). Amorphous colourless solid (69 mg, 86 %).

***rac*-1-(2-{[4-(N,N-dimethylsulfamoyl)phenyl]bis[4-methoxyphenyl]methoxy}ethyl)-piperidine-3-carboxylic acid (5c):** GP4 was followed using **12c** (66 mg, 0.11 mmol), barium hydroxide octahydrate (137 mg, 0.434 mmol), MeOH/H_2O 4:1 (3.0 ml). The crude compound was purified by flash column chromatography on silica (eluent MeOH). Amorphous colourless solid (55 mg, 88 %).

***rac*-1-(2-{Imidazo[1,2-a]pyridin-6-ylbis(4-methoxyphenyl)methoxy}ethyl)piperidine-3-carboxylic acid (5d):** GP4 was followed using **12d** (78 mg, 0.14 mmol), barium hydroxide octahydrate (170 mg, 0.54 mmol), MeOH/H_2O 4:1 (5.0 ml). The crude compound was purified by flash column chromatography on silica (eluent MeOH/CH_2Cl_2 1:1). Amorphous colourless solid (59 mg, 80 %).

***rac*-1-{2-[(4-Carboxyphenyl)bis(4-methoxyphenyl)methoxy]ethyl}piperidine-3-carboxylic acid (5e):** GP4 was followed using **12e** (200 mg, 0.350 mmol), barium hydroxide octahydrate (222 mg, 0.704 mmol), MeOH/H_2O 4:1 (5.0 ml). The crude compound was purified by flash column chromatography on silica (eluent MeOH). Amorphous colourless solid (110 mg, 61 %).

***rac*-1-(2-{[4-(Methoxymethyl)phenyl]bis[4-methoxyphenyl]methoxy}ethyl)piperidine-3-carboxylic acid (5f):** GP4 was followed using **12f** (72 mg, 0.13 mmol), barium hydroxide octahydrate (83 mg, 0.26 mmol), MeOH/H_2O 4:1 (12.0 ml). The crude compound was purified by flash column chromatography on silica (eluent MeOH). Amorphous colourless solid (56 mg, 81 %).

***rac*-1-{2-[(4-Cyanophenyl)bis(4-methoxyphenyl)methoxy]ethyl}piperidine-3-carboxylic acid (5g):** GP4 was followed using **12g** (48 mg, 0.090 mmol), barium hydroxide octahydrate (57 mg, 0.18 mmol), MeOH/H_2O 4:1 (2.0 ml). The crude compound was purified by flash column chromatography on silica (eluent MeOH). Amorphous colourless solid (39 mg, 86 %).

***rac*-1-(2-{Bis[4-(methoxymethyl)phenyl][4-methoxyphenyl]methoxy}ethyl)piperidine-3-carboxylic acid (5h):** GP4 was followed using **12h** (56 mg, 0.10 mmol), barium hydroxide octahydrate (127 mg, 0.403 mmol), MeOH/H_2O 4:1 (5.0 ml). The crude compound was purified by flash column chromatography on silica (eluent MeOH). Amorphous colourless solid (51 mg, 94 %).

***rac*-1-(2-{Tris[4-(methoxymethyl)phenyl]methoxy}ethyl)piperidine-3-carboxylic acid (5i):** GP4 was followed using **12i** (61 mg, 0.11 mmol), barium hydroxide octahydrate (75 mg, 0.44 mmol), MeOH/H_2O 4:1 (5.0 ml). The crude compound was purified by flash column chromatography on silica (eluent MeOH). Amorphous colourless solid (52 mg, 90 %).

***rac*-1-{2-[(4-Carbamoylphenyl)bis(4-methoxyphenyl)methoxy]ethyl}piperidine-3-carboxylic acid (5j):** GP4 was followed using **12j** (63 mg, 0.12 mmol), barium hydroxide octahydrate (146 mg, 0.46 mmol), MeOH/H_2O 4:1 (5.0 ml). The crude compound was purified by flash column chromatography on silica (eluent MeOH). Amorphous colourless solid (52 mg, 87 %).

***rac*-1-{2-[Carboxybis(4-methoxyphenyl)methoxy]ethyl}piperidine-3-carboxylic acid (5k):** GP4 was followed using **12k** (370 mg, 0.760 mmol), barium hydroxide octahydrate (481 mg, 1.52 mmol), MeOH/H_2O 4:1 (5.0 ml). The crude compound was purified by flash column chromatography on silica (eluent MeOH). Amorphous colourless solid (327 mg, 97 %).

***rac*-1-[4-Hydroxy-4,4-bis(4-methoxyphenyl)butyl]piperidine-3-carboxylic acid (5l):** GP4 was followed using **12l** (103 mg, 0.230 mmol), barium hydroxide octahydrate (148 mg, 0.469 mmol), MeOH/H_2O 4:1 (3.6 ml). The crude compound was purified by flash column chromatography on silica (eluent MeOH). Amorphous colourless solid (81 mg, 84 %).

rac-1-(2-{[4-(Hydroxymethyl)phenyl]bis[4-methoxyphenyl]methoxy}ethyl)piperidine-3-carboxylic acid (5m): GP4 was followed using **12m** (58 mg, 0.11 mmol), barium hydroxide octahydrate (69 mg, 0.22 mmol), MeOH/H_2O 4:1 (3.0 ml). The crude compound was purified by flash column chromatography on silica (eluent MeOH). Amorphous colourless solid (38 mg, 69 %).

***rac*-1-{2-[(4-{[(Carboxymethyl)amino]methyl}phenyl)bis(4-methoxyphenyl)methoxy]-ethyl}piperidine-3-carboxylic acid (5n):** GP4 was followed using **12n** (35 mg, 0.060 mmol), barium hydroxide octahydrate (37 mg, 0.12 mmol), MeOH/H_2O 4:1 (5.0 ml). The crude compound was purified by flash column chromatography on silica (eluent MeOH). Amorphous colourless solid (29 mg, 65 %).

***rac*-1-{2-[(4-{[(2-Carboxyethyl)amino]methyl}phenyl)bis(4-methoxyphenyl)-methoxy]-ethyl}piperidine-3-carboxylic acid (5o):** GP4 was followed using **12o** (83 mg, 0.13 mmol), barium hydroxide octahydrate (171 mg, 0.542 mmol), MeOH/H_2O 4:1 (5.0 ml). The crude

compound was purified by flash column chromatography on silica (eluent MeOH). Amorphous colourless solid (57 mg, 74 %).

***rac*-1-{2-[(4-{[(1-Carboxycyclopropyl)amino]methyl}phenyl)bis(4-methoxyphenyl)-methoxy]ethyl}piperidine-3-carboxylic acid (5p):** GP4 was followed using **12p** (51 mg, 0.079 mmol), barium hydroxide octahydrate (100 mg, 0.317 mmol), MeOH/H_2O 4:1 (6.0 ml). The crude compound was purified by flash column chromatography on silica (eluent MeOH). Amorphous colourless solid (50 mg, 82 %).

***rac*-1-{2-[(4-{[(2-Carboxypropan-2-yl)amino]methyl}phenyl)bis(4-methoxyphenyl)-methoxy]ethyl}piperidine-3-carboxylic acid (5q):** GP4 was followed using **12q** (35 mg, 0.054 mmol), barium hydroxide octahydrate (136 mg, 0.431 mmol), MeOH/H_2O 4:1 (5.0 ml). The crude compound was purified by flash column chromatography on silica (eluent MeOH). Amorphous colourless solid (29.3 mg, 92 %).

***rac*-1-[2-(Bis{4-methoxyphenyl}{4-[(2-oxopyrrolidin-1-yl)methyl]phenyl}methoxy)ethyl]-piperidine-3-carboxylic acid (5r):** GP5 was followed using **12a** (173 mg, 0.330 mmol), ethyl 4-aminobutanoate hydrochloride (109 mg, 0.650 mmol), sodium triacetoxyborohydride (155 mg, 0.730 mmol), CH_2Cl_2 (2.0 ml). The crude compound was purified by flash column chromatography on silica (eluent ethyl acetate + 5% triethylamine), yielding 107 mg of a mixture of *rac*-ethyl 1-[2-(bis{4-methoxyphenyl}{4-[(2-oxopyrrolidin-1-yl)methyl]-phenyl}methoxy)ethyl]piperidine-3-carboxylate and *rac*-ethyl 1-{2-[(4-{[(4-methoxy-4-oxobutyl)amino]methyl}phenyl)bis(4-methoxyphenyl)methoxy]ethyl}-piperidine-3-carboxylate. 84 mg thereof were subjected to GP4 using barium hydroxide octahydrate (178 mg, 0.564 mmol), MeOH/H_2O 4:1 (3.5 ml). The crude compound was purified by flash column chromatography on silica (eluent MeOH). Amorphous colourless solid (69 mg, 47 % over both steps).

***rac*-1-{2-[(4-{[(3-Carboxypropyl)amino]methyl}phenyl)bis(4-methoxyphenyl)methoxy]-ethyl}piperidine-3-carboxylic acid (5s):** GP4 was followed using **12s** (50 mg, 0.081 mmol), barium hydroxide octahydrate (103 mg, 0.326 mmol), MeOH/H_2O 4:1 (5.0 ml). Amorphous colourless solid (40 mg, 84 %).

***rac*-1-{2-[(4-{[(4-Carboxyphenyl)amino]methyl}phenyl)bis(4-methoxyphenyl)methoxy]-ethyl}piperidine-3-carboxylic acid (5t): 12t** (37.2 mg, 0.057 mmol) was dissolved in THF (1.5 ml) and H_2O (1.5 ml) and barium hydroxide octahydrate (38.4 mg, 4.0 eq) were added. The mixture was stirred at room temperature until TLC indicated complete consumption of **12t**. Carbon dioxide was passed through the solution until no further precipitate formed. The suspension was filtered through a syringe filter (Perfect-Flow®, WICOM Germany GmbH, PTFE, 0.2µM) and lyophilized. Amorphous colourless solid (34.0 mg, 96 %).

[4-(Dimethoxymethyl)phenyl]bis(4-methoxyphenyl)methanol (8a): GP2 was followed using *tert*-butyllithium solution (1.7M in pentane, 1.2 ml, 2.04 mmol), 1-bromo-4-(dimethoxymethyl)benzene **9a** (235 mg, 1.02 mmol), THF (3.0 ml). Addition of 4,4´-dimethoxybenzophenone **10a** (245 mg, 1.00 mmol) in THF (5.0 ml). The crude compound was purified by flash column chromatography on silica (eluent pentane/Et_2O 7:3). Colourless oil (393 mg, 99 %).

Bis(4-methoxyphenyl)[4-(2-methyl-1,3-dioxan-2-yl)phenyl]methanol (8b): GP2 was followed using t*ert*-butyllithium solution (1.7M in pentane, 3.3 ml, 5.6 mmol), 2-(4-bromophenyl)-2-methyl-1,3-dioxane **9b** (713 mg, 2.77 mmol), THF (12.0 ml). Addition of 4,4´-dimethoxybenzophenone **10a** (700 mg, 2.83 mmol) in THF (12.0 ml). The crude compound was purified by flash column chromatography on silica (eluent pentane/Et_2O 8:2). Colourless semi-solid (1.02 g, 87 %).

4-[Hydroxybis(4-methoxyphenyl)methyl]-N,N-dimethylbenzenesulfonamide (8c): GP2 was followed using *tert*-butyllithium solution (1.7M in pentane, 2.7 ml, 4.6 mmol), **9c** (561 mg, 2.27 mmol), THF (30.0 ml). Addition of 4,4´- dimethoxybenzophenone **10a** (561 mg, 2.27 mmol) in THF (12.0 ml). The crude compound was precipitated from isohexane/THF. Amorphous colourless solid (514 mg, 53 %).

Imidazo[1,2-a]pyridin-6-ylbis(4-methoxyphenyl)methanol (8d): *N*-butyllithium solution (2.4 M in hexane, 1.0 ml, 2.4 mmol) was added dropwise to a suspension of 6-bromoimidazo[1,2-a]pyridine **9d** (483 mmg, 2.40 mmol) in Et_2O (24.0 ml) at -78°C. After 30min a suspension of 4,4´-dimethoxybenzophenone **10a** (494 mg, 2.0 mmol) in Et_2O was added. The mixture was stirred 1h at -78°C, warmed to room temperature, quenched with water (20.0 ml) and extracted thrice with ethyl acetate (20.0 ml). The combined organic phases were washed

with saturated Na_2CO_3 solution, dried over $MgSO_4$, filtered and reduced in vacuum. The crude compound was purified by flash column chromatography on silica (eluent CH_2Cl_2 + 2% MeOH). Amorphous slightly yellowish solid (400 mg, 56 %).

Ethyl 4-[hydroxybis(4-methoxyphenyl)methyl]benzoate (8e): Isopropylmagnesium chloride (2.0M solution in THF, 1.0 ml, 2.0 mmol) was added dropwise to a solution of ethyl 4-iodobenzoate **9e** (547 mg, 2.02 mmol) in THF (5.0 ml) at -20°C. The mixture was stirred for 1.5h and a solution of 4,4´-dimethoxybenzophenone **10a** (445 mg, 1.80 mmol) in THF (5.0 ml) was slowly added via syringe. Stirring was continued at 0°C over night. The reaction mixture was allowed to slowly warm up to room temperature, quenched with saturated NH_4Cl solution and extracted thrice with CH_2Cl_2. The combined organic phases were dried over $MgSO_4$, filtered and reduced in vacuum. The resulting crude compound was purified by flash column chromatography on silica (eluent pentane/Et_2O 8:2). Colourless semi-solid (328 mg, 77 %).

[4-(Methoxymethyl)phenyl]bis(4-methoxyphenyl)methanol (8f): GP2 was followed using t*ert*-butyllithium solution (1.7M in pentane, 5.0 ml, 8.50 mmol), 1-bromo-4-(methoxymethyl)benzene **9f** (848 mg, 4.22 mmol), THF (24.0 ml). Addition of 4,4´-dimethoxybenzophenone **10a** (1.05 g, 4.25 mmol) in THF (12.0 ml). The crude compound was purified by flash column chromatography on silica (eluent pentane/Et_2O 7:3). Amorphous colourless solid (1.42 g, 92 %).

4-[Hydroxybis(4-methoxyphenyl)methyl]benzonitrile (8g): GP1 was followed using a Grignard reagent prepared from 4-bromoanisol **9g** (1.72 g, 9.01 mmol) and magnesium (219 mg, 9.01 mmol) in THF (20.0 ml). A solution of 4-cyanobenzoyl chloride **10c** (736 mg, 4.40 mmol) in THF (8.0 ml) was added dropwise at 0°C. The reaction mixture was stirred 2h at 0°C and 30min at 25°C. The crude compound was purified by flash column chromatography on silica (eluent pentane/Et_2O 6:4). Amorphous colourless solid (1.42 g, 94 %).

Bis[4-(methoxymethyl)phenyl](4-methoxyphenyl)methanol (8h): GP1 was followed using a Grignard reagent prepared from 1-bromo-4-(methoxymethyl)benzene **9h** (745 mg, 3.70 mmol) and magnesium (90 mg, 3.7 mmol) in THF (6.0 ml). A solution of methyl 4-methoxybenzoate (560 mg, 3.30 mmol) in THF (6.0 ml) was added dropwise. The reaction mixture was stirred at room temperature for 16h and refluxed 90min. The crude compound

was purified by flash column chromatography on silica (eluent pentane/Et_2O 6:4). Pale yellowish oil (492 mg, 70 %).

Tris[4-(methoxymethyl)phenyl]methanol (8i): GP1 was followed using a Grignard reagent prepared from 1-bromo-4-(methoxymethyl)benzene **9h** (1.41 g, 7.00 mmol) and magnesium (170 mg, 6.99 mmol) in THF (10.0 ml). Dimethyl carbonate (209 mg, 2.30 mmol) was added dropwise at room temperature. The reaction mixture was refluxed 90 min, then stirred at room temperature over night. The crude compound was purified by flash column chromatography on silica (eluent pentane/Et_2O 1:1). Colourless oil (771 mg, 85 %).

4-[Hydroxybis(4-methoxyphenyl)methyl]benzamide (8j): A mixture of 4-[hydroxybis(4-methoxyphenyl)methyl]benzonitrile **8g** (171 mg, 0.500 mmol) and potassium *tert*-butoxide (340 mg, 3.00 mmol) was stirred in *tert*-butanol (4.0 ml) at 50°C for 40h. Water (25 ml) was added ad the mixture was extracted thrice with CH_2Cl_2 (30.0 ml). The combined organic phases were dried over $MgSO_4$ and reduced in vacuum. The crude compound was purified flash column chromatography on silica (eluent isohexane/ethyl acetate 3:7). Amorphous colourless solid (173 mg, 96 %).

Methyl 2-hydroxy-2,2-bis(4-methoxyphenyl)acetate (8k): A mixture of 4,4´-dimethoxybenzilic acid (2.78 g, 9.64 mmol) and 1,8-diazabicyclo[5.4.0]undec-7-ene (DBU, 2.65 g, 17.4 mmol) in MeCN (4.5 ml) was cooled to 0°C and iodomethane (5.02 g, 35.0 mmol) was added. The ice bath was removed and stirring was continued for 48h at ambient temperature. The reaction mixture was reduced in vacuum and purified by flash column chromatography on silica (eluent pentane/Et_2O 2:1 to 1:1). Amorphous colourless solid (2.64 g, 91 %).

4-Chloro-1,1-bis(4-methoxyphenyl)butan-1-ol (8l): GP1 was followed using a Grignard reagent prepared from 4-bromoanisol (0.94 g, 4.98 mmol) and magnesium (122 mg, 5.02 mmol) in THF (12.0 ml). A solution of 4-chloro-1-(4-methoxyphenyl)butan-1-one (1.06 g, 5.00 mmol) in THF (12.0 ml) was added dropwise at 0°C. The reaction mixture was stirred 1h at ambient temperature. The crude compound was purified by flash column chromatography on silica (eluent isohexane/ethyl acetate 9:1). Colourless oil (1.06 g, 66 %).

4-Bromo-N,N-dimethylbenzenesulfonamide (9d): A mixture of 4-bromobenzenesulfonamide (2.40 g, 10.2 mmol), tetrabutylammonium tetrafluoroborate (329 mg, 1.02 mmol), K_2CO_3 (5.58 g, 40.4 mmol) and dimethyl sulfate (2.53 g, 20.0 mmol) in MeCN (15.0 ml) was refluxed for 3h. After cooling to room temperature concentrated ammonium hydroxide solution (5.0 ml) was added and stirring was continued for 16h. The reaction mixture was poured into water (20.0 ml) and extracted thrice with CH_2Cl_2 (30.0 ml). The combined organic phases were dried over $MgSO_4$, filtered and reduced in vacuum. The crude compound was purified by flash column chromatography on silica (eluent pentane/Et_2O 7:3). Amorphous colourless solid (2.66 g, 99 %).

1-{4-[Hydroxybis(4-methoxyphenyl)methyl]phenyl}ethan-1-one (11): Concentrated hydrochlorid acid (3.0 ml) was added to a solution of **8b** (430 mg, 1.02 mmol) in THF (12.0 ml). The mixture was refluxed overnight, basified with 2M NaOH and extracted thrice with CH_2Cl_2. The combined organic phases were dried over $MgSO_4$, filtered and reduced in vacuum. The crude compound was purified by flash column chromatography on silica (eluent pentane/Et_2O 1:1). Amorphous colourless solid (345 mg, 93 %).

***rac*-Ethyl 1-{2-[(4-formylphenyl)bis(4-methoxyphenyl)methoxy]ethyl}piperidine-3-carboxylate (*rac*-12a):** GP3 was followed using **8a** (2.68 g, 6.35 mmol), acetylchloride (10.0 ml), *rac*-ethyl 1-(2-hydroxyethyl)nipecotinate (1.41 g, 6.99 mmol), K_2CO_3 (2.20 g, 15.9 mmol), acetontrile (20.0 ml). The crude compound was purified by two consecutive flash column chromatographies on silica (eluent pentane/Et_2O 1:1 + 5% triethyl amine; Et_2O 100%). Colourless oil (2.35 g, 70 %).

(*S*)-Ethyl 1-{2-[(4-formylphenyl)bis(4-methoxyphenyl)methoxy]ethyl}piperidine-3-carboxylate [(*S*)-12a]: GP3 was followed using **8a** (509 mg, 1.21 mmol), acetylchloride (3.0 ml), (S)-ethyl 1-(2-hydroxyethyl)nipecotinate (318 mg, 1.58 mmol), K_2CO_3 (498 mg, 3.60 mmol), MeCN (5.0 ml). The crude compound was purified by two consecutive flash column chromatographies on silica (eluent pentane/Et_2O 1:1 + 5% triethyl amine; Et_2O 100%). Colourless oil (324 mg, 41 %).

(*R*)-Ethyl 1-{2-[(4-formylphenyl)bis(4-methoxyphenyl)methoxy]ethyl}piperidine-3-carboxylate [(*S*)-12a]: GP3 was followed using **8a** (380 mg, 0.900 mmol), acetylchloride (1.0 ml), (*R*)-ethyl 1-(2-hydroxyethyl)nipecotinate (201 mg, 1.00 mmol), K_2CO_3 (311 mg, 2.25 mmol),

MeCN (1.0 ml). The crude compound was purified by two consecutive flash column chromatographies on silica (eluent pentane/Et_2O 1:1 + 5% triethyl amine;Et_2O 100%). Colourless oil (270 mg, 56 %).

***rac*-Ethyl 1-{2-[(4-acetylphenyl)bis(4-methoxyphenyl)methoxy]ethyl}piperidine-3-carboxylate (12b):** GP3 was followed using **8b** (344 mg, 0.950 mmol), acetylchloride (3.0 ml), *rac*-ethyl 1-(2-hydroxyethyl)nipecotinate (211 mg, 1.05 mmol), K_2CO_3 (329 mg, 2.38 mmol), MeCN (3.0 ml). The crude compound was purified by flash column chromatography on silica (eluent pentane/Et_2O 6:4 + 5% trimethylamine). Colourless oil (261 mg, 50 %).

***rac*-Ethyl 1-(2-{[4-(N,N-dimethylsulfamoyl)phenyl]bis[4-methoxyphenyl]methoxy}ethyl)-piperidine-3-carboxylate (12c):** GP3 was followed using **8c** (455 mg, 1.06 mmol), acetylchloride (3.0 ml), *rac*-ethyl 1-(2-hydroxyethyl)nipecotinate (213 mg, 1.06 mmol), K_2CO_3 (366 mg, 2.65 mmol), MeCN (3.0 ml). The crude compound was purified by flash column chromatography on silica (eluent pentane/Et_2O 1:1 + 5% trimethylamine). Yellowish semi-solid (411 mg, 64 %).

***rac*-Ethyl 1-(2-{imidazo[1,2-a]pyridin-6-ylbis(4-methoxyphenyl)methoxy}ethyl)piperidine-3-carboxylate (12d):** GP5 was followed using **8d** (254 mg, 0.710 mmol), acetylchloride (3.0 ml), *rac*-ethyl 1-(2-hydroxyethyl)nipecotinate (157 mg, 0.780 mmol), K_2CO_3 (488 mg, 3.53 mmol), MeCN (5.0 ml). The crude compound was purified by flash column chromatography on silica (eluent Et_2O/MeOH 9:1). Yellow semi-solid (160 mg, 48 %).

***rac*-Ethyl 1-(2-{[4-(ethoxycarbonyl)phenyl]bis[4-methoxyphenyl]methoxy}ethyl)piperidine-3-carboxylate (12e):** GP3 was followed using **8e** (217 mg, 0.550 mmol), acetylchloride (1.0 ml), *rac*-ethyl 1-(2-hydroxyethyl)nipecotinate (133 mg, 0.661 mmol), K_2CO_3 (191 mg, 1.38 mmol), MeCN (2.0 ml). The crude compound was purified by two consecutive flash column chromatographies on silica (eluent pentane/Et_2O 4:6; pentane/Et_2O 8:2 + 5% dimethylethylamine). Colourless semi-solid (173 mg, 54 %).

***rac*- Ethyl 1-(2-{[4-(methoxymethyl)phenyl]bis[4-methoxyphenyl]methoxy}ethyl)-piperidine-3-carboxylate (12f):** GP3 was followed using **8f** (310 mg, 0.850 mmol), acetylchloride (5.0 ml), *rac*-ethyl 1-(2-hydroxyethyl)nipecotinate (191 mg, 0.949 mmol), K_2CO_3 (294 mg, 2.13 mmol), MeCN (5.0 ml). The crude compound was purified by two

consecutive flash column chromatographies on silica (eluent Et_2O 100%, pentane/Et_2O 7:3 + 5% triethylamine). Colourless oil (207 mg, 44 %).

***rac*-Ethyl 1-{2-[(4-cyanophenyl)bis(4-methoxyphenyl)methoxy]ethyl}piperidine-3-carboxylate (12g):** GP3 was followed using **8g** (364 mg, 1.00 mmol), acetylchloride (1.0 ml), *rac*-ethyl 1-(2-hydroxyethyl)nipecotinate (242 mg, 1.20 mmol), K_2CO_3 (346 mg, 2.50 mmol), MeCN (5.0 ml). The crude compound was purified by flash column chromatography on silica (eluent pentane/Et_2O/triethyl amine 4:4:2). Yellowish semi-solid (447 mg, 85 %).

***rac*-Ethyl 1-(2-{bis[4-(methoxymethyl)phenyl][4-methoxyphenyl]methoxy}ethyl)-piperidine-3-carboxylate (12h):** GP3 was followed using **8h** (380 mg, 1.00 mmol), acetylchloride (3.0 ml), *rac*-ethyl 1-(2-hydroxyethyl)nipecotinate (221 mg, 1.10 mmol), K_2CO_3 (346 mg, 2.5 mmol), MeCN (5.0 ml). The crude compound was purified flash column chromatography on silica (eluent Et_2O). Colourless oil (260 mg, 46 %).

***rac*-Ethyl 1-(2-{tris[4-(methoxymethyl)phenyl]methoxy}ethyl)piperidine-3-carboxylate (12i):** GP3 was followed using **8i** (243 mg, 0.620 mmol), acetylchloride (3.0 ml), *rac* ethyl 1-(2-hydroxyethyl)nipecotinate (452 mg, 2.25 mmol), K_2CO_3 (774 mg, 5.60 mmol), MeCN (5.0 ml). The crude compound was purified by flash column chromatography on silica (eluent isohexane/Et_2O 8:1 to Et_2O 100%). Colourless oil (151 mg, 42 %).

***rac*-Ethyl 1-{2-[(4-carbamoylphenyl)bis(4-methoxyphenyl)methoxy]ethyl}piperidine-3-carboxylate (12j):** GP3 was followed using **8j** (512 mg, 1.41 mmol), acetylchloride (5.0 ml), *rac*-ethyl 1-(2-hydroxyethyl)nipecotinate (321 mg, 1.55 mmol), K_2CO_3 (488 mg, 3.53 mmol), MeCN (5.0 ml). The crude compound was purified flash column chromatography on silica (eluent ethyl acetate + 5% MeOH). Amorphous slightly yellowish solid (375 mg, 49 %).

***rac*-Ethyl 1-{2-[2-methoxy-1,1-bis(4-methoxyphenyl)-2-oxoethoxy]ethyl}piperidine-3-carboxylate (12k):** GP3 was followed using **8k** (680 mg, 2.24 mmol), acetylchloride (5.0 ml), *rac*-ethyl 1-(2-hydroxyethyl)nipecotinate (452 mg, 2.25 mmol), K_2CO_3 (774 mg, 5.60 mmol), MeCN (5.0 ml). The crude compound was purified by flash column chromatography on silica (eluent pentane/Et_2O 1:1 to pentane/ Et_2O 1:1 + 20% triethylamine). Colourless semi-solid (956 mg, 88 %).

***rac*-Ethyl 1-[4-hydroxy-4,4-bis(4-methoxyphenyl)butyl]piperidine-3-carboxylate (12l):** A mixture of **8l** (435 mg, 1.29 mmol), *rac*-ethyl nipecotinate (233 mg, 1.42 mmol), K_2CO_3 (446 mg, 3.23 mmol) and KI (21 mg, 0.13 mmol) in MeCN (5.0 ml) was irradiated in the microwave at 80°C for 24h, filtered and reduced in vacuum. The crude compound was purified by flash column chromatography on silica (eluent pentane/ Et_2O 2:1 + 5% triethylamine). Amorphous slightly yellowish solid (374 mg, 66 %).

***rac*-Ethyl 1-(2-{[4-(hydroxymethyl)phenyl]bis[4-methoxyphenyl]methoxy}ethyl)piperidine-3-carboxylate (12m):** Sodium borohydride (46 mg, 1.2 mmol) was added to a solution of **12a** (254 mg, 0.480 mmol) in MeOH (7.5 ml) at 0°C. The ice bath was removed and stirring was continued at ambient temperature for 3h. The mixture was poured into water (30.0 ml) and extracted thrice with Et_2O (30.0 ml). The combined organic phases were dried over $MgSO_4$, filtered and reduced in vacuum. Colourless oil (226 mg, 89 %).

***rac*-Ethyl 1-{2-[(4-{[(2-methoxy-2-oxoethyl)amino]methyl}phenyl)bis(4-methoxyphenyl)-methoxy]ethyl}piperidine-3-carboxylate (12n):** GP5 was followed using **12a** (449 mg, 0.850 mmol), methyl glycinate hydrochloride (212 mg, 1.69 mmol), sodium triacetoxyborohydride (250 mg, 1.18 mmol), CH_2Cl_2 (5.0 ml). The crude compound was purified by flash column chromatography on silica (eluent isohexane/ethyl acetate 7:3 + 5% triethylamine). Colourless semi-solid (289 mg, 57 %).

***rac*-Ethyl 1-{2-[(4-{[(3-ethoxy-3-oxopropyl)amino]methyl}phenyl)bis(4-methoxyphenyl)-methoxy]ethyl}piperidine-3-carboxylate (12o):** GP5 was followed using **12a** (480 mg, 0.900 mmol), β-alanine methyl ester hydrochloride (314 mg, 2.25 mmol), sodium triacetoxyborohydride (267 mg, 1.26 mmol), CH_2Cl_2 (10.0 ml). The crude compound was purified by flash column chromatography on silica (eluent Et_2O + 4% triethylamine). Pale yellow oil (236 mg, 42 %).

***rac*-Ethyl 1-(2-{[4-({[1-(ethoxycarbonyl)cyclopropyl]amino}methyl)phenyl]bis[4-methoxy-phenyl]methoxy}ethyl)piperidine-3-carboxylate (12p):** GP5 was followed using **12a** (233 mg, 0.44 mmol), ethyl 1-aminocyclopropanecarboxylate hydrochloride (145 mg, 0.88 mmol), sodium triacetoxyborohydride (131 mg, 0.620 mmol), CH_2Cl_2 (2.0 ml). The crude compound was purified by flash column chromatography on silica (eluent pentane/Et_2O + 4% triethylamine). Colourless semi-solid (168 mg, 59 %).

***rac*-Ethyl 1-{2-[(4-{[(1-ethoxy-2-methyl-1-oxopropan-2-yl)amino]methyl}phenyl)bis(4-methoxyphenyl)methoxy]ethyl}piperidine-3-carboxylate (12q):** GP5 was followed using **12a** (152 mg, 0.290 mmol), ethyl 2-amino-2-methylpropanoate hydrochloride (96 mg, 0.57 mmol), sodium triacetoxyborohydride (85 mg, 0.40 mmol), CH_2Cl_2 (2.0 ml). The crude compound was purified by flash column chromatography on silica (eluent pentane/Et_2O 1:1 + 4% triethylamine). Colourless semi-solid (119 mg, 64 %).

***rac*-4-{[4-({2-[3-(Ethoxycarbonyl)piperidin-1-yl]ethoxy}bis{4-methoxyphenyl}methyl)-benzyl]amino}butanoic acid (12s):** GP6 was followed 4-aminobutanoic acid (83 mg, 0.80 mmol), **12a** (213 mg, 0.40 mmol), sodium cyanoborohydride (37 mg, 0.56 mmol), MeOH (5.0 ml). The crude compound was purified by flash column chromatography on silica (eluent MeOH). Amorphous colourless solid (100 mg, 40 %).

***rac*-4-{[4-({2-[3-(Ethoxycarbonyl)piperidin-1-yl]ethoxy}bis{4-methoxyphenyl}methyl)-benzyl]amino}benzoic acid (12t):** GP6 was followed using 4-aminobutanoic acid (217 mg, 1.58 mmol), **12a** (420 mg, 0.790 mmol), sodium cyanoborohydride (73 mg, 1.1 mmol), MeOH (10.0 ml). The crude compound was purified by flash column chromatography on silica (eluent MeCN/H_2O 9:1). Amorphous slightly yellowish solid (132 mg, 25 %).

Biological evaluation

[^{3}H]GABA uptake assays: The [^{3}H]GABA uptake assays were performed in a 96-well plate format with intact HEK293 cells expressing mGAT1, mGAT2, mGAT3, mGAT4 and hGAT3, respectively.

MS Binding Assays: The MS Binding Assays were performed with mGAT1 membrane preparations obtained from a stable HEK293 cell line and NO711 as unlabeled marker in competitive binding experiments.

Conflict of interest

The authors declare no conflict of interest.

Literature

[1] P. Krogsgaard-Larsen, *Medicinal Research Reviews* **1988**, Vol. 8, No. 1, 27-56

[2] B.S. Meldrum, A.G. Chapman, Epilepsia **1999**, *40*, 9, 2-6

[3] D.M. Treiman**,** *Epilepsia* **2001**, *42*, 8-12

[4] S.R. Kleppner, A.J. Tobin**,** *Expert Opinion on Therapeutic Targets* **2001**, *5*, 219-239

[5] M.A. Daemen, G. Hoogland, J.M. Cijntje, G.H. Spincemaille, *Neuroscience Letters* **2008**, *444*, 112-115

[6] P. Nuss, *Neuropsychiatric Disease and Treatment* **2015**, *11*, 165–175

[7] A.V. Kalueff, D. J. Nutt, *Depression and Anxiety* **2007**, *24*, 495–517

[8] K.L. Lanctot, N. Herrmann, P. Mazzotta, L.R. Khan, N. Ingber, *Canadian Journal of Psychiatry* **2004**, *49*, 439-453

[9] Ł. Fijałkowski, K. Sałat, A. Podkowa, P. Zaręba, A. Nowaczyk, *European Journal of Pharmaceutical Sciences* **2017**, *96*, 362-372

[10] K. Sałat, A. Podkowa, P. Kowalczyk, K. Kulig, A. Dzubina, B. Filipek, T. Librowski, *Pharmakological Reports* **2015**, 67, 465-472

[11] A. Schousboe, K.K. Madsen, M.L. Barker-Haliski, H.S. White, *Neurochemical Research* **2014**, *39*, 1980-1987

[12] A.S. Kristensen, J. Andersen, T.N. Jørgensen, L. Sørensen, J. Eriksen, C.J. Loland, K. Strømgaard, U. Gether, *Pharmacological Reviews* **2011**, *63*, 3, 585-640

[13] S. Bröer, U. Gether, *British Journal of Pharmacology* **2012**, *167*, 2, 256-278

[14] L. Shi, M. Quick, Y. Zhao, H. Weinstein, J.A. Javitch, *Molecular Cell* **2008**, *30*, 667–677

[15] K.K. Madsen, R.P. Clausen, O.M. Larsson, P. Krogsgaard-Larsen, A. Schousboe, H.S. White, *Journal of Neurochemistry* **2009**, *109*, 139-144

[16] N. O. Dalby, Eur. J. Pharmacol., 2003, 479, 127-137

[17] B. Christiansen, A. K. Meinild, A. A. Jensen, H. Bräuner-Osbore, *Journal of Biological Chemistry* **2007**, *282*, 19331-19341

[18] L.A. Borden, *Neurochemistry International* **1996**, *29*, 4, 335-356

[19] Y. Zhou, N.C. Danbolt, *Front Endocrinol* **2013**, *4*, 165

[20] S.A. Kempson SA, Y. Zhou Y, N.C. Danbolt, *Frontiers in Physiology* **2014**, *5*, 159

[21] Y. Zhou, S. Holmseth, R. Hua, A. C. Lehre, A. M. Olofsson, I. Poblete-Naredo, S. A. Kempson, N. C. Danbolt, *American Journal of Physiology – Renal Physiology* **2012**, *302*, 313-328

[22] K.K. Madsen, H.S. White, A. Schousboe, *Pharmacology & Therapeutics* **2010**, *125*, 394-401

[23] I.E. Leppik, L. Gram, R. Deaton, K.W. Sommerville, *Epilepsy Research* **1999**, *33*, 235–246

[24] T.G.M. Dhar, L.A. Borden, S. Tyagarajan, K.E. Smith, T.A. Branchek, R.L. Weinshank, C. Gluchowski, *Journal of Medicinal Chemistry* **1994**, *37*, 2334-2342

[25] J. Pabel, M. Faust, C. Prehn, B. Woerlein, L. Allmendinger, G. Höfner, K.T. Wanner, *ChemMedChem* **2012**, *7*, 1245-1255

[26] M. Petrera, T. Wein, L. Allmendinger, M. Sindelar, J. Pabel, G. Höfner, K.T. Wanner *ChemMedChem*. **2016**, *11*, 519-538

[27] R. Schirrmacher, W. Hamkens, M. Piel, U. Schmitt, H. Lüddens, C. Hiemke, F. Rösch, *Journal of Labelled Compounds and Radiopharceutical*s **2001**, *44*, 627-642

[28] L.J.S. Knutsen, K.E. Andersen, J. Lau, B.F. Lundt, R.F. Henry, H.E. Morton, L. Nrum, H. Petersen, H. Stephensen, P.D. Suzdak, Journal of Medicinal Chemistry 1999, 42, 18, 3447-3462

[29] G.C. Midya, A. Kapat, S. Maiti, J. Dash, *Journal of Organic Chemistry* **2015**, 80, 8, 4148-4151

[30] T. Ohwada, K. Shudo, *Journal of the American Chemical Society* **1988**, *110*, 6, 1862-70

[31] G. Speck, C. Eickmeier, S. Pestel, S. Germeyer, M.P. Pieper, S. Breitenfelder, M. Grauert, *PCT Int. Appl.* **2007**, 2003064418

[32] A.F. Abdel-Magid, K.G. Carson, B.D. Harris, C.A. Maryanoff, R.D. Shah, *Journal of Organic Chemistry* **1996**, *61*, 3849-3862

[33] A. Kragler, G. Höfner, K.T. Wanner, *European Journal of Medical Chemistry* **2008**, *43*, 2404-2411

[34] C. Zepperitz, G. Höfner, K.T. Wanner*, ChemMedChem* **2006**, *1*, 298-217

[35] MarvinSketch, version 6.1.4; ChemAxon, Budapest (Hungary), http://www.chemaxon.com/products/marvin/marvinsketch/ (accessed July 30, 2019)

[36] S. A. Hitchcock, L. D. Pennington, *J. Med. Chem.* **2006**, *49*, 7559–7583

[37] J. Mensch, J. Oyarzabal, C. Mackie, P. Augustijns, *J. Pharm. Sci.* **2009**, *98*, 4429–4468

[38] publication is to follow

Analytical data for compounds **5a-t**, **8a-l**, **9c**, **11**, **12a-q** and **12s-t**

***rac*-1-{2-[(4-Formylphenyl)bis(4-methoxyphenyl)methoxy]ethyl}piperidine-3-carboxylic acid (5a):** ^{1}H NMR (400 MHz, MeOD + NaOD) δ = 1.25 – 1.41 (m, 1H, $NCH_2CH_2CH_{ax}H_{eq}$), 1.54 (qt, *J*=12.1, 3.9, 1H, $NCH_2CH_{ax}H_{eq}CH_2$), 1.61 – 1.70 (m, 1H, $NCH_2CH_{ax}H_{eq}CH_2$), 1.88 – 2.02 (m, 2H, $NCH_2CH_2CH_{ax}H_{eq}$ + $NCH_{ax}H_{eq}CH_2CH_2$), 2.08 (t, *J*=11.3, 1H, $NCH_{ax}H_{eq}CHCOO$), 2.34 (tt, *J*=11.6, 3.7, 1H, NCH_2CHCOO), 2.63 (t, *J*=6.3, 2H, NCH_2CH_2O), 2.82 (d, *J*=11.3, 1H, $NCH_{ax}H_{eq}CH_2CH_2$), 2.99 – 3.07 (m, 1H, $NCH_{ax}H_{eq}CHCOO$), 3.18 – 3.31 (m, 2H, NCH_2CH_2O), 3.78 (s, 6H, $C_{Ar}OCH_3$), 6.81 – 6.91 (m, 4H, $CCHCHCOCH_3$), 7.23 – 7.34 (m, 4H, $CCHCHCOCH_3$), 7.54 – 7.64 (m, 2H, CCHCHCCHO), 7.70 (d, *J*=8.2, 2H, CCHCHCCHO), 8.70 (br s, 1H, CHO). ^{13}C NMR (101 MHz, CD_2Cl_2) δ = 22.56 ($NCH_2CH_2CH_2$), 27.08 ($NCH_2CH_2CH_2$), 40.90 (NCH_2CHCOO), 53.32 ($NCH_2CH_2CH_2$), 55.81 ($C_{Ar}OCH_3$), 56.10 (NCH_2CHCOO), 57.70 (NCH_2CH_2O), 59.97 (NCH_2CH_2O), 87.02 (NCH_2CH_2OC), 113.87 ($CCHCHCOCH_3$), 128.66 (CCHCHCCHO), 129.77 (CCHCHCCHO), 130.84 (d, *J*=3.6, $CCHCHCOCH_3$), 135.10 (d, *J*=5.5, $CCHCHCOCH_3$), 135.51 (CCHCHCCHO), 153.17 (CCHCHCCHO), 159.54 ($CCHCHCOCH_3$), 176.74 (COO), 192.29 (CHO). IR (KBr): ṽ = 2933, 2835, 1702, 1606, 1574, 1509, 1463, 1410, 1303, 1251, 1213, 1175, 1153, 1115, 1068, 1033, 916, 822, 732, 677, 582, 536 cm^{-1}. HRMS-ESI- *m/z* [*M*-H]$^-$ calcd for $C_{30}H_{33}NO_6$: 502.2235, found: 502.2241.

(*S*)-1-{2-[(4-Formylphenyl)bis(4-methoxyphenyl)methoxy]ethyl}piperidine-3-carboxylic acid [(*S*)-5a]: The analytical data are consistent with racemic compound **5a**. $[\alpha]_D^{22}$ = +0.14 (c=1.93 g/100 ml in EtOH).

(*R*)-1-{2-[(4-Formylphenyl)bis(4-methoxyphenyl)methoxy]ethyl}piperidine-3-carboxylic acid [(*R*)-5a]: The analytical data are consistent with racemic compound **5a**. $[\alpha]_D^{22}$ = -0.15 (c=2.03 g/100 ml in EtOH).

***rac*-1-{2-[(4-Acetylphenyl)bis(4-methoxyphenyl)methoxy]ethyl}piperidine-3-carboxylic acid (5b):** ^{1}H NMR (400 MHz, MeOD + NaOD) δ = 1.25 – 1.41 (m, 1H, $NCH_2CH_2CH_{ax}H_{eq}$), 1.48 – 1.63 (m, 1H, $NCH_2CH_{ax}H_{eq}CH_2$), 1.63 – 1.73 (m, 1H, $NCH_2CH_{ax}H_{eq}CH_2$), 1.92 – 2.05 (m, 2H, $NCH_2CH_2CH_{ax}H_{eq}$ + $NCH_{ax}H_{eq}CH_2CH_2$), 2.10 (t, *J*=11.3, 1H, $NCH_{ax}H_{eq}CHCOO$), 2.36 (ddt, *J*=12.0, 7.4, 3.9, 1H, NCH_2CHCOO), 2.66 (t, *J*=6.3, 2H, NCH_2CH_2O), 2.85 (d, *J*=11.4, 1H, $NCH_{ax}H_{eq}CH_2CH_2$), 3.03 – 3.11 (m, 1H, $NCH_{ax}H_{eq}CHCOO$), 3.21-3.31 (m, 2H, NCH_2CH_2O), 3.80 (s, 6H, $C_{Ar}OCH_3$), 6.85 – 6.93 (m, 4H, $CCHCHCOCH_3$), 7.27 – 7.37 (m, 4H, $CCHCHCOCH_3$), 7.58 – 7.66 (m, 2H, $CCHCHCCCH_3$), 7.90 – 7.95 (m, 2H, $CCHCHCCCH_3$). ^{13}C NMR (101 MHz, MeOD + NaOD) δ = 25.98 ($NCH_2CH_2CH_2$), 29.33 ($NCH_2CH_2CH_2$), 46.38 (NCH_2CHCOO), 55.49 ($NCH_2CH_2CH_2$), 55.80 ($C_{Ar}OCH_3$), 58.80 (NCH_2CHCOO), 59.49 (NCH_2CH_2O), 62.51 (NCH_2CH_2O), 87.60 (NCH_2CH_2OC), 114.30 ($CCHCHCOCH_3$), 128.08 ($CCHCHCCCH_3$), 128.09 ($CCHCHCCCH_3$), 131.46 ($CCHCHCOCH_3$), 136.15 ($CCHCHCOCH_3$), 136.35 ($CCHCHCCCH_3$), 153.14 ($CCHCHCCCH_3$), 160.37 ($CCHCHCOCH_3$), 182.81 ($COOCH_2CH_3$), 200.68 (CCH_3). IR (KBr): ṽ = 2934, 2361, 2342, 1683, 1606, 1509, 1407, 1251, 1176, 1070, 1034, 828, 668, 605 cm^{-1}. HRMS-ESI+ *m/z* [*M*+H]$^+$ calcd for $C_{31}H_{35}NO_6$: 518.2534, found: 518.2537.

***rac*-1-(2-{[4-(N,N-dimethylsulfamoyl)phenyl]bis[4-ethoxyphenyl]methoxy}ethyl)piperidine-3-carboxylic acid (5c):** ^{1}H NMR (500 MHz, MeOD + NaOD) δ = 1.25 – 1.41 (m, 1H, $NCH_2CH_2CH_{ax}H_{eq}$), 1.55 (qt, *J*=13.0, 3.9, 1H, $NCH_2CH_{ax}H_{eq}CH_2$), 1.62 – 1.70 (m, 1H,

$NCH_2CH_{ax}H_{eq}CH_2$), 1.92 – 2.02 (m, 2H, $NCH_2CH_2CH_{ax}H_{eq}$ + $NCH_{ax}H_{eq}CH_2CH_2$), 2.08 (t, *J*=11.4, 1H, $NCH_{ax}H_{eq}CHCOO$), 2.35 (tt, *J*=11.8, 3.7, 1H, NCH_2CHCOO), 2.61 – 2.69 (m, 8H, NCH_2CH_2O + SO_2NCH_3), 2.79 – 2.85 (m, 1H, $NCH_{ax}H_{eq}CH_2CH_2$), 3.06 (dt, *J*=11.4, 1.8, 1H, $NCH_{ax}H_{eq}CHCOO$), 3.21 – 3.30 (m, 2H, NCH_2CH_2O), 3.79 (s, 6H, $C_{Ar}OCH_3$), 6.85 – 6.93 (m, 4H, $CCHCHCOCH_3$), 7.26 – 7.34 (m, 4H, $CCHCHCOCH_3$), 7.66 – 7.77 (m, 4H, CCHCHCS + CCHCHCS). ^{13}C NMR (126 MHz, MeOD + NaOD) δ = 25.99 ($NCH_2CH_2CH_2$), 29.33 ($NCH_2CH_2CH_2$), 38.30 (NSO_2CH_3), 46.38 (NCH_2CHCOO), 54.49 ($NCH_2CH_2CH_2$), 55.82 ($C_{Ar}OCH_3$), 58.80 (NCH_2CHCOO), 59.46 (NCH_2CH_2O), 62.56 (NCH_2CH_2O), 87.48 (NCH_2CH_2OC), 114.42 ($CCHCHCOCH_3$), 128.45 ($CCHCHCS$), 129.49 ($CCHCHCS$), 131.51($CCHCHCOCH_3$), 134.64 ($CCHCHCS$), 135.98 ($CCHCHCOCH_3$), 153.19 ($CCHCHCS$), 160.48 ($CCHCHCOCH_3$), 182.82 (*C*OO). IR (KBr): ṽ = 2934, 2361, 2341, 1607, 1578, 1508, 1460, 1411, 1342, 1251, 1165, 1033, 953, 829, 753, 693, 599, 586 cm^{-1}. HRMS-ESI+ *m/z* $[M+H]^+$ calcd for $C_{31}H_{38}N_2O_7S$: 583.2473, found: 583.2474.

***rac*-1-(2-{Imidazo[1,2-a]pyridin-6-ylbis(4-methoxyphenyl)methoxy}ethyl)piperidine-3-carboxylic acid (5d):** ^{1}H NMR (500 MHz, MeOD + NaOD) δ = 1.25 – 1.39 (m, 1H, $NCH_2CH_2CH_{ax}H_{eq}$), 1.56 (qt, *J*=13.0, 3.8, 1H, $NCH_2CH_{ax}H_{eq}CH_2$), 1.64 – 1.70 (m, 1H, $NCH_2CH_{ax}H_{eq}CH_2$), 1.93 – 2.03 (m, 2H, $NCH_2CH_2CH_{ax}H_{eq}$ + $NCH_{ax}H_{eq}CH_2CH_2$), 2.10 (t, *J*=11.4, 1H, $NCH_{ax}H_{eq}CHCOO$), 2.37 (tt, *J*=11.9, 3.7, 1H, NCH_2CHCOO), 2.62 – 2.72 (m, 2H, NCH_2CH_2O), 2.82 (br d, *J*=11.3, 1H, $NCH_{ax}H_{eq}CH_2CH_2$), 3.09 – 3.15 (m, 1H, $NCH_{ax}H_{eq}CHCOO$), 3.32 – 3.36 (m, 2H, NCH_2CH_2O), 3.79 (s, 6H, $C_{Ar}OCH_3$), 6.88 – 6.94 (m, 4H, $CCHCHCOCH_3$), 7.13 (dd, *J*=9.6, 1.8, 1H, CCHCHCN), 7.33 – 7.40 (m, 5H, $CCHCHCOCH_3$ + CCHCHCN), 7.52 (d, *J*=1.4, 1H, CCHNCHCHN), 7.86 (dd, *J*=1.4, 0.7, 1H, CCHNCHCHN), 8.69 (dd, *J*=1.9, 1.0, 1H, CCHNCHCHN). ^{13}C NMR (126 MHz, MeOD + NaOD) δ = 25.97 ($NCH_2CH_2CH_2$), 29.34 ($NCH_2CH_2CH_2$), 46.34 (NCH_2CHCOO), 55.46 ($NCH_2CH_2CH_2$), 55.83 ($C_{Ar}OCH_3$), 58.79 (NCH_2CHCOO), 59.47 (NCH_2CH_2O), 62.46 (NCH_2CH_2O), 86.23 (NCH_2CH_2OC), 114.51 ($CCHCHCOCH_3$), 115.23 (CCHNCHCHN), 116.24 (CCHCHCN), 126.20 (CCHNCHCHN), 128.27 (CCHCHCN), 130.43 ($CCHCHCOCH_3$), 133.17 (CCHNCHCHN), 133.49 (CCHNCHCHN), 135.38 ($CCHCHCOCH_3$), 145.38 (CCHCHCN), 160.58 ($CCHCHCOCH_3$), 182.82 (*C*OO). IR (KBr): ṽ = 2936, 1608, 1578, 1508, 1458, 1397, 1315, 1251, 1177, 1131, 1085, 1031, 925, 829, 732, 676, 621, 586 cm^{-1}. HRMS-ESI- *m/z* $[M-H]^-$ calcd for $C_{30}H_{33}O_5N_3$: 514.2347, found: 514.2352.

***rac*-1-{2-[(4-Carboxyphenyl)bis(4-methoxyphenyl)methoxy]ethyl}piperidine-3-carboxylic acid (5e):** ^{1}H NMR (500 MHz, D_2O + NaOD) δ = 0.88 – 1.02 (m, 1H, $NCH_2CH_2CH_{ax}H_{eq}$), 1.05 – 1.17 (m, 1H, $NCH_2CH_{ax}H_{eq}CH_2$), 1.18 – 1.27 (m, 1H, $NCH_2CH_{ax}H_{eq}CH_2$), 1.41 (t, *J*=11.3, 1H, $NCH_{ax}H_{eq}CH_2CH_2$), 1.63 (br d, *J*=11.7, 1H, $NCH_2CH_2CH_{ax}H_{eq}$), 1.75 (t, *J*=11.5, 1H, $NCH_{ax}H_{eq}CHCOO$), 1.99 – 2.20 (m, 2H, NCH_2CHCOO + $NCH_{ax}H_{eq}CH_2CH_2$), 2.25 – 2.37 (m, 2H, NCH_2CH_2O), 2.68 (br d, *J*=10.7, 1H, $NCH_{ax}H_{eq}CHCOO$), 2.95 (br s, 2H, NCH_2CH_2O), 3.30 (s, 6H, $C_{Ar}OCH_3$), 6.38 – 6.52 (m, 4H, $CCHCHCOCH_3$), 7.02 (br d, *J*=8.4, 4H, $CCHCHCOCH_3$), 7.21 (br d, *J*=8.1, 2H, CCHCHCCOO), 7.61 (br d, *J*=8.1, 2H, CCHCHCCOO). ^{13}C NMR (126 MHz, D_2O + NaOD) δ = 23.89 ($NCH_2CH_2CH_2$), 27.40 ($NCH_2CH_2CH_2$), 44.34 (NCH_2CHCOO), 52.53 ($NCH_2CH_2CH_2$), 54.73 (d, $C_{Ar}OCH_3$), 56.76 (NCH_2CHCOO), 57.19 (NCH_2CH_2O), 60.37 (NCH_2CH_2O), 86.19 (NCH_2CH_2OC), 113.00 ($CCHCHCOCH_3$), 127.65 (CCHCHCCOO), 128.66 (CCHCHCCOO), 129.65 (d, $CCHCHCOCH_3$), 134.88 (CCHCHCCOO), 135.60 (d, $CCHCHCOCH_3$), 147.10 (CCHCHCCOO), 157.89 ($CCHCHCOCH_3$), 174.28 ($C_{Ar}COO$), 182.68 (CHCOO). IR (KBr): ṽ = 2935, 1718, 1607, 1543, 1509, 1396, 1301, 1251, 1176, 1089, 1034, 828, 796 cm^{-1}. HRMS-ESI+ *m/z* $[M+H]^+$ calcd for $C_{30}H_{33}NO_7$: 520.2330, found: 520.2331.

***rac*-1-(2-{[4-(Methoxymethyl)phenyl]bis[4-methoxyphenyl]methoxy}ethyl)piperidine-3-carboxylic acid (5f):** ^{1}H NMR (400 MHz, MeOD + NaOD) δ = 1.25 – 1.40 (m, 1H, $NCH_2CH_2CH_{ax}H_{eq}$), 1.53 (qt, *J*=13.2, 3.9, 1H, $NCH_2CH_{ax}H_{eq}CH_2$), 1.61 – 1.68 (m, 1H, $NCH_2CH_{ax}H_{eq}CH_2$), 1.89-2.02 (m, 2H, $NCH_2CH_2CH_{ax}H_{eq}$ + $NCH_{ax}H_{eq}CH_2CH_2$), 2.07 (t, *J*=11.4, 1H, $NCH_{ax}H_{eq}CHCOO$), 2.34 (tt, *J*=11.8, 3.7, 1H, NCH_2CHCOO), 2.63 (t, *J*=6.4, 2H, NCH_2CH_2O), 2.83 (br d, *J*=11.4, 1H, $NCH_{ax}H_{eq}CH_2CH_2$), 3.01 – 3.08 (m, 1H, $NCH_{ax}H_{eq}CHCOO$), 3.20 – 3.30 (m, 2H, NCH_2CH_2O), 3.35 (s, 3H, CH_2OCH_3), 3.77 (s, 6H, $C_{Ar}OCH_3$), 4.42 (s, 2H, CH_2OCH_3), 6.79 – 6.88 (m, 4H, $CCHCHCOCH_3$), 7.23 – 7.33 (m, 6H, $CCHCHCOCH_3$ + $CCHCHCCH_2OCH_3$), 7.38 – 7.45 (m, 2H, $CCHCHCCH_2OCH_3$). ^{13}C NMR (101 MHz, MeOD + NaOD) δ = 25.95 ($NCH_2CH_2CH_2$), 29.32 ($NCH_2CH_2CH_2$), 46.35 (NCH_2CHCOO), 55.47 ($NCH_2CH_2CH_2$), 55.77 ($C_{Ar}OCH_3$), 58.35 (CH_2OCH_3), 58.82 (NCH_2CHCOO), 59.56 (NCH_2CH_2O), 62.38 (NCH_2CH_2O), 75.35 (CH_2OCH_3), 87.55 (NCH_2CH_2OC), 114.11 ($CCHCHCOCH_3$), 128.40 ($CCHCHCCH_2OCH_3$), 129.32 ($CCHCHCCH_2OCH_3$), 131.22 ($CCHCHCOCH_3$), 137.44 ($CCHCHCOCH_3$), 137.80 ($CCHCHCCH_2OCH_3$), 146.32 ($CCHCHCCH_2OCH_3$), 160.10 ($CCHCHCOCH_3$), 182.82 (*C*OO). IR (KBr): ṽ = 2933, 1608, 1508, 1457, 1405, 1302, 1250, 1176, 1153, 1091, 1033, 916, 826, 582 cm^{-1}. HRMS-ESI- *m/z* [*M*-H]$^{-}$ calcd for $C_{31}H_{37}NO_6$: 518.2548, found: 518.2556.

***rac*-1-{2-[(4-Cyanophenyl)bis(4-methoxyphenyl)methoxy]ethyl}piperidine-3-carboxylic acid (5g):** ^{1}H NMR (500 MHz, MeOD + NaOD) δ = 1.24 – 1.40 (m, 1H, $NCH_2CH_2CH_{ax}H_{eq}$), 1.55 (qt, *J*=12.9, 3.8, 1H, $NCH_2CH_{ax}H_{eq}CH_2$), 1.62 – 1.70 (m, 1H, $NCH_2CH_{ax}H_{eq}CH_2$), 1.97 (td, *J*=11.9, 3.0, 2H, $NCH_2CH_2CH_{ax}H_{eq}$ + $NCH_{ax}H_{eq}CH_2CH_2$), 2.08 (t, *J*=11.4, 1H, $NCH_{ax}H_{eq}CHCOO$), 2.35 (tt, *J*=11.8, 3.8, 1H, NCH_2CHCOO), 2.64 (t, *J*=6.2, 2H, NCH_2CH_2O), 2.81 (d, *J*=11.1, 1H, $NCH_{ax}H_{eq}CH_2CH_2$), 3.01 – 3.09 (m, 1H, $NCH_{ax}H_{eq}CHCOO$), 3.19 – 3.29 (m, 2H, NCH_2CH_2O), 3.79 (s, 6H, $C_{Ar}OCH_3$), 6.83 – 6.96 (m, 4H, $CCHCHCOCH_3$), 7.23 – 7.36 (m, 4H, $CCHCHCOCH_3$), 7.61 – 7.71 (m, 4H, $CCHCHCCN$ + $CCHCHCCN$). ^{13}C NMR (126 MHz, MeOD + NaOD) δ = 25.98 ($NCH_2CH_2CH_2$), 29.33 ($NCH_2CH_2CH_2$), 46.39 (NCH_2CHCOO), 55.49 ($NCH_2CH_2CH_2$), 55.79 ($C_{Ar}OCH_3$), 58.78 (NCH_2CHCOO), 59.42 (NCH_2CH_2O), 62.54 (NCH_2CH_2O), 87.45 (NCH_2CH_2OC), 111.14 ($CCHCHCCN$), 114.42 ($CCHCHCOCH_3$), 119.83 ($C_{Ar}CN$), 129.62 ($CCHCHCCN$), 131.37 ($CCHCHCOCH_3$), 132.79 ($CCHCHCCN$), 135.75 ($CCHCHCOCH_3$), 153.50 ($CCHCHCCN$), 160.52 ($CCHCHCOCH_3$), 182.79 (*C*OO). IR (KBr): ṽ = 2928, 2362, 2343, 1718, 1608, 1508 1458, 1395, 1300, 1251, 1176, 1032, 826, 668 cm^{-1}. HRMS-ESI+ *m/z* [*M*+H]$^{+}$ calcd for $C_{30}H_{32}N_2O_5$: 501.2384, found: 501.2386.

***rac*-1-(2-{Bis[4-(methoxymethyl)phenyl][4-methoxyphenyl]methoxy}ethyl)piperidine-3-carboxylic acid (5h):** ^{1}H NMR (500 MHz, MeOD + NaOD) δ = 1.25 – 1.40 (m, 1H, $NCH_2CH_2CH_{ax}H_{eq}$), 1.53 (qt, *J*=13.2, 4.0, 1H, $NCH_2CH_{ax}H_{eq}CH_2$), 1.65 (dt, *J*=13.4, 2.6, 1H, $NCH_2CH_{ax}H_{eq}CH_2$), 1.89-2.02 (m, 2H, $NCH_2CH_2CH_{ax}H_{eq}$ + $NCH_{ax}H_{eq}CH_2CH_2$), 2.07 (t, *J*=11.4, 1H, $NCH_{ax}H_{eq}CHCOO$), 2.34 (tt, *J*=11.8, 3.7, 1H, NCH_2CHCOO), 2.59 – 2.68 (m, 2H, NCH_2CH_2O), 2.82 (br d, *J*=11.4, 1H, $NCH_{ax}H_{eq}CH_2CH_2$), 2.99 – 3.07 (m, 1H, $NCH_{ax}H_{eq}CHCOO$), 3.19 – 3.30 (m, 2H, NCH_2CH_2O), 3.35 (s, 6H, CH_2OCH_3), 3.78 (s, 3H, $C_{Ar}OCH_3$), 4.43 (s, 4H, CH_2OCH_3), 6.83 – 6.89 (m, 2H, $CCHCHCOCH_3$), 7.25 – 7.31 (m, 6H, $CCHCHCOCH_3$ + $CCHCHCCH_2OCH_3$), 7.39 – 7.44 (m, 4H, $CCHCHCCH_2OCH_3$). ^{13}C NMR (126 MHz, MeOD + NaOD) δ = 25.95 ($NCH_2CH_2CH_2$), 29.31 ($NCH_2CH_2CH_2$), 46.34 (NCH_2CHCOO), 55.45 ($NCH_2CH_2CH_2$), 55.82 ($C_{Ar}OCH_3$), 58.38 (CH_2OCH_3), 58.83 (NCH_2CHCOO), 59.52 (NCH_2CH_2O), 62.49 (NCH_2CH_2O), 75.31 (CH_2OCH_3), 87.74 (NCH_2CH_2OC), 114.17 ($CCHCHCOCH_3$), 128.44 ($CCHCHCCH_2OCH_3$), 129.56 ($CCHCHCCH_2OCH_3$), 131.55 ($CCHCHCOCH_3$), 136.76 ($CCHCHCOCH_3$), 138.06 ($CCHCHCCH_2OCH_3$), 145.66 ($CCHCHCCH_2OCH_3$), 160.26 ($CCHCHCOCH_3$), 182.85 (*C*OO). IR (KBr): ṽ = 2930, 1609, 1508, 1458,

1405, 1296, 1250, 1176, 1036, 827 cm^{-1}. HRMS-ESI+ *m/z* $[M+H]^+$ calcd for $C_{32}H_{39}NO_6$: 534.2850, found: 534.2848.

***rac*-1-(2-{Tris[4-(methoxymethyl)phenyl]methoxy}ethyl)piperidine-3-carboxylic acid (5i):** ^1H NMR (500 MHz, MeOD + NaOD) δ = 1.24 – 1.37 (m, 1H, $NCH_2CH_2CH_{ax}H_{eq}$), 1.53 (qt, *J*=13.0, 3.8, 1H, $NCH_2CH_{ax}H_{eq}CH_2$), 1.61 – 1.70 (m, 1H, $NCH_2CH_{ax}H_{eq}CH_2$), 1.89-2.01 (m, 2H, $NCH_2CH_2CH_{ax}H_{eq}$ + $NCH_{ax}H_{eq}CH_2CH_2$), 2.07 (t, *J*=11.4, 1H, $NCH_{ax}H_{eq}CHCOO$), 2.34 (tt, *J*=11.8, 3.7, 1H, NCH_2CHCOO), 2.59 – 2.71 (m, 2H, NCH_2CH_2O), 2.82 (br d, *J*=11.4, 1H, $NCH_{ax}H_{eq}CH_2CH_2$), 3.00 - 3.06 (m, 1H, $NCH_{ax}H_{eq}CHCOO$), 3.21 – 3.30 (m, 2H, NCH_2CH_2O), 3.36 (s, 9H, CH_2OCH_3), 4.44 (s, 6H, CH_2OCH_3), 7.24 – 7.32 (m, 6H, $CCHCHCCH_2OCH_3$), 7.38 – 7.46 (m, 6H, $CCHCHCCH_2OCH_3$). ^{13}C NMR (126 MHz, MeOD + NaOD) δ = 25.96 ($NCH_2CH_2CH_2$), 29.32 ($NCH_2CH_2CH_2$), 46.36 (NCH_2CHCOO), 55.44 ($NCH_2CH_2CH_2$), 58.40 (CH_2OCH_3), 58.86 (NCH_2CHCOO), 59.49 (NCH_2CH_2O), 62.65 (NCH_2CH_2O), 75.27 (CH_2OCH_3), 87.91 (NCH_2CH_2OC), 128.45 ($CCHCHCCH_2OCH_3$), 129.84 ($CCHCHCCH_2OCH_3$), 138.35 ($CCHCHCCH_2OCH_3$), 144.99 ($CCHCHCCH_2OCH_3$), 182.81 (*C*OO). IR (KBr): ṽ = 2930, 2361, 2343, 1609, 1508, 1405, 1296, 1250, 1036, 827, 575 cm^{-1}. HRMS-ESI+ *m/z* $[M+H]^+$ calcd for $C_{33}H_{41}NO_6$: 548.3007, found: 548.3001.

***rac*-1-{2-[(4-Carbamoylphenyl)bis(4-methoxyphenyl)methoxy]ethyl}piperidine-3-carboxylic acid (5j):** ^1H NMR (500 MHz, MeOD + NaOD) δ = 1.26 – 1.42 (m, 1H, $NCH_2CH_2CH_{ax}H_{eq}$), 1.57 (qt, *J*=12.9, 3.8, 1H, $NCH_2CH_{ax}H_{eq}CH_2$), 1.64 – 1.72 (m, 1H, $NCH_2CH_{ax}H_{eq}CH_2$), 1.94 – 2.04 (m, 2H, $NCH_2CH_2CH_{ax}H_{eq}$ + $NCH_{ax}H_{eq}CH_2CH_2$), 2.10 (t, *J*=11.4, 1H, $NCH_{ax}H_{eq}CHCOO$), 2.38 (tt, *J*=12.0, 3.7, 1H, NCH_2CHCOO), 2.66 (t, *J*=6.3, 2H, NCH_2CH_2O), 2.85 (d, *J*=11.4, 1H, $NCH_{ax}H_{eq}CH_2CH_2$), 3.06 – 3.12 (m, 1H, $NCH_{ax}H_{eq}CHCOO$), 3.24 – 3.31 (m, 2H, NCH_2CH_2O), 3.80 (s, 6H, $C_{Ar}OCH_3$), 6.85 – 6.94 (m, 4H, $CCHCHCOCH_3$), 7.28 – 7.37 (m, 4H, $CCHCHCOCH_3$), 7.55 – 7.62 (m, 2H, $CCHCHCNH_2$), 7.78 – 7.85 (m, 2H, m, 2H, $CCHCHCNH_2$). ^{13}C NMR (126 MHz, MeOD + NaOD) δ = 25.99 ($NCH_2CH_2CH_2$), 29.34 ($NCH_2CH_2CH_2$), 46.42 (NCH_2CHCOO), 55.52 ($NCH_2CH_2CH_2$), 55.76 ($C_{Ar}OCH_3$), 58.80 (NCH_2CHCOO), 59.51 (NCH_2CH_2O), 62.50 (NCH_2CH_2O), 87.53 (NCH_2CH_2OC), 114.24 ($CCHCHCOCH_3$), 128.20 ($CCHCHCC(O)NH_2$), 129.02 ($CCHCHCCNH_2$), 131.40 ($CCHCHCOCH_3$), 133.11 ($CCHCHCCNH_2$), 136.63 ($CCHCHCOCH_3$), 151.35 ($CCHCHCCNH_2$), 160.32 ($CCHCHCOCH_3$), 172.21 (CNH_2), 182.77 (*C*OO). IR (KBr): ṽ = 2934, 2360, 1670, 1609, 1567, 1508, 1464, 1409, 1302, 1250, 1175, 1070, 1034, 829, 770, 583 cm^{-1}. HRMS-ESI- *m/z* $[M-H]^-$ calcd for $C_{30}H_{34}N_2O_6$: 517.2344, found: 517.2350.

***rac*-1-{2-[Carboxybis(4-methoxyphenyl)methoxy]ethyl}piperidine-3-carboxylic acid (5k):** ^1H NMR (500 MHz, D_2O + NaOD) δ = 0.95 – 1.05 (m, 1H, $NCH_2CH_2CH_{ax}H_{eq}$), 1.17 – 1.30 (m, 1H, $NCH_2CH_{ax}H_{eq}CH_2$), 1.38 – 1.52 (m, 2H, $NCH_2CH_{ax}H_{eq}CH_2$ + $NCH_{ax}H_{eq}CH_2CH_2$), 1.61 (t, *J*=11.4, 1H, $NCH_{ax}H_{eq}CHCOO$), 1.69 (br d, *J*=9.9, 1H, $NCH_2CH_2CH_{ax}H_{eq}$), 2.08 (tt, *J*=12.0, 4.5, 2H, NCH_2CHCOO + NCH_2CH_2O), 2.17 (dt, *J*=11.9, 5.7, 1H, NCH_2CH_2O), 2.38 (br d, *J*=11.1, 1H, $NCH_{ax}H_{eq}CH_2CH_2$), 2.56 – 2.66 (m, 1H, $NCH_{ax}H_{eq}CHCOO$), 2.85 (t, *J*=5.7, 2H, NCH_2CH_2O), 3.58 (d, *J*=7.2, 6H, $C_{Ar}OCH_3$), 6.67 – 6.75 (m, 4H, $CCHCHCOCH_3$), 7.12 (dq, *J*=8.5, 3.2, 4H, $CCHCHCOCH_3$). ^{13}C NMR (101 MHz, CH_2Cl_2) δ = 22.50 ($NCH_2CH_2CH_2$), 26.87 ($NCH_2CH_2CH_2$), 40.84 (d, *J*=12.7, NCH_2CHCOO), 53.54 ($NCH_2CH_2CH_2$), 55.70 ($C_{Ar}OCH_3$), 56.38 (NCH_2CHCOO), 58.10 (NCH_2CH_2O), 61.08 (NCH_2CH_2O), 90.11 (NCH_2CH_2OC), 112.70 (d, *J*=1.4, $CCHCHCOCH_3$), 132.19 ($CCHCHCOCH_3$), 133.91 (d, *J*=7.2, $CCHCHCOCH_3$), 158.91 ($CCHCHCOCH_3$), 176.67 (COO). IR (KBr): ṽ = 2956, 1588, 1508, 1252, 1176, 1030, 829, 810, 780, 601, 567 cm^{-1}. HRMS-ESI- *m/z* $[M-H]^-$ calcd for $C_{24}H_{29}O_7N$: 443.1871, found: 442.1878.

***rac*-1-[4-Hydroxy-4,4-bis(4-methoxyphenyl)butyl]piperidine-3-carboxylic acid (5l):** ^{1}H NMR (400 MHz, MeOD + NaOD) δ = 1.26 – 1.40 (m, 1H, $NCH_2CH_2CH_{ax}H_{eq}CH$), 1.47 – 1.69 (m, 4H, $NCH_2CH_{ax}H_{eq}CH_2CH$ + $NCH_2CH_2CH_2COH$ + $NCH_2CH_{ax}H_{eq}CH_2CH$), 1.80 (td, *J*=11.6, 3.2, 1H, $NCH_{ax}H_{eq}CH_2CH_2CH$), 1.89 – 2.02 (m, 2H, $NCH_2CH_2CH_{ax}H_{eq}CH$ + $NCH_{ax}H_{eq}CHCOO$), 2.24 – 2.43 (m, 5H, $NCH_2CH_2CH_2COH$ + $NCH_2CH_2CH_2COH$ + NCH_2CHCOO), 2.70 (br d, *J*=11.2, 1H, $NCH_{ax}H_{eq}CH_2CH_2CH$), 2.94 – 3.01 (m, 1H, $NCH_{ax}H_{eq}CHCOO$), 3.75 (d, *J*=3.5, 6H, $C_{Ar}OCH_3$), 6.78 – 6.86 (m, 4H, $CCHCHCOCH_3$), 7.25 – 7.33 (m, 4H, $CCHCHCOCH_3$). ^{13}C NMR (126 MHz, Methanol-d_4) δ = 22.59 ($NCH_2CH_2CH_2COH$), 25.91 ($NCH_2CH_2CH_2CH$), 29.54 ($NCH_2CH_2CH_2CH$), 42.58 ($NCH_2CH_2CH_2COH$), 46.21 (NCH_2CHCOO), 54.64 ($NCH_2CH_2CH_2CH$), 55.82 ($C_{Ar}OCH_3$), 58.12 (NCH_2CHCOO), 60.63 ($NCH_2CH_2CH_2COH$), 78.12 (*C*OH), 114.20 (d, $CCHCHCOCH_3$), 128.56 (d, $CCHCHCOCH_3$), 141.57 (d, $CCHCHCOCH_3$), 159.54 (d, $CCHCHCOCH_3$), 182.92 (*C*OO). IR (KBr): ṽ = 2937, 2834, 1608, 1582, 1508, 1463, 1403, 1301, 1247, 1175, 1092, 1033, 829, 781, 668, 635, 592, 574 cm^{-1}. HRMS-ESI- *m/z* [*M*-H]$^-$ calcd for $C_{24}H_{31}NO_5$: 412.2129, found: 412.2137.

***rac*-1-(2-{[4-(Hydroxymethyl)phenyl]bis[4-methoxyphenyl]methoxy}ethyl)piperidine-3-carboxylic acid (5m):** ^{1}H NMR (500 MHz, MeOD + NaOD) δ = 1.32 (td, *J*=12.7, 4.1, 1H, $NCH_2CH_2CH_{ax}H_{eq}$), 1.54 (qt, *J*=13.0, 3.9, 1H, $NCH_2CH_{ax}H_{eq}CH_2$), 1.64 (dt, *J*=13.4, 3.4, 1H, $NCH_2CH_{ax}H_{eq}CH_2$), 1.93 – 2.00 (m, 2H, $NCH_2CH_2CH_{ax}H_{eq}$ + $NCH_{ax}H_{eq}CH_2CH_2$), 2.07 (t, *J*=11.4, 1H, $NCH_{ax}H_{eq}CHCOO$), 2.34 (tt, *J*=11.9, 3.8, 1H, NCH_2CHCOO), 2.63 (t, *J*=6.4, 2H, NCH_2CH_2O), 2.83 (br d, *J*=11.4, 1H, $NCH_{ax}H_{eq}CH_2CH_2$), 3.00 – 3.08 (m, 1H, $NCH_{ax}H_{eq}CHCOO$), 3.26 (qt, *J*=9.5, 6.5, 2H, NCH_2CH_2O), 3.77 (s, 6H, $C_{Ar}OCH_3$), 4.57 (s, 2H, CH_2OH), 6.80 – 6.87 (m, 4H, $CCHCHCOCH_3$), 7.24 – 7.33 (m, 6H, $CCHCHCOCH_3$ + $CCHCHCCH_2OH$), 7.38 – 7.44 (m, 2H, $CCHCHCCH_2OH$). ^{13}C NMR (126 MHz, MeOD + NaOD) δ = 25.94 ($NCH_2CH_2CH_2$), 29.31 ($NCH_2CH_2CH_2$), 46.35 (NCH_2CHCOO), 55.45 ($NCH_2CH_2CH_2$), 55.73 ($C_{Ar}OCH_3$), 58.78 (NCH_2CHCOO), 59.55 (NCH_2CH_2O), 62.32 (NCH_2CH_2O), 64.90 (CH_2OH), 87.54 (NCH_2CH_2OC), 114.04 ($CCHCHCOCH_3$), 127.48 ($CCHCHCCH_2OH$), 129.32 ($CCHCHCCH_2OH$), 131.18 ($CCHCHCOCH_3$), 137.57 ($CCHCHCOCH_3$), 141.26 ($CCHCHCCH_2OH$), 145.61 ($CCHCHCCH_2OH$), 160.05 ($CCHCHCOCH_3$), 182.77 (*C*OO). IR (KBr): ṽ = 3332, 2935, 2836, 1733, 1607, 1581, 1508, 1463, 1441, 1411, 1301, 1250, 1176, 1153, 1115, 1068, 1034, 916, 828, 735, 701 cm^{-1}. HRMS-ESI- *m/z* [*M*-H]$^-$ calcd for $C_{30}H_{35}NO_6$: 504.2392, found: 504.2396.

***rac*-1-{2-[(4-{[(Carboxymethyl)amino]methyl}phenyl)bis(4-methoxyphenyl)methoxy]-ethyl}piperidine-3-carboxylic acid (5n):** ^{1}H NMR (400 MHz, MeOD + NaOD) δ = 1.23 – 1.39 (m, 1H, $NCH_2CH_2CH_{ax}H_{eq}$), 1.46 – 1.61 (m, 1H, $NCH_2CH_{ax}H_{eq}CH_2$), 1.61 – 1.69 (m, 1H, $NCH_2CH_{ax}H_{eq}CH_2$), 1.91 – 2.02 (m, 2H, $NCH_2CH_2CH_{ax}H_{eq}$ + $NCH_{ax}H_{eq}CH_2CH_2$), 2.07 (t, *J*=11.4, 1H, $NCH_{ax}H_{eq}CHCOO$), 2.35 (tt, *J*=11.8, 3.8, 1H, NCH_2CHCOO), 2.63 (td, *J*=6.5, 2.5, 2H, NCH_2CH_2O), 2.83 (br d, *J*=11.3, 1H, $NCH_{ax}H_{eq}CH_2CH_2$), 3.01 – 3.08 (m, 1H, $NCH_{ax}H_{eq}CHCOO$), 3.15 (s, 2H, CH_2NHCH_2COO), 3.19 – 3.30 (m, 2H, NCH_2CH_2O), 3.70 (s, 2H, CH_2NHCH_2COO), 3.77 (s, 6H, $C_{Ar}OCH_3$), 6.81 – 6.87 (m, 4H, $CCHCHCOCH_3$), 7.26 – 7.32 (m, 6H, $CCHCHCOCH_3$ + $CCHCHCCH_2NH$), 7.37 – 7.42 (m, 2H, $CCHCHCCH_2NH$). ^{13}C NMR (101 MHz, MeOD + NaOD) δ = 25.97 ($NCH_2CH_2CH_2$), 29.35 ($NCH_2CH_2CH_2$), 46.38 (NCH_2CHCOO), 53.43 (CH_2NHCH_2COO), 53.87 (CH_2NHCH_2COO), 55.46 ($NCH_2CH_2CH_2$), 55.71 ($C_{Ar}OCH_3$), 58.89 (NCH_2CHCOO), 59.59 (NCH_2CH_2O), 62.38 (NCH_2CH_2O), 87.52 (NCH_2CH_2OC), 114.05 ($CCHCHCOCH_3$), 128.95 ($CCHCHCCH_2NH$), 129.34 ($CCHCHCCH_2NH$), 131.25 (d, $CCHCHCOCH_3$), 137.49 (d, $CCHCHCOCH_3$), 139.06 ($CCHCHCCH_2NH$), 145.73 ($CCHCHCCH_2NH$), 160.11 ($CCHCHCOCH_3$), 178.84 ($NHCH_2COO$), 182.74 (NCH_2CHCOO). IR (KBr): ṽ = 2933, 1607, 1581, 1508, 1411, 1301, 1250, 1176, 1070, 1035, 827, 582 cm^{-1}. HRMS-ESI- *m/z* [*M*-H]$^-$ calcd for $C_{32}H_{38}N_2O_7$: 561.2606, found: 561.2599.

***rac*-1-{2-[(4-{[(2-Carboxyethyl)amino]methyl}phenyl)bis(4-methoxyphenyl)methoxy]-ethyl}piperidine-3-carboxylic acid (5o):** ^{1}H NMR (500 MHz, MeOD + NaOD) δ = 1.24 – 1.37 (m, 1H, $NCH_2CH_2CH_{ax}H_{eq}$), 1.53 (qt, *J*=12.8, 3.8, 1H, $NCH_2CH_{ax}H_{eq}CH_2$), 1.61 – 1.68 (m, 1H, $NCH_2CH_{ax}H_{eq}CH_2$), 1.88 – 2.00 (m, 2H, $NCH_2CH_2CH_{ax}H_{eq}$ + $NCH_{ax}H_{eq}CH_2CH_2$), 2.07 (t, *J*=11.4, 1H, $NCH_{ax}H_{eq}CHCOO$), 2.33 (ddt, *J*=11.9, 7.5, 3.7, 1H, NCH_2CHCOO), 2.39 (t, *J*=6.8, 2H, $NHCH_2CH_2COO$), 2.57 – 2.67 (m, 2H, NCH_2CH_2O), 2.76 – 2.86 (m, 3H $NCH_{ax}H_{eq}CH_2CH_2$ + $NHCH_2CH_2COO$), 2.99 – 3.07 (m, 1H, $NCH_{ax}H_{eq}CHCOO$), 3.19 – 3.30 (m, 2H, NCH_2CH_2O), 3.72 (s, 2H, $C_{Ar}CH_2NH$), 3.77 (s, 6H, $C_{Ar}OCH_3$), 6.81 – 6.86 (m, 4H, $CCHCHCOCH_3$), 7.25 – 7.31 (m, 6H, $CCHCHCOCH_3$ + $CCHCHCCH_2NH$), 7.36 – 7.40 (m, 2H, $CCHCHCCH_2NH$). ^{13}C NMR (101 MHz, MeOD + NaOD) δ = 25.94 ($NCH_2CH_2CH_2$), 29.30 ($NCH_2CH_2CH_2$), 38.19 ($NHCH_2CH_2COO$), 46.32 (NCH_2CHCOO), 47.10 ($NHCH_2CH_2COO$), 54.02 (CH_2NHCH_2COO), 55.45 ($NCH_2CH_2CH_2$), 55.82 ($C_{Ar}OCH_3$), 58.82 (NCH_2CHCOO), 59.57 (NCH_2CH_2O), 62.35 (NCH_2CH_2O), 87.55 (NCH_2CH_2OC), 114.08 ($CCHCHCOCH_3$), 128.92 ($CCHCHCCH_2NH$), 129.36 ($CCHCHCCH_2NH$), 131.22 ($CCHCHCOCH_3$), 137.51 (d, $CCHCHCOCH_3$), 139.19 ($CCHCHCCH_2NH$), 145.54 ($CCHCHCCH_2NH$), 160.07 ($CCHCHCOCH_3$), 181.09 ($NHCH_2COO$), 182.89 (NCH_2CHCOO). IR (KBr): ṽ = 2936, 1560, 1508, 1406, 1302, 1250, 11176, 1068, 1035, 826, 583 cm^{-1}. HRMS-ESI+ *m/z* $[M+H]^+$ calcd for $C_{33}H_{40}N_2O_7$: 577.2908, found: 577.2909.

***rac*-1-{2-[(4-{[(1-Carboxycyclopropyl)amino]methyl}phenyl)bis(4-methoxyphenyl)-methoxy]ethyl}piperidine-3-carboxylic acid (5p):** ^{1}H NMR (400 MHz, MeOD + NaOD) δ = 0.80 (q, *J*=3.8, 2H, $NHCCH_{ax}$), 1.11 (q, *J*=3.8, 2H, , $NHCCH_{eq}$), 1.25 – 1.39 (m, 1H, $NCH_2CH_2CH_{ax}H_{eq}$), 1.46 – 1.71 (m, 2H, $NCH_2CH_{ax}H_{eq}CH_2$ + $NCH_2CH_{ax}H_{eq}CH_2$), 1.89 – 2.01 (m, 2H, $NCH_2CH_2CH_{ax}H_{eq}$ + $NCH_{ax}H_{eq}CH_2CH_2$), 2.07 (t, *J*=11.3, 1H, $NCH_{ax}H_{eq}CHCOO$), 2.34 (tt, *J*=11.7, 3.5, 1H, NCH_2CHCOO), 2.58 – 2.67 (m, 2H, NCH_2CH_2O), 2.83 (br d, *J*=11.4, 1H, $NCH_{ax}H_{eq}CH_2CH_2$), 2.99 – 3.07 (m, 1H, $NCH_{ax}H_{eq}CHCOO$), 3.20 – 3.29 (m, 2H, NCH_2CH_2O), 3.77 (s, 6H, $C_{Ar}OCH_3$), 3.78 (s, 2H, $C_{Ar}CH_2NH$), 6.81 – 6.87 (m, 4H, $CCHCHCOCH_3$), 7.25 – 7.33 (m, 6H, $CCHCHCOCH_3$ + $CCHCHCCH_2NH$), 7.35 – 7.39 (m, 2H, $CCHCHCCH_2NH$). ^{13}C NMR (101 MHz, MeOD + NaOD) δ = 15.41 ($NHCCH_2$), 25.94 ($NCH_2CH_2CH_2$), 29.31 ($NCH_2CH_2CH_2$), 43.73 (NHC), 46.33 (NCH_2CHCOO), 52.57 ($C_{Ar}CH_2NH$), 55.43 ($NCH_2CH_2CH_2$), 55.81 ($C_{Ar}OCH_3$), 58.84 (NCH_2CHCOO), 59.57 (NCH_2CH_2O), 62.35 (NCH_2CH_2O), 87.57 (NCH_2CH_2OC), 114.07 ($CCHCHCOCH_3$), 129.14 ($CCHCHCCH_2NH$), 129.33 ($CCHCHCCH_2NH$), 131.22 ($CCHCHCOCH_3$), 137.56 ($CCHCHCOCH_3$), 139.79 ($CCHCHCCH_2NH$), 145.41 ($CCHCHCCH_2NH$), 160.06 ($CCHCHCOCH_3$), 182.03 ($CHCOO$), 182.87 ($C(CH_2)_2COO$). IR (KBr): ṽ = 2933, 1608. 1557, 1508, 1442, 1406, 1338, 1301, 1250, 1175, 1034, 916, 827, 582, 518 cm^{-1}. HRMS-ESI- *m/z* $[M-H]^-$ calcd for $C_{34}H_{40}N_2O_7$: 587.2763, found: 587.2773.

***rac*-1-{2-[(4-{[(2-Carboxypropan-2-yl)amino]methyl}phenyl)bis(4-methoxyphenyl)-methoxy]ethyl}piperidine-3-carboxylic acid (5q):** ^{1}H NMR (500 MHz, MeOD + NaOD) δ = 1.26 – 1.36 (m, 7H, CCH_3 + $NCH_2CH_2CH_{ax}H_{eq}$), 1.53 (qt, *J*=13.0, 3.9, 1H, $NCH_2CH_{ax}H_{eq}CH_2$), 1.60 – 1.68 (m, 1H, $NCH_2CH_{ax}H_{eq}CH_2$), 1.90 – 2.00 (m, 2H, $NCH_2CH_2CH_{ax}H_{eq}$ + $NCH_{ax}H_{eq}CH_2CH_2$), 2.07 (t, *J*=11.4, 1H, $NCH_{ax}H_{eq}CHCOO$), 2.34 (tt, *J*=11.9, 3.7, 1H, , NCH_2CHCOO), 2.57 – 2.68 (m, 2H, NCH_2CH_2O), 2.83 (br d, *J*=11.4, 1H, $NCH_{ax}H_{eq}CH_2CH_2$), 3.00 – 3.06 (m, 1H, $NCH_{ax}H_{eq}CHCOO$), 3.20 – 3.29 (m, 2H, NCH_2CH_2O), 3.57 (s, 2H, $C_{Ar}CH_2NH$), 3.77 (s, 6H, $C_{Ar}OCH_3$), 6.77 – 6.93 (m, 4H, $CCHCHCOCH_3$), 7.26 – 7.33 (m, 6H, $CCHCHCOCH_3$ + $CCHCHCCH_2NH$), 7.36 – 7.41 (m, 2H, $CCHCHCCH_2NH$). ^{13}C NMR (126 MHz, MeOD + NaOD) δ = 25.89 ($NHCCH_3$), 25.91 ($NCH_2CH_2CH_2$), 29.27 ($NCH_2CH_2CH_2$), 46.29 (NCH_2CHCOO), 49.27 ($C_{Ar}CH_2NH$), 55.40 ($NCH_2CH_2CH_2$), 55.79 ($C_{Ar}OCH_3$), 58.81 (NCH_2CHCOO), 59.54 (NCH_2CH_2O), 61.74 ($NHC(CH_3)_2$), 62.32 (NCH_2CH_2O),

87.53 (NCH_2CH_2OC), 114.05 ($CCHCHCOCH_3$), 129.13 ($CCHCHCCH_2NH$), 129.35 ($CCHCHCCH_2NH$), 131.20 ($CCHCHCOCH_3$), 137.48 ($CCHCHCOCH_3$), 160.04 ($CCHCHCOCH_3$), 182.85 ($CHCOO$), 184.22 ($C(CH_3)_2COO$). IR (KBr): $\tilde{\nu}$ = 2932, 1608, 1578, 1508, 1464, 1403, 1302, 1250, 1174, 1116, 1069, 1033, 916, 827, 583, 519 cm^{-1}. HRMS-ESI- *m/z* $[M-H]^-$ calcd for $C_{34}H_{42}N_2O_7$: 589.2919, found: 589.2926.

***rac*-1-[2-(Bis{4-methoxyphenyl}{4-[(2-oxopyrrolidin-1-yl)methyl]phenyl}methoxy)ethyl]-piperidine-3-carboxylic acid (5r):** ^1H NMR (400 MHz, MeOD + NaOD) δ = 1.25 – 1.40 (m, 1H, $NCH_2CH_2CH_{ax}H_{eq}CH$), 1.46 – 1.60 (m, 1H, $NCH_2CH_{ax}H_{eq}CH_2CH$), 1.60 – 1.69 (m, 1H, $NCH_2CH_{ax}H_{eq}CH_2CH$), 1.88 – 2.17 (m, 5H, $NCH_2CH_2CH_{ax}H_{eq}CH$ + $NCH_{ax}H_{eq}CHCOO$ + $NCH_{ax}H_{eq}CH_2CH_2CH$ + $NCH_2CH_2CH_2CO$), 2.28 – 2.38 (m, 1H, NCH_2CHCOO), 2.42 (t, *J*=8.1, 2H, $NCH_2CH_2CH_2CO$), 2.61 (t, *J*=6.4, 2H, NCH_2CH_2O), 2.81 (br d, *J*=12.5, 1H, $NCH_{ax}H_{eq}CH_2CH_2CH$), 2.98 – 3.05 (m, 1H, $NCH_{ax}H_{eq}CHCOO$), 3.18 – 3.29 (m, 2H, NCH_2CH_2O), 3.32 – 3.35 (m, 2H, $NCH_2CH_2CH_2CO$), 3.77 (s, 6H, $C_{Ar}OCH_3$), 4.42 (s, 2H, $C_{Ar}CH_2N$), 6.80 – 6.87 (m, 4H, $CCHCHCOCH_3$), 7.14 – 7.20 (m, 2H, $CCHCHCCH_2N$), 7.24 – 7.31 (m, 4H, $CCHCHCOCH_3$), 7.38 – 7.43 (m, 2H, $CCHCHCCH_2N$). ^{13}C NMR (101 MHz, MeOD + NaOD) δ = 18.69 ($NCH_2CH_2CH_2CO$), 25.94 ($NCH_2CH_2CH_2CH$), 29.29 ($NCH_2CH_2CH_2CH$), 31.96 ($NCH_2CH_2CH_2CO$), 46.30 (NCH_2CHCOO), 47.06 ($C_{Ar}CH_2N$), 48.31 ($NCH_2CH_2CH_2CO$), 55.46 ($NCH_2CH_2CH_2$), 55.86 ($C_{Ar}OCH_3$), 58.80 (NCH_2CHCOO), 59.54 (NCH_2CH_2O), 62.37 (NCH_2CH_2O), 87.50 (NCH_2CH_2OC), 114.16 ($CCHCHCOCH_3$), 128.43 ($CCHCHCCH_2NH$), 129.60 ($CCHCHCCH_2NH$), 131.22 ($CCHCHCOCH_3$), 136.12 ($CCHCHCCH_2NH$), 137.33 ($CCHCHCOCH_3$), 146.29 ($CCHCHCCH_2NH$), 160.10 ($CCHCHCOCH_3$), 177.68 (NCO), 182.91 (COO). IR (KBr): $\tilde{\nu}$ = 2933, 1670, 1608, 1581, 1508, 1463, 1410, 1300, 1249, 1175, 1115, 1069, 1032, 915, 828, 667, 635, 582, 515 cm^{-1}. HRMS-ESI+ *m/z* $[M+H]^+$ calcd for $C_{34}H_{40}NO_6$: 573.2959, found: 573.2957.

***rac*-1-{2-[(4-{[(3-Carboxypropyl)amino]methyl}phenyl)bis(4-methoxyphenyl)methoxy]-ethyl}piperidine-3-carboxylic acid (5s):** ^1H NMR (400 MHz, MeOD + NaOD) δ = 1.24 – 1.38 (m, 1H, $NCH_2CH_2CH_{ax}H_{eq}$), 1.46 – 1.60 (m, 1H, $NCH_2CH_{ax}H_{eq}CH_2$), 1.60 – 1.70 (m, 1H, $NCH_2CH_{ax}H_{eq}CH_2$), 1.70 – 1.85 (m, 2H, $NHCH_2CH_2CH_2COO$), 1.89 – 2.01 (m, 2H, $NCH_2CH_2CH_{ax}H_{eq}$ + $NCH_{ax}H_{eq}CH_2CH_2$), 2.07 (t, *J*=11.3, 1H, $NCH_{ax}H_{eq}CHCOO$), 2.14 – 2.21 (m, 2H, $NHCH_2CH_2CH_2COO$), 2.34 (tt, *J*=11.7, 3.7, 1H, NCH_2CHCOO), 2.57 – 2.67 (m, 4H, $NHCH_2CH_2CH_2COO$ + NCH_2CH_2O), 2.83 (br d, *J*=11.3, 1H, $NCH_{ax}H_{eq}CH_2CH_2$), 2.99 – 3.07 (m, 1H, $NCH_{ax}H_{eq}CHCOO$), 3.20 – 3.29 (m, 2H, NCH_2CH_2O), 3.70 (s, 2H, $C_{Ar}CH_2NH$), 3.77 (s, 6H, $C_{Ar}OCH_3$), 6.81 – 6.88 (m, 4H, $CCHCHCOCH_3$), 7.24 – 7.33 (m, 6H, $CCHCHCOCH_3$ + $CCHCHCCH_2NH$), 7.36 – 7.41 (m, 2H, $CCHCHCCH_2NH$). ^{13}C NMR (101 MHz, MeOD + NaOD) δ = 25.94 ($NCH_2CH_2CH_2$), 27.33 ($NHCH_2CH_2CH_2COOH$), 29.31 ($NCH_2CH_2CH_2$), 36.94 ($NHCH_2CH_2CH_2COOH$), 46.32 (NCH_2CHCOO), 50.14 ($NHCH_2CH_2CH_2COOH$), 54.05 ($C_{Ar}CH_2NH$), 55.44 ($NCH_2CH_2CH_2$), 55.81 ($C_{Ar}OCH_3$), 58.83 (NCH_2CHCOO), 59.58 (NCH_2CH_2O), 62.35 (NCH_2CH_2O), 87.55 (NCH_2CH_2OC), 114.09 ($CCHCHCOCH_3$), 128.93 (d, $CCHCHCCH_2NH$), 129.35 ($CCHCHCCH_2NH$), 131.23 ($CCHCHCOCH_3$), 137.52 ($CCHCHCCH_2NH$), 139.23 ($CCHCHCOCH_3$), 145.52 ($CCHCHCCH_2NH$), 160.07 ($CCHCHCOCH_3$), 182.53 (CH_2COO), 182.87 ($CHCOO$). IR (KBr): $\tilde{\nu}$ = 2926, 1628, 1508, 1458, 1250, 1175, 1033, 701, 470 cm^{-1}. HRMS-ESI- *m/z* $[M-H]^-$ calcd for $C_{36}H_{42}N_2O_7$: 589.2919, found: 589.2917.

***rac*-1-{2-[(4-{[(4-Carboxyphenyl)amino]methyl}phenyl)bis(4-methoxyphenyl)methoxy]-ethyl}piperidine-3-carboxylic acid (5t):** ^1H NMR (500 MHz, D_2O + NaOD) δ = 1.19 – 1.34 (m, 1H, $NCH_2CH_2CH_{ax}H_{eq}$), 1.34 – 1.47 (m, 1H, $NCH_2CH_{ax}H_{eq}CH_2$), 1.52 – 1.61 (m, 1H, $NCH_2CH_{ax}H_{eq}CH_2$), 1.80 – 1.88 (m, 1H, $NCH_{ax}H_{eq}CH_2CH_2$), 1.88 – 1.99 (m, 1H, $NCH_2CH_2CH_{ax}H_{eq}$),

2.07-2.23 (m, 1H, NC*H*$_{ax}$H$_{eq}$CHCOO), 2.27 – 2.38 (m, 1H, NCH$_2$C*H*COO), 2.50 – 2.70 (m, 3H, NCH$_{ax}$*H*$_{eq}$CH$_2$CH$_2$ + NC*H*$_2$CH$_2$O), 2.88 (br d, *J*=11.1, 1H, NCH$_{ax}$*H*$_{eq}$CHCOO), 3.15 – 3.27 (m, 2H, NCH$_2$C*H*$_2$O), 3.58 (s, 6H, C$_{Ar}$OCH$_3$), 4.11 (s, 2H, C$_{Ar}$C*H*$_2$NH), 6.52 (br d, *J*=8.7, 2H, NHCC*H*CHCCOO), 6.67 (br d, *J*=8.3, 4H, CCHC*H*COCH$_3$), 7.09 (br d, *J*=8.0, 2H, CCHC*H*CCCH$_2$NH), 7.22 (br dd, *J*=22.2, 8.2, 6H, CCHC*H*COCH$_3$ + CC*H*CHCCCH$_2$NH), 7.58 – 7.67 (m, 2H, NHCCHC*H*CCOO). ^{13}C NMR (126 MHz, D$_2$O + NaOD) δ = 24.49 (NCH$_2$*C*H$_2$CH$_2$), 27.89 (NCH$_2$CH$_2$*C*H$_2$), 44.94 (NCH$_2$*C*HCOO), 46.88 (C$_{Ar}$*C*H$_2$NH), 53.02 (N*C*H$_2$CH$_2$CH$_2$), 55.21 (C$_{Ar}$O*C*H$_3$), 57.33 (N*C*H$_2$CHCOO), 57.80 (N*C*H$_2$CH$_2$O), 60.93 (NCH$_2$*C*H$_2$O), 86.68 (NCH$_2$CH$_2$O*C*), 112.31 (NHC*C*HCHCCOO), 113.49 (CCH*C*HCOCH$_3$), 125.08 (CCHCH*C*COO), 127.43 (CCH*C*HCCCH$_2$NH), 128.71 (C*C*HCHCCCH$_2$NH), 130.13 (C*C*HCHCOCH$_3$), 131.46 (NHC*C*HCHCCOO), 143.67 (*C*CHCHCCH$_2$NH), 136.56 (d, *C*CHCHCOCH$_3$), 138.18 (CCHCH*C*CH$_2$NH), 150.90 (NH*C*CHCHCCOO), 158.30 (CCHCH*C*OCH$_3$), 175.58 (C$_{Ar}$*C*OO) 183.20 (CH*C*OO). IR (KBr): ṽ = 2934, 1606, 1508, 1464, 1385, 1332, 1302, 1250, 1177, 1084, 1032, 917, 827, 788, 703, 583 cm^{-1}. HRMS-ESI- *m/z* [*M*-H]$^-$ calcd for C$_{37}$H$_{40}$N$_2$O$_7$: 623.2763, found: 623.2764.

[4-(Dimethoxymethyl)phenyl]bis(4-methoxyphenyl)methanol (8a): ^{1}H NMR (500 MHz, CD$_2$Cl$_2$) δ = 2.81 (s, 1H, COH), 3.30 (s, 6H, CHOC*H*$_3$), 3.78 (s, 6H, C$_{Ar}$OC*H*$_3$), 5.34 (s, 1H, C*H*OCH$_3$), 6.78 – 6.88 (m, 4H, CCHC*H*COCH$_3$), 7.11 – 7.20 (m, 4H, CC*H*CHCOCH$_3$), 7.22 – 7.29 (m, 2H, CC*H*CHCCHO), 7.32 – 7.40 (m, 2H, CCHC*H*CCHO). ^{13}C NMR (126 MHz, CD$_2$Cl$_2$) δ = 53.13 (CHO*C*H$_3$), 55.61 (C$_{Ar}$O*C*H$_3$), 81.51 (COH), 103.56 (CCHCHC*C*HO), 113.47 (CCH*C*HCOCH$_3$), 126.53 (C*C*HCHCCHO), 127.89 (CCH*C*HCCHO), 129.41 (C*C*HCHCOCH$_3$), 137.61 (CCHCH*C*CHO), 139.81 (*C*CHCHCOCH$_3$), 148.02 (*C*CHCHCCHO), 159.14 (CCHCH*C*OCH$_3$). IR (KBr): ṽ = 3448, 2935, 2833, 1608, 1508, 1436, 1353, 1299, 1250, 1214, 1176, 1101, 1035, 984, 907, 828, 587 cm^{-1}. HRMS-ESI- *m/z* [*M*-H]$^-$ calcd for C$_{24}$H$_{26}$O$_5$: 393.1707, found: 393.1706.

Bis(4-methoxyphenyl)[4-(2-methyl-1,3-dioxan-2-yl)phenyl]methanol (8b): ^{1}H NMR (500 MHz, CD$_2$Cl$_2$) δ = 1.21 – 1.28 (m, 1H, COCH$_2$C*H*$_{ax}$H$_{eq}$CH$_2$), 1.44 (s, 3H, CCH$_3$), 1.97 – 2.09 (m, 1H, COCH$_2$CH$_{ax}$*H*$_{eq}$CH$_2$), 2.79 (s, 1H, OH), 3.72 – 3.85 (m, 10H, COC*H*$_2$CH$_2$CH$_2$ + COCH$_2$CH$_2$C*H*$_2$ + C$_{Ar}$OCH$_3$), 6.82 – 6.86 (m, 4H, CCHC*H*COCH$_3$), 7.16 – 7.20 (m, 4H, CC*H*CHCOCH$_3$), 7.26 – 7.30 (m, 2H, CC*H*CHCCCH$_3$), 7.33 – 7.37 (m, 2H, CCHC*H*CCCH$_3$). ^{13}C NMR (126 MHz, CD$_2$Cl$_2$) δ = 26.10 (COCH$_2$*C*H$_2$), 32.61 (C*C*H$_3$), 55.79 (C$_{Ar}$O*C*H$_3$), 61.72 (CO*C*H$_2$CH$_2$), 81.76 (COH), 100.81 (*C*CH$_3$), 113.64 (CCH*C*HCOCH$_3$), 126.89 (CCH*C*HCCCH$_3$), 128.53 (C*C*HCHCCCH$_3$), 129.56 (C*C*HCHCOCH$_3$), 140.06 (*C*CHCHCOCH$_3$), 140.89 (CCHCHC*C*CH$_3$), 147.28 (*C*CHCHCCCH$_3$), 159.32 (CCHCH*C*OCH$_3$). IR (KBr): ṽ = 3463, 2958, 1608, 1509, 1463, 1370, 1298, 1249, 1189, 1145, 1081, 1034, 969, 940, 897, 860, 829, 606, 585 cm^{-1}. HRMS-ESI- *m/z* [*M*-H]$^-$ calcd for C$_{26}$H$_{28}$O$_5$: 419.1864, found: 419.1875.

4-[Hydroxybis(4-methoxyphenyl)methyl]-N,N-dimethylbenzenesulfonamide (8c): ^{1}H NMR (400 MHz, THF-*d*$_8$) δ = 2.62 (s, 6H, NSO$_2$CH$_3$), 3.74 (s, 6H, C$_{Ar}$OCH$_3$), 6.75 – 6.84 (m, 4H, CCHC*H*COCH$_3$), 7.10 – 7.18 (m, 4H, CC*H*CHCOCH$_3$), 7.48 – 7.56 (m, 2H, CCHC*H*CS), 7.61 – 7.68 (m, 2H, CC*H*CHCS). ^{13}C NMR (101 MHz, THF-*d*$_8$) δ = 37.04 (NSO$_2$CH$_3$), 54.37 (C$_{Ar}$O*C*H$_3$), 80.09 (COH), 112.70 (CCH*C*HCOCH$_3$), 126.92 (C*C*HCHCS), 128.22 (CCH*C*HCS), 129.02 (C*C*HCHCOCH$_3$), 134.18 (CCHCH*C*S), 139.66 (*C*CHCHCOCH$_3$), 153.42 (*C*CHCHCS), 158.81 (CCHCH*C*OCH$_3$). IR (KBr): ṽ = 3514, 2961, 2834, 1608, 1580, 1508, 1463, 1397, 1329, 1297, 1255, 1171, 1090, 1032, 951, 913, 837, 800, 754, 737, 720, 695, 638, 619, 596, 585, 520, 508, 492 cm^{-1}. HRMS-ESI+ *m/z* [*M*+H]$^+$ calcd for C$_{23}$H$_{25}$NO$_5$S: 428.1526, found: 428.1529.

Imidazo[1,2-a]pyridin-6-ylbis(4-methoxyphenyl)methanol (8d): ^{1}H NMR (500 MHz, CD_2Cl_2) δ = 3.79 (s, 6H, $C_{Ar}OC\mathit{H}_3$), 3.91 (s, 1H, OH), 6.58 (td, *J*=6.9, 1.2, 1H, CCHNC*H*CHN), 6.79 (s, 1H, CC*H*NCHCHN), 6.83 – 6.88 (m, 4H, CCHC*H*COCH$_3$), 7.09 (ddd, *J*=9.1, 6.7, 1.3, 1H, CC*H*CHCN), 7.18 – 7.24 (m, 4H, CC*H*CHCOCH$_3$), 7.41 (dt, *J*=9.1, 1.2, 1H, CCHC*H*CN), 8.04 (dt, *J*=7.0, 1.2, 1H, CCHNCHC*H*N). ^{13}C NMR (126 MHz, CD_2Cl_2) δ = 55.80 ($C_{Ar}OC\mathit{H}_3$), 77.25 (COH), 111.97 (CCHN*C*HCHN), 114.06 (CCH*C*HCOCH$_3$), 117.86 (CCH*C*HCN), 125.03 (C*C*HCHCN), 127.58 (CCHNC*H*CHN), 128.46 (C*C*HCHCOCH$_3$), 129.16 (*C*CHNCHCHN), 135.33 (C*C*HNCHCHN), 136.91 (*C*CHCHCOCH$_3$), 147.42 (CCHCH*C*N), 159.69 (CCHCH*C*OCH$_3$). HRMS-EI+ *m/z* [*M*]$^+$ calcd for $C_{22}H_{20}N_2O_3$ 360.1468, found: 360.1472.

Ethyl 4-[hydroxybis(4-methoxyphenyl)methyl]benzoate (8e): ^{1}H NMR (500 MHz, CD_2Cl_2) δ = 1.36 (t, *J*=7.1, 3H, COOCH$_2$CH_3), 2.91 (s, 1H, CO*H*), 3.78 (s, 6H, $C_{Ar}OCH_3$), 4.33 (q, *J*=7.1, 2H, COOCH_2CH$_3$), 6.79 – 6.88 (m, 4H, CCHC*H*COCH$_3$), 7.11 – 7.18 (m, 2H, CC*H*CHCOCH$_3$), 7.36 – 7.42 (m, 2H, CC*H*CHCCOO), 7.91 – 7.97 (m, 2H, CCHC*H*CCOO). ^{13}C NMR (126 MHz, CD_2Cl_2) δ = 14.51 (COOCH$_2$*C*H$_3$), 55.64 ($C_{Ar}OC\mathit{H}_3$), 61.32 (COO*C*H$_2$CH$_3$), 81.55 (COH), 113.63 (CCH*C*HCOCH$_3$), 128.06 (C*C*HCHCCOO), 129.32 (CCH*C*HCCOO), 129.45 (C*C*HCHCOCH$_3$), 129.67 (CCHCH*C*COO), 139.29 (*C*CHCHCOCH$_3$), 152.67 (*C*CHCHCCOO), 159.31 (CCHCH*C*OCH$_3$), 166.62 (*C*OOCH$_2$CH$_3$). IR (KBr): ṽ = 3475, 2835, 2361, 2342, 1716, 1608, 1509, 1277, 1250, 1176, 1104, 1032, 828, 765 cm^{-1}. HRMS-EI+ *m/z* [*M*]$^+$ calcd for $C_{24}H_{24}O_5$: 392.1624, found: 392.1655.

[4-(Methoxymethyl)phenyl]bis(4-methoxyphenyl)methanol (8f): ^{1}H NMR (500 MHz, CD_2Cl_2) δ = 2.78 (s, 1H, OH), 3.36 (s, 3H, CH$_2$OCH_3), 3.78 (s, 6H, $C_{Ar}OC\mathit{H}_3$), 4.42 (s, 2H, CH_2OCH$_3$), 6.80 – 6.85 (m, 4H, CCHC*H*COCH$_3$), 7.13 – 7.18 (m, 4H, CC*H*CHCOCH$_3$), 7.22 – 7.28 (m, 4H, CC*H*CHCCH$_2$OCH$_3$ + CCHC*H*CCH$_2$OCH$_3$). ^{13}C NMR (126 MHz, CD_2Cl_2) δ = 55.63 ($C_{Ar}OC\mathit{H}_3$), 58.41 (CH$_2$O*C*H$_3$), 74.61 (*C*H$_2$OCH$_3$), 81.54 (COH), 113.48 (CCH*C*HCOCH$_3$), 127.52 (CCH*C*HCCH$_2$OCH$_3$), 128.08 (C*C*HCHCCH$_2$OCH$_3$), 129.43 (C*C*HCHCOCH$_3$), 137.79 (CCHCH*C*CH$_2$OCH$_3$), 139.90 (*C*CHCHCOCH$_3$), 147.24 (*C*CHCHCCH$_2$OCH$_3$), 159.15 (CCHCH*C*OCH$_3$). IR (KBr): ṽ = 3437, 2342, 1608, 1508, 1299, 1250, 1176, 1033, 828, 585 cm^{-1}. HRMS+ESI- *m/z* [*M*-H]$^-$ calcd for $C_{23}H_{24}O_4$: 363.1602, found: 363.1605.

4-[Hydroxybis(4-methoxyphenyl)methyl]benzonitrile (8g): ^{1}H NMR (500 MHz, CD_2Cl_2) δ = 2.86 (s, 1H, OH), 3.78 (s, 6H, $C_{Ar}OC\mathit{H}_3$), 6.81 – 6.88 (m, 4H, CCHC*H*COCH$_3$), 7.10 – 7.16 (m, 4H, CC*H*CHCOCH$_3$), 7.43 – 7.47 (m, 2H, CC*H*CHCCN), 7.57 – 7.63 (m, 2H, CCHC*H*CCN). ^{13}C NMR (126 MHz, CD_2Cl_2) δ = 55.42 ($C_{Ar}OC\mathit{H}_3$), 81.45 (COH), 111.20 (CCHCH*C*CN), 113.79 (CCH*C*HCOCH$_3$), 119.20 (CCHCHC*C*N), 128.79 (CCH*C*HCCN), 129.43 (CCH*C*HCOCH$_3$), 132.09 (CCH*C*HCCN), 138.74 (*C*CHCHCOCH$_3$), 152.93 (*C*CHCHCCN), 159.49 (CCHCH*C*OCH$_3$). IR (KBr): ṽ = 3461, 2835, 2227, 1607, 1582, 1509, 1462, 1298, 1250, 1175, 1152, 1114, 1032, 905, 828, 732, 619 cm^{-1}. HRMS+ESI- *m/z* [*M*-H]$^-$ calcd for $C_{22}H_{19}NO_3$: 344.1292, found: 344.1295.

Bis[4-(methoxymethyl)phenyl](4-methoxyphenyl)methanol (8h): ^{1}H NMR (500 MHz, CD_2Cl_2) δ = 2.82 (s, 1H, OH), 3.36 (s, 6H, CH$_2$OCH_3), 3.78 (s, 3H, $C_{Ar}OC\mathit{H}_3$), 4.42 (s, 4H, CH_2OCH$_3$), 6.80 – 6.85 (m, 2H, CCHC*H*COCH$_3$), 7.13 – 7.18 (m, 2H, CC*H*CHCOCH$_3$), 7.22 – 7.28 (m, 8H, CC*H*CHCCH$_2$OCH$_3$ + CCHC*H*CCH$_2$OCH$_3$). ^{13}C NMR (126 MHz, CD_2Cl_2) δ = 55.64 ($C_{Ar}OC\mathit{H}_3$), 58.43 (CH$_2$O*C*H$_3$), 74.60 (*C*H$_2$OCH$_3$), 81.73 (COH), 113.54 (CCH*C*HCOCH$_3$), 127.56 (CCH*C*HCCH$_2$OCH$_3$), 128.14 (C*C*HCHCCH$_2$OCH$_3$), 129.51 (C*C*HCHCOCH$_3$), 137.93 (CCHCH*C*CH$_2$OCH$_3$), 139.63 (*C*CHCHCOCH$_3$), 146.95 (*C*CHCHCCH$_2$OCH$_3$), 159.23 (CCHCH*C*OCH$_3$). IR (KBr): ṽ = 3447, 2929, 2834, 1608, 1508, 1299, 1250, 1179, 1033, 828, 581 cm^{-1}. HRMS-EI+ *m/z* [*M*]$^+$ calcd for $C_{24}H_{26}O_4$: 378.1831, found: 378.1825.

Tris[4-(methoxymethyl)phenyl]methanol (8i): ^{1}H NMR (400 MHz, CD_2Cl_2) δ = 2.86 (s, 1H, OH), 3.36 (s, 9H, $CH_2OC\mathit{H_3}$), 4.42 (s, 6H, $C\mathit{H_2}OCH_3$), 7.19 – 7.31 (m, 12H, $CC\mathit{H}CHCCH_2OCH_3$ + $CCHC\mathit{H}CCH_2OCH_3$). ^{13}C NMR (101 MHz, CD_2Cl_2) δ = 58.56 ($C_{Ar}O\mathit{C}H_3$), 74.73 ($\mathit{C}H_2OCH_3$), 82.05 (COH), 127.75 ($CCH\mathit{C}HCCH_2OCH_3$), 128.37 ($C\mathit{C}HCHCCH_2OCH_3$), 138.14 ($CCHCH\mathit{C}CH_2OCH_3$), 146.87 ($\mathit{C}CHCHCCH_2OCH_3$). IR (KBr): ṽ = 2929, 2834, 1717, 1700, 1654, 1608, 1582, 1508, 1458, 1412, 1379, 1300, 1250, 1212, 1179, 1155, 1096, 1033, 967, 907, 828, 730, 638, 581, 546 cm^{-1}. HRMS-EI+ *m/z* $[M]^+$ calcd for $C_{25}H_{28}O_4$: 392.1988, found: 392.1985.

4-[Hydroxybis(4-methoxyphenyl)methyl]benzamide (8j): ^{1}H NMR (400 MHz, tetrachloroethane-d_2, 80°C) δ = 2.74 (s, 1H, COH), 3.84 (s, 6H, $C_{Ar}OCH_3$), 5.75 (br s, 2H, CNH_2), 6.84 – 6.92 (m, 4H, $CCHC\mathit{H}COCH_3$), 7.17 – 7.24 (m, 4H, $CC\mathit{H}CHCOCH_3$), 7.42 – 7.49 (m, 2H, $CC\mathit{H}CHCCNH_2$), 7.73 – 7.79 (m, 2H, $CCHC\mathit{H}CCNH_2$). ^{13}C NMR (101 MHz, tetrachloroethane-d_2, 80°C) δ = 55.23 ($C_{Ar}O\mathit{C}H_3$), 81.11 (COH), 113.45 ($CCH\mathit{C}HCOCH_3$), 126.68 ($CCH\mathit{C}HCCNH_2$), 127.86 ($C\mathit{C}HCHCCNH_2$), 128.94 ($C\mathit{C}HCHCOCH_3$), 131.95 ($CCHCH\mathit{C}CNH_2$), 138.79 ($\mathit{C}CHCHCOCH_3$), 151.25 ($C\mathit{C}HCHCCNH_2$), 158.80 ($CCHCH\mathit{C}OCH_3$), 168.56 ($\mathit{C}ONH_2$). IR (KBr): ṽ = 3451, 3197, 2360, 1650, 1610, 1566, 1509, 1408, 1388, 1296, 1251, 1177, 1030, 916, 831, 774 cm^{-1}. HRMS-EI+ *m/z* $[M]^+$ calcd for $C_{17}H_{18}O_5$: 363.1471, found: 363.1468.

Methyl 2-hydroxy-2,2-bis(4-methoxyphenyl)acetate (8k): ^{1}H NMR (500 MHz, $CDCl_3$) δ = 3.81 (s, 6H, $C_{Ar}OC\mathit{H_3}$), 3.84 (s, 3H, $COOC\mathit{H_3}$), 4.08 (s, 1H, OH), 6.82 – 6.92 (m, 4H, $CCHC\mathit{H}COCH_3$), 7.30 – 7.37 (m, 4H, $CC\mathit{H}CHCOCH_3$). ^{13}C NMR (126 MHz, $CDCl_3$) δ = 53.48 ($COO\mathit{C}H_3$), 55.28 ($C_{Ar}O\mathit{C}H_3$), 80.46 ($\mathit{C}OH$), 113.42 ($CCH\mathit{C}HCOCH_3$), 128.61 ($C\mathit{C}HCHCOCH_3$), 134.29 ($C\mathit{C}HCHCOCH_3$), 159.29 ($CCHCH\mathit{C}OCH_3$), 175.38 ($\mathit{C}OOCH_3$). IR (KBr): ṽ = 3496, 2361, 1731, 1610, 1510, 1248, 1175, 1160, 1071, 1030, 839, 776 cm^{-1}. HRMS-EI+ *m/z* $[M]^+$ calcd for $C_{17}H_{18}O_5$: 302.1154, found: 302.1138.

4-Chloro-1,1-bis(4-methoxyphenyl)butan-1-ol (8l): ^{1}H NMR (400 MHz, CD_2Cl_2) δ = 1.91 (p, *J*=7.2, 2H, $ClCH_2C\mathit{H_2}CH_2$), 2.42 – 2.51 (m, 2H, $ClCH_2CH_2C\mathit{H_2}$), 3.75 (s, 6H, $C_{Ar}OC\mathit{H_3}$), 3.97 (t, *J*=7.1, 2H, $ClC\mathit{H_2}CH_2CH_2$), 6.77 – 6.86 (m, 4H, $CCHC\mathit{H}COCH_3$), 7.24 – 7.33 (m, 4H, $CC\mathit{H}CHCOCH_3$). ^{13}C NMR (101 MHz, CD_2Cl_2) δ = 26.04 ($ClCH_2\mathit{C}H_2CH_2$), 39.16 ($ClCH_2CH_2\mathit{C}H_2$), 55.73 ($C_{Ar}O\mathit{C}H_3$), 67.71 ($Cl\mathit{C}H_2CH_2CH_2$), 87.89 (COH), 113.84 ($CCH\mathit{C}HCOCH_3$), 127.44 ($C\mathit{C}HCHCOCH_3$), 139.60 ($\mathit{C}CHCHCOCH_3$), 158.86 ($CCHCH\mathit{C}OCH_3$). IR (KBr): ṽ = 3444, 2930, 2360, 1607, 1508, 1462, 1301, 1246, 1180, 1028, 988, 829, 740, 597, 574 cm^{-1}. HRMS-EI+ *m/z* $[M\text{-}HCl]^+$ calcd for $C_{18}H_{21}ClO_3$: 284.1407, found: 284.1407.

4-Bromo-N,N-dimethylbenzenesulfonamide (9c): ^{1}H NMR (400 MHz, CD_2Cl_2) δ = 2.68 (s, 6H, NSO_2CH_3), 7.58 – 7.65 (m, 2H, $CCHC\mathit{H}CS$), 7.69 – 7.76 (m, 2H, $CC\mathit{H}CHCS$). ^{13}C NMR (101 MHz, CD_2Cl_2) δ = 38.31 ($NSO_2\mathit{C}H_3$), 128.14 ($\mathit{C}CHCHCS$), 129.80 ($CCH\mathit{C}HCS$), 132.90 ($C\mathit{C}HCHCS$), 135.20 ($CCHCH\mathit{C}S$). IR (KBr): ṽ = 2963, 1574, 1458, 1389, 1343, 1262, 1163, 1085, 1067, 1007, 944, 821, 749, 707, 690, 595, 528, 469 cm^{-1}. HRMS-ESI+ *m/z* $[M+H]^+$ calcd for $C_8H_{10}BrNO_2S$: 263.9688, found: 263.9691.

1-{4-[Hydroxybis(4-methoxyphenyl)methyl]phenyl}ethan-1-one (11): ^{1}H NMR (400 MHz, CD_2Cl_2) δ = 2.56 (s, 3H, CCH_3), 2.84 (s, 1H, COH), 3.78 (s, 6H, $C_{Ar}OC\mathit{H_3}$), 6.81 – 6.88 (m, 4H, $CCHC\mathit{H}COCH_3$), 7.12 – 7.18 (m, 4H, $CC\mathit{H}CHCOCH_3$), 7.39 – 7.46 (m, 2H, $CC\mathit{H}CHCCCH_3$), 7.84 – 7.90 (m, 2H, $CCHC\mathit{H}CCCH_3$). ^{13}C NMR (101 MHz, CD_2Cl_2) δ = 27.05 ($C\mathit{C}H_3$), 55.81 ($C_{Ar}O\mathit{C}H_3$), 81.71 (COH), 113.82 ($CCH\mathit{C}HCOCH_3$), 128.35 ($CCH\mathit{C}HCCCH_3$), 128.36 ($C\mathit{C}HCHCCCH_3$), 129.59

(C*C*HCHCOCH$_3$), 136.45 (CCHCHC*C*CH$_3$), 139.37 (*C*CHCHCOCH$_3$), 152.99 (*C*CHCHCCCH$_3$), 159.52 (CCHCH*C*OCH$_3$), 198.04 (*C*CH$_3$). IR (KBr): $\tilde{\nu}$ = 3358, 2830, 1686, 1661, 1606, 1508, 1279, 1248, 1175, 1037, 908, 844, 824, 605, 582 cm^{-1}. HRMS-ESI- *m/z* [*M*-H]$^-$ calcd for $C_{23}H_{22}O_4$: 361.1445, found: 361.1447.

***rac*-Ethyl 1-{2-[(4-formylphenyl)bis(4-methoxyphenyl)methoxy]ethyl}piperidine-3-carboxylate (12a):** ^{1}H NMR (400 MHz, CD_2Cl_2) δ = 1.20 (t, *J*=7.1, 3H, COOCH$_2$C*H$_3$*), 1.34 – 1.47 (m, 1H, NCH$_2$CH$_2$C*H$_{ax}$*H$_{eq}$), 1.48 – 1.61 (m, 1H, NCH$_2$C*H$_{ax}$*H$_{eq}$CH$_2$), 1.64 – 1.74 (m, 1H, NCH$_2$CH$_2$CH$_{ax}$*H$_{eq}$*), 1.82 – 1.92 (m, 1H, NCH$_2$CH$_2$CH$_{ax}$*H$_{eq}$*), 2.05 (td, *J*=11.0, 3.1, 1H, NC*H$_{ax}$*H$_{eq}$CH$_2$CH$_2$), 2.20 (t, *J*=10.5, 1H, NC*H$_{ax}$*H$_{eq}$CHCOO), 2.52 (tt, *J*=10.5, 3.8, 1H, NCH$_2$C*H*COO), 2.56 – 2.62 (m, 2H, NC*H$_2$*CH$_2$O), 2.69 (dt, *J*=10.5, 4.1, 1H, NCH$_{ax}$*H$_{eq}$*CH$_2$CH$_2$), 2.96 (br dd, *J*=11.1, 3.6, 1H, NCH$_{ax}$*H$_{eq}$*CHCOO), 3.06 – 3.19 (m, 2H, NCH$_2$C*H$_2$*O), 3.78 (s, 6H, C$_{Ar}$OCH$_3$), 4.04 – 4.10 (m, 2H, COOC*H$_2$*CH$_3$), 6.80 – 6.89 (m, 4H, CCHC*H*COCH$_3$), 7.28 – 7.37 (m, 4H, CC*H*CHCOCH$_3$), 7.67 – 7.71 (m, 2H, CC*H*CHCCHO), 7.76 – 7.81 (m, 2H, CCHC*H*CCHO), 9.96 (s, 1H, CHO). ^{13}C NMR (101 MHz, CD_2Cl_2) δ = 14.59 (COOCH$_2$*C*H$_3$), 25.31 (NCH$_2$*C*H$_2$CH$_2$), 27.39 (NCH$_2$CH$_2$*C*H$_2$), 42.66 (NCH$_2$*C*HCOO), 54.84 (N*C*H$_2$CH$_2$CH$_2$), 55.77 (C$_{Ar}$O*C*H$_3$), 56.87 (N*C*H$_2$CHCOO), 58.97 (N*C*H$_2$CH$_2$O), 60.69 (COO*C*H$_2$CH$_3$), 62.50 (NCH$_2$*C*H$_2$O), 86.48 (N*C*H$_2$CH$_2$O*C*), 113.74 (CCH*C*HCOCH$_3$), 128.87 (C*C*HCHCCHO), 129.69 (CCH*C*HCCHO), 130.81 (C*C*HCHCOCH$_3$), 135.43 (*C*CHCHCCHO), 135.74 (*C*CHCHCOCH$_3$), 153.63 (CCHCH*C*CHO), 159.40 (CCHCH*C*OCH$_3$), 174.54 (COO), 192.31 (CHO). IR (KBr): $\tilde{\nu}$ = 2938, 2835, 1730, 1701, 1606, 1509, 1464, 1372, 1303, 1251, 1213, 1176, 1153, 1069, 1033, 823 cm^{-1}. HRMS-EI+ *m/z* [*M*]$^+$ calcd for $C_{32}H_{37}NO_6$: 531.2621, found: 531.2643.

(*S*)-Ethyl 1-{2-[(4-formylphenyl)bis(4-methoxyphenyl)methoxy]ethyl}piperidine-3-carboxylate [(*S*)-12a]: The analytical data are consistent with the racemic compound **12a**. $[\alpha]_D^{22}$ = -0.17 (c=2.26 g/100 ml in EtOH).

(*R*)-Ethyl 1-{2-[(4-formylphenyl)bis(4-methoxyphenyl)methoxy]ethyl}piperidine-3-carboxylate [(*R*)-12a]: The analytical data are consistent with the racemic compound **12a**. $[\alpha]_D^{22}$ = +0.15 (c=1.80 g/100 ml in EtOH).

***rac*-Ethyl 1-{2-[(4-acetylphenyl)bis(4-methoxyphenyl)methoxy]ethyl}piperidine-3-carboxylate (12b):** ^{1}H NMR (400 MHz, CD_2Cl_2) δ = 1.20 (t, *J*=7.1, 3H, COOCH$_2$C*H$_3$*), 1.35 – 1.47 (m, 1H, NCH$_2$CH$_2$C*H$_{ax}$*H$_{eq}$), 1.48 – 1.73 (m, 2H, NCH$_2$C*H$_{ax}$*H$_{eq}$CH$_2$ + NCH$_2$CH$_{ax}$*H$_{eq}$*CH$_2$), 1.82 – 1.93 (m, 1H, NCH$_2$CH$_2$CH$_{ax}$*H$_{eq}$*), 2.05 (td, *J*=10.9, 3.0, 1H, NC*H$_{ax}$*H$_{eq}$CH$_2$CH$_2$), 2.19 (t, *J*=10.6, 1H, NC*H$_{ax}$*H$_{eq}$CHCOO), 2.54 (s, 4H, NCH$_2$C*H*COO + CCH$_3$), 2.59 (t, *J*=5.8, 2H, NC*H$_2$*CH$_2$O), 2.66 – 2.74 (m, 1H, NCH$_{ax}$*H$_{eq}$*CH$_2$CH$_2$), 2.91-2.99 (m, 1H, NCH$_{ax}$*H$_{eq}$*CHCOO), 3.06 – 3.18 (m, 2H, NCH$_2$C*H$_2$*O), 3.78 (s, 6H, C$_{Ar}$OCH$_3$), 4.04 – 4.10 (m, 2H, COOC*H$_2$*CH$_3$), 6.80 – 6.88 (m, 4H, CCHC*H*COCH$_3$), 7.27 – 7.36 (m, 4H, CC*H*CHCOCH$_3$), 7.57 – 7.64 (m, 2H, CC*H*CHCCCH$_3$), 7.83 – 7.90 (m, 2H, CCHC*H*CCCH$_3$). ^{13}C NMR (101 MHz, CD_2Cl_2) δ = 14.43 (COOCH$_2$C*H$_3$*), 25.17 (NCH$_2$*C*H$_2$CH$_2$), 26.86 (C*C*H$_3$), 27.26 (NCH$_2$CH$_2$*C*H$_2$), 42.52 (NCH$_2$*C*HCOO), 54.69 (N*C*H$_2$CH$_2$CH$_2$), 55.62 (C$_{Ar}$O*C*H$_3$), 56.72 (N*C*H$_2$CHCOO), 58.83 (N*C*H$_2$CH$_2$O), 60.53 (COO*C*H$_2$CH$_3$), 62.33 (NCH$_2$*C*H$_2$O), 86.28 (NCH$_2$CH$_2$O*C*), 113.53 (CCH*C*HCOCH$_3$), 128.20 (CCH*C*HCC(O)CH$_3$), 128.33 (C*C*HCHCCCH$_3$), 130.60 (C*C*HCHCOCH$_3$), 135.87 (CCHCHC*C*CH$_3$ + *C*CHCHCOCH$_3$), 151.73 (*C*CHCHCCCH$_3$), 159.19 (CCHCH*C*OCH$_3$), 174.41 (COO), 197.84 (*C*CH$_3$). IR (KBr): $\tilde{\nu}$ = 2937, 2360, 1730, 1684, 1607, 1508, 1251, 1176, 1032, 827, 601 cm^{-1}. HRMS-ESI+ *m/z* [*M*+H]$^+$ calcd for $C_{33}H_{39}NO_6$: 546.2850, found: 546.2847.

***rac*-Ethyl 1-(2-{[4-(N,N-dimethylsulfamoyl)phenyl]bis[4-methoxyphenyl]methoxy}ethyl)-piperidine-3-carboxylate (12c):** ^{1}H NMR (500 MHz, CD_2Cl_2) δ = 1.20 (t, *J*=7.1, 3H, $COOCH_2CH_3$), 1.36 – 1.47 (m, 1H, $NCH_2CH_2CH_{ax}H_{eq}$), 1.48 – 1.61 (m, 1H, $NCH_2CH_{ax}H_{eq}CH_2$), 1.65 – 1.74 (m, 1H, $NCH_2CH_{ax}H_{eq}CH_2$), 1.82 – 1.96 (m, 1H, $NCH_2CH_2CH_{ax}H_{eq}$), 2.05 (td, *J*=11.0, 3.0, 1H, $NCH_{ax}H_{eq}CH_2CH_2$), 2.20 (t, *J*=10.5, 1H, $NCH_{ax}H_{eq}CHCOO$), 2.52 (tt, *J*=10.5, 3.8, 1H, NCH_2CHCOO), 2.56 – 2.62 (m, 2H, NCH_2CH_2O), 2.64 – 2.72 (m, 7H, SO_2NCH_3 + $NCH_{ax}H_{eq}CH_2CH_2$), 2.95 (dd, *J*=11.2, 3.6, 1H, $NCH_{ax}H_{eq}CHCOO$), 3.06 – 3.16 (m, 2H, NCH_2CH_2O), 3.79 (s, 6H, $C_{Ar}OCH_3$), 4.04 – 4.10 (m, 2H, $COOCH_2CH_3$), 6.80 – 6.96 (m, 4H, $CCHCHCOCH_3$), 7.26 – 7.37 (m, 4H, $CCHCHCOCH_3$), 7.61 – 7.74 (m, 4H, $CCHCHCS$ + $CCHCHCS$). ^{13}C NMR (125 MHz, CD_2Cl_2) δ = 14.44 ($COOCH_2CH_3$), 25.17 ($NCH_2CH_2CH_2$), 27.24 ($NCH_2CH_2CH_2$), 38.21 (NSO_2CH_3), 42.51 (NCH_2CHCOO), 54.69 ($NCH_2CH_2CH_2$), 55.64 ($C_{Ar}OCH_3$), 56.73 (NCH_2CHCOO), 58.82 (NCH_2CH_2O), 60.55 ($COOCH_2CH_3$), 62.36 (NCH_2CH_2O), 86.15 (NCH_2CH_2OC), 113.59 ($CCHCHCOCH_3$), 127.66 ($CCHCHCS$), 128.80 ($CCHCHCS$), 130.67 ($CCHCHCOCH_3$), 134.08 ($CCHCHCS$), 135.52 ($CCHCHCOCH_3$), 151.73 ($CCHCHCS$), 159.27 ($CCHCHCOCH_3$), 174.38 (COO). IR (KBr): ṽ = 2935, 2360, 2044, 1729, 1608, 1509, 1464, 1344, 1252, 1164, 1031, 951, 827, 752, 691, 584, 531 cm^{-1}. HRMS-ESI+ *m/z* $[M+H]^+$ calcd for $C_{33}H_{42}N_2O_7S$: 611.2786, found: 611.2786.

***rac*-Ethyl 1-(2-{imidazo[1,2-a]pyridin-6-ylbis(4-methoxyphenyl)methoxy}ethyl)piperidine-3-carboxylate (12d):** ^{1}H NMR (500 MHz, CD_2Cl_2) δ = 1.19 (t, *J*=7.1, 3H, $COOCH_2CH_3$), 1.37 – 1.49 (m, 1H, $NCH_2CH_2CH_{ax}H_{eq}$), 1.50 – 1.60 (m, 1H, $NCH_2CH_{ax}H_{eq}CH_2$), 1.66-1.74 (m, 1H, $NCH_2CH_{ax}H_{eq}CH_2$), 1.80 – 1.93 (m, 1H, $NCH_2CH_2CH_{ax}H_{eq}$), 2.07 (td, *J*=10.9, 3.0, 1H, $NCH_{ax}H_{eq}CH_2CH_2$), 2.20-2.30 (m, 1H, $NCH_{ax}H_{eq}CHCOO$), 2.53 (tt, *J*=10.4, 3.9, 1H, NCH_2CHCOO), 2.61 (td, *J*=5.7, 2.2, 2H, NCH_2CH_2O), 2.66 – 2.74 (m, 1H, $NCH_{ax}H_{eq}CH_2CH_2$), 2.99 (br dd, *J*=11.2, 3.6, 1H, $NCH_{ax}H_{eq}CHCOO$), 3.19 (qt, *J*=9.5, 5.7, 2H, NCH_2CH_2O), 3.79 (s, 6H, $C_{Ar}OCH_3$), 4.04 – 4.10 (m, 2H, $COOCH_2CH_3$), 6.83 – 6.89 (m, 4H, $CCHCHCOCH_3$), 7.03 (dd, *J*=9.5, 1.8, 1H, $CCHCHCN$), 7.32 – 7.42 (m, 5H, $CCHCHCOCH_3$ + $CCHCHCN$), 7.54 (d, *J*=1.2, 1H, $CCHNCHCHN$), 7.61 (t, *J*=1.0, 1H, $CCHNCHCHN$), 8.46 (dd, *J*=1.9, 1.0, 1H, $CCHNCHCHN$). ^{13}C NMR (126 MHz, CD_2Cl_2) δ = 14.42 ($COOCH_2CH_3$), 25.17 ($NCH_2CH_2CH_2$), 27.21 ($NCH_2CH_2CH_2$), 42.48 (NCH_2CHCOO), 54.70 ($NCH_2CH_2CH_2$), 55.64 ($C_{Ar}OCH_3$), 56.82 (NCH_2CHCOO), 58.88 (NCH_2CH_2O), 60.57 ($COOCH_2CH_3$), 62.46 (NCH_2CH_2O), 84.92 (NCH_2CH_2OC), 113.53 ($CCHNCHCHN$), 113.65 ($CCHCHCOCH_3$), 116.68 ($CCHCHCN$), 125.21 ($CCHNCHCHN$), 126.37 ($CCHCHCN$), 130.47 ($CCHCHCOCH_3$), 130.97 ($CCHNCHCHN$), 134.05 ($CCHNCHCHN$), 135.19 ($CCHCHCOCH_3$), 144.82 ($CCHCHCN$), 159.32 ($CCHCHCOCH_3$), 174.40 (COO). IR (KBr): ṽ = 2935, 1728, 1608, 1508, 1464, 1311, 1249, 1176, 1069, 1032, 923, 828, 808, 671, 619, 584 cm^{-1}. HRMS-ESI+ *m/z* $[M+H]^+$ calcd for $C_{32}H_{37}O_5N_3$: 544.2806, found: 544.2811.

***rac*-Ethyl 1-(2-{[4-(ethoxycarbonyl)phenyl]bis[4-methoxyphenyl]methoxy}ethyl)piperidine-3-carboxylate (12e):** ^{1}H NMR (500 MHz, CD_2Cl_2) δ = 1.20 (t, *J*=7.1, 3H, $CHCOOCH_2CH_3$), 1.35 (t, *J*=7.1, 3H, $C_{Ar}COOCH_2CH_3$), 1.37 – 1.45 (m, 1H, $NCH_2CH_2CH_{ax}H_{eq}$), 1.48 – 1.58 (m, 1H, $NCH_2CH_{ax}H_{eq}CH_2$), 1.64 – 1.72 (m, 1H, $NCH_2CH_{ax}H_{eq}CH_2$), 1.84 – 1.93 (m, 1H, $NCH_2CH_2CH_{ax}H_{eq}$), 2.04 (td, *J*=11.0, 3.0, 1H, $NCH_{ax}H_{eq}CH_2CH_2$), 2.14 – 2.24 (m, 1H, $NCH_{ax}H_{eq}CHCOO$), 2.51 (tt, *J*=10.5, 3.8, 1H, NCH_2CHCOO), 2.56 – 2.62 (m, 2H, NCH_2CH_2O), 2.66 – 2.73 (m, 1H, $NCH_{ax}H_{eq}CH_2CH_2$), 2.92 – 2.99 (m, 1H, $NCH_{ax}H_{eq}CHCOO$), 3.07 – 3.17 (m, 2H, NCH_2CH_2O), 3.78 (s, 6H, $C_{Ar}OCH_3$), 4.04 – 4.10 (m, 2H, $CHCOOCH_2CH_3$), 4.32 (q, *J*=7.1, 2H, $C_{Ar}COOCH_2CH_3$), 6.79 – 6.88 (m, 4H, $CCHCHCOCH_3$), 7.28 – 7.36 (m, 4H, $CCHCHCCH_2OCH_3$), 7.53 – 7.61 (m, 2H, $CCHCHCCOO$), 7.89 – 7.97 (m, 2H, $CCHCHCCOO$). ^{13}C NMR (126 MHz, CD_2Cl_2) δ = 14.43 ($CHCOOCH_2CH_3$), 14.53 ($C_{Ar}COOCH_2CH_3$), 25.16 ($NCH_2CH_2CH_2$), 27.25 ($NCH_2CH_2CH_2$), 42.50 (NCH_2CHCOO), 54.68 ($NCH_2CH_2CH_2$), 55.61 ($C_{Ar}OCH_3$), 56.71 (NCH_2CHCOO), 58.82 (NCH_2CH_2O),

60.53 (CHCOO*C*H_2CH$_3$), 61.22 (C_{Ar}COO*C*H_2CH$_3$), 62.31 (NCH$_2$*C*H_2O), 86.28 (N*C*H_2CH$_2$O*C*), 113.51 (CCH*C*HCOCH$_3$), 128.22 (C*C*HCHCCOO), 129.26 (CCHCH*C*COO), 129.32 (CCH*C*HCCOO), 130.57 (C*C*HCHCOCH$_3$), 135.94 (*C*CHCHCOCH$_3$), 151.40 (*C*CHCHCCOO), 159.15 (CCHCH*C*OCH$_3$), 166.61 (C_{Ar}*C*OO), 174.40 (CH*C*OO). IR (KBr): ṽ = 2938, 1718, 1608, 1509, 1465, 1275, 1251, 1176, 1103, 1033, 827, 765, 704 cm^{-1}. HRMS-ESI+ *m/z* [*M*+H]$^+$ calcd for $C_{34}H_{41}NO_7$: 576.2956, found: 576.2962.

***rac*-Ethyl 1-(2-{[4-(methoxymethyl)phenyl]bis[4-methoxyphenyl]methoxy}ethyl)-piperidine-3-carboxylate (12f):** ^{1}H NMR (400 MHz, CD_2Cl_2) δ = 1.20 (t, *J*=7.1, 3H, COOCH$_2$C*H*$_3$), 1.31 – 1.46 (m, 1H, NCH$_2$CH$_2$C*H*$_{ax}$H$_{eq}$), 1.46 – 1.60 (m, 1H, NCH$_2$C*H*$_{ax}$H$_{eq}$CH$_2$), 1.63 – 1.72 (m, 1H, NCH$_2$CH$_{ax}$*H*$_{eq}$CH$_2$), 1.82 – 1.93 (m, 1H, NCH$_2$CH$_2$CH$_{ax}$*H*$_{eq}$), 2.03 (td, *J*=10.9, 3.0, 1H, NC*H*$_{ax}$H$_{eq}$CH$_2$CH$_2$), 2.18 (t, *J*=10.6, 1H, NC*H*$_{ax}$H$_{eq}$CHCOO), 2.51 (tt, *J*=10.5, 3.8, 1H, NCH$_2$C*H*COO), 2.58 (t, *J*=6.0, 2H, NC*H*$_2$CH$_2$O), 2.70 (br dt, *J*=11.4, 3.8, 1H, NCH$_{ax}$*H*$_{eq}$CH$_2$CH$_2$), 2.91 – 3.04 (m, 1H, NCH$_{ax}$*H*$_{eq}$CHCOO), 3.06 – 3.21 (m, 2H, NCH$_2$C*H*$_2$O), 3.35 (s, 3H, CH$_2$OC*H*$_3$), 3.77 (s, 6H, C_{Ar}OCH$_3$), 4.04 – 4.10 (m, 2H, COOC*H*$_2$CH$_3$), 4.39 (s, 2H, C_{Ar}C*H*$_2$OCH$_3$), 6.76 – 6.89 (m, 4H, CCHC*H*COCH$_3$), 7.21 – 7.30 (m, 2H, CCHC*H*CCH$_2$OCH$_3$), 7.29 – 7.37 (m, 4H, CC*H*CHCOCH$_3$), 7.38 – 7.46 (m, 2H, CC*H*CHCCH$_2$OCH$_3$). ^{13}C NMR (101 MHz, CD_2Cl_2) δ = 14.43 (COOCH$_2$C*H*$_3$), 25.16 (NCH$_2$*C*H$_2$CH$_2$), 27.28 (NCH$_2$CH$_2$*C*H$_2$), 42.51 (NCH$_2$*C*HCOO), 54.68 (N*C*H$_2$CH$_2$CH$_2$), 55.60 (C_{Ar}O*C*H$_3$), 56.71 (N*C*H$_2$CHCOO), 58.43 (CH$_2$O*C*H$_3$), 58.89 (N*C*H$_2$CH$_2$O), 60.52 (COO*C*H$_2$CH$_3$), 62.18 (NCH$_2$*C*H$_2$O), 74.67 (*C*H$_2$OCH$_3$), 86.22 (N*C*H$_2$CH$_2$O*C*), 113.37 (CCH*C*HCOCH$_3$), 127.48 (CCH*C*HCCH$_2$OCH$_3$), 128.59 (C*C*HCHCCH$_2$OCH$_3$), 130.38 (C*C*HCHCOCH$_3$), 136.93 (*C*CHCHCOCH$_3$), 137.37 (CCHCH*C*CH$_2$OCH$_3$), 145.12 (*C*CHCHCCH$_2$OCH$_3$), 158.94 (CCHCH*C*OCH$_3$), 174.43 (COO). IR (KBr): ṽ = 2936, 2835, 1730, 1608, 1582, 1509, 1464, 1413, 1373, 1302, 1250, 1177, 1154, 1093, 1034, 968, 915, 827, 732, 582 cm^{-1}. HRMS-ESI+ *m/z* [*M*+H]$^+$ calcd for $C_{33}H_{41}NO_6$: 548.3007, found: 548.3003.

***rac*-Ethyl 1-{2-[(4-cyanophenyl)bis(4-methoxyphenyl)methoxy]ethyl}piperidine-3-carboxylate (12g):** ^{1}H NMR (400 MHz, CD_2Cl_2) δ = 1.20 (t, *J*=7.1, 3H, COOCH$_2$C*H*$_3$), 1.33 – 1.47 (m, 1H, NCH$_2$CH$_2$C*H*$_{ax}$H$_{eq}$), 1.48 – 1.60 (m, 1H, NCH$_2$C*H*$_{ax}$H$_{eq}$CH$_2$), 1.64 – 1.74 (m, 1H, NCH$_2$CH$_{ax}$*H*$_{eq}$CH$_2$), 1.82 – 1.93 (m, 1H, NCH$_2$CH$_2$CH$_{ax}$*H*$_{eq}$), 2.05 (td, *J*=11.0, 2.7, 1H, NC*H*$_{ax}$H$_{eq}$CH$_2$CH$_2$), 2.20 (t, *J*=10.5, 1H, NC*H*$_{ax}$H$_{eq}$CHCOO), 2.51 (tt, *J*=10.3, 3.7, 1H, NCH$_2$C*H*COO), 2.58 (td, *J*=5.8, 1.5, 2H, NC*H*$_2$CH$_2$O), 2.68 (td, *J*=8.0, 3.8, 1H, NCH$_{ax}$*H*$_{eq}$CH$_2$CH$_2$), 2.94 (dd, *J*=10.8, 3.6, 1H, NCH$_{ax}$*H*$_{eq}$CHCOO), 3.02 – 3.17 (m, 2H, NCH$_2$C*H*$_2$O), 3.78 (s, 6H, C_{Ar}OCH$_3$), 4.04 – 4.10 (m, 2H, COOC*H*$_2$CH$_3$), 6.74 – 6.91 (m, 4H, CCHC*H*COCH$_3$), 7.23 – 7.38 (m, 4H, CC*H*CHCOCH$_3$), 7.51 – 7.61 (m, 2H, CCHC*H*CCN), 7.62 – 7.68 (m, 2H, CC*H*CHCCN). ^{13}C NMR (101 MHz, CD_2Cl_2) δ = 14.44 (COOCH$_2$C*H*$_3$), 25.15 (NCH$_2$*C*H$_2$CH$_2$), 27.22 (NCH$_2$CH$_2$*C*H$_2$), 42.51 (NCH$_2$*C*HCOO), 54.68 (N*C*H$_2$CH$_2$CH$_2$), 55.64 (C_{Ar}O*C*H$_3$), 56.73 (N*C*H$_2$CHCOO), 58.79 (N*C*H$_2$CH$_2$O), 60.55 (COO*C*H$_2$CH$_3$), 62.35 (NCH$_2$*C*H$_2$O), 86.12 (N*C*H$_2$CH$_2$O*C*), 110.67 (CCHCH*C*CN), 113.64 (CCH*C*HCOCH$_3$), 119.27 (Ar*C*N), 128.79 (C*C*HCHCCN), 130.66 (C*C*HCHCOCH$_3$), 132.08 (CCH*C*HCCN), 135.22 (*C*CHCHCOCH$_3$), 152.16 (*C*CHCHCCN), 159.33 (CCHCH*C*OCH$_3$), 174.38 (COO). IR (KBr): ṽ = 2938, 2227, 1729, 1607, 1509, 1464, 1303, 1252, 1177, 1153, 1069, 1032, 827 cm^{-1}. HRMS-EI+ *m/z* [*M*+H]$^+$ calcd for $C_{32}H_{36}N_2O_5$: 529.2697, found: 529.2702.

***rac*-Ethyl 1-(2-{bis[4-(methoxymethyl)phenyl][4-methoxyphenyl]methoxy}ethyl)piperidine-3-carboxylate (12h):** ^{1}H NMR (400 MHz, CD_2Cl_2) δ = 1.20 (t, *J*=7.1, 3H, COOCH$_2$C*H*$_3$), 1.34 – 1.47 (m, 1H, NCH$_2$CH$_2$C*H*$_{ax}$H$_{eq}$), 1.46 – 1.62 (m, 1H, NCH$_2$C*H*$_{ax}$H$_{eq}$CH$_2$), 1.64 – 1.74 (m, 1H, NCH$_2$CH$_{ax}$*H*$_{eq}$CH$_2$), 1.84 – 1.93 (m, 1H, NCH$_2$CH$_2$CH$_{ax}$*H*$_{eq}$), 1.97 – 2.09 (m, 1H, NC*H*$_{ax}$H$_{eq}$CH$_2$CH$_2$), 2.19 (t, *J*=10.6, 1H, NC*H*$_{ax}$H$_{eq}$CHCOO), 2.45 – 2.55 (m, 1H, NCH$_2$C*H*COO), 2.56 – 2.62 (m, 2H,

NC*H*$_2$CH$_2$O), 2.66 – 2.75 (m, 1H, NCH$_{ax}$*H*$_{eq}$CH$_2$CH$_2$), 2.92 – 3.00 (m, 1H, NCH$_{ax}$*H*$_{eq}$CHCOO), 3.08 – 3.19 (m, 2H, NCH$_2$C*H*$_2$O), 3.36 (s, 6H, CH$_2$OC*H*$_3$), 3.78 (s, 3H, C$_{Ar}$OCH$_3$), 4.04 – 4.10 (m, 2H, COOC*H*$_2$CH$_3$), 4.40 (s, 4H, C$_{Ar}$C*H*$_2$OCH$_3$), 6.79 – 6.86 (m, 2H, CCHC*H*COCH$_3$), 7.22 – 7.26 (m, 4H, CCHC*H*CCH$_2$OCH$_3$), 7.29 – 7.34 (m, 2H, CC*H*CHCOCH$_3$), 7.39 – 7.45 (m, 4H, CC*H*CHCCH$_2$OCH$_3$). ^{13}C NMR (101 MHz, CD$_2$Cl$_2$) δ = 14.43 (COOCH$_2$C*H*$_3$), 25.13 (NCH$_2$*C*H$_2$CH$_2$), 27.25 (NCH$_2$CH$_2$*C*H$_2$), 42.47 (NCH$_2$*C*HCOO), 54.65 (N*C*H$_2$CH$_2$CH$_2$), 55.60 (C$_{Ar}$O*C*H$_3$), 56.70 (N*C*H$_2$CHCOO), 58.43 (CH$_2$O*C*H$_3$), 58.84 (N*C*H$_2$CH$_2$O), 60.53 (COO*C*H$_2$CH$_3$), 62.26 (NCH$_2$*C*H$_2$O), 74.65 (*C*H$_2$OCH$_3$), 86.45 (N*C*H$_2$CH$_2$O*C*), 113.39 (CCH*C*HCOCH$_3$), 127.48 (CCH*C*HCCH$_2$OCH$_3$), 128.80 (C*C*HCHCCH$_2$OCH$_3$), 130.62 (C*C*HCHCOCH$_3$), 136.41 (*C*CHCHCOCH$_3$), 137.54 (CCHCH*C*CH$_2$OCH$_3$), 144.59 (*C*CHCHCCH$_2$OCH$_3$), 159.04 (CCHCH*C*OCH$_3$), 174.41 (COO). IR (KBr): ṽ = 2931, 1729, 1676, 1608, 1509, 1464, 1377, 1301, 1251, 1221, 1180, 1153, 1096, 1033, 967, 917, 812, 668, 639, 586. 542, 530 cm^{-1}. HRMS-ESI+ *m/z* [*M*+H]$^+$ calcd for C$_{34}$H$_{43}$NO$_6$: 562.3163, found: 562.3161.

***rac*-Ethyl 1-(2-{tris[4-(methoxymethyl)phenyl]methoxy}ethyl)piperidine-3-carboxylate (12i):** ^{1}H NMR (400 MHz, CD$_2$Cl$_2$) δ = 1.20 (t, *J*=7.1, 3H, COOCH$_2$C*H*$_3$), 1.35 – 1.45 (m, 1H, NCH$_2$CH$_2$C*H*$_{ax}$H$_{eq}$), 1.47 – 1.61 (m, 1H, NCH$_2$C*H*$_{ax}$H$_{eq}$CH$_2$), 1.63 – 1.75 (m, 1H, NCH$_2$CH$_{ax}$*H*$_{eq}$CH$_2$), 1.83 – 1.93 (m, 1H, NCH$_2$CH$_2$CH$_{ax}$*H*$_{eq}$), 1.98 – 2.10 (m, 1H, NC*H*$_{ax}$H$_{eq}$CH$_2$CH$_2$), 2.19 (t, *J*=10.6, 1H, NC*H*$_{ax}$H$_{eq}$CHCOO), 2.44 - 2.63 (m, 3H, NCH$_2$C*H*COO + NC*H*$_2$CH$_2$O), 2.70 (br d, *J*=11.3, 1H, NCH$_{ax}$*H*$_{eq}$CH$_2$CH$_2$), 2.96 (br d, *J*=11.2, 1H, NCH$_{ax}$*H*$_{eq}$CHCOO), 3.06 – 3.20 (m, 2H, NCH$_2$C*H*$_2$O), 3.36 (s, 9H, CH$_2$OC*H*$_3$), 4.04 – 4.10 (m, 2H, COOC*H*$_2$CH$_3$), 4.40 (s, 6H, C$_{Ar}$C*H*$_2$OCH$_3$), 7.22 – 7.29 (m, 6H, CCHC*H*CCH$_2$OCH$_3$), 7.38 – 7.46 (m, 6H, CC*H*CHCCH$_2$OCH$_3$). ^{13}C NMR (101 MHz, CD$_2$Cl$_2$) δ = 14.43 (COOCH$_2$C*H*$_3$), 25.13 (NCH$_2$*C*H$_2$CH$_2$), 27.24 (NCH$_2$CH$_2$*C*H$_2$), 42.47 (NCH$_2$*C*HCOO), 54.64 (N*C*H$_2$CH$_2$CH$_2$), 56.71 (N*C*H$_2$CHCOO), 58.44 (CH$_2$O*C*H$_3$), 58.45 (N*C*H$_2$CH$_2$O), 58.81 (COO*C*H$_2$CH$_3$), 62.40 (NCH$_2$*C*H$_2$O), 74.63 (*C*H$_2$OCH$_3$), 86.65 (N*C*H$_2$CH$_2$O*C*), 127.48 (CCH*C*HCCH$_2$OCH$_3$), 129.02 (C*C*HCHCCH$_2$OCH$_3$), 137.71 (CCHCH*C*CH$_2$OCH$_3$), 144.09 (*C*CHCHCCH$_2$OCH$_3$), 174.39 (COO). IR (KBr): ṽ = 2933, 2820, 1731, 1634, 1508, 1452, 1413, 1377, 1311, 1221, 1190, 1154, 1100, 1022, 969, 918, 797, 668, 519 cm^{-1}. HRMS-ESI+ *m/z* [*M*+H]$^+$ calcd for C$_{35}$H$_{45}$NO$_6$: 576.3320, found: 576.3316.

***rac*-Ethyl 1-{2-[(4-carbamoylphenyl)bis(4-methoxyphenyl)methoxy]ethyl}piperidine-3-carboxylate (12j):** ^{1}H NMR (400 MHz, tetrachloroethane-*d*$_2$) δ = 1.22 (t, *J*=7.1, 1H, 3H, COOCH$_2$C*H*$_3$), 1.33 – 1.46 (m, 1H, NCH$_2$CH$_2$C*H*$_{ax}$H$_{eq}$), 1.46 – 1.61 (m, 1H, NCH$_2$C*H*$_{ax}$H$_{eq}$CH$_2$), 1.65 – 1.81 (m, 1H, NCH$_2$CH$_{ax}$*H*$_{eq}$CH$_2$), 1.87 – 1.97 (m, 1H, NCH$_2$CH$_2$CH$_{ax}$*H*$_{eq}$), 1.99 – 2.12 (m, 1H, NC*H*$_{ax}$H$_{eq}$CH$_2$CH$_2$), 2.19 (t, *J*=10.7, 1H, NC*H*$_{ax}$H$_{eq}$CHCOO), 2.53 (tt, *J*=10.6, 3.8, 1H, NCH$_2$C*H*COO), 2.63 (t, *J*=6.0, 2H, NC*H*$_2$CH$_2$O), 2.73 (br d, *J*=11.2, 1H, NCH$_{ax}$*H*$_{eq}$CH$_2$CH$_2$), 2.91 – 3.01 (m, 1H, NCH$_{ax}$*H*$_{eq}$CHCOO), 3.07 – 3.20 (m, 2H, NCH$_2$C*H*$_2$O), 3.81 (s, 6H, C$_{Ar}$OCH$_3$), 4.04 – 4.17 (m, 2H, COOC*H*$_2$CH$_3$), 5.62 (br s, 1H, CONH$_2$), 6.10 (br s, 1H, CONH$_2$), 6.81 – 6.89 (m, 4H, CCHC*H*COCH$_3$), 7.29 – 7.37 (m, 4H, CC*H*CHCOCH$_3$), 7.55 – 7.62 (m, 2H, CC*H*CHCNH$_2$), 7.68 – 7.75 (m, 2H, CCHC*H*CNH$_2$). ^{13}C NMR (101 MHz, tetrachloroethne-*d*$_2$) δ = 14.16 (COOCH$_2$C*H*$_3$), 24.53 (NCH$_2$*C*H$_2$CH$_2$), 26.68 (NCH$_2$CH$_2$*C*H$_2$), 41.81 (NCH$_2$*C*HCOO), 53.99 (N*C*H$_2$CH$_2$CH$_2$), 55.22 (C$_{Ar}$O*C*H$_3$), 55.96 (N*C*H$_2$CHCOO), 58.17 (N*C*H$_2$CH$_2$O), 60.23 (COO*C*H$_2$CH$_3$), 61.72 (NCH$_2$*C*H$_2$O), 85.57 (NCH$_2$CH$_2$O*C*), 113.07 (CCH*C*HCOCH$_3$), 126.75 (CCH*C*HCNH$_2$), 128.00 (C*C*HCHCNH$_2$), 130.08 (C*C*HCHCOCH$_3$), 131.28 (CCHCH*C*CNH$_2$), 135.29 (*C*CHCHCOCH$_3$), 150.01 (*C*CHCHCC(O)NH$_2$), 158.27 (CCHCH*C*OCH$_3$), 168.84 (*C*NH$_2$), 174.14 (COO). IR (KBr): ṽ = 2937, 2835, 1728, 1664, 1609, 1509, 1465, 1383, 1302, 1251, 1176, 1156, 1071, 1033, 829, 767, 582 cm^{-1}. HRMS-ESI+ *m/z* [*M*+H]$^+$ calcd for C$_{32}$H$_{38}$N$_2$O$_6$: 547.2803, found: 547.2796.

***rac*-Ethyl 1-{2-[2-methoxy-1,1-bis(4-methoxyphenyl)-2-oxoethoxy]ethyl}piperidine-3-carboxylate (12k):** ^{1}H NMR (500 MHz, CD_2Cl_2) δ = 1.20 (t, *J*=7.1, 3H, $COOCH_2CH_3$), 1.34 – 1.46 (m, 1H, $NCH_2CH_2CH_{ax}H_{eq}$), 1.50 (dtt, *J*=13.0, 11.0, 3.9, 1H, $NCH_2CH_{ax}H_{eq}CH_2$), 1.65 (dp, *J*=15.1, 3.9, 1H, $NCH_2CH_{ax}H_{eq}CH_2$), 1.86 (dq, *J*=12.4, 4.0, 1H, $NCH_2CH_2CH_{ax}H_{eq}$), 2.02 (td, *J*=11.0, 3.0, 1H, $NCH_{ax}H_{eq}CH_2CH_2$), 2.15 (br t, *J*=10.6, 1H, $NCH_{ax}H_{eq}CHCOO$), 2.43 – 2.52 (m, 1H, NCH_2CHCOO), 2.56 (t, *J*=6.1, 2H, NCH_2CH_2O), 2.66 – 2.76 (m, 1H, $NCH_{ax}H_{eq}CH_2CH_2$), 2.90 – 2.98 (m, 1H, $NCH_{ax}H_{eq}CHCOO$), 3.30 (t, *J*=6.1, 2H, NCH_2CH_2O), 3.71 (s, 3H, $COOCH_3$), 3.79 (s, 6H, $C_{Ar}OCH_3$), 4.04 – 4.10 (m, 2H, $COOCH_2CH_3$), 6.79 – 6.87 (m, 4H, $CCHCHCOCH_3$), 7.26 – 7.35 (m, 4H, $CCHCHCOCH_3$). ^{13}C NMR (126 MHz, CD_2Cl_2) δ = 14.41 ($COOCH_2CH_3$), 25.12 ($NCH_2CH_2CH_2$), 27.27 ($NCH_2CH_2CH_2$), 42.43 (NCH_2CHCOO), 52.64 ($COOCH_3$), 54.45 ($NCH_2CH_2CH_2$), 55.62 ($C_{Ar}OCH_3$), 56.33 (NCH_2CHCOO), 58.67 (NCH_2CH_2O), 60.50 ($COOCH_2CH_3$), 63.46 (NCH_2CH_2O), 86.51 ($CCOOCH_3$), 113.46 ($CCHCHCOCH_3$), 130.06 ($CCHCHCOCH_3$), 133.51 ($CCHCHCOCH_3$), 159.66 ($CCHCHCOCH_3$), 172.95 ($COOCH_3$), 174.42 ($COOCH_2CH_3$). IR (KBr): ṽ = 2950, 1731, 1609, 1510, 1465, 1303, 1252, 1175, 1093, 1033, 831, 807, 781, 597, 570 cm^{-1}. HRMS-ESI+ *m/z* $[M+H]^+$ calcd for $C_{27}H_{35}O_7N$: 486.2486, found: 486.2499.

***rac*-Ethyl 1-[4-hydroxy-4,4-bis(4-methoxyphenyl)butyl]piperidine-3-carboxylate (12l):** ^{1}H NMR (400 MHz, CD_2Cl_2) δ = 1.28 (t, *J*=7.1, 3H, $COOCH_2CH_3$), 1.34 – 1.48 (m, 1H, $NCH_2CH_2CH_{ax}H_{eq}CH$), 1.54 – 1.77 (m, 4H, $NCH_2CH_{ax}H_{eq}CH_2CH$ + $NCH_2CH_2CH_2COH$ + $NCH_2CH_{ax}H_{eq}CH_2CH$), 1.87 (td, *J*=11.2, 3.6, 1H, $NCH_{ax}H_{eq}CH_2CH_2CH$), 1.94 – 2.07 (m, 2H, $NCH_2CH_2CH_{ax}H_{eq}CH$ + $NCH_{ax}H_{eq}CHCOO$), 2.32 – 2.51 (m, 4H, $NCH_2CH_2CH_2COH$ + $NCH_2CH_2CH_2COH$), 2.58 – 2.71 (m, 2H, NCH_2CHCOO + $NCH_{ax}H_{eq}CH_2CH_2CH$), 2.82 – 2.93 (m, 1H, $NCH_{ax}H_{eq}CHCOO$), 3.79 (d, *J*=1.5, 6H, $C_{Ar}OCH_3$), 4.13 (q, *J*=7.1, 2H, $COOCH_2CH_3$), 6.80 – 6.89 (m, 4H, $CCHCHCOCH_3$), 7.37 – 7.46 (m, 4H, $CCHCHCOCH_3$). ^{13}C NMR (101 MHz, CD_2Cl_2) δ = 14.56 ($COOCH_2CH_3$), 22.38 ($NCH_2CH_2CH_2COH$), 24.80 ($NCH_2CH_2CH_2CH$), 27.55 ($NCH_2CH_2CH_2CH$), 42.07 (NCH_2CHCOO), 43.28 ($NCH_2CH_2CH_2COH$), 58.78 ($NCH_2CH_2CH_2CH$), 55.58 (NCH_2CHCOO), 55.68 (d, $C_{Ar}OCH_3$), 59.88 ($NCH_2CH_2CH_2COH$), 60.85 ($COOCH_2CH_3$). 76.29 (COH), 113.61 (d, $CCHCHCOCH_3$), 127.67 (d, $CCHCHCOCH_3$), 141.91 (d, $CCHCHCOCH_3$), 158.46 (d, $CCHCHCOCH_3$), 174.10 (COO). IR (KBr): ṽ = 3055, 2937, 2830, 1729, 1606, 1505, 1453, 1370, 1324, 1241, 1177, 1149, 1122, 1030, 851, 840, 818, 633, 591, 577 cm^{-1}. HRMS-ESI+ *m/z* $[M+H]^+$ calcd for $C_{26}H_{35}NO_5$: 442.2588, found: 442.2587.

***rac*-Ethyl 1-(2-{[4-(hydroxymethyl)phenyl]bis[4-methoxyphenyl]methoxy}ethyl)piperidine-3-carboxylate (12m):** ^{1}H NMR (500 MHz, CD_2Cl_2) δ = 1.20 (t, *J*=7.1, 3H, $COOCH_2CH_3$), 1.34 – 1.45 (m, 1H, $NCH_2CH_2CH_{ax}H_{eq}$), 1.47 – 1.59 (m, 1H, $NCH_2CH_{ax}H_{eq}CH_2$), 1.63 – 1.71 (m, 1H, $NCH_2CH_{ax}H_{eq}CH_2$), 1.82 – 1.91 (m, 1H, $NCH_2CH_2CH_{ax}H_{eq}$), 2.03 (td, *J*=11.1, 3.0, 1H, $NCH_{ax}H_{eq}CH_2CH_2$), 2.16 (t, *J*=10.6, 1H, $NCH_{ax}H_{eq}CHCOO$), 2.50 (tt, *J*=10.6, 3.9, 1H, NCH_2CHCOO), 2.58 (td, *J*=6.0, 1.7, 2H, NCH_2CH_2O), 2.66 – 2.74 (m, 1H, $NCH_{ax}H_{eq}CH_2CH_2$), 2.90 – 2.98 (m, 1H, $NCH_{ax}H_{eq}CHCOO$), 3.06 – 3.19 (m, 2H, NCH_2CH_2O), 3.77 (s, 6H, $C_{Ar}OCH_3$), 4.03 – 4.09 (m, 2H, $COOCH_2CH_3$), 4.61 (s, 2H, CH_2OH), 6.78 – 6.87 (m, 4H, $CCHCHCOCH_3$), 7.25 – 7.29 (m, 2H, $CCHCHCCH_2OH$), 7.30 – 7.35 (m, 4H, $CCHCHCOCH_3$), 7.42 – 7.45 (m, 2H, $CCHCHCCH_2OH$). ^{13}C NMR (126 MHz, CD_2Cl_2) δ = 14.43 ($COOCH_2CH_3$), 25.16 ($NCH_2CH_2CH_2$), 27.27 ($NCH_2CH_2CH_2$), 42.49 (NCH_2CHCOO), 54.67 ($NCH_2CH_2CH_2$), 55.60 ($C_{Ar}OCH_3$), 56.65 (NCH_2CHCOO), 58.87 (NCH_2CH_2O), 60.54 ($CH_2COOCH_2CH_3$), 62.14 (NCH_2CH_2O), 65.17 (CH_2OH), 86.22 (NCH_2CH_2OC), 113.38 ($CCHCHCOCH_3$), 126.77 ($CCHCHCCH_2OH$), 128.72 ($CCHCHCCH_2OH$), 130.37 ($CCHCHCOCH_3$), 136.87 ($CCHCHCOCH_3$), 140.08 ($CCHCHCCH_2OH$), 145.17 ($CCHCHCCH_2OH$), 158.94 ($CCHCHCOCH_3$), 174.45 (COO). IR (KBr): ṽ = 2936, 2360, 1729, 1608, 1508, 1302, 1250,

1176, 1153, 1070, 1033, 915, 827, 582 cm^{-1}. HRMS-ESI+ *m/z* $[M+H]^+$ calcd for $C_{32}H_{39}NO_6$: 534.2850, found: 534.2861.

***rac*- Ethyl 1-{2-[(4-{[(2-ethoxy-2-oxoethyl)amino]methyl}phenyl)bis(4-methoxyphenyl)-methoxy]ethyl}piperidine-3-carboxylate (12n):** ^{1}H NMR (500 MHz, CD_2Cl_2) δ = 1.20 (t, *J*=7.2, 3H, $CHCOOCH_2CH_3$), 1.24 (t, *J*=7.1, 3H, $CH_2COOCH_2CH_3$), 1.34 – 1.45 (m, 1H, $NCH_2CH_2H_{ax}H_{eq}$), 1.48 – 1.58 (m, 1H, $NCH_2CH_{ax}H_{eq}CH_2$), 1.67 (ddd, *J*=17.0, 7.4, 3.6, 1H, $NCH_2CH_{ax}H_{eq}CH_2$), 1.83 – 1.91 (m, 1H, $NCH_2CH_2CH_{ax}H_{eq}$), 2.03 (td, *J*=10.9, 2.4, 1H, $NCH_{ax}H_{eq}CH_2CH_2$), 2.18 (t, *J*=10.6, 1H, $NCH_{ax}H_{eq}CHCOO$), 2.51 (tt, *J*=10.5, 3.8, 1H, NCH_2CHCOO), 2.57 (t, *J*=6.0, 2H, NCH_2CH_2O), 2.66 – 2.73 (m, 1H, $NCH_{ax}H_{eq}CH_2CH_2$), 2.95 (br d, *J*=10.7, 1H, $NCH_{ax}H_{eq}CHCOO$), 3.11 (tt, *J*=9.6, 4.7, 2H, NCH_2CH_2O), 3.37 (s, 2H, CH_2NHCH_2COO), 3.75 (s, 2H, CH_2NHCH_2COO), 3.77 (s, 6H, $C_{Ar}OCH_3$), 4.03 – 4.11 (m, 2H, $CHCOOCH_2CH_3$), 4.14 (q, *J*=7.2, 2H, $CH_2COOCH_2CH_3$), 6.79 – 6.86 (m, 4H, $CCHCHCOCH_3$), 7.22 – 7.27 (m, 2H, $CCHCHCCH_2NH$), 7.30 – 7.35 (m, 4H, $CCHCHCOCH_3$), 7.37 – 7.41 (m, 2H, $CCHCHCCH_2NH$). ^{13}C NMR (126 MHz, CD_2Cl_2) δ = 14.44 (d, $CHCOOCH_2CH_3$ + $CHCOOCH_2CH_3$), 25.16 ($NCH_2CH_2CH_2$), 27.27 ($NCH_2CH_2CH_2$), 42.49 (NCH_2CHCOO), 50.66 (CH_2NHCH_2COO), 53.19 (CH_2NHCH_2COO), 54.67 ($NCH_2CH_2CH_2$), 55.59 ($C_{Ar}OCH_3$), 56.71 (NCH_2CHCOO), 58.89 (NCH_2CH_2O), 60.52 ($CHCOOCH_2CH_3$), 60.98 ($CH_2COOCH_2CH_3$), 62.17 (NCH_2CH_2O), 86.21 (NCH_2CH_2OC), 113.35 ($CCHCHCOCH_3$), 127.95 ($CCHCHCCH_2NH$), 128.62 ($CCHCHCCH_2NH$), 130.36 ($CCHCHCOCH_3$), 137.00 ($CCHCHCOCH_3$), 138.85 ($CCHCHCCH_2NH$), 144.53 ($CCHCHCCH_2NH$), 158.91 ($CCHCHCOCH_3$), 172.76 ($NHCH_2COO$), 174.43 (NCH_2CHCOO). IR (KBr): ṽ = 2948, 2835, 1731, 1608, 1582, 1509, 1464, 1440, 1367, 1302, 1250, 1176, 1071, 1034, 916, 828, 583 cm^{-1}. HRMS-ESI+ *m/z* $[M+H]^+$ calcd for $C_{36}H_{46}N_2O_7$: 619.3378, found: 619.3394.

***rac*-Ethyl 1-{2-[(4-{[(3-methoxy-3-oxopropyl)amino]methyl}phenyl)bis(4-methoxyphenyl)-methoxy]ethyl}piperidine-3-carboxylate (12o):** ^{1}H NMR (500 MHz, CD_2Cl_2) δ = 1.20 (t, *J*=7.1, 3H, $COOCH_2CH_3$), 1.33 – 1.45 (m, 1H, $NCH_2CH_2CH_{ax}H_{eq}$), 1.48 – 1.59 (m, 1H, $NCH_2CH_{ax}H_{eq}CH_2$), 1.63 – 1.71 (m, 1H, $NCH_2CH_{ax}H_{eq}CH_2$), 1.83 – 1.91 (m, 1H, $NCH_2CH_2CH_{ax}H_{eq}$), 2.00 – 2.06 (m, 1H, $NCH_{ax}H_{eq}CH_2CH_2$), 2.17 (t, *J*=10.6, 1H, $NCH_{ax}H_{eq}CHCOO$), 2.46 – 2.54 (m, 3H, NCH_2CHCOO + $NHCH_2CH_2COO$), 2.57 (t, *J*=5.9, 2H, NCH_2CH_2O), 2.66 – 2.73 (m, 1H, $NCH_{ax}H_{eq}CH_2CH_2$), 2.87 (t, *J*=6.5, 2H, $NHCH_2CH_2COO$), 2.92 – 2.98 (m, 1H, $NCH_{ax}H_{eq}CHCOO$), 3.06 – 3.18 (m, 2H, NCH_2CH_2O), 3.64 (s, 3H, $COOCH_3$), 3.74 (s, 2H, $C_{Ar}CH_2NH$), 3.77 (s, 6H, $C_{Ar}OCH_3$), 4.04 – 4.10 (m, 2H, $CH_2COOCH_2CH_3$), 6.79 – 6.84 (m, 4H, $CCHCHCOCH_3$), 7.21 – 7.25 (m, 2H, $CCHCHCCH_2NH$), 7.30 – 7.35 (m, 4H, $CCHCHCOCH_3$), 7.36 – 7.40 (m, 2H, $CCHCHCCH_2NH$). ^{13}C NMR (126 MHz, CD_2Cl_2) δ = 14.43 ($COOCH_2CH_3$), 25.16 ($NCH_2CH_2CH_2$), 27.27 ($NCH_2CH_2CH_2$), 35.08 ($NHCH_2CH_2COO$) 42.49 (NCH_2CHCOO), 45.10 ($NHCH_2CH_2COO$), 51.78 ($COOCH_3$), 53.62 ($C_{Ar}CH_2NH$), 54.66 ($NCH_2CH_2CH_2$), 55.59 ($C_{Ar}OCH_3$), 56.70 (NCH_2CHCOO), 58.89 (NCH_2CH_2O), 60.52 ($CHCOOCH_2CH_3$), 62.15 (NCH_2CH_2O), 86.21 (NCH_2CH_2OC), 113.34 ($CCHCHCOCH_3$), 127.77 ($CCHCHCCH_2NH$), 128.59 ($CCHCHCCH_2NH$), 130.35 ($CCHCHCOCH_3$), 137.04 ($CCHCHCOCH_3$), 139.46 ($CCHCHCCH_2NH$), 144.30 ($CCHCHCCH_2NH$), 158.90 ($CCHCHCOCH_3$), 173.46 ($NH_2CH_2CH_2COO$), 174.43 (NCH_2CHCOO). IR (KBr): ṽ = 2936, 1607, 1560, 1508, 1406, 1302, 1250, 1176, 1068, 1035, 826, 583 cm^{-1}. HRMS-ESI+ *m/z* $[M+H]^+$ calcd for $C_{36}H_{46}N_2O_7$: 619.3378, found: 619.3381.

***rac*-Ethyl 1-(2-{[4-({[1-(ethoxycarbonyl)cyclopropyl]amino}methyl)phenyl]bis[4-methoxy-phenyl]methoxy}ethyl)piperidine-3-carboxylate (12p):** ^{1}H NMR (400 MHz, CD_2Cl_2) δ = 0.98 (q, *J*=3.9, 2H, $NHCCH_{ax}H_{eq}$), 1.17 – 1.28 (m, 8H, $CHCOOCH_2CH_3$ + $CCOOCH_2CH_3$ + $NHCCH_{ax}H_{eq}$), 1.33 – 1.45 (m, 1H, $NCH_2CH_2CH_{ax}H_{eq}$), 1.46 – 1.62 (m, 1H, $NCH_2CH_{ax}H_{eq}CH_2$), 1.67 (dt, *J*=12.5, 3.7,

1H, $NCH_2CH_{ax}H_{eq}CH_2$), 1.82 – 1.92 (m, 1H, $NCH_2CH_2CH_{ax}H_{eq}$), 2.03 (td, *J*=10.9, 2.9, 1H, $NCH_{ax}H_{eq}CH_2CH_2$), 2.17 (t, *J*=10.6, 1H, $NCH_{ax}H_{eq}CHCOO$), 2.50 (tt, *J*=10.4, 3.8, 1H, NCH_2CHCOO), 2.57 (t, *J*=6.0, 2H, NCH_2CH_2O), 2.65 – 2.74 (m, 1H, $NCH_{ax}H_{eq}CH_2CH_2$), 2.91 – 2.99 (m, 1H, $NCH_{ax}H_{eq}CHCOO$), 3.11 (tt, *J*=5.8, 3.1, 2H, NCH_2CH_2O), 3.77 (s, 6H, $C_{Ar}OCH_3$), 3.82 (s, 2H, $C_{Ar}CH_2NH$), 4.03 – 4.14 (m, 4H, $CHCOOCH_2CH_3$ + $CCOOCH_2CH_3$), 6.78 – 6.85 (m, 4H, $CCHCHCOCH_3$), 7.18 – 7.26 (m, 2H, $CCHCHCCH_2NH$), 7.30 – 7.34 (m, 4H, $CCHCHCOCH_3$), 7.35 – 7.39 (m, 2H, $CCHCHCCH_2NH$). ^{13}C NMR (101 MHz, CD_2Cl_2) δ = 14.47 (d, $NHCCH_2$), 17.79 ($CHCOOCH_2CH_3$ + $CCOOCH_2CH_3$), 25.17 ($NCH_2CH_2CH_2$), 27.28 ($NCH_2CH_2CH_2$), 41.38 (NHC), 42.50 (NCH_2CHCOO), 51.74 ($C_{Ar}CH_2NH$), 54.67 ($NCH_2CH_2CH_2$), 55.59 ($C_{Ar}OCH_3$), 56.71 (NCH_2CHCOO), 58.89 (NCH_2CH_2O), 60.51 ($CHCOOCH_2CH_3$), 61.10 ($CCOOCH_2CH_3$), 62.17 (NCH_2CH_2O), 86.21 (NCH_2CH_2OC), 113.34 ($CCHCHCOCH_3$), 127.97 ($CCHCHCCH_2NH$), 128.55 ($CCHCHCCH_2NH$), 130.34 ($CCHCHCOCH_3$), 137.04 ($CCHCHCOCH_3$), 139.67 ($CCHCHCCH_2NH$), 144.31 ($CCHCHCCH_2NH$), 158.90 ($CCHCHCOCH_3$), 174.43 (CHCOO), 175.45 (CCOO). IR (KBr): ṽ = 2938, 1724, 1608, 1508, 1464, 1368, 1301, 1250, 1176, 1152, 1091, 1071, 1033, 969, 916, 827, 751, 733, 582 cm^{-1}. HRMS-ESI+ *m/z* $[M+H]^+$ calcd for $C_{38}H_{48}N_2O_7$: 645.3534, found: 645.3535.

***rac*-Ethyl 1-{2-[(4-{[(1-ethoxy-2-methyl-1-oxopropan-2-yl)amino]methyl}phenyl)bis(4-methoxyphenyl)methoxy]ethyl}piperidine-3-carboxylate (12q):** ^{1}H NMR (400 MHz, CD_2Cl_2) δ = 1.20 (t, *J*=7.1, 3H, $CHCOOCH_2CH_3$), 1.26 (t, *J*=7.1, 3H, $CCOOCH_2CH_3$), 1.31 (s, 6H, CCH_3), 1.34 – 1.44 (m, 1H, $NCH_2CH_2CH_{ax}H_{eq}$), 1.47 – 1.59 (m, 1H, $NCH_2CH_{ax}H_{eq}CH_2$), 1.63 – 1.72 (m, 1H, $NCH_2CH_{ax}H_{eq}CH_2$), 1.83 – 1.92 (m, 1H, $NCH_2CH_2CH_{ax}H_{eq}$), 2.03 (td, *J*=11.0, 3.0, 1H, $NCH_{ax}H_{eq}CH_2CH_2$), 2.18 (t, *J*=10.6, 1H, $NCH_{ax}H_{eq}CHCOO$), 2.50 (tt, *J*=10.4, 3.8, 1H, NCH_2CHCOO), 2.58 (t, *J*=6.0, 2H, NCH_2CH_2O), 2.65 – 2.75 (m, 1H, $NCH_{ax}H_{eq}CH_2CH_2$), 2.91 – 2.99 (m, 1H, $NCH_{ax}H_{eq}CHCOO$), 3.11 (tt, *J*=6.4, 3.3, 2H, NCH_2CH_2O), 3.58 (s, 2H, $C_{Ar}CH_2NH$), 3.77 (s, 6H, $C_{Ar}OCH_3$), 4.04 – 4.10 (m, 2H, $CHCOOCH_2CH_3$), 4.14 (q, *J*=7.1, 2H, $CCOOCH_2CH_3$), 6.78 – 6.85 (m, 4H, $CCHCHCOCH_3$), 7.22 – 7.27 (m, 2H, $CCHCHCCH_2NH$), 7.29 – 7.35 (m, 4H, $CCHCHCOCH_3$), 7.36 – 7.40 (m, 2H, $CCHCHCCH_2NH$). ^{13}C NMR (101 MHz, CD_2Cl_2) δ = 14.44 ($CHCOOCH_2CH_3$), 14.55 ($CCOOCH_2CH_3$), 25.17 ($NCH_2CH_2CH_2$), 25.58 (CCH_3), 27.28 ($NCH_2CH_2CH_2$), 42.50 (NCH_2CHCOO), 48.76 ($C_{Ar}CH_2NH$), 54.67 ($NCH_2CH_2CH_2$), 55.59 ($C_{Ar}OCH_3$), 56.71 (NCH_2CHCOO), 58.88 (NCH_2CH_2O), 59.43 ($NHCCH_3$), 60.51 ($CHCOOCH_2CH_3$), 61.02 ($CCOOCH_2CH_3$), 62.18 (NCH_2CH_2O), 86.21 (NCH_2CH_2OC), 113.35 ($CCHCHCOCH_3$), 128.05 ($CCHCHCCH_2NH$), 128.61 ($CCHCHCCH_2NH$), 130.36 ($CCHCHCOCH_3$), 137.02 ($CCHCHCOCH_3$), 139.65 ($CCHCHCCH_2NH$), 144.42 ($CCHCHCCH_2NH$), 158.91 ($CCHCHCOCH_3$), 174.43 (CHCOO), 177.14 (CCOO). IR (KBr): ṽ = 2979, 2937, 1729, 1608, 1582, 1509, 1464, 1302, 1250, 1176, 1140, 1071, 1033, 915, 826, 660, 582 cm^{-1}. HRMS-ESI+ *m/z* $[M+H]^+$ calcd for $C_{38}H_{50}N_2O_7$: 647.3691, found: 647.3688.

***rac*-4-{[4-({2-[3-(Ethoxycarbonyl)piperidin-1-yl]ethoxy}bis{4-methoxyphenyl}methyl)-benzyl]amino}butanoic acid (12s):** ^{1}H NMR (400 MHz, MeOD) δ = 1.20 (t, *J*=7.1, 3H, $COOCH_2CH_3$), 1.36 – 1.47 (m, 1H, $NCH_2CH_2CH_{ax}H_{eq}$), 1.48 – 1.64 (m, 1H, $NCH_2CH_{ax}H_{eq}CH_2$), 1.70 (dt, *J*=13.3, 3.7, 1H, $NCH_2CH_{ax}H_{eq}CH_2$), 1.79 – 1.94 (m, 3H, $NCH_2CH_2CH_{ax}H_{eq}$ + $NHCH_2CH_2CH_2COOH$), 2.08 (td, *J*=11.2, 3.0, 1H, $NCH_{ax}H_{eq}CH_2CH_2$), 2.17 – 2.31 (m, 3H, $NCH_{ax}H_{eq}CHCOO$ + $NHCH_2CH_2CH_2COOH$), 2.52 (ddt, *J*=10.6, 7.6, 3.8, 1H, NCH_2CHCOO), 2.64 (td, *J*=5.7, 3.0, 2H, NCH_2CH_2O), 2.70 – 2.78 (m, 1H, $NCH_{ax}H_{eq}CH_2CH_2$), 2.81 (t, *J*=6.9, 2H, $NHCH_2CH_2CH_2COOH$), 2.99 – 3.08 (m, 1H, $NCH_{ax}H_{eq}CHCOO$), 3.23 (qt, *J*=9.9, 5.7, 2H, NCH_2CH_2O), 3.77 (s, 6H, $C_{Ar}OCH_3$), 3.88 (s, 2H, $C_{Ar}CH_2NH$), 4.06 – 4.12 (m, 2H, $CH_2COOCH_2CH_3$), 6.82 – 6.88 (m, 4H, $CCHCHCOCH_3$), 7.28 – 7.35 (m, 6H, $CCHCHCOCH_3$ + $CCHCHCCH_2NH$), 7.44 – 7.49 (m, 2H, $CCHCHCCH_2NH$). ^{13}C NMR (126 MHz, Methanol-d_4) δ = 14.52 ($COOCH_2CH_3$), 25.25

(NCH$_2$*C*H$_2$CH$_2$), 25.61 (NHCH$_2$*C*H$_2$CH$_2$COOH), 27.68 (NCH$_2$CH$_2$*C*H$_2$), 37.06 (NHCH$_2$CH$_2$*C*H$_2$COOH), 42.82 (NCH$_2$*C*HCOO), 49.80 (NH*C*H$_2$CH$_2$CH$_2$COOH), 53.00 (C$_{Ar}$*C*H$_2$NH), 55.19 (N*C*H$_2$CH$_2$CH$_2$), 55.71 (C$_{Ar}$O*C*H$_3$), 57.05 (N*C*H$_2$CHCOO), 59.34 (N*C*H$_2$CH$_2$O), 61.57 (CHCOO*C*H$_2$CH$_3$), 62.51 (NCH$_2$*C*H$_2$O), 87.51 (NCH$_2$CH$_2$O*C*), 114.09 (CCH*C*HCOCH$_3$), 129.49 (d, CCH*C*HCCH$_2$NH + C*C*HCHCCH$_2$NH), 131.30 (C*C*HCHCOCH$_3$), 135.94 (CCHCH*C*CH$_2$NH), 137.17 (*C*CHCHCOCH$_3$), 146.80 (*C*CHCHCCH$_2$NH), 160.19 (CCHCH*C*OCH$_3$), 175.36 (*C*OOCH$_2$CH$_3$), 181.74 (CH$_2$*C*OOH). IR (KBr): ṽ = 2939, 1730, 1609, 1578, 1508, 1465, 1404, 1302, 1250, 1176, 1153, 1070, 1033, 916, 828, 582 cm^{-1}. HRMS-ESI+ *m/z* [*M*+H]$^+$ calcd for C$_{36}$H$_{46}$N$_2$O$_7$: 619.3378, found: 619.3382.

***rac*-4-{[4-({2-[3-(Ethoxycarbonyl)piperidin-1-yl]ethoxy}bis{4-methoxyphenyl}methyl)-benzyl]amino}benzoic acid (12t):** ^{1}H NMR (400 MHz, CD$_2$Cl$_2$) δ = 1.20 (t, *J*=7.1, 3H, COOCH$_2$C*H$_3$*), 1.35 – 1.47 (m, 1H, NCH$_2$CH$_2$C*H$_{ax}$*H$_{eq}$), 1.56 – 1.73 (m, 2H, NCH$_2$C*H$_{ax}$*H$_{eq}$CH$_2$ + NCH$_2$CH$_{ax}$*H$_{eq}$*CH$_2$), 1.89 – 1.99 (m, 1H, NCH$_2$CH$_2$CH$_{ax}$*H$_{eq}$*), 2.08 (td, *J*=10.9, 4.2, 1H, NC*H$_{ax}$*H$_{eq}$CH$_2$CH$_2$), 2.20 (t, *J*=11.0, 1H, NC*H$_{ax}$*H$_{eq}$CHCOO), 2.60 – 2.76 (m, 3H, NCH$_2$C*H*COO + NC*H$_2$*CH$_2$O), 2.90 (br d, *J*=11.5, 1H, NCH$_{ax}$*H$_{eq}$*CH$_2$CH$_2$), 3.09 – 3.17 (m, 1H, NCH$_{ax}$*H$_{eq}$*CHCOO), 3.21 (t, *J*=6.0, 2H, NCH$_2$C*H$_2$*O), 3.76 (s, 6H, C$_{Ar}$OCH$_3$), 4.04 – 4.10 (m, 2H, COOC*H$_2$*CH$_3$), 4.22 (s, 2H, C$_{Ar}$C*H$_2$*NH), 6.54 – 6.65 (m, 2H, CC*H*CHCCOOH), 6.77 – 6.85 (m, 4H, CCHC*H*COCH$_3$), 7.15 – 7.23 (m, 2H, CCHC*H*CCH$_2$NH), 7.27 – 7.36 (m, 4H, CC*H*CHCOCH$_3$), 7.37 – 7.45 (m, 2H, CC*H*CHCCH$_2$NH), 7.77 – 7.87 (m, 2H, CCHC*H*CCOOH). ^{13}C NMR (101 MHz, CD$_2$Cl$_2$) δ = 14.55 (COOCH$_2$*C*H$_3$), 24.56 (NCH$_2$*C*H$_2$CH$_2$), 27.32 (NCH$_2$CH$_2$*C*H$_2$), 41.75 (NCH$_2$*C*HCOO), 47.91 (C$_{Ar}$*C*H$_2$NH), 54.33 (N*C*H$_2$CH$_2$CH$_2$), 55.74 (C$_{Ar}$O*C*H$_3$), 56.02 (N*C*H$_2$CHCOO), 58.40 (N*C*H$_2$CH$_2$O), 60.86 (COO*C*H$_2$CH$_3$), 61.42 (NCH$_2$*C*H$_2$O), 86.57 (NCH$_2$CH$_2$O*C*), 112.02 (C*C*HCHCCOOH), 113.58 (CCH*C*HCOCH$_3$), 119.69 (CCHCH*C*COO), 127.71 (CCH*C*HCCH$_2$NH), 129.16 (C*C*HCHCCH$_2$NH), 130.45 (d, *J*=2.9, C*C*HCHCOCH$_3$), 132.39 (CCH*C*HCCOOH), 136.88 (d, *J*=4.5, *C*CHCHCOCH$_3$), 137.35 (CCHCH*C*CH$_2$NH), 144.91 (*C*CHCHCCH$_2$NH), 152.58 (*C*CHCHCCOO), 159.12 (CCHCH*C*OCH$_3$), 170.67 (C$_{Ar}$*C*OO), 174.24 (CH*C*OO). IR (KBr): ṽ = 2935, 2836, 1728, 1606, 1508, 1464, 1413, 1372, 1303, 1251, 1175, 1113, 1072, 1033, 918, 827, 776, 701, 583 cm^{-1}. HRMS-ESI- *m/z* [*M*-H]$^-$ calcd for C$_{39}$H$_{44}$N$_2$O$_7$: 651.3076, found: 651.3078.

Synthesis and Biological Evaluation of N-Substituted Nipecotic Acids as (*S*)-SNAP-5114 Analogues Containing Sterically Demanding Aliphatic Moieties in the Lipophilic Domain

Michael C. Böck, Georg Höfner, Klaus T. Wanner
Department of Pharmacy – Center for Drug Research
Ludwig-Maximilians-Universität München
Butenandtstraße 5-13, 81377 Munich, Germany

Abstract

A variety of N-substituted nipecotic acid derivatives were synthesized and biologically evaluated for their potential as mGAT4 inhibitors. Featuring in the lipophilic domain a sterically demanding, aliphatic group in addition to one or two aromatic moieties, the molecular structure of these compounds differs significantly from the typical triaryl pattern found in previously developed mGAT4 inhibitors such as (*S*)-SNAP-5114, DDPM-1457 and DDPM-859. The biological evaluation of the synthesized compounds revealed a tight correlation between the size and the lipophilicity of the sterically demanding group and the inhibitory potency exerted at mGAT4. In this context (*S*)-1-{2-[(adamantan-1-yl)bis(4-methoxyphenyl)methoxy]ethyl}piperidine-3-carboxylic acid was found to have a pIC_{50} value of 6.18 ± 0.11, hence constituting a distinctly more potent inhibitor than the lead substance (*S*)-SNAP-5114.

Introduction

According to the latest data from the World Health Organisation (WHO) an estimated five million people worldwide are diagnosed with epilepsy each year. Globally, more than 50 million people suffer from epilepsy,[1] affecting 1% of the population by the age 20 and 3% of the population by the age 75[2]. Epilepsy can hence be considered one of the most common neurological disorders[3], accounting for a significant proportion of the world's disease burden[1]. Treatment of epilepsy aims to enable the patient to lead an unimpaired life free of seizures and keeping the side effects of the medication to a minimum. In about 70% of cases this can

be achieved by the use of antiepileptic drugs currently available. Nevertheless, in up to 30% of the patients seizures cannot be controlled by medication effectively, leaving surgery as only expedient.[4] Hence, there is a strong need for new and effective antiepileptic drugs.

Deficient GABAergic neurotransmission is known to play a key role in the pathogenesis of epilepsy.[5,6,7] GABA (γ-aminobutyric acid) is the main inhibitory neurotransmitter in the mammalian central nervous system (CNS)[8], with estimates assuming that approximately 40% of neurons for synaptic communication are based on GABA[9]. As it is the case with most neurotransmitters, GABAergic signaling is terminated by the rapid reuptake of the molecule into presynaptic neurons, and in the present case also into surrounding glia cells.[10] This process is accomplished by specific, high-affinity transport proteins termed GABA transporters (GATs). The inhibition of these transport proteins by pharmacological agents causes an increase of the GABA concentration in the synaptic cleft, enhances GABAergic neurotransmission, and thus counteracts the development of epileptic seizures.[11,12] Hence, GAT inhibitors have emerged as promising drug candidates for the treatment of epilepsy.

Belonging to the solute carrier 6 (SLC6) gene family[13] and consisting of 12 transmembrane helices[14] the GABA transporters use the co-transport of sodium ions as a driving force to translocate their substrate against the chemical gradient existing across the cell membrane.[15] There are four GAT subtypes, termed mGAT1-4 when cloned from murine brain cells.[16,17] For all other species, including humans according to a proposal from the Human Genome Organization (HUGO), a deviant nomenclature is used that denotes these transporters as GAT1 (≙ mGAT1), BGT1 (≙ mGAT2), GAT2 (≙ mGAT3) and GAT3 (≙ mGAT4), respectively[18]. mGAT1 and mGAT4 are the dominant GAT subtypes in the mammalian brain. mGAT1 is primarily found on presynaptic neurons mediating the neuronal GABA uptake, whereas the latter is commonly expressed on astrocytes, where it conducts the glial GABA uptake.[11] mGAT1 and mGAT4 also differ in the regions of the CNS they are most prevalent. In case of mGAT1, densities are highest in spinal cord, cerebellum, basal ganglia and hippocampus, while mGAT4 is found particularly in olfactory bulb, brainstem, and diencephalon.[9,19] Since being present in low densities only and confined to specific brain structures, mGAT2 and mGAT3 play only a subordinate role in the termination of GABAergic neurotransmission in the CNS.[20,21]

To this date, Tiagabine [(*R*)-**1**, table 1, entry 1] has been the only approved anti-epileptic drug targeting the GABA uptake transporters. Being a selective and high affinity inhibitor of mGAT1,

it is used for the add-on treatment of partial-onset seizures.[22,23] Unfortunately, its side effects, including dizziness, tremor, somnolence, headache, memory loss, diarrhea, and depression,[24,25] seem to be closely linked to the function of mGAT1. Hence, other GAT subtypes, in particular mGAT4, have come into focus[18,26,27], but the role these transporter subtypes might play as potential targets for anticonvulsive therapy is still to be elucidated. This requires selective and high potency compounds as pharmacological tools. For mGAT4 (*S*)-SNAP5114 [(*S*)-**2**, table 1, entry 3] has fulfilled that role to a certain extend.[28] However, the compound is linked to a number of serious drawbacks, including moderate potency and selectivity, and a lack of chemical stability due to the tritylether function present in its lipophilic domain, which is prone to decomposition. The latter issue was successfully addressed by the development of DDPM-1457 [(*S*)-**3**, table 1, entry 4], which avoids the labile ether function by featuring an unsaturated all carbon spacer instead of an oxyethyl linker between the trityl moiety and the nipecotic acid partial structure. Furthermore, modifications of the trityl moiety, e.g. by introduction of a methyl group in the ortho position of one of the three aryl groups [(*S*)-**4**, table 1, entry 5], led to compounds with slightly improved subtype selectivity.[29] More recently, a new class of non-competitive hGAT3 (=mGAT4) inhibitors derived from isatin has been reported, with 5-(thiophen-2-yl)indoline-2,3-dione (**5**, table 1, entry 6) being the most potent compound thereof.[30]

***Table 1**. Binding affinities (pK_i) and inhibitory potencies (pIC_{50}) of reference compounds **1-5** from the literature*

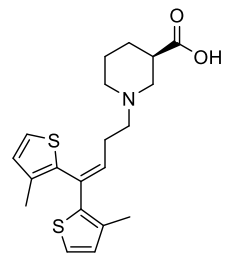

Tiagagbine [(R)-**1**]

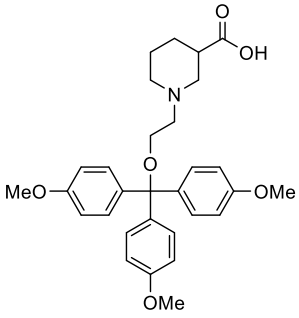

rac-SNAP-5114 [(*rac)*-**2**]

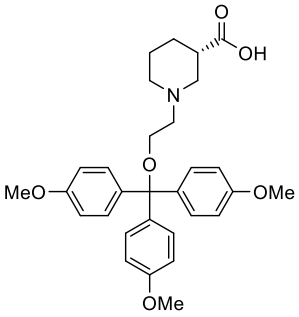

(*S*)-SNAP-5114 [(*S*)-**2**]

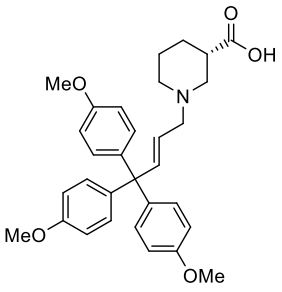

DDPM-1457 [(*S*)-**3**]

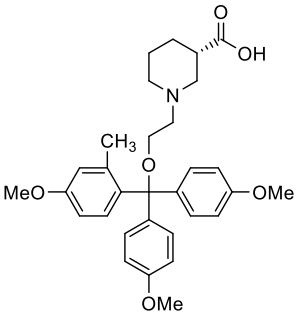

DDPM-859 [(*S*)-**4**]

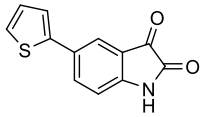

5-(Thiophen-2-yl)indoline-2,3-dione [**5**]

Entry	Compound	pK_i[a]	pIC_{50}[b]			
		mGAT1	mGAT1	mGAT2	mGAT3	mGAT4
1	Tiagabine [(*R*)-**1**][c]	7.43 ± 0.11	6.88 ± 0.12	50%	64%	73%
2	*rac*-SNAP-5114 [(*rac*)-**2**][d]	-	4.08	-	4.96	5.64 ± 0.05
3	(*S*)-SNAP-5114 [(*S*)-**2**][d]	4.56[e] ± 0.02	4.07 ± 0.09	56%	5.29 ± 0.04	5.71 ± 0.07
4	DDPM-1457 [(*S*)-**3**][d]	4.33 ± 0.06	4.40 ± 0.05	4.42 ± 0.11	5.47 ± 0.02	5.87 ± 0.08
5	DDPM-859 [(*S*)-**4**][d]	-	4.19 ± 0.07	4.12 ± 0.08	4.85 ± 0.04	5.78 ± 0.03
6	5-(Thiophen-2-yl)indoline-2,3-dione [**5**]	-	65%[f]	3.21 ± 0.19[e] 103%[f]	3.74 ± 0.14[e] 4.68 ± 0.08[f]	5.20 ± 0.05[e] 5.53 ± 0.08[f]

(a) Results of the MS Binding Assays are given as pKi ± SEM. (b) Results of the [^{3}H]GABA Uptake Assays are given as pIC_{50} ± SEM. Percent values represent remaining [^{3}H]GABA uptake in presence of 100µM compound. (c) Reference literature[31]. (d) Reference literature[29]. (e) The pIC_{50} values are taken from reference literature[30] and refer to the four human GAT subtypes hGAT1, hBGT1, hGAT2 and hGAT3, respectively. (f) The pIC_{50} values were determined using the test system developed in our research group.[32]

Despite these advances, the inhibitory potencies of the compounds developed so far remain unsatisfying, prompting the necessity for further research into the structure activity relationship (SAR) of mGAT4 inhibitors. To this end, this study aimed to synthesize and evaluate a variety of (*S*)-SNAP-5114 [(*S*)-**2**] analogues with structurally strongly modified lipophilic domains. As common denominator of these modifications sterically demanding aliphatic residues should replace one of the aromatic groups present in the parent compound, thereby departing substantially from the established trityl pattern found in previously developed (*S*)-**2** analogues (scheme 1).

For ease of discussion, the compounds to be synthesized will be divided into three subgroups hereafter which are denoted as type I, II, and III. The structure of type I compounds deviates from the parent substance only by having one of its 4-methoxyphenyl groups substituted by a sterically demanding moiety, such as a *tert*-butyl or an adamant-1-yl residue. In that context, it should also be studied how the replacement of the carboxylic acid function by an amide group and variations of the spacer length influence the inhibitory potency and selectivity of the resulting compounds. Secondly, compounds classified as type II should be synthesized that vary more substantially from the original (*S*)-**2** scaffold by one of the two remaining aromatic groups being replaced with a hydrogen atom. This will result in potential mGAT4 inhibitors exhibiting lipophilic domains with distinctly modified space requirements and reduced molecular weight. The third type concerns even smaller molecules that have an adamantane scaffold as sterically demanding group that integrates the central methyl group of the trityl moiety and thus substitutes two of the aryl residues of the lipophilic domain.

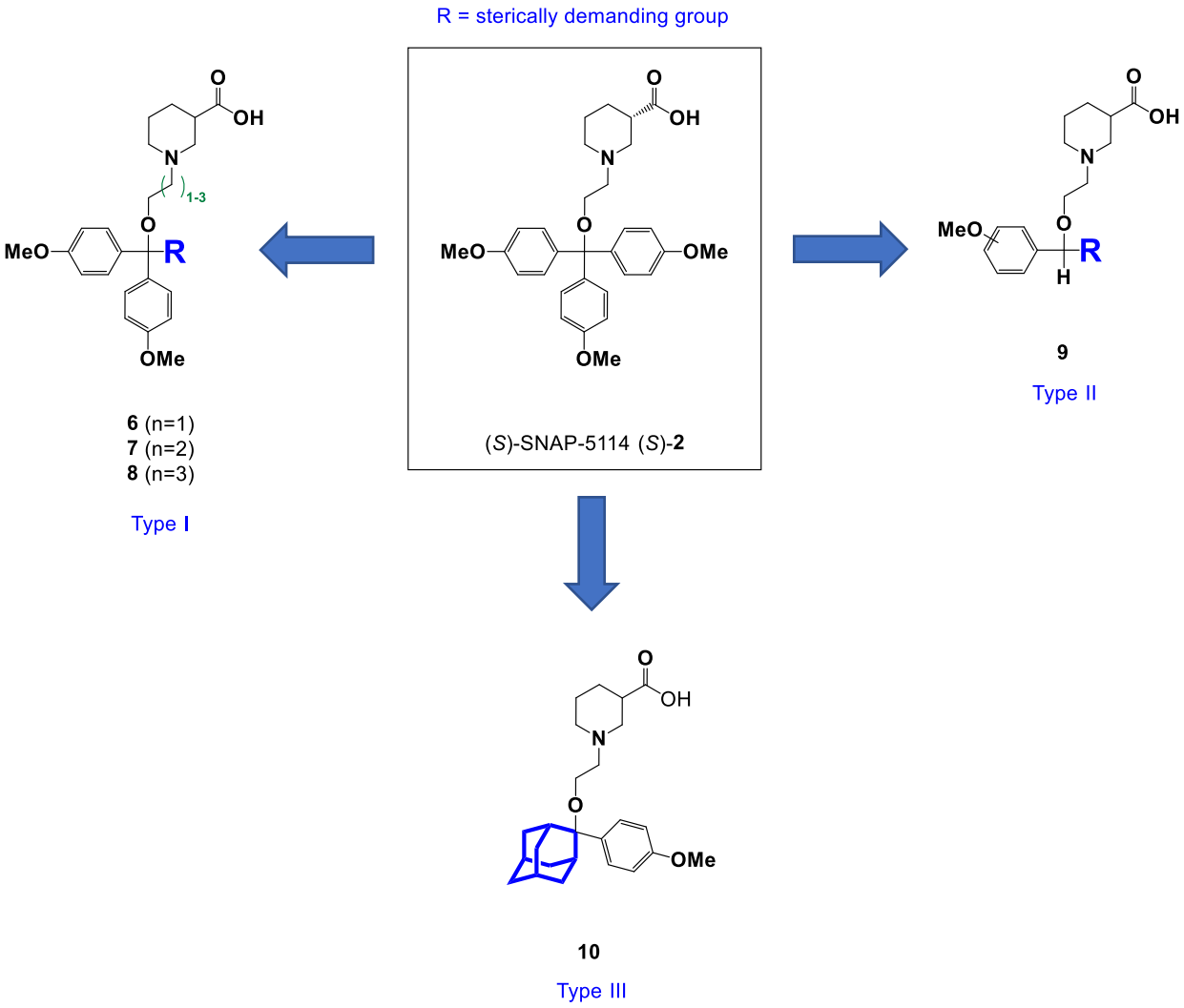

***Scheme 1**. Overview of the structure modifications of the (S)-SNAP-5114 [(S)-**2**] conducted in this study*

Results and Discussion

Chemistry

As the desired N-substituted nipecotic acids termed type I, type II, and type III are considerably different with regard to their molecular structure, the strategy for their synthesis had to be adopted accordingly. Type I compounds **6**-**8** should be accessed following the reaction sequence first described by Schirrmacher et al.[12] for the synthesis of [^{18}F] labelled (*S*)-**2** analogues (scheme 2a). By this method tertiary alcohols **15** exhibiting the required substituents are transformed into the corresponding chlorides **14**, e.g. by reaction with acetyl

chloride. Subsequent alcoholysis of the thus obtained tertiary chlorides with N-(2-hydroxyethyl)nipecotinate **11**, N-(2-hydroxypropyl)nipecotinate **12**, and N-(2-hydroxybutyl)nipecotinate **13**, respectively, provides the desired test compounds in form of their ester precursors, which, upon hydrolysis of the ester function, will furnish the free N-substituted nipecotic acids **6**-**8**.

In case of type II compounds **9** with the lipophilic domains being derived from secondary alcohols **19**, a different synthetic approach is required (scheme 2b). The etherification of benzylic alcohols with aliphatic alcohols is known to proceed under solvent free reaction conditions in presence of a Lewis acid catalyst, such as indium(III)-chloride[33]. In order to avoid side reactions affecting the ester function when reacting the benzylic alcohol with N-(2-hydroxyethyl)nipecotinate **11**, the benzyclic alcohol should be reacted with 2-chloroethanol **18** to at first establish the spacer. Introduction of the nipecotic acid partial structure in form of its ethyl ester was to follow in the subsequent reaction which should be accomplished by reacting ethyl nipecotinate **16** with the β-chloroethyl ether **17**. As it is the case with type I compounds, hydrolysis of the nipecotic acid ester function should furnish the desired nipecotic acid derivatives **9** with the free carboxylic acid function. Finally, type III compounds were intended to be synthesized analogous to the reaction sequence depicted for type II inhibitors.

Though the stereochemistry of the nipecotic acid partial structure represents an important factor when it comes to the biological activity of mGAT4 inhibitors[34], we decided to synthesize the target compounds in racemic form as this provides information on the biological activity of both enantiomers. For racemic compounds displaying similar or higher potency at mGAT4 than the benchmark inhibitor (*S*)-**2** however, additionally the pure (*R*)- and (*S*)-isomers should be synthesized and biologically evaluated. Synthesis of the enantiopure forms should be accomplished following the depicted synthetic pathway, except that the respective nipecotic acid building block (e.g. *rac*-**11**) should be replaced by the enantiopure (*R*)- and (*S*)-isomers, respectively.

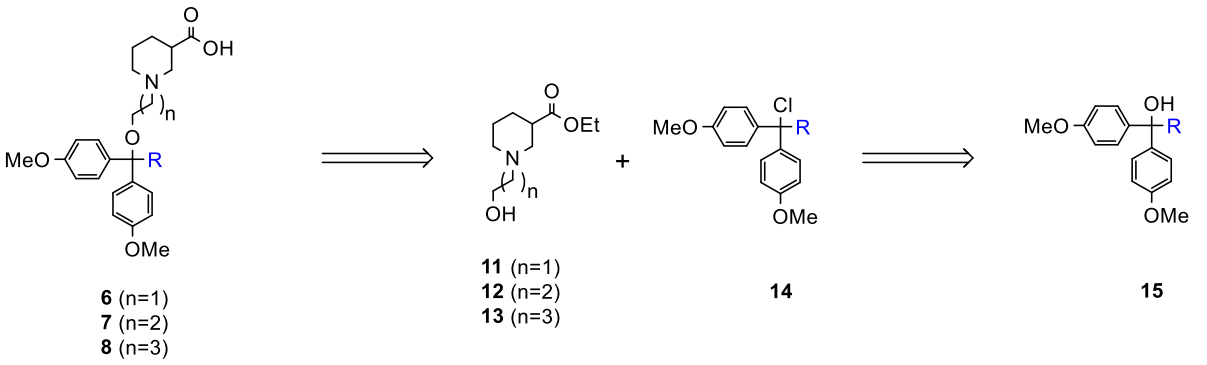

Scheme 2a**. Retrosynthetic analysis for the preparation of (S)-SNAP-5114 analogues **6 - 8

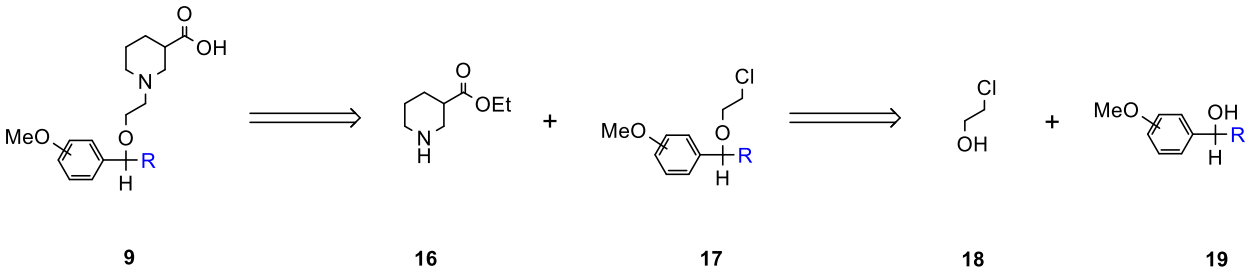

Scheme 2b**. Retrosynthetic analysis for the preparation of (S)-SNAP-5114 analogues **9

Synthesis of type I compounds

In order to construct the target compounds that differ from *rac*-SNAP-5114 [(*rac*)-**2**] by having one of the three 4-methoxyphenyl substituents in the lipophilic domain replaced by a sterically demanding aliphatic group, initially the corresponding tertiary alcohols **15a-f** had to be synthesized as building blocks. This was achieved in moderate to good yields of 48 – 91% by reaction of the appropriate electrophiles **21-26**, featuring the desired sterically hindered moieties, with 4-methoxyphenylmagnesium bromide **20** (table 2, step a). In the ensuing reaction step alcohols **15a-f** were transformed into the corresponding chlorides **14a-f** by reaction with acetyl chloride in the presence of a catalytic amount of dimethyl formamide (table 2, step b). Due to their high reactivity and susceptibility to moisture, the tertiary chlorides were without prior purification or characterization directly used for the next step, which involved alcoholysis with racemic N-(2-hydroxyethyl)nipecotic acid ethyl ester (**11**), N-(2-hydroxypropyl)nipecotic acid ethyl ester (**12**) and N-(2-hydroxybutyl)nipecotic acid ethyl ester (**13**), respectively. Thereupon, by establishing an ether bridge as part of the linker between the lipophilic domain and the nipecotic acid subunit (table 2, step c), the ethyl esters

27a-f, **28** and **29** of the desired target compounds were obtained with yields amounting to 24% to 75% over both reaction steps (referring to **15a-f** as starting material). Finally, hydrolysis of the ester function of **27a**-**f**, **28** and **29** was conducted using barium hydroxide octahydrate in methanol/water 4:1, followed by workup with carbon dioxide, which provided the target compounds **6a-f**, **7** and **8** in yields from 72% to 98% (table 3, step g). For the examination of whether the carboxylic acid group is essential for the biological activity of the respective test compounds, or may be replaced by other polar moieties that are not ionizable under physiological conditions, **27a** and the ethyl ester of *rac*-**2**[28]**,** were exemplarily transformed into the corresponding nipecotic acid amides **30** and **31** by subjection to aminolysis with ammonia. Even after prolonged time at 70 °C no product formation was observed when applying methanolic ammonia solution alone. However, upon addition of sodium cyanide (0.1 equiv), which according to literature[35] is a mild catalyst for the aminolysis of ester functions, the desired products were formed in yields of 59% (**30**) and 20% (**31**), respectively.

Table 2. *Synthesis of type I inhibitors*

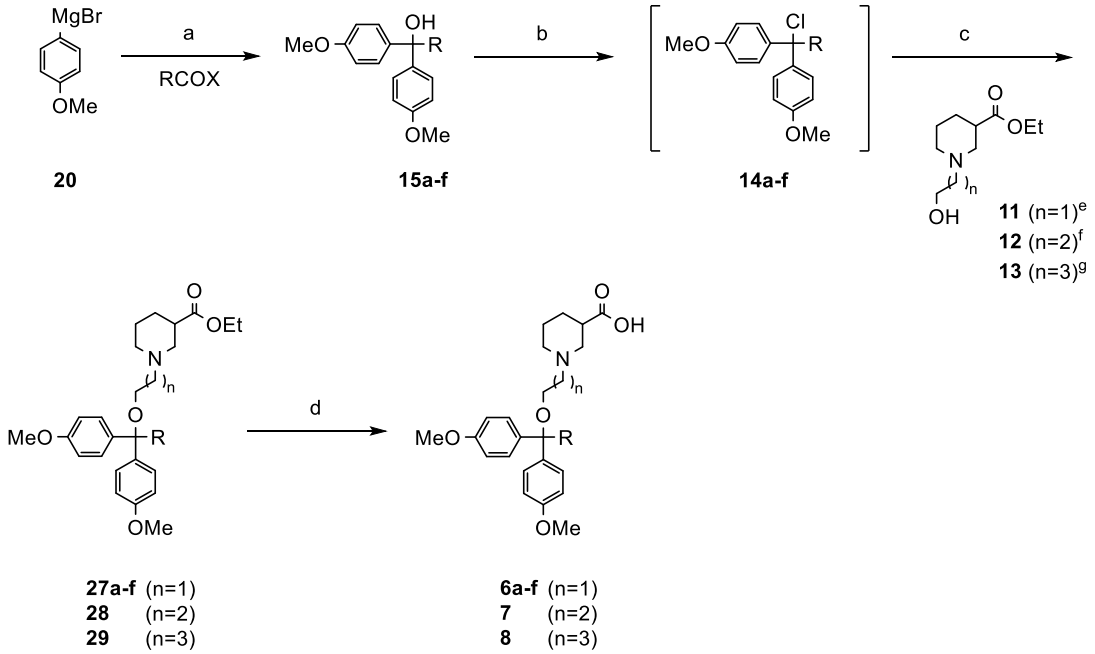

20 **15a-f** **14a-f**

11 (n=1)[e]
12 (n=2)[f]
13 (n=3)[g]

27a-f (n=1)
28 (n=2)
29 (n=3)

6a-f (n=1)
7 (n=2)
8 (n=3)

Ent.	R =	RCOX	Product step a	Yield (%)	Product step b	n	Product step c	Yield (%)[h]	Product step d	Yield (%)
1		R-COOEt **21**	**15a**	83	**14a**	1	**27a**	75	**6a**	98
2						2	**28**	86	**7**	88
3						3	**29**	24	**8**	86
4		R-COOMe **22**[i]	**15b**	80	**14b**	1	**27b**	31	**6b**	72
5		R-COOMe **23**[j]	**15c**	66	**14c**	1	**27c**	42	**6c**	89
6		R-COOMe **24**[k]	**15d**	48	**14d**	1	**27d**	35	**6d**	95
7	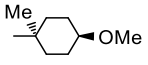	R-COOMe **25**[l]	**15e**	89	**14e**	1	**27e**	38	**6e**	84
8		R-COCl **26**	**15f**	91	**14f**	1	**27f**	39	**6f**	96

Reagents and conditions: (a) ***21-26*** *(0.45 eq), THF, rt. (b) AcCl, DMF (cat.). (c) entry 1, 4-7:* ***11*** *(1.1 eq), K_2CO_3 (2.5 eq), MeCN, rt; entry 2:* ***12*** *(1.1 eq), K_2CO_3 (2.5 eq), MeCN, rt; entry 3:* ***13*** *(1.1 eq), K_2CO_3 (2.5 eq), MeCN, rt. (d) 1. $Ba(OH)_2$ * 8 H_2O (4.0 eq), MeOH/H_2O 4:1, 2. CO_2. (e) Synthesized according to literature [36]. (f) Synthesized from ethyl nipecotinate, 3-bromopropanol (1.2 eq), K_2CO_3 (2.0 eq), KI (10mol-%), acetone, rt. (g) Synthesized from ethyl nipecotinate, 4-bromobutanol (1.2 eq), K_2CO_3 (2.0 eq), KI (10mol-%), acetone, rt. (h) Yield over step b and c. (i) Synthesized according to literature[37]. (j) Synthesized according to literature[38]. (k) Synthesized according to literature[39]. (l) Synthesized in a two-step synthesis by hydration of 4-methoxybenzoic acid methyl ester in presence of 10mol-% rhodium furnishing methyl 4-methoxycyclohexane-1-carboxylate (98% yield), followed by α-methylation according to a literature procedure described for the n-propyl derivative[40] (77 % yield).*

Synthesis of type II and type III compounds

As it is the case with type I inhibitors also for the synthesis of type II inhibitors a variety of alcohols containing the desired sterically demanding aliphatic moieties were required as building blocks for the construction of the desired analogues of *rac*-SNAP-5114 (*rac*-**2**). The preparation of these secondary alcohols was achieved in a two-step synthesis using the appropriate acid chlorides **26** and **32**-**34** as starting material, which upon reaction with 2-, 3- and 4-methoxyphenylmagnesium bromide (at 0 °C or 0 °C - rt) provided ketones **35a-f** in yields from 73 - 95% (table 3, step a). In order to obtain ketone **35g** featuring a methoxy group in the 3-position of its adamantane scaffold, **35f**, containing a bromine atom in this position, was subjected to silver tetra fluoroborate in methanol, furnishing **35g** in 92% yield. Ketones **35a-e** and **35g** were subsequently reduced to the corresponding secondary alcohols **19a-e** and **19g** in very good yields using sodium borohydride as reductant in methanol or methanol/diethyl ether (table 3, step b). The etherification of the hydroxy functions of alcohols **19a-e** and **19g** with 2-chloroethanol **18** was accomplished by treatment of the reactants with indium(III)-chloride as lewis acid catalyst furnishing the β-chloroethyl ethers **17a-e** and **17g**, again in very good yields of 90 - 99% (table 3, step c). Finally β-chloroethyl ethers **17a-e** and **17g** were reacted with *rac*-ethylnipecotinate **16** in the presence of K_2CO_3 and KI in acetonitrile under reflux conditions (table 3, step e). The N-substituted nipecotic acid esters **36a-e** and **36g**, obtained hereby in yields of 53-99 % as ~1:1 mixtures of racemic diastereomers, furnished the free nipecotic acids **9a-e** and **9g** upon hydrolysis according to the procedure described above using barium hydroxide (table 3, step e). As separation of the diastereomers by flash column chromatography proved hardly feasible at the stage of the nipecotic acid esters **36a-e** and **36g** alike the free acids **9a-e** and **9g**, the biological evaluation was performed with the aforementioned mixtures.

Table 3. *Synthesis of type II inhibitors*

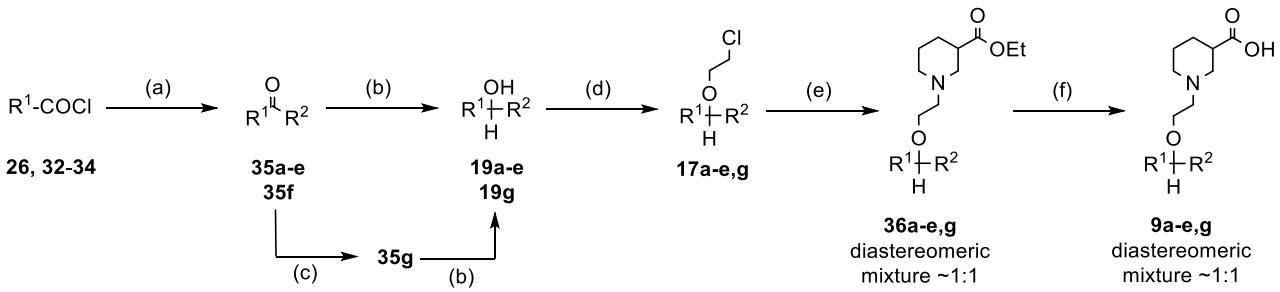

Ent.	R^1 =	R^2 =	R^1COCl	Prod. step a	Yield (%)	Prod. step b	Yield (%)	Prod. step d	Yield (%)	Prod. step e	Yield (%)	Prod. step f	Yield (%)
1		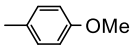	**32**[g]	**35a**	84	**19a**	91	**17a**	90	**36a**	53	**9a**	92
2		"	**26**	**35b**	95	**19b**	97	**17b**	93	**36b**	88	**9b**	97
3	"	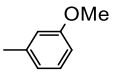	**26**	**35c**	78	**19c**	quant.	**17c**	95	**36c**	99	**9c**	79
4	"		**26**	**35d**	88	**19d**	quant.	**17d**	98	**36d**	82	**9d**	70
5	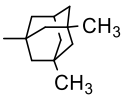	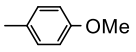	**33**[h]	**35e**	73	**19e**	quant.	**17e**	98	**36e**	87	**9e**	82
6		„	**34**[i]	**35f**	79								
7		„		**(35g**[c]**)**		**19g**	97	**17g**	97	**36g**	65	**9g**	90

Reagents and conditions: (a) entry 1-2, 5-6: 4-methoxyphenylmagnesium bromide (0.9 eq), THF, 0°C-rt; entry 3: 3-methoxyphenylmagnesium bromide (0.9 eq), THF, 0°C-rt; entry 4: 2-methoxyphenylmagnesium bromide (0.9 eq), THF, 0°C-rt; (b) $NaBH_4$ (2.0 eq), MeOH or MeOH/Et_2O 2:1, rt. (c) ***35g*** *was synthesized from* ***35f*** *by reaction with MeOH in presence of silver tetrafluoroborate (1.1 eq). (d) 2-Chloroethanol, $InCl_3$ (2mol-%). (e)* ***18*** *(1.1 eq), K_2CO_3 (2.5 eq), KI (5.0 mol-%), MeCN, reflux. (f) 1. $Ba(OH)_2$ * 8 H_2O (4.0 eq), MeOH/H_2O 4:1, 2. CO_2. (g) Synthesized according to literature[41]. (h) Synthesized according to literature[42]. (i) Synthesized according to literature[43]. (j)*

Target compound **10**, as a single example of type III derivatives, was synthesized following the procedure described for type II compounds. Hence, alcohol **37**[44] was reacted with 2-chloroethanol under indium(III)-chloride acid catalysis. Though this procedure had worked exceptionally well in case of the formation of **17a**-**e** and **17g** from the secondary alcohols **19a-e** and **19g**, this time the desired 2-chloroethyl derivate **38** could be obtained in a mediocre

yield of 44% only. The yield could, however, be raised to 71% by employing *p*-toluenesulfonic acid as catalyst. Reaction of β-chloroethyl ether **38** with ethyl nipecotinate **16** resulted in the N-substituted nipecotic acid ester **39** in 95% yield, which, after hydrolysis of the ester function with barium hydroxide, gave the desired free nipecotic acid derivative **10** (Scheme 3).

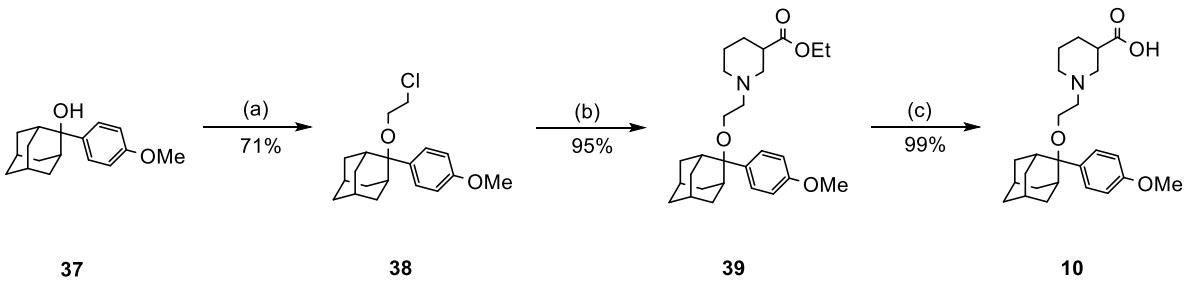

***Scheme 3**. Synthesis of **11**. Reagents and conditions: (a) **18** (2.0 eq), 4-toluenesulfonic acid (5.0 mol-%), MeCN. (b) **16** (1.1 eq), K_2CO_3 (2.5 eq), KI (5.0 mol-%), MeCN, reflux. (c) 1. $Ba(OH)_2$ * 8 H_2O (4.0 eq), MeOH/H_2O 4:1, 2. CO_2.*

Biological evaluation

The N-substituted nipecotic acids derivatives **6a-f**, **7**, **8**, **9a-e**, **9g**, and **10**, as well as their ester precursors **27a-f**, **28**, **29**, **36a-e**, **36g**, and **39**, and the nipecotic acid amides **30** and **31** were evaluated for their inhibitory potency on the four GABA transporter subtypes mGAT1-4 using a [^{3}H]GABA uptake assay previously developed by our group[32]. Based on HEK293 cells stably expressing one of the four tested GABA transporter subtypes, the tests were performed in a standardized manner. Additionally, binding affinity at mGAT1 was examined employing a MS Binding Assay with NO711 as native MS marker. The results are listed in table 4. In case of compounds that did not reduce the [^{3}H]GABA uptake to a value below 50% at 100µM compound concentration, which equates to a pIC_{50} value ≤ 4.0, only the percentage of the remaining [^{3}H]GABA uptake is given. Similarly, the percentage of the remaining marker is given if the tested compound did not cause a reduction of the MS marker binding beyond 50%. For all other compounds, potency (pIC_{50}) and binding affinity (pK_i) were determined. If the results of an experiment suggested a pIC_{50} or $pK_i \geq 5$, the experiment was repeated two times and the

standard error of mean (SEM) of the three experiments is given. Compounds displaying high pIC_{50} values at mGAT4 were additionally tested at the human analogue hGAT3.

As outlined above, the structure of the prototypic mGAT4 inhibitor *rac*-SNAP-5114 [(*S*)-**2**] was modified with respect to the triarylmethyl moiety representing the lipophilic domain, which is attached to the polar nipecotic acid unit via a linker, in order to examine the effects of such alterations on the inhibitory potency and selectivity of the compound. In particular, one of the 4-methoxyphenyl moieties of the parent compound was substituted for an aliphatic, sterically demanding group, while another was either retained or substituted for a hydrogen atom. The replacement of one of the 4-methoxyphenyl moieties of (*rac*)-**2** by a *tert*-butyl group, resulting in **6a**, was not tolerated well by mGAT4 and caused the pIC_{50} value to decline by more than one log unit from 5.64 ± 0.05 for (*rac*)-**2** (table 1, entry 2) to 4.37 for **6a** (table 4, entry 2).

To examine the role played by the length of the spacer that connects the ether oxygen atom carrying the lipophilic domain with the nipecotic acid partial structure, the homologues **7** and **8** had been synthesized. As mentioned, **6a**, which retains the C_2O-spacer of the parent compound and hence only deviates from *rac*-**2** by featuring a *tert*-butyl group in place of one of the 4-methoxyphenyl moieties, exhibits a pIC_{50} value of 4.37 (table 4, entry 2). Homologue **7**, comprising a propyleneoxy spacer instead of an ethyleneoxy spacer, is characterized by a pIC_{50} value of 4.01 (table 4, entry 4), while the potency of the butyleneoxy analogue **8** is somewhat higher with a pIC_{50} of 4.76 (table 4, entry 6). Hence, the length of the spacer exerts only little influence on the activity of these compounds.

Replacing the carboxylic acid group of the nipecotic acid partial structure by another polar moiety i.e. a carboxamide function, was performed to study the effect of the negative charge of the carboxylic acid function on the bioactivity. Interestingly, the carboxamide **30** derived from **6a** exhibits a pIC_{50} value of 4.43 (table 4, entry 35), which amounts to an activity very similar to that of the corresponding acid (**6a**, pIC_{50} = 4.37, Table 4, entry 2). However, since the potency of both of these compounds is comparatively low, this does not necessarily point to the carboxamide group being a suitable replacement for the carboxyl function of the nipecotic acid partial structure. Hence, carboxamide **31** derived from the more potent benchmark inhibitor *rac*-SNAP-5114 (*rac*-**2**) was also synthesized and tested. Showing a pIC_{50} value of 4.41 (**31**, table 4, entry 36), its potency is more than one log unit lower than that of the corresponding acid (*rac*-**2**, pIC_{50} = 5.64 ± 0.05, table 1, entry 2). Thus, in case of weak

binders such as **6a**, binding seems to be dominated by unspecified ligand-target interactions that are hardly affected by the exchange of the carboxylate by a carboxamide function.

With regard to the sterically demanding moieties introduced in place of one of the three 4-methoxyphenyl groups of *rac*-**2**, the data of the biological testing show a clear correlation between their size and the biological activity of the resulting compounds. Nipecotic acid derivative **6a**, that features a *tert*-butyl moiety in this position, has a comparatively low pIC_{50} of 4.37 (table 4, entry 2). Formally enlarging this residue to a 1-methylcyclopent-1-yl moiety leads to a compound with a distinctly higher pIC_{50} value of 5.16 ± 0.04 (**6b**, table 4, entry 8). Further expansion of the cyclopentyl ring by a methylene group causes the potency to increase to a pIC_{50} of 5.70 ± 0.10 (**6c**, table 4, entry 10), which is on par with the pIC_{50} value determined for the benchmark inhibitor *rac*-**2** (pIC_{50} = 5.64 ± 0.05, table 1, entry 2). Interestingly, **6f**, that has one of the 4-methoxyphenyl groups of the parent compound *rac*-**2** substituted by the even bulkier adamantan-1-yl rest, is characterized by a pIC_{50} value of 5.77 ± 0.09 (table 4, entry 18). This amounts to a potency nominally equal to that of **6c**, despite the difference in the size and rigidity of the respective substituents. On the grounds of their high inhibitory potency, **6c** and **6f** were also synthesized and evaluated in form of their enantiopure (*R*)- and (*S*)-isomers. As is the case with the lead compound SNAP-5114, the (*S*)-enantiomers exhibit more pronounced bioacitivity than the respective (*R*)-enantiomers. In that context, the pIC_{50} value of (*R*)-**6c** amounts to 4.89 ± 0.08 (table 4, entry 12), whereas its (*S*)-isomer is characterized by a distinctly higher pIC_{50} value of 5.76 ± 0.09 [(*S*)-**6c**, table 4, entry 11], which is equal to that of the enantiopure benchmark compound (*S*)-**2** (pIC_{50} = 5.71 ± 0.07, table 1, entry 3). Similarly, the enantiomers of **6f** exhibit pIC_{50} values of 5.26 ± 0.08 [(*R*)-**6f,** table 4, entry 19] and 6.13 ± 0.10 [(*S*)-**6f,** table 4, entry 19], respectively. Hence, (*S*)-**6f** constitutes one of the most potent mGAT4 inhibitors developed so far, with its inhibitory potency surpassing that of (*S*)-**2** by a notable margin of nominally ~0.4 log units.

The high inhibitory potency of the racemic compounds **6c** and **6f** and, even more so, of the respective enantiopure isomers (*S*)-**6c** and (S)-**6f** was confirmed by additionally testing the compounds at hGAT3, which constitutes the corresponding human transporter analogue to mGAT4. At hGAT3 the pIC_{50} value of the racemic compound **6c** amounts to 5.74 ± 0.09 (table 4, entry 10), whereas (*S*)-**6c** displays a slightly higher pIC_{50} value of 5.94 ± 0.04 (table 4, entry 11). As expected, the pIC_{50} value for (*R*)-**6c** is considerably lower (4.96 ± 0.02, table 4, entry 12) as compared to the (*S*)-enantiomer. Similarly, the pIC_{50} values at hGAT3 of the racemic

compound **6f** and its enantiopure isomers (*S*)-**6f** and (*R*)-**6f** was found to be 5.82 ± 0.09 (**6f**, table 4, entry 18), 6.18 ± 0.11 [(*S*)-**6f**, table 4, entry 19] and 5.29 ± 0.12 [(*R*)-**6f**, table 4, entry 20], respectively. Hence, for all concerning compounds the inhibitory potency displayed at hGAT3 corresponds very tightly with the results at mGAT4.

A correlation between the inhibitory potency and the size of the sterically demanding moiety in the lipophilic domain is also found with type II inhibitors, in which one of the three 4-methoxy phenyl groups of the lipophilic domain of *rac*-**2** is replaced by a sterically demanding aliphatic group and another by a hydrogen atom. While the pIC_{50} value of **9a**, that features the comparatively small 1-methylcyclohex-1-yl group as a substitute for a 4-methoxyphenyl residue, only amounts to 4.88 ± 0.08 (table 4, entry 22), a notable increase to 5.49 ± 0.01 is observed if this position is occupied by the bulkier adamantan-1-yl residue (**9b**, table 4, entry 24). However, further enlargement of the substituent by introduction of two methyl groups into 3- and 5-position of the adamantane scaffold, resulting in **9e**, causes a decrease of inhibitory potency to 5.17 ± 0.09 (table 4, entry 30), which implies that the tolerable size of the sterically demanding moiety has been exceeded in this case.

Since the three-dimensional molecular structure of type II inhibitors deviates significantly from the *rac*-**2** scaffold they were originally derived from, it could not necessarily be assumed that the contribution of the aromatic methoxy group to the biological activity is highest when located in the 4-position. In order to examine this issue, also the 3- and 2-methoxy analogues of **9b**, compounds **9c** and **9d**, were synthesized and biologically studied. As the data indicate, these variations of the position of the methoxy group are associated with a decrease of the pIC_{50} value from 5.49 ± 0.01 to 4.80 for the 3-methoxy (**9c**, table 4, entry 26) and further to 4.74 for the 2-methoxy derivative (**9d**, table 4, entry 28), indicating that the contribution of the methoxy group to the inhibitory potency of the compound is most pronounced when occupying the 4-position.

Nipecotic acid derivative **10**, that has an adamantane structure integrating the quaternary carbon atom of the $COCH_2CH_2$ linker constitutes the sole example of type III compounds, exerts comparatively weak inhibitory potency at mGAT4, its pIC_{50} amounting to 3.64 ± 0.08 (table 4, entry 34). This might be ascribed to the reduction of the overall size of the lipophilic domain of this compound as compared to the more potent type I and II inhibitors, hence resulting in an insufficient filling of the target binding site.

Compound **6d**, that has one of the 4-methoxy phenyl groups of the *rac*-**2** molecule replaced by a 4-methyltetrahydro-2H-pyran-4-yl rest, displays a pIC_{50} value of 4.76 ± 0.09 (table 4, entry 14), which equates to a potency loss of one entire log unit as compared to the carba analogue **6c** (pIC_{50} = 5.70 ± 0.10, table 4, entry 10). An almost identical pIC_{50} value of 4.70 was determined for **6e** (table 4, entry 16), which has the polar moiety located outside the cyclohexyl ring by featuring a methoxy group in the 4-position. Likewise, the introduction of a methoxy group in the 3-position of the adamant-1-yl scaffold of **9b** leads to a compound with greatly reduced potency, **9g** (75% [^{3}H]GABA at 100µM, table 4, entry 32). Therefore, it appears that mGAT4 does not tolerate the introduction of polar atoms or moieties into the sterically hindered, aliphatic residue of type I and type II inhibitors.

The ester precursors of type I inhibitors **27a**-**27f** and **28**-**29** display only moderate inhibitory potency at mGAT4, with the respective pIC_{50} values not exceeding 4.97 (**27e**, table 4, entry 15). In case of the most potent type I inhibitors **6c** and **6f**, which are characterized by an 1-methylcyclohexyl and an 1-adamantyl residue in the lipophilic domain, the potency of the corresponding esters is distinctly lower than that of the free acids, the esters reducing the [^{3}H]GABA uptake at 100µM test compound concentration only to 73.6% (**27c**, table 4, entry 9) and 95.3% (**27f**, table 4, entry 17), respectively.

On the other hand, the ester precursors of type II inhibitors **36a**-**36e** and **36g** reveal a high inhibitory potency, with the respective pIC_{50} values ranging from 4.29 (**36g** table 4, entry 31) to 5.32 ± 0.09 (**36d**, table 4, entry 27). This places the inhibitory activity of the esters in the same order of magnitude as that of the analogous free nipecotic acids. Interestingly, for all type II ester precursors the biological activity at mGAT4 is slightly or at least nominally slightly higher than that of the corresponding free carboxylic acid. There is only one exception, the most potent type II inhibitor **9b.** It possesses a distinctly higher activity than its ester analogue **36b**, with its pIC_{50} value amounting to 5.49 ± 0.01 (table 4, entry 24), whereas the corresponding ester possesses a pIC_{50} value of 4.92 (table 4, entry 23). Finally, also in case of type III inhibitor **10**, the corresponding ester **39** (pIC_{50} = 4.85, table 4, entry 33) displays a distinctly higher inhibitory potency than the free acid (**10**, pIC_{50} = 3.64 ± 0.08, table 4 entry 34). In view of the fact that the free nipecotic acid function has been shown to be essential for mGAT4 inhibitors constituting a triaryl or diaryl alkyl moiety as its lipophilic domain, it is likely that a different binding mode is involved when it comes to the ester precursors of the type II and type III inhibitors.

For the mGAT4 inhibitors with a $pIC_{50} \geq 5.0$, which includes the carboxylic acids **6b**, **6c**, **6f**, **9b**, and **9e** and the esters **36c**-**36e**, no clear subtype selectivity in favor of mGAT4 is observed. **6c**, which displays a 1-methylcyclohexyl moiety in its lipophilic domain, is characterized by a pIC_{50} value of 5.70 ± 0.10 at mGAT4. It also shows considerable activity at mGAT1 and mGAT3, with the pIC_{50} values amounting to 4.85 ± 0.02 (mGAT1) and 5.01 ± 0.03 (mGAT3), respectively, whereas the value determined for mGAT2 is somewhat lower (pIC_{50} = 4.42 ± 0.04, table 4, entry 10). Likewise, its analogue **6f**, featuring in its lipophilic domain a sterically more demanding 1-adamantyl residue, exhibits the highest activity besides at mGAT4 (pIC_{50} = 5.77 ± 0.09) at mGAT3 (pIC_{50} = 5.62 ± 0.02). The pIC_{50} values determined for the other GAT subtypes amount to 4.93 ± 0.13 (mGAT1) and 5.06 ± 0.06 (mGAT2), respectively (table 4, entry 16). Notably, the enantiopure compounds (*S*)-**6c** and (*S*)-**6f** are characterized by almost identical pIC_{50} values at mGAT1-3 as the respective racemates **6c** and **6f**, with only two exceptions: A slight increase of the inhibitory effects exerted at mGAT2 is observed in case of (*S*)-**6c** (pIC_{50} = 4.72 ± 0.06) as compared to the racemic compound **6c** (pIC_{50} = 4.42 ± 0.04). Contrarily, the activity of (*S*)-**6f** at the same transporter subtype is marginally lower than that of the corresponding racemate **6f**, with the pIC_{50} values amounting to 4.82 ± 0.04 [(*S*)-**6f**] and 5.06 ± 0.06 (**6f**), respectively.

Inhibitor **6b** on the other hand, comprising a 1-methylcyclopentyl group in its lipophilic domain, displays a somewhat more distinct selectivity pattern by exerting a pIC_{50} of 4.95 at mGAT2, which comes close to that of mGAT4 (pIC_{50} = 5.16 ± 0.04, table 4, entry 8), whereas pIC_{50} values at mGAT3 (pIC_{50} = 4.29) and mGAT1 (pIC_{50} = 4.47) are lower. A similar subtype selectivity is observed for **9b** (table 4, entry 24), that deviates more widely from the original structure of *rac*-SNAP-5114 (*rac*-**2**) by being devoid of a second aromatic moiety in the lipophilic domain. Showing in addition to its activity at mGAT4 (pIC_{50} = 5.49 ± 0.01) a relatively high inhibitory potency at mGAT2 (pIC_{50} = 5.27 ± 0.06), it is less active at mGAT1 (pIC_{50} = 4.31 ± 0.04) and mGAT3 (pIC_{50} = 5.03 ± 0.12).

Of the ester precursors of type II compounds, **36d** stands out for being a potent mGAT3 inhibitor. The pIC_{50} value at this GAT subtype amounts to 5.68 (table 4, entry 27), which is higher than the respective values for mGAT1 (pIC_{50} = 5.25), mGAT2 (pIC_{50} = 4.88) and even mGAT4 (pIC_{50} = 5.32). Interestingly, in case of its regioisomer **36c**, which differs from **36d** only by featuring the methoxy group in the aromatic 3-position instead of the 2-position, potency at mGAT3 is reduced by half a log unit to a pIC_{50} value of 5.15, whereas the potency exerted

at mGAT4 stays nearly the same (pIC_{50} = 5.24 ± 0.12, table 4, entry 25). With regard to the inhibitory activity shown at mGAT1 and mGAT2, the variations between **36c** and **36d** are somewhat smaller. In summary, no clear trend is observable for the subtype selectivity of the mGAT4 inhibitors presented in this study, and even minor structure alterations in the lipophilic domain appear to cause considerable alterations of the selectivity pattern. Regarding the binding affinity for mGAT1, there is only a mediocre correlation with the respective inhibitory potency observable. Generally, the pK_i values determined in this context are low, with only **9e** exceeding 5.0 by a noteworthy margin (pK_i = 5.36, table 4, entry 30).

***Table 4**. Binding affinities (pK_i) and inhibitory potencies (pIC_{50}) of the N-substituted nipecotic acids **6a-f, 7, 8, 9a-e, 9g** and **10**, the corresponding nipecotic acid ethyl esters **27a-f, 28, 29, 36a-e, 36g** and **39**, and amides **30** and **31**.*

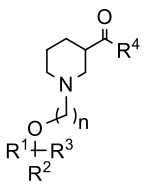

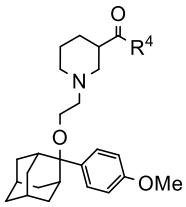

6a-f, 7, 8, 9a-e, 9g
27 a-f, 28, 29, 36a-e, **36g**
30, 31
(R^4 = OH)
(R^4 = OEt)
(R^4 = NH_2)

10 (R^4 = OH)
39 (R^4 = OEt)

Entry	Cmpd	n	R1	R2	R3	R4	pKi[a]	pIC_{50}[b] mGAT1	mGAT2	mGAT3	mGAT4	hGAT3
1	**27a**	2	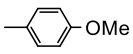	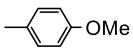		-OEt	111.9%	74.3%	68.7%	4.82	4.25	-
2	**6a**					-OH	59.0%	75.4%	68.2%	48.3%	4.37	-
3	**28**	3				-OEt	98.7%	4.42	53.9%	4.85	4.67	-
4	**7**					-OH	4.38	3.95	4.17	52.4	4.01	-
5	**29**	4				-OEt	96.7%	59.4%	4.88	4.72	4.88	-
6	**8**					-OH	5.02 ±0.04	4.27	4.32	4.18	4.76	-
7	**27b**	2	"	"		-OEt	84.3%	4.96	53.6%	4.59	4.43	-
8	**6b**					-OH	4.45	4.47	4.95	4.29	5.16 ±0.04	-
9	**27c**				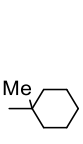	-OEt	101.0%	75.0%	54.7%	68.3%	73.6%	-
10	**6c**					-OH	4.60	4.85 ±0.02	4.42 ±0.04	5.01 ±0.03	**5.70 ±0.10**	**5.74 ±0.09**
11	(*S*)-**6c**					"	4.67	4.86 ±0.01	4.72 ±0.06	5.18 ±0.09	**5.76 ±0.09**	**5.94 ±0.04**
12	(*R*)-**6c**					"	4.79	4.67 ±0.09	4.51 ±0.02	4.70 ±0.05	4.89 ±0.08	4.96 ±0.02
13	**27d**		"	"		-OEt	91.4%	48.9%	53.6%	4.63	4.53	-
14	**6d**					-OH	78.9%	50.3%	82.3%	4.31	4.76 ±0.09	4.72 ±0.05

***Table 4** (continued).*

Entry	Cmpd	n	R1	R2	R3	R4	pKi[a]	pIC$_{50}$[b] mGAT1	mGAT2	mGAT3	mGAT4	hGAT3
15	**27e**	2	"	"	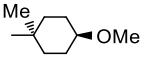	-OEt	82.8%	53.9%	4.45	5.13	4.97	-
16	**6e**					-OH	67.1%	55.3%	66.7%	57.8%	4.70	-
17	**27f**					-OEt	105.0%	77.7%	66.4%	100.0%	95.3%	-
18	**6f**		"	"		-OH	4.50	4.93 ±0.13	5.06 ±0.06	**5.62 ±0.02**	**5.77 ±0.09**	**5.82 ±0.09**
19	(*S*)-**6f**					"	4.66	5.01 ±0.08	4.82 ±0.08	5.61 ±0.03	**6.13 ±0.10**	**6.18 ±0.11**
20	(*R*)-**6f**					"	4.64	4.93 ±0.07	4.93 ±0.11	5.06 ±0.05	5.26 ±0.08	5.29 ±0.12
21	**36a**		-H	"		-OEt	4.21	4.60	4.93 ±0.14	4.87	4.90 ±0.10	-
22	**9a**					-OH	4.90	4.13	4.06	4.82	4.88 ±0.08	4.96 ±0.08
23	**36b**		"	"		-OEt	66.3%	4.62	4.57	5.03 ±0.05	4.92	-
24	**9b**					-OH	4.49 ±0.05	4.31 ±0.04	5.27 ±0.06	5.03 ±0.12	5.49 ±0.01	5.65 ±0.04
25	**36c**		"	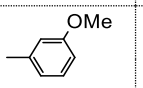	"	-OEt	71.1%	4.87	5.11 ±0.06	5.15	5.24 ±0.12	-
26	**9c**					-OH	4.44	4.93	4.93	4.99	4.80	-
27	**36d**		"		"	-OEt	76.9%	5.25	4.88	**5.68**	5.32 ±0.09	-
28	**9d**					-OH	5.05 ±0.06	4.40	4.36	5.05	4.74	-
29	**36e**		"	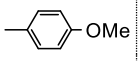	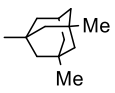	-OEt	83.1%	4.70 ±0.09	4.34 ±0.09	4.86 ±0.08	5.24 ±0.04	-
30	**9e**					-OH	5.36	4.72	4.77 ±0.02	4.96 ±0.11	5.17 ±0.09	-
31	**36g**		"	"	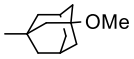	-OEt	76.4%	4.01	93.8%	4.71	4.29	-
32	**9g**					-OH	78.5%	89.0%	91.8%	75.5%	75.0%	-
33	**39**	-				-OEt	4.21	4.56	4.98	4.86	4.85	-
34	**10**					-OH	4.81 ±0.12	4.36 ±0.08	4.37 ±0.03	3.81± 0.09	3.64 ±0.08	-
35	**30**	2	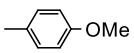	"		$-NH_2$	53.2%	4.57	4.59	4.44	4.43	-
36	**31**		"	"	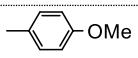	$-NH_2$	53.7%	4.21	4.14	4.36	4.41	-

(a) Results of the MS Binding Assays are given as pKi ± SEM. For compounds with low pK$_i$ values only one measurement was performed, therefore no SEM can be reported. Percent values represent remaining specific NO711 binding in presence of 100µM compound. (b) Results of the [^{3}H]GABA Uptake Assays are given as pIC$_{50}$ ± SEM. For compounds with low pIC$_{50}$ values only one measurement was performed, therefore no SEM can be reported. Percent values represent remaining [^{3}H]GABA uptake in presence of 100µM compound.

Conclusion

In order to gain insights into the structure activity relationship (SAR) of mGAT4 inhibitors, a series of N-substituted nipecotic acid derivatives was synthesized and biologically evaluated. The core feature of these compounds, having a sterically demanding aliphatic group present in the lipophilic domain in addition to one or two aromatic moieties, distinguishes them significantly from previously developed nipecotic acid derivatives such as (*S*)-SNAP-5114 [(*S*)-**2**], DDPM-1457 [(*S*)-**3**] and DDPM-859 [(*S*)-**4**], which all comprise a typical triaryl structure.

The central step in the reaction sequence leading to the test substances consisted of the etherification of secondary and tertiary alcohols featuring the required sterically hindered moieties with the appropriate alcohols containing a nipecotic acid partial structure, or a leaving group which was substituted with the appropriate nipecotic acid derivative in the ensuing reaction step. The biological evaluation of the test compounds synthesized this way revealed a tight correlation between the size of the sterically demanding group and the inhibitory potency exerted at mGAT4, whereas the introduction of polar moieties into the sterically demanding group consistently led to a notable decline in biological activity. Among the tested compounds, we identified (*S*)-1-{2-[(adamantan-1-yl)bis(4-methoxyphenyl)methoxy]ethyl}piperidine-3-carboxylic acid [(*S*)-**6f**] as an especially potent mGAT4 inhibitor. Being characterized by a pIC_{50} value of 6.13 ± 0.10, it nominally surpasses the inhibitory potency of the benchmark substance (*S*)-SNAP-5114 [(*S*)-**2**] by ~0.4 log units, albeit this comes at the expense of some loss in subtype selectivity.

Furthermore, we found N-substituted nipecotic acid derivatives that comprise only one aryl group in the lipophilic domain besides the sterically demanding aliphatic moiety to constitute potent mGAT4 inhibitors as well, with the ~1:1 mixture of the racemic diastereomers of 1-{2-[(adamantan-1-yl)(4-methoxyphenyl)methoxy]ethyl}piperidine-3-carboxylic acid (**9b**) being characterized by a pIC_{50} value of 5.49 ± 0.01. Due to the extent that the structure of these compounds differs from the prototypic mGAT4 inhibitor (*S*)-SNAP-5114, they can be regarded as a new class of mGAT4 inhibitors. Considering the desirable properties associated with the new structure motif, which include a reduced molecular weight as well as the possibility of increased chemical stability, these compounds may constitute a promising starting point for future developments.

Experimental Section

Chemistry

Moisture-sensitive reactions were carried out in oven-dried glassware under inert gas atmosphere. Commercially available starting materials were used without further purification. Dry acetonitrile (MeCN) was purchased from VWR (HiPerSolv Chromanonorm, water content > 30ppm) and Tetrahydrofuran (THF) was freshly distilled from sodium benzophenone ketyl. All other solvents were distilled prior to use. Flash column chromatography was performed on Merck silica gel 60 (mesh 0.040 - 0.063 mm) as stationary phase; thin-layer chromatography (TLC) was carried out on Merck silica gel 60 F_{254} sheets. ^{1}H and ^{13}C NMR spectra were, unless stated otherwise, recorded at room temperature with JNMR-GX (JEOL 400 or 500 MHz) or Bruker BioSpin Avance III HD (400 or 500 MHz) and integrated with the NMR software MestReNova. IR samples were measured as KBr pellets or film with Perkin-Elmer FT-IR 1600. HRMS data were obtained with JMS-GCmate II (EI, Jeol) or Thermo Finnigan LTQ FT Ultra (ESI, Thermo Finnigan).

*General procedure for the synthesis of trityl alcohols by Grignard reaction (**GP1**):* Magnesium turnings were scraped with a glass rod and suspended in dry THF. The appropriate amount of 4-bromoanisol was added. After completion of the Grignard reagent formation, a solution of the electrophile in THF was added dropwise. The mixture was stirred for the prescribed time and temperature, quenched with saturated ammonium chloride solution, diluted with water and extracted thrice with CH_2Cl_2. The combined organic phases were dried over magnesium sulfate, filtered and reduced in vacuum. The crude compound was purified by flash column chromatography.

*General procedure for the etherification of tertiary alcohols (**GP2**):* The tertiary alcohol (1.0 eq) was charged with a catalytic amount of dimethylformamide (DMF). Acetyl chloride was added and the reaction mixture was stirred at the given temperature for 24 hours, reduced in vacuum and dried under high vacuum. The oily or solid residue was solved in dry acetonitrile. Racemic, (*R*)- or (*S*)-ethyl 1-(hydroxyalkyl)nipecotinate (1.1 eq) and oven-dried potassium carbonate (2.5 eq) were added consecutively. After stirring for 16 hours at room temperature, the mixture was filtered, reduced in vacuum and purified by flash column chromatography.

*General procedure for the synthesis of ketones from acid chlorides (**GP3**):* Magnesium turnings were scraped with a glass rod and suspended in dry THF. The appropriate amount of 2-, 3-, or 4-bromoanisol (1.0 eq) was added. After completion of the Grignard reagent formation the solution was added dropwise and under intense stirring to an ice-cooled solution of the appropriate acid chloride (1.1 eq) in dry THF. The reaction mixture was allowed to warm to room temperature overnight, quenched with saturated ammonium chloride solution, diluted with water and extracted thrice with CH_2Cl_2. The combined organic phases were dried over magnesium sulfate, filtered and reduced in vacuum. The crude compound was purified by flash column chromatography.

*General procedure for reduction of ketones (**GP4**):* Sodium borohydride (2.0 eq) was added portion wise to a solution of the ketone in methanol or methanol/diethyl ether 2:1. The reaction mixture was stirred at room temperature until TLC indicated complete consumption of the educt, quenched with water (5.0 ml) and extracted thrice with CH_2Cl_2 (15.0 ml). The combined organic phases were dried over magnesium sulfate, filtered and reduced in vacuum.

*General procedure for the etherification of secondary alcohols (**GP5**):* A mixture of the secondary alcohol, 2-chloroethanol and indium(III)-chloride (2.0 mol-%) was stirred at 60°C for 24 h, reduced in vacuum and purified by flash column chromatography.

*General procedure for the N-alkylation of rac-ethyl nipecotinate (**GP6**):* A mixture the alkylating agent (1.0 eq), ethyl nipecotinate (1.1 eq), potassium iodide (5.0 mol-%) and oven-dried potassium carbonate (2.5 eq) was stirred in dry acetonitrile under reflux conditions for 48 h, filtered and reduced in vacuum. The residue was purified by flash column chromatography.

*General procedure for the hydrolysis of the ethyl ester function (**GP7**):* The ester (1.0 eq) was dissolved in methanol. Distilled water and barium hydroxide octahydrate (2.0-4.0 eq) were added and the mixture was stirred at room temperature until TLC showed full conversion. Carbon dioxide was passed through the solution until no further precipitate formed. The suspension was diluted with methanol (1:1), filtered through a paper filter and reduced in vacuum. If necessary, the crude acid was purified by flash column chromatography. The solid

residue was solved in methanol (1.0 ml), filtered through a syringe filter (Perfect-Flow®, WICOM Germany GmbH, PTFE, 0.2µM), diluted with bidest. water (4.0 ml) and lyophilized.

*General procedure for the synthesis of nipecotic acid carbamides (**GP8**):* The appropriate nipecotic acid ethyl ester was solved in saturated ammonia solution in methanol. Sodium cyanide (0.5 eq) was added and the mixture was heated in the microwave at 50°C for the appropriate time and reduced in vacuum. The residue was finally purified by flash column chromatography.

***rac*-1-{2-[1,1-Bis(4-methoxyphenyl)-2,2-dimethylpropoxy]ethyl}piperidine-3-carboxylic acid (6a)** According to GP7 from **27a** (143 mg, 0.301 mmol), barium hydroxide octahydrate (374 mg, 1.18 mmol), methanol/water 4:1 (7.5 ml). **6a** was obtained as white solid (132 mg, 98 %). ^{1}H NMR (400 MHz, MeOD + NaOD, 25°C) δ = 1.04 (s, 9H), 1.32 (qd, *J*=12.3, 3.8, 1H), 1.54 (qt, *J*=13.7, 4.5, 1H), 1.60 – 1.71 (m, 1H), 1.87 – 2.04 (m, 2H), 2.08 (t, *J*=11.3, 1H), 2.33 (tt, *J*=11.8, 3.7, 1H), 2.59 (t, *J*=6.6, 2H), 2.84 (d, *J*=11.4, 1H), 2.96 – 3.07 (m, 1H), 3.18 (ddt, *J*=9.4, 6.6, 2.9, 2H), 3.80 (s, 6H), 6.82 – 6.89 (m, 4H), 7.36 – 7.43 (m, 4H). ^{13}C NMR (101 MHz, CD_2Cl_2, 25°C) δ = 22.50, 26.87, 28.86, 40.78, 40.90, 53.54, 55.70, 56.38, 58.10, 61.08, 90.11, 112.70 (d, *J*=1.4), 132.19, 133.91 (d, *J*=7.2), 158.91, 176.67. IR (KBr): ṽ = 2957, 2836, 2041, 1714, 1608, 1510, 1463, 1393, 1364, 1297, 1251, 1175, 1086, 1037, 987, 902, 832, 811, 655, 577, 523 cm^{-1}. HRMS-ESI+ *m/z* [*M*+H]$^{+}$ calcd for $C_{27}H_{37}NO_5$: 456.2745, found: 456.2743.

***rac*-1-{2-[Bis(4-methoxyphenyl)(1-methylcyclopentyl)methoxy]ethyl}piperidine-3-carboxylic acid (6b)** According to GP7 from **27b** (31 mg, 0.060 mmol), barium hydroxide octahydrate (77 mg, 0.24 mmol), methanol/water 4:1 (3.0 ml). **6b** was obtained as white solid (21 mg, 72 %). ^{1}H NMR (400 MHz, MeOD + NaOD, 25°C) δ = 1.03 (s, 3H), 1.05 – 1.17 (m, 2H), 1.30 (qd, *J*=12.8, 4.2, 1H), 1.45 – 1.68 (m, 6H), 1.87 – 2.00 (m, 2H), 2.05 (t, *J*=11.4, 1H), 2.27 – 2.45 (m, 3H), 2.52 (td, *J*=6.5, 2.3, 2H), 2.82 (br d, *J*=11.3, 1H), 2.97 – 3.03 (m, 1H), 3.08 – 3.23 (m, 2H), 3.80 (s, 6H), 6.80 – 6.87 (m, 4H), 7.25 – 7.33 (m, 4H). ^{13}C NMR (101 MHz, MeOD + NaOD, 25°C) δ = 25.96, 26.56 (d, *J*=7.3), 26.73, 29.32, 39.15 (d, *J*=6.0), 46.41, 53.09, 55.54, 55.68, 58.85, 59.80, 62.97, 90.45, 113.23, 132.95 (d, *J*=6.5), 135.17, 159.90 (d, *J*=1.4), 182.75. IR (KBr): ṽ = 2938, 2362, 1609, 1578, 1509, 1459, 1407, 1297, 1250, 1177, 1069, 1037, 834, 785, 577 cm^{-1}. HRMS-ESI- *m/z* [*M*-H]$^{-}$ calcd for $C_{29}H_{39}NO_5$: 480.2755, found: 480.2757.

***rac*-1-{2-[Bis(4-methoxyphenyl)(1-methylcyclohexyl)methoxy]ethyl}piperidine-3-carboxylic acid (6c)** According to GP7 from **27c** (60 mg, 0.12 mmol), barium hydroxide octahydrate (146 mg, 0.463 mmol), methanol/water 4:1 (5.0 ml). **6c** was obtained as white solid (51 mg, 89 %). ^{1}H NMR (400 MHz, MeOD + NaOD, 25°C) δ = 0.93 – 1.07 (m, 4H), 1.24 – 1.72 (m, 12H), 1.87 – 2.04 (m, 2H), 2.09 (t, *J*=11.3, 1H), 2.34 (tt, *J*=11.8, 3.7, 1H), 2.62 (dd, *J*=7.2, 6.0, 2H), 2.86 (br d, *J*=11.3, 1H), 2.98 – 3.07 (m, 1H), 3.19 (tq, *J*=6.4, 2.8, 2H), 3.80 (s, 6H), 6.80 – 6.90 (m, 4H), 7.38 – 7.46 (m, 4H). ^{13}C NMR (126 MHz, MeOD + NaOD, 25°C) δ = 20.29, 23.56, 25.95, 27.01, 29.30, 34.52, 44.45, 46.38, 55.61, 55.73, 58.86, 59.73, 63.47, 91.42, 113.10, 133.16 (d, *J*=2.6), 134.44, 159.74, 182.84. IR (KBr): ṽ = 2931, 2858, 2353, 1607, 1505, 1403, 1296, 1250, 1176, 1037, 829, 772, 667, 576 cm^{-1}. HRMS-ESI- *m/z* [*M*-H]$^{-}$ calcd for $C_{30}H_{41}NO_5$: 494.2912, found: 494.2916.

(*S*)-1-{2-[Bis(4-methoxyphenyl)(1-methylcyclohexyl)methoxy]ethyl}piperidine-3-carboxylic acid [(*S*)-6c] According to GP7 from **(*S*)-27c** (27 mg, 0.052 mmol), barium hydroxide octahydrate (75 mg, 0.24 mmol), methanol/water 4:1 (2.5 ml). **(*S*)-6c** was obtained as white solid (22 mg, 88 %). The analytical data are consistent with the racemate **6c**.

(*R*)-1-{2-[Bis(4-methoxyphenyl)(1-methylcyclohexyl)methoxy]ethyl}piperidine-3-carboxylic acid [(*R*)-6c] According to GP7 from **(*R*)-27c** (38 mg, 0.072 mmol), barium hydroxide octahydrate (91 mg, 0.29 mmol), methanol/water 4:1 (5.0 ml). **(*R*)-6c** was obtained as white solid (29 mg, 81 %). The analytical data are consistent with the racemate **6c**.

***rac*-1-{2-[Bis(4-methoxyphenyl)(4-methyltetrahydro-2H-pyran-4-yl)methoxy]ethyl}piperidine-3-carboxylic acid (6d)** According to GP7 from **27d** (30 mg, 0.057 mmol), barium hydroxide octahydrate (65 mg, 0.21 mmol), methanol/water 4:1 (2.0 ml). **6d** was obtained as white solid (27 mg, 95 %). ^{1}H NMR (400 MHz, MeOD + NaOD, 25°C) δ = 1.01 – 1.14 (m, 5H), 1.24 – 1.40 (m, 1H), 1.46 – 1.70 (m, 2H), 1.88 – 2.12 (m, 3H), 2.22 – 2.40 (m, 3H), 2.62 (t, *J*=6.5, 2H), 2.83 (br d, *J*=11.5, 1H), 2.98 – 3.07 (m, 1H), 3.17 (tq, *J*=5.5, 3.2, 2H), 3.52 (t, *J*=12.0, 2H), 3.76 (dd, *J*=11.7, 5.0, 2H), 3.81 (s, 6H), 6.83 – 6.92 (m, 4H), 7.40 – 7.48 (m, 4H). ^{13}C NMR (126 MHz, MeOD + NaOD, 25°C) δ = 19.71, 25.96, 29.27, 34.95, 42.30, 46.35, 55.61, 55.83, 58.85, 59.61, 63.37, 65.36, 90.60, 113.44, 133.00, 133.40, 159.98, 182.95. IR (KBr): ṽ = 2951, 2853, 2360, 1731, 1609, 1579, 1509, 1466, 1375, 1297, 1297, 1250, 1179, 1112, 1067, 1034, 932,

857, 832, 784, 575, 561 cm^{-1}. HRMS-ESI+ *m/z* $[M+H]^+$ calcd for $C_{29}H_{39}NO_6$: 498.2850, found: : 498.2848.

***rac*-1-(2-{[(1*S*,4*S*)-4-Methoxy-1-methylcyclohexyl]bis[4-methoxyphenyl]methoxy}ethyl)-piperidine-3-carboxylic acid (6e)** According to GP7 from **27e** (30 mg, 0.054 mmol), barium hydroxide octahydrate (69 mg, 0.22 mmol), methanol/water 4:1 (5.0 ml). **6e** was obtained as white solid (24 mg, 84 %). ^{1}H NMR (500 MHz, MeOD + NaOD, 25°C) δ = 0.96 (s, 3H), 1.15 (br d, *J*=13.5, 2H), 1.32 (qd, *J*=13.0, 4.2, 1H), 1.47 – 1.61 (m, 3H), 1.62 – 1.70 (m, 1H), 1.81 (br d, *J*=14.3, 2H), 1.91 – 2.04 (m, 2H), 2.08 (t, *J*=11.4, 1H), 2.22 (br t, *J*=13.4, 2H), 2.34 (tt, *J*=11.9, 3.7, 1H), 2.55 – 2.64 (m, 2H), 2.87 (br d, *J*=11.3, 1H), 2.98 – 3.02 (m, 1H), 3.19 – 3.28 (m, 2H), 3.35 (s, 3H), 3.39 – 3.43 (m, 1H), 3.79 (s, 6H), 6.78 – 6.85 (m, 4H), 7.36 – 7.44 (m, 4H). ^{13}C NMR (126 MHz, MeOD + NaOD, 25°C) δ = 20.99, 25.96, 26.58 (d, *J*=1.9), 28.46, 29.30, 43.49, 46.36, 49.85, 55.58 (d, *J*=4.4), 55.72, 58.84, 59.86, 63.90, 75.77, 91.38, 113.03, 133.13 (d, *J*=3.2), 135.28, 159.69, 182.85. IR (KBr): ṽ = 2935, 2361, 2343, 1609, 1577, 1560, 1508, 1458, 1406, 1363, 1297, 1250, 1170, 1089, 1036, 880, 830, 787, 669, 577 cm^{-1}. HRMS-ESI+ *m/z* $[M+H]^+$ calcd for $C_{31}H_{43}NO_6$: 526.3163, found: 526.3165.

***rac*-1-{2-[(Adamantan-1-yl)bis(4-methoxyphenyl)methoxy]ethyl}piperidine-3-carboxylic acid (6f)** According to GP7 from **27f** (51 mg, 0.091 mmol), barium hydroxide octahydrate (114 mg, 0.361 mmol), methanol/water 4:1 (2.5 ml). **6f** was obtained as white solid (46 mg, 96 %). ^{1}H NMR (400 MHz, MeOD + NaOD, 25°C) δ = 1.33 (qd, *J*=13.7, 13.2, 4.7, 1H), 1.48 – 2.14 (m, 20H), 2.34 (tt, *J*=11.7, 3.8, 1H), 2.63 (br t, *J*=6.6, 2H), 2.86 (br d, *J*=11.2, 1H), 2.98 – 3.07 (m, 1H), 3.11 – 3.24 (m, 2H), 3.81 (s, 6H), 6.81 – 6.93 (m, 4H), 7.42 – 7.53 (m, 4H). ^{13}C NMR (101 MHz, MeOD + NaOD, 25°C) δ = 25.95, 29.29, 30.53, 38.19, 39.13, 43.68, 46.36, 55.63, 55.75, 58.88, 59.68, 63.30, 90.44, 113.12, 133.05, 133.80, 159.73, 182.87. IR (KBr): ṽ = 2906, 2847, 1718, 1608, 1579, 1508, 1452, 1360, 1344, 1297, 1249, 1182, 1172, 1036, 896, 836, 809, 768, 667 cm^{-1}. HRMS-ESI+ *m/z* $[M+H]^+$ calcd for $C_{33}H_{43}NO_5$: 534.3214, found: 534.3227.

(*S*)-1-{2-[(Adamantan-1-yl)bis(4-methoxyphenyl)methoxy]ethyl}piperidine-3-carboxylic acid [(*S*)-6f] According to GP7 from **(*S*)-27f** (96 mg, 0.17 mmol), barium hydroxide octahydrate (216 mg, 0.68 mmol), methanol/water 4:1 (10.0 ml). **(*S*)-6f** was obtained as white solid (82 mg, 90 %). The analytical data are consistent with *the* racemtate **6f**.

(*R*)-1-{2-[(Adamantan-1-yl)bis(4-methoxyphenyl)methoxy]ethyl}piperidine-3-carboxylic acid [(*R*)-6f] According to GP7 from **(*R*)-27f** (59 mg, 0.11 mmol), barium hydroxide octahydrate (72 mg, 0.42 mmol), methanol/water 4:1 (2.5 ml). **(*R*)-6f** was obtained as white solid (48 mg, 85 %). The analytical data are consistent with the racemate **6f**.

***rac*-1-{3-[1,1-Bis(4-methoxyphenyl)-2,2-dimethylpropoxy]propyl}piperidine-3-carboxylic acid (7)** According to GP7 from **28** (76 mg, 0.15 mmol), barium hydroxide octahydrate (194 mg, 0.615 mmol), methanol/water 4:1 (5.0 ml). **7** was obtained as white solid (62 mg, 86 %). ^{1}H NMR (400 MHz, MeOD + NaOD, 25°C) δ = 1.03 (s, 9H), 1.34 (qd, *J*=12.6, 4.0, 1H), 1.50 – 1.65 (m, 1H), 1.65 – 1.81 (m, 3H), 1.86 – 2.06 (m, 3H), 2.37 (tt, *J*=11.8, 3.8, 1H), 2.42 – 2.52 (m, 2H), 2.87 (br d, *J*=11.3, 1H), 3.01 (t, *J*=6.1, 2H), 3.07 – 3.15 (m, 1H), 3.80 (s, 6H), 6.79 – 6.88 (m, 4H), 7.34 – 7.43 (m, 4H). ^{13}C NMR (101 MHz, MeOD + NaOD, 25°C) δ = 25.97, 28.44, 29.04, 29.47, 41.57, 46.25, 55.02, 55.79, 57.68, 58.33, 63.79, 89.74, 113.15, 132.80, 135.00, 159.73, 183.00. IR (KBr): ṽ = 2934, 2361, 1630, 1509, 1461, 1397, 1295, 1250, 1175, 1077, 1038, 832, 668 cm^{-1}. HRMS-ESI- *m/z* [*M*-H]$^{-}$ calcd for $C_{28}H_{39}NO_5$: 468.2755, found: 468.2760.

***rac*-1-{4-[1,1-Bis(4-methoxyphenyl)-2,2-dimethylpropoxy]butyl}piperidine-3-carboxylic acid (8)** According to GP7 from **29** (76 mg, 0.15 mmol), barium hydroxide octahydrate (188 mg, 0.596 mmol), methanol/water 4:1 (3.0 ml). **8** was obtained as white solid (63 mg, 88 %). ^{1}H NMR (400 MHz, MeOD + NaOD, 25°C) δ = 1.04 (s, 9H), 1.35 (qd, *J*=12.7, 4.2, 1H), 1.49 – 1.75 (m, 6H), 1.89 (td, *J*=11.8, 2.9, 1H), 1.94 – 2.05 (m, 2H), 2.29 – 2.45 (m, 3H), 2.88 (br d, *J*=11.4, 1H), 2.99 (t, *J*=6.1, 2H), 3.09 – 3.17 (m, 1H), 3.80 (s, 6H), 6.81 – 6.87 (m, 4H), 7.35 – 7.43 (m, 4H). ^{13}C NMR (126 MHz, MeOD + NaOD, 25°C) δ = 24.47, 25.94, 29.03, 29.53, 29.55, 41.56, 46.32, 55.03, 55.68, 58.30, 60.36, 65.11, 89.65, 113.09, 132.82, 135.10, 159.74, 182.86. IR (KBr): ṽ = 2954, 1608, 1579, 1508, 1462, 1441, 1401, 1296, 1251, 1174, 1076, 1038, 930, 902, 832, 811, 794, 632, 595, 577, 525, 495 cm^{-1}. HRMS-ESI+ *m/z* [*M*+H]$^{+}$ calcd for $C_{29}H_{41}NO_5$: 484.3058, found: 484.3053.

***rac*-1-{2-[(1*R*)(4-Methoxyphenyl)(1-methylcyclohexyl)methoxy]ethyl}(3*R*)-piperidine-3-carboxylic acid and *rac*-1-{2-[(1*S*)(4-Methoxyphenyl)(1-methylcyclohexyl)methoxy]ethyl}-(3*R*)-piperidine-3-carboxylic acid ~1:1 (9a)** According to GP7 from **36a** (62 mg, 0.15 mmol), barium hydroxide octahydrate (188 mg, 0.596 mmol), methanol/water 4:1 (5.0 ml). **9a** was

obtained as white solid (53 mg, 93 %). ^{1}H NMR (500 MHz, MeOD + NaOD, 25°C) δ = 0.80 (s, 3H), 0.96 – 1.06 (m, 1H), 1.13 – 1.62 (m, 11H), 1.63 – 1.71 (m, 1H), 1.90 – 2.05 (m, 2H), 2.10 (q, *J*=11.6, 1H), 2.30 – 2.40 (m, 1H), 2.51 – 2.64 (m, 2H), 2.89 (br t, *J*=12.4, 1H), 3.03 (br d, *J*=11.3, 1H), 3.29 – 3.36 (m, 1H), 3.43 (dq, *J*=9.9, 6.1, 1H), 3.78 (s, 3H), 3.92 (s, 1H), 6.83 – 6.94 (m, 2H), 7.11 – 7.21 (m, 2H). ^{13}C NMR (126 MHz, MeOD + NaOD, 25°C) δ = 19.86, 22.93 (d, *J*=7.6), 25.92, 27.62, 29.27 (d, *J*=2.7), 35.43, 35.63, 39.13, 46.23, 55.25 (d, *J*=9.4), 55.87, 58.64 (d, *J*=14.1), 59.42 (d, *J*=10.2), 67.91 (d, *J*=17.7), 91.27, 113.97, 130.78, 132.44, 160.34, 183.03. IR (KBr): ṽ = 2928, 2857, 2360, 2342, 1610, 1568, 1511, 1466, 1404, 1247, 1174, 1094, 1037, 836, 668, 652 cm^{-1}. HRMS-ESI+ *m/z* [*M*+H]$^{+}$ calcd for $C_{23}H_{35}NO_4$: 390.2639, found: 390.2636.

***rac*-1-{2-[(1*R*)(Adamantan-1-yl)(4-methoxyphenyl)methoxy]ethyl}(3*R*)-piperidine-3-carboxylic acid and *rac*-1-{2-[(1*S*)(Adamantan-1-yl)(4-methoxyphenyl)methoxy]ethyl}(3*R*)-piperidine-3-carboxylic acid ~1:1 (9b)** According to GP7 from **36b** (78 mg, 0.17 mmol), barium hydroxide octahydrate (217 mg, 0.688 mmol), methanol/water 4:1 (5.0 ml). **9b** was obtained as white solid (71 mg, 97 %). ^{1}H NMR (400 MHz, MeOD + NaOD, 25°C) δ = 1.29 – 1.74 (m, 15H), 1.87 – 2.17 (m, 6H), 2.34 – 2.45 (m, 1H), 2.53 – 2.69 (m, 2H), 2.92 (br t, *J*=11.3, 1H), 3.05 – 3.14 (m, 1H), 3.28 – 3.39 (m, 1H), 3.40 – 3.53 (m, 1H), 3.71 (d, *J*=2.2, 1H), 3.81 (s, 3H), 6.84 – 6.93 (m, 2H), 7.09 – 7.18 (m, 2H). ^{13}C NMR (101 MHz, MeOD + NaOD, 25°C) δ = 25.96, 29.36 (d, *J*=2.4), 29.90, 38.35 (d, *J*=1.9), 39.72, 46.35, 55.32 (d, *J*=1.6), 55.72, 58.67 (d, *J*=11.1), 59.41 (d, *J*=7.4), 67.93 (d, *J*=11.4), 92.35, 113.91, 130.70, 131.91, 160.44, 182.81. IR (KBr): ṽ = 2904, 2847, 2360, 2342, 1615, 1560, 1510, 1457, 1405, 1247, 1172, 1092, 1037, 832, 668 cm^{-1}. HRMS-ESI+ *m/z* [*M*+H]$^{+}$ calcd for $C_{26}H_{37}NO_4$: 428.2795, found: 428.2798.

***rac*-1-{2-[(1*R*)(Adamantan-1-yl)(3-methoxyphenyl)methoxy]ethyl}(3*R*)-piperidine-3-carboxylic acid and *rac*-1-{2-[(1*S*)(Adamantan-1-yl)(3-methoxyphenyl)methoxy]ethyl}(3*R*)-piperidine-3-carboxylic acid ~1:1 (9c)** According to GP7 from **36c** (70 mg, 0.15 mmol), barium hydroxide octahydrate (197 mg, 0.624 mmol), methanol/water 4:1 (5.0 ml). **9c** was obtained as white solid (52 mg, 79 %). ^{1}H NMR (500 MHz, MeOD + NaOD, 25°C) δ = 1.26 – 1.38 (m, 1H), 1.42 – 1.50 (m, 3H), 1.50 – 1.62 (m, 4H), 1.63 – 1.72 (m, 7H), 1.86 – 1.93 (m, 3H), 1.93 – 2.05 (m, 2H), 2.11 (td, *J*=11.3, 7.9, 1H), 2.36 (tq, *J*=11.4, 3.7, 1H), 2.53 – 2.67 (m, 2H), 2.91 (br t, *J*=10.2, 1H), 3.02 – 3.11 (m, 1H), 3.31 – 3.37 (m, 1H), 3.46 (dq, *J*=9.8, 6.3, 1H), 3.71 (d, *J*=1.7, 1H), 3.78 (s, 3H), 6.75 – 6.84 (m, 3H), 7.21 (t, *J*=7.8, 1H). ^{13}C NMR (126 MHz, MeOD + NaOD,

25°C) δ = 25.95 (d, *J*=2.3), 29.33, 29.89, 38.27, 38.31, 39.79, 46.28, 55.30, 55.73 (d, *J*=2.2), 58.68 (d, *J*=10.0), 59.40 (d, *J*=6.6), 68.13 (d, *J*=3.3), 92.73 (d, *J*=1.9), 113.67 (d, *J*=3.2), 115.25, 122.28, 129.45, 141.69, 160.58, 182.89. IR (KBr): ṽ = 2906, 2847, 1583, 1488, 1451, 1403, 1315, 1283, 1256, 1151, 1942, 873, 793, 779, 742, 702, 632, 595, 525, 495 cm^{-1}. HRMS-ESI+ *m/z* $[M+H]^+$ calcd for $C_{26}H_{37}NO_4$: 428.2795, found: 428.2794.

***rac*-1-{2-[(1*R*)(Adamantan-1-yl)(2-methoxyphenyl)methoxy]ethyl}(3*R*)-piperidine-3-carboxylic acid and *rac*-1-{2-[(1*S*)(Adamantan-1-yl)(2-methoxyphenyl)methoxy]ethyl}(3*R*)-piperidine-3-carboxylic acid ~1:1 (9d)** According to GP7 from **36d** (50 mg, 0.11 mmol), barium hydroxide octahydrate (140 mg, 0.444 mmol), methanol/water 4:1 (5.0 ml). **9d** was obtained as white solid (33 mg, 70 %). ^{1}H NMR (400 MHz, MeOD + NaOD, 25°C) δ = 1.25 – 1.80 (m, 15H), 1.83 – 2.15 (m, 6H), 2.35 (ddt, *J*=15.2, 11.3, 3.6, 1H), 2.48 – 2.65 (m, 2H), 2.89 (t, *J*=12.6, 1H), 3.00 – 3.09 (m, 1H), 3.24 – 3.33 (m, 1H), 3.33 – 3.41 (m, 1H), 3.78 (s, 3H), 4.37 (s, 1H), 6.88 – 6.98 (m, 2H), 7.18 – 7.29 (m, 2H). ^{13}C NMR (126 MHz, MeOD + NaOD, 25°C) δ = 25.92, 29.31, 29.92, 38.42, 39.02, 39.36, 46.26, 55.28, 55.74, 58.67 (d, *J*=18.0), 59.38 (d, *J*=10.9), 67.91 (d, *J*=12.3), 84.04, 111.30, 120.83, 128.27, 129.25, 129.90, 159.77, 182.95. IR (KBr): ṽ = 2904, 2848, 2360, 1600, 1489, 1458, 1397, 1362, 1315, 1281, 1238, 1089, 1000, 932, 755, 668 cm^{-1}. HRMS-ESI+ *m/z* $[M+H]^+$ calcd for $C_{26}H_{37}NO_4$: 428.2795, found: 428.2793.

***rac*-1-{2-[(1*R*)(3,5-Dimethyladamantan-1-yl)(4-methoxyphenyl)methoxy]ethyl}(3*R*)-piperidine-3-carboxylic acid and *rac*-1-{2-[(1*S*)(3,5-Dimethyladamantan-1-yl)(4-methoxyphenyl)methoxy]ethyl}(3*R*)-piperidine-3-carboxylic acid ~1:1 (9e)** According to GP7 from **36e** (68 mg, 0.14 mmol), barium hydroxide octahydrate (178 mg, 0.564 mmol), methanol/water 4:1 (5.0 ml). **9e** was obtained as white solid (52 mg, 82 %). ^{1}H NMR (400 MHz, MeOD + NaOD, 25°C) δ = 0.78 (s, 6H), 0.97 – 1.14 (m, 4H), 1.22 – 1.42 (m, 8H), 1.47 – 1.74 (m, 3H), 1.93 – 2.05 (m, 3H), 2.11 (td, *J*=11.4, 6.3, 1H), 2.33 – 2.45 (m, 1H), 2.53 – 2.67 (m, 2H), 2.92 (br t, *J*=12.6, 1H), 3.03 – 3.13 (m, 1H), 3.28 – 3.37 (m, 1H), 3.45 (dq, *J*=9.8, 6.1, 1H), 3.76 (d, *J*=1.9, 1H), 3.81 (s, 3H), 6.85 – 6.92 (m, 2H), 7.10 – 7.17 (m, 2H). ^{13}C NMR (126 MHz, MeOD + NaOD, 25°C) δ = 25.96, 29.37 (d, *J*=3.6), 30.95, 31.39, 31.92 (d, *J*=1.2), 38.27, 40.36, 44.54, 46.04 (d, *J*=4.0), 46.32, 52.47, 55.29, 55.72, 58.65 (d, *J*=15.5), 59.38 (d, *J*=9.8), 67.88 (d, *J*=17.4), 91.92, 113.93, 130.68, 131.98, 160.46, 182.78. IR (KBr): ṽ = 2899, 2365, 1611, 1510, 1458, 1400, 1356, 1247,

1173, 1099, 1037, 834, 669, 569 cm^{-1}. HRMS-ESI+ *m/z* $[M+H]^+$ calcd for $C_{28}H_{41}NO_4$: 456.3108, found: 456.3109.

***rac*-1-{2-[(1*R*)(3-Methoxyadamantan-1-yl)(4-methoxyphenyl)methoxy]ethyl}(3*R*)-piperidine-3-carboxylic acid and *rac*-1-{2-[(1*S*)(3-Methoxyadamantan-1-yl)(4-methoxyphenyl)methoxy]ethyl}(3*R*)-piperidine-3-carboxylic acid ~1:1 (9g)** According to GP7 from **36g** (56 mg, 0.12 mmol), barium hydroxide octahydrate (146 mg, 0.463 mmol), methanol/water 4:1 (5.0 ml). **9g** was obtained as white solid (48 mg, 90 %). ^{1}H NMR (400 MHz, MeOD + NaOD, 25°C) δ = 1.23 – 1.74 (m, 15H), 1.92 – 2.19 (m, 5H), 2.37 (tt, *J*=11.5, 3.8, 1H), 2.53 – 2.67 (m, 2H), 2.90 (br t, *J*=10.2, 1H), 3.03 – 3.11 (m, 1H), 3.19 (s, 3H), 3.32 – 3.37 (m, 1H), 3.44 (dt, *J*=11.4, 5.6, 1H), 3.79 (s, 3H), 3.81 (d, *J*=2.0, 1H), 6.85 – 6.92 (m, 2H), 7.10 – 7.17 (m, 2H). ^{13}C NMR (126 MHz, MeOD + NaOD, 25°C) δ = 25.96, 29.34, 31.65, 37.03, 38.62 (d, *J*=5.0), 38.77, 41.55 (d, *J*=2.4), 41.97, 42.96 (d, *J*=4.6), 46.32, 55.31, 55.76, 58.65 (d, *J*=10.8), 59.38 (d, *J*=6.9), 67.90 (d, *J*=11.7), 74.72, 91.34, 114.07, 130.66, 131.60, 160.59, 182.83. IR (KBr): ṽ = 2925, 2852, 2357, 2339, 1614, 1513, 1455, 1403, 1247, 1171, 1079, 838, 787, 561 cm^{-1}. HRMS-ESI+ *m/z* $[M+H]^+$ calcd for $C_{27}H_{39}NO_5$: 458.2901, found: 458.2902.

***rac*-1-(2-{[2-(4-Methoxyphenyl)adamantan-2-yl]oxy}ethyl)piperidine-3-carboxylic acid (10)** According to GP7 from **39** (75 mg, 0.17 mmol), barium hydroxide octahydrate (214 mg, 0.678 mmol), methanol/water 4:1 (5.0 ml). **10** was obtained as white solid (70 mg, 99 %). ^{1}H NMR (500 MHz, CD_2Cl_2, 25°C) δ = 1.43 – 1.90 (m, 14H), 2.10 (br s, 1H), 2.22 – 2.62 (m, 9H), 2.76 (br s, 1H), 3.05 (t, *J*=5.5, 2H), 3.79 (s, 3H), 6.83 – 6.92 (m, 2H), 7.40 (br d, *J*=8.2, 2H). ^{13}C NMR (101 MHz, CD_2Cl_2, 25°C) δ = 22.82, 27.12, 27.41, 28.32, 33.29 (d, *J*=1.9), 33.97, 34.86, 34.94, 38.15, 41.31, 52.78, 55.55, 56.07 (d, *J*=11.1), 57.75, 80.36, 113.59, 128.99, 133.67, 159.02, 177.84. IR (KBr): ṽ = 2908, 2853, 1608, 1514, 1448, 1393, 1300, 1256, 1202, 1183, 1034, 937, 917, 825, 737, 621, 580, 549 cm^{-1}. HRMS-ESI+ *m/z* $[M+H]^+$ calcd for $C_{25}H_{35}NO_4$: 414.2639, found: 414.2643.

***rac*-Ethyl 1-(3-hydroxypropyl)piperidine-3-carboxylate (12)** A mixture of ethyl nipecotinate (1.82 g, 11.1 mmol), 3-bromo-1-butanol (1.38 g, 10.0 mmol) and potassium carbonate (3.46 g, 25.0 mmol) in acetone (20.0 ml) was stirred at rt for 72 h, filtered and reduced in vacuum. After purification by flash column chromatography (eluent: diethyl ether + 5 % triethyl amine)

12 was obtained as pale yellowish oil (1.49 g, 69 %). ^{1}H NMR (400 MHz, CD_2Cl_2, 25°C) δ = 1.24 (t, *J*=7.1, 3H), 1.38 – 1.60 (m, 2H), 1.61 – 1.79 (m, 3H), 1.81 – 1.96 (m, 1H), 2.04 (br t, *J*=9.7, 1H), 2.19 (br t, *J*=10.2, 1H), 2.50 (tt, *J*=10.2, 4.0, 1H), 2.55 – 2.60 (m, 2H), 2.81 (br d, *J*=11.2, 1H), 3.03 (br d, *J*=10.6, 1H), 3.71 (t, *J*=5.2, 2H), 4.10 (q, *J*=7.1, 2H), 4.68 (br s, 1H). ^{13}C NMR (101 MHz, CD_2Cl_2, 25°C) δ = 14.55, 25.16, 27.38, 28.06, 42.45, 54.37, 56.38, 59.67, 60.86, 64.84, 174.24. IR (KBr): ṽ = 3414, 2946, 2816, 1731, 1471, 1448, 1373, 1311, 1183, 1151, 1105, 1066, 1031, 862, 803, 752, 669, 496 cm^{-1}. HRMS+EI *m/z* $[M]^+$ calcd for $C_{11}H_{21}NO_3$: 215.1521, found: 215.1530.

***rac*-Ethyl 1-(4-hydroxybutyl)piperidine-3-carboxylate (13)** A mixture of ethyl nipecotinate (810 mg, 5.00 mmol), 4-chloro-1-butanol (543 mg, 5.00 mmol), potassium carbonate (2.07 g, 15.0 mmol) and potassium iodide (166 mg, 1.00 mmol) in acetonitrile (10.0 ml) was heated under reflux for 24 h, filtered and reduced in vacuum. After purification by flash column chromatography (eluent: ethyl acetate + 4 % triethyl amine) **13** was obtained as pale yellowish oil (886 mg, 77 %). ^{1}H NMR (400 MHz, CD_2Cl_2, 25°C) δ = 1.23 (t, *J*=7.1, 3H), 1.36 – 1.48 (m, 1H), 1.50 – 1.77 (m, 7H), 1.87 – 2.06 (m, 2H), 2.15 (t, *J*=10.9, 1H), 2.32 – 2.40 (m, 2H), 2.54 (tt, *J*=10.7, 3.9, 1H), 2.81 (br d, *J*=11.1, 1H), 3.02 (br d, *J*=11.4, 1H), 3.41 – 3.52 (m, 2H), 4.09 (m, 2H). ^{13}C NMR (101 MHz, CD_2Cl_2, 25°C) δ = 14.54, 24.87, 25.97, 27.52, 33.22, 42.09, 54.16, 55.85, 59.39, 60.85, 63.03, 174.22. IR (KBr): ṽ = 3427, 2940, 1732, 1635, 1470, 1455, 1372, 1311, 1181, 1152, 1093, 1033, 862, 790, 668, 579 cm^{-1}. HRMS-ESI+ *m/z* $[M+H]^+$ calcd for $C_{12}H_{23}NO_3$: 230.1751, found: 230.1751.

1,1-Bis(4-methoxyphenyl)-2,2-dimethylpropan-1-ol (15a) According to GP1 from magnesium (941 mg, 38.7 mmol), 4-bromoanisol (7.47 g, 38.7 mmol), THF (40.0 ml) and ethyl pivalate (2.48 g, 19.1 mmol). After purification by flash column chromatography (eluent: pentane/diethyl ether 6 : 1) **15a** was obtained as white solid (5.17 g, 90 %). ^{1}H NMR (400 MHz, $CDCl_3$, 25°C) δ = 1.15 (s, 9H), 2.17 (s, 1H), 3.78 (s, 6H), 6.74 – 6.82 (m, 4H), 7.38 – 7.46 (m, 4H). ^{13}C NMR (101 MHz, $CDCl_3$, 25°C) δ = 27.63, 39.45, 55.30, 82.62, 112.55, 129.80, 138.74, 158.06. IR (KBr): ṽ = 3528, 2957, 2835, 1608, 1508, 1463, 1294, 1250, 1177, 1037, 998, 890, 830, 811, 787 cm^{-1}. HRMS+EI *m/z* $[M]^+$ calcd for $C_{19}H_{24}O_3$: 300.1726, found: 300.1729.

Bis(4-methoxyphenyl)(1-methylcyclopentyl)methanol (15b) According to GP1 from magnesium (156 mg, 6.42 mmol), 4-bromoanisol (1.23 g, 6.38 mmol), THF (6.0 ml) and methyl 1-methylcyclopentane-1-carboxylate (412 mg, 2.90 mmol). After purification by flash column chromatography (eluent: pentane/diethyl ether 7 : 3) **15b** was obtained as colorless oil (1.05 g, 80 %). ^{1}H NMR (400 MHz, CD_2Cl_2, 25°C) δ = 1.15 (s, 3H), 1.35 – 1.47 (m, 4H), 1.55 – 1.66 (m, 2H), 2.07 – 2.19 (m, 2H), 2.26 (s, 1H), 3.77 (s, 6H), 6.74 – 6.83 (m, 4H), 7.27 – 7.38 (m, 4H). ^{13}C NMR (101 MHz, CD_2Cl_2, 25°C) δ = 26.12, 26.69, 37.66, 51.39, 55.67, 83.61, 112.93, 130.25, 139.54, 158.62. IR (KBr): ṽ = 2956, 2357, 1608, 1508, 1463, 1455, 1278, 1296, 1248, 1177, 1118, 1036, 829, 810, 782 cm^{-1}. HRMS+EI *m/z* [*M-OH*]$^{+}$ calcd for $C_{21}H_{26}O_3$: 309.1806, found: 309.1807.

Bis(4-methoxyphenyl)(1-methylcyclohexyl)methanol (15c) According to GP1 from magnesium (301 mg, 12.4 mmol), 4-bromoanisol (2.39 g, 12.4 mmol), THF (12.0 ml) and methyl 1-methylcyclohexane-1-carboxylate (950 mg, 6.08 mmol). After purification by flash column chromatography (eluent: pentane/diethyl ether 9 : 1) **15c** was obtained as white solid (135 mg, 66 %). ^{1}H NMR (500 MHz, CD_2Cl_2, 25°C) δ = 1.10 (qt, *J*=12.9, 3.8, 1H), 1.17 (s, 3H), 1.42 – 1.77 (m, 9H), 2.33 (s, 1H), 3.81 (s, 6H), 6.79 – 6.87 (m, 4H), 7.43 – 7.51 (m, 4H). ^{13}C NMR (126 MHz, CD_2Cl_2, 25°C) δ = 19.46, 22.75, 26.49, 33.13, 42.46, 55.66, 83.53, 112.77, 130.49, 138.93, 158.52. IR (KBr): ṽ = 3482, 2881, 1607, 1582, 1510, 1453, 1464, 1360, 1298, 1253, 1186, 826, 810, 765, 639, 608, 582, 533 cm^{-1}. HRMS-ESI+ *m/z* [*M-OH*]$^{+}$ calcd for $C_{22}H_{28}O_3$: 323.2006, found: 323.2005.

Bis(4-methoxyphenyl)(4-methyltetrahydro-2H-pyran-4-yl)methanol (15d) According to GP1 from magnesium (98 mg, 4.0 mmol), 4-bromoanisol (777 mg, 4.03 mmol), THF (12.0 ml) and methyl 4-methyltetrahydro-2H-pyran-4-carboxylate (319 mg, 2.01 mmol). After purification by flash column chromatography (eluent: pentane/diethyl ether 7 : 3) **15d** was obtained as white solid (329 mg, 48 %). ^{1}H NMR (400 MHz, CD_2Cl_2, 25°C) δ = 1.20 (s, 3H), 1.28 – 1.37 (m, 2H), 2.13 (td, *J*=13.1, 5.3, 2H), 2.29 (s, 1H), 3.54 (ddd, *J*=12.6, 11.7, 2.2, 2H), 3.77 (s, 8H), 6.76 – 6.84 (m, 4H), 7.37 – 7.45 (m, 4H). ^{13}C NMR (101 MHz, CD_2Cl_2, 25°C) δ = 19.34, 33.57, 40.32, 55.70, 64.54, 82.98, 113.02, 130.38, 138.26, 158.75. IR (KBr): ṽ = 3419, 2957, 2857, 1608, 1580, 1508, 1463, 1296, 1248, 1179, 1105, 1034, 928, 830, 778, 735 cm^{-1}. HRMS-ESI+ *m/z* [*M-OH*]$^{+}$ calcd for $C_{21}H_{26}O_4$: 325.1798, found: 325.1798.

[(1*s*,4*s*)-4-Methoxy-1-methylcyclohexyl]bis[4-methoxyphenyl]methanol (15e) According to GP1 from magnesium (146 mg, 6.01 mmol), 4-bromoanisol (1.16 g, 6.02 mmol), THF (6.0 ml) and methyl (1*s*,4*s*)-4-methoxy-1-methylcyclohexane-1-carboxylate (373 mg, 2.00 mmol). After purification by flash column chromatography (eluent: pentane/diethyl ether 7 : 3) **15e** was obtained as colorless semi-solid (662 mg, 89 %). ^{1}H NMR (400 MHz, CD_2Cl_2, 25°C) δ = 1.04 (s, 3H), 1.12 – 1.22 (m, 2H), 1.45 – 1.57 (m, 2H), 1.78 – 1.88 (m, 2H), 2.18 (td, *J*=13.5, 4.3, 2H), 2.25 (s, 1H), 3.32 (s, 3H), 3.42 (br p, *J*=2.7, 1H), 3.76 (s, 6H), 6.70 – 6.81 (m, 4H), 7.36 – 7.48 (m, 4H). ^{13}C NMR (101 MHz, CD_2Cl_2, 25°C) δ = 20.08, 25.97, 27.06, 41.33, 55.67, 74.65, 83.76, 112.73, 130.65, 139.12, 158.53. IR (KBr): ṽ = 3483, 2483, 2931, 2834, 1608, 1581, 1508, 1459, 1412, 1363, 1296, 1249, 1177, 1089, 1036, 883, 829, 784, 599, 583 cm^{-1}. HRMS-ESI+ *m/z* [*M-OH*]$^{+}$ calcd for $C_{23}H_{30}O_4$: 353.2111, found: 353.2113.

(Adamantan-1-yl)bis(4-methoxyphenyl)methanol (15f) According to GP1 from magnesium (622 mg, 25.6 mmol), 4-bromoanisol (4.93 g, 25.6 mmol), THF (20.0 ml) and methyl 1-methylcyclopentane-1-carboxylate (2.20 g, 10.7 mmol). After purification by flash column chromatography (eluent: pentane/diethyl ether 9 : 1) **15f** was obtained as white solid (3.68 g, 91 %). ^{1}H NMR (400 MHz, $CDCl_3$, 25°C) δ = 1.53 – 1.71 (m, 6H), 1.84 (d, *J*=3.0, 6H), 1.98 (br p, *J*=6.0, 2.9, 3H), 2.16 (s, 1H), 3.78 (s, 6H), 6.75 – 6.85 (m, 4H), 7.41 – 7.53 (m, 4H). ^{13}C NMR (101 MHz, $CDCl_3$, 25°C) δ = 28.98, 37.11, 37.56, 41.29, 55.27, 81.93, 112.50, 129.86, 137.99, 157.99. IR (KBr): ṽ = 3482, 2881, 1607, 1582, 1510, 1453, 1464, 1360, 1298, 1253, 1186, 826, 810, 765, 639, 608, 582, 533 cm^{-1}. HRMS-ESI- *m/z* [*M-H*]$^{-}$ calcd for $C_{25}H_{30}O_3$: 377.2117, found: 377.2122.

***rac*-1-[(2-Chloroethoxy)(1-methylcyclohexyl)methyl]-4-methoxybenzene (17a)** According to GP5 from **19a** (329 mg, 1.40 mmol), indium (III)-chloride (6.6 mg, 0.027 mmol), 2-chloroethanol (6.00 g, 74.6 mmol). After purification by flash column chromatography (eluent: pentane/diethyl ether 95 : 5) **17a** was obtained as white solid (374 mg, 90 %). ^{1}H NMR (400 MHz, CD_2Cl_2, 25°C) δ = 0.83 (s, 3H), 1.01 – 1.10 (m, 1H), 1.13 – 1.27 (m, 1H), 1.29 – 1.61 (m, 8H), 3.41 (ddd, *J*=10.5, 5.9, 5.3, 1H), 3.50 – 3.62 (m, 3H), 3.78 (s, 3H), 3.96 (s, 1H), 6.81 – 6.89 (m, 2H), 7.14 – 7.21 (m, 2H). ^{13}C NMR (101 MHz, CD_2Cl_2, 25°C) δ = 19.15, 22.18, 22.26, 26.90, 34.50, 34.75, 38.62, 43.94, 55.55, 69.73, 90.10, 113.17, 130.07, 131.32, 159.36. IR (KBr): ṽ = 2967, 2937, 2849, 1610, 1513, 1459, 1291, 1238, 1175, 1108, 1088, 1057, 1025, 984, 917, 892,

842, 824, 771, 665, 628, 598, 578, 558, 526, 495 cm^{-1}. HRMS+EI *m/z* $[M]^+$ calcd for $C_{17}H_{25}ClO_2$: 296.1538, found: 296.1529.

***rac*-1-[(2-Chloroethoxy)(4-methoxyphenyl)methyl]adamantane (17b)** According to GP5 from **19b** (574 mg, 2.10 mmol), indium (III)-chloride (9.3 mg, 0.038 mmol) and 2-chloroethanol (7.10 g, 88.2 mmol). After purification by flash column chromatography (eluent: pentane/diethyl ether 7 : 3) **17b** was obtained as colorless oil (657 mg, 93 %). ^{1}H NMR (500 MHz, CD_2Cl_2, 25°C) δ = 1.40 – 1.46 (m, 3H), 1.53 – 1.60 (m, 3H), 1.63 – 1.69 (m, 6H), 1.91 (p, *J*=3.0, 3H), 3.36 – 3.42 (m, 1H), 3.51 – 3.56 (m, 1H), 3.56 – 3.61 (m, 2H), 3.73 (s, 1H), 3.79 (s, 3H), 6.81 – 6.87 (m, 2H), 7.09 – 7.17 (m, 2H). ^{13}C NMR (126 MHz, $CDCl_3$, 25°C) δ = 28.39, 37.15, 37.35, 38.40, 43.20, 55.20, 69.28, 90.72, 112.84, 129.52, 130.41, 158.85. IR (KBr): ṽ = 2907, 2849, 1612, 1584, 1511, 1454, 1346, 1290, 1246, 1172, 1111, 1036, 920, 833, 812, 782, 762, 750 cm^{-1}. HRMS+EI *m/z* $[M]^+$ calcd for $C_{20}H_{27}ClO_2$: 334.1694, found: 334.1693.

***rac*-1-[(2-Chloroethoxy)(3-methoxyphenyl)methyl]adamantane (17c)** According to GP5 from **19c** (408 mg, 1.50 mmol), indium (III)-chloride (6.6 mg, 0.027 mmol) and 2-chloroethanol (7.20 g, 89.5 mmol). After purification by flash column chromatography (eluent: pentane/diethyl ether 9 : 1) **17c** was obtained as colorless oil (478 mg, 95 %). ^{1}H NMR (400 MHz, CD_2Cl_2, 25°C) δ = 1.46 (dq, *J*=12.3, 2.6, 3H), 1.52 – 1.61 (m, 3H), 1.62 – 1.76 (m, 6H), 1.92 (p, *J*=3.2, 3H), 3.37 – 3.48 (m, 1H), 3.51 – 3.64 (m, 3H), 3.75 (s, 1H), 3.78 (s, 3H), 6.76 – 6.83 (m, 3H), 7.16 – 7.26 (m, 1H). ^{13}C NMR (101 MHz, CD_2Cl_2, 25°C) δ = 29.14, 37.71, 37.83, 39.05, 44.07, 55.65, 70.03, 91.49, 113.05, 114.64, 121.70, 128.81, 140.77, 159.70. IR (KBr): ṽ = 2902, 2847, 1599, 1584, 1489, 1452, 1436, 1346, 1314, 1283, 1257, 1152, 1114, 1051, 875, 792, 779, 742, 701, 671, 591, 564, 469 cm^{-1}. HRMS+EI *m/z* $[M]^+$ calcd for $C_{20}H_{27}ClO_2$: 334.1694, found: 334.1691.

***rac*-1-[(2-Chloroethoxy)(2-methoxyphenyl)methyl]adamantane (17d)** According to GP5 from **19d** (646 mg, 2.37 mmol), indium (III)-chloride (11 mg, 0.045 mmol), 2-chloroethanol (12.0 g, 149 mmol). After purification by flash column chromatography (eluent: pentane/diethyl ether 9 : 1) **17d** was obtained as colorless oil (780 mg, 98 %). ^{1}H NMR (400 MHz, CD_2Cl_2, 25°C) δ = 1.44 (dq, *J*=12.4, 2.7, 3H), 1.53 – 1.70 (m, 6H), 1.76 (dq, *J*=12.3, 2.6, 3H), 1.90 (p, *J*=3.2, 3H), 3.38 (dt, *J*=10.7, 5.8, 1H), 3.46 (ddd, *J*=10.7, 6.4, 5.3, 1H), 3.52 – 3.60 (m, 2H), 3.77 (s, 3H), 4.41 (s, 1H), 6.87 (dd, *J*=8.2, 1.1, 1H), 6.90 – 6.98 (m, 1H), 7.23 (ddd, *J*=8.3, 7.4, 1.8, 1H), 7.30 (dd,

J=7.6, 1.8, 1H). ^{13}C NMR (101 MHz, CD_2Cl_2, 25°C) δ = 29.18, 37.81, 38.57, 44.01, 55.63, 69.89, 82.92, 110.58, 120.27, 127.54, 128.50, 129.63, 158.88. IR (KBr): ṽ = 2903, 2850, 1598, 1585, 1489, 1464, 1454, 1347, 1280, 1237, 1048, 1029, 975, 945, 920, 809, 758, 665, 653, 624, 562, 526, 490 cm^{-1}. HRMS+EI *m/z* $[M]^+$ calcd for $C_{20}H_{27}O_2Cl$: 334.1694, found: 334.1692.

***rac*-1-[(2-Chloroethoxy)(4-methoxyphenyl)methyl]-3,5-dimethyladamantane (17e)** According to GP5 from **19e** (300 mg, 1.01 mmol), indium (III)-chloride (4.4 mg, 0.018 mmol) and 2-chloroethanol (6.02 g, 74.6 mmol). After purification by flash column chromatography (eluent: pentane/diethyl ether 10 : 1) **17e** was obtained as colorless oil (357 mg, 98 %). ^{1}H NMR (400 MHz, CD_2Cl_2, 25°C) δ = 0.77 (s, 6H), 0.98 – 1.12 (m, 4H), 1.19 – 1.33 (m, 7H), 1.47 – 1.54 (m, 1H), 2.01 (hept, *J*=3.1, 1H), 3.40 (dt, *J*=10.6, 5.7, 1H), 3.51 (ddd, *J*=10.7, 6.6, 5.0, 1H), 3.55 – 3.60 (m, 2H), 3.77 (s, 1H), 3.79 (s, 3H), 6.82 – 6.89 (m, 2H), 7.09 – 7.17 (m, 2H). ^{13}C NMR (126 MHz, CD_2Cl_2, 25°C) δ = 30.17, 31.10, 31.40, 37.64, 39.84, 43.88, 44.00, 45.14 (d, *J*=3.6), 51.74, 55.70, 69.89, 90.76, 113.32, 130.13, 131.01, 159.52. IR (KBr): ṽ = 2942, 2898, 2861, 1612, 1511, 1455, 1357, 1295, 1247, 1173, 1115, 1038, 833, 758, 670, 660, 594, 523 cm^{-1}. HRMS+EI *m/z* $[M]^+$ calcd for $C_{22}H_{31}O_2Cl$: 362.2013, found: 362.2006.

***rac*-1-[(2-Chloroethoxy)(4-methoxyphenyl)methyl]-3-methoxyadamantane (17g)** A mixture of **19g** (245 mg, 0.81 mmol), indium (III)-chloride (8.9 mg, 0.036 mmol) and 2-chloroethanol (12.0 g, 149 mmol) was stirred for 60 min at rt. Water (30.0 ml) was added and the mixture was extracted twice with diethyl ether (30.0 ml). The combined ether phases were dried over magnesium sulfate and reduced in vacuum. After purification by flash column chromatography (eluent: pentane/diethyl ether 75 : 25) **17g** was obtained as colorless oil (288 mg, 97 %). ^{1}H NMR (400 MHz, CD_2Cl_2, 25°C) δ = 1.30 – 1.68 (m, 12H), 2.11 – 2.19 (m, 2H), 3.15 (s, 3H), 3.40 (ddd, *J*=10.5, 5.9, 5.3, 1H), 3.50 – 3.63 (m, 3H), 3.79 (s, 3H), 3.81 (s, 1H), 6.82 – 6.90 (m, 2H), 7.10 – 7.16 (m, 2H). ^{13}C NMR (101 MHz, CD_2Cl_2, 25°C) δ = 30.71, 36.40, 37.77, 37.92, 40.86, 41.23, 42.40, 43.87, 47.99, 55.57, 69.72, 72.89, 90.16, 113.29, 129.91, 130.52, 159.50. IR (KBr): ṽ = 2907, 2853, 1611, 1584, 1511, 1458, 1355, 1290, 1247, 1173, 1113, 1080, 1036, 882, 834, 802, 756, 668, 655, 592, 562, 526 cm^{-1}. HRMS+EI *m/z* $[M]^+$ calcd for $C_{21}H_{29}O_3Cl$: 364.1805, found: 364.1795.

***rac*-(4-Methoxyphenyl)(1-methylcyclohexyl)methanol (19a)** According to GP4 from **35a** (375 mg, 1.60 mmol), sodium borohydride (124 mg, 3.2 mmol), methanol (3.0 ml). After purification by flash column chromatography (eluent: pentane/diethyl ether 9:1) **19a** was obtained as colorless oil (343 mg, 91 %). ^{1}H NMR (500 MHz, CD_2Cl_2, 25°C) δ = 0.83 (s, 3H), 1.04 – 1.61 (m, 10H), 1.83 (d, *J*=3.1, 1H), 3.78 (s, 3H), 4.36 (d, *J*=3.0, 1H), 6.77 – 6.88 (m, 2H), 7.16 – 7.27 (m, 2H). ^{13}C NMR (126 MHz, CD_2Cl_2, 25°C) δ = 18.42, 22.21 (d, *J*=6.1), 26.84, 34.30, 34.70, 38.46, 55.56, 82.09, 113.10, 129.27, 134.53, 159.23. IR (KBr): ṽ = 2926, 2857, 1611, 1584, 1512, 1465, 1444, 1302, 1247, 1174, 1111, 1037, 907, 835, 766, 749, 709, 644, 625, 573, 546, 512 cm^{-1}. HRMS+EI *m/z* $[M]^+$ calcd for $C_{15}H_{22}O_2$: 234.1620, found: 234.1614.

***rac*-(Adamantan-1-yl)(4-methoxyphenyl)methanol (19b)** According to GP4 from **35b** (588 mg, 2.17 mmol), sodium borohydride (168 mg, 4.34 mmol), methanol (7.0 ml). **19b** was obtained as white solid (574 mg, 97 %). ^{1}H NMR (500 MHz, $CDCl_3$, 25°C) δ = 1.47 (dq, *J*=12.1, 2.6, 3H), 1.54 – 1.70 (m, 9H), 1.73 (s, 1H), 1.96 (br p, *J*=3.2, 3H), 3.81 (s, 3H), 4.17 (s, 1H), 6.82 – 6.89 (m, 2H), 7.15 – 7.21 (m, 2H). ^{13}C NMR (126 MHz, $CDCl_3$, 25°C) δ = 28.47, 37.23, 37.35, 38.26, 55.38, 82.74, 113.01, 128.92, 133.47, 158.95. IR (KBr): ṽ = 3483, 3444, 2900, 2845, 2360, 2342, 1611, 1511, 1455, 1288, 1238, 1174, 1128, 1030, 831, 742, 653, 569 cm^{-1}. HRMS+EI *m/z* $[M]^+$ calcd for $C_{18}H_{24}O_2$: 272.1771, found: 272.1767.

***rac*-(Adamantan-1-yl)(3-methoxyphenyl)methanol (19c)** According to GP4 from **35c** (567 mg, 2.11 mmol), sodium borohydride (162 mg, 4.24 mmol), methanol/diethyl ether 2:1 (6.0 ml). **19c** was obtained as colorless oil (570 mg, 100 %). ^{1}H NMR (400 MHz, CD_2Cl_2, 25°C) δ = 1.45 – 1.74 (m, 12H), 1.86 (d, *J*=3.2, 1H), 1.94 (p, *J*=3.2, 3H), 3.79 (s, 3H), 4.16 (d, *J*=3.1, 1H), 6.77 – 6.89 (m, 3H), 7.21 (td, *J*=7.6, 0.9, 1H). ^{13}C NMR (126 MHz, CD_2Cl_2, 25°C) δ = 28.94, 37.49, 38.60, 55.53, 83.08, 112.69, 113.97, 120.70, 128.62, 143.57, 159.43. IR (KBr): ṽ = 3449, 2903, 2846, 1601, 1583, 1488, 1452, 1361, 1345, 1314, 1282, 1256, 1150, 1125, 1031, 977, 939, 874, 816, 789, 762, 746, 730, 700, 666, 591, 562, 467 cm^{-1}. HRMS+EI *m/z* $[M]^+$ calcd for $C_{18}H_{24}O_2$: 272.1771, found: 272.1771.

***rac*-(Adamantan-1-yl)(2-methoxyphenyl)methanol (19d)** According to GP4 from **35d** (641 mg, 2.37 mmol), sodium borohydride (183 mg, 4.74 mmol), methanol/diethyl ether 2:1 (18.0 ml). **19d** was obtained as white solid (645 mg, 100 %). ^{1}H NMR (500 MHz, CD_2Cl_2, 25°C) δ =

1.41 – 1.74 (m, 12H), 1.93 (hept, *J*=3.2, 3H), 2.59 (br s, 1H), 3.79 (s, 3H), 4.47 (s, 1H), 6.86 – 6.97 (m, 2H), 7.16 – 7.28 (m, 2H). ^{13}C NMR (126 MHz, CD_2Cl_2, 25°C) δ = 29.20, 37.73, 38.72, 38.84, 55.66, 111.09, 120.41, 128.45, 129.83, 130.11, 157.85. IR (KBr): ṽ = 3364, 2901, 2846, 1598, 1584, 1488, 1462, 1435, 1384, 1354, 1343, 1281, 1238, 1172, 1125, 1113, 1036, 975, 935, 914, 817, 809, 776, 751, 714, 658, 612, 580, 552, 510, 472 cm^{-1}. HRMS+EI *m/z* $[M]^+$ calcd for $C_{18}H_{24}O_2$: 272.1771, found: 272.1770.

***rac*-(3,5-Dimethyladamantan-1-yl)(4-methoxyphenyl)methanol (19e)** According to GP4 from **35e** (306 mg, 1.02 mmol), sodium borohydride (77 mg, 2.02 mmol), methanol/diethyl ether 2:1 (6.0 ml). **19e** was obtained as colorless oil (310 mg, 100 %). ^{1}H NMR (400 MHz, CD_2Cl_2, 25°C) δ = 0.78 (s, 6H), 0.98 – 1.13 (m, 4H), 1.17 – 1.33 (m, 7H), 1.41 – 1.48 (m, 1H), 1.80 (d, *J*=3.1, 1H), 2.03 (p, *J*=3.2, 1H), 3.79 (s, 3H), 4.18 (d, *J*=2.9, 1H), 6.81 – 6.88 (m, 2H), 7.13 – 7.21 (m, 2H). ^{13}C NMR (101 MHz, CD_2Cl_2, 25°C) δ = 30.15, 31.08, 31.42, 37.30, 39.75, 43.83, 44.93 (d, *J*=3.9), 51.69, 55.71, 82.50, 113.26, 129.34, 134.17, 159.39. IR (KBr): ṽ = 3450, 2942, 2896, 2838, 1612, 1585, 1512, 1454, 1357, 1341, 1302, 1247, 1174, 1111, 1074, 1040, 876, 832, 790, 756, 732, 692, 661, 630, 583, 555, 535 cm^{-1}. HRMS+EI *m/z* $[M]^+$ calcd for $C_{20}H_{28}O_2$: 300.2089, found: 300.2081.

***rac*-(3-Methoxyadamantan-1-yl)(4-methoxyphenyl)methanol (19g)** According to GP4 from **35g** (344 mg, 1.15 mmol), sodium borohydride (89 mg, 2.32 mmol), methanol (7.0 ml). **19g** was obtained as white solid (338 mg, 97 %). ^{1}H NMR (400 MHz, CD_2Cl_2, 25°C) δ = 1.31 – 1.60 (m, 10H), 1.59 – 1.69 (m, 2H), 1.87 (d, *J*=3.0, 1H), 2.17 (p, *J*=3.2, 2H), 3.15 (s, 3H), 3.79 (s, 3H), 4.22 (d, *J*=2.9, 1H), 6.81 – 6.87 (m, 2H), 7.14 – 7.21 (m, 2H). ^{13}C NMR (126 MHz, CD_2Cl_2, 25°C) δ = 30.69 (d, *J*=2.1), 36.36, 37.61 (d, *J*=6.2), 40.85 (d, *J*=5.9), 41.14, 42.03, 48.00, 55.58, 72.92, 81.97, 113.23, 129.13, 133.75, 159.36. IR (KBr): ṽ = 3433, 2923, 2854, 2830, 2360, 1608, 1583, 1511, 1400, 1356, 1300, 1249, 1169, 1169, 1130, 1111, 1065, 1035, 995, 929, 892, 879, 839, 779, 751, 707, 656, 616, 572, 500 cm^{-1}. HRMS+EI *m/z* $[M]^+$ calcd for $C_{19}H_{26}O_3$: 302.1882, found: 302.1873.

Methyl (1*S*,4*S*)-4-methoxy-1-methylcyclohexane-1-carboxylate (25) A solution of n-butyl lithium (2.6 M in hexanes, 3.6 ml, 9.0 mmol) was added dropwise to a stirred solution of diisopropylamine (1.52 ml, 10.8 mmol) in THF (5.0 ml) at -78 °C. After 30 min methyl 4-

methoxycyclohexane-1-carboxylate (706 mg, 4.11 mmol) was added by syringe. Stirring was continued for 60 min before addition of iodomethane (0.90 ml, 14.3 mmol). The mixture was allowed to warm up to room temperature overnight, quenched with 1M HCl (10.0 ml) and extracted thrice with CH_2Cl_2 (20.0 ml). The combined organic phases were dried with magnesium sulfate and reduced in vacuum. The crude product was purified by flash column chromatography (eluent: pentane/diethyl ether 9:1). **25** was obtained as colorless oil (591 mg, 77 %). ^{1}H NMR (400 MHz, CD_2Cl_2, 25°C) δ = 1.13 (s, 3H), 1.15 – 1.29 (m, 4H), 1.81 – 1.92 (m, 2H), 2.11 – 2.21 (m, 2H), 3.06 – 3.15 (m, 1H), 3.27 (s, 3H), 3.65 (s, 3H). ^{13}C NMR (101 MHz, CD_2Cl_2, 25°C) δ = 27.03, 29.43, 33.86, 43.45, 52.09, 55.83, 78.79, 177.85. IR (KBr): ṽ = 2925, 2359, 2341, 1731, 1633, 1505, 1455, 1249, 1174, 1037, 832, 668 cm^{-1}. HRMS-EI *m/z* [*M*-H]$^-$ calcd for $C_{10}H_{18}O_3$: 185.1183, found: 185.1172.

***rac*-Ethyl 1-{2-[1,1-bis(4-methoxyphenyl)-2,2-dimethylpropoxy]ethyl}piperidine-3-carboxylate (27a)** According to GP2 from **15a** (179 mg, 0.602 mmol), acetyl chloride (1.0 ml), rt, ethyl 2-hydroxyethylnipecotinate (132 mg, 0.656 mmol), potassium carbonate (206 mg, 1.49 mmol), acetonitrile (1.30 ml). After purification by flash column chromatography (eluent: pentane/diethyl ether 5 : 1 + 3 % triethylamine) **27a** was obtained as colorless oil (191 mg, 76 %). ^{1}H NMR (400 MHz, CD_2Cl_2, 25°C) δ = 1.07 (s, 9H), 1.24 (t, *J*=7.1, 3H), 1.38 – 1.62 (m, 2H), 1.67 – 1.75 (m, 1H), 1.87 – 1.95 (m, 1H), 2.08 (td, *J*=10.9, 3.0, 1H), 2.22 (t, *J*=10.6, 1H), 2.48 – 2.61 (m, 3H), 2.73 (d, *J*=11.3, 1H), 2.97 – 3.05 (m, 1H), 3.12 (t, *J*=6.1, 2H), 3.84 (s, 6H), 4.11 (m, 2H), 6.80 – 6.91 (m, 4H), 7.40 – 7.53 (m, 4H). ^{13}C NMR (126 MHz, $CDCl_3$, 25°C) δ = 14.36, 24.85, 26.97, 28.61, 40.61, 42.22, 54.43, 55.29, 56.38, 58.91, 60.41, 63.02, 88.83, 112.19, 131.83, 134.07, 158.18, 174.41. IR (KBr): ṽ = 2954, 1731, 1609, 1580, 1509, 1465, 1392, 1366, 1297, 1251, 1175, 1070, 1037, 832, 810, 794, 578 cm^{-1}. HRMS-ESI+ *m/z* [*M*+H]$^+$ calcd for $C_{29}H_{41}NO_5$: 484.3069, found: 484.3063.

***rac*-Ethyl 1-{2-[bis(4-methoxyphenyl)(1-methylcyclopentyl)methoxy]ethyl}piperidine-3-carboxylate (27b)** According to GP2 from **15b** (144 mg, 0.440 mmol), acetyl chloride (2.5 ml), -20°C, ethyl 2-hydroxyethylnipecotinate (93 mg, 0.46 mmol), potassium carbonate (152 mg, 1.10 mmol), acetonitrile (3.0 ml). After purification by flash column chromatography (eluent: pentane/diethyl ether 4 : 6) **27b** was obtained as colorless oil (69 mg, 31 %). ^{1}H NMR (400 MHz, CD_2Cl_2, 25°C) δ = 1.01 (s, 3H), 1.05 – 1.14 (m, 2H), 1.20 (t, *J*=7.1, 3H), 1.33 – 1.70 (m, 7H),

1.86 (dq, *J*=12.6, 4.2, 3.7, 1H), 2.01 (td, *J*=11.0, 3.0, 1H), 2.15 (t, *J*=10.6, 1H), 2.29 – 2.39 (m, 2H), 2.43 – 2.53 (m, 3H), 2.66 (dt, *J*=10.4, 4.0, 1H), 2.93 (dt, *J*=11.2, 2.1, 1H), 3.04 (t, *J*=6.0, 2H), 3.79 (s, 6H), 4.06 (m, 2H), 6.77 – 6.84 (m, 4H), 7.27 – 7.34 (m, 4H). ^{13}C NMR (101 MHz, CD_2Cl_2, 25°C) δ = 14.59, 25.35, 26.11, 26.46, 27.43, 38.53 (d, *J*=1.8), 42.72, 52.42, 54.88, 55.66, 56.88, 59.25, 60.65, 62.99, 89.29, 112.55, 132.36, 134.90, 158.80, 174.61. IR (KBr): ṽ = 2944, 2868, 1731, 1609, 1578, 1509, 1465, 1375, 1298, 1250, 1178, 1070, 1037, 994, 901, 835, 786, 632, 577, 533 cm^{-1}. HRMS-ESI+ *m/z* [*M*+H]$^+$ calcd for $C_{31}H_{43}NO_5$: 510.3214, found: 510.3213.

***rac*-Ethyl 1-{2-[bis(4-methoxyphenyl)(1-methylcyclohexyl)methoxy]ethyl}piperidine-3-carboxylate (27c)** According to GP2 from **15c** (320 mg, 0.940 mmol), acetyl chloride (3.0 ml), 0°C, ethyl 2-hydroxyethylnipecotinate (207 mg, 1.03 mmol), potassium carbonate (325 mg, 2.35 mmol), acetonitrile (5.0 ml). After purification by flash column chromatography (eluent: pentane/diethyl ether 1 : 1) **27c** was obtained as pale yellowish oil (208 mg, 42 %). ^{1}H NMR (400 MHz, CD_2Cl_2, 25°C) δ = 1.03 (s, 3H), 1.20 (t, *J*=7.1, 3H), 1.29 – 1.71 (m, 13H), 1.81 – 1.91 (m, 1H), 2.01 – 2.10 (m, 1H), 2.19 (t, *J*=10.7, 1H), 2.46 – 2.59 (m, 3H), 2.65 – 2.74 (m, 1H), 2.91 – 3.01 (m, 1H), 3.08 (t, *J*=6.1, 2H), 3.80 (s, 6H), 4.07 (m, 2H), 6.79 – 6.86 (m, 4H), 7.40 – 7.50 (m, 4H). ^{13}C NMR (101 MHz, CD_2Cl_2, 25°C) δ = 14.42, 19.83, 22.92, 25.21, 26.31, 27.27, 33.64, 42.56, 43.69, 54.80, 55.50, 56.81, 59.07, 60.50, 63.39, 90.10, 112.25, 132.45, 133.92 (d, *J*=1.7), 158.51, 174.46. IR (KBr): ṽ = 2946, 2834, 1732, 1608, 1578, 1508, 1465, 1443, 1374, 1298, 1251, 1177, 1154, 1068, 1036, 829, 657, 631, 575, 540 cm^{-1}. HRMS-ESI+ *m/z* [*M*+H]$^+$ calcd for $C_{32}H_{45}NO_5$: 524.3371, found: 524.3371.

(*S*)-Ethyl 1-{2-[bis(4-methoxyphenyl)(1-methylcyclohexyl)methoxy]ethyl}piperidine-3-carboxylate [(*S*)-27c] According to GP2 from **15c** (170 mg, 0.501 mmol), acetyl chloride (2.0 ml), 0°C, ethyl 2-hydroxyethylnipecotinate (111 mg, 0.551 mmol), potassium carbonate (173 mg, 1.25 mmol), acetonitrile (2.0 ml). After purification by flash column chromatography (eluent: pentane/diethyl ether 1 : 1) **(*S*)-27c** was obtained as pale yellowish oil (105 mg, 40 %). The analytical data are consistent with the racemate **27c**.

(*R*)-Ethyl 1-{2-[bis(4-methoxyphenyl)(1-methylcyclohexyl)methoxy]ethyl}piperidine-3-carboxylate [(*R*)-27c] According to GP2 from **15c** (134 mg, 0.390 mmol), acetyl chloride (1.0 ml), 0°C, ethyl 2-hydroxyethylnipecotinate (87 mg, 0.43 mmol), potassium carbonate (136 mg,

0.984 mmol), acetonitrile (5.0 ml). After purification by flash column chromatography (eluent: pentane/diethyl ether 15 : 35) **(*R*)-27c** was obtained as pale yellowish oil (91 mg, 44 %). The analytical data are consistent with the racemate **27c**.

***rac*-Ethyl 1-{2-[bis(4-methoxyphenyl)(4-methyltetrahydro-2H-pyran-4-yl)methoxy]ethyl}-piperidine-3-carboxylate (27d)** According to GP2 from **15d** (223 mg, 0.650 mmol), acetyl chloride (2.0 ml), rt, ethyl 2-hydroxyethylnipecotinate (145 mg, 0.720 mmol), potassium carbonate (225 mg, 1.63 mmol), acetonitrile (3.0 ml). After purification by flash column chromatography (eluent: pentane/diethyl ether 75 : 25 + 3% triethylamine) **27d** was obtained as pale yellowish oil (120 mg, 35 %). ^{1}H NMR (500 MHz, CD_2Cl_2, 25°C) δ = 0.98 - 1.08 (m, 5H), 1.20 (t, *J*=7.1, 3H), 1.33 – 1.58 (m, 2H), 1.63 – 1.73 (m, 1H), 1.83 – 1.93 (m, 1H), 2.03 (td, *J*=10.8, 2.9, 1H), 2.13 – 2.30 (m, 3H), 2.44 – 2.61 (m, 3H), 2.63 – 2.74 (m, 1H), 2.89 – 2.99 (m, 1H), 3.06 (t, *J*=6.1, 2H), 3.45 (ddd, *J*=13.4, 11.9, 2.3, 2H), 3.72 (dd, *J*=11.6, 5.3, 2H), 3.80 (s, 6H), 4.07 (m, 2H), 6.80 – 6.89 (m, 4H), 7.42 – 7.51 (m, 4H). ^{13}C NMR (101 MHz, CD_2Cl_2, 25°C) δ = 14.57, 19.51, 25.33, 27.41, 34.22 (d, *J*=1.8), 41.75, 42.68, 54.94, 55.67, 56.88, 59.13, 60.66, 63.27, 64.72, 89.37, 112.66, 132.43, 133.06, 158.86, 174.57. IR (KBr): ṽ = 2951, 1733, 1609, 1509, 1442, 1374, 1300, 1250, 1178, 1155, 1112, 1068, 1035, 932, 862, 832, 632, 595, 525, 495 cm^{-1}. HRMS-ESI+ *m/z* $[M+H]^+$ calcd for $C_{31}H_{43}NO_6$: 562.3163, found: 562.3159.

***rac*-Ethyl 1-(2-{[(1*S*,4*S*)-4-methoxy-1-methylcyclohexyl]bis[4-methoxyphenyl]methoxy}-ethyl)piperidine-3-carboxylate (27e)** According to GP2 from **15c** (157 mg, 0.421 mmol), acetyl chloride (3.0 ml), 0°C, ethyl 2-hydroxyethylnipecotinate (94 mg, 0.47 mmol), potassium carbonate (147 mg, 1.06 mmol), acetonitrile (3.0 ml). After purification by flash column chromatography (eluent: diethyl ether) **27e** was obtained as pale yellowish oil (89 mg, 38 %). ^{1}H NMR (400 MHz, CD_2Cl_2, 25°C) δ = 0.94 (s, 3H), 1.09 – 1.07 (m, 2H), 1.20 (t, *J*=7.1, 3H), 1.34 – 1.61 (m, 4H), 1.62 – 1.71 (m, 1H), 1.74 – 1.82 (m, 2H), 1.82 – 1.91 (m, 1H), 2.04 (td, *J*=10.9, 2.9, 1H), 2.13 – 2.25 (m, 3H), 2.44 – 2.57 (m, 3H), 2.65 – 2.75 (m, 1H), 2.88 – 2.97 (m, 1H), 3.15 (t, *J*=6.2, 2H), 3.29 (s, 3H), 3.34 – 3.40 (m, 1H), 3.79 (s, 6H), 4.07 (m, 2H), 6.76 – 6.83 (m, 4H), 7.38 – 7.47 (m, 4H). ^{13}C NMR (101 MHz, CD_2Cl_2, 25°C) δ = 14.43, 20.63, 25.19, 26.06 (d, *J*=2.7), 27.27, 27.72, 42.53, 42.62, 54.78, 55.38, 55.49, 56.73, 59.20, 60.49, 63.81, 74.54, 90.08, 112.17, 132.39, 134.91, 158.45, 174.47. IR (KBr): ṽ = 2936, 1731, 1608, 1579, 1508, 1464, 1364,

1297, 1250, 1177, 1091, 1036, 829, 787, 651, 576, 536 cm^{-1}. HRMS-ESI+ *m/z* $[M+H]^+$ calcd for $C_{33}H_{47}NO_6$: 554.3476, found: 554.3483.

***rac*-Ethyl 1-{2-[(adamantan-1-yl)bis(4-methoxyphenyl)methoxy]ethyl}piperidine-3-carboxylate (27f)** According to GP2 from **15f** (369 mg, 0.980 mmol), acetyl chloride (3.0 ml), rt, ethyl 2-hydroxyethylnipecotinate (216 mg, 1.07 mmol), potassium carbonate (337 mg, 2.44 mmol), acetonitrile (5.0 ml). After purification by flash column chromatography (eluent: pentane/diethyl ether 1 : 1) **27f** was obtained as colorless oil (231 mg, 42 %). ^{1}H NMR (500 MHz, CD_2Cl_2, 25°C) δ = 1.20 (t, *J*=7.1, 3H), 1.35 – 1.46 (m, 1H), 1.47 – 1.61 (m, 7H), 1.64 – 1.77 (m, 7H), 1.82 – 1.94 (m, 4H), 2.06 (td, *J*=11.0, 3.0, 1H), 2.20 (t, *J*=10.6, 1H), 2.49 (tt, *J*=10.4, 3.8, 1H), 2.57 (t, *J*=6.1, 2H), 2.65 – 2.75 (m, 1H), 2.97 (br dd, *J*=11.7, 3.6, 1H), 3.07 (t, *J*=6.1, 2H), 3.80 (s, 6H), 4.06 (m, 2H), 6.80 – 6.88 (m, 4H), 7.47 – 7.54 (m, 4H). ^{13}C NMR (126 MHz, $CDCl_3$, 25°C) δ = 14.58, 25.35, 27.42, 29.82, 37.59, 38.40, 42.70, 43.03, 54.96, 55.64, 56.97, 59.16, 60.66, 63.38, 89.31, 112.42, 132.47, 133.39, 158.65, 174.61. IR (KBr): ṽ = 2906, 2361, 2343, 1734, 1609, 1508, 1458, 1298, 1249, 1172, 1035, 834, 669, 574 cm^{-1}. HRMS-ESI+ *m/z* $[M+H]^+$ calcd for $C_{35}H_{47}NO_5$: 562.3527, found: 562.3541.

(*S*)-Ethyl 1-{2-[(adamantan-1-yl)bis(4-methoxyphenyl)methoxy]ethyl}piperidine-3-carboxylate [(*S*)-27f] According to GP2 from **15f** (260 mg, 0.681 mmol), acetyl chloride (3.0 ml), rt, ethyl 2-hydroxyethylnipecotinate (152 mg, 0.755 mmol), potassium carbonate (238 mg, 1.72 mmol), acetonitrile (5.0 ml). After purification by flash column chromatography (eluent: pentane/diethyl ether 4 : 1) **(*S*)-27f** was obtained as pale yellowish oil (300 mg, 71 %). The analytical data are consistent with the racemate **27f**.

(*R*)-Ethyl 1-{2-[(adamantan-1-yl)bis(4-methoxyphenyl)methoxy]ethyl}piperidine-3-carboxylate [(*R*)-27f] According to GP2 from **15f** (189 mg, 0.502 mmol), acetyl chloride (1.0 ml), rt, ethyl 2-hydroxyethylnipecotinate (111 mg, 0.551 mmol), potassium carbonate (173 mg, 1.25 mmol), acetonitrile (2.0 ml). After purification by flash column chromatography (eluent: diethyl ether) **(*R*)-27f** was obtained as pale yellowish oil (120 mg, 43 %). The analytical data are consistent with the racemate **27f**.

***rac*-Ethyl 1-{3-[1,1-bis(4-methoxyphenyl)-2,2-dimethylpropoxy]propyl}piperidine-3-carboxylate (28)** According to GP2 from **15a** (510 mg, 1.70 mmol), acetyl chloride (3.0 ml), rt, ethyl 2-hydroxyethylnipecotinate (409 mg, 1.90 mmol), potassium carbonate (587 mg, 4.25 mmol), acetonitrile (8.0 ml). After purification by flash column chromatography (eluent: pentane/diethyl ether 85 : 15 + 3 % triethylamine) **28** was obtained as colorless oil (730 mg, 86 %). ^{1}H NMR (400 MHz, CD_2Cl_2, 25°C) δ = 1.03 (s, 9H), 1.21 (t, *J*=7.1, 3H), 1.36 – 1.56 (m, 2H), 1.64 – 1.74 (m, 3H), 1.84 – 2.01 (m, 2H), 2.10 (t, *J*=10.6, 1H), 2.37 – 2.53 (m, 3H), 2.70 (dt, *J*=11.4, 4.3, 1H), 2.87 – 2.96 (m, 1H), 3.01 (td, *J*=6.3, 2.1, 2H), 3.80 (s, 6H), 4.07 (m, 2H), 6.78 – 6.86 (m, 4H), 7.37 – 7.43 (m, 4H). ^{13}C NMR (101 MHz, CD_2Cl_2, 25°C) δ = 14.58, 25.32, 27.65, 28.31, 28.71, 41.03, 42.61, 54.38, 55.66, 56.16, 60.66, 62.81, 88.70, 112.46, 132.21 (d, *J*=2.3), 134.62, 158.68, 174.67. IR (KBr): ṽ = 2952, 2359, 1732, 1609, 1508, 1465, 1297, 1251, 1175, 1074, 1038, 902, 832, 811, 794, 657, 578, 520 cm^{-1}. HRMS-ESI+ *m/z* $[M+H]^+$ calcd for $C_{30}H_{43}NO_5$: 498.3214, found: 498.3208.

***rac*-Ethyl 1-{4-[1,1-bis(4-methoxyphenyl)-2,2-dimethylpropoxy]butyl}piperidine-3-carboxylate (29)** According to GP2 from **15a** (415 mg, 1.38 mmol), acetyl chloride (1.0 ml), rt, ethyl 2-hydroxyethylnipecotinate (440 mg, 1.52 mmol), potassium carbonate (477 mg, 3.45 mmol), acetonitrile (5.0 ml). After purification by flash column chromatography (eluent: pentane/diethyl ether 6 : 4) **29** was obtained as colorless oil (167 mg, 24 %). ^{1}H NMR (400 MHz, CD_2Cl_2, 25°C) δ = 1.04 (s, 9H), 1.22 (t, *J*=7.1, 3H), 1.34 – 1.61 (m, 6H), 1.64 – 1.75 (m, 1H), 1.81 – 2.00 (m, 2H), 2.05 – 2.17 (m, 1H), 2.24 – 2.34 (m, 2H), 2.48 (tt, *J*=10.2, 3.8, 1H), 2.64 – 2.72 (m, 1H), 2.85 – 2.94 (m, 1H), 2.95 – 3.01 (m, 2H), 3.79 (s, 6H), 4.08 (q, *J*=7.1, 2H), 6.75 – 6.87 (m, 4H), 7.33 – 7.45 (m, 4H). ^{13}C NMR (101 MHz, CD_2Cl_2, 25°C) δ = 14.61, 24.28, 25.25, 27.65, 28.78, 40.99, 42.55, 54.37, 55.65, 56.17, 59.27, 60.65, 64.77, 88.73, 112.47, 132.19, 134.76, 158.67, 174.69. IR (KBr): ṽ = 2948, 2868, 1731, 1609, 1579, 1509, 1465, 1442, 1392, 1370, 1297, 1251, 1175, 1073, 1038, 902, 832, 811, 794, 632, 577, 524, 495 cm^{-1}. HRMS-ESI+ *m/z* $[M+H]^+$ calcd for $C_{31}H_{45}NO_5$: 512.3371, found: 512.3368.

***rac*-1-{2-[1,1-Bis(4-methoxyphenyl)-2,2-dimethylpropoxy]ethyl}piperidine-3-carboxamide (30)** According to GP8 from saturated ammonia solution in methanol (2.0 ml), **27a** (145 mg, 0.301 mmol) and sodium cyanide (7.4 mg, 0.15 mmol), 70 h. After purification by flash column chromatography (eluent: ethyl acetate/methanol 98 : 2 + 5 % triethylamine) **30** was obtained

as white solid (80 mg, 59 %). ^{1}H NMR (500 MHz, CD_2Cl_2, 25°C) δ = 1.04 (s, 9H), 1.46 – 1.64 (m, 2H), 1.68 – 1.94 (m, 2H), 2.07 (br t, *J*=11.9, 1H), 2.33 (br d, *J*=11.7, 1H), 2.40 – 2.50 (m, 2H), 2.51 – 2.60 (m, 1H), 2.78 (br s, 1H), 2.87 – 3.00 (m, 1H), 3.07 – 3.21 (m, 2H), 3.80 (s, 6H), 6.82 (d, *J*=8.5, 4H), 7.34 – 7.46 (m, 4H). ^{13}C NMR (101 MHz, tetrachloroethane, 60°C) δ = 23.21, 27.30, 29.10, 40.87, 42.10, 54.22, 55.75, 56.23, 59.11, 62.08, 89.65, 112.76 (d, *J*=4.4), 120.81, 132.04 (d, *J*=8.1), 134.38 (d, *J*=13.0), 158.61. IR (KBr): ṽ = 3242, 2936, 2361, 1663, 1609, 1508, 1464, 1296, 1250, 1175, 1069, 1037, 902, 831, 668, 578 cm^{-1}. HRMS-ESI+ *m/z* [*M*+H]$^{+}$ calcd for $C_{27}H_{38}N_2O_4$: 455.2904, found: 455.2900.

***rac*-1-{2-[Tris(4-methoxyphenyl)methoxy]ethyl}piperidine-3-carboxamide (31)** According to GP8 from saturated ammonia solution in methanol (5.0 ml), ethyl 1-(2-(tris(4-methoxyphenyl)methoxy)ethyl)piperidine-3-carboxylate (125 mg, 0.230 mmol) and sodium cyanide (5.7 mg, 0.12 mmol), 18 h. After purification by flash column chromatography (eluent: ethyl acetate/methanol 98 : 2 + 5 % triethylamine) **31** was obtained as white solid (24 mg, 20 %). ^{1}H NMR (400 MHz, tetrachloroethane-d_2, 60°C) δ = 1.49 – 1.61 (m, 2H), 1.64 – 1.79 (m, 1H), 1.85 – 1.95 (m, 1H), 2.01 – 2.13 (m, 1H), 2.27 (dd, *J*=11.6, 3.1, 1H), 2.39 – 2.45 (br p, *J*=3.9, 1H), 2.45 – 2.60 (m, 2H), 2.68 – 2.77 (m, 1H), 2.83 – 2.90 (m, 1H), 3.13 (ddd, *J*=10.3, 6.1, 4.5, 1H), 3.22 (ddd, *J*=10.8, 6.6, 4.6, 1H), 3.79 (s, 9H), 5.13 (br s, 1H), 6.73 – 6.91 (m, 6H), 7.20 – 7.36 (m, 6H), 8.08 (br s, 1H). ^{13}C NMR (101 MHz, tetrachloroethane-d_2, 40°C) δ = 23.12, 27.38, 41.93, 54.24, 55.32, 55.82, 58.40, 60.58, 86.31, 113.61, 130.18, 137.23, 158.72, 178.15. IR (KBr): ṽ = 3446, 2934, 2834, 1675, 1607, 1508, 1463, 1302, 1249, 1175, 1071, 1034, 915, 827, 784, 730, 583 cm^{-1}. HRMS-ESI+ *m/z* [*M*+H]$^{+}$ calcd for $C_{30}H_{36}N_2O_5$: 505.2697, found: 505.2693.

(Adamantan-1-yl)(4-methoxyphenyl)methanone (35b) According to GP3 from magnesium (122 mg, 5.02 mmol), 4-bromoanisol (956 mg, 5.04 mmol), THF (12.0 ml) and adamantane-1-carbonyl chloride (1093 mg, 5.50 mmol) in THF (10.0 ml). After purification by flash column chromatography (eluent: pentane/diethyl ether 95 : 5) **35b** was obtained as white solid (1.28 g, 95 %). ^{1}H NMR (500 MHz, $CDCl_3$, 25°C) δ = 1.71 – 1.84 (m, 6H), 2.02 – 2.13 (m, 9H), 3.85 (s, 3H), 6.85 – 6.92 (m, 2H), 7.71 – 7.80 (m, 2H). ^{13}C NMR (101 MHz, $CDCl_3$, 25°C) δ = 28.46, 36.81, 39.66, 46.97, 55.49, 113.31, 130.47, 131.29, 161.73, 207.30. IR (KBr): ṽ = 2906, 2845, 1655, 1597, 1510, 1455, 1321, 1304, 1264, 1234, 1166, 1114, 1029, 986, 928, 829, 814, 745, 681, 604, 506 cm^{-1}. HRMS+EI *m/z* [*M*]$^{+}$ calcd for $C_{18}H_{22}O_2$: 270.1620, found: 270.1612.

(Adamantan-1-yl)(3-methoxyphenyl)methanone (35c) According to GP3 from magnesium (68 mg, 2.80 mmol), 4-bromoanisol (524 mg, 2.77 mmol), THF (6.0 ml) and adamantane-1-carbonyl chloride (635 mg, 3.11 mmol) in THF (5.0 ml). After purification by flash column chromatography (eluent: pentane/diethyl ether 93 : 7) **35c** was obtained as white solid (587 g, 78 %). ^{1}H NMR (400 MHz, CD_2Cl_2, 25°C) δ = 1.68 – 1.83 (m, 6H), 1.97 (d, *J*=3.0, 6H), 2.05 (br p, *J*=2.6, 3H), 3.81 (s, 3H), 6.94 – 7.02 (m, 2H), 7.05 – 7.13 (m, 1H), 7.25 – 7.36 (m, 1H). ^{13}C NMR (101 MHz, CD_2Cl_2, 25°C) δ = 28.88, 37.07, 39.62, 47.42, 55.88, 113.12, 116.02, 119.67, 129.49, 141.73, 159.82, 210.27. IR (KBr): ṽ = 2905, 2851, 1682, 1674, 1595, 1580, 1487, 1455, 1428, 1322, 1288, 1272, 1256, 1213, 1175, 1105, 1044, 994, 872, 783, 762, 736, 686, 655 cm^{-1}. HRMS+EI *m/z* $[M]^+$ calcd for $C_{18}H_{22}O_2$: 270.1620, found: 270.1616.

(Adamantan-1-yl)(2-methoxyphenyl)methanone (35d) According to GP3 from magnesium (68 mg, 2.80 mmol), 4-bromoanisol (541 mg, 2.86 mmol), THF (5.0 ml) and adamantane-1-carbonyl chloride (616 mg, 3.1 mmol) in THF (5.0 ml). After purification by flash column chromatography (eluent: pentane/diethyl ether 93 : 7) **35d** was obtained as white solid (665 g, 88 %). ^{1}H NMR (400 MHz, CD_2Cl_2, 25°C) δ = 1.68 – 1.83 (m, 6H), 1.97 (d, *J*=3.0, 6H), 2.05 (br p, *J*=2.6, 3H), 3.81 (s, 3H), 6.94 – 7.02 (m, 2H), 7.05 – 7.13 (m, 1H), 7.25 – 7.36 (m, 1H). ^{13}C NMR (101 MHz, CD_2Cl_2, 25°C) δ = 28.76, 37.08, 38.70, 47.51, 55.85, 111.46, 120.54, 126.78, 130.18, 131.38, 155.99, 213.00. IR (KBr): ṽ = 2890, 2848, 1690, 1599, 1582, 1490, 1472, 1450, 1434, 1346, 1287, 1250, 1231, 1183, 1130, 1104, 1043, 1018, 985, 951, 923, 853, 835, 811, 741, 639, 558, 510, 477 cm^{-1}. HRMS+EI *m/z* $[M]^+$ calcd for $C_{18}H_{22}O_2$: 270.1620, found: 270.1614.

(3,5-Dimethyladamantan-1-yl)(4-methoxyphenyl)methanone (35e) According to GP3 from magnesium (49 mg, 2.02 mmol), 4-bromoanisol (386 mg, 2.02 mmol), THF (6.0 ml) and adamantane-1-carbonyl chloride (499 mg, 2.21 mmol) in THF (6.0 ml). After purification by flash column chromatography (eluent: pentane/diethyl ether 9 : 1) **35e** was obtained as white solid (438 g, 73 %). ^{1}H NMR (500 MHz, CD_2Cl_2, 25°C) δ = 0.86 (s, 6H), 1.16 – 1.24 (m, 2H), 1.34 – 1.46 (m, 4H), 1.58 – 1.70 (m, 4H), 1.83 – 1.88 (m, 2H), 2.16 (hept, *J*=3.2, 1H), 3.84 (s, 3H), 6.85 – 6.92 (m, 2H), 7.67 – 7.73 (m, 2H). ^{13}C NMR (126 MHz, CD_2Cl_2, 25°C) δ = 30.23, 30.97, 31.67, 38.71, 43.36, 46.15, 49.27, 51.22, 55.91, 113.63, 130.72, 131.89, 162.18, 207.15. IR

(KBr): ṽ = 2942, 2896, 2838, 1612, 1512, 1454, 1357, 1302, 1247, 1147, 1040, 832, 790, 756, 732, 692, 661, 583 cm^{-1}. HRMS+EI *m/z* $[M]^+$ calcd for $C_{20}H_{26}O_2$: 298.1933, found: 298.1925.

(3-Bromoadamantan-1-yl)(4-methoxyphenyl)methanone (35f) According to GP3 from magnesium (106 mg, 4.34 mmol), 4-bromoanisol (837 mg, 4.34 mmol), THF (6.0 ml) and 3-bromoadamantane-1-carbonyl chloride (1.32 g, 4.77 mmol) in THF (5.0 ml). After purification by flash column chromatography (eluent: pentane/diethyl ether 90 : 10) **35f** was obtained as white solid (1.20 g, 79 %). ^{1}H NMR (500 MHz, CD_2Cl_2, 25°C) δ = 1.73 – 1.78 (m, 2H), 1.97 – 2.12 (m, 4H), 2.26 (br p, *J*=3.2, 2H), 2.32 – 2.41 (m, 4H), 2.57 – 2.61 (m, 2H), 3.84 (s, 3H), 6.89 – 6.96 (m, 2H), 7.70 – 7.77 (m, 2H). ^{13}C NMR (126 MHz, CD_2Cl_2, 25°C) δ = 32.83, 35.07, 38.30, 48.85, 50.96, 51.66, 55.96, 65.76, 113.85, 130.90, 162.57, 204.43. IR (KBr): ṽ = 2940, 1745, 1658, 1597, 1569, 1505, 1442, 1413, 1344, 1331, 1309, 1254, 1230, 1172, 1103, 1029, 973, 949, 843, 828, 749, 702, 671, 635, 613, 541, 508, 478 cm^{-1}. HRMS+EI *m/z* $[M]^+$ calcd for $C_{18}H_{21}BrO_2$: 348.0725, found: 348.0719.

(3-Methoxyadamantan-1-yl)(4-methoxyphenyl)methanone (35g) A solution of silver tetrafluoroborate (276 mg, 1.42 mmol) in 5.0 ml methanol was added to an intensely stirred solution of **35f** (450 mg, 1.29 mmol) in methanol (15.0 ml). The reaction mixture was stirred for 16 h under light exclusion and filtered through a paper filter. The filtrate was diluted with diethyl ether (80.0 mL), washed with water (20.0 ml) and brine (20.0 ml), dried over magnesium sulfate and reduced in vacuum. After purification by flash column chromatography (eluent: pentane/diethyl ether 75 : 25) **35g** was obtained as white solid (357 mg, 92 %). ^{1}H NMR (400 MHz, CD_2Cl_2, 25°C) δ = 1.59 – 1.81 (m, 6H), 1.86 – 2.00 (m, 6H), 2.25 – 2.37 (m, 2H), 3.21 (s, 3H), 3.84 (s, 3H), 6.84 – 6.97 (m, 2H), 7.68 – 7.78 (m, 2H). ^{13}C NMR (101 MHz, $CDCl_3$, 25°C) δ = ^{13}C NMR (101 MHz, CD_2Cl_2, 25°C) δ = 31.00, 36.07, 39.23, 40.74, 43.47, 48.27, 50.32, 55.93, 72.78, 113.73, 130.87, 131.41, 162.38, 205.77. IR (KBr): ṽ = 2933, 2855, 1655, 1601, 1573, 1508, 1453, 1307, 1251, 1172, 1121, 1077, 1030, 1012, 979, 952, 894, 836, 738 cm^{-1}. HRMS+EI *m/z* $[M]^+$ calcd for $C_{19}H_{24}O_3$: 300.1725, found: 300.1726.

***rac*-Ethyl 1-{2-[(1*R*)(4-methoxyphenyl)(1-methylcyclohexyl)methoxy]ethyl}(3*R*)-piperidine-3-carboxylate and *rac*-Ethyl 1-{2-[(1*S*)(4-methoxyphenyl)(1-methylcyclohexyl)methoxy]-ethyl}(3*R*)-piperidine-3-carboxylate ~1:1 (36a)** According to GP6 from **17a** (180 mg, 0.611

mmol), ethyl nipecotinate (111 mg, 0.678 mmol), potassium carbonate (210 mg, 1.52 mmol), potassium iodide (5.0 mg, 0.030 mmol), acetonitrile (8.0 ml). After purification by flash column chromatography (eluent: pentane/diethyl ether 1 : 1) **36a** was obtained as colorless oil (134 mg, 53 %). ^{1}H NMR (400 MHz, CD_2Cl_2, 25°C) δ = 0.80 (s, 3H), 0.99 – 1.08 (m, 1H), 1.12 – 1.60 (m, 14H), 1.61 – 1.72 (m, 1H), 1.82 – 1.92 (m, 1H), 2.03 (tt, *J*=10.4, 2.1, 1H), 2.16 (t, *J*=10.7, 1H), 2.43 – 2.56 (m, 3H), 2.67 – 2.77 (m, 1H), 2.92 – 3.07 (m, 1H), 3.25 (dtd, *J*=10.0, 5.9, 1.6, 1H), 3.36 (dt, *J*=9.9, 5.9, 1H), 3.78 (s, 3H), 3.91 (s, 1H), 4.07 (m, 2H), 6.79 – 6.88 (m, 2H), 7.13 – 7.20 (m, 2H). ^{13}C NMR (101 MHz, CD_2Cl_2, 25°C) δ = 14.43, 19.31, 22.24, 22.31, 25.18, 26.95, 27.25, 27.30, 34.65, 34.84, 38.44, 42.52, 54.54, 55.53, 56.43, 58.63 (d, *J*=3.8), 60.50, 67.83, 67.88, 90.05, 113.05, 130.09 (d, *J*=1.4), 132.04, 159.18, 174.48. IR (KBr): ṽ = 2931, 2858, 2362, 1733, 1610, 1511, 1466, 1374, 1303, 1290, 1247, 1174, 1154, 1095, 1035, 873, 753, 668, 541 cm^{-1}. HRMS-ESI+ *m/z* $[M+H]^+$ calcd for $C_{25}H_{39}NO_4$: 418.2952, found: 418.2946.

***rac*-Ethyl 1-{2-[(1*R*)(adamantan-1-yl)(4-methoxyphenyl)methoxy]ethyl}(3*R*)-piperidine-3-carboxylate and *rac*-Ethyl 1-{2-[(1*S*)(adamantan-1-yl)(4-methoxyphenyl)methoxy]ethyl}-(3*R*)-piperidine-3-carboxylate ~1:1 (36b)** According to GP6 from **17b** (500 mg, 1.49 mmol), ethyl nipecotinate (264 mg, 1.63 mmol), potassium carbonate (516 mg, 3.73 mmol), potassium iodide (13 mg, 0.075 mmol), acetonitrile (5.0 ml). After purification by flash column chromatography (eluent: pentane/diethyl ether 9:1 + 3 % triethylamine) **36b** was obtained as colorless oil (550 mg, 81 %). ^{1}H NMR (500 MHz, $CDCl_3$, 25°C) δ = 1.24 (t, *J*=7.1, 3H), 1.36 – 1.47 (m, 4H), 1.48 – 1.73 (m, 11H), 1.87 – 1.96 (m, 4H), 2.06 (td, *J*=11.2, 3.0, 1H), 2.21 (t, *J*=10.7, 1H), 2.48 – 2.61 (m, 3H), 2.72 – 2.82 (m, 1H), 2.99 – 3.09 (m, 1H), 3.26 (dt, *J*=9.9, 6.1, 1H), 3.42 (dtd, *J*=10.0, 6.1, 2.7, 1H), 3.66 (s, 1H), 3.81 (s, 3H), 4.06 – 4.17 (m, 2H), 6.78 – 6.89 (m, 2H), 7.06 – 7.15 (m, 2H). ^{13}C NMR (126 MHz, $CDCl_3$, 25°C) δ = 14.22, 24.73 (d, *J*=1.9), 26.87 (d, *J*=7.1), 28.43, 37.19, 38.52, 42.10, 54.10, 55.18, 55.96 (d, *J*=4.1), 58.18 (d, *J*=3.4), 60.25, 67.40, 90.78 (d, *J*=1.8), 112.72, 129.54, 131.04, 158.66, 174.30 (d, *J*=2.4). IR (KBr): ṽ = 2904, 2847, 1731, 1611, 1584, 1511, 1453, 1302, 1302, 1289, 1247, 1172, 1154, 1095, 1035, 832, 811, 749, 733 cm^{-1}. HRMS-ESI+ *m/z* $[M+H]^+$ calcd for $C_{28}H_{41}NO_4$: 456.3114, found: 456.3111.

***rac*-Ethyl 1-{2-[(1*R*)(adamantan-1-yl)(3-methoxyphenyl)methoxy]ethyl}(3*R*)-piperidine-3-carboxylate and *rac*-Ethyl 1-{2-[(1*S*)(adamantan-1-yl)(3-methoxyphenyl)methoxy]ethyl}-(3*R*)-piperidine-3-carboxylate ~1:1 (36c)** According to GP6 from **17c** (231 mg, 0.690 mmol),

ethyl nipecotinate (124 mg, 0.758 mmol), potassium carbonate (236 mg, 1.71 mmol), potassium iodide (5.6 mg, 0.034 mmol), acetonitrile (5.0 ml). After purification by flash column chromatography (eluent: pentane/diethyl ether 1 : 1) **36c** was obtained as pale yellowish oil (310 mg, 99 %). ^{1}H NMR (500 MHz, CD_2Cl_2, 25°C) δ = 1.21 (td, *J*=7.1, 0.9, 3H), 1.34 – 1.70 (m, 15H), 1.84 – 1.94 (m, 4H), 2.04 (tt, *J*=11.1, 2.9, 1H), 2.17 (td, *J*=10.7, 5.6, 1H), 2.44 – 2.57 (m, 3H), 2.68 – 2.76 (d, *J*=11.3, 1H), 2.96 – 3.03 (m, 1H), 3.25 (dtd, *J*=10.0, 5.9, 1.3, 1H), 3.39 (dt, *J*=9.9, 5.9, 1H), 3.69 (s, 1H), 3.79 (d, *J*=0.8, 3H), 4.07 (m, 2H), 6.74 – 6.81 (m, 3H), 7.21 (t, *J*=7.8, 1H). ^{13}C NMR (126 MHz, CD_2Cl_2, 25°C) δ = 14.43, 25.17 (d, *J*=3.9), 27.29 (d, *J*=8.2), 29.02, 37.52, 37.59, 39.00, 42.51 (d, *J*=4.1), 54.54 (d, *J*=3.3), 55.48, 56.45, 58.56 (d, *J*=5.1), 60.50, 68.06, 91.44 (d, *J*=3.9), 112.56 (d, *J*=5.2), 114.60, 121.60, 128.51, 141.35, 159.47, 174.47 (d, *J*=2.2). IR (KBr): ṽ = 2904, 2848, 2361, 2342, 1732, 1600, 1587, 1489 1465, 1455, 1361, 1314, 1281, 1238, 1182, 1154, 1090, 1049, 1032, 940, 861, 809, 755, 719, 659, 624 cm^{-1}. HRMS-ESI+ *m/z* [*M*+H]$^{+}$ calcd for $C_{28}H_{41}NO_4$: 456.3114, found: 456.3106.

***rac*-Ethyl 1-{2-[(1*R*)(adamantan-1-yl)(2-methoxyphenyl)methoxy]ethyl}(3*R*)-piperidine-3-carboxylate and *rac*-Ethyl 1-{2-[(1*S*)(adamantan-1-yl)(2-methoxyphenyl)methoxy]ethyl}-(3*R*)-piperidine-3-carboxylate ~1:1 (36d)** According to GP6 from **17d** (340 mg, 1.00 mmol), ethyl nipecotinate (180 mg, 1.10 mmol), potassium carbonate (346 mg, 2.50 mmol), potassium iodide (8.3 mg, 0.050 mmol), acetonitrile (6.0 ml). After purification by flash column chromatography (eluent: pentane/diethyl ether 1 : 1) **36d** was obtained as colorless oil (379 mg, 82 %). ^{1}H NMR (400 MHz, CD_2Cl_2, 25°C) δ = 1.21 (t, *J*=7.1, 3H), 1.33 – 1.77 (m, 15H), 1.82 – 1.92 (m, 4H), 2.02 (tt, *J*=11.1, 3.2, 1H), 2.15 (td, *J*=10.7, 6.0, 1H), 2.43 – 2.52 (m, 3H), 2.67 – 2.75 (m, 1H), 2.94 – 3.03 (m, 1H), 3.17 – 3.33 (m, 2H), 3.77 (s, 3H), 4.07 (m, 2H), 4.35 (d, *J*=3.1, 1H), 6.86 (d, *J*=8.2, 1H), 6.93 (t, *J*=7.5, 1H), 7.18 – 7.24 (m, 1H), 7.29 (dt, *J*=7.9, 2.3, 1H). ^{13}C NMR (126 MHz, CD_2Cl_2, 25°C) δ = 14.43, 25.16, 27.30 (d, *J*=7.5), 29.08, 37.71, 38.28, 38.53, 42.50, 54.54, 55.48, 56.41 (d, *J*=2.8), 58.57, 60.49, 67.84, 82.88, 110.40, 120.07, 128.09, 129.50 (d, *J*=3.1), 158.84, 174.48. IR (KBr): ṽ = 2888, 2848, 1733, 1600, 1587, 1489, 1458, 1361, 1314, 1281, 1238, 1183, 1154, 1090, 1033, 939, 862, 809, 755, 719, 658, 626, 495 cm^{-1}. HRMS-ESI+ *m/z* [*M*+H]$^{+}$ calcd for $C_{28}H_{41}O_4N$: 456.3114, found: 456.3106.

***rac*-Ethyl 1-{2-[(1*R*)(3,5-dimethyladamantan-1-yl)(4-methoxyphenyl)methoxy]ethyl}(3*R*)-piperidine-3-carboxylate and *rac*-Ethyl 1-{2-[(1*S*)(3,5-dimethyladamantan-1-yl)(4-methoxy-phenyl)methoxy]ethyl}(3*R*)-piperidine-3-carboxylate ~1:1 (36e)** According to GP6 from **17e**

(327 mg, 0.90 mmol), ethyl nipecotinate (162 mg, 1.00 mmol), potassium carbonate (311 mg, 2.25 mmol), potassium iodide (7.5 mg, 0.045 mmol), acetonitrile (5.0 ml). After purification by flash column chromatography (eluent: pentane/diethyl ether 1 : 1) **36e** was obtained as colorless oil (377 mg, 87 %). ^{1}H NMR (400 MHz, CD_2Cl_2, 25°C) δ = 0.76 (s, 6H), 0.94 – 1.10 (m, 4H), 1.16 – 1.72 (m, 14H), 1.81 – 1.92 (m, 1H), 1.95 – 2.09 (m, 2H), 2.10 – 2.22 (m, 1H), 2.42 – 2.56 (m, 3H), 2.65 – 2.76 (m, 1H), 2.90 – 3.03 (m, 1H), 3.22 (dtd, *J*=10.0, 6.0, 2.6, 1H), 3.35 (dt, *J*=10.0, 6.0, 1H), 3.71 (s, 1H), 3.79 (d, *J*=0.6, 3H), 4.08 (m, 2H), 6.77 – 6.91 (m, 2H), 7.04 – 7.18 (m, 2H). ^{13}C NMR (126 MHz, CD_2Cl_2, 25°C) δ = 14.59 (d, *J*=1.6), 25.32 (d, *J*=2.7), 27.46 (d, *J*=8.4), 30.19, 31.11, 31.39, 37.64, 39.69, 42.64, 43.91, 45.28, 51.76, 54.65 (d, *J*=4.0), 55.66, 56.55 (d), 58.64 (d, *J*=4.7), 60.64, 67.94 (d, *J*=5.2), 90.77 (d, *J*=3.3), 113.19, 130.13 (d, *J*=1.6), 131.71, 159.32, 174.61. IR (KBr): ṽ = 2941, 2898, 2839, 2861, 1732, 1612, 1584, 1511, 1455, 1357, 1302, 1247, 1173, 1154, 1096, 1035, 966, 943, 833, 790, 759, 735, 696, 663, 636, 605, 569, 535 cm^{-1}. HRMS-ESI+ *m/z* [*M*+H]$^{+}$ calcd for $C_{30}H_{45}O_4N$: 484.3421, found: 484.3422.

***rac*-Ethyl 1-{2-[(1*R*)(3-methoxyadamantan-1-yl)(4-methoxyphenyl)methoxy]ethyl}(3*R*)-piperidine-3-carboxylate and *rac*-Ethyl 1-{2-[(1*S*)(3-methoxyadamantan-1-yl)(4-methoxyphenyl)methoxy]ethyl}(3*R*)-piperidine-3-carboxylate ~1:1 (36g)** According to GP6 from **17g** (250 mg, 0.690 mmol), ethyl nipecotinate (121 mg, 0.753 mmol), potassium carbonate (236 mg, 1.71 mmol), potassium iodide (5.6 mg, 0.033 mmol), acetonitrile (5.0 ml). After purification by flash column chromatography (eluent: diethyl ether) **36g** was obtained as pale yellowish oil (215 mg, 65 %). ^{1}H NMR (400 MHz, CD_2Cl_2, 25°C) δ = 1.21 (td, *J*=7.1, 1.4, 3H), 1.27 – 1.72 (m, 15H), 1.84 – 1.92 (m, 1H), 1.99 – 2.09 (m, 1H), 2.10 – 2.23 (m, 3H), 2.43 – 2.57 (m, 3H), 2.71 (br d, *J*=11.1, 1H), 2.92 – 3.03 (m, 1H), 3.14 (s, 3H), 3.20 – 3.29 (m, 1H), 3.33 – 3.41 (m, 1H), 3.76 (s, 1H), 3.79 (d, *J*=0.5, 3H), 4.03 – 4.13 (m, 2H), 6.79 – 6.89 (m, 2H), 7.07 – 7.17 (m, 2H). ^{13}C NMR (101 MHz, CD_2Cl_2, 25°C) δ = 14.43, 25.15, 27.28 (d, *J*=5.7), 30.75, 36.44, 37.89 (d, *J*=4.0), 38.02, 40.92 (d, *J*=2.4), 41.09, 42.45 (d, *J*=3.0), 47.95, 55.55, 56.42 (d, *J*=4.4), 58.53 (d, *J*=2.8), 60.51, 67.85, 72.93, 90.21 (d, *J*=2.9), 113.18, 129.93, 131.22, 159.32, 174.44. IR (KBr): ṽ = 2934, 2357, 1731, 1611, 1584, 1511, 1465, 1454, 1355, 1303, 1247, 1173, 1154, 1112, 1080, 1035, 882, 834, 802, 736, 660, 636 cm^{-1}. HRMS-ESI+ *m/z* [*M*+H]$^{+}$ calcd for $C_{29}H_{43}NO_5$: 486.3214, found: 486.3215.

2-(2-Chloroethoxy)-2-(4-methoxyphenyl)adamantane (38) 2-Chloroethanol (506 mg, 6.28 mmol) and 4-toluenesulfonic acid monohydrate (29.9 mg, 0.158 mmol) were added to a solution of **37** (810 mg, 3.14 mmol) in 6.0 ml acetonitrile. The reaction mixture was stirred for 2 h, added to phosphate buffer pH 7.0 and extracted thrice with CH_2Cl_2 (25.0 ml). The combined organic phases were dried over sodium sulfate and reduced in vacuum. The crude product was purified by flash column chromatography (eluent: pentane/diethyl ether 9:1). **38** was obtained as white solid (717 mg, 71 %). ^{1}H NMR (400 MHz, $CDCl_3$, 25°C) δ = 1.62 – 1.78 (m, 9H), 1.83 – 1.93 (m, 1H), 2.37 (br d, *J*=12.4, 2H), 2.58 (br s, 2H), 3.14 (t, *J*=6.1, 2H), 3.36 (t, *J*=6.1, 2H), 3.82 (s, 3H), 6.84 – 6.93 (m, 2H), 7.34 – 7.43 (m, 2H). ^{13}C NMR (101 MHz, $CDCl_3$, 25°C) δ = 26.98, 27.87, 32.94, 33.54, 34.65, 37.87, 43.82, 55.29, 60.91, 80.09, 113.46, 128.53, 133.36, 158.68. IR (KBr): ṽ = 2912, 2853, 1606, 1513, 1458, 1299, 1263, 1097, 1032, 991, 854, 822, 670, 541 cm^{-1}. HRMS+EI *m/z* $[M]^+$ calcd for $C_{19}H_{25}O_2Cl$: 320.1543, found: 320.1538.

***rac*-Ethyl 1-(2-{[2-(4-methoxyphenyl)adamantan-2-yl]oxy}ethyl)piperidine-3-carboxylate (39)** According to GP6 from **38** (697 mg, 2.17 mmol), ethyl nipecotinate (436 mg, 2.66 mmol), potassium carbonate (750 mg, 5.42 mmol), potassium iodide (18 mg, 0.11 mmol), acetonitrile (10.8 ml). After purification by flash column chromatography (eluent: pentane/diethyl ether 92 : 8 + 3% triethyl amine) **39** was obtained as colorless oil (914 mg, 95 %). ^{1}H NMR (400 MHz, $CDCl_3$, 25°C) δ = 1.23 (t, *J*=7.1, 3H), 1.34 (m, 1H), 1.40 – 1.56 (m, 1H), 1.57 – 1.77 (m, 10H), 1.84 – 1.98 (m, 3H), 2.07 (t, *J*=10.9, 1H), 2.28 – 2.41 (m, 4H), 2.46 (tt, *J*=10.9, 3.8, 1H), 2.53 – 2.59 (m, 2H), 2.58 – 2.67 (m, 1H), 2.88 – 2.94 (m, 1H), 2.97 – 3.07 (m, 2H), 3.81 (s, 3H), 4.10 (q, *J*=7.1, 2H), 6.83 – 6.90 (m, 2H), 7.34 – 7.40 (m, 2H). ^{13}C NMR (101 MHz, $CDCl_3$, 25°C) δ = 14.36, 24.80, 27.04, 27.07, 27.96, 33.16, 33.36, 33.63, 34.68, 37.98, 42.12, 54.24, 55.30, 56.06, 58.13, 58.78, 60.35, 79.65, 113.33, 128.62, 133.82, 158.49, 174.45. IR (KBr): ṽ = 2907, 2853, 1731, 1608, 1581, 1513, 1466, 1448, 1366, 1300, 1254, 1182, 1035, 973, 916, 825, 738 cm^{-1}. HRMS+EI *m/z* $[M]^+$ calcd for $C_{27}H_{39}NO_4$: 441.2879, found: 441.2871.

References

[1] Fact Sheet Epilepsy www.who.int/news-room/fact-sheets/detail/epilepsy (accessed July 19, 2019)

[2] T.R. Holmes, G.L. Browne, *Handbook of epilepsy* (4th ed.) **2008**, Philadelphia: Lippincott Williams & Wilkins, p. 7

[3] D. Hirtz, D.J. Thurman, K. Gwinn-Hardy, M. Mohamed, A.R. Chaudhuri, R. Zalutsky, *Neurology* **2007**, 68 (5), 326-337

[4] Atlas: Epilepsy Care in the World, World Health Organization, **2005** www.who.int/mental_health/neurology/Epilepsy_atlas_r1.pdf (accessed July 19, 2019)

[5] D.M. Treiman**,** *Epilepsia* **2001**, *42*, 8-12

[6] S.R. Kleppner, A.J. Tobin**,** *Expert Opinion on Therapeutic Targets* **2001**, *5*, 219-239

[7] H.E. Scharfman, Curr Neurol Neurosci Rep **2007**, 7, 348-354

[8] P. Krogsgaard-Larsen, *Medicinal Research Reviews* **1988**, Vol. 8, No. 1, 27-56

[9] B.S. Meldrum, A.G. Chapman, Epilepsia **1999**, *40*, 9, 2-6

[10] J.M. Kuhar, Life Sci. **1973**, *13*, 1623

[11] K.K. Madsen, H.S. White, A. Schousboe, *Pharmacology & Therapeutics* **2010**, *125*, 394-401

[12] R. Schirrmacher, W. Hamkens, M. Piel, U. Schmitt, H. Lüddens, C. Hiemke, F. Rösch*, Journal of Labelled Compounds and Radiopharceuticals* **2001**, *44*, 627-642

[13] S. Bröer, U. Gether, *British Journal of Pharmacology* **2012**, *167*, 2, 256-278

[14] A.S. Kristensen, J. Andersen, T.N. Jørgensen, L. Sørensen, J. Eriksen, C.J. Loland, K. Strømgaard, U. Gether, *Pharmacological Reviews* **2011**, *63*, 3, 585-640

[15] L.A. Borden, *Neurochemistry International* **1996**, *29*, 4, 335-356

[16] N. O. Dalby, *Eur. J. Pharmacol.* **2003**, 479, 127-137

[17] B. Christiansen, A. K. Meinild, A. A. Jensen, H. Bräuner-Osbore, *Journal of Biological Chemistry* **2007**, *282*, 19331-19341

[18] K.K. Madsen, R.P. Clausen, O.M. Larsson, P. Krogsgaard-Larsen, A. Schousboe, H.S. White, *Journal of Neurochemistry* **2009**, *109*, 139-144

[19] Y. Zhou, N.C. Danbolt, *Front Endocrinol* **2013**, *4*, 165

[20] S.A. Kempson SA, Y. Zhou Y, N.C. Danbolt, *Frontiers in Physiology* **2014**, *5*, 159

[21] Y. Zhou, S. Holmseth, R. Hua, A. C. Lehre, A. M. Olofsson, I. Poblete-Naredo, S. A. Kempson, N. C. Danbolt, *American Journal of Physiology – Renal Physiology* **2012**, *302*, 313-328

[22] P. Genton, R. Guerrini, E. Perucca, *Epilepsia* **2001**, *42*, 42-45

[23] S.M. LaRoche, S.L. Helmers, *JAMA* **2004**, *291*, 605-614

[24] I.E. Leppik, L. Gram, R. Deaton, K.W. Sommerville, *Epilepsy Research* **1999**, *33*, 235–246

[25] J.P. Leach, M.J. Brodie, *Lancet* **1998**, *351*, 203-207

[26] A.S. Kristensen, J. Andersen, T.N. Jørgensen, L. Sørensen, J. Eriksen, C.J. Loland, K. Strømgaard, U. Gether, *Pharmacological Reviews* **2011**, *63*, 3, 585-640

[27] K.K. Madsen, H.S. White, A. Schousboe, *Pharmacology & Therapeutics* **2010**, *125*, 394-401

[28] T.G.M. Dhar, L.A. Borden, S. Tyagarajan, K.E. Smith, T.A. Branchek, R.L. Weinshank, C. Gluchowski, *Journal of Medicinal Chemistry* **1994**, 37, 2334-2342

[29] J. Pabel, M. Faust, C. Prehn, B. Woerlein, L. Allmendinger, G. Höfner, K.T. Wanner, *ChemMedChem* **2012**, *7*, 1245-1255

[30] M. Damgaard, R.P. Clausen, *ACS Chem. Neurosci.* **2015**, *6*, 1591−1599

[31] M. Petrera, T. Wein, L. Allmendinger, M. Sindelar, J. Pabel, G. Höfner, K.T. Wanner *ChemMedChem*. **2016**, *11*, 519-538

[32] A. Kragler, G. Höfner, K.T. Wanner, *European Journal of Medical Chemistry* **2008**, *43*, 2404-2411

[33] G. Bhaksar, M. Solomon, G. Babu, D. Muralidharan, P.T. Perumal, *Indian Journal of Chemistry* **2010**, *48B*, 795-801

[34] T.G.M. Dhar, L.A. Borden, S. Tyagarajan, K.E. Smith, T.A. Branchek, R.L. Weinshank, C. Gluchowski, *Journal of Medicinal Chemistry* **1994**, *37*, 2334-2342

[35] T. Högberg, P. Ström, M. Ebner, S. Rämsby, *Journal of Organic Chemistry* **1987**, *52*, 2033-2036

[36] L.J.S. Knutsen, K.E. Andersen, J. Lau, B.F. Lundt, R.F. Henry, H.E. Morton, L. Nrum, H. Petersen, H. Stephensen, P.D. Suzdak*, Journal of Medicinal Chemistry* **1999**, *42*, 18, 3447-3462

[37] W.E. Bondinell, R.F. Hall, Q. Jin, J.K. Kerns, H. Nie, K.L. Widdowson, *PCT Int. Appl.* **2004**, WO2004017911

[38] B.P. Reddy, V.M. Sharma, K.R. Reddy, L.V.L. Subrahmanyam, N. Sudhakar, *PCT Int. Appl.* **2012**, WO2012025857

[39] J. Regan, S. Breitenfelder, P. Crillo, T. Gilmore, A.G. Graham, E. Hickey, B. Klaus, J. Madwed, M. Moriak, N. Moss, C. Pargellis, S. Pav, A- Pronto, A. Swinamer, L. Tong, C. Torcellini, *Journal of Medicinal Chemistry* **2002**, *45*, 2994-3008

[40] D.G. Cooper, I.T. Forbes, V. Garzya, J. Jin, Y. Louchart, G. Walker, P.A. Wyman, *PCT Int. Appl*. **2007**, WO2007107566

[41] B. Liegault, K. Fagnou, *Organometallics* **2008**, *27*, 4841–4843

[42] V. Sperandio, J.R. Falk, *U.S. Pat. Appl. Publ.* **2014**, 20140275189

[43] J.M. Balkovec, R. Thieringer, S.S. Mundt, A. Hermanowski-Vosatka, D.W. Graham, G.F. Patel, S.D. Aster, S.T. Waddell, S.H. Olson, M. Maletic, *PCT Int. Appl.* **2003**, 2003065983

[44] N. Basarić, I. Žabčić, K. Mlinarić-Majerski, P. Wan*, Journal of Organic Chemistry* **2010,** *75*, 1, 102-116

Spectra

***rac*-1-{2-[1,1-Bis(4-methoxyphenyl)-2,2-dimethylpropoxy]ethyl}piperidine-3-carboxylic acid (6a)**

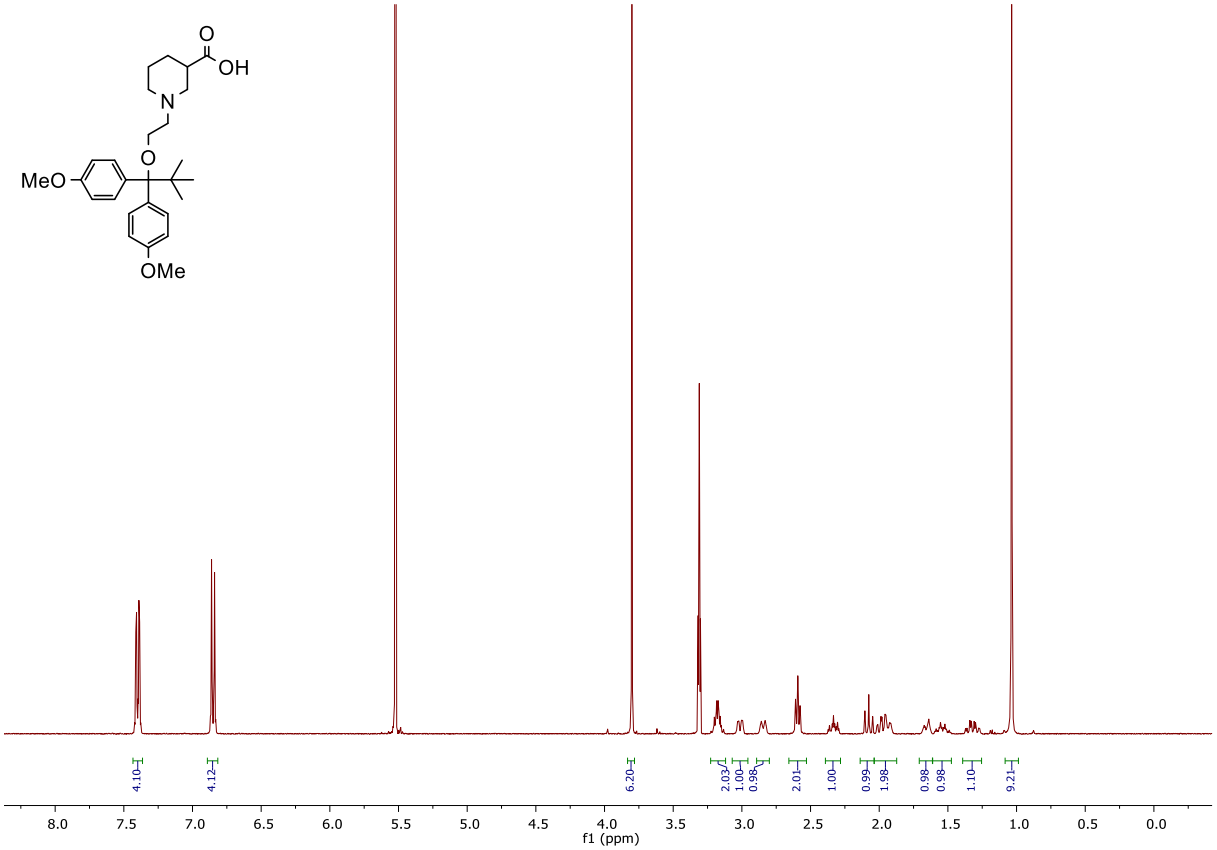

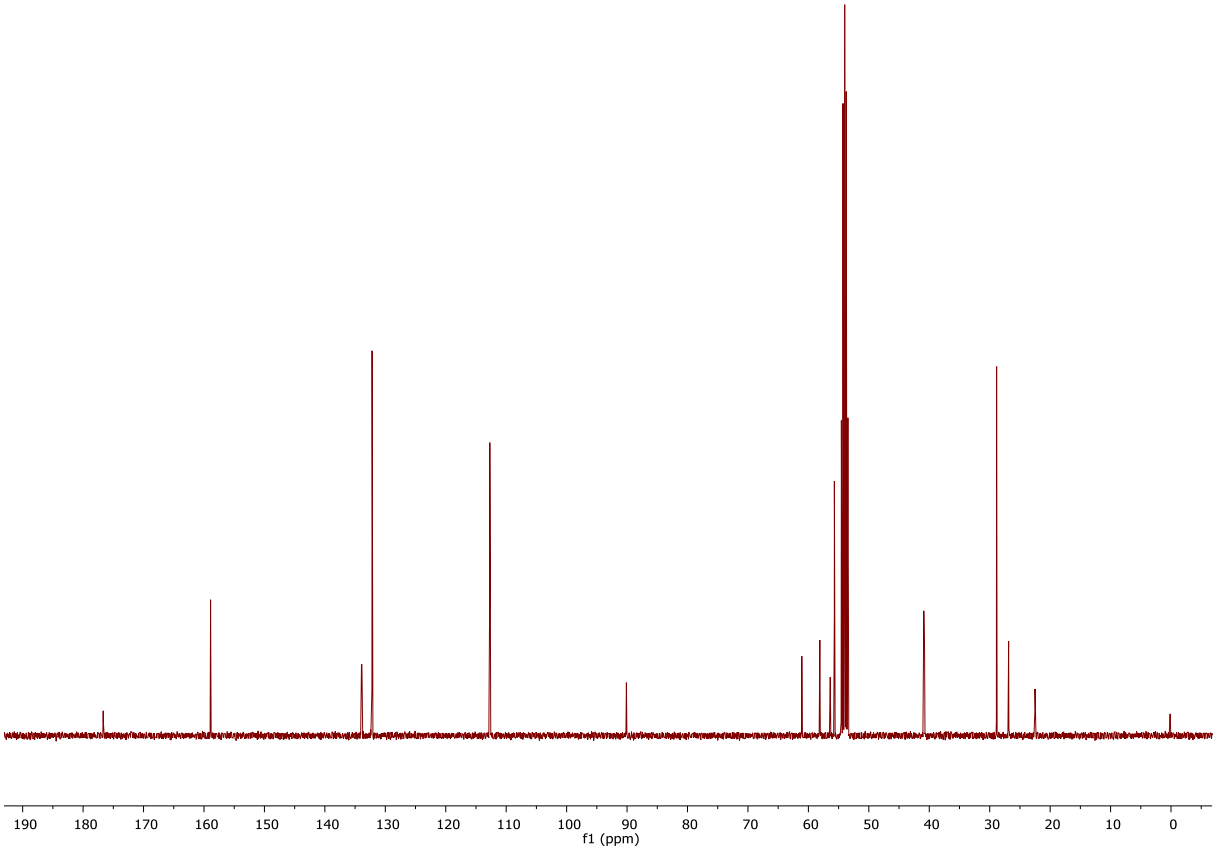

***rac*-1-{2-[Bis(4-methoxyphenyl)(1-methylcyclopentyl)methoxy]ethyl}piperidine-3-carboxylic acid (6b)**

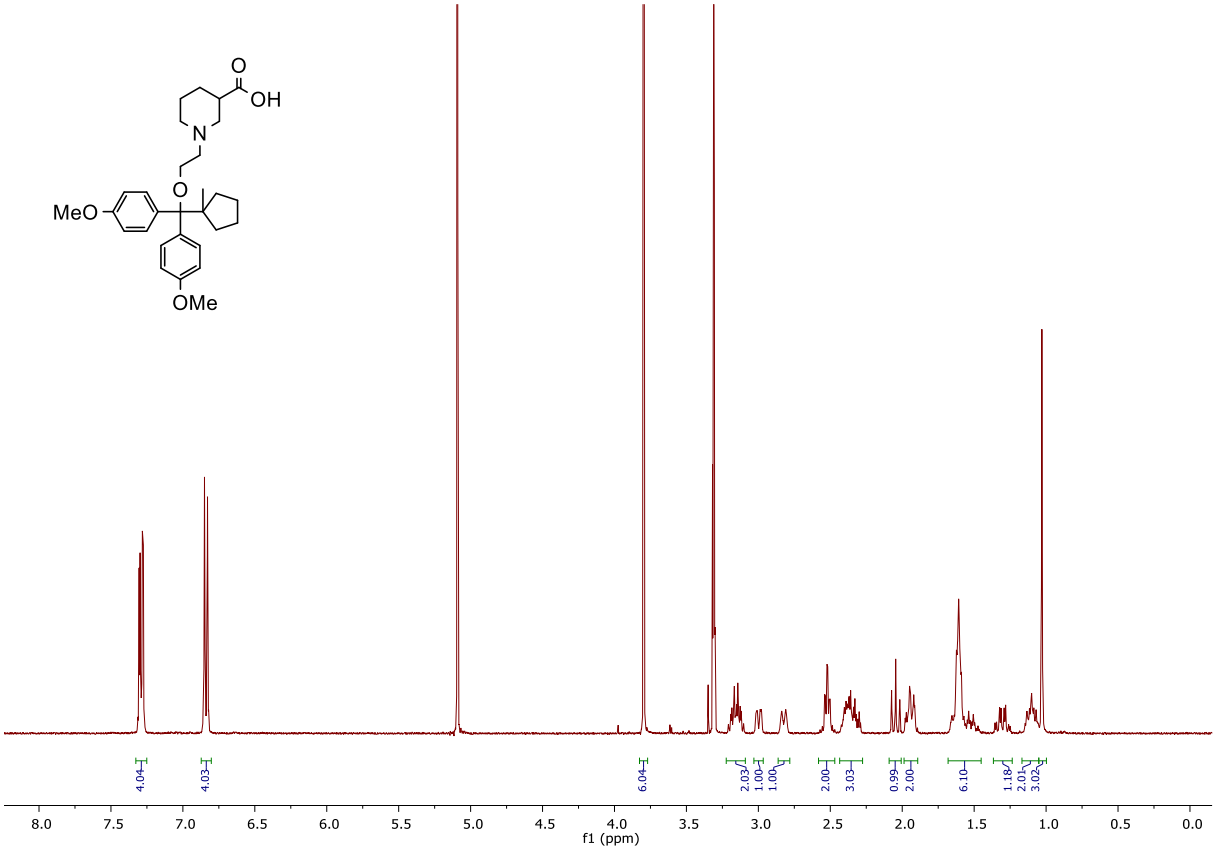

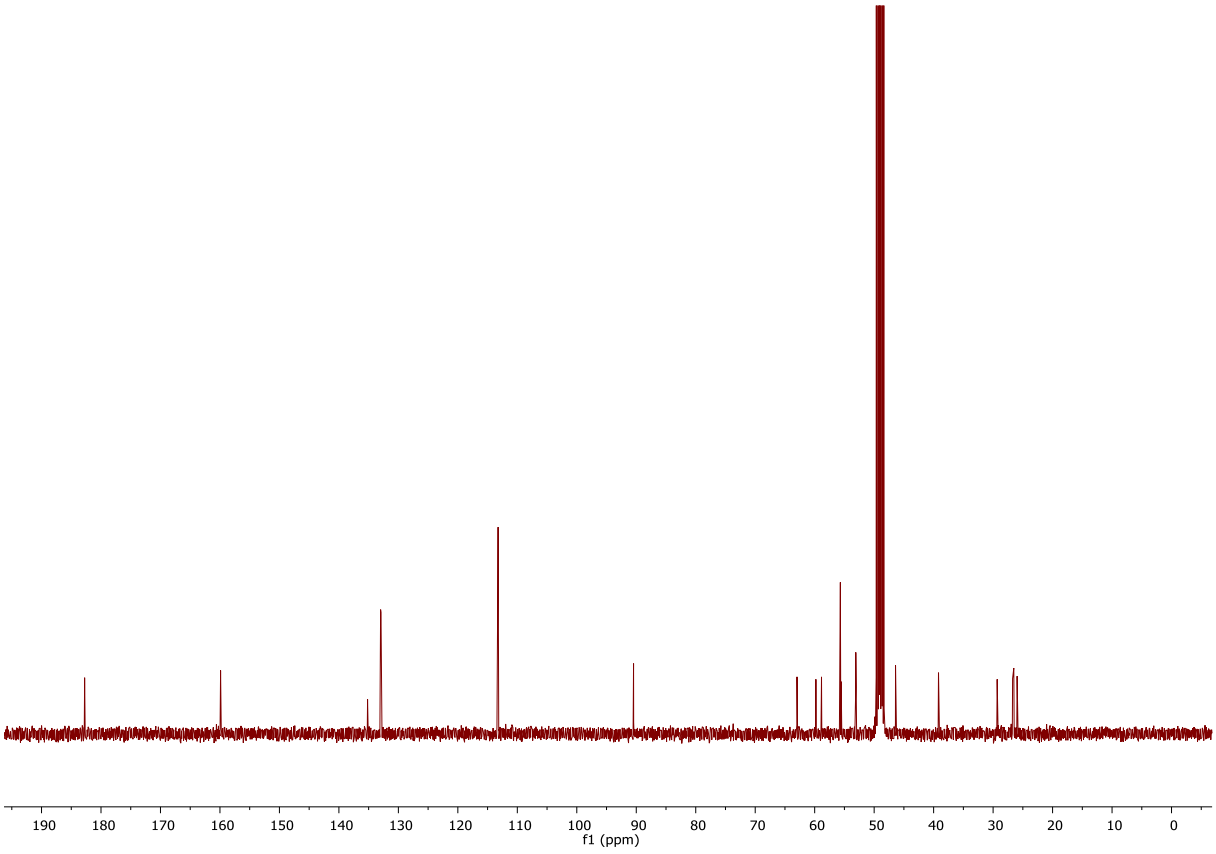

***rac*-1-{2-[Bis(4-methoxyphenyl)(1-methylcyclohexyl)methoxy]ethyl}piperidine-3-carboxylic acid (6c)**

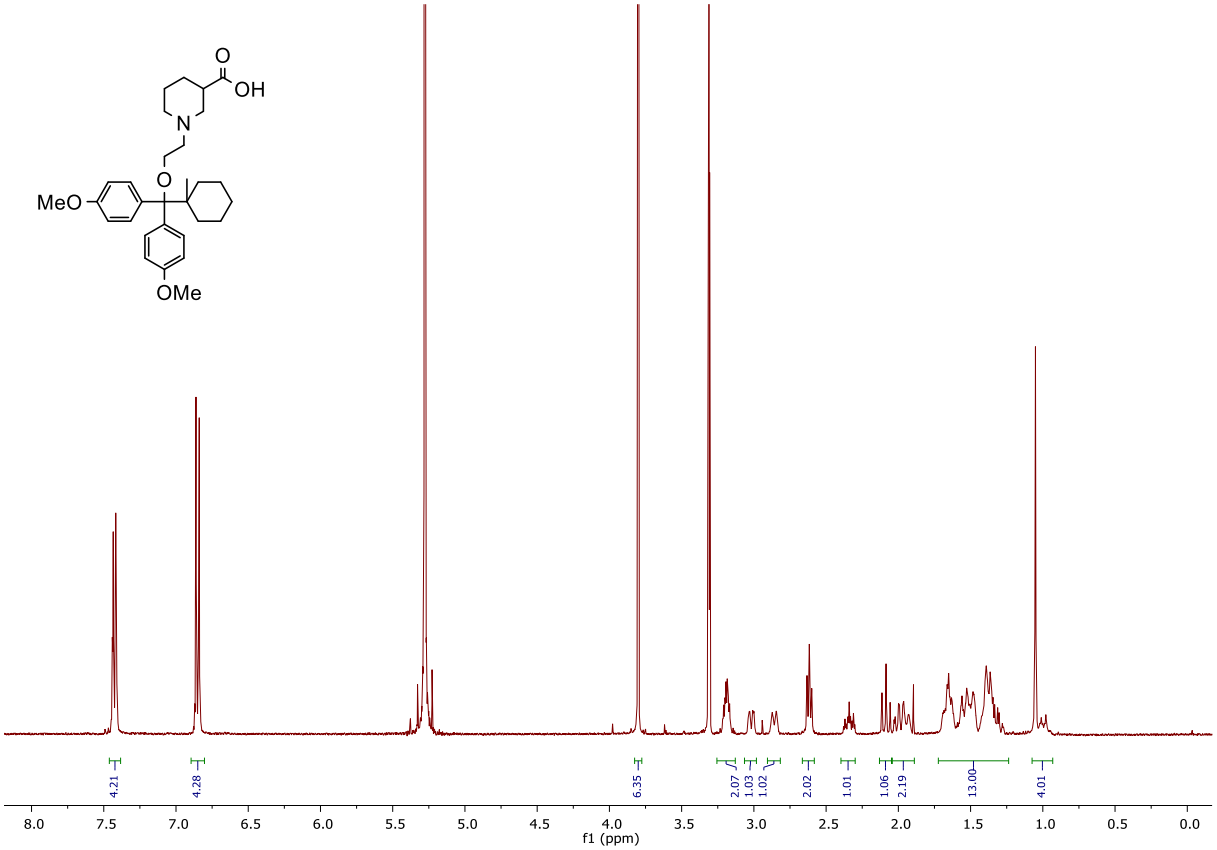

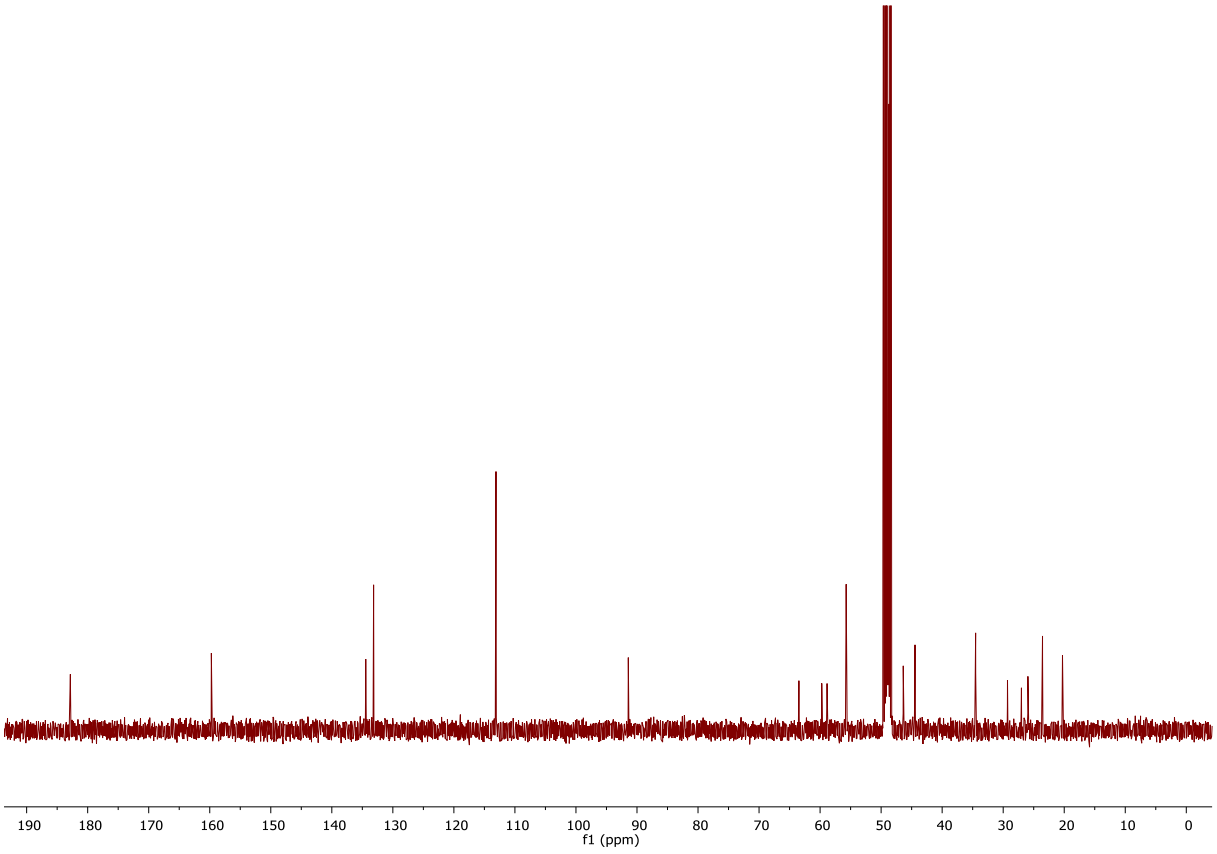

***rac*-1-{2-[Bis(4-methoxyphenyl)(4-methyltetrahydro-2H-pyran-4-yl)methoxy]ethyl}piperidine-3-carboxylic acid (6d)**

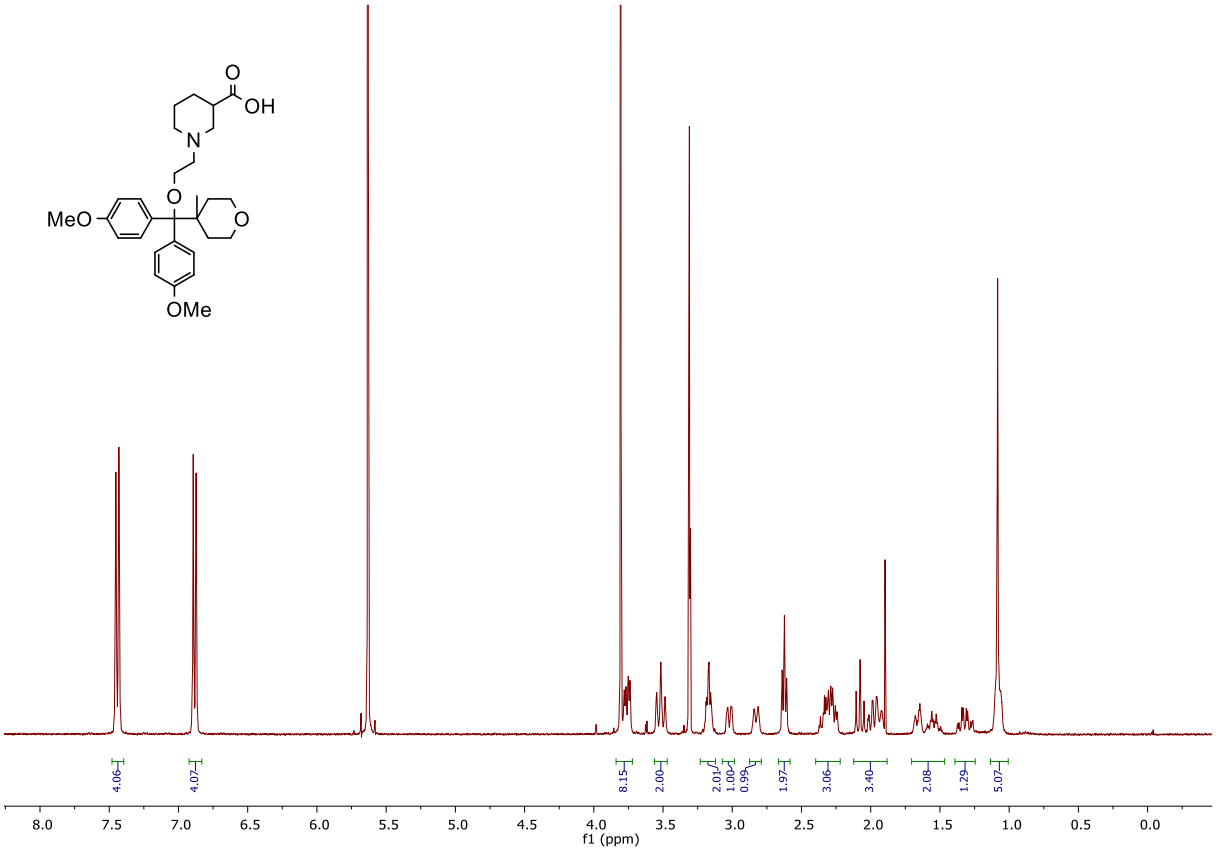

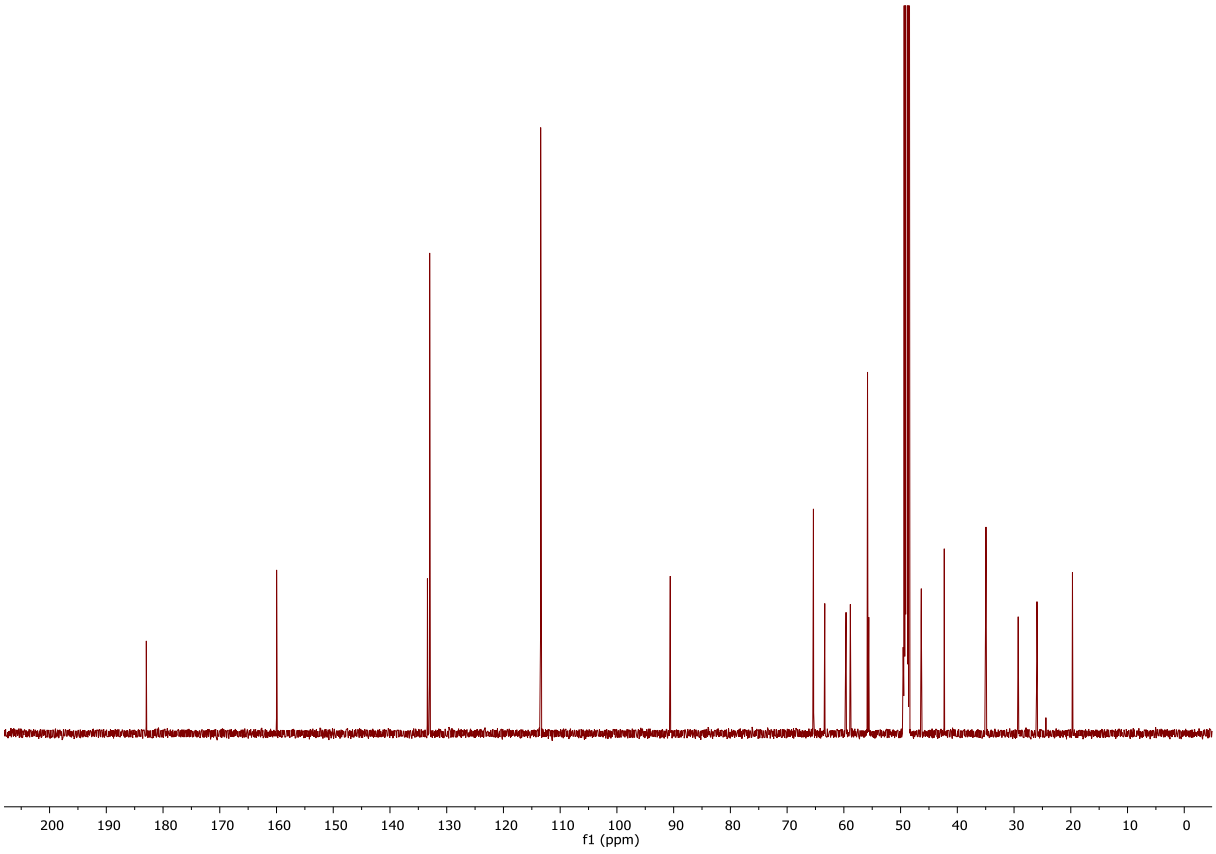

***rac*-1-(2-{[(1*S*,4*S*)-4-Methoxy-1-methylcyclohexyl]bis[4-methoxyphenyl]methoxy}ethyl)piperidine-3-carboxylic acid (6e)**

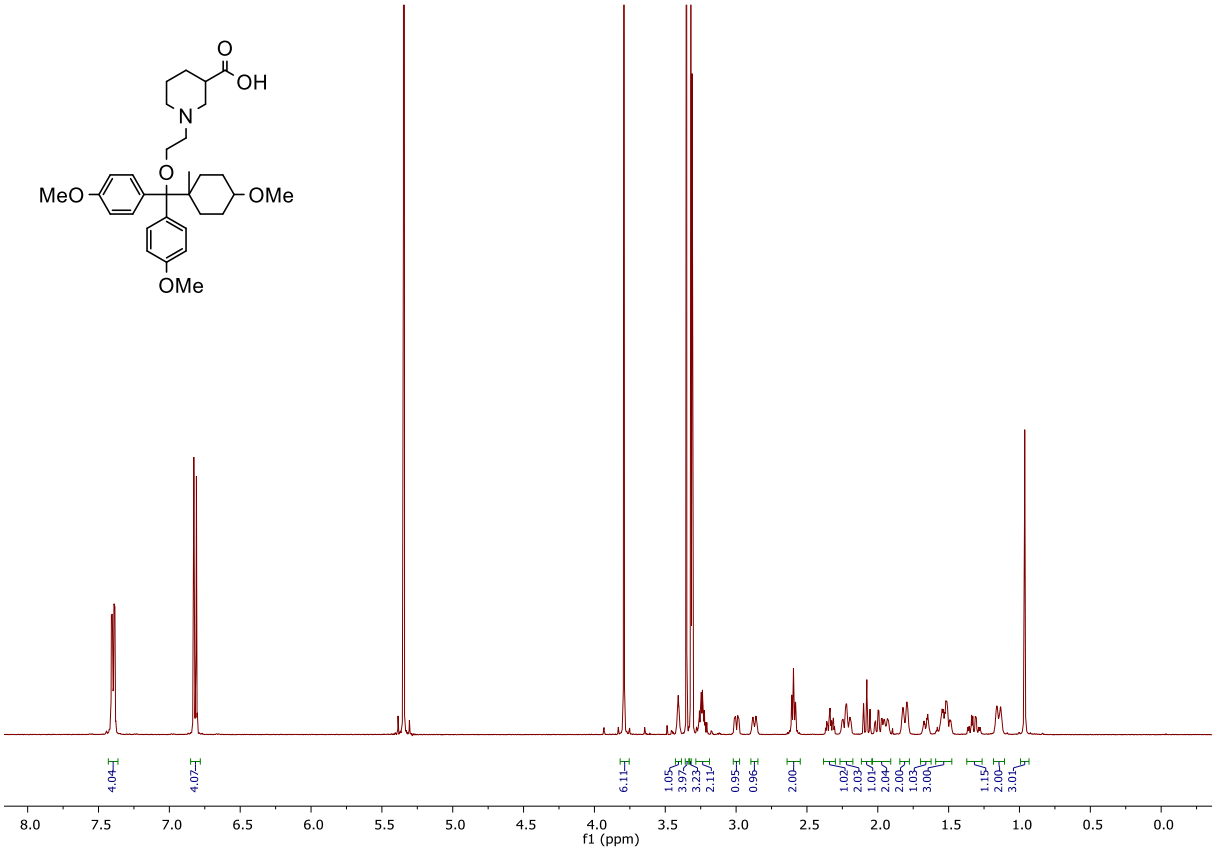

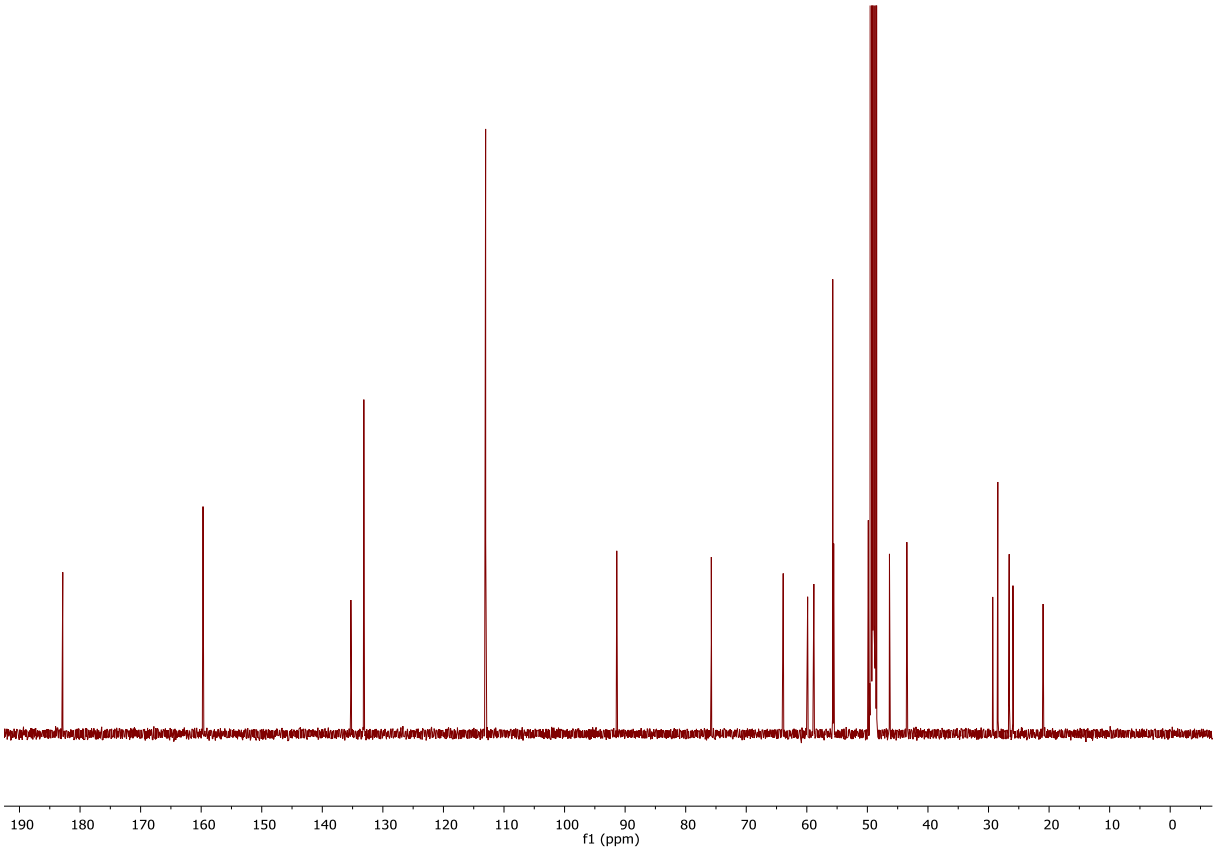

***rac*-1-{2-[(Adamantan-1-yl)bis(4-methoxyphenyl)methoxy]ethyl}piperidine-3-carboxylic acid (6f)**

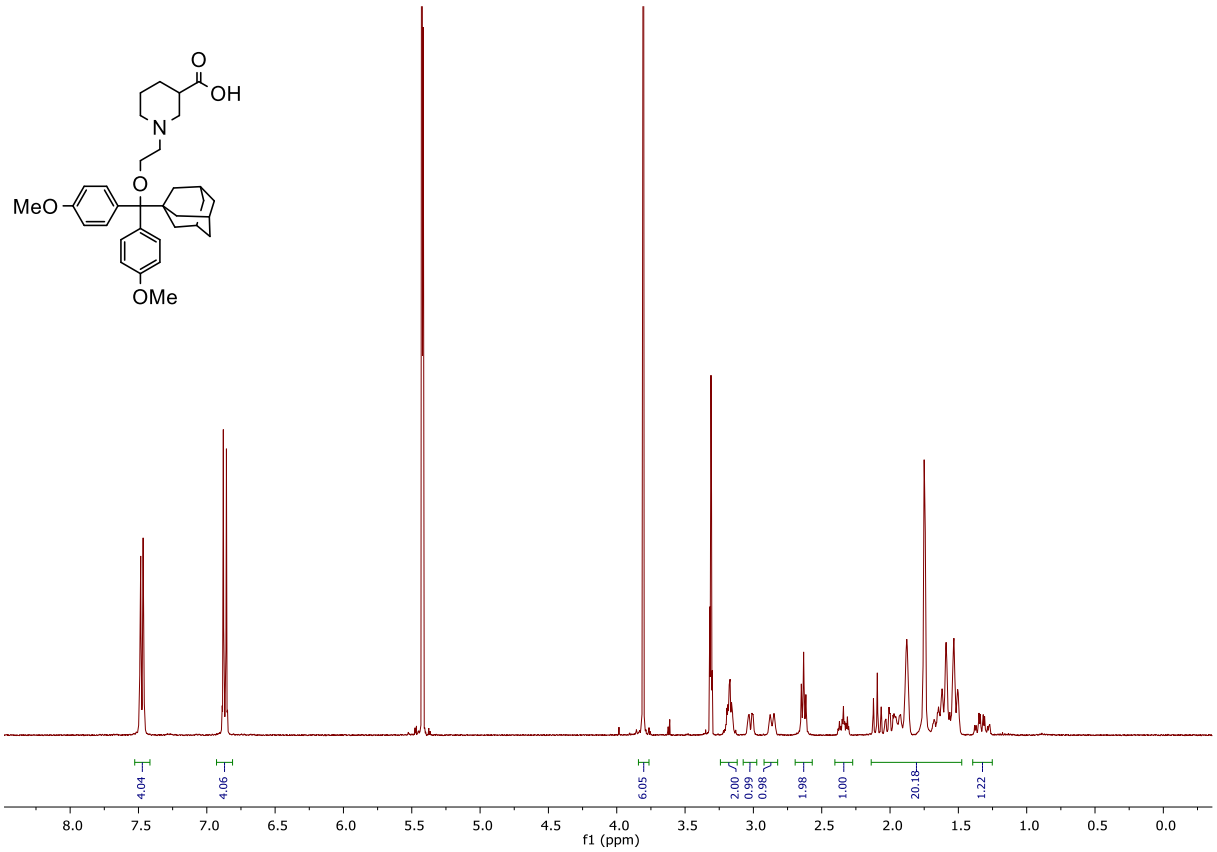

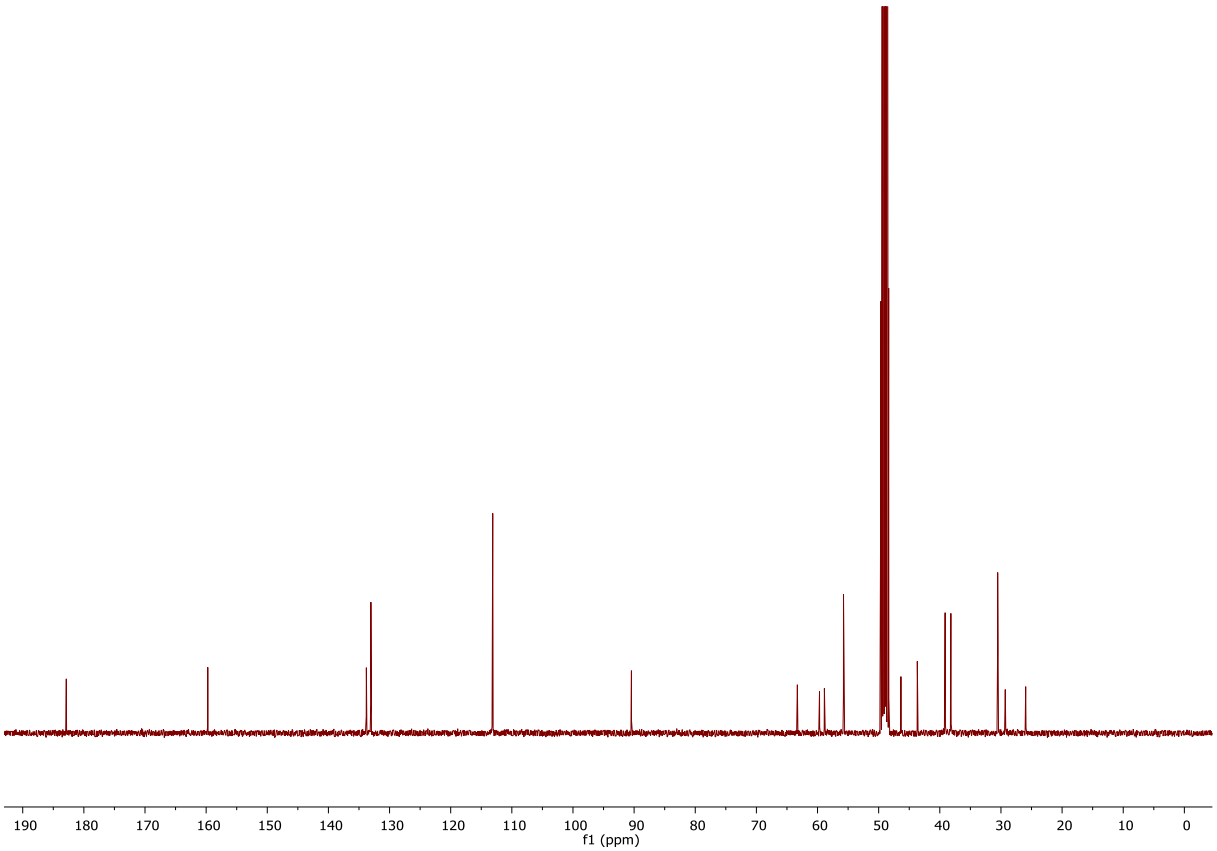

***rac*-1-{3-[1,1-Bis(4-methoxyphenyl)-2,2-dimethylpropoxy]propyl}piperidine-3-carboxylic acid (7)**

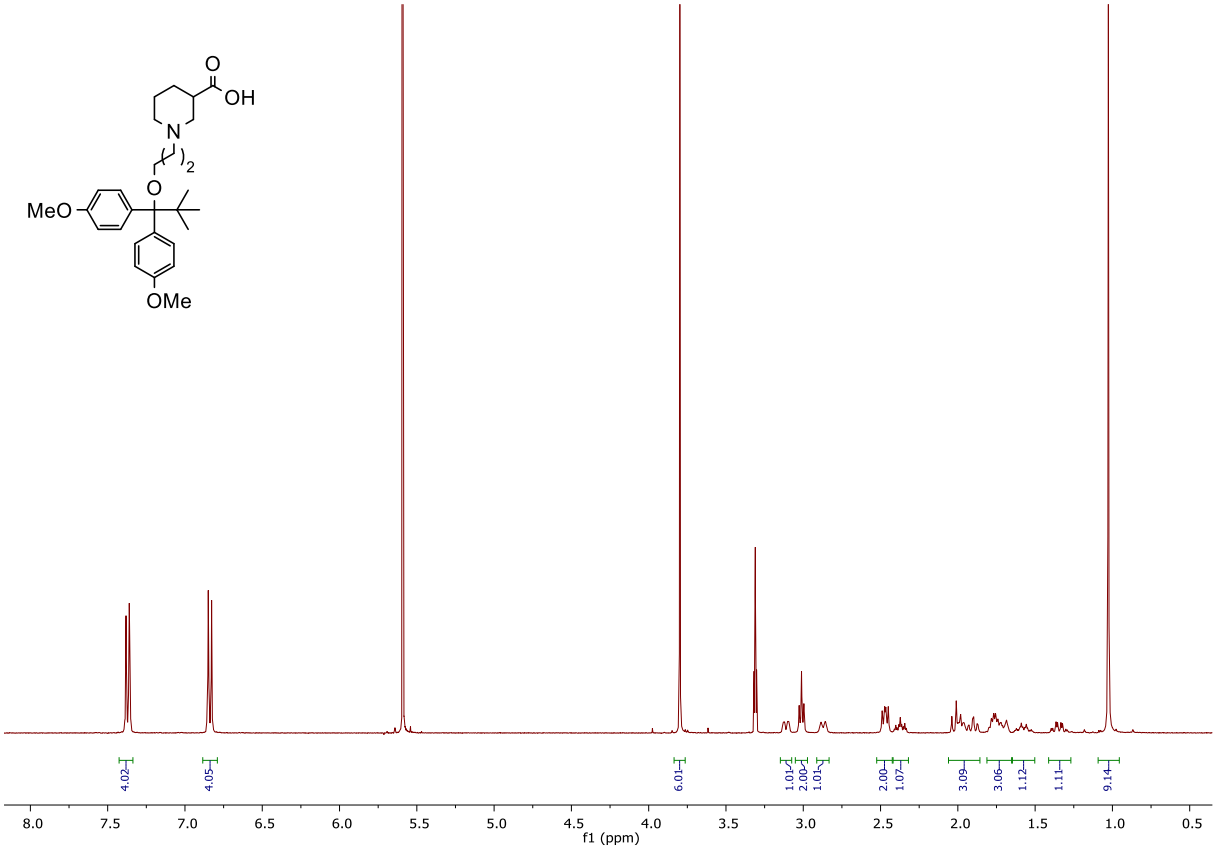

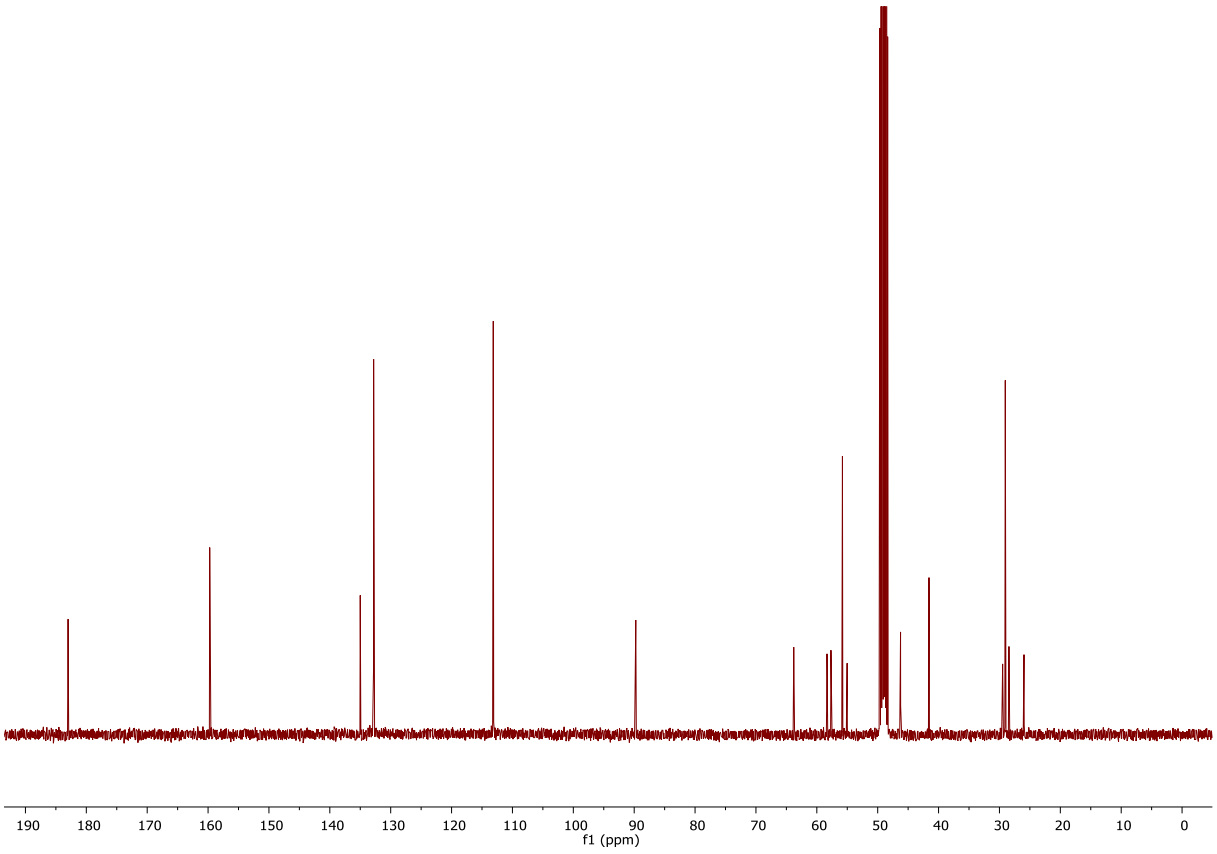

***rac*-1-{4-[1,1-Bis(4-methoxyphenyl)-2,2-dimethylpropoxy]butyl}piperidine-3-carboxylic acid (8)**

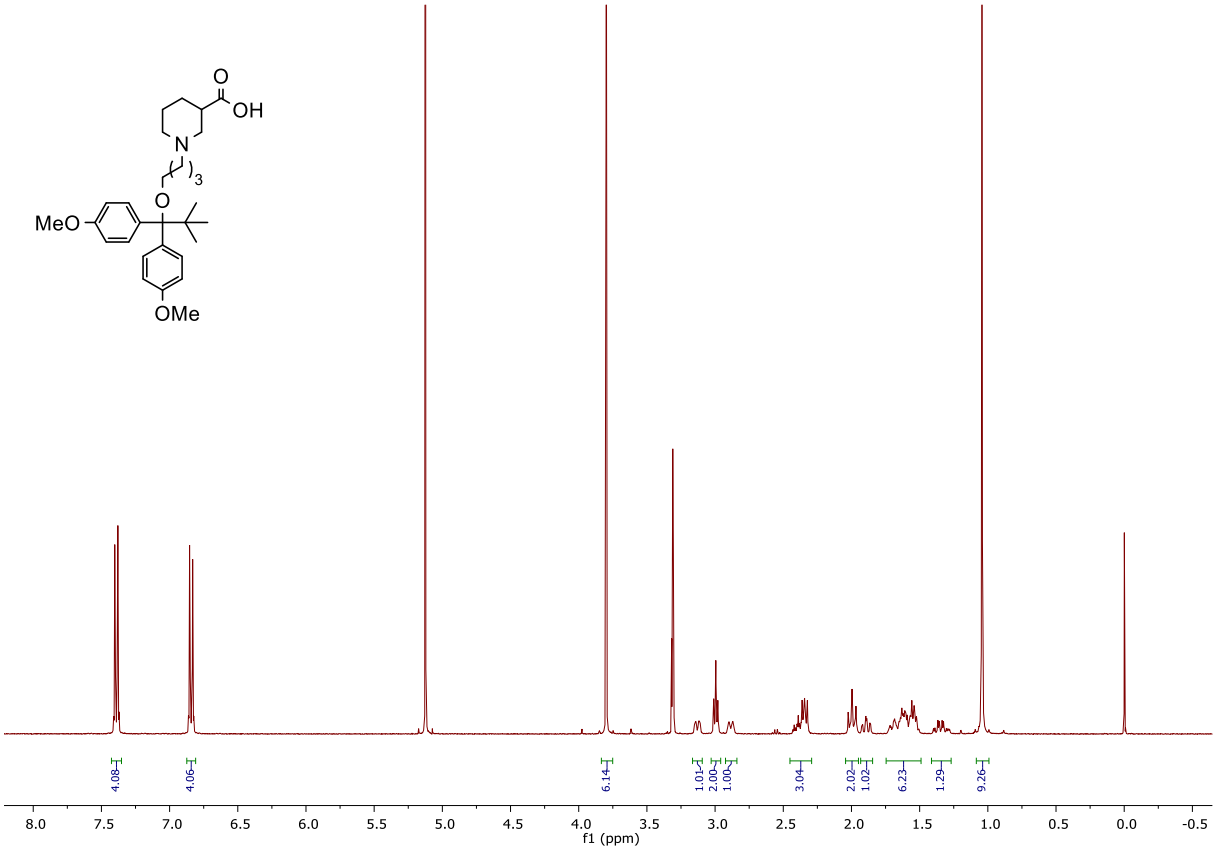

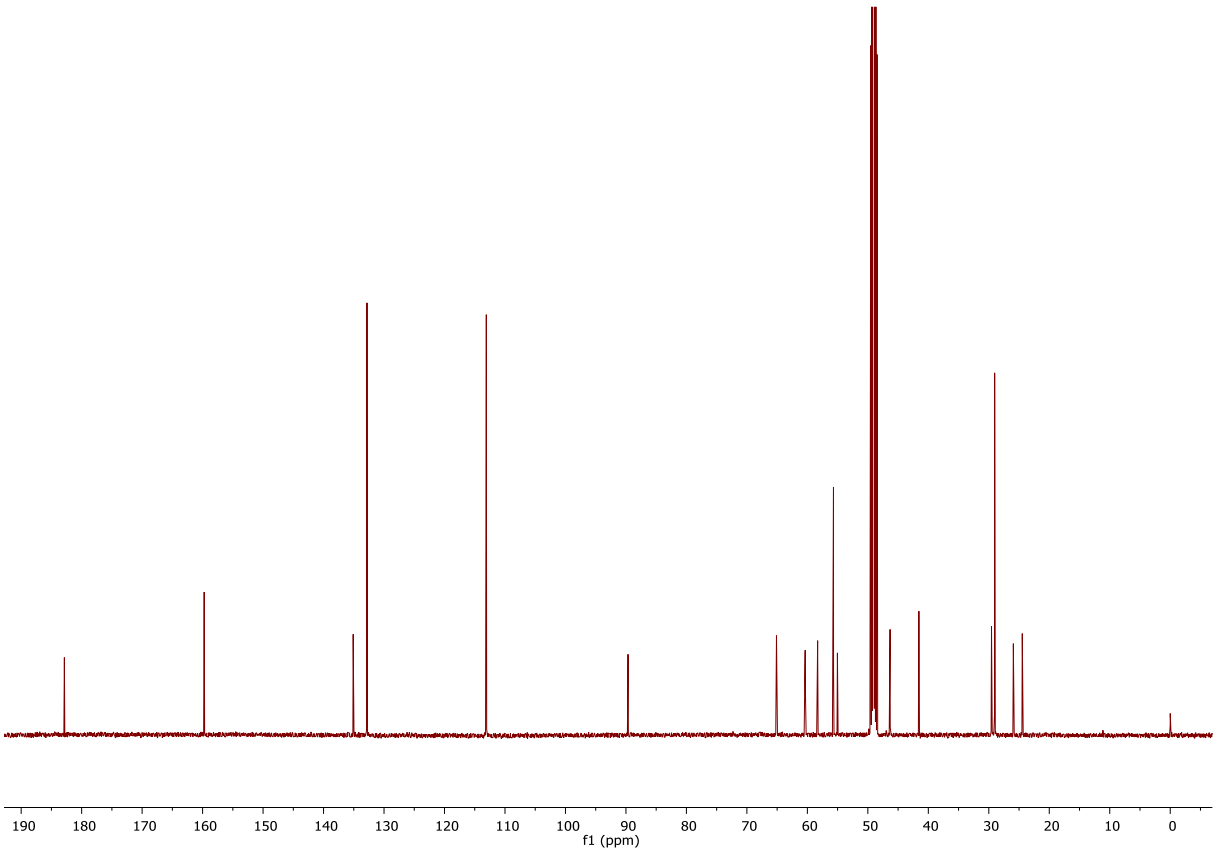

rac-1-{2-[(1_R_)(4-Methoxyphenyl)(1-methylcyclohexyl)methoxy]ethyl}(3_R_)-piperidine-3-carboxylic acid and _rac_-1-{2-[(1_S_)(4-Methoxyphenyl)(1-methylcyclohexyl)methoxy]ethyl}(3_R_)-piperidine-3-carboxylic acid ~1:1 (9a)

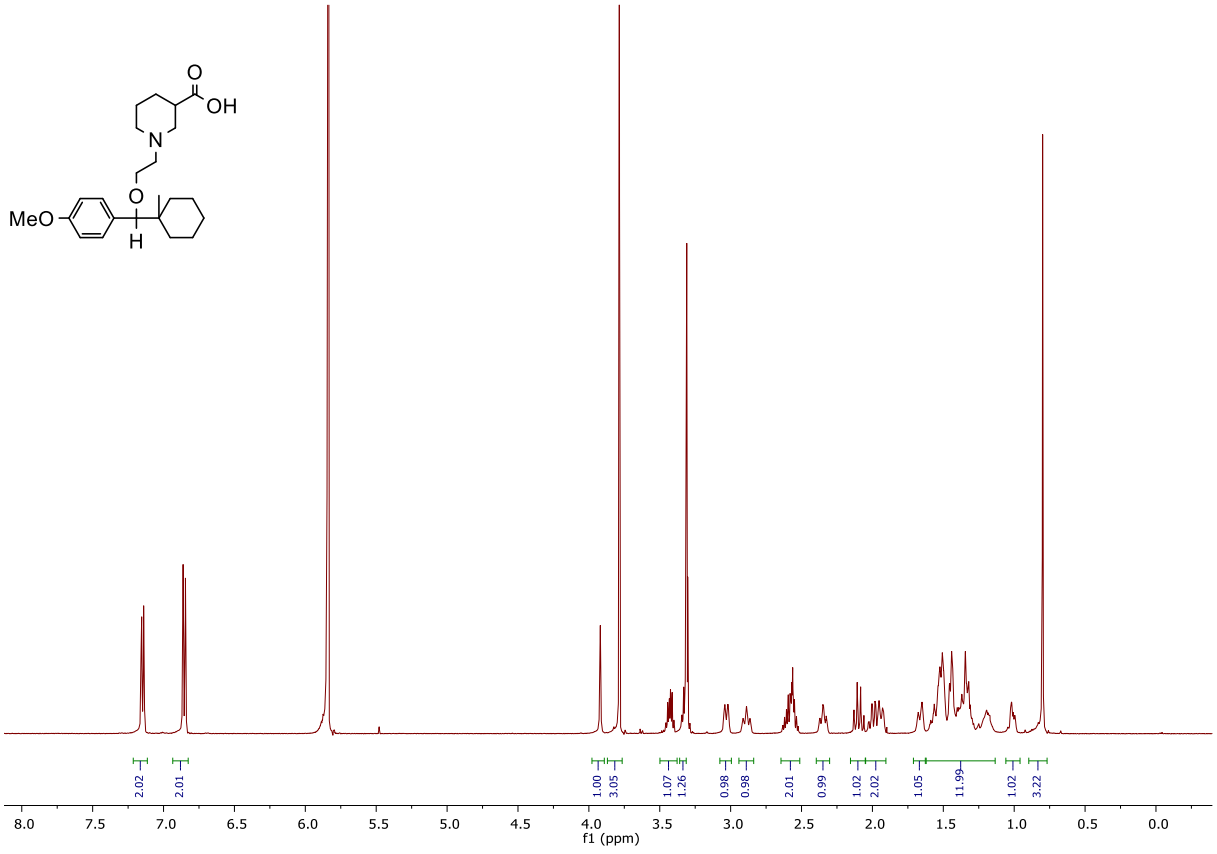

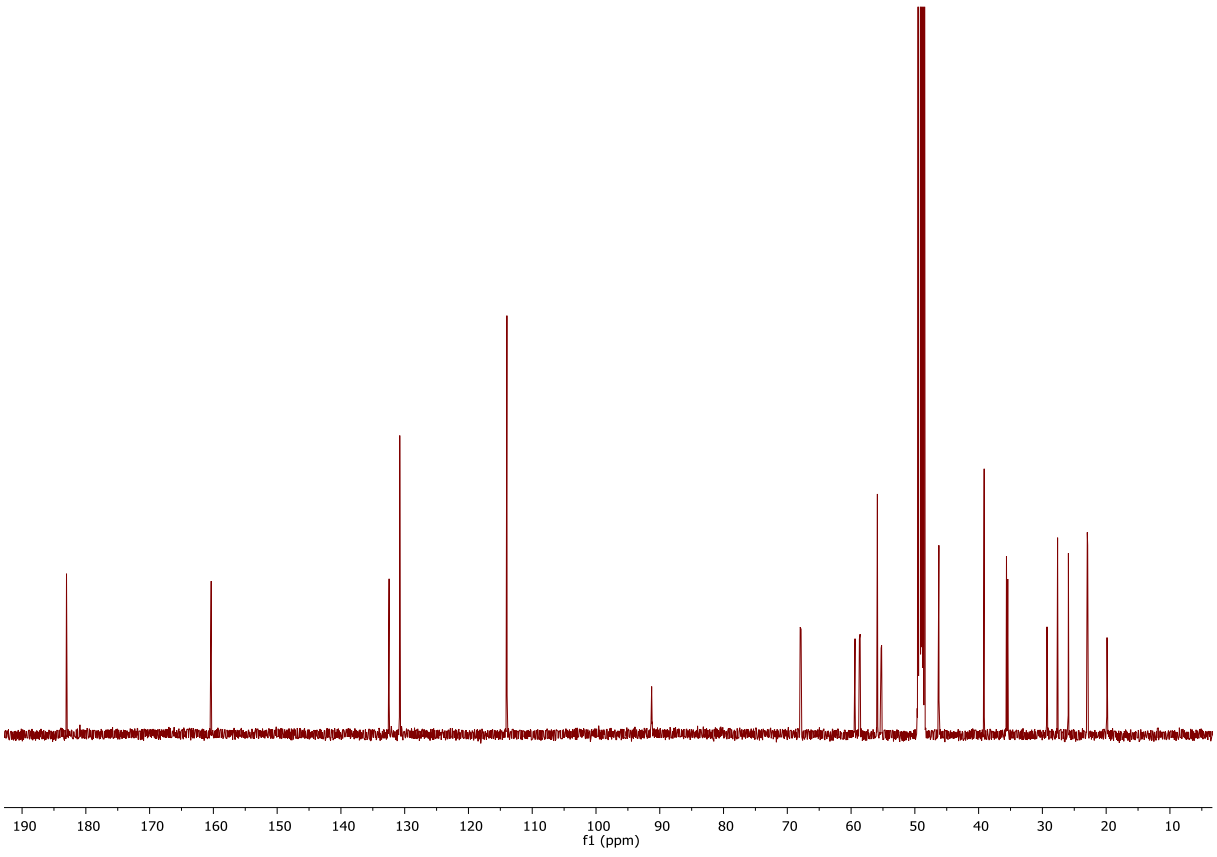

rac-1-{2-[(1_R_)(Adamantan-1-yl)(4-methoxyphenyl)methoxy]ethyl}(3_R_)-piperidine-3-carboxylic acid and _rac_-1-{2-[(1_S_)(Adamantan-1-yl)(4-methoxyphenyl)methoxy]ethyl}(3_R_)-piperidine-3-carboxylic acid ~1:1 (9b)

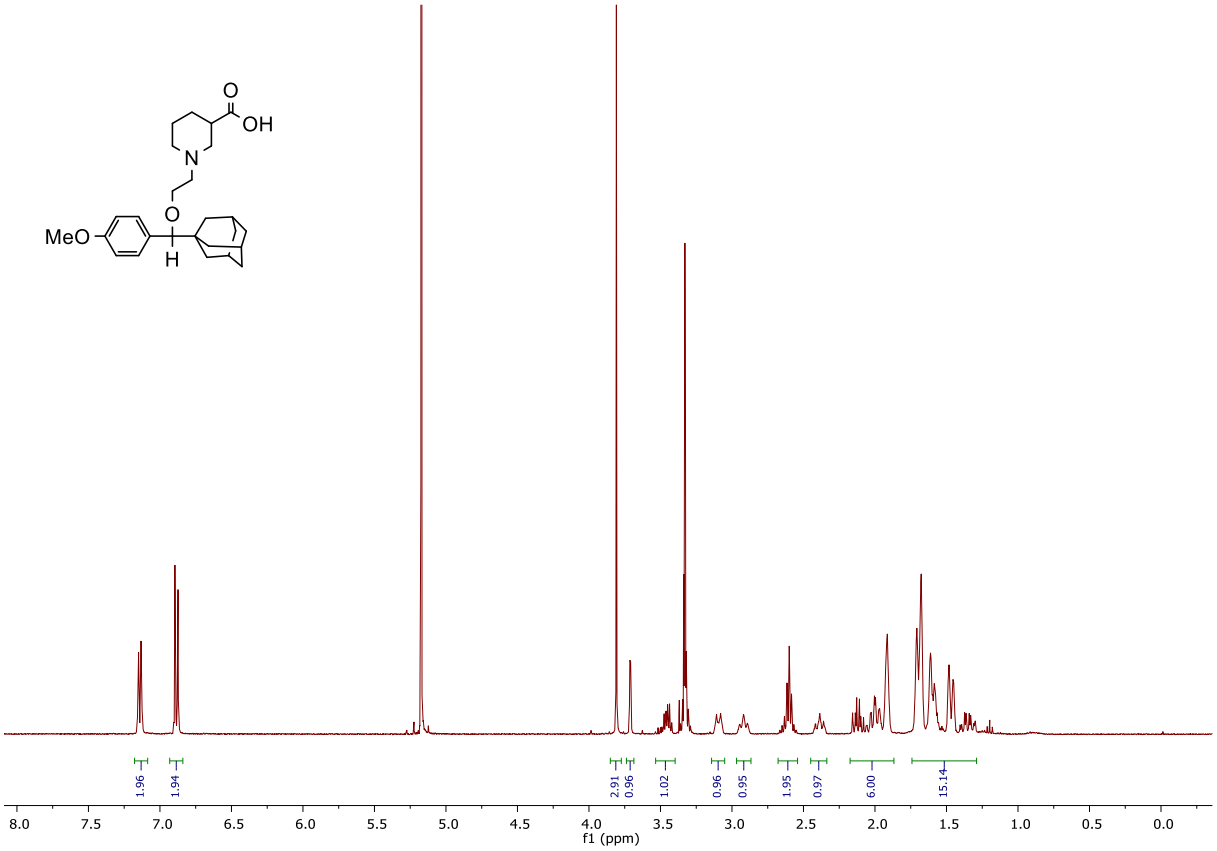

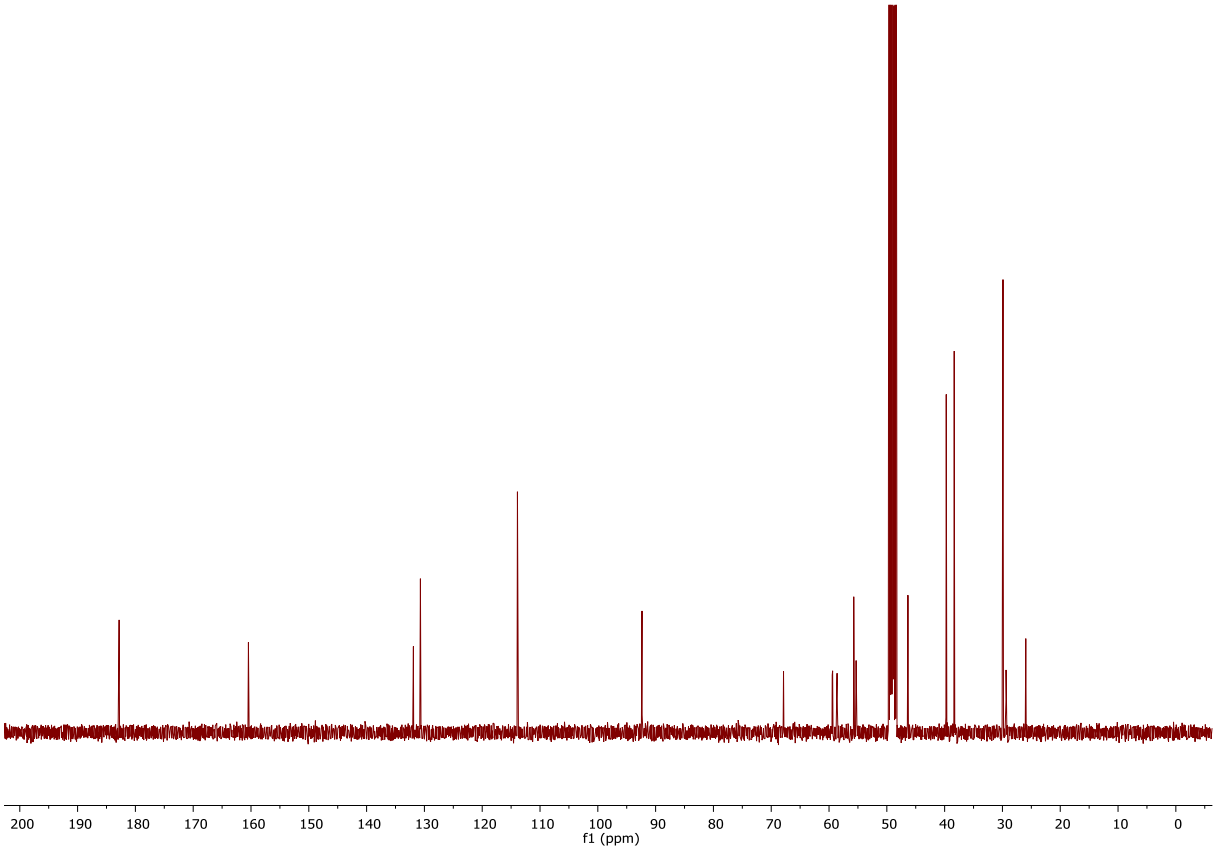

rac-1-{2-[(1_R_)(Adamantan-1-yl)(3-methoxyphenyl)methoxy]ethyl}(3_R_)-piperidine-3-carboxylic acid and _rac_-1-{2-[(1_S_)(Adamantan-1-yl)(3-methoxyphenyl)methoxy]ethyl}(3_R_)-piperidine-3-carboxylic acid ~1:1 (9c)

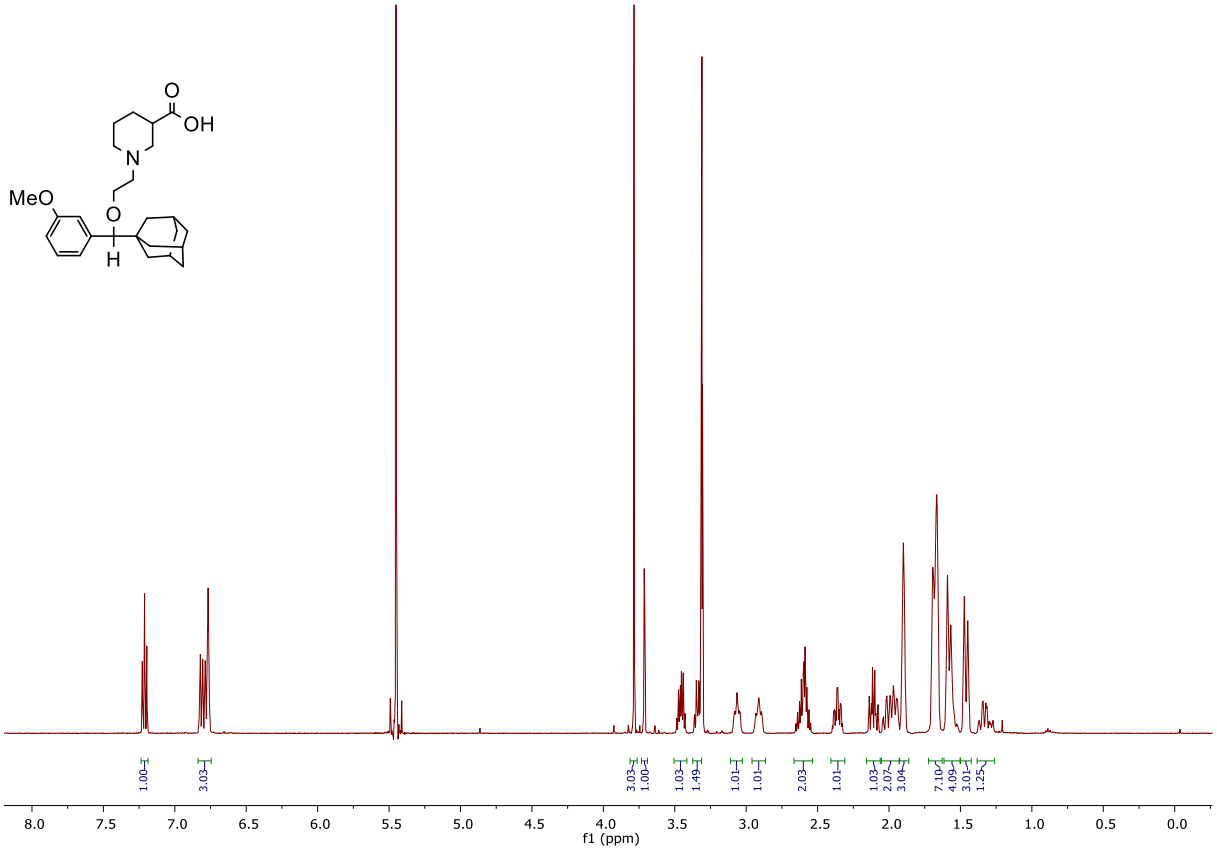

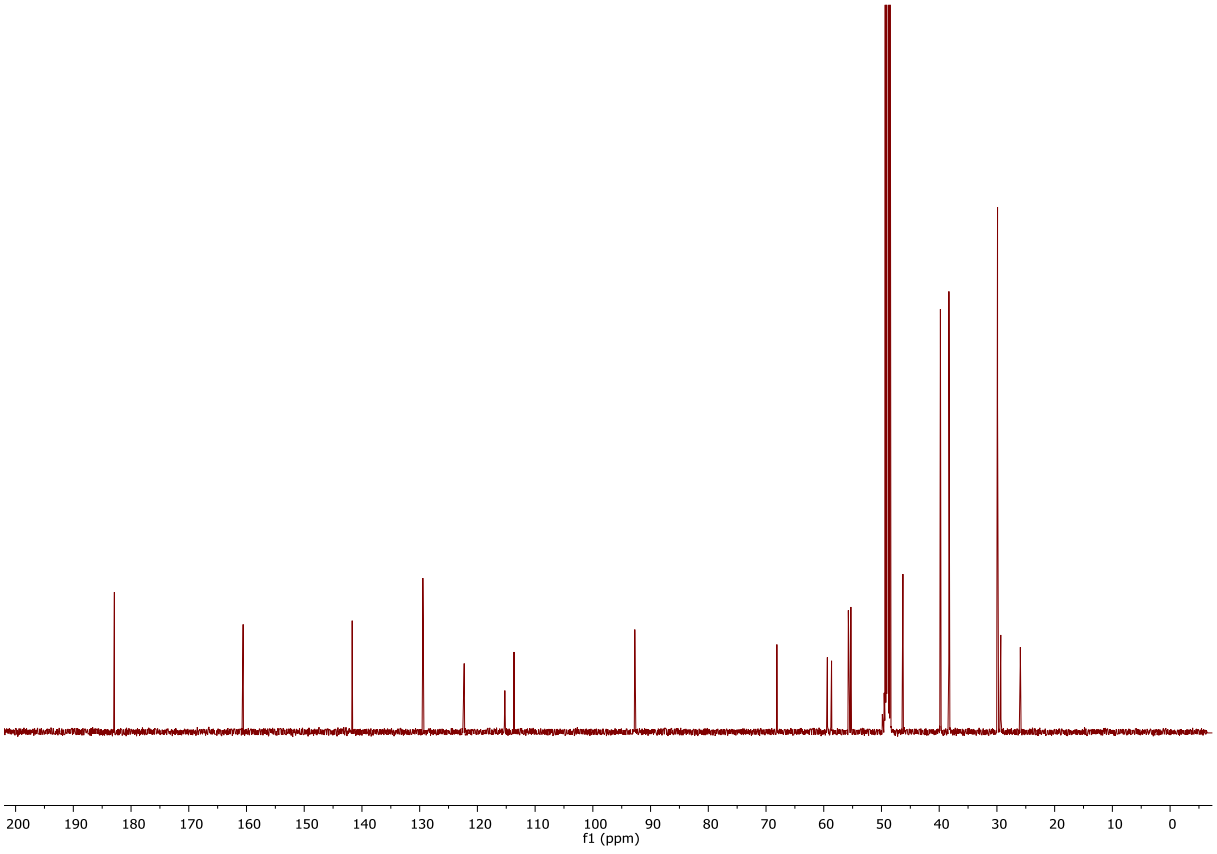

rac-1-{2-[(1_R_)(Adamantan-1-yl)(2-methoxyphenyl)methoxy]ethyl}(3_R_)-piperidine-3-carboxylic acid and _rac_-1-{2-[(1_S_)(Adamantan-1-yl)(2-methoxyphenyl)methoxy]ethyl}(3_R_)-piperidine-3-carboxylic acid ~1:1 (9d)

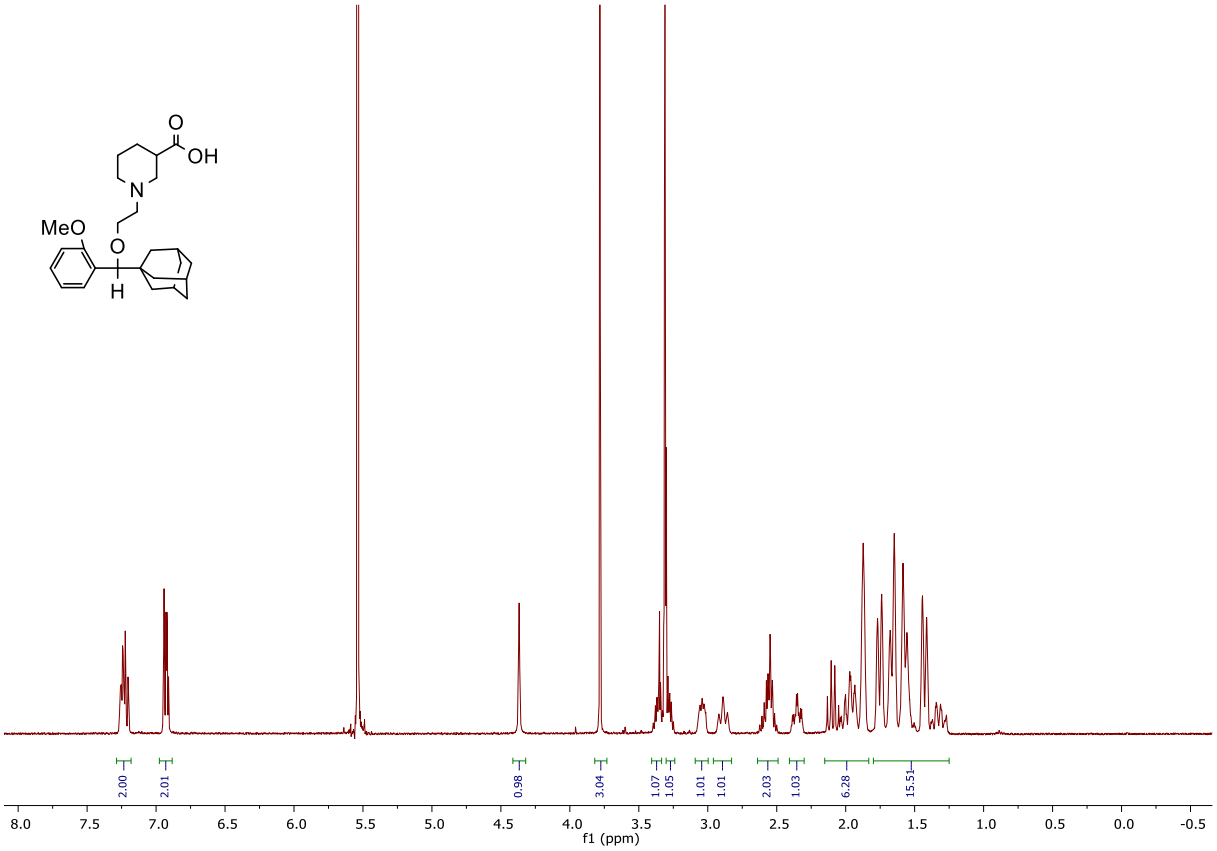

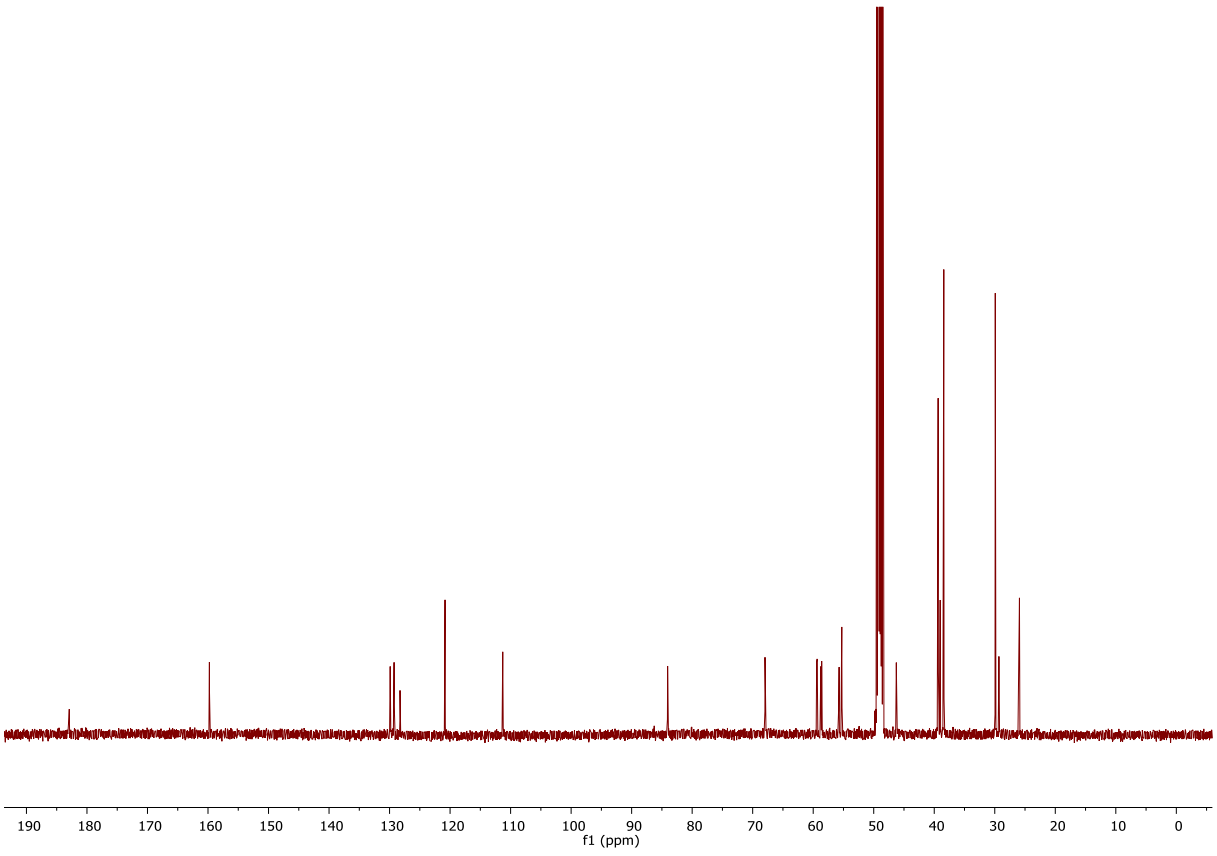

rac-1-{2-[(1_R_)(3,5-Dimethyladamantan-1-yl)(4-methoxyphenyl)methoxy]ethyl}(3_R_)-piperidine-3-carboxylic acid and _rac_-1-{2-[(1_S_)(3,5-Dimethyladamantan-1-yl)(4-methoxyphenyl)methoxy]ethyl}(3_R_)-piperidine-3-carboxylic acid ~1:1 (9e)

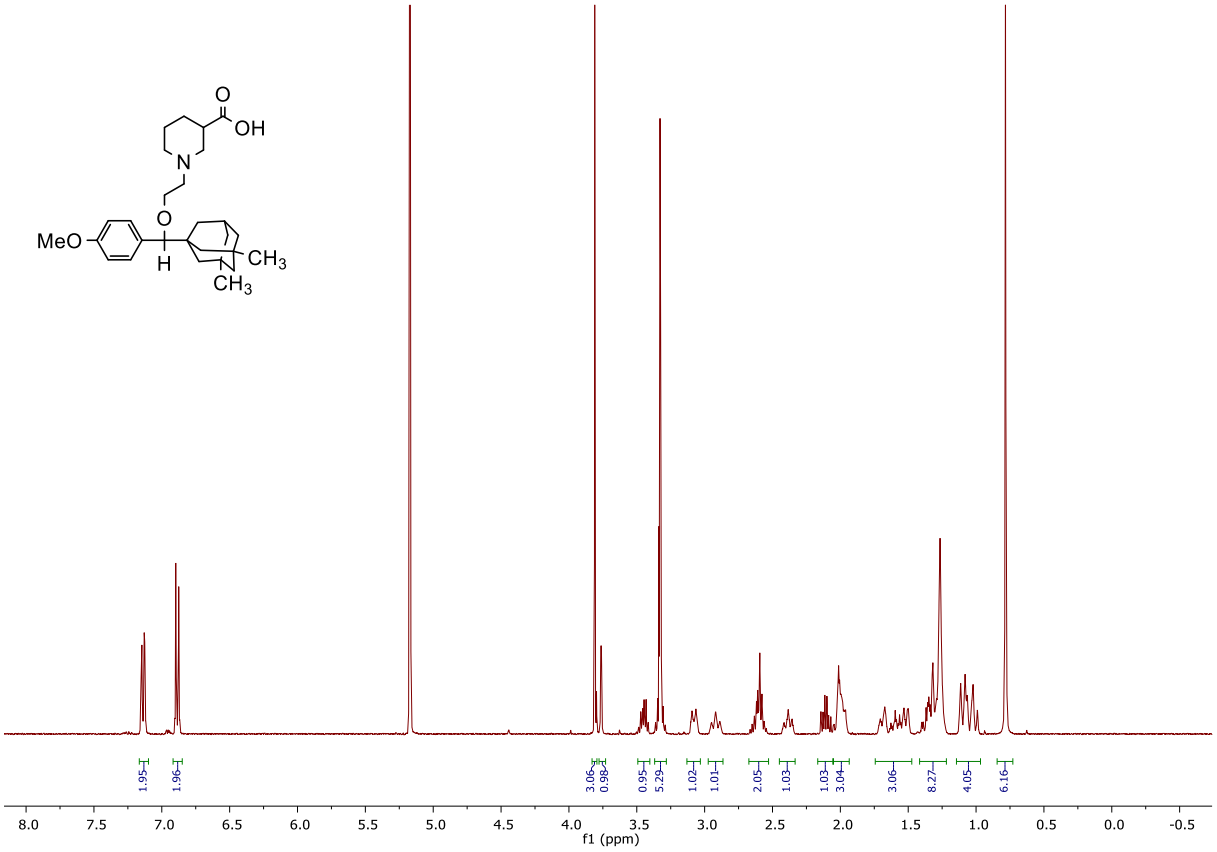

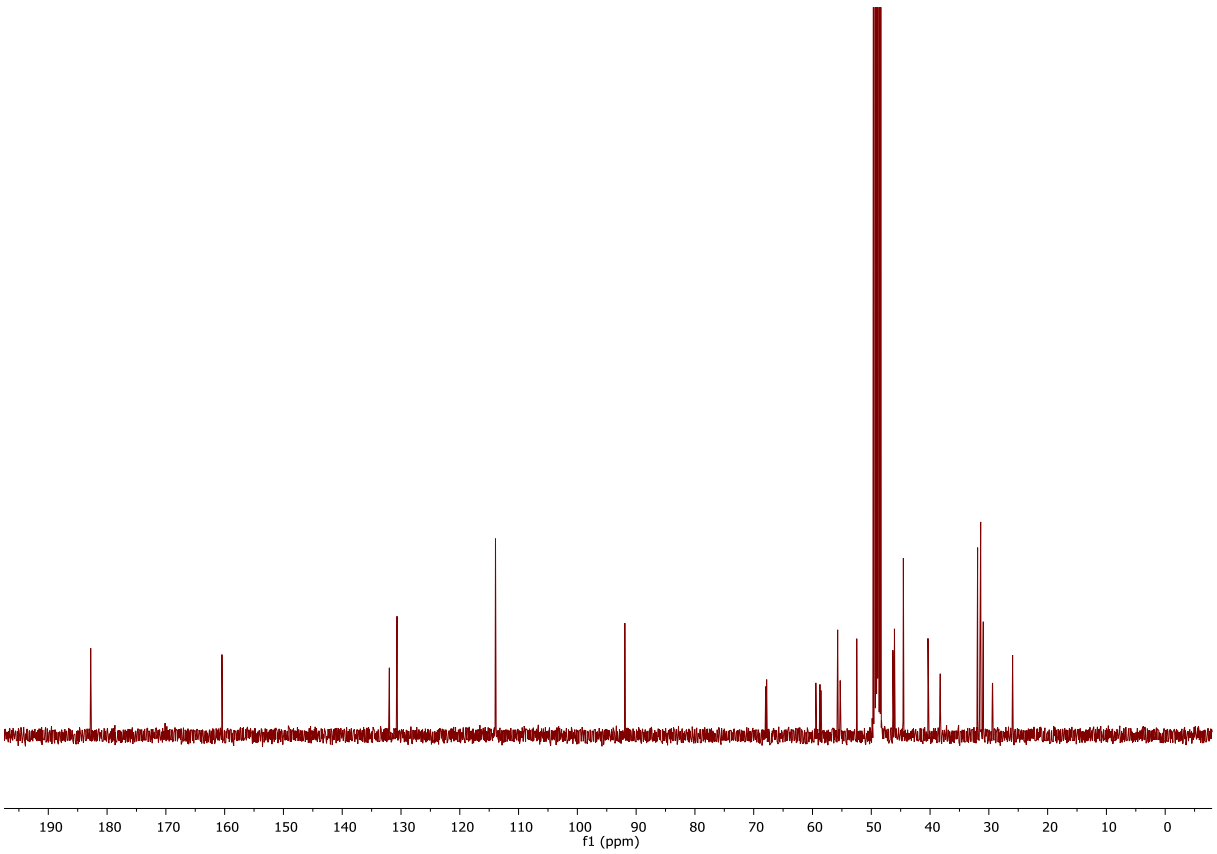

rac-1-{2-[(1_R_)(3-Methoxyadamantan-1-yl)(4-methoxyphenyl)methoxy]ethyl}(3_R_)-piperidine-3-carboxylic acid and _rac_-1-{2-[(1_S_)(3-Methoxyadamantan-1-yl)(4-methoxyphenyl)methoxy]ethyl}(3_R_)-piperidine-3-carboxylic acid ~1:1 (9g)

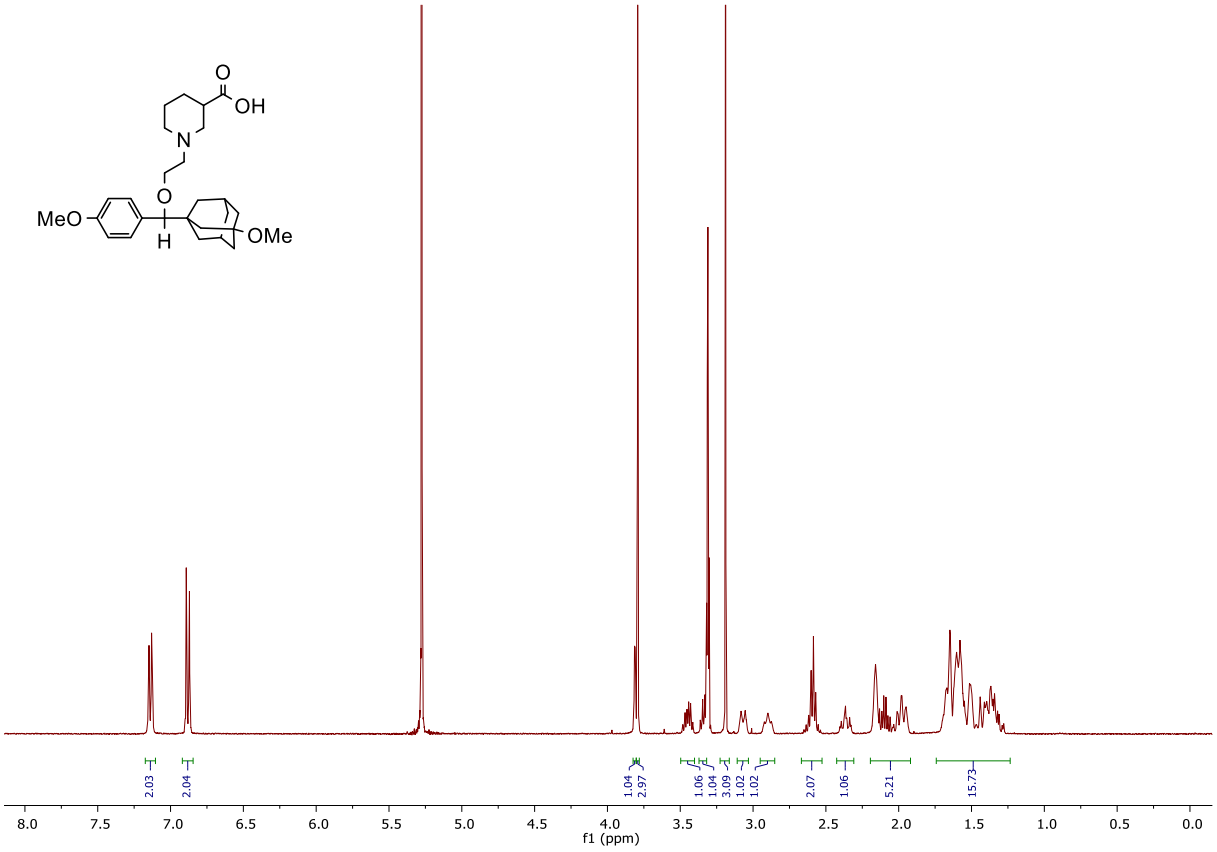

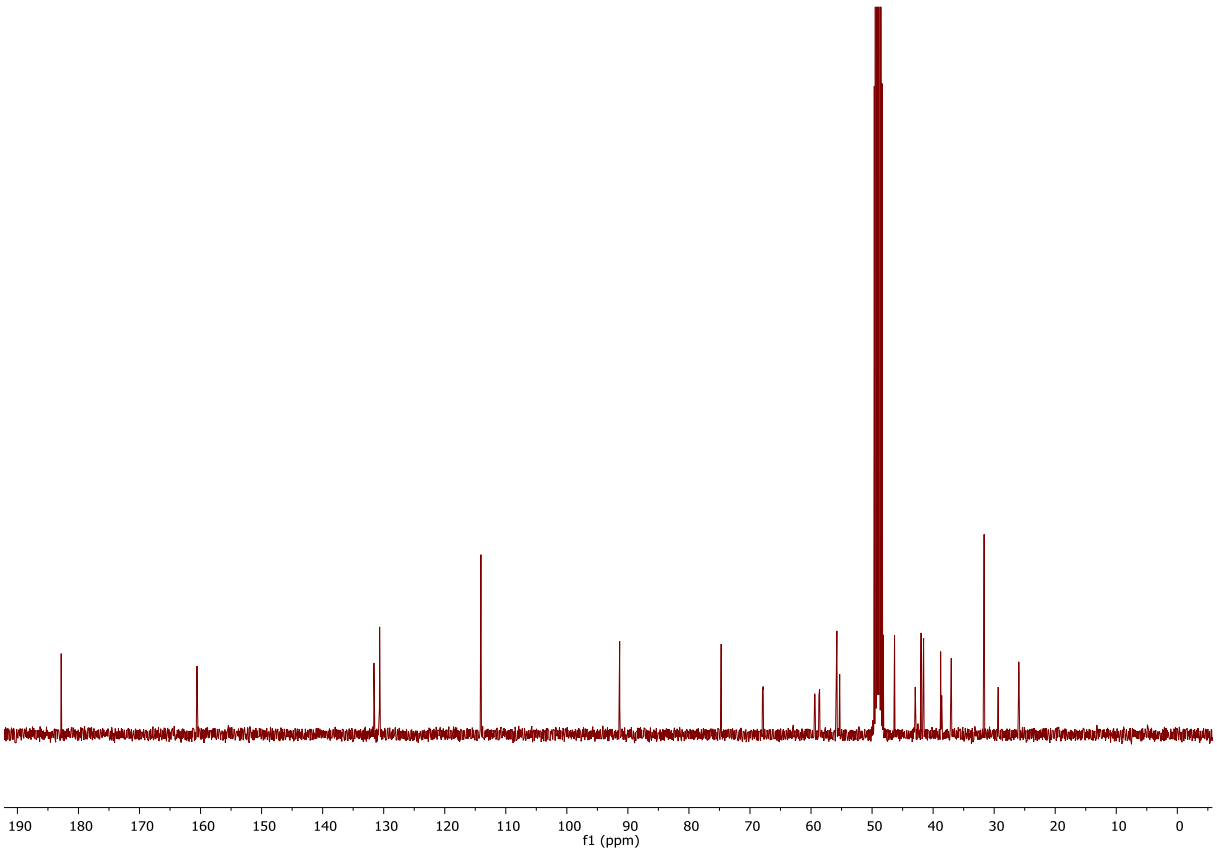

***rac*-1-(2-{[2-(4-Methoxyphenyl)adamantan-2-yl]oxy}ethyl)piperidine-3-carboxylic acid (10)**

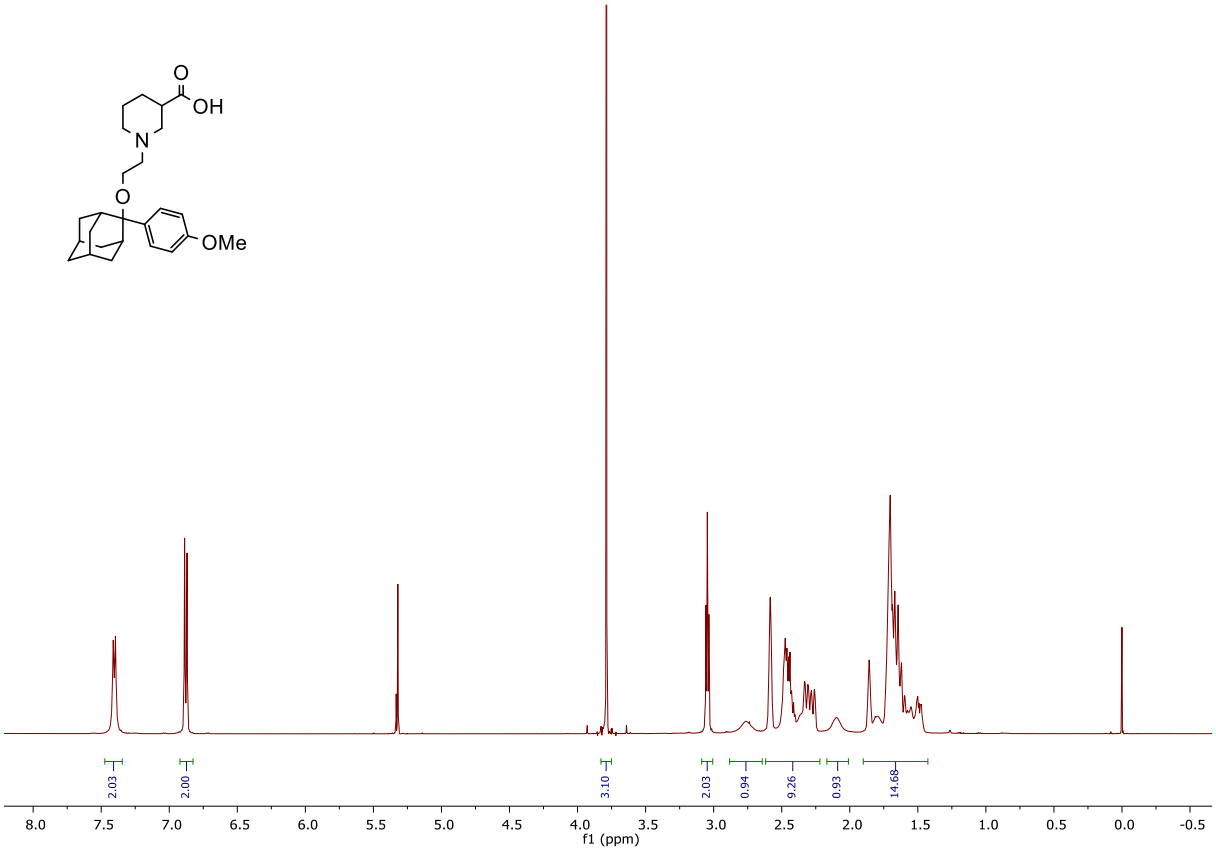

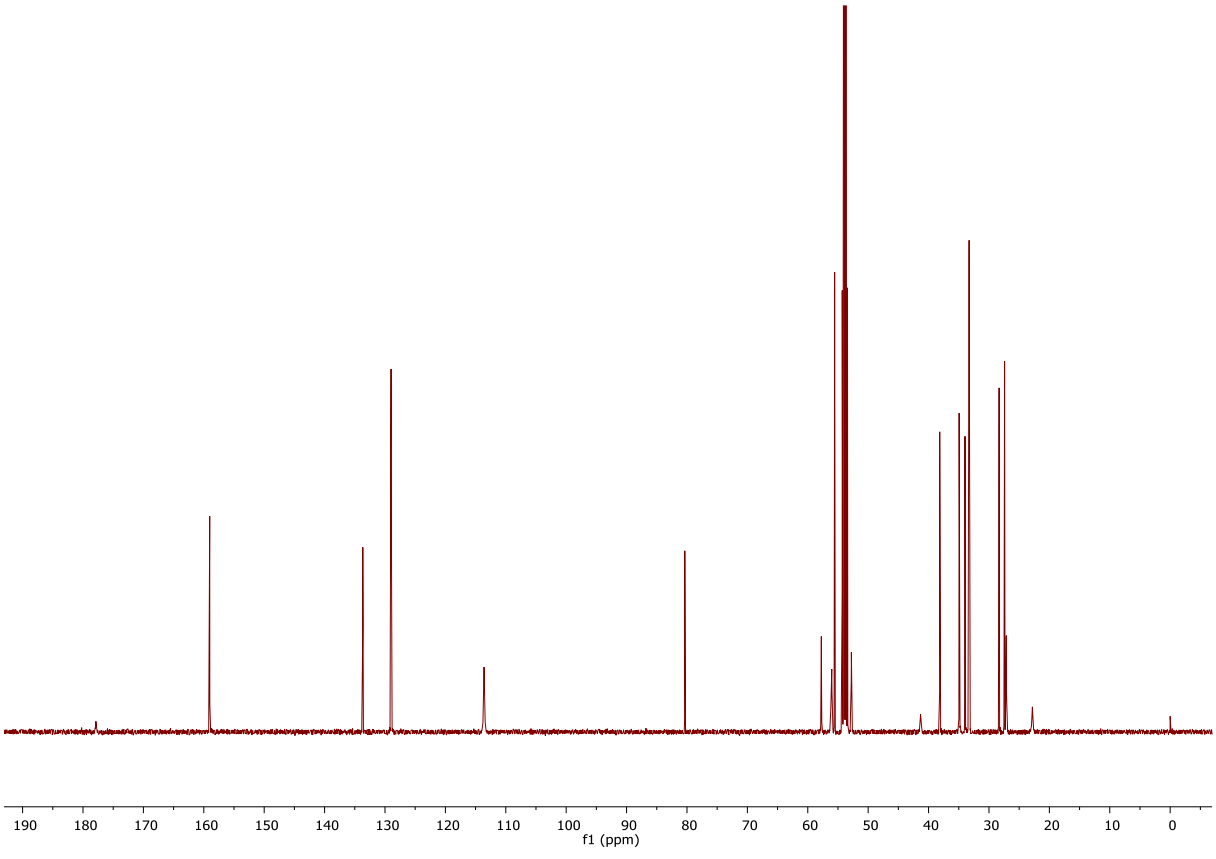

rac-Ethyl 1-(3-hydroxypropyl)piperidine-3-carboxylate (12)

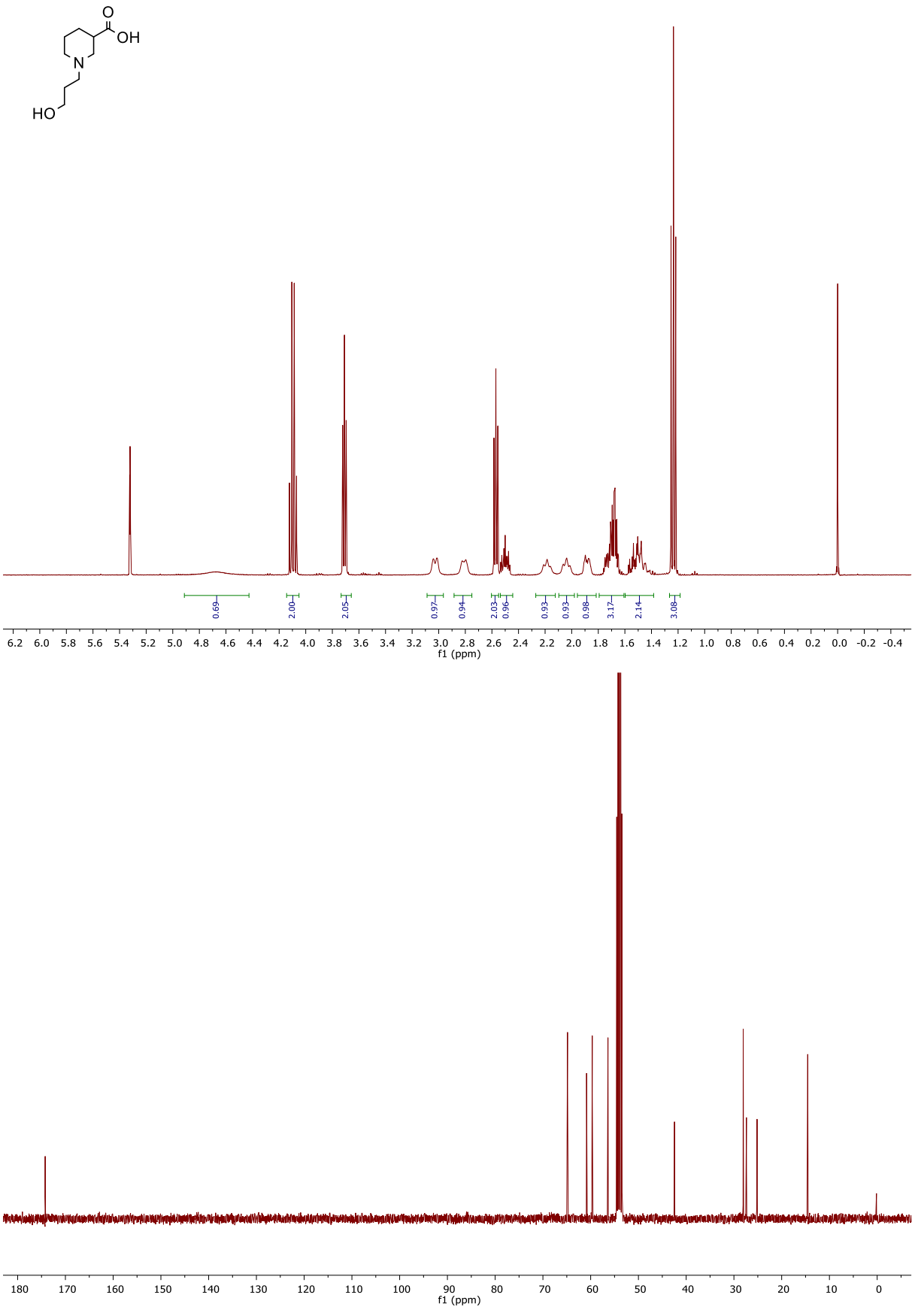

***rac*-Ethyl 1-(4-hydroxybutyl)piperidine-3-carboxylate (13)**

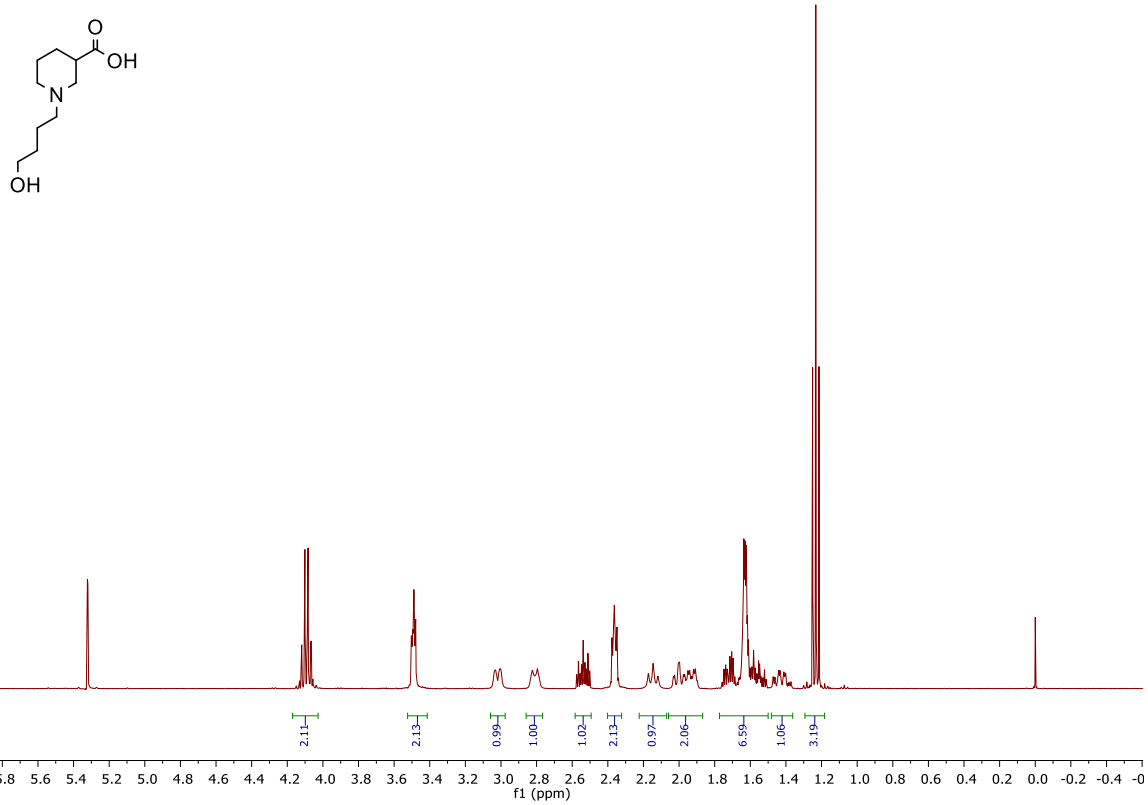

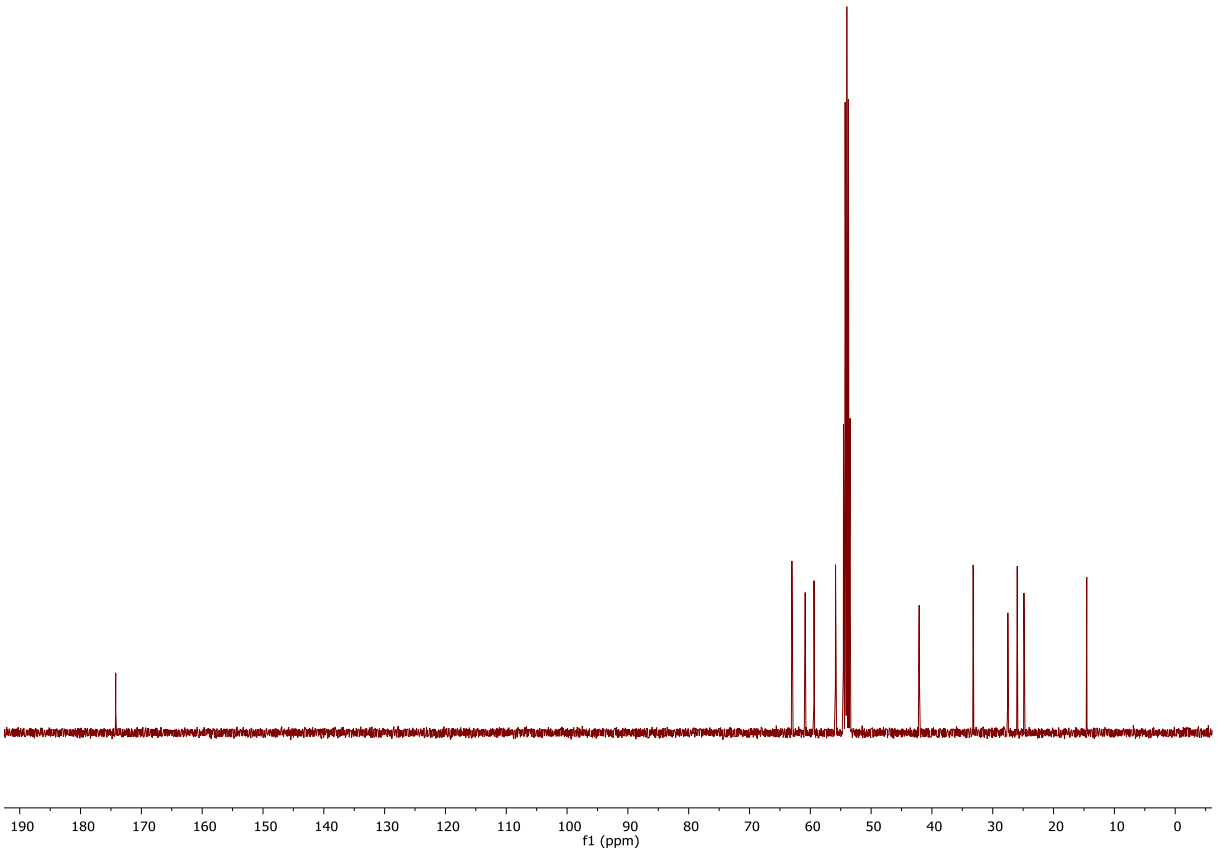

1,1-Bis(4-methoxyphenyl)-2,2-dimethylpropan-1-ol (15a)

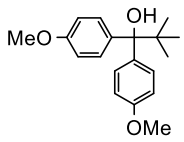

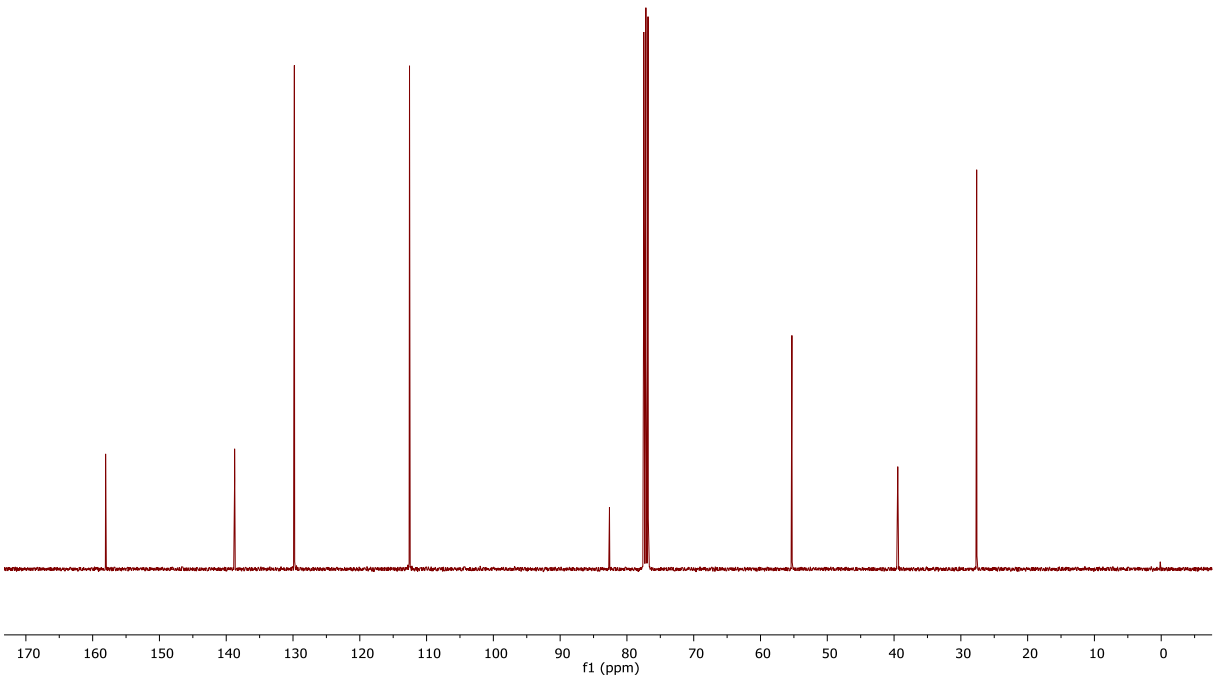

Bis(4-methoxyphenyl)(1-methylcyclopentyl)methanol (15b)

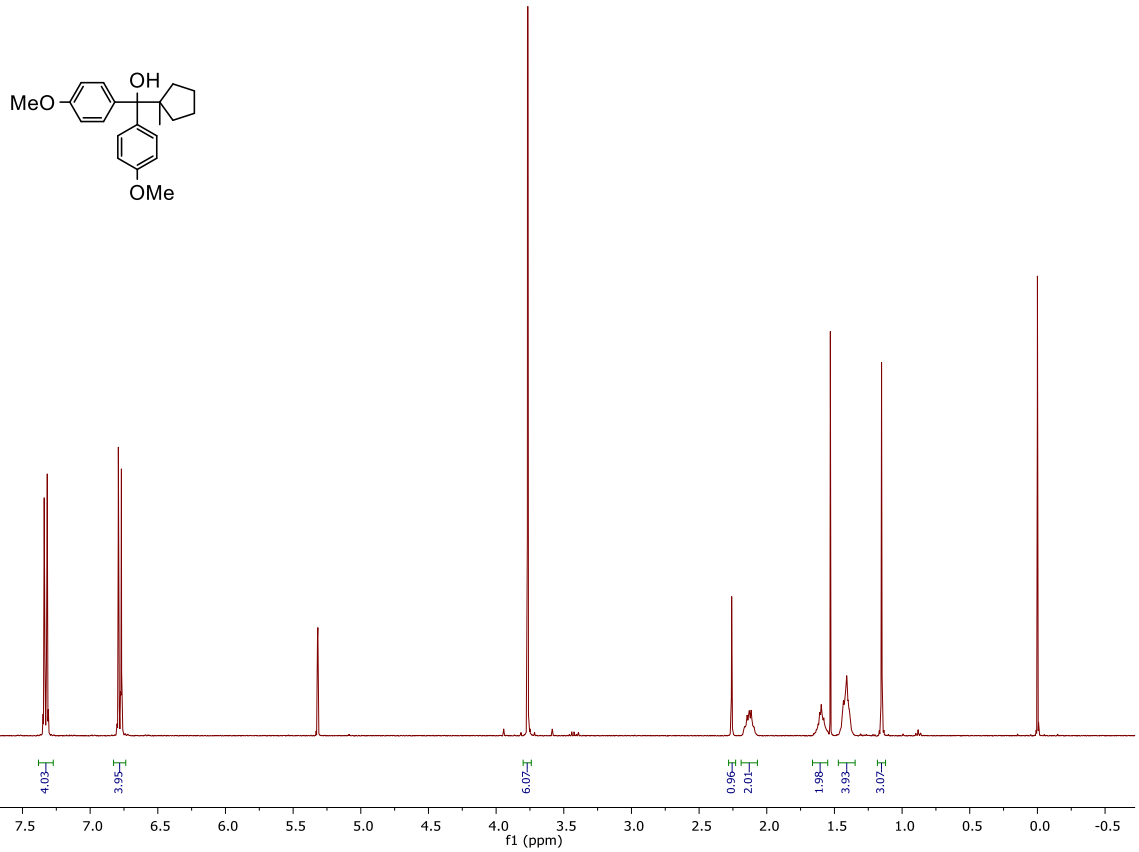

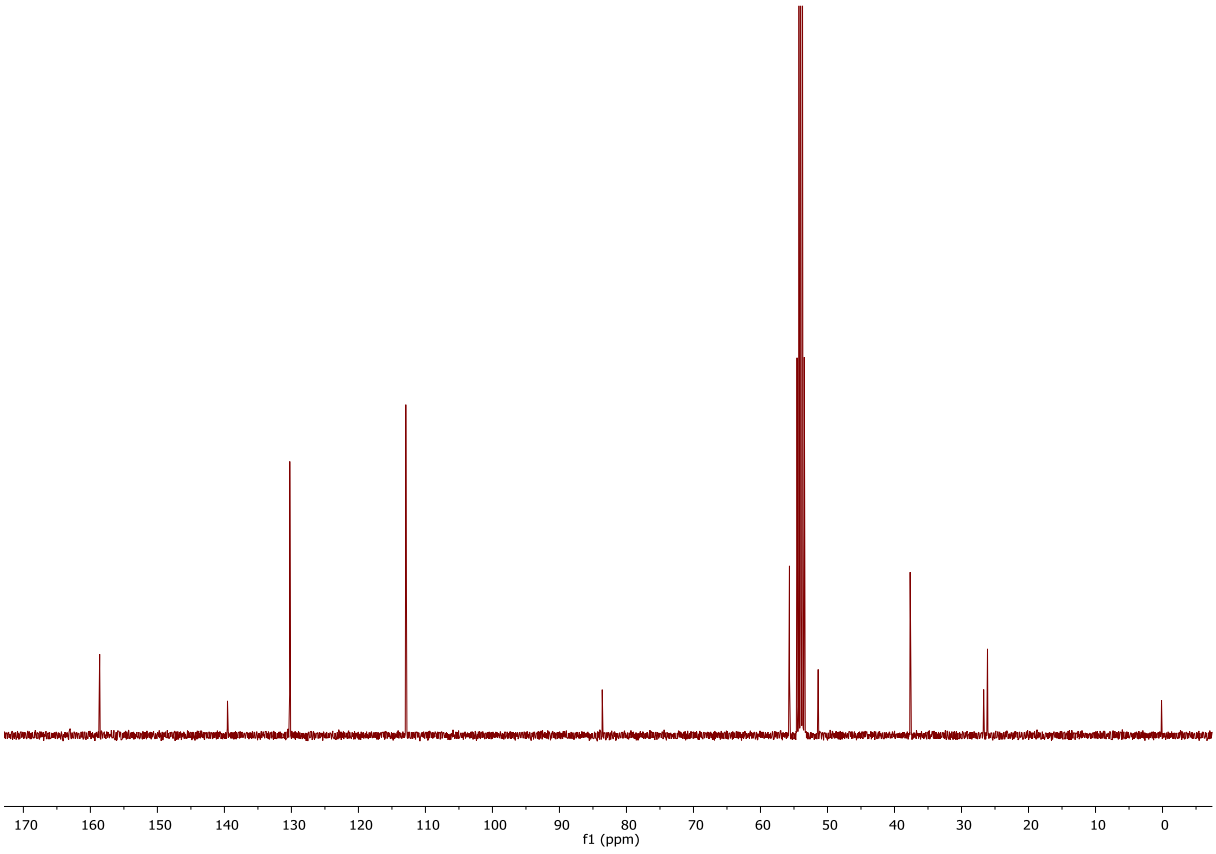

Bis(4-methoxyphenyl)(1-methylcyclohexyl)methanol (15c)

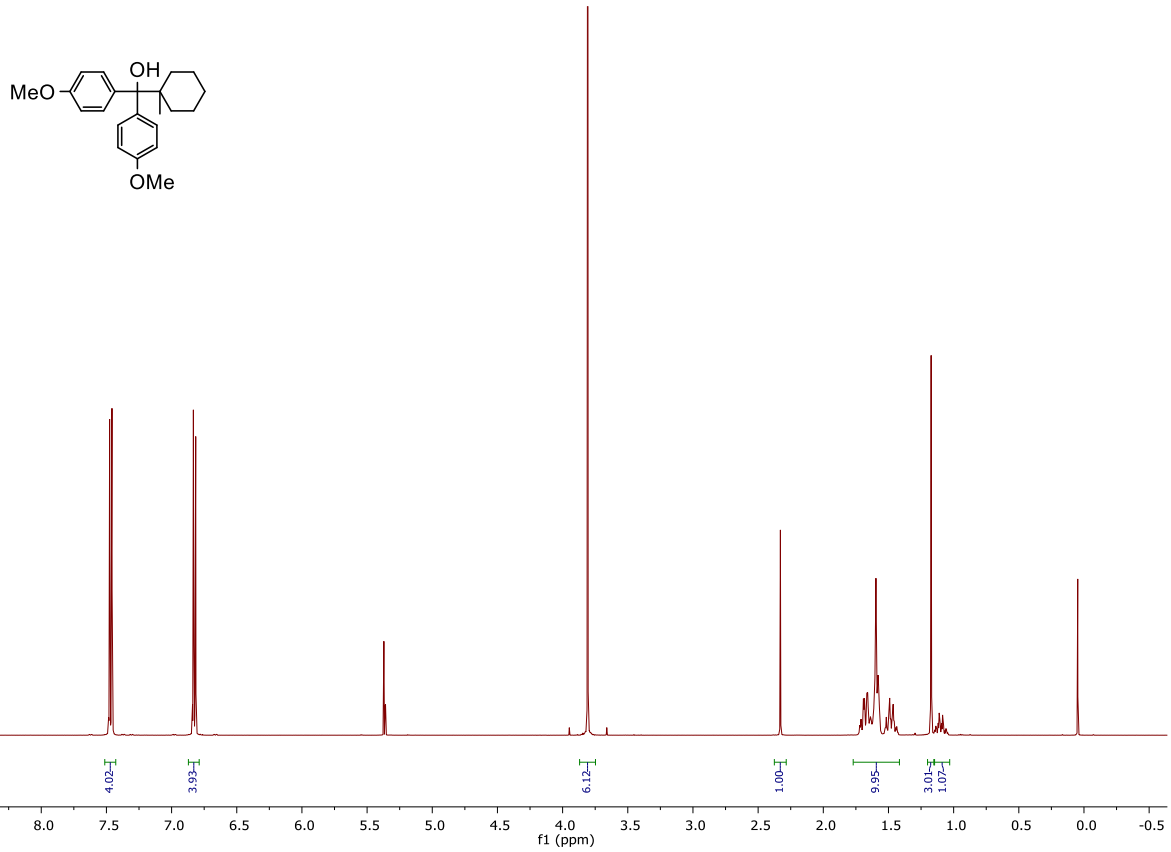

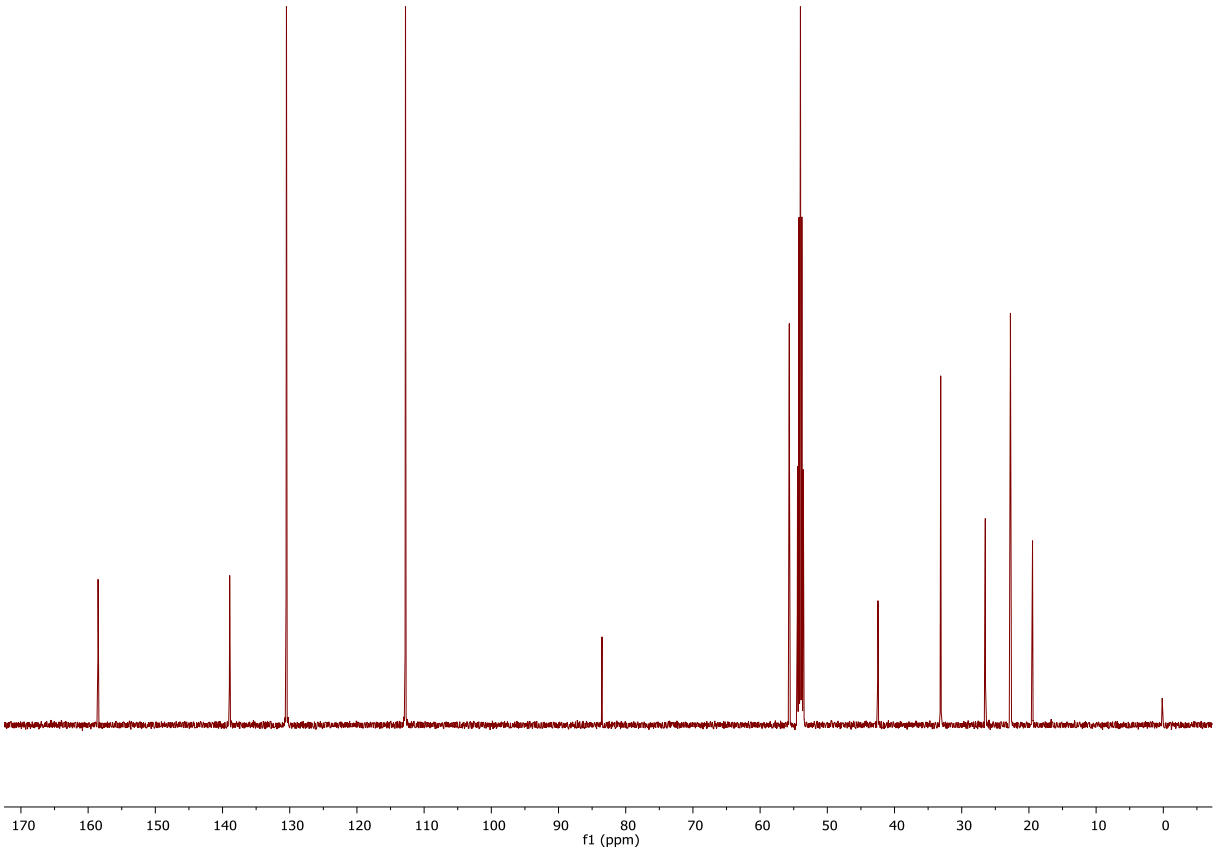

Bis(4-methoxyphenyl)(4-methyltetrahydro-2H-pyran-4-yl)methanol (15d)

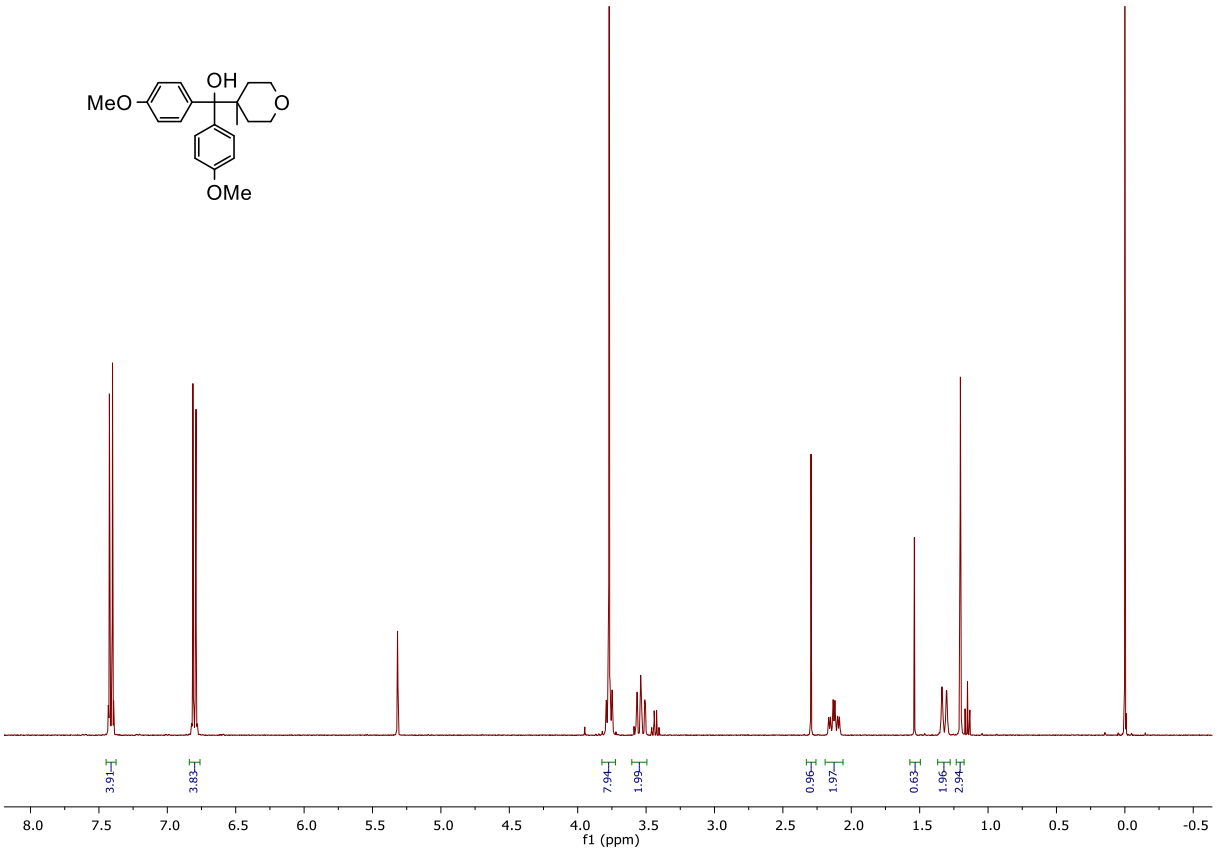

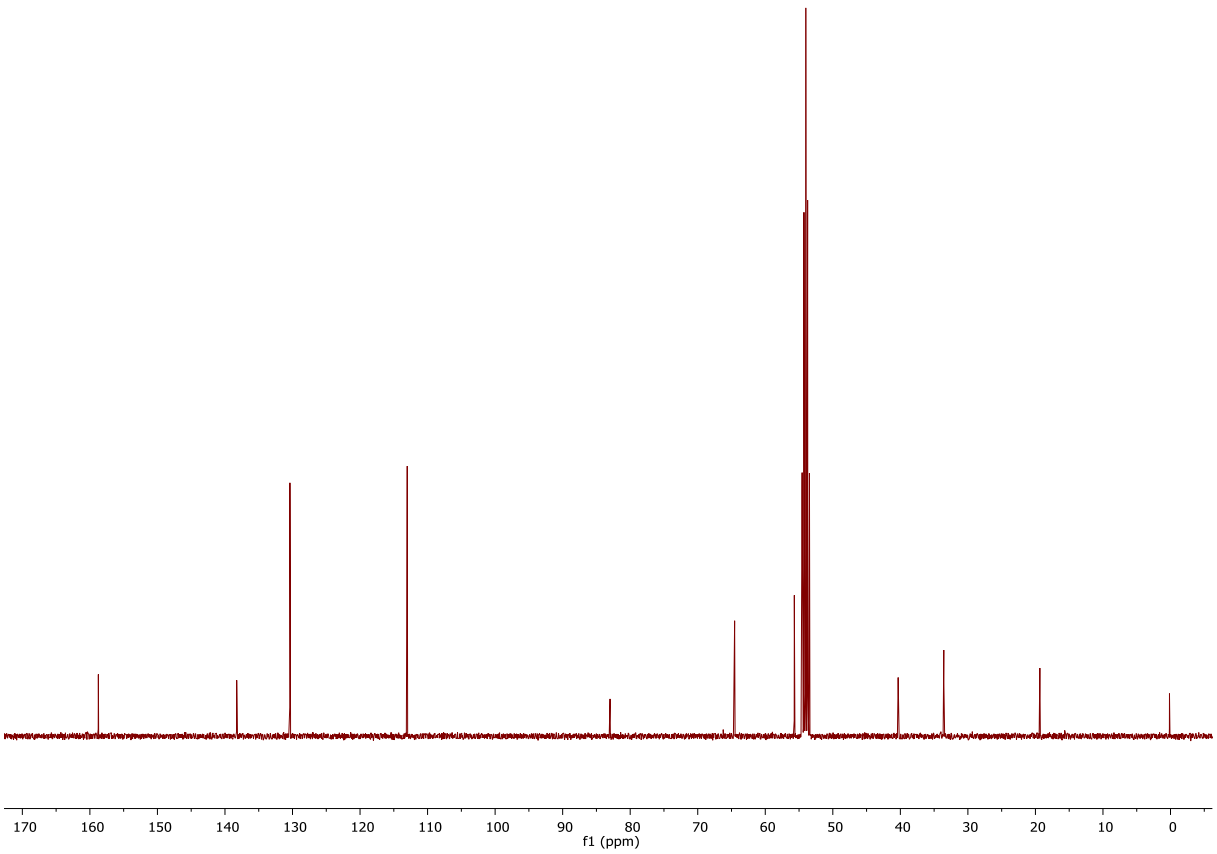

[(1*S*,4*S*)-4-Methoxy-1-methylcyclohexyl]bis[4-methoxyphenyl]methanol (15e)

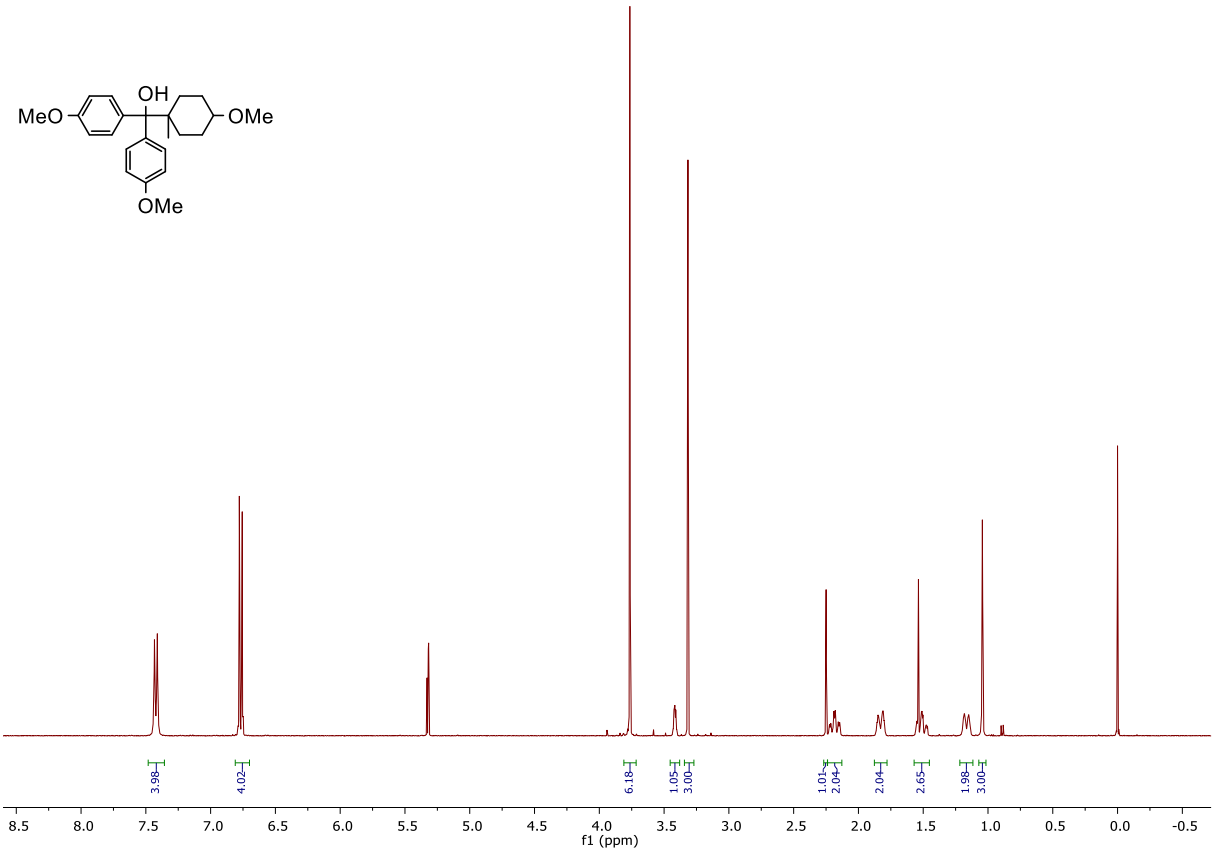

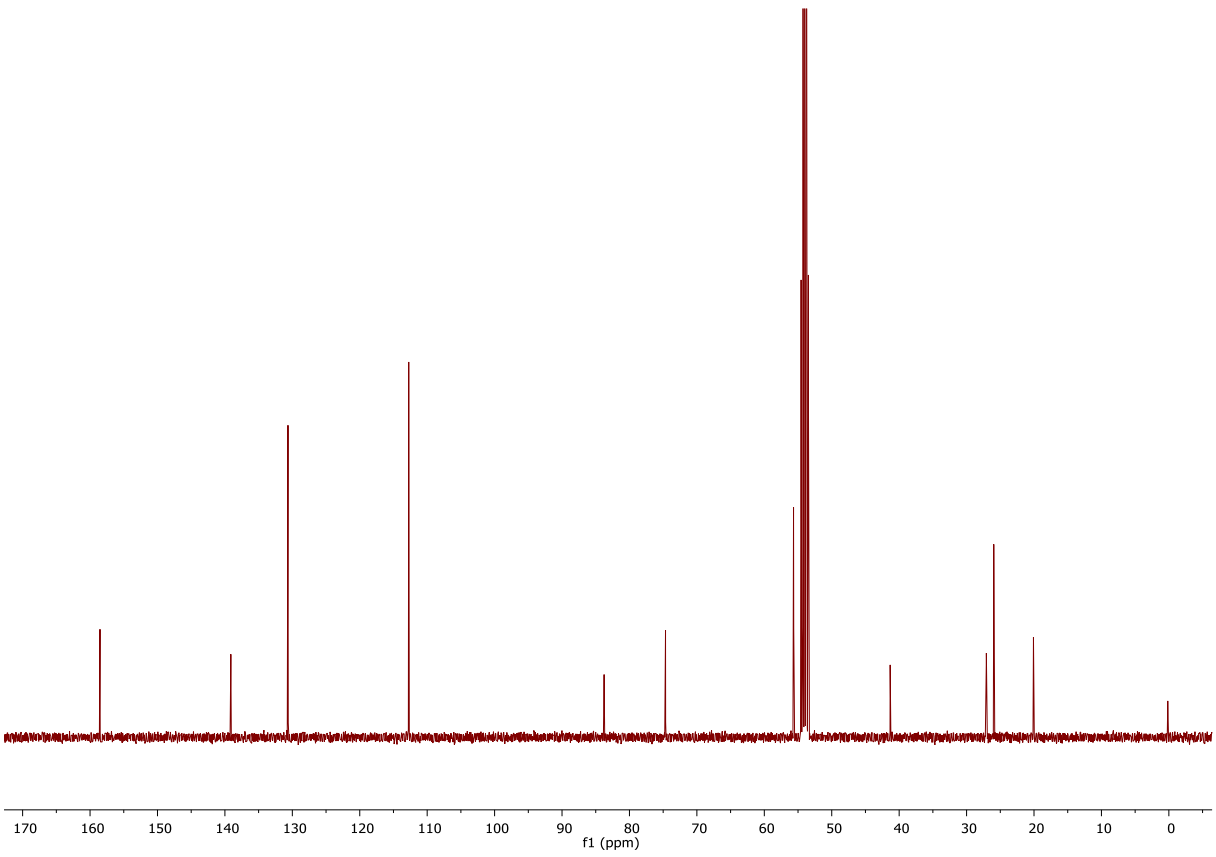

(Adamantan-1-yl)bis(4-methoxyphenyl)methanol (15f)

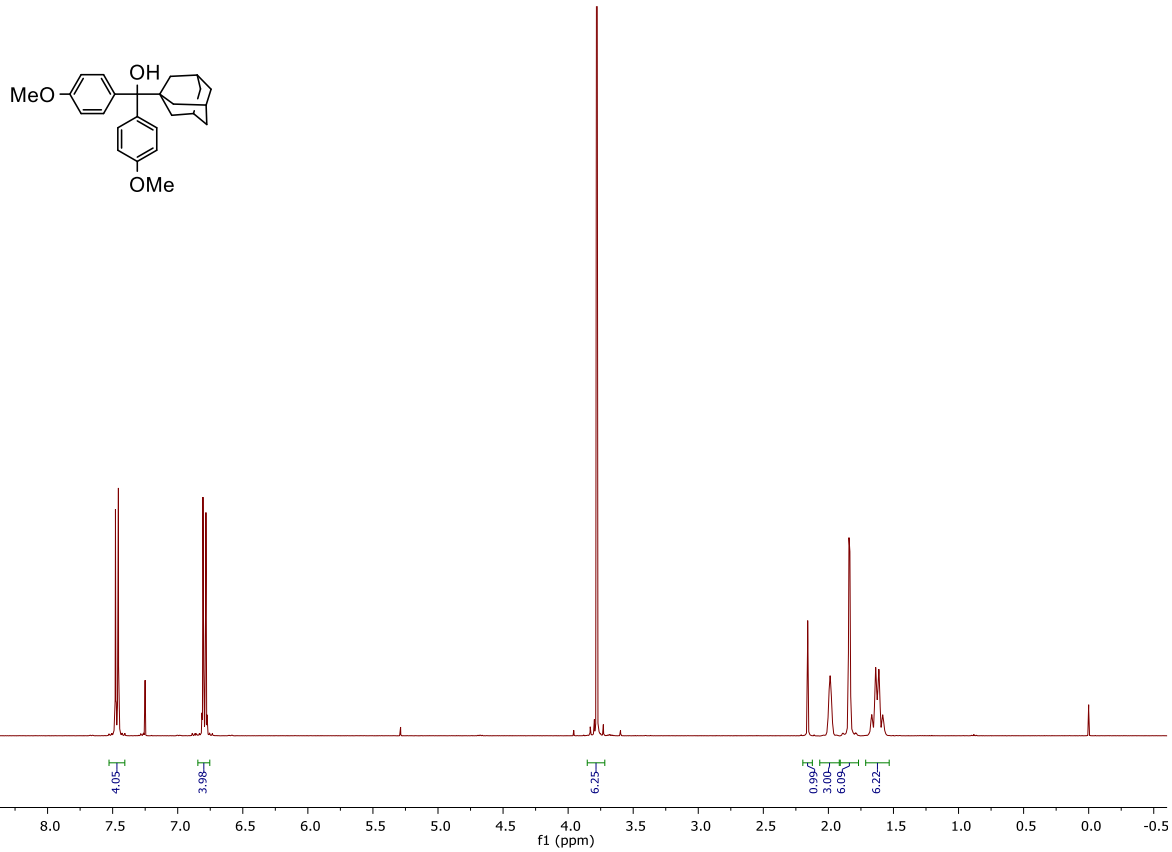

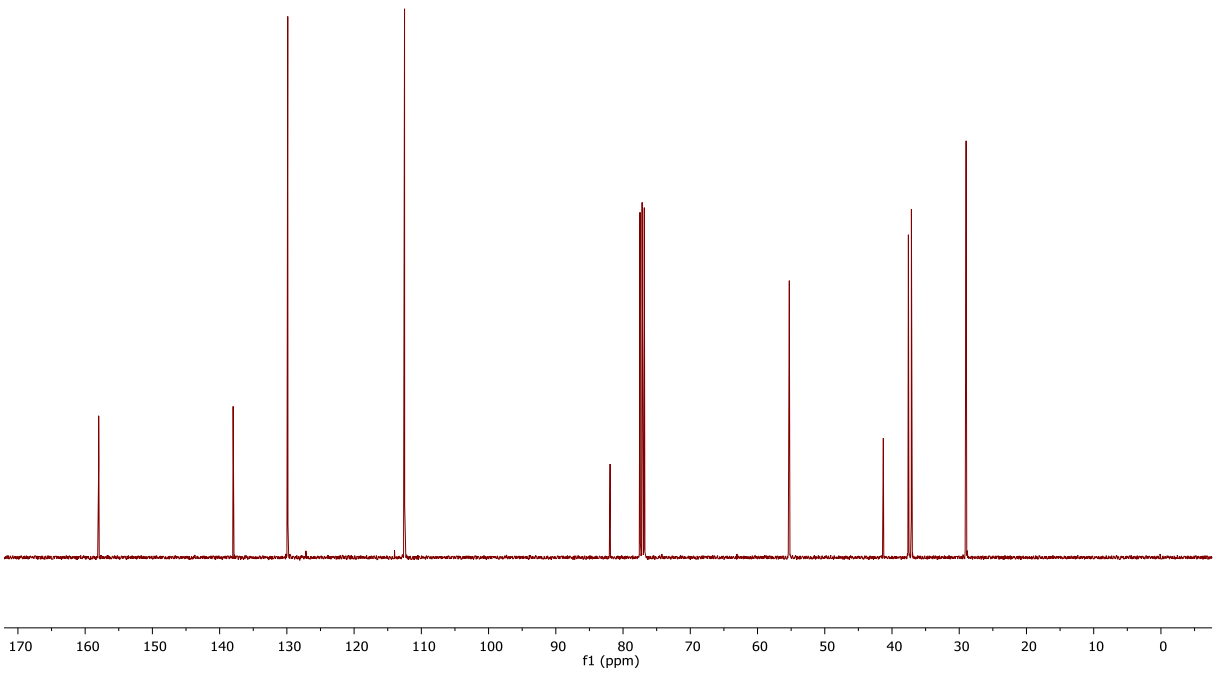

***rac*-1-[(2-Chloroethoxy)(1-methylcyclohexyl)methyl]-4-methoxybenzene (17a)**

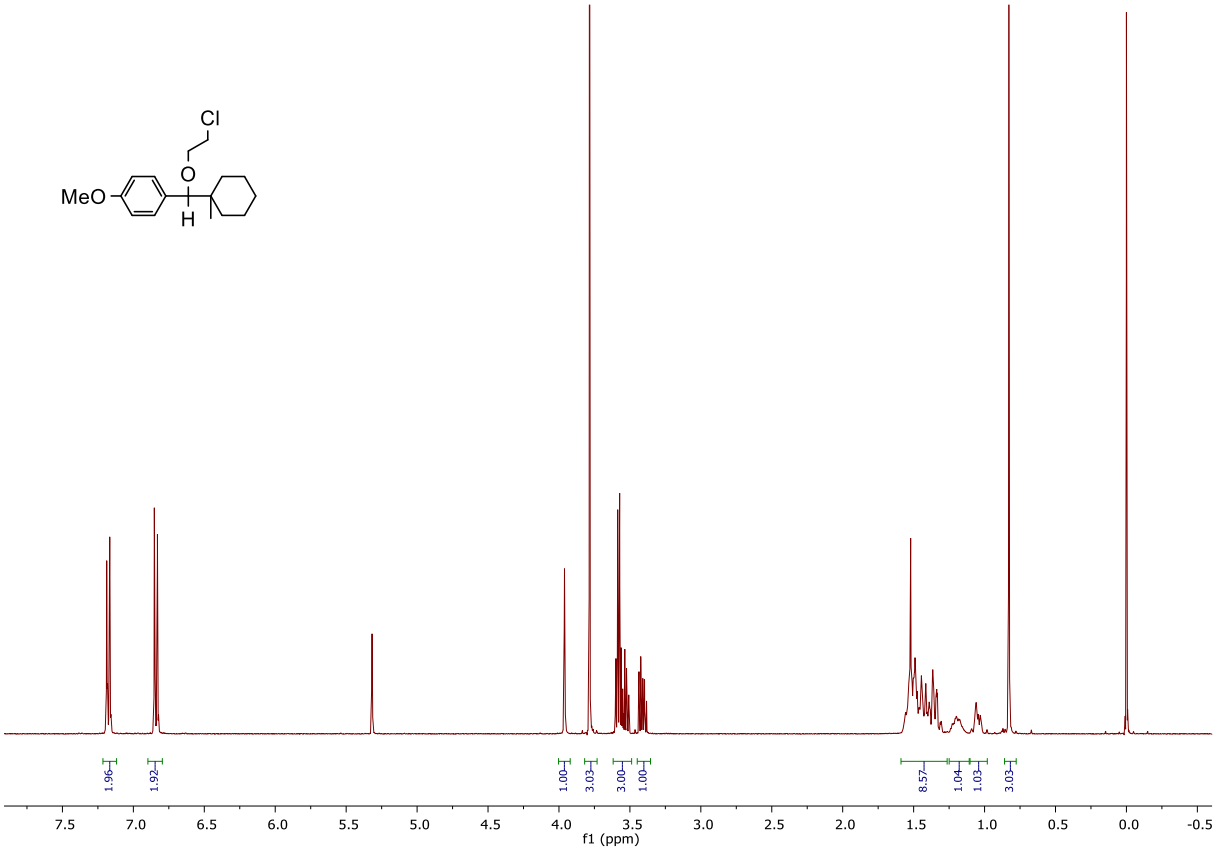

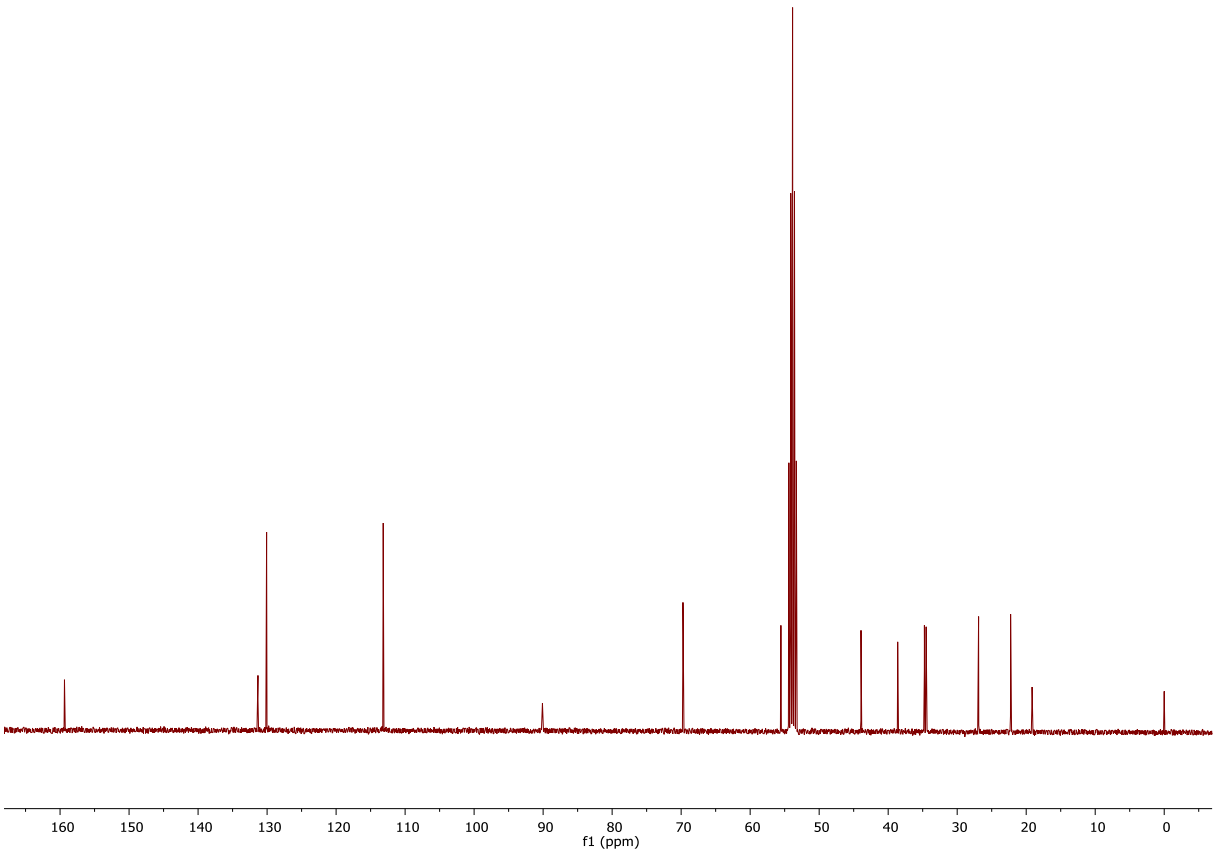

***rac*-1-[(2-Chloroethoxy)(4-methoxyphenyl)methyl]adamantane (17b)**

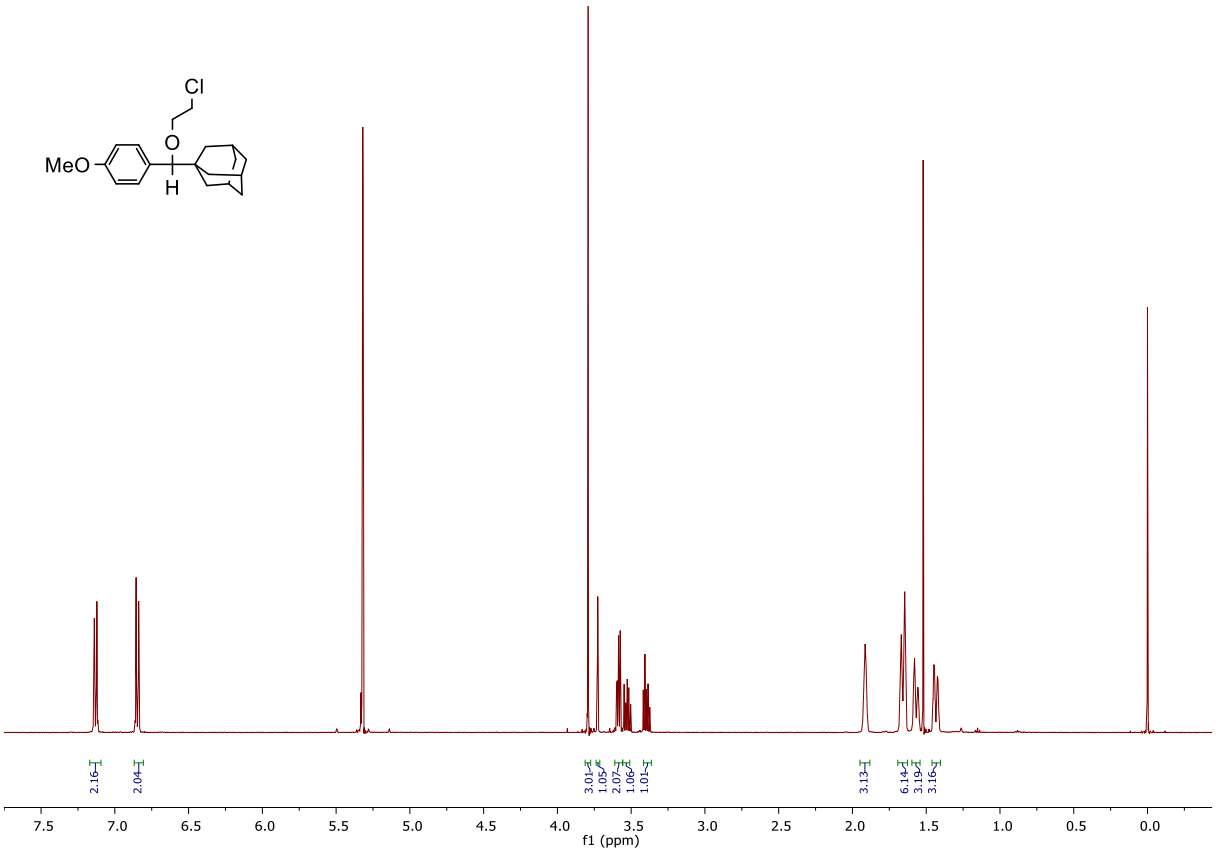

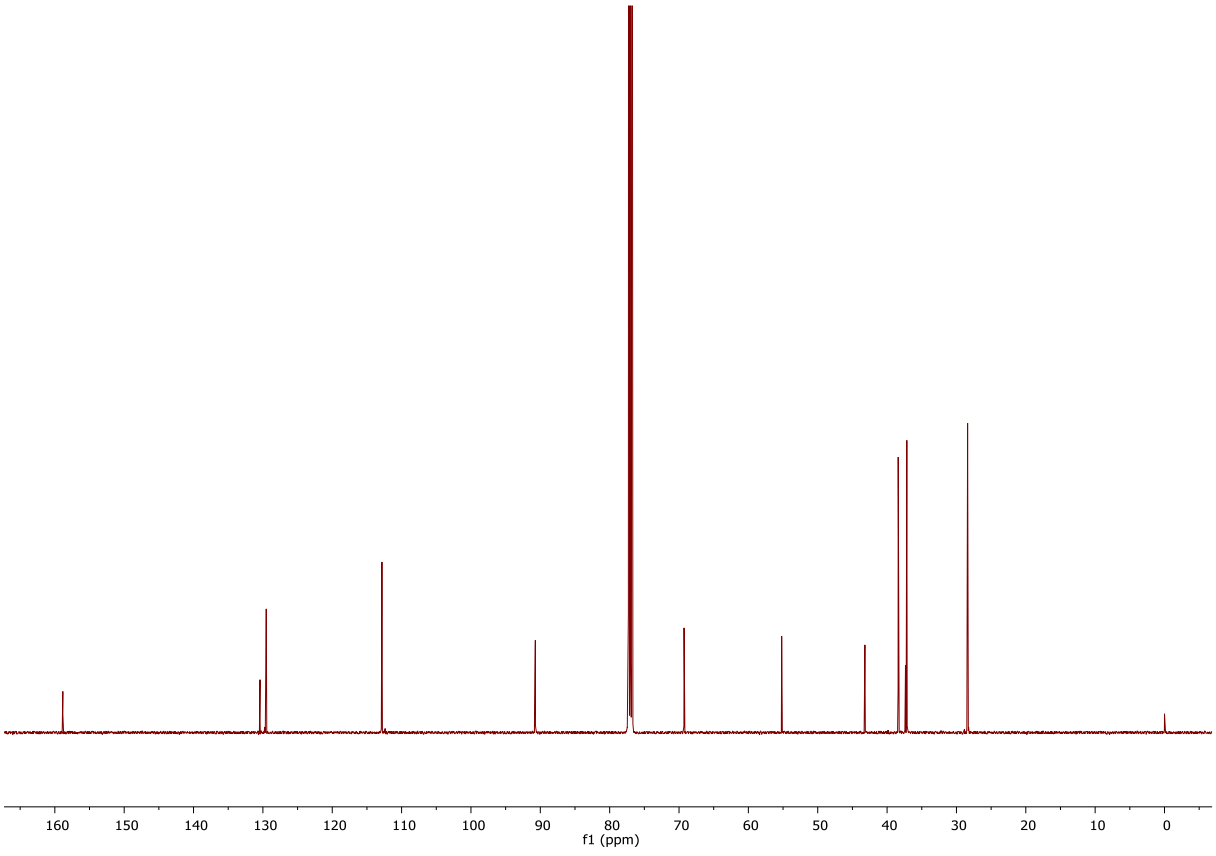

***rac*-1-[(2-Chloroethoxy)(3-methoxyphenyl)methyl]adamantane (17c)**

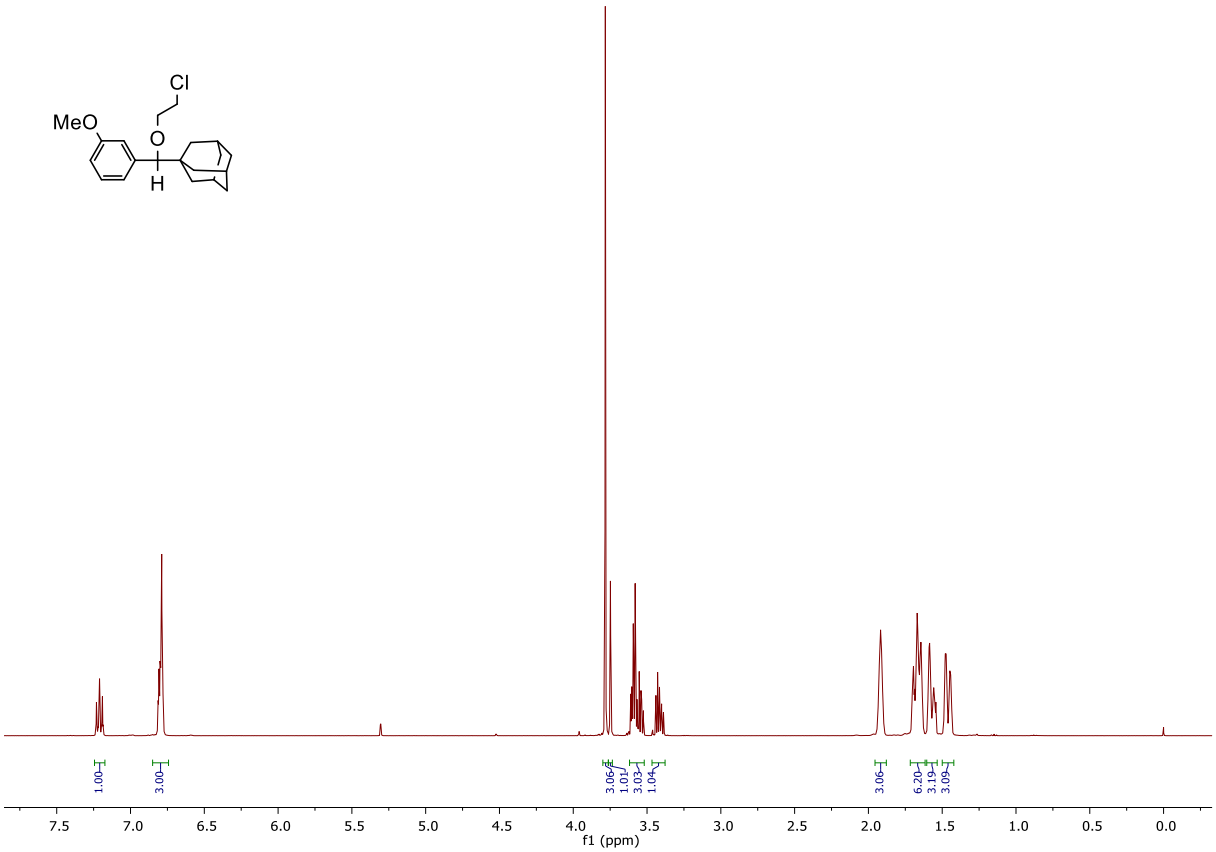

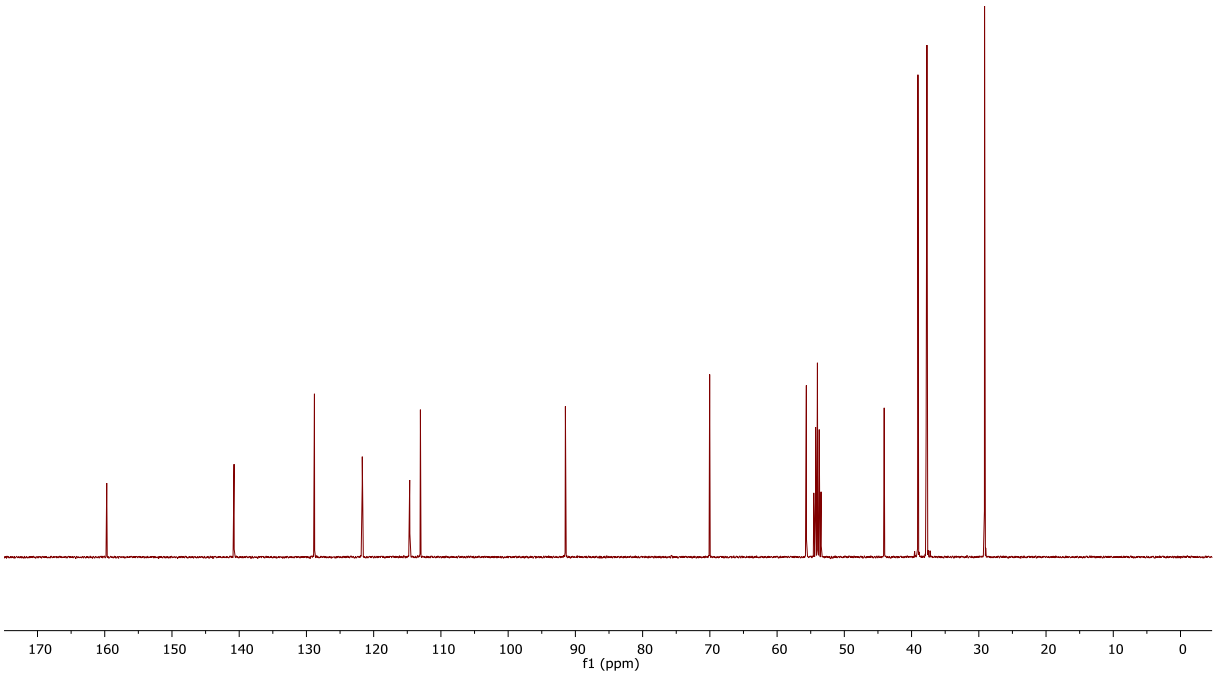

***rac*-1-[(2-Chloroethoxy)(2-methoxyphenyl)methyl]adamantane (17d)**

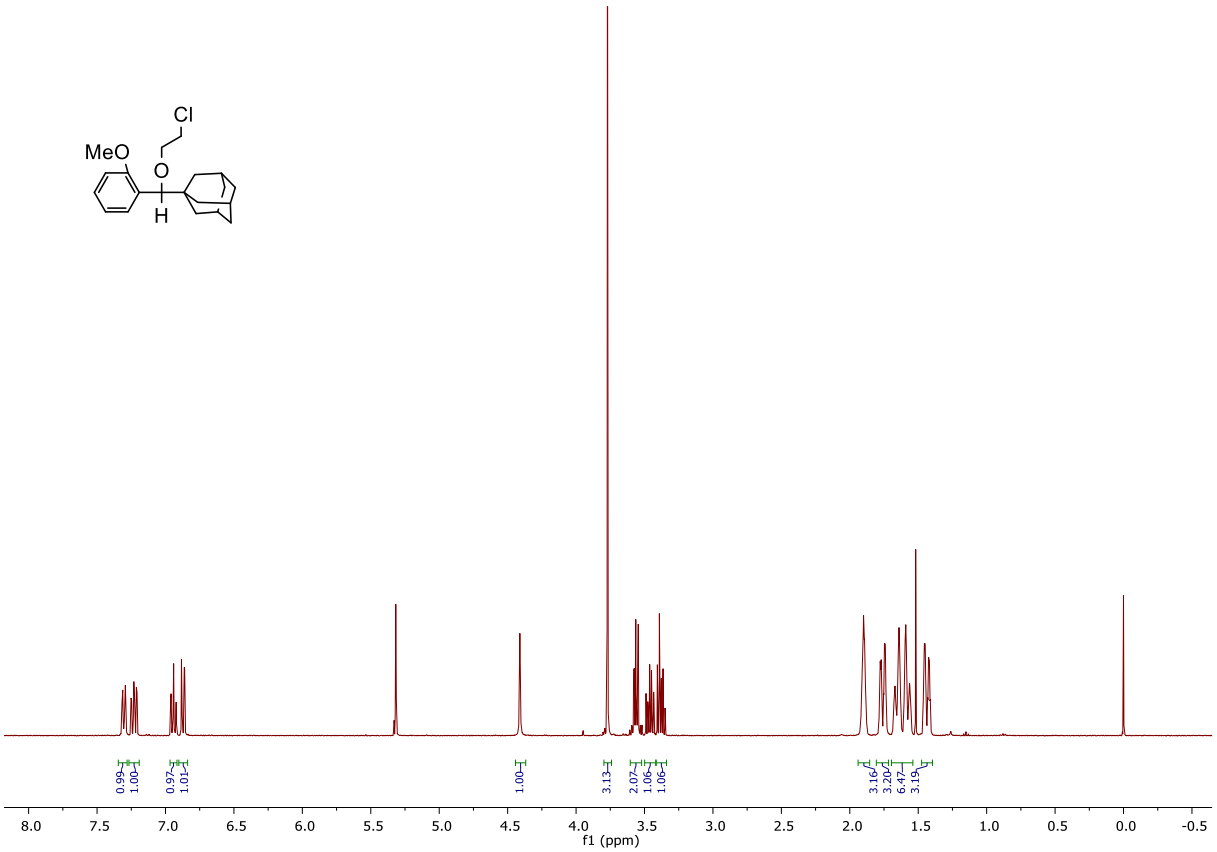

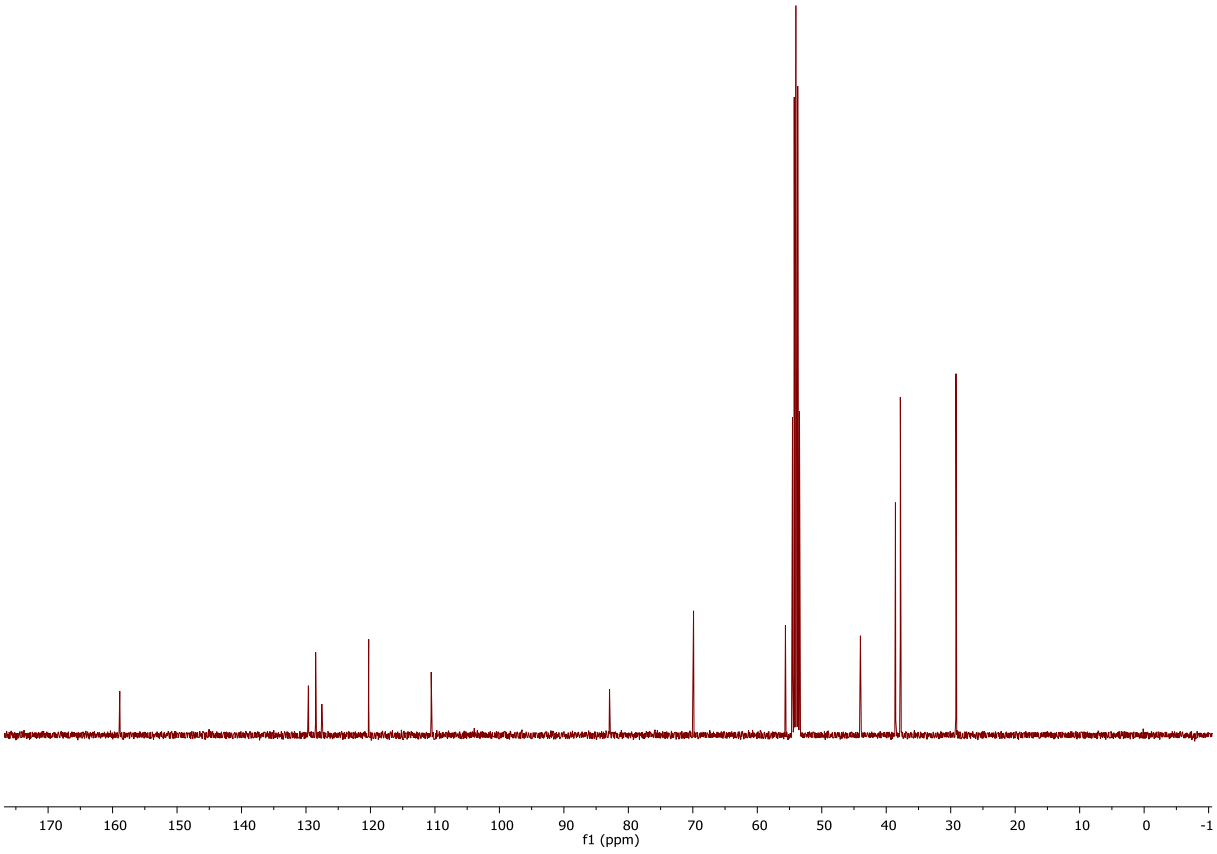

***rac*-1-[(2-Chloroethoxy)(4-methoxyphenyl)methyl]-3,5-dimethyladamantane (17e)**

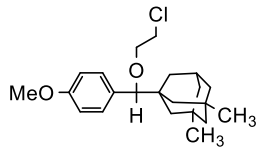

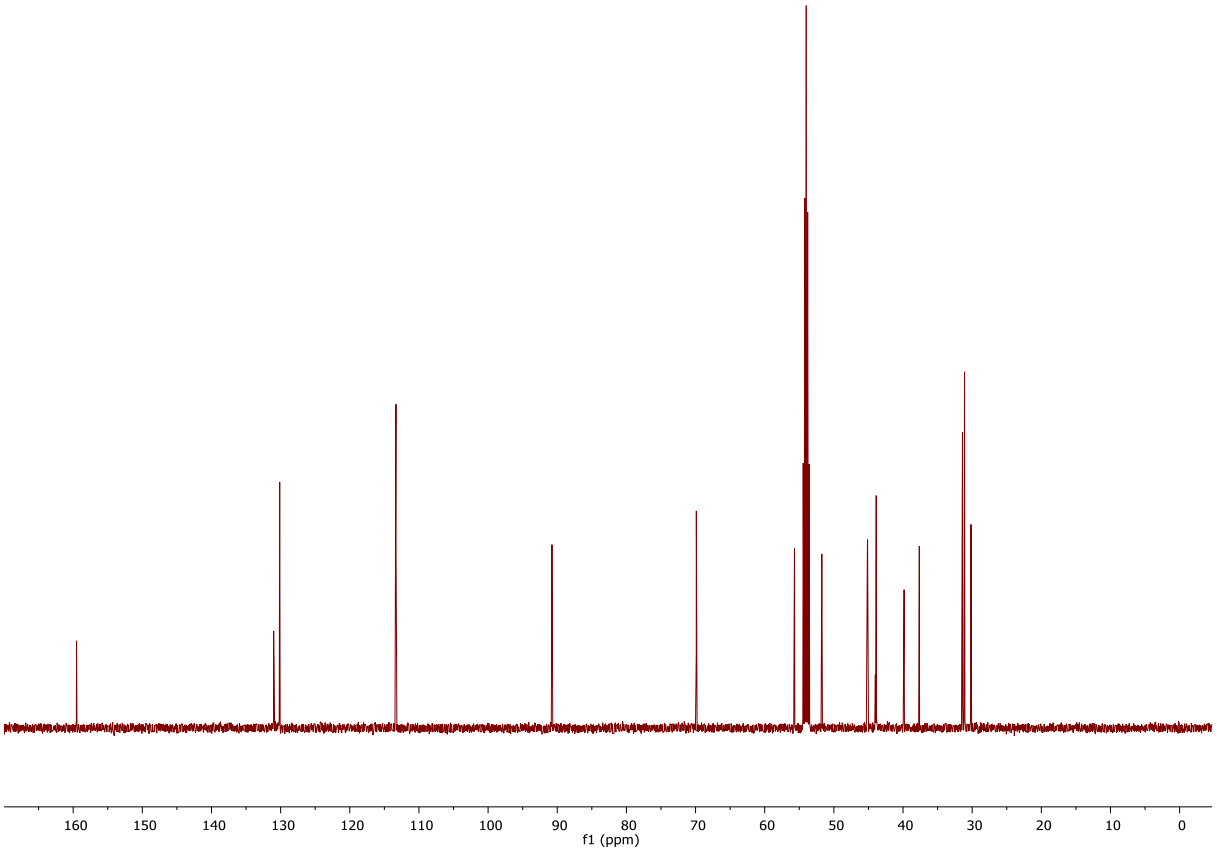

***rac*-1-[(2-Chloroethoxy)(4-methoxyphenyl)methyl]-3-methoxyadamantane (17g)**

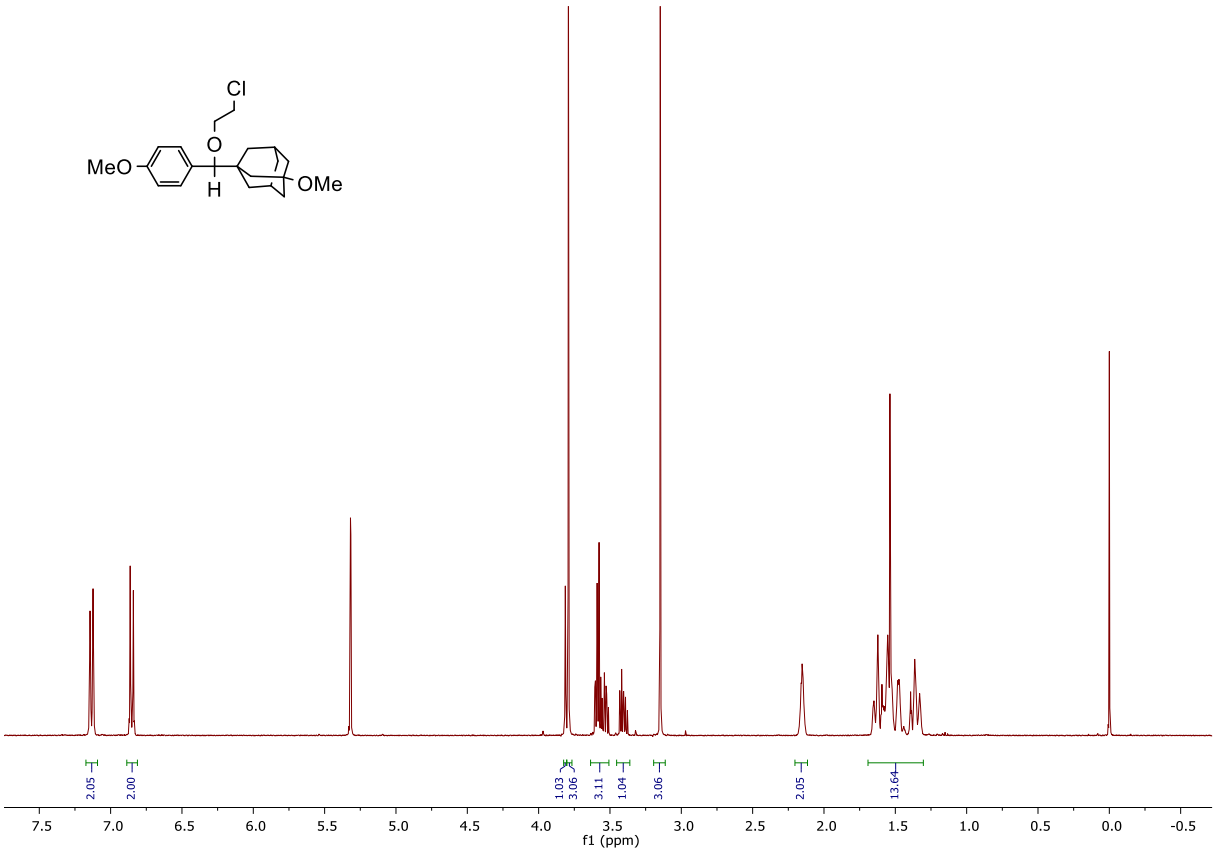

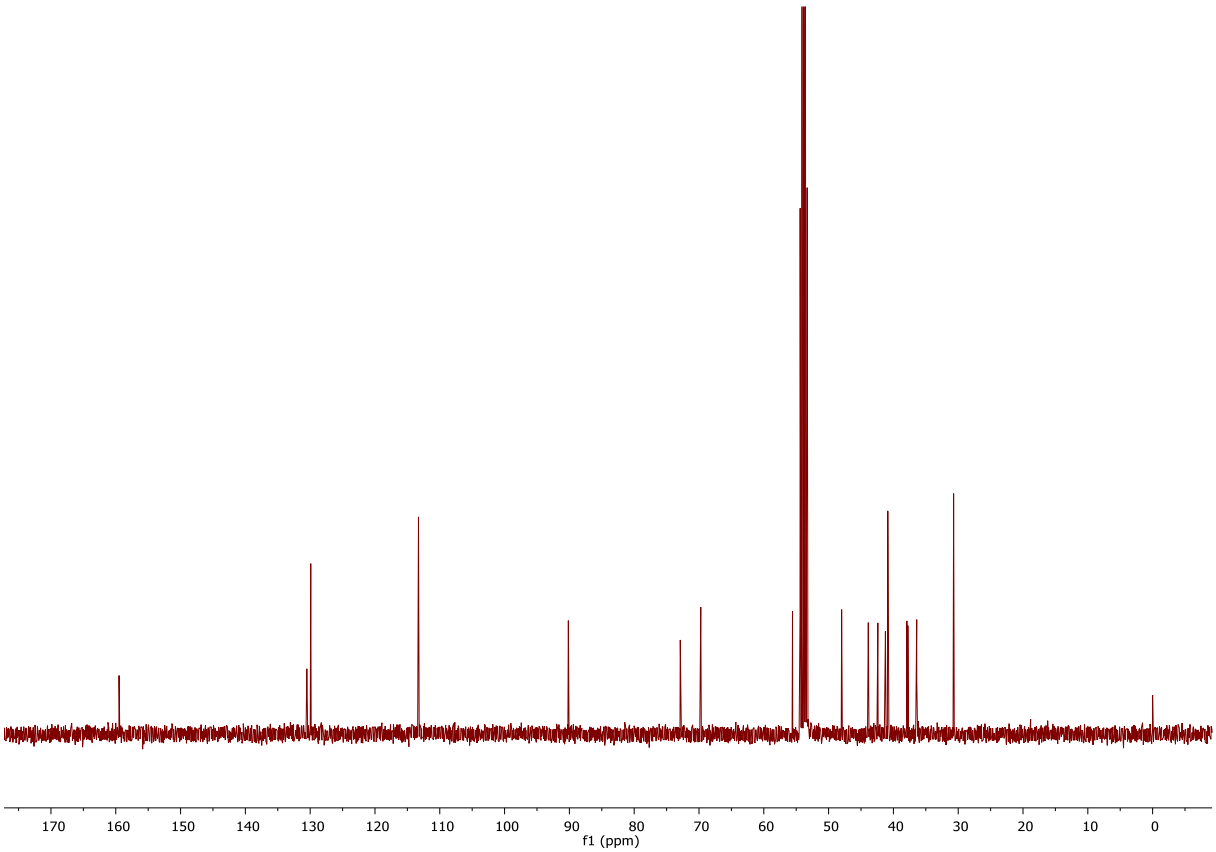

***rac*-(4-Methoxyphenyl)(1-methylcyclohexyl)methanol (19a)**

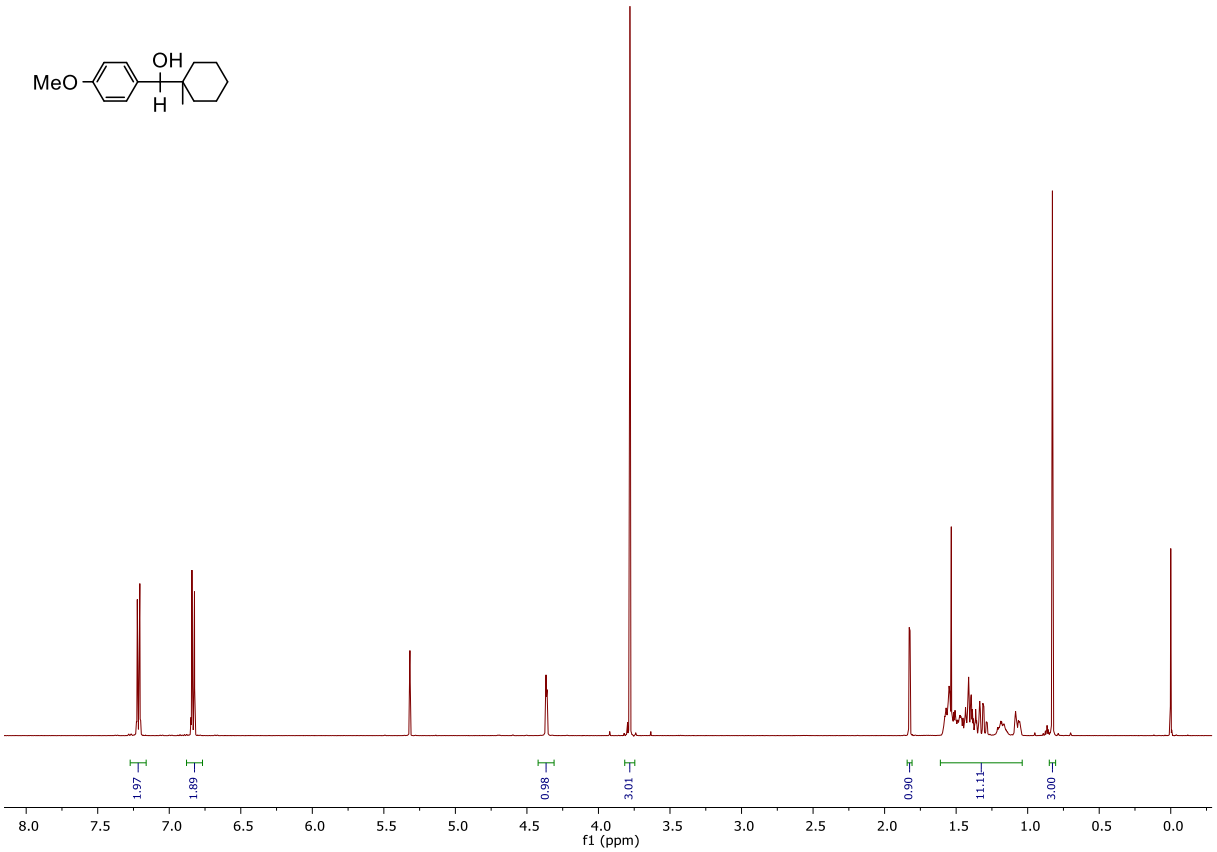

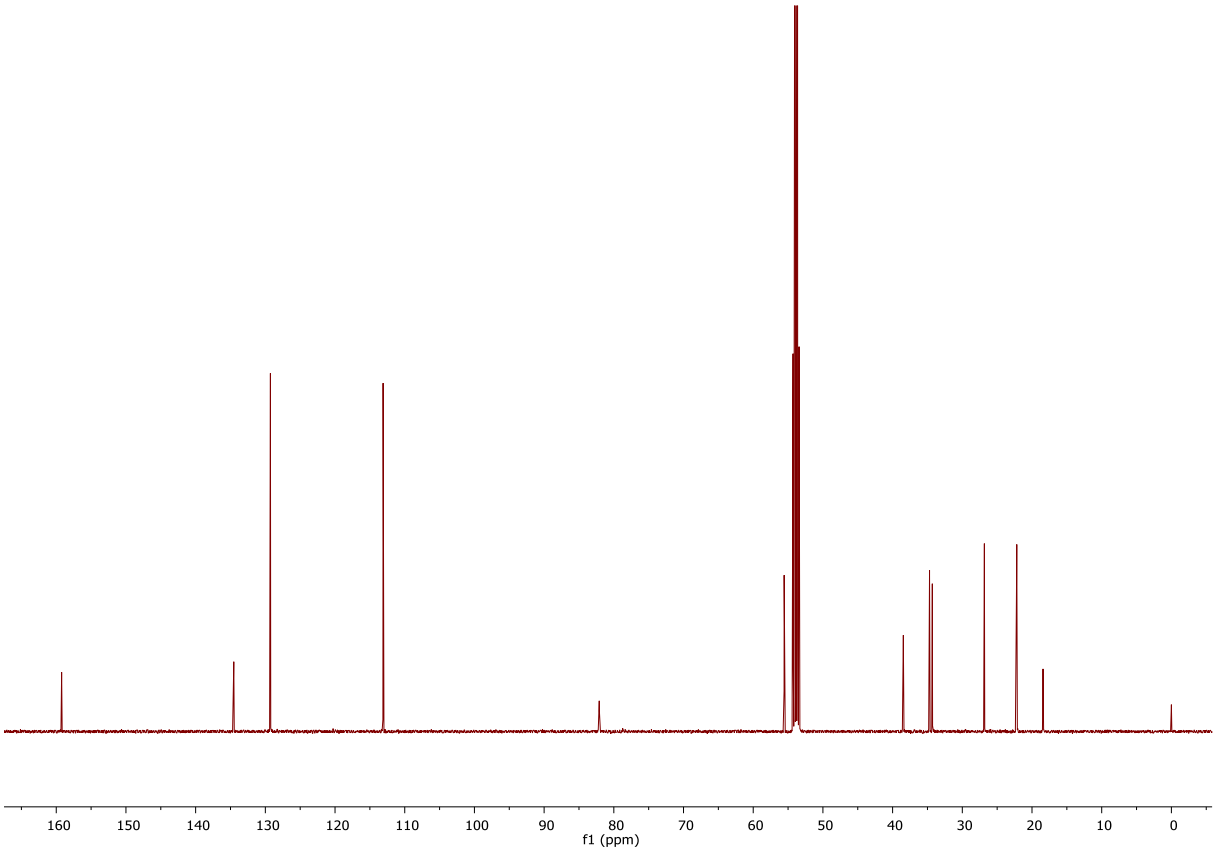

***rac*-(Adamantan-1-yl)(4-methoxyphenyl)methanol (19b)**

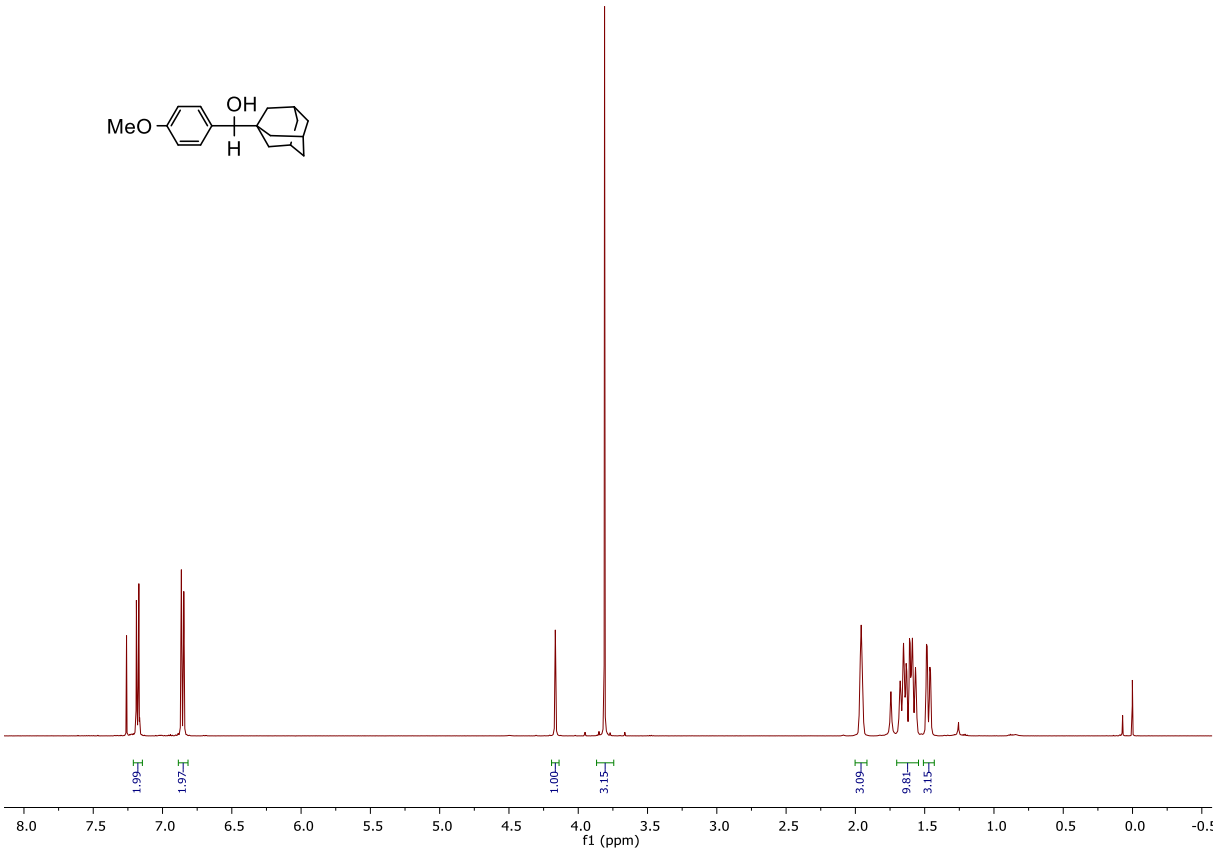

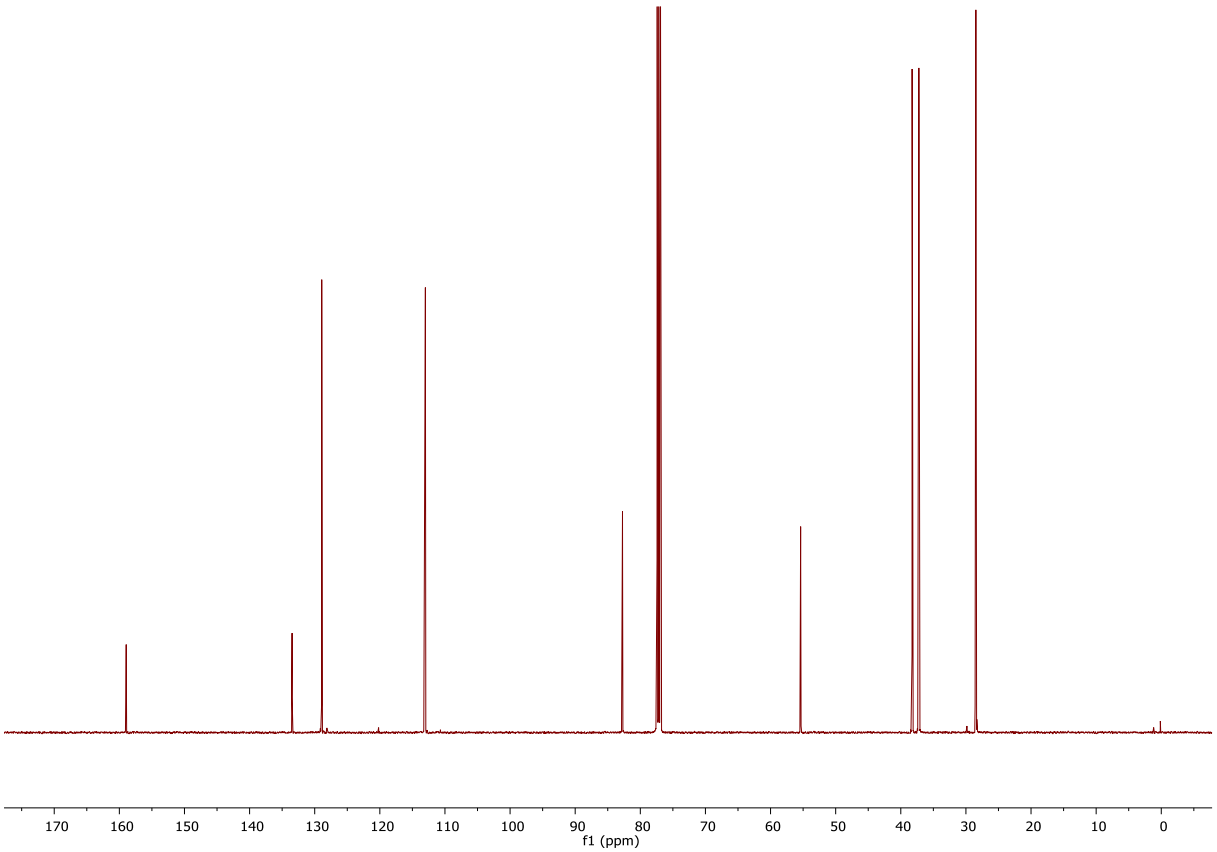

***rac*-(Adamantan-1-yl)(3-methoxyphenyl)methanol (19c)**

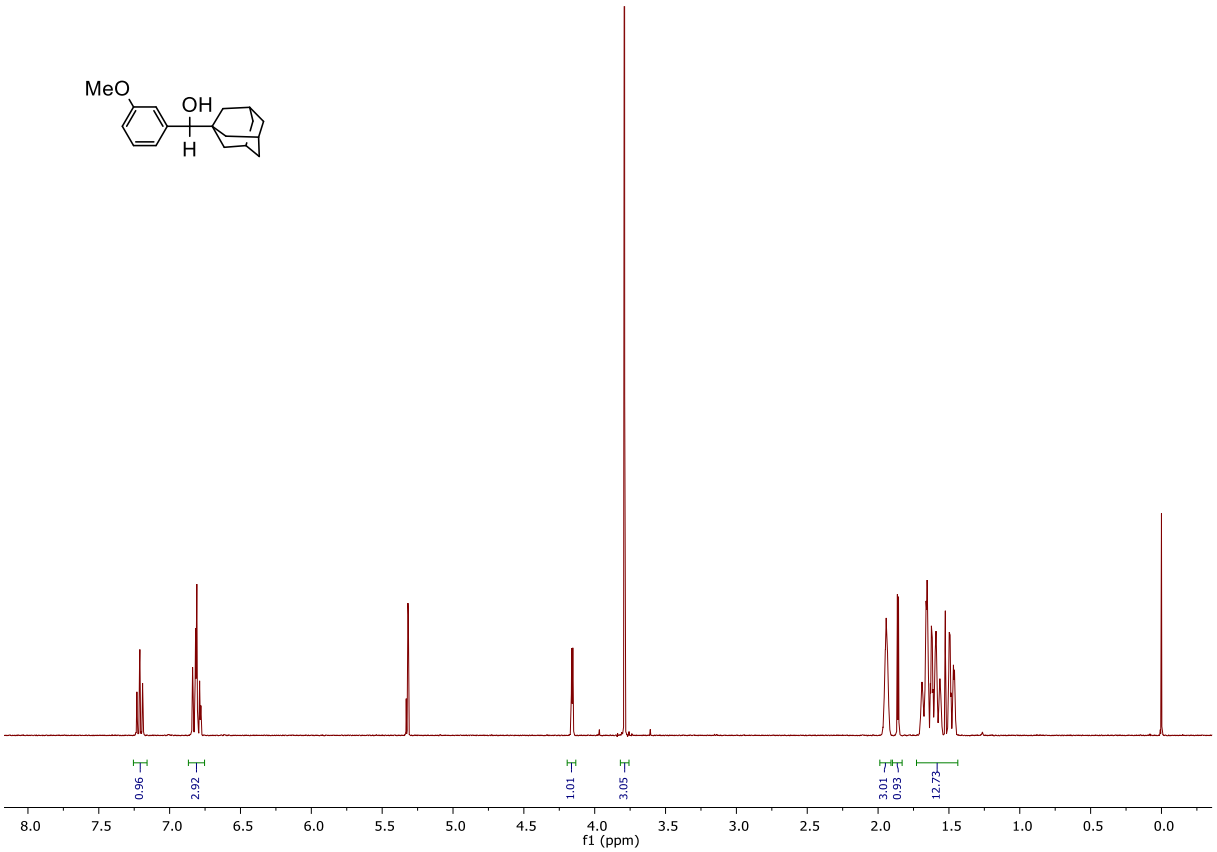

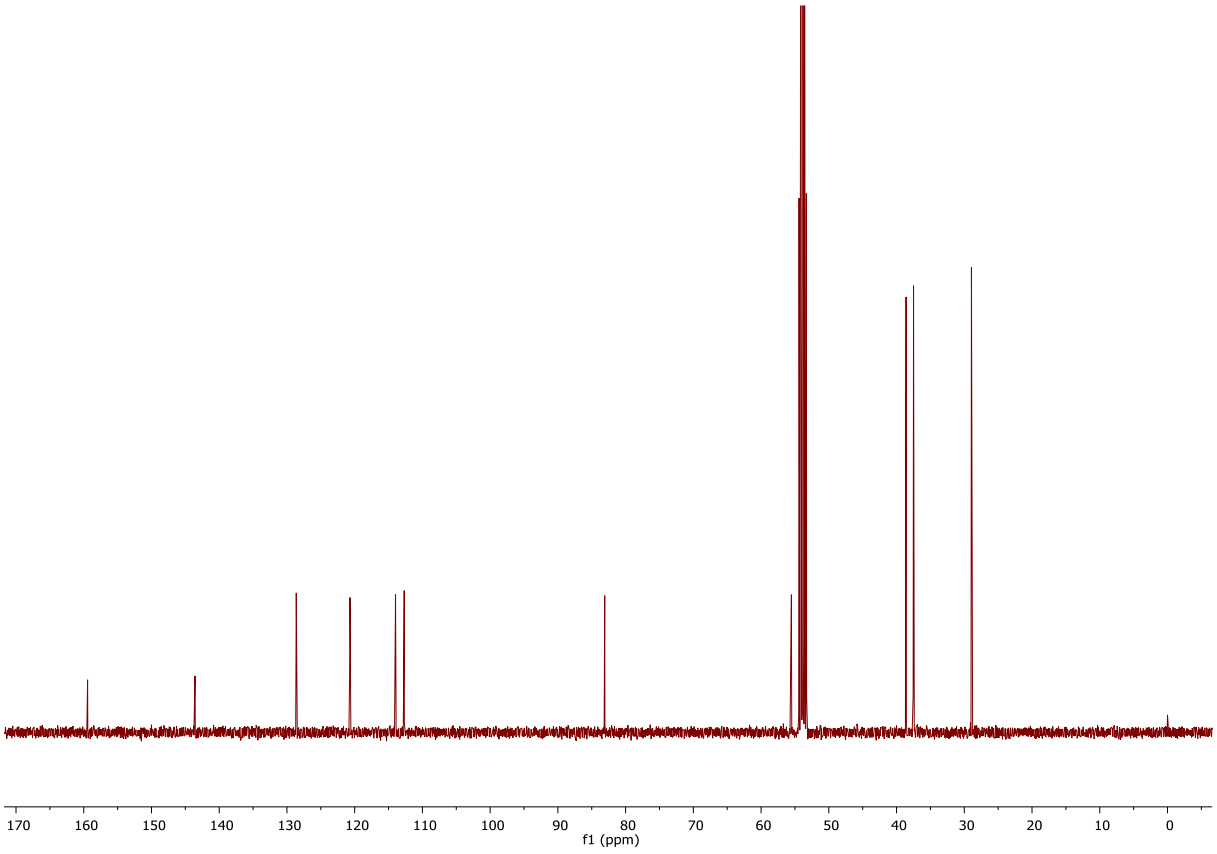

***rac*-(Adamantan-1-yl)(2-methoxyphenyl)methanol (19d)**

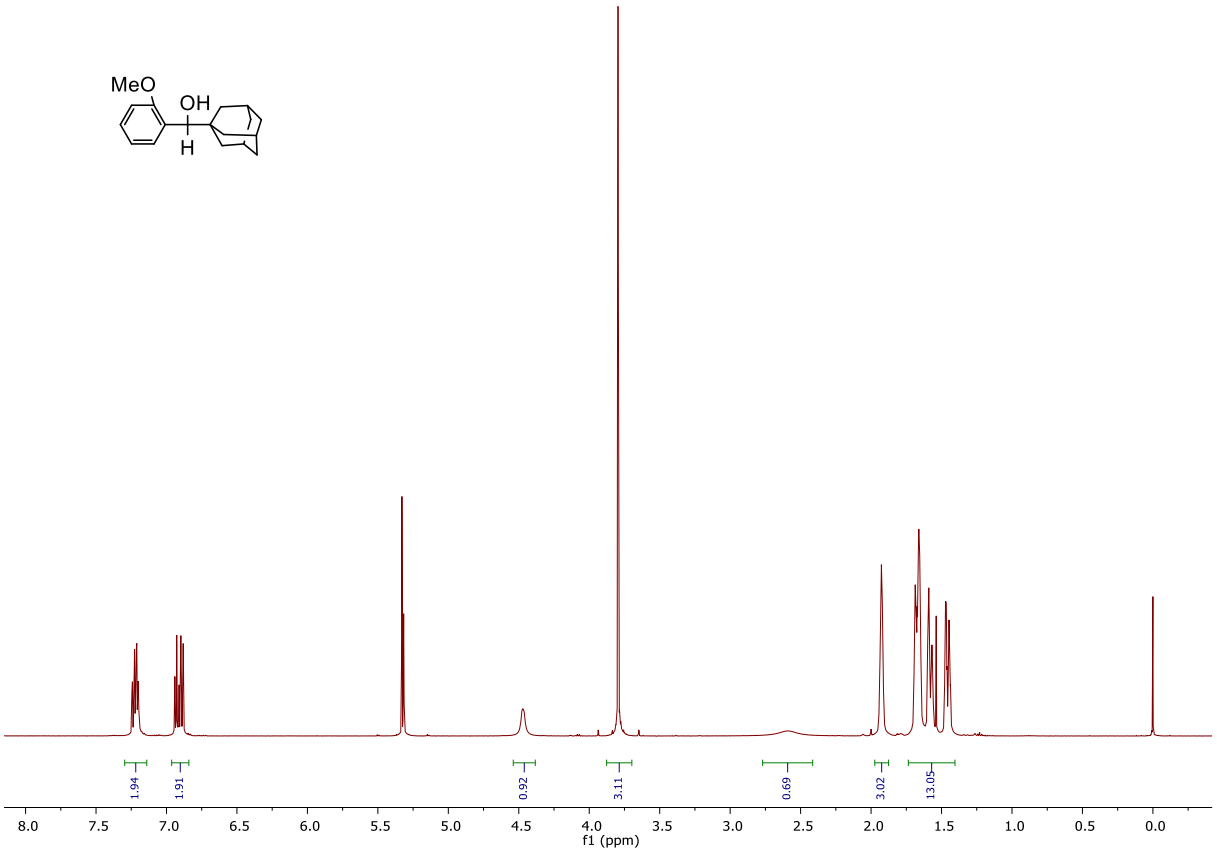

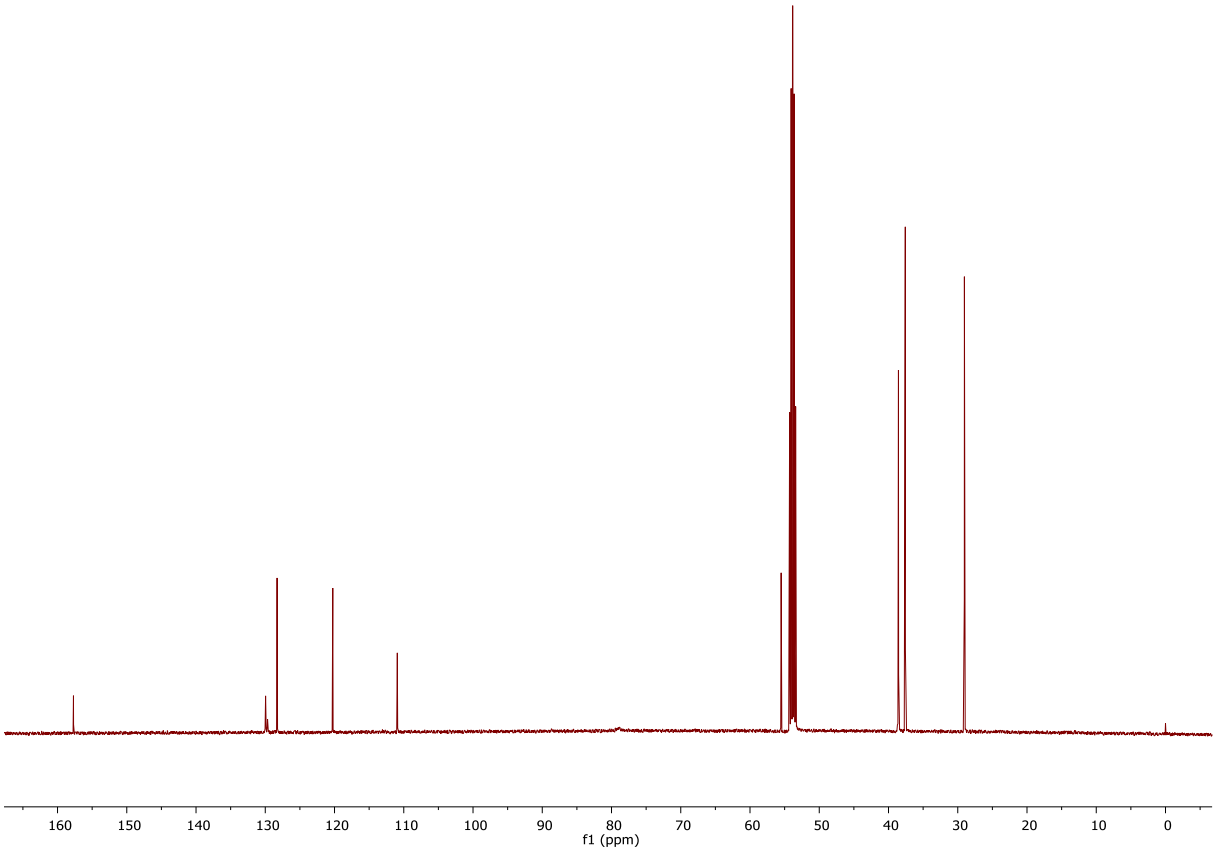

***rac*-(3,5-Dimethyladamantan-1-yl)(4-methoxyphenyl)methanol (19e)**

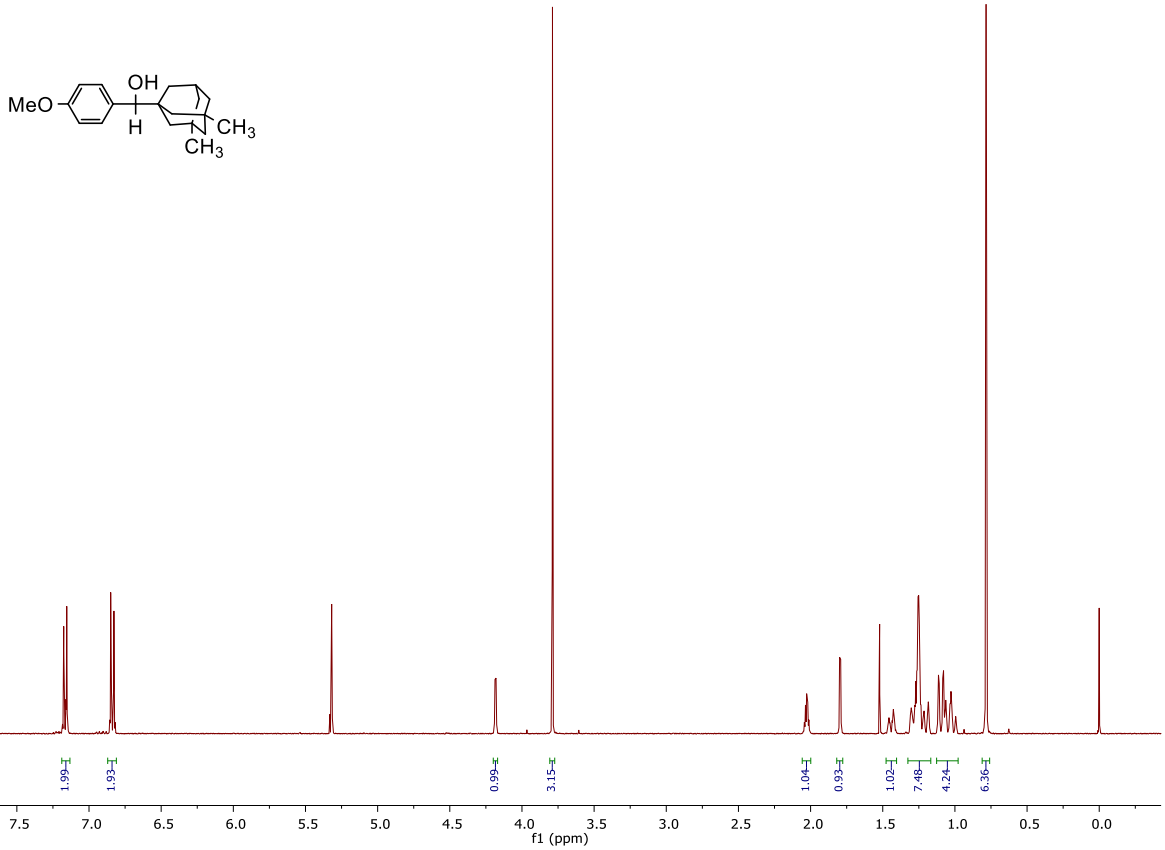

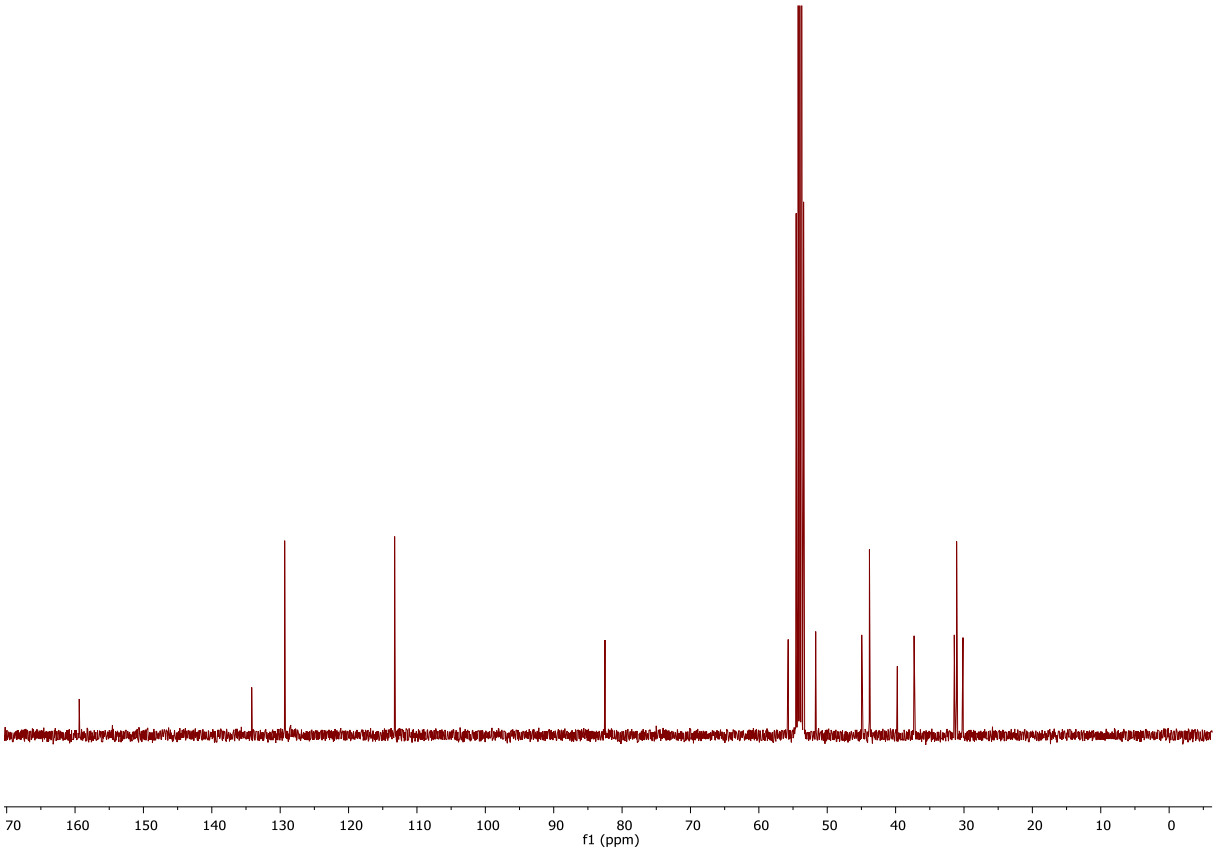

***rac*-(3-Methoxyadamantan-1-yl)(4-methoxyphenyl)methanol (19g)**

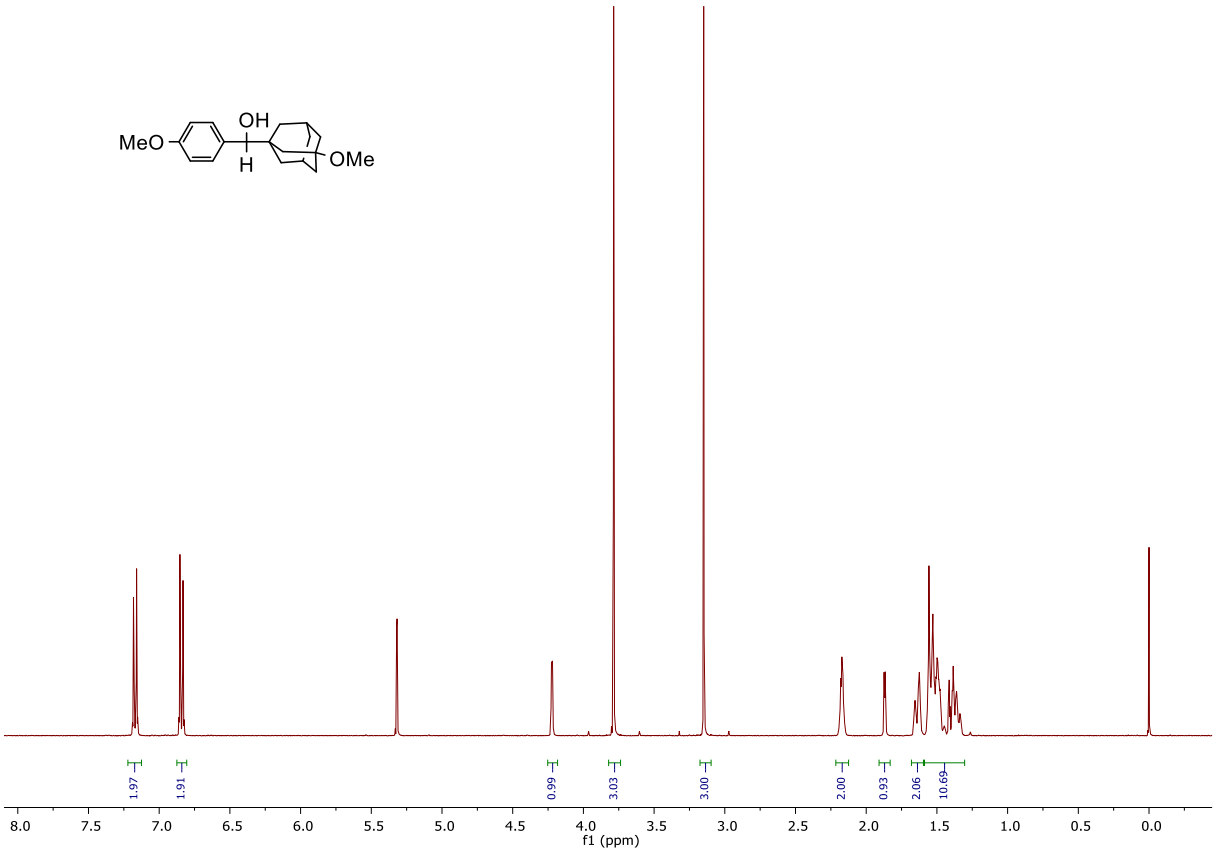

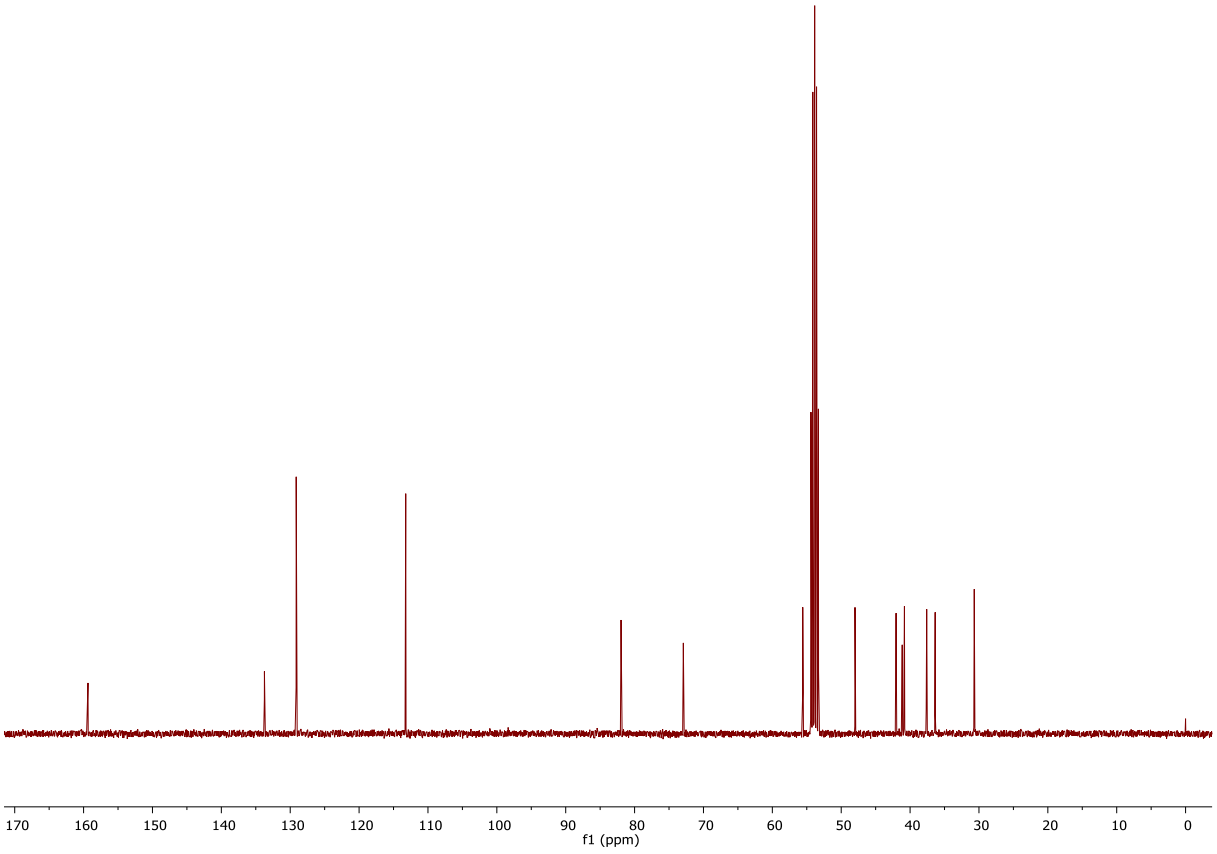

Methyl (1*S*,4*S*)-4-methoxy-1-methylcyclohexane-1-carboxylate (25)

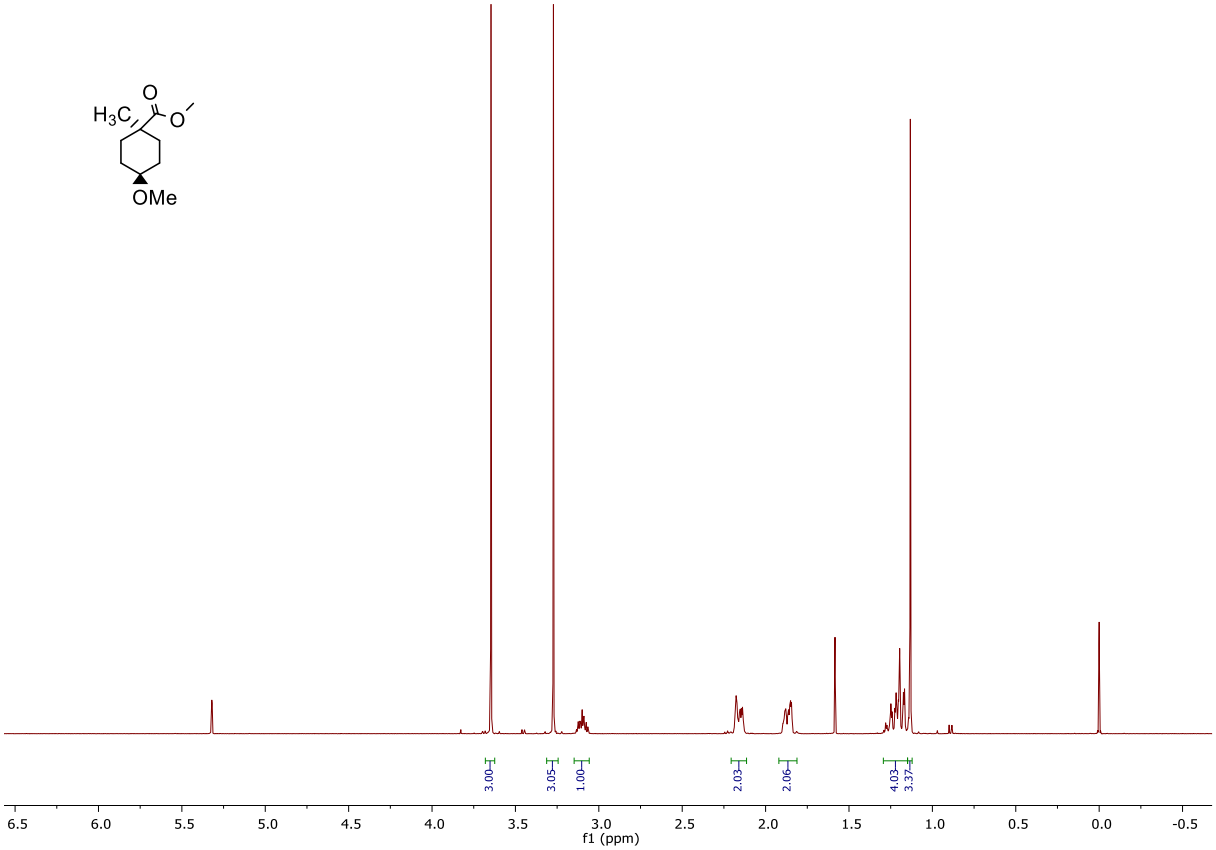

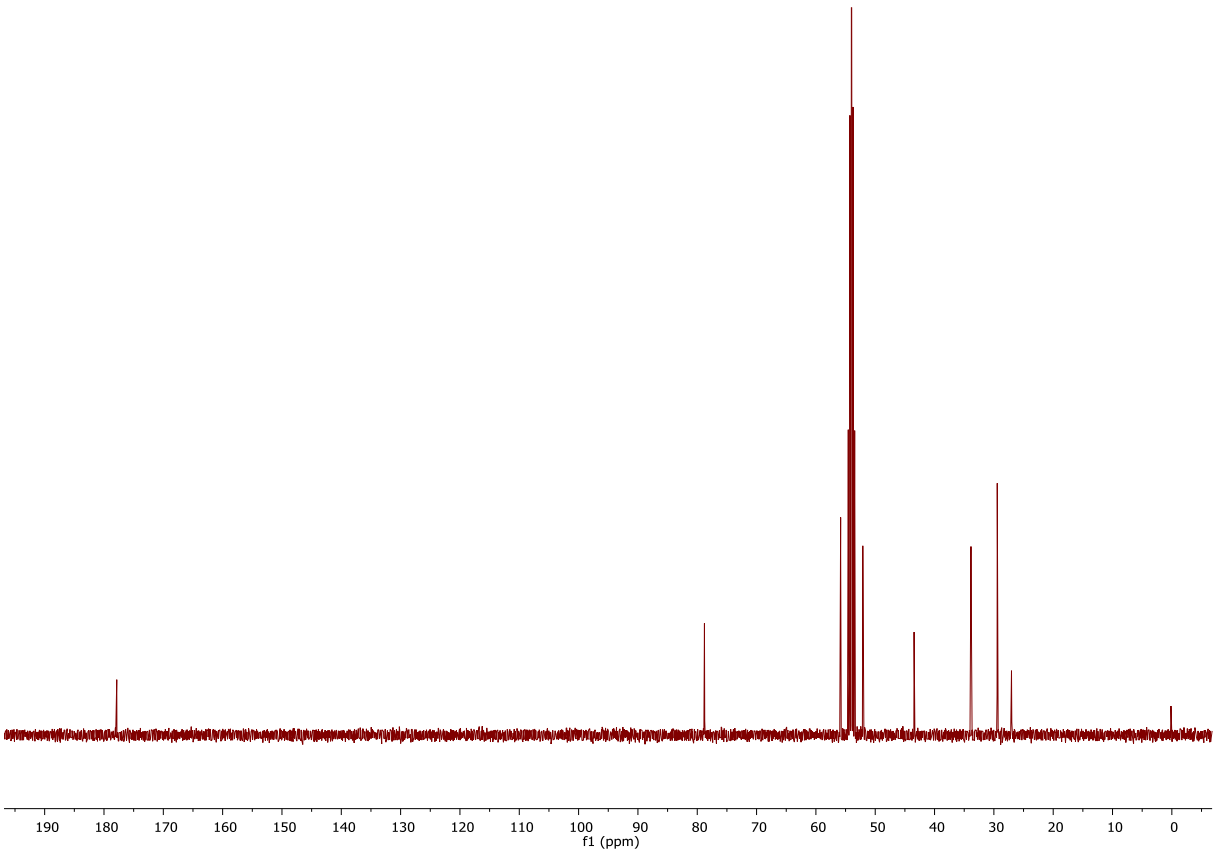

***rac*-Ethyl 1-{2-[1,1-bis(4-methoxyphenyl)-2,2-dimethylpropoxy]ethyl}piperidine-3-carboxylate (27a)**

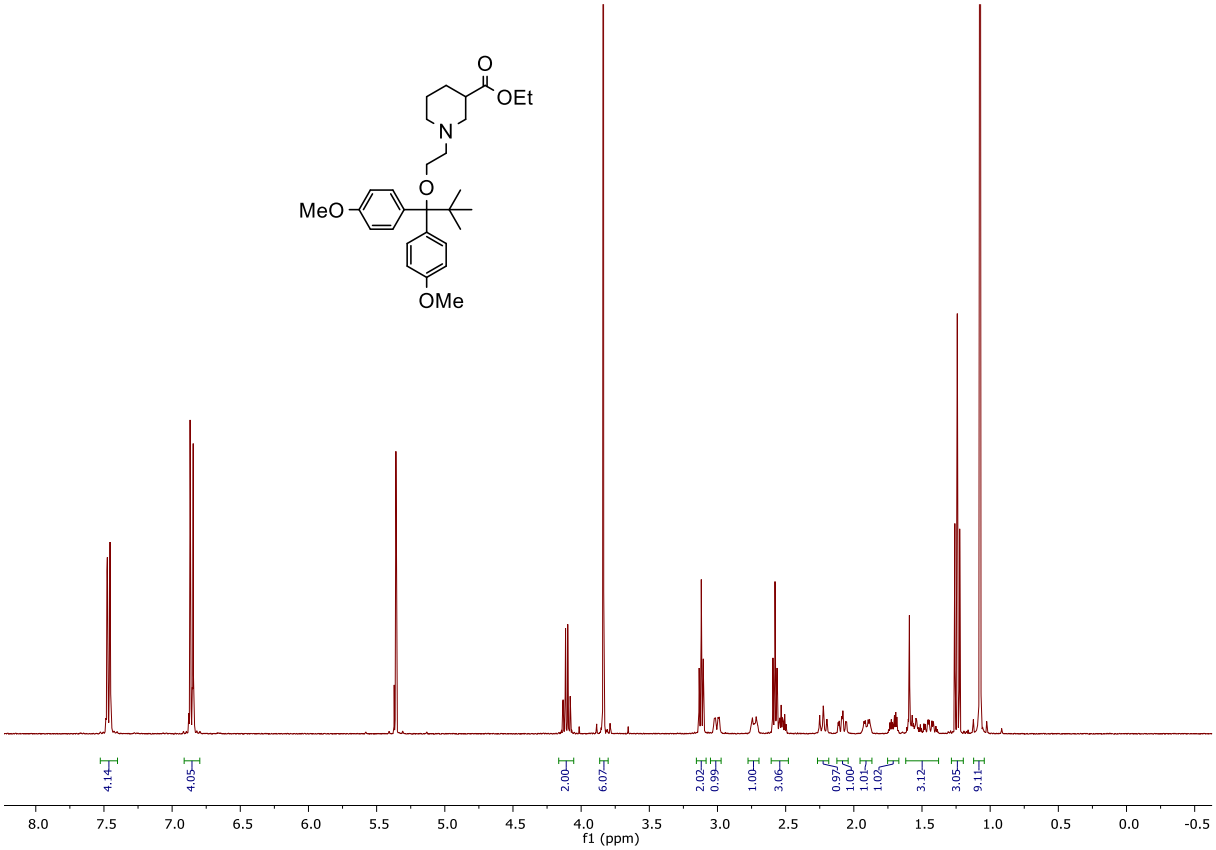

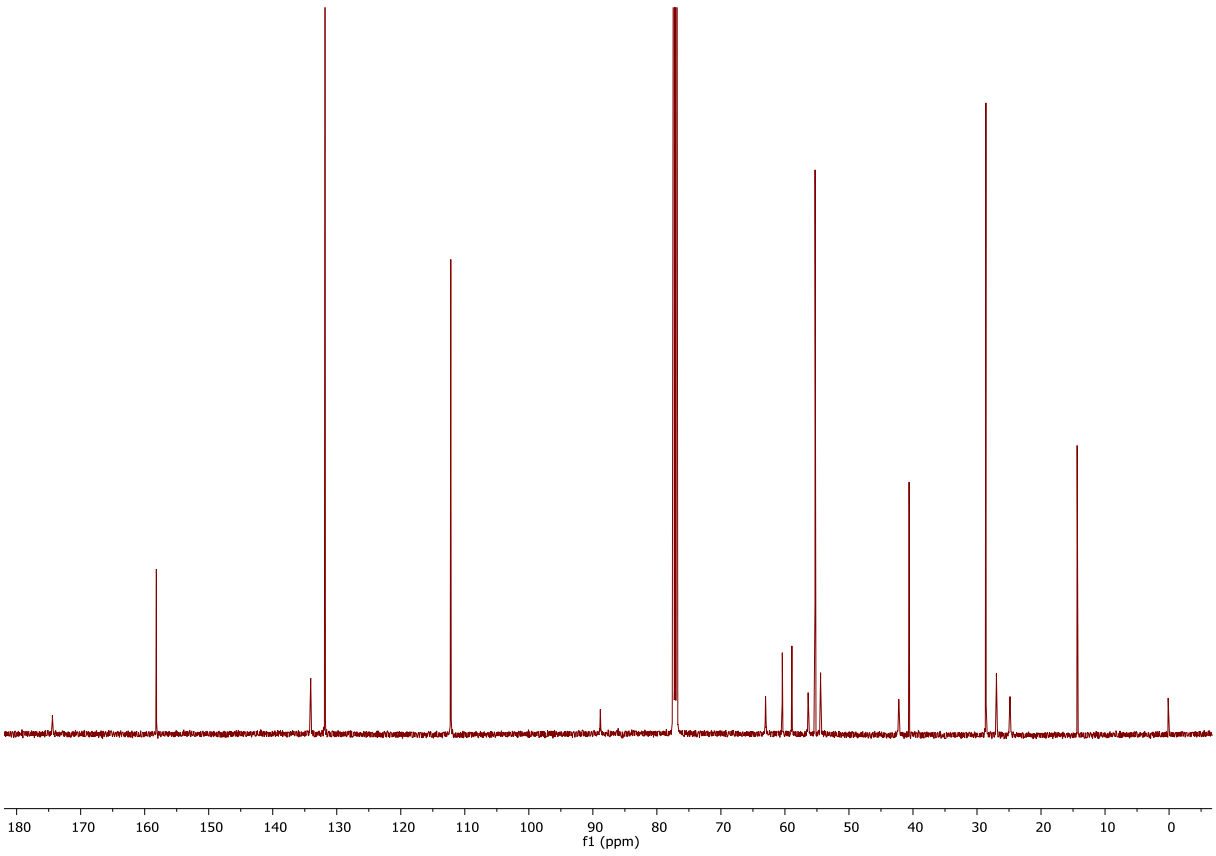

***rac*-Ethyl 1-{2-[bis(4-methoxyphenyl)(1-methylcyclopentyl)methoxy]ethyl}piperidine-3-carboxylate (27b)**

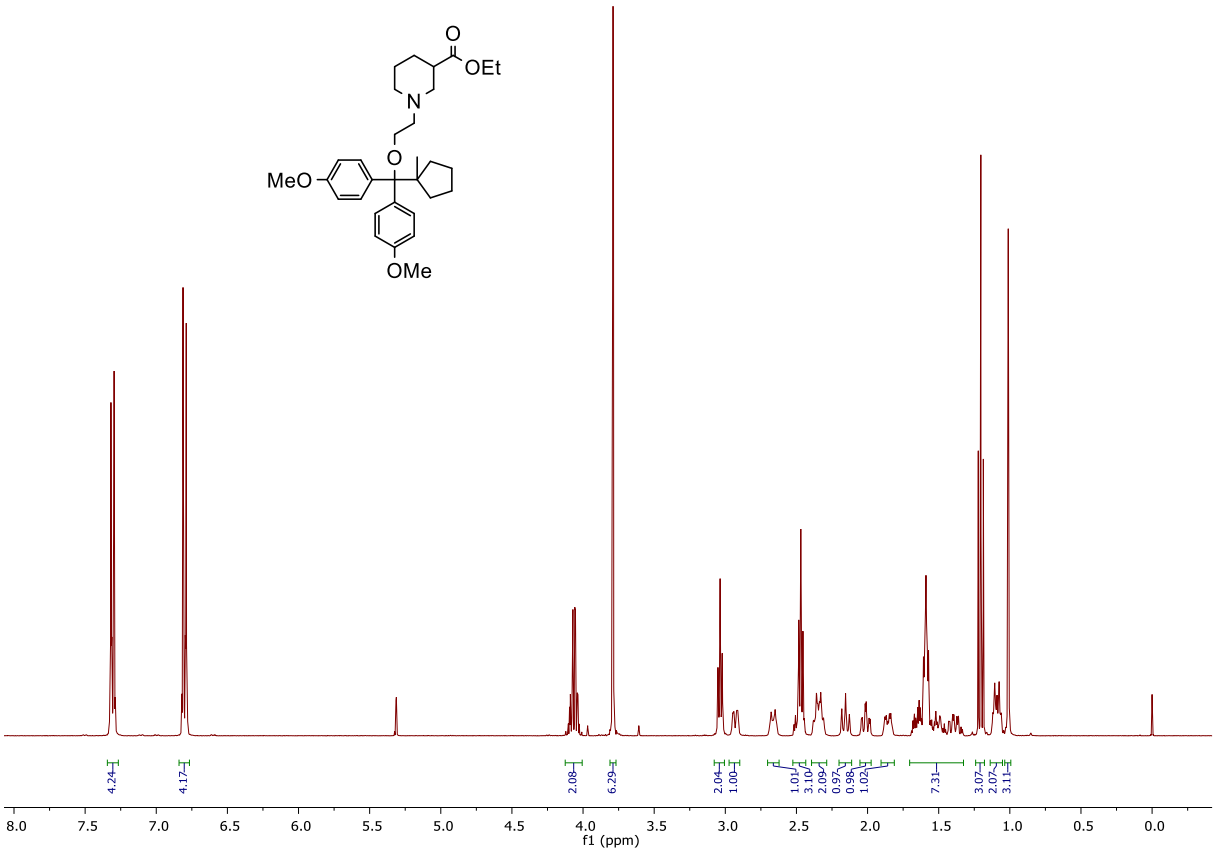

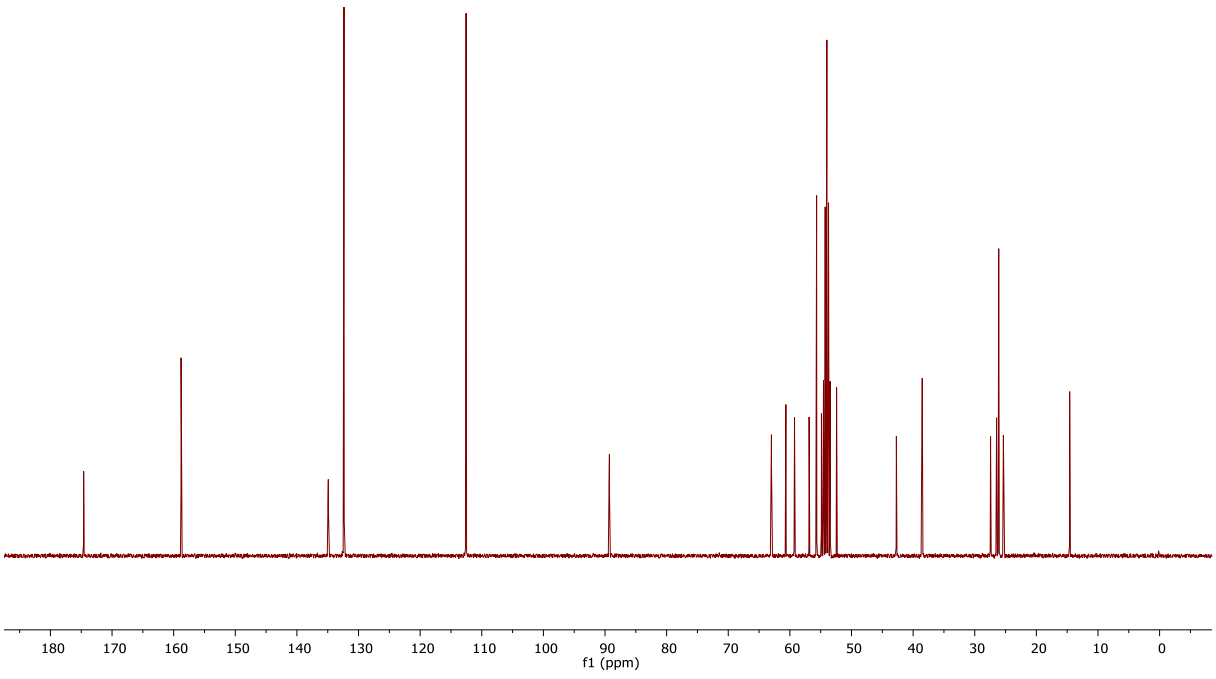

***rac*-Ethyl 1-{2-[bis(4-methoxyphenyl)(1-methylcyclohexyl)methoxy]ethyl}piperidine-3-carboxylate (27c)**

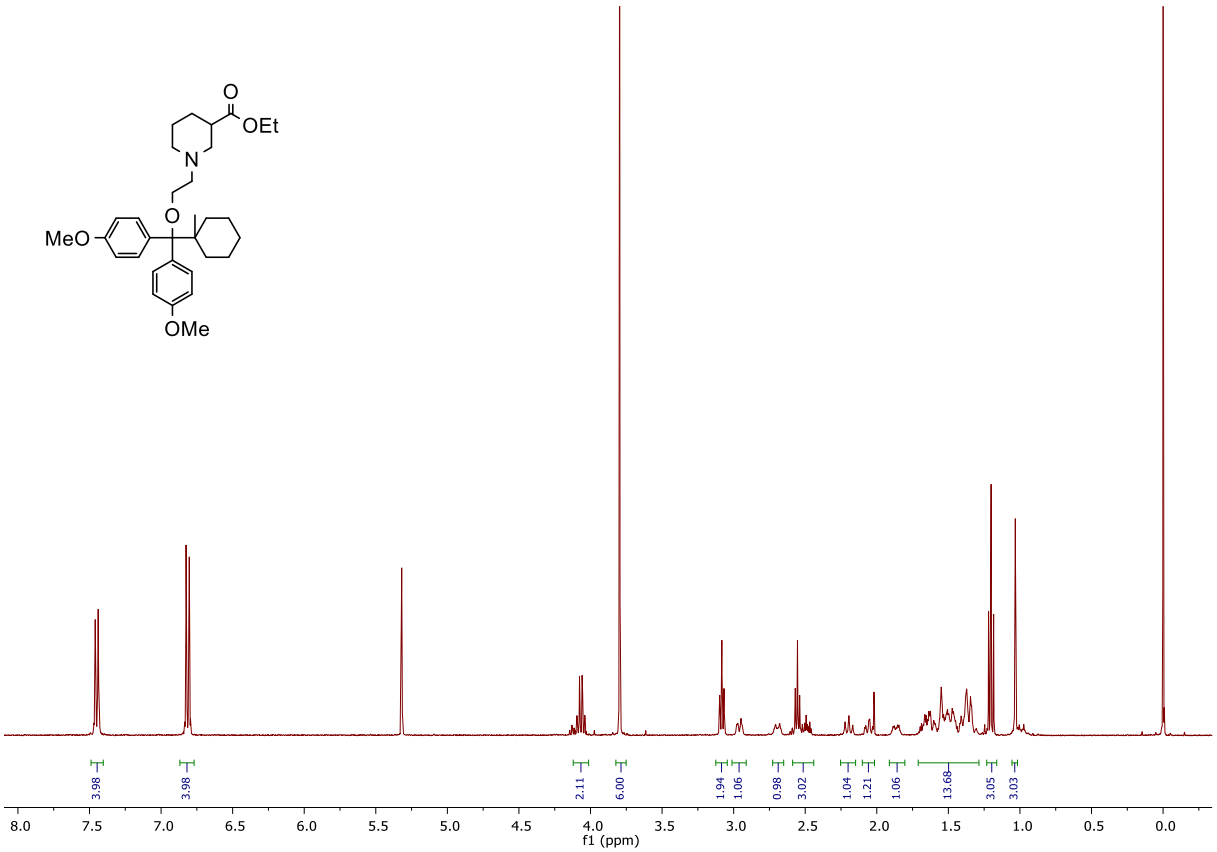

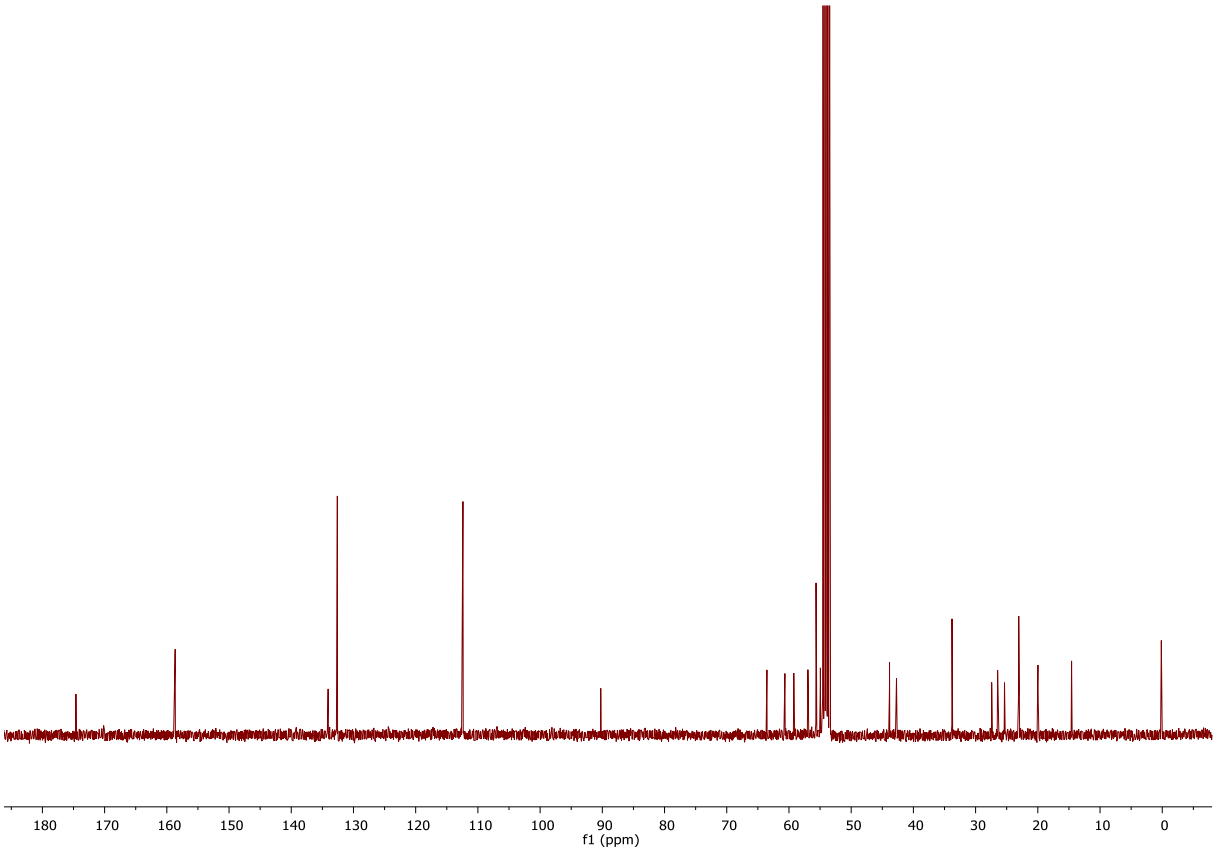

***rac*-Ethyl 1-{2-[bis(4-methoxyphenyl)(4-methyltetrahydro-2H-pyran-4-yl)methoxy]ethyl}piperidine-3-carboxylate (27d)**

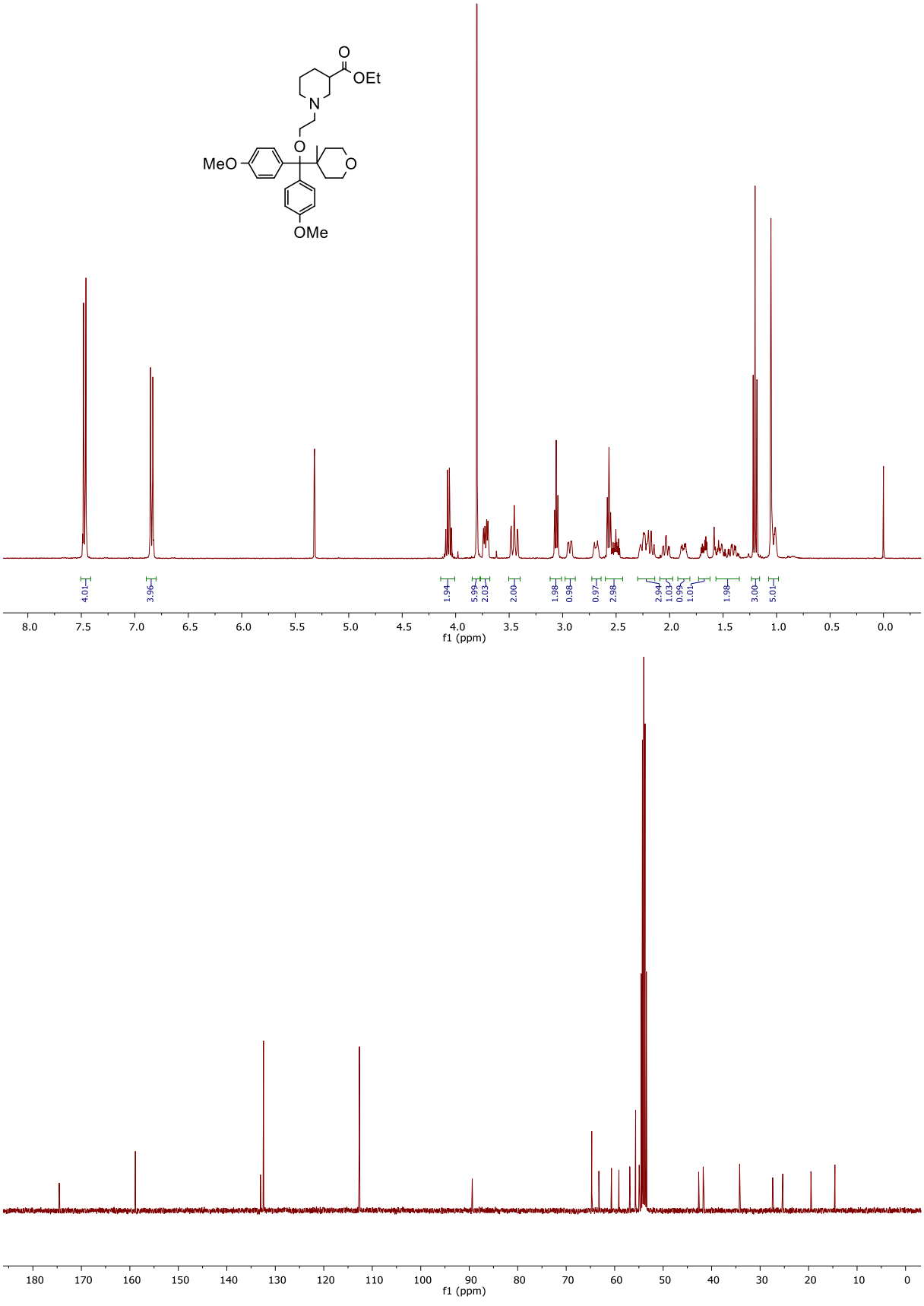

***rac*-Ethyl 1-(2-{[(1*S*,4*S*)-4-methoxy-1-methylcyclohexyl]bis[4-methoxyphenyl]methoxy}ethyl)piperidine-3-carboxylate (27e)**

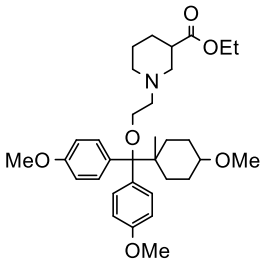

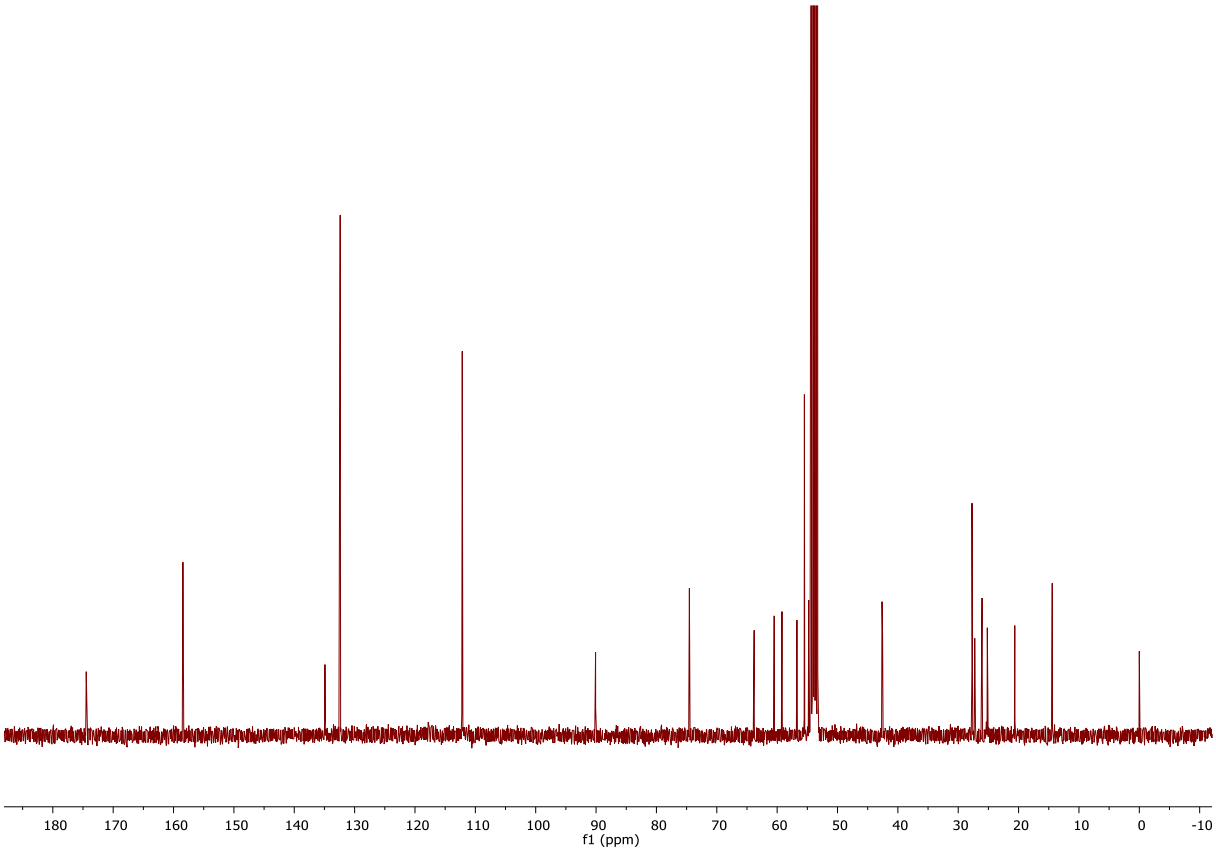

***rac*-Ethyl 1-{2-[(adamantan-1-yl)bis(4-methoxyphenyl)methoxy]ethyl}piperidine-3-carboxylate (27f)**

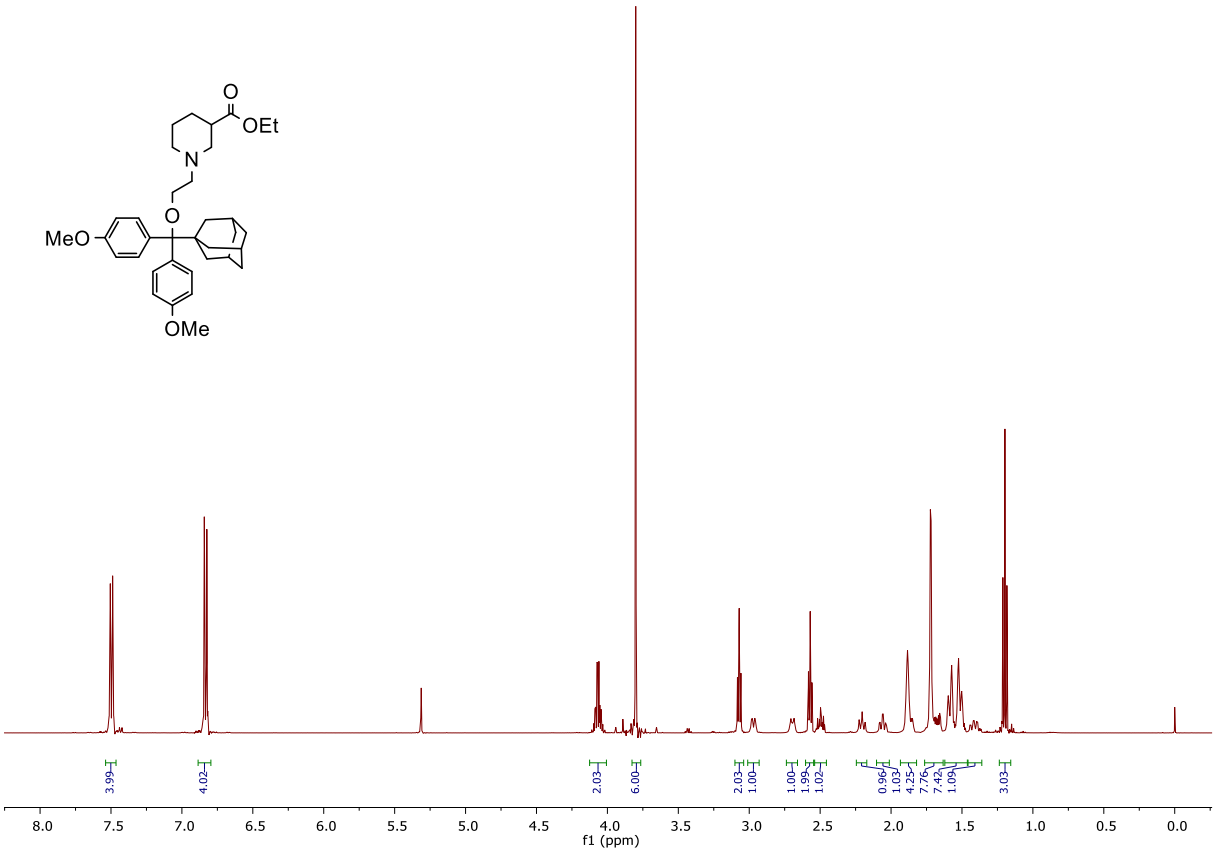

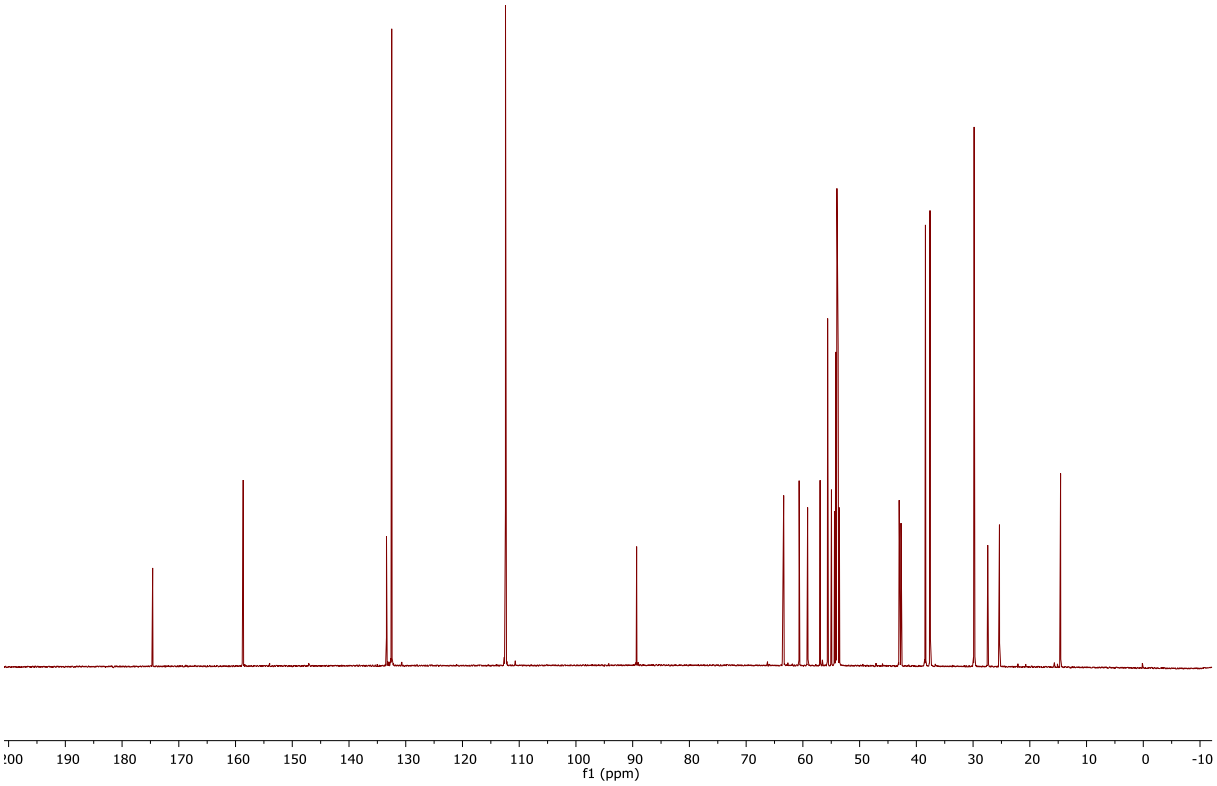

***rac*-Ethyl 1-{3-[1,1-bis(4-methoxyphenyl)-2,2-dimethylpropoxy]propyl}piperidine-3-carboxylate (28)**

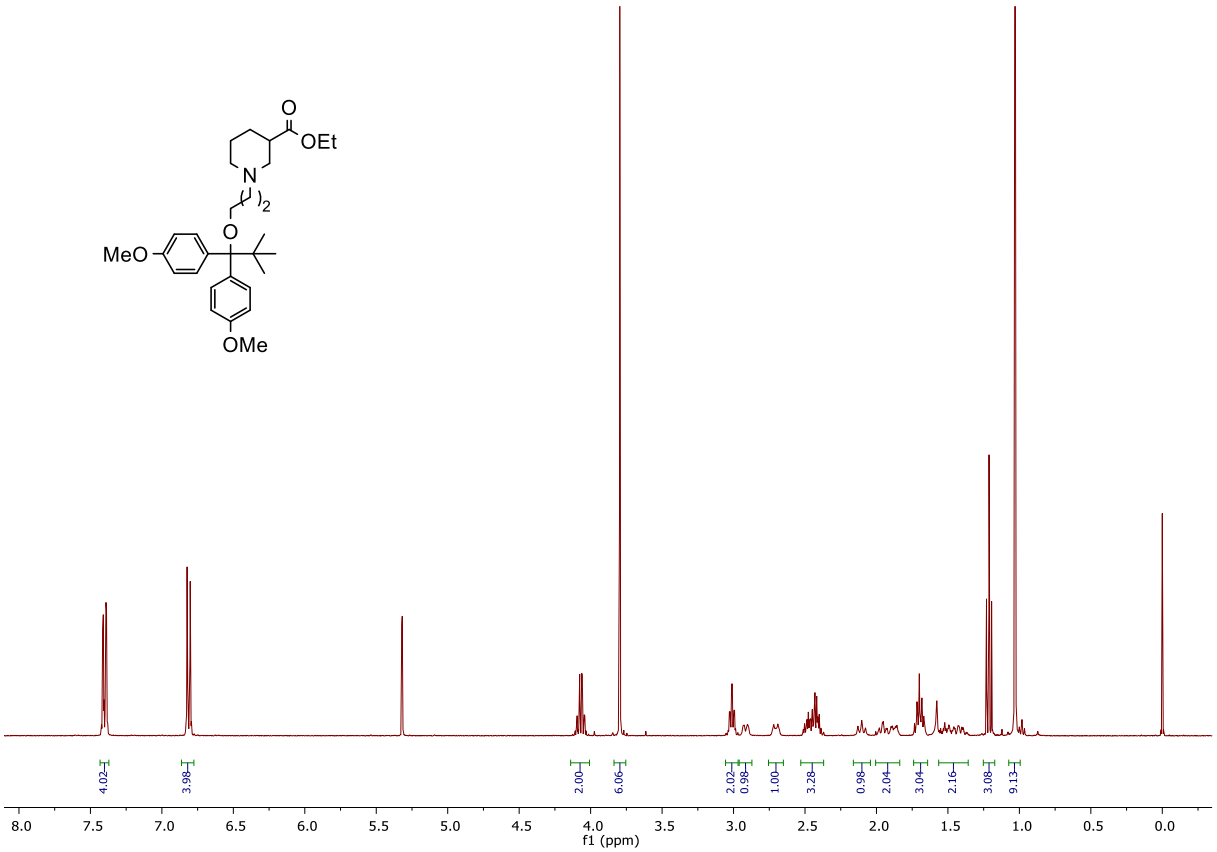

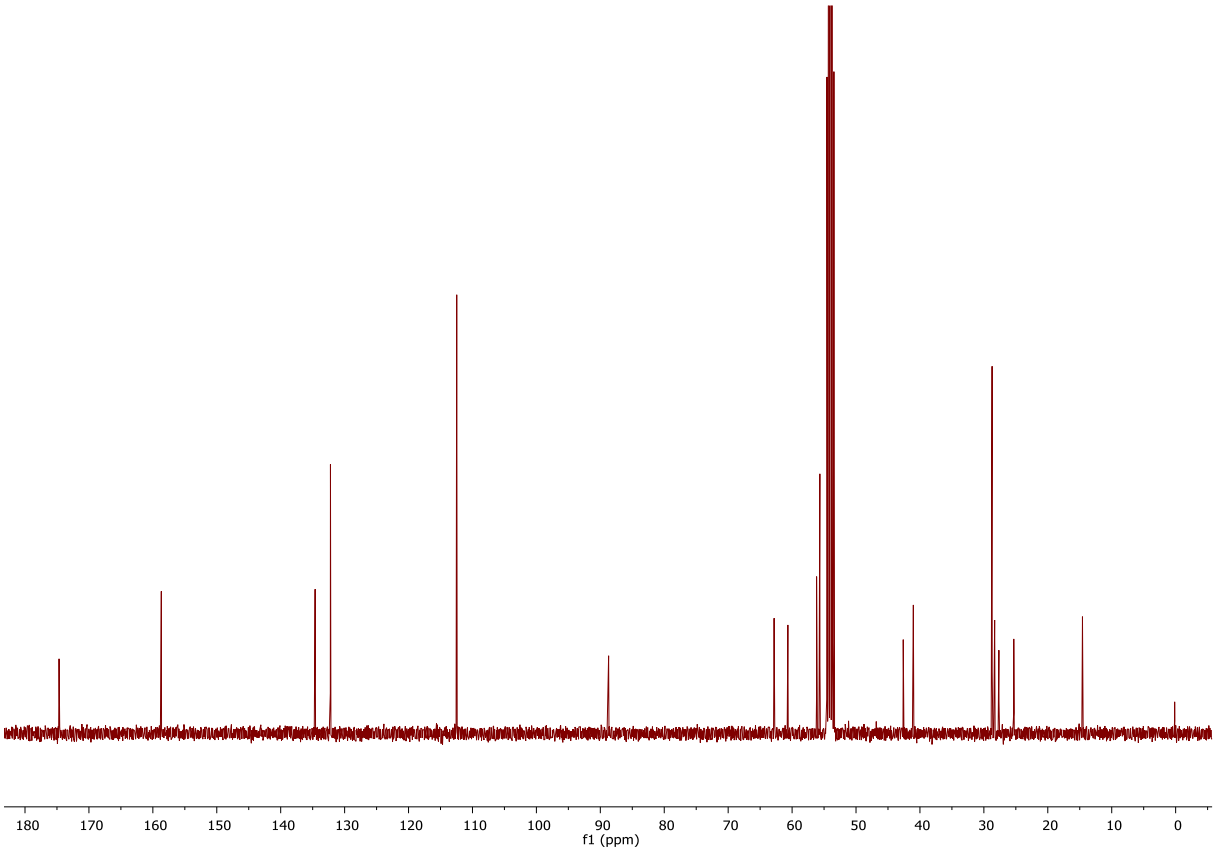

***rac*-Ethyl 1-{4-[1,1-bis(4-methoxyphenyl)-2,2-dimethylpropoxy]butyl}piperidine-3-carboxylate (29)**

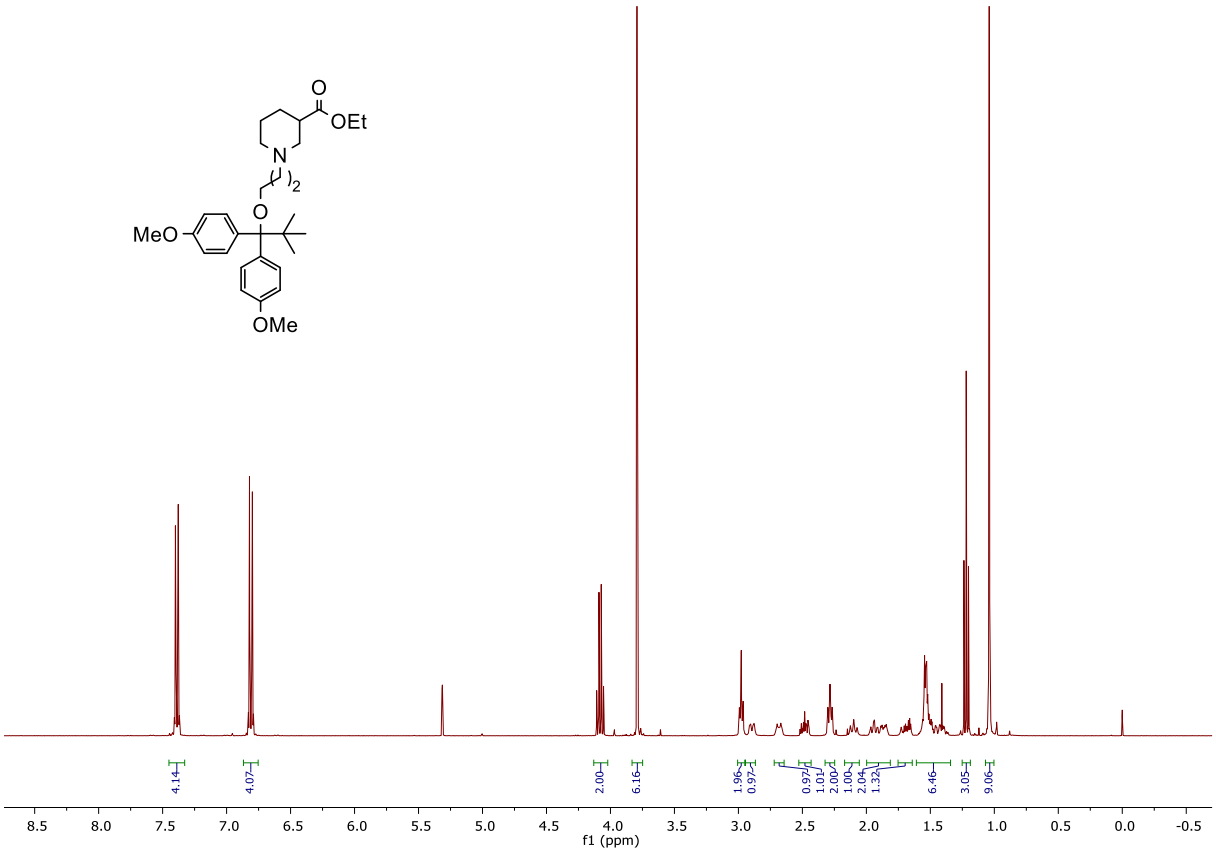

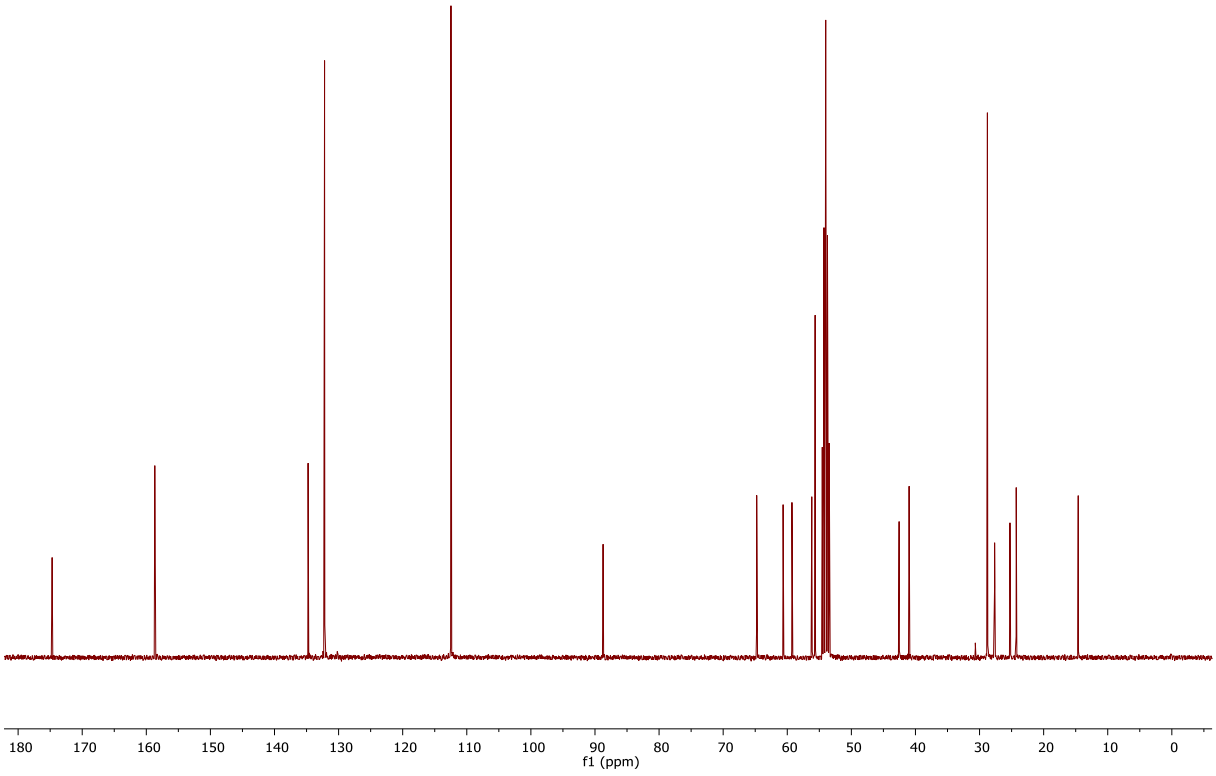

***rac*-1-{2-[1,1-Bis(4-methoxyphenyl)-2,2-dimethylpropoxy]ethyl}piperidine-3-carboxamide (30)**

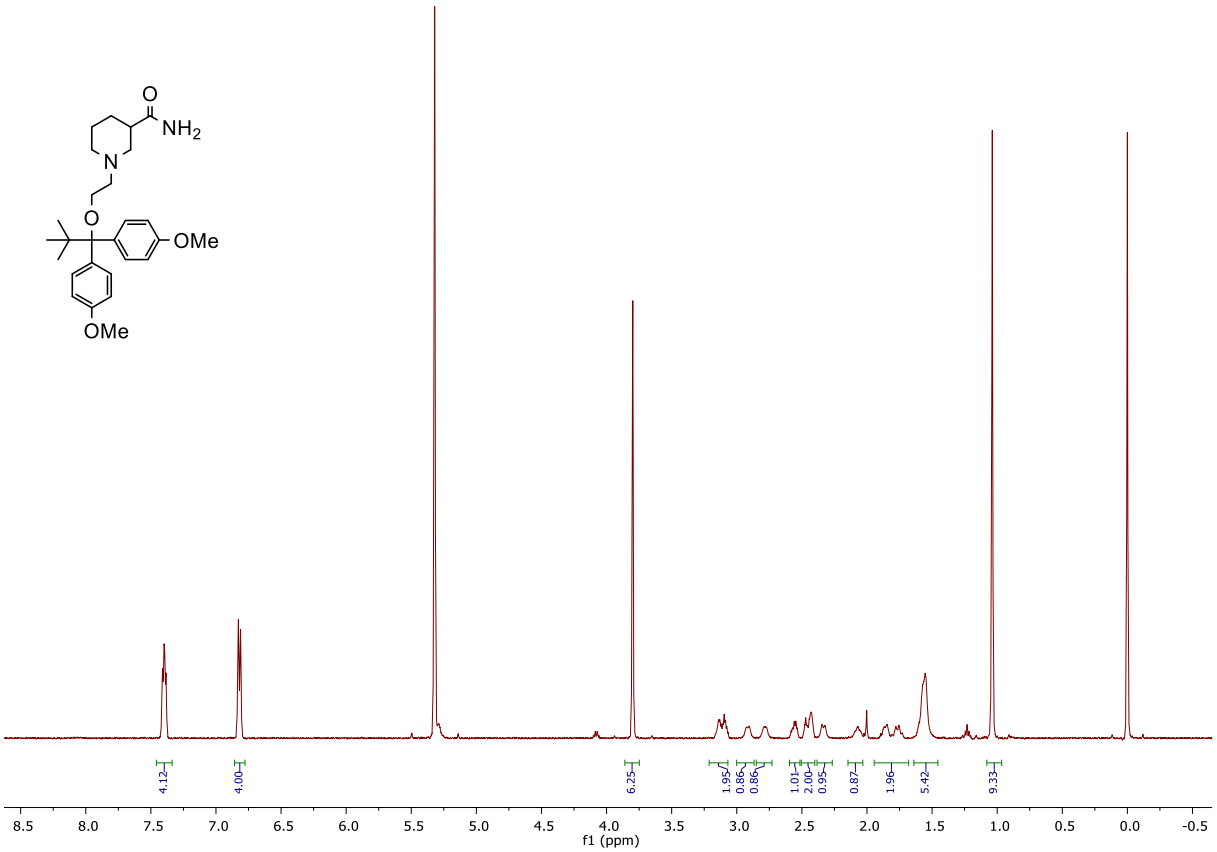

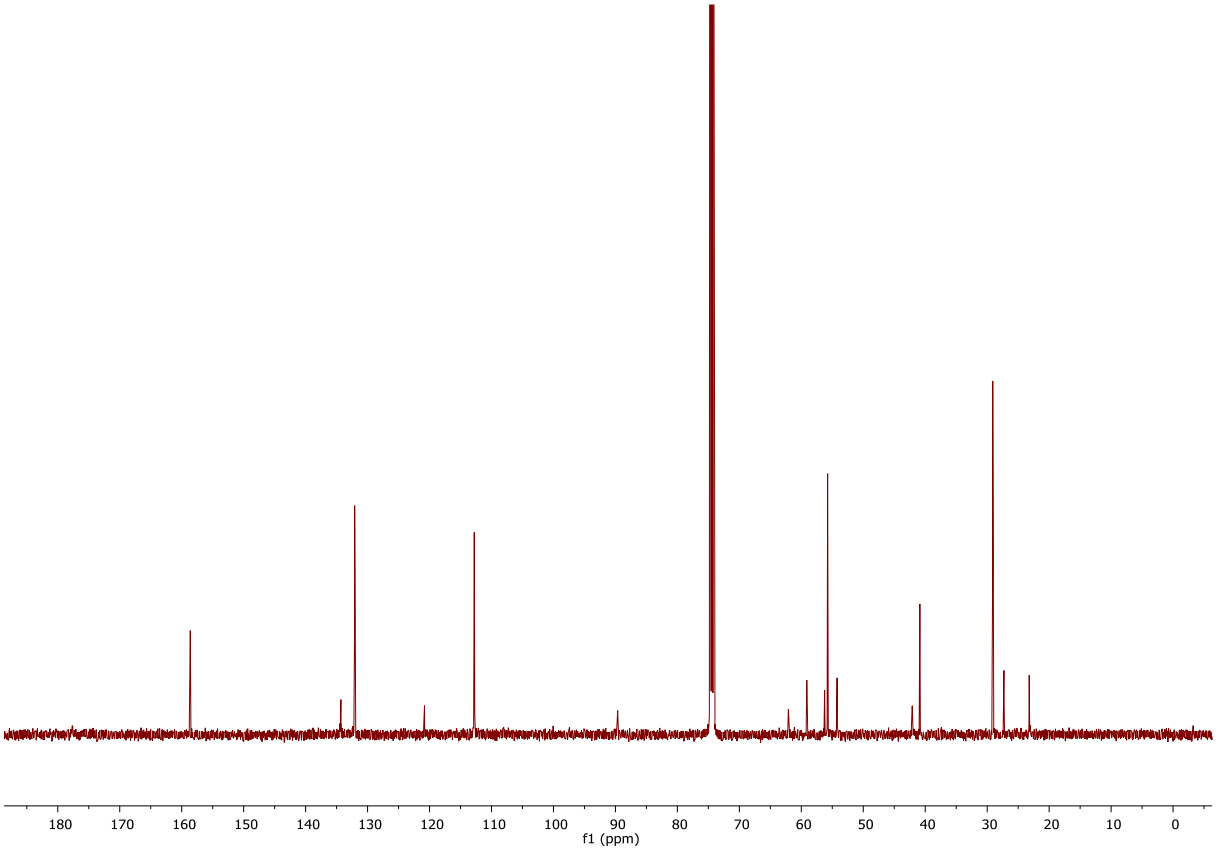

***rac*-1-{2-[Tris(4-methoxyphenyl)methoxy]ethyl}piperidine-3-carboxamide (31)**

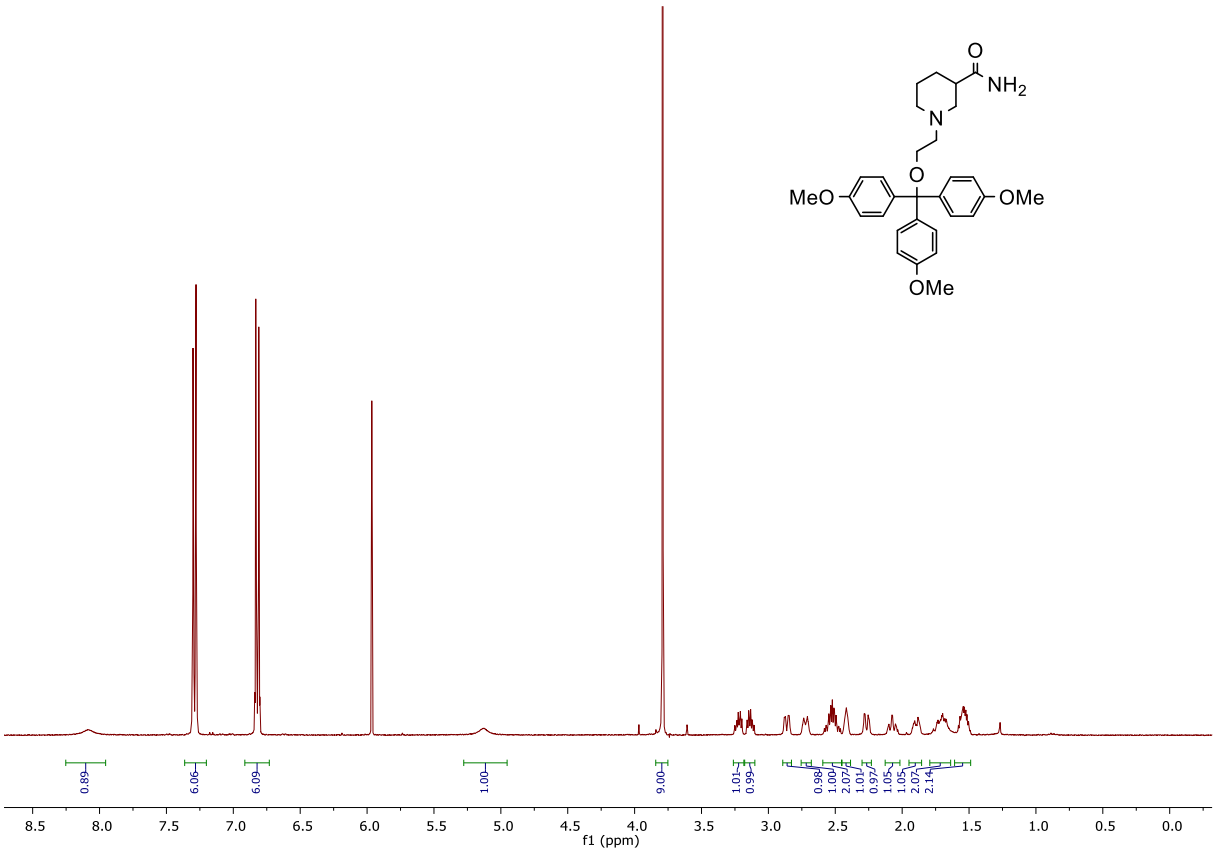

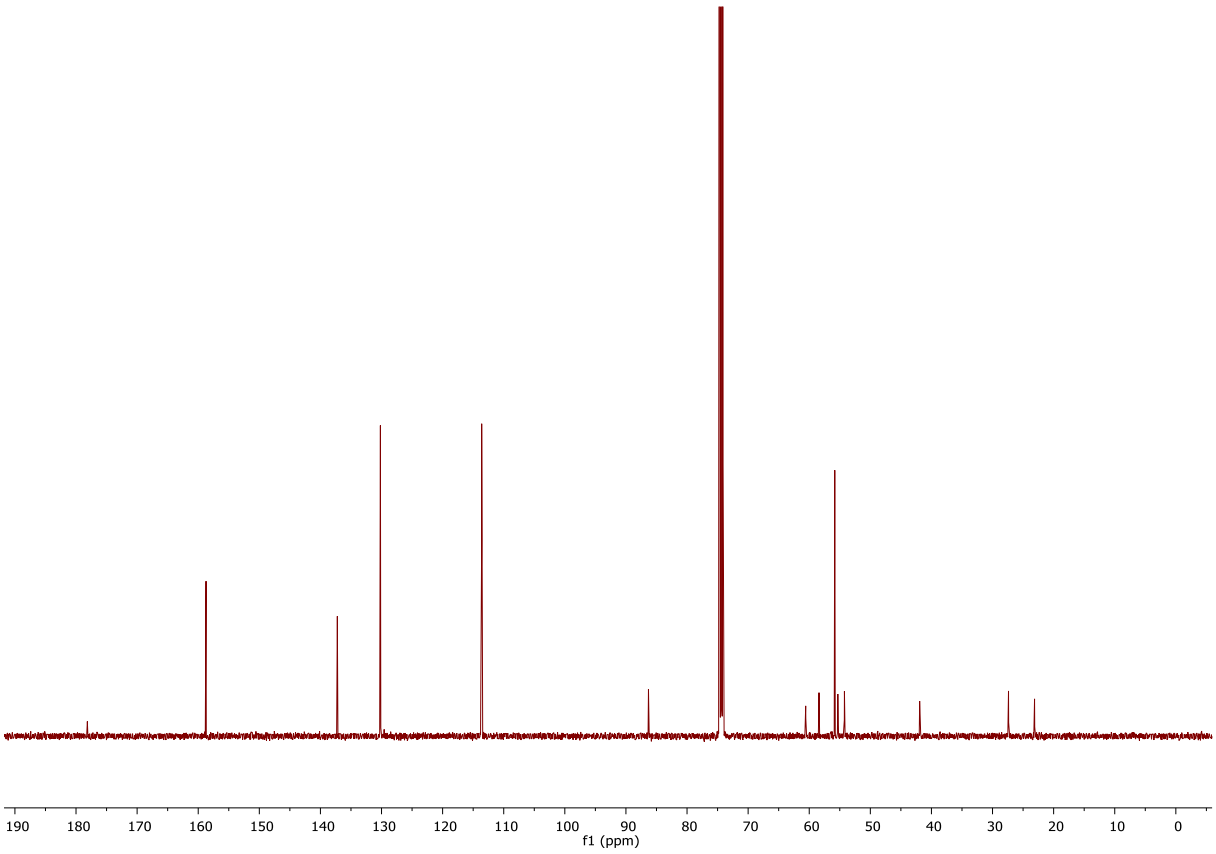

(Adamantan-1-yl)(4-methoxyphenyl)methanone (35b)

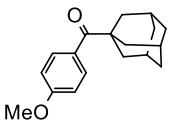

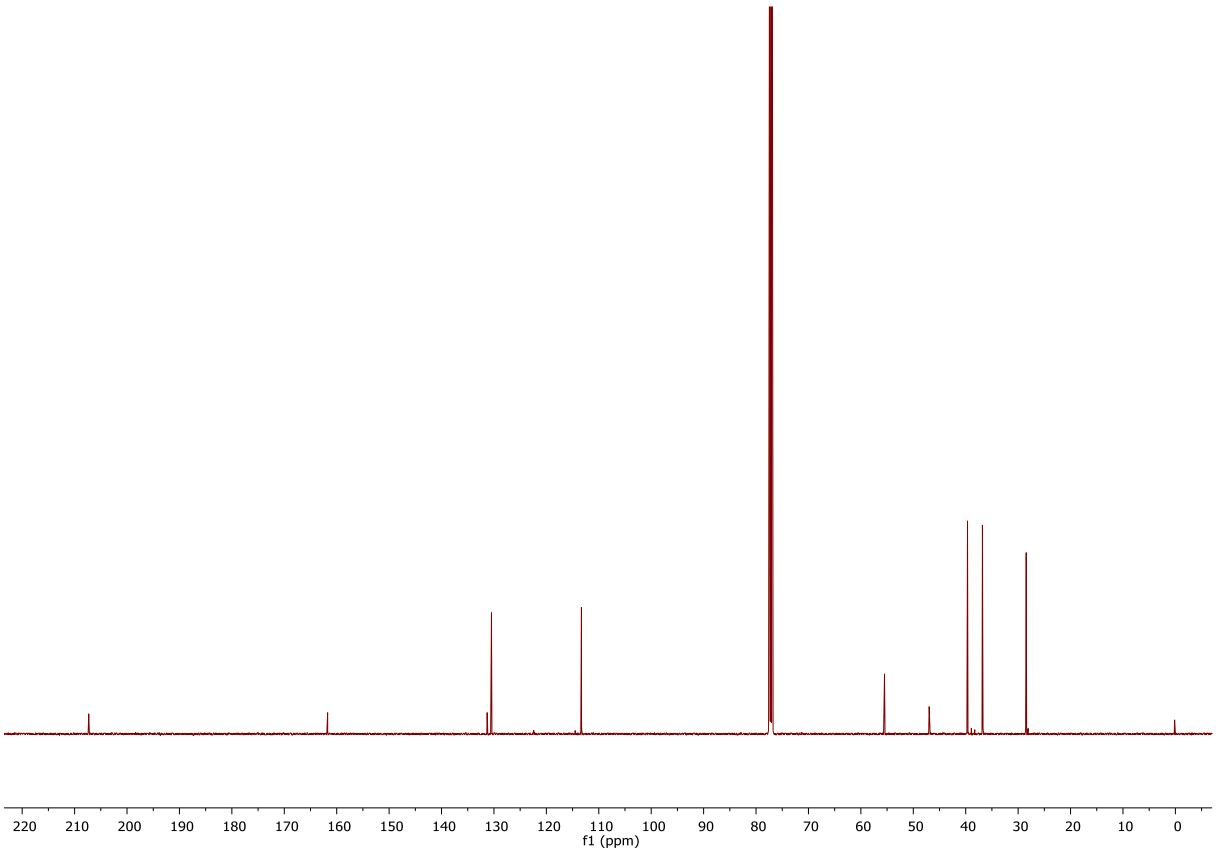

(Adamantan-1-yl)(3-methoxyphenyl)methanone (35c)

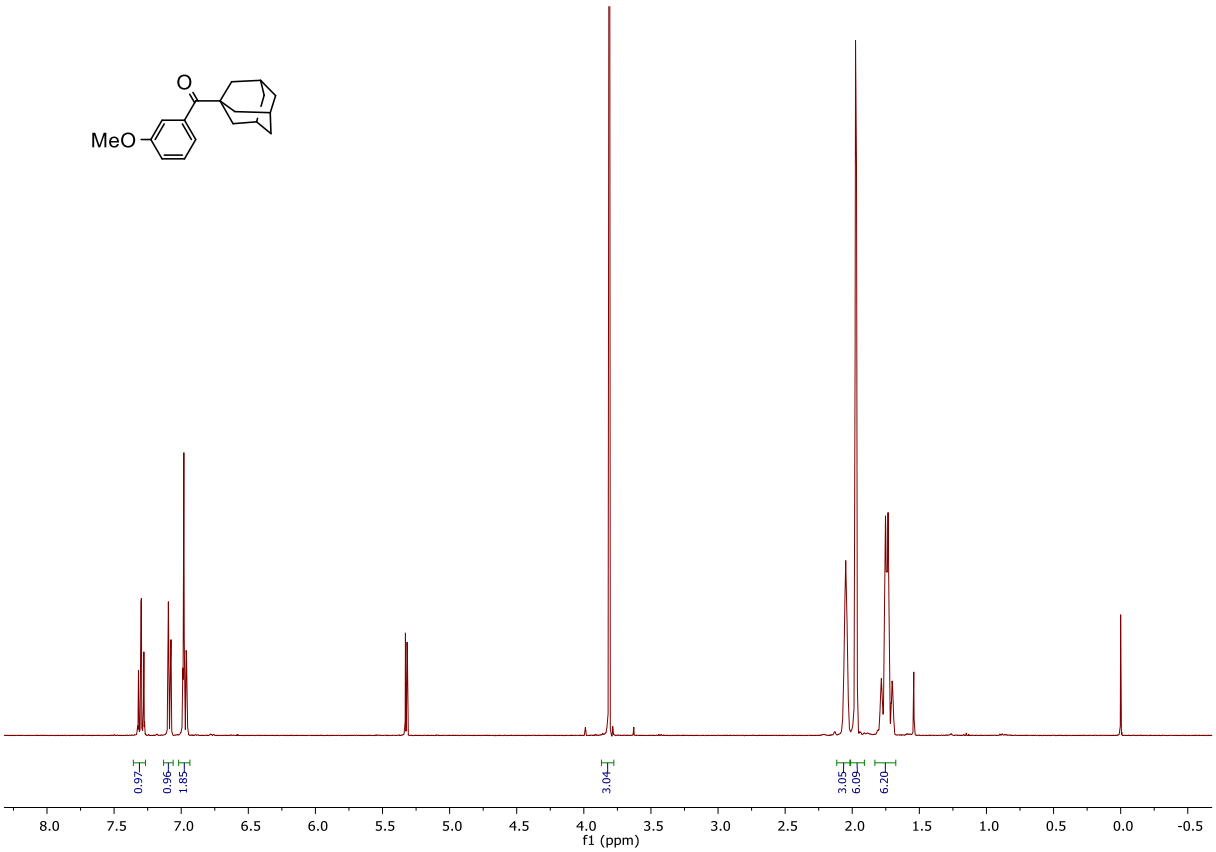

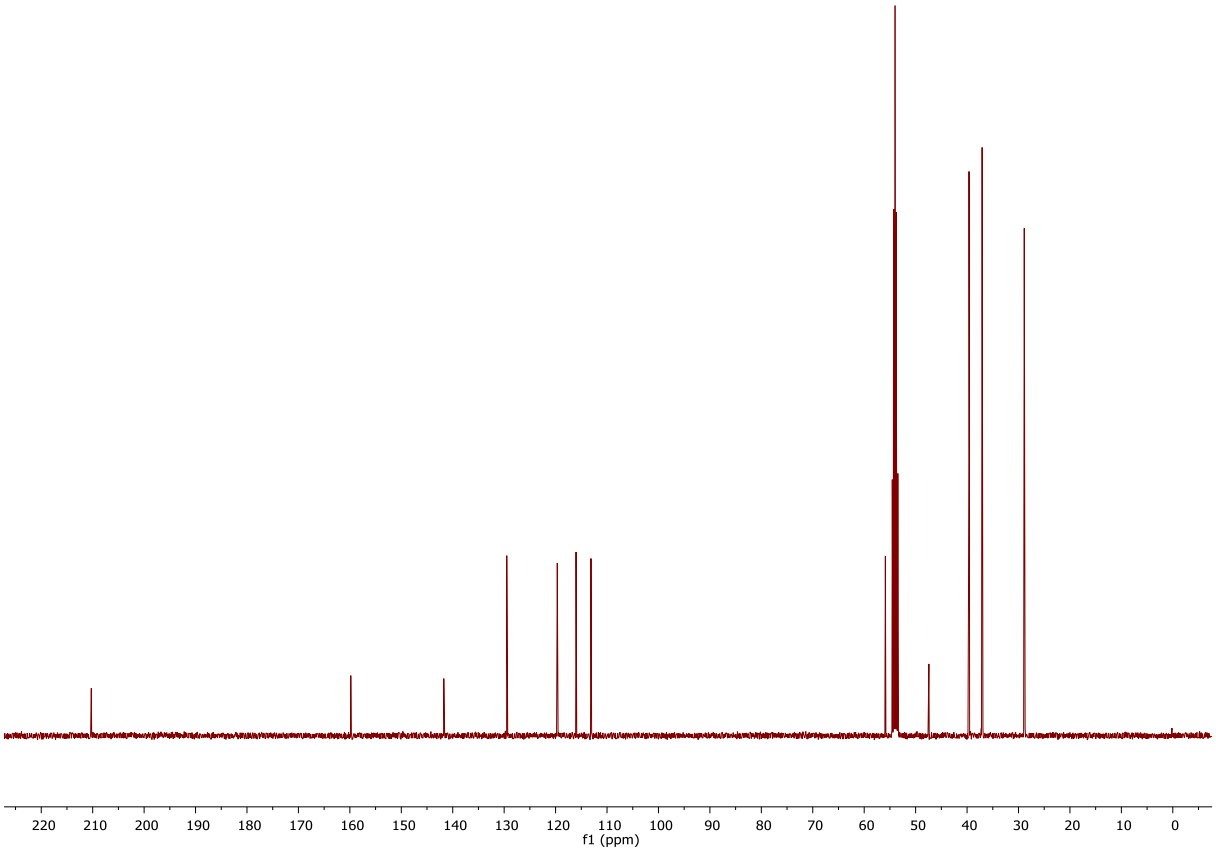

(Adamantan-1-yl)(2-methoxyphenyl)methanone (35d)

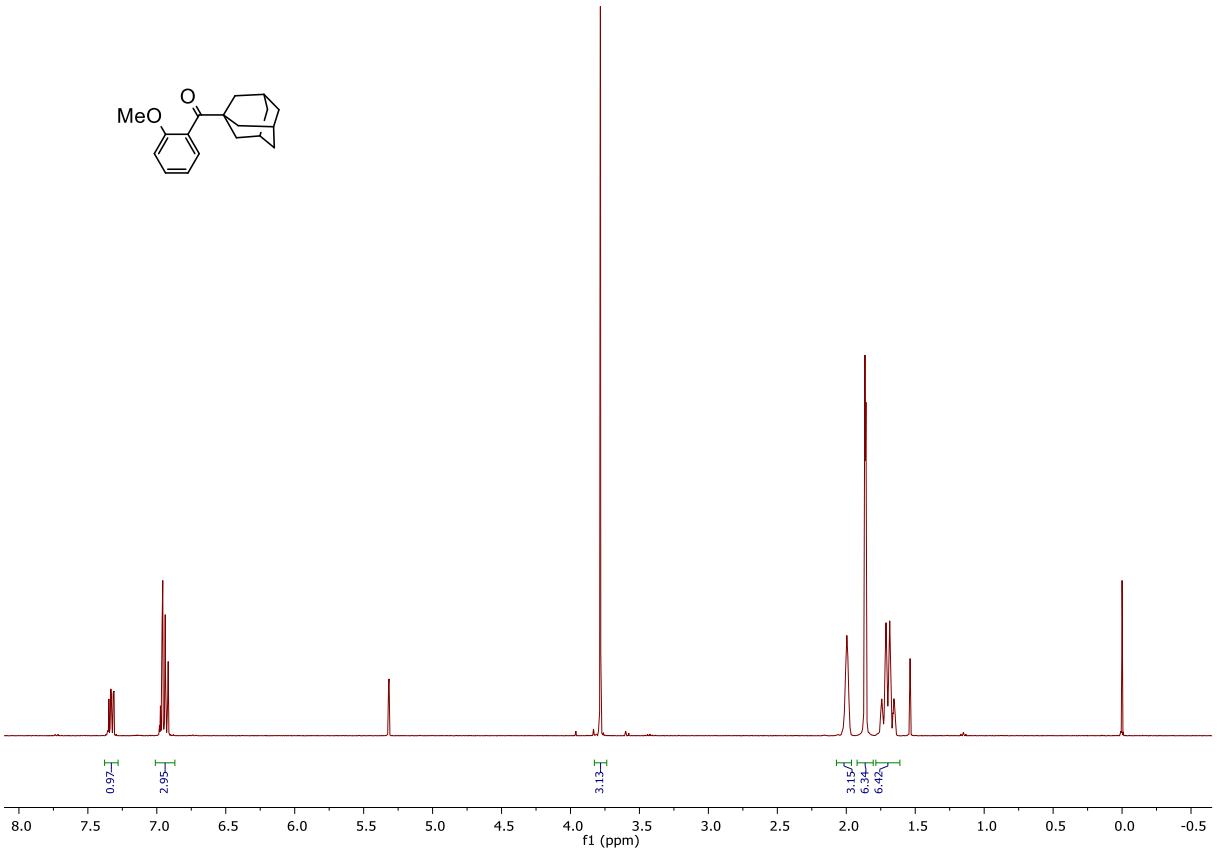

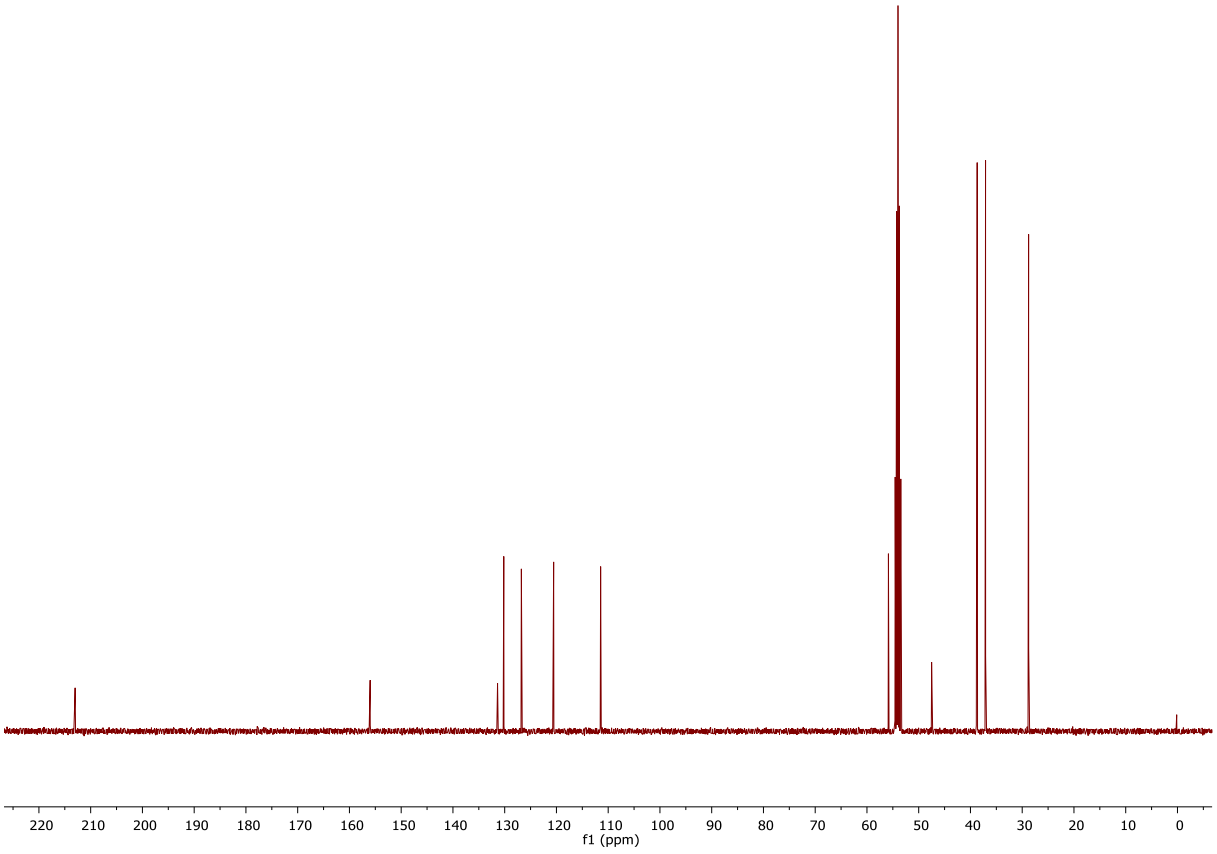

(3,5-Dimethyladamantan-1-yl)(4-methoxyphenyl)methanone (35e)

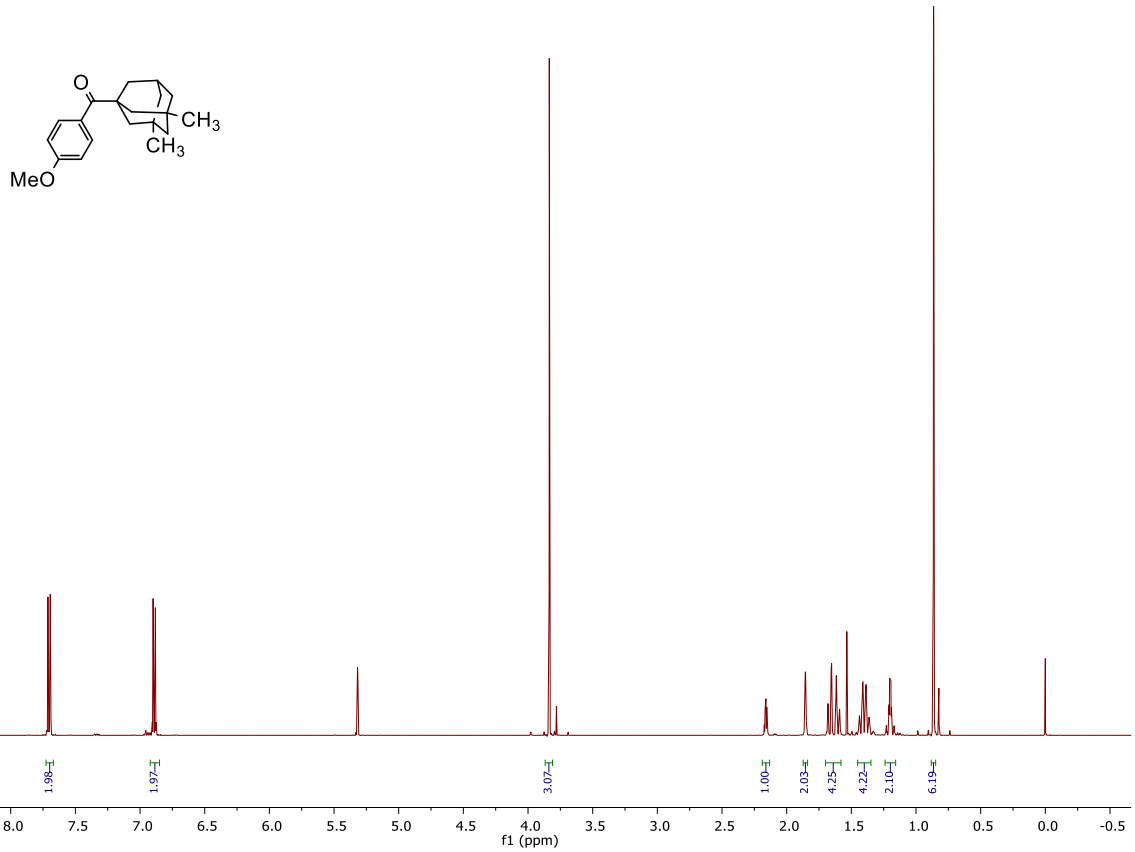

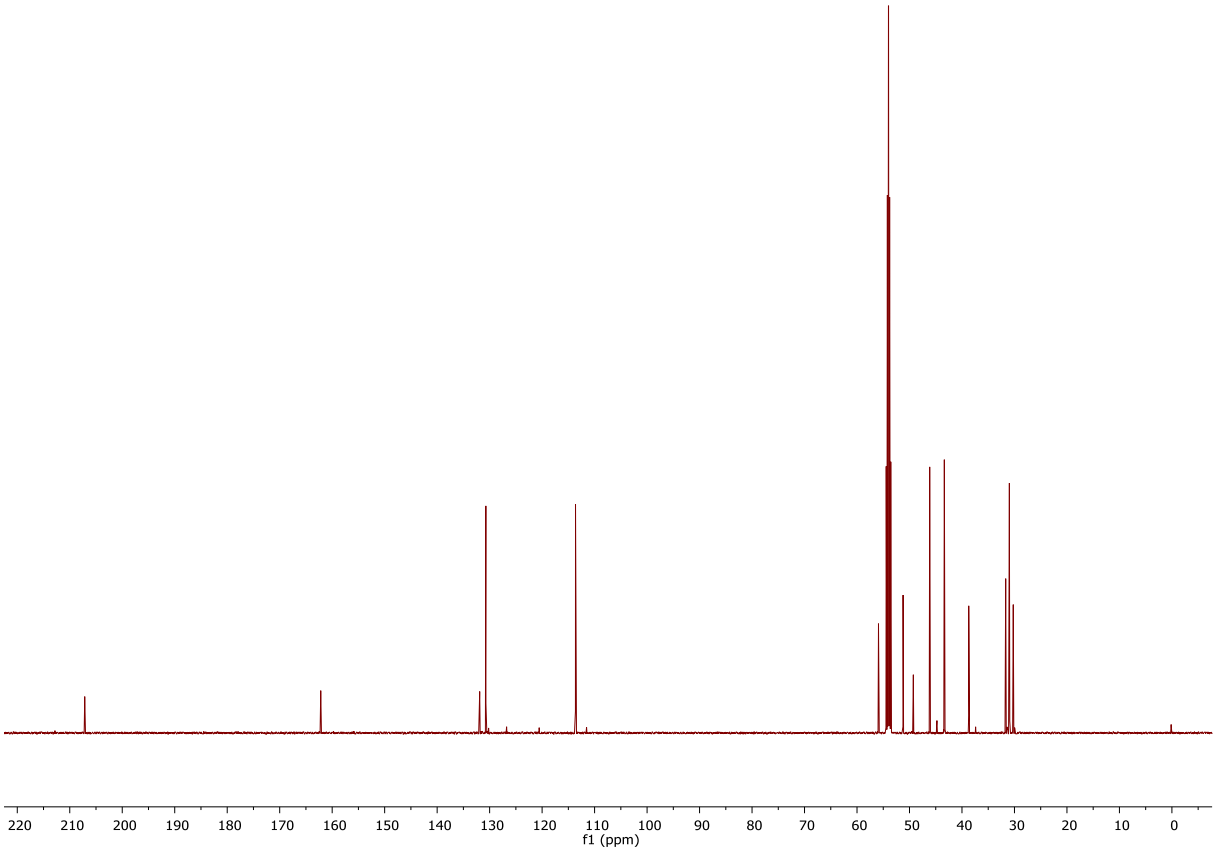

(3-Bromoadamantan-1-yl)(4-methoxyphenyl)methanone (35f)

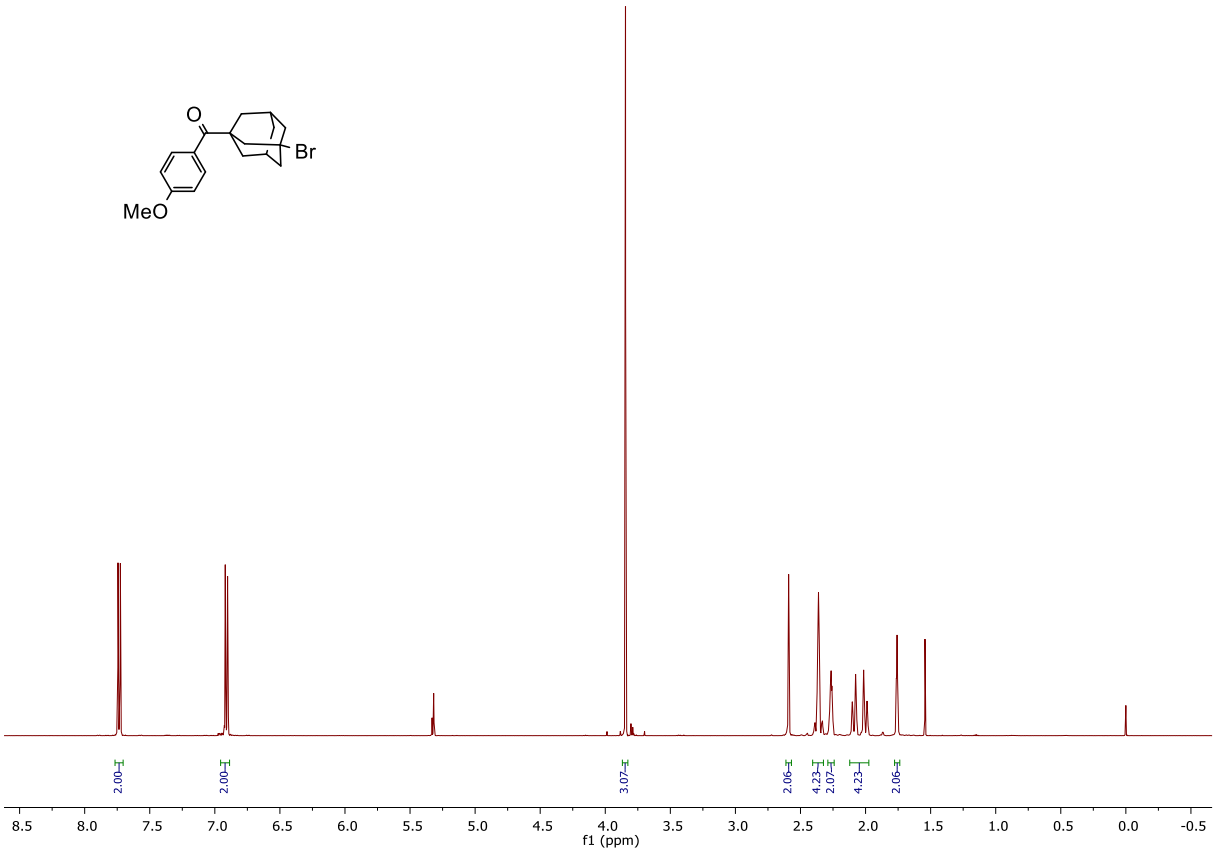

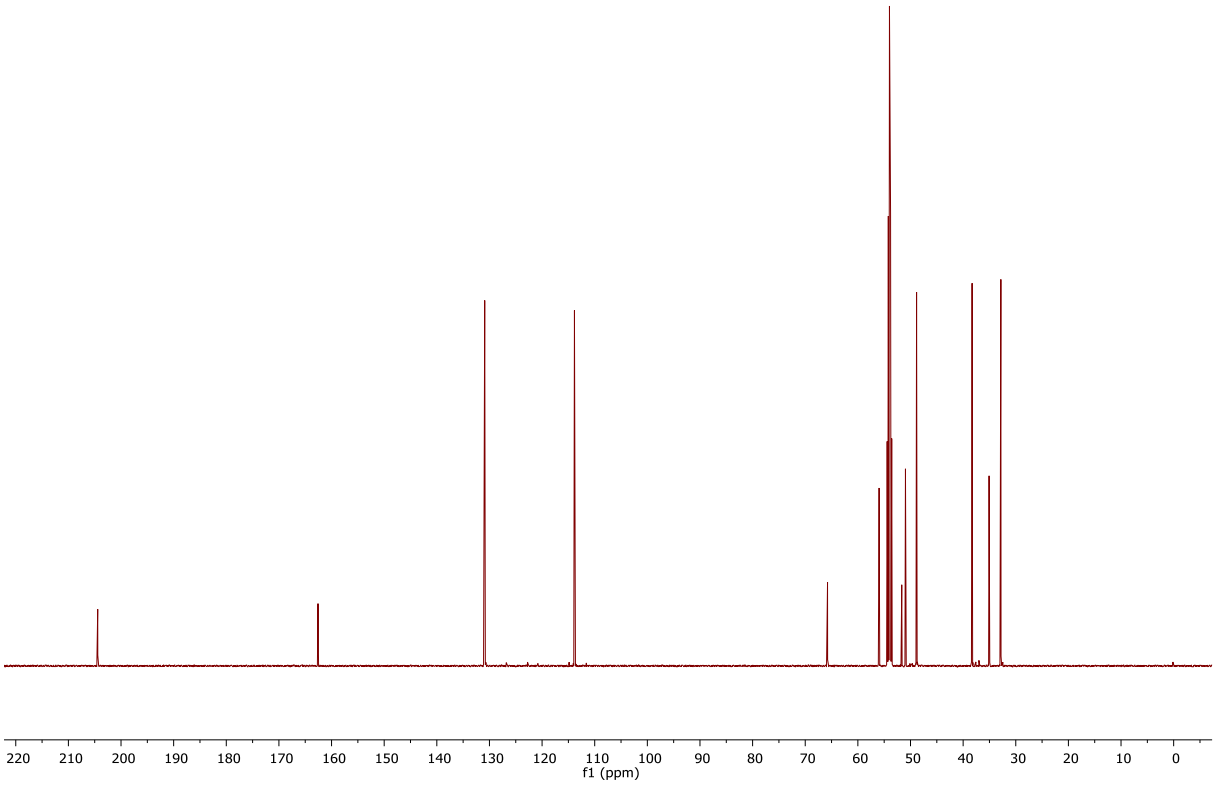

(3-Methoxyadamantan-1-yl)(4-methoxyphenyl)methanone (35g)

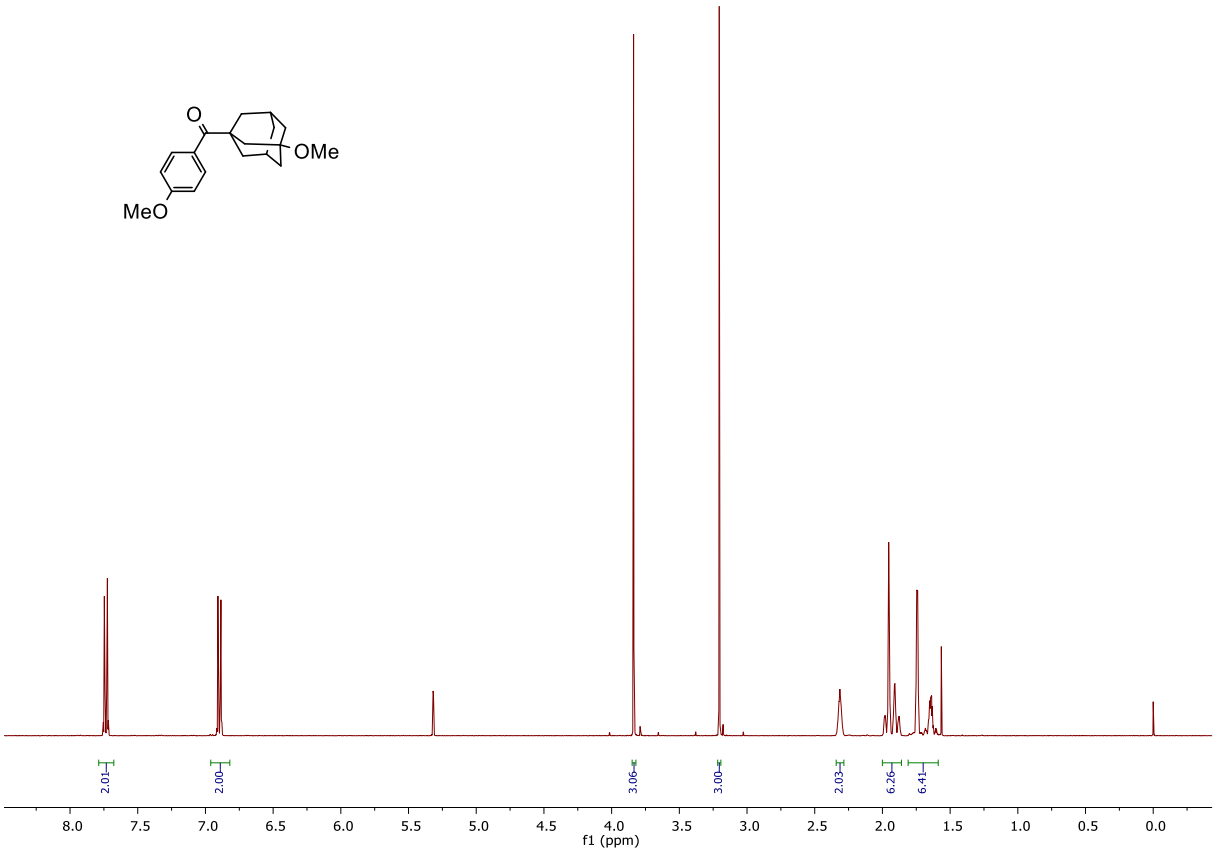

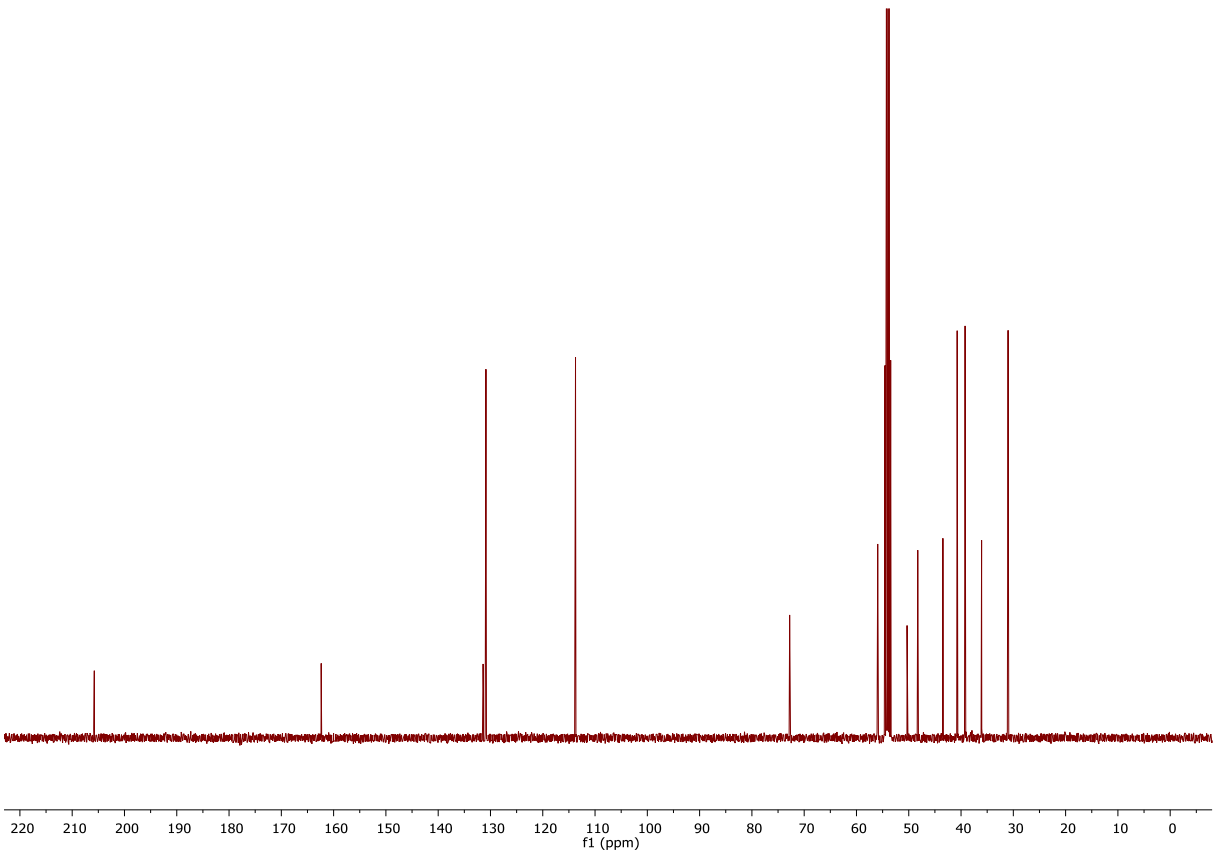

rac-Ethyl 1-{2-[(1_R_)(4-methoxyphenyl)(1-methylcyclohexyl)methoxy]ethyl}(3_R_)-piperidine-3-carboxylate and _rac_-Ethyl 1-{2-[(1_S_)(4-methoxyphenyl)(1-methylcyclohexyl)methoxy]ethyl}(3_R_)-piperidine-3-carboxylate ~1:1 (36a)

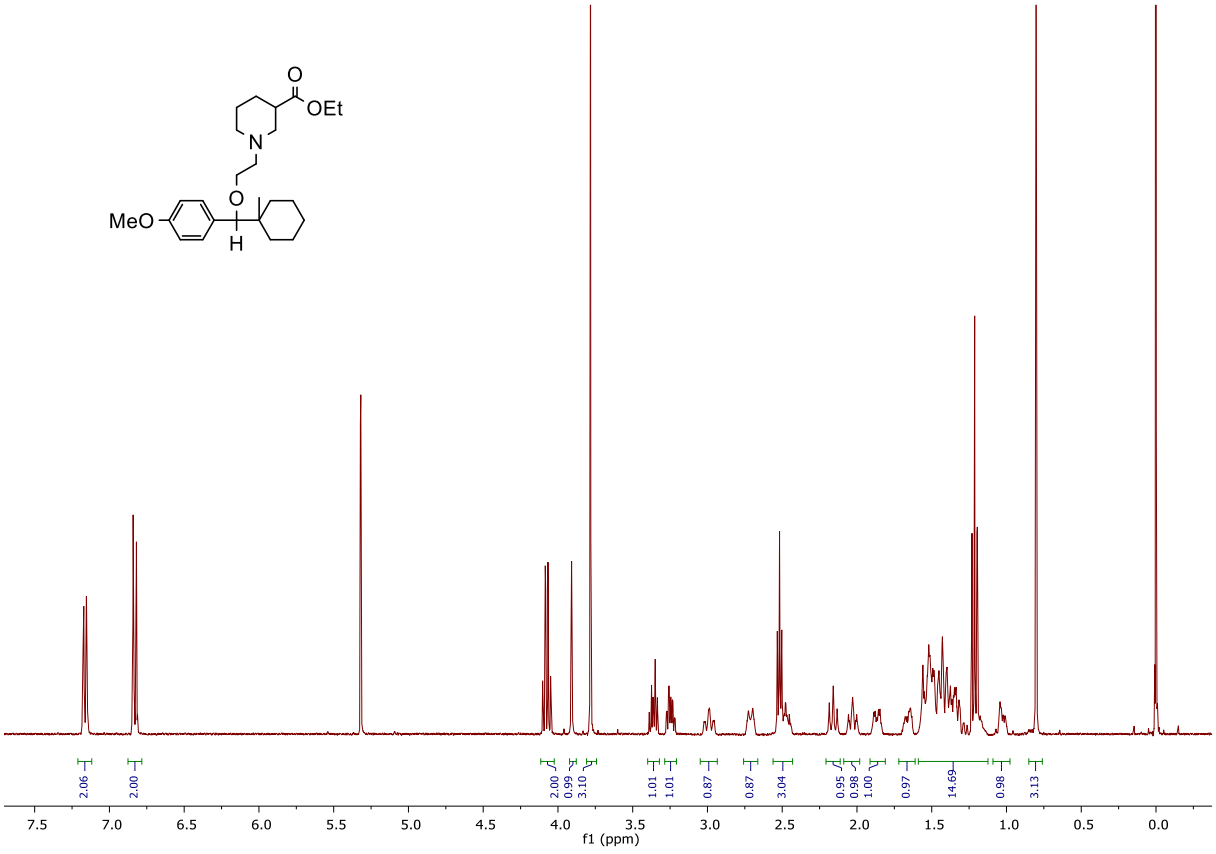

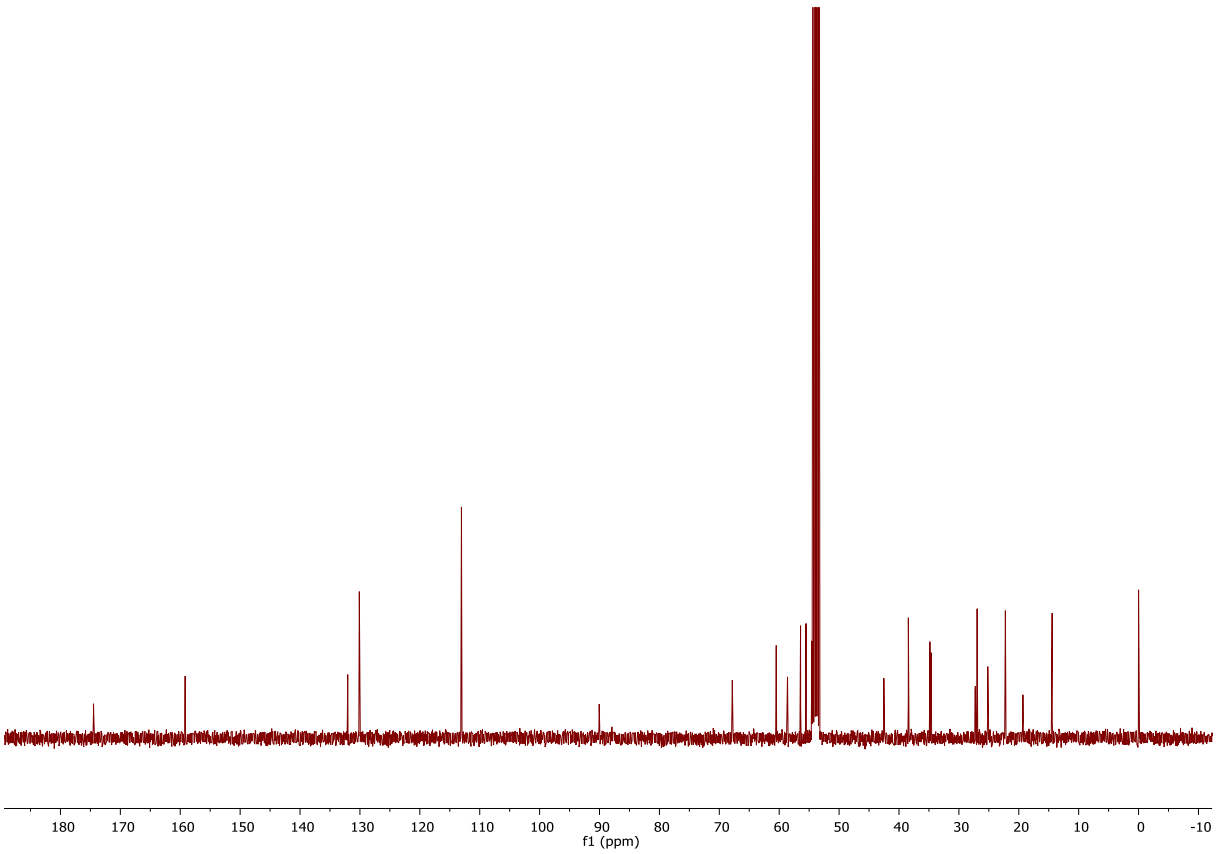

rac-Ethyl 1-{2-[(1_R_)(adamantan-1-yl)(4-methoxyphenyl)methoxy]ethyl}(3_R_)-piperidine-3-carboxylate and _rac_-Ethyl 1-{2-[(1_S_)(adamantan-1-yl)(4-methoxyphenyl)methoxy]ethyl}(3_R_)-piperidine-3-carboxylate ~1:1 (36b)

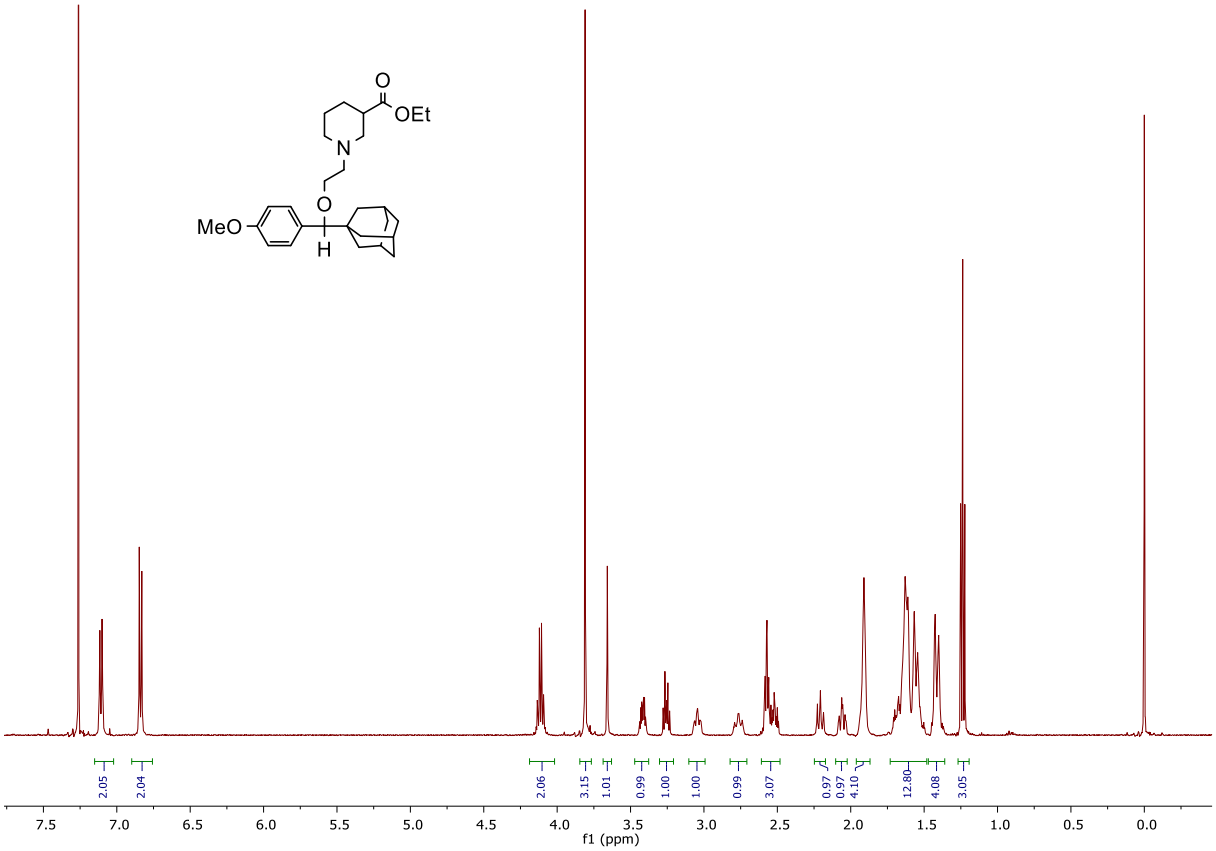

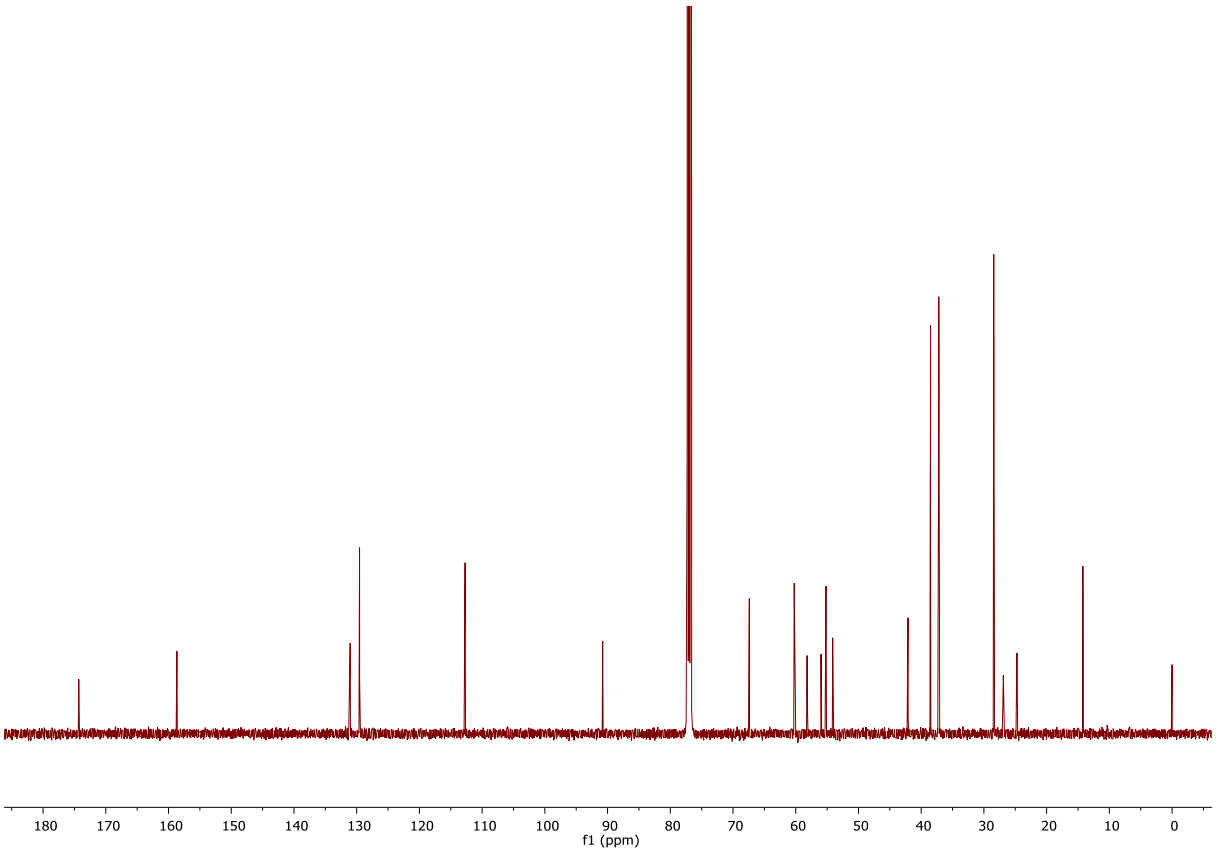

rac-Ethyl 1-{2-[(1_R_)(adamantan-1-yl)(3-methoxyphenyl)methoxy]ethyl}(3_R_)-piperidine-3-carboxylate and _rac_-Ethyl 1-{2-[(1_S_)(adamantan-1-yl)(3-methoxyphenyl)methoxy]ethyl}(3_R_)-piperidine-3-carboxylate ~1:1 (36c)

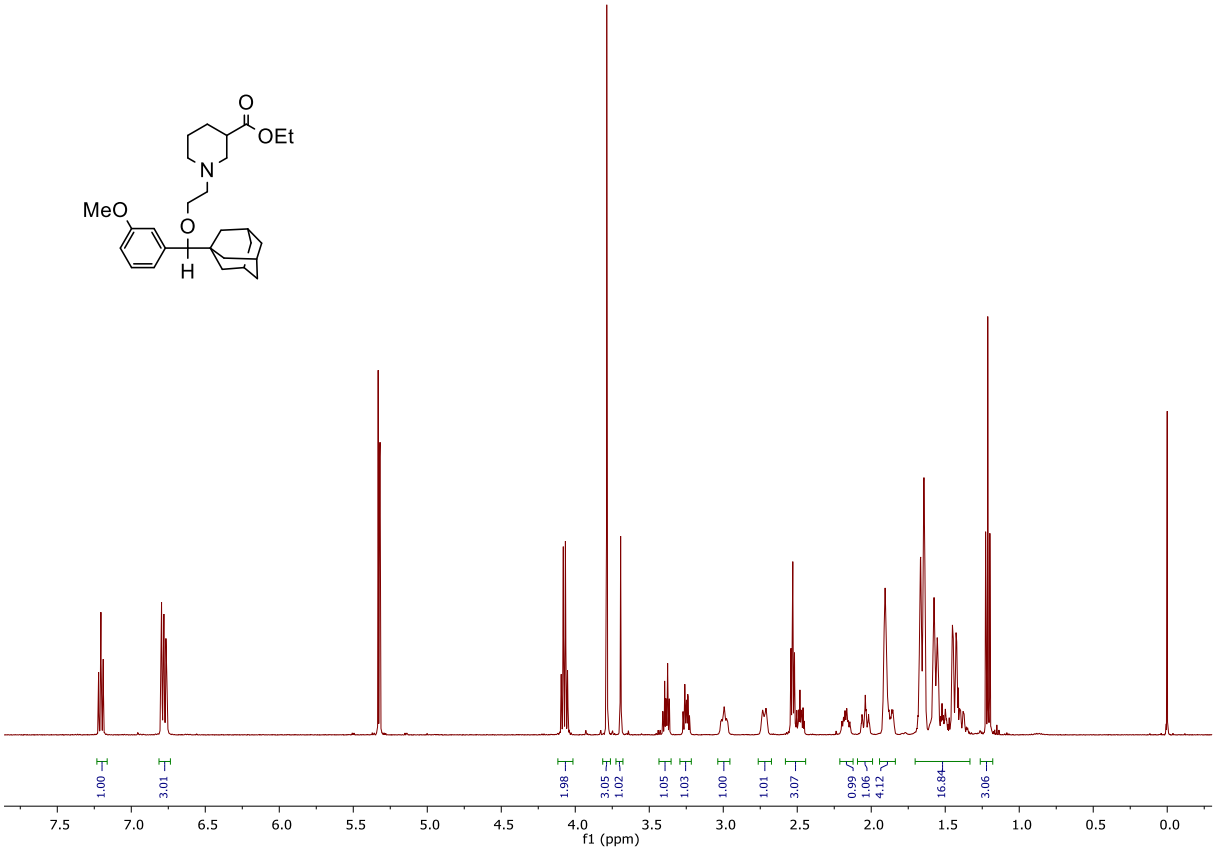

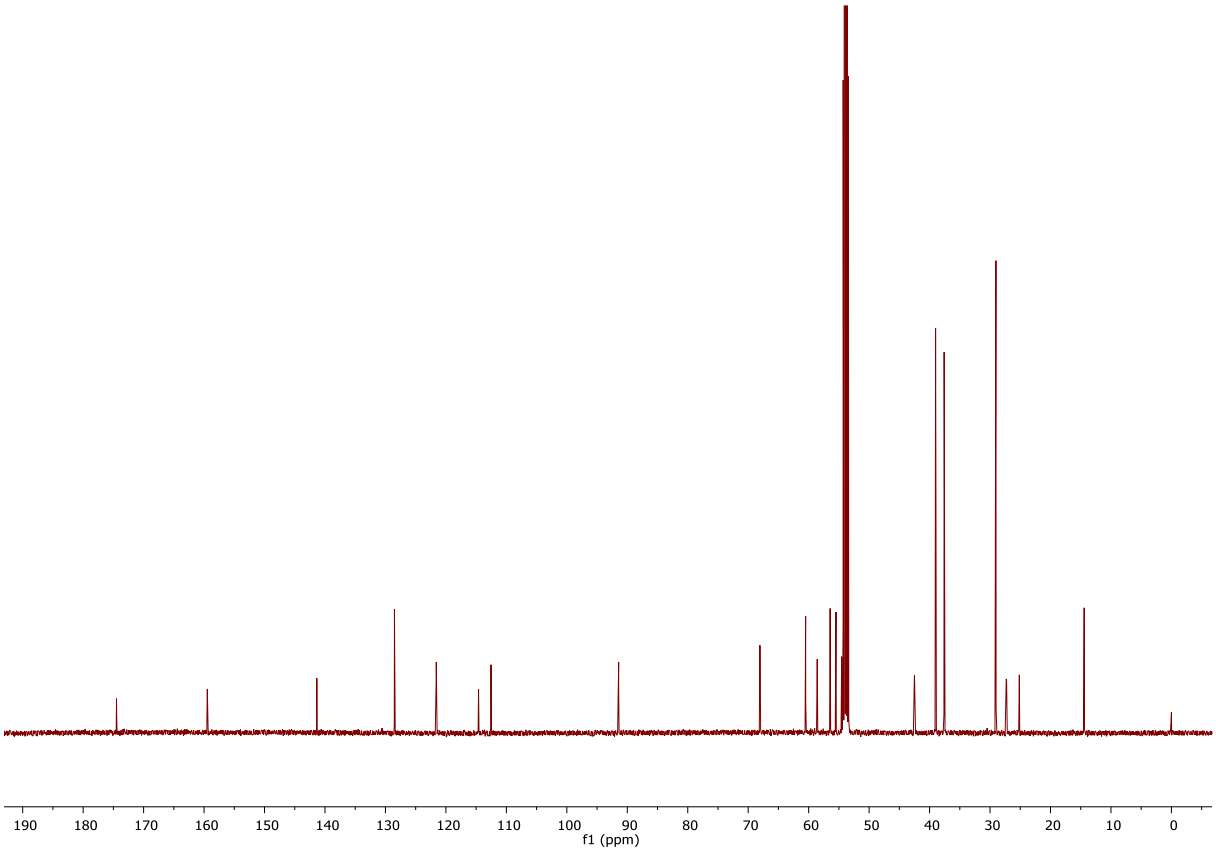

rac-Ethyl 1-{2-[(1_R_)(adamantan-1-yl)(2-methoxyphenyl)methoxy]ethyl}(3_R_)-piperidine-3-carboxylate and _rac_-Ethyl 1-{2-[(1_S_)(adamantan-1-yl)(2-methoxyphenyl)methoxy]ethyl}(3_R_)-piperidine-3-carboxylate ~1:1 (36d)

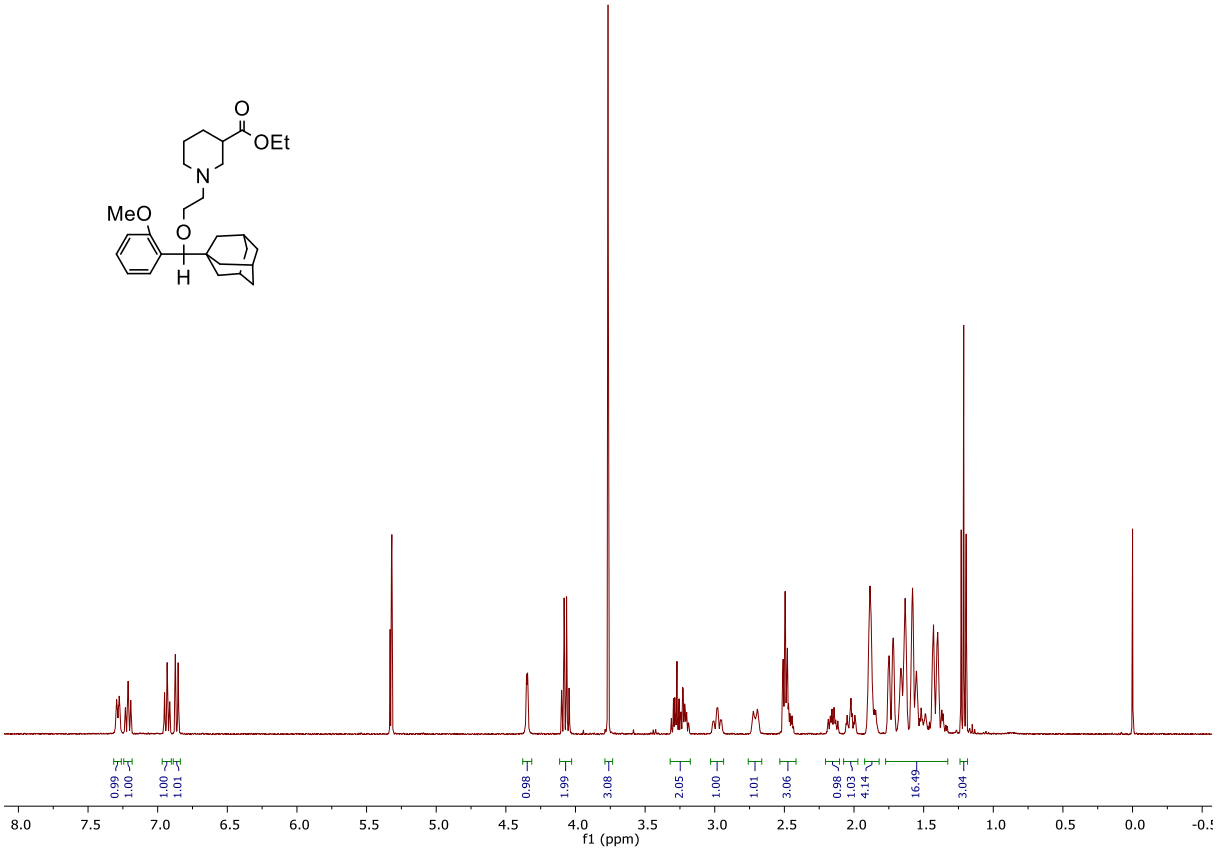

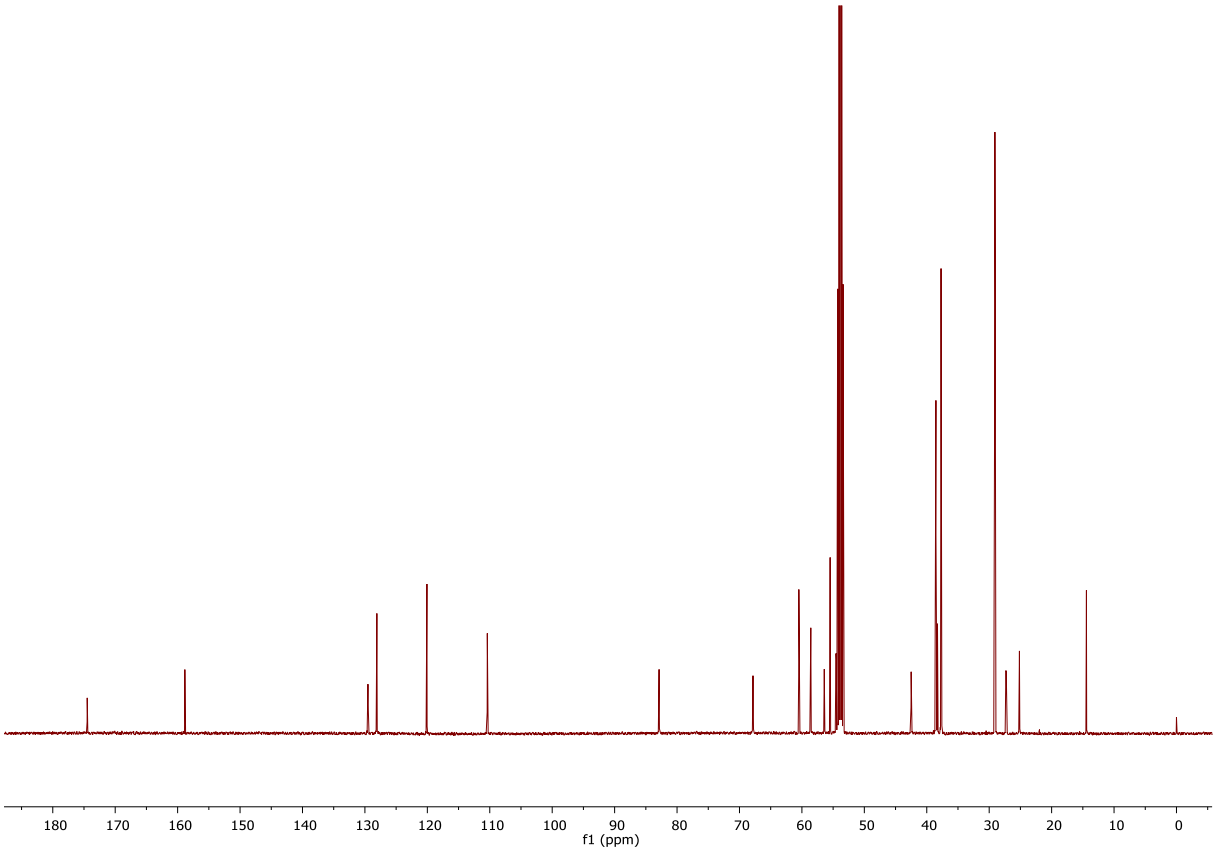

rac-Ethyl 1-{2-[(1*R*)(3,5-dimethyladamantan-1-yl)(4-methoxyphenyl)methoxy]ethyl}(3*R*)-piperidine-3-carboxylate and _rac_-Ethyl 1-{2-[(1*S*)(3,5-dimethyladamantan-1-yl)(4-methoxyphenyl)methoxy]ethyl}(3*R*)-piperidine-3-carboxylate ~1:1 (36e)

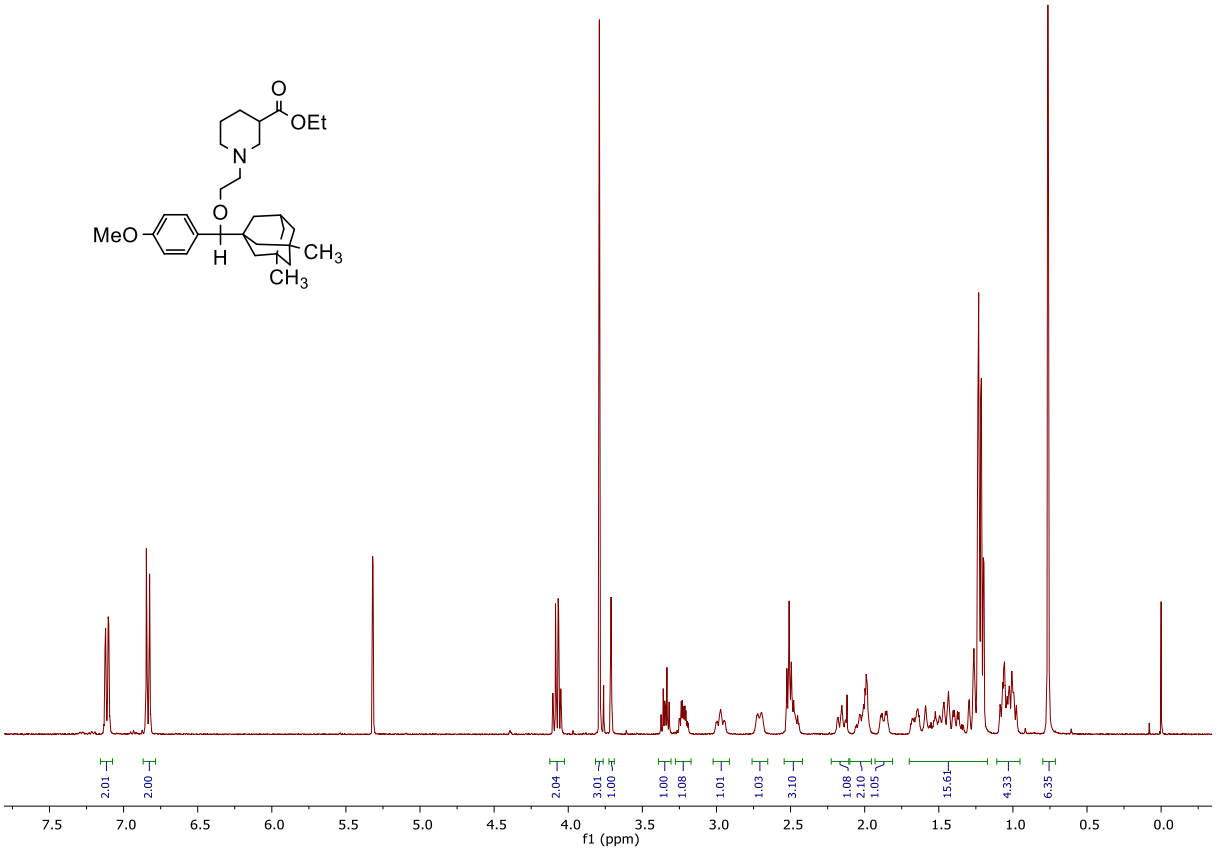

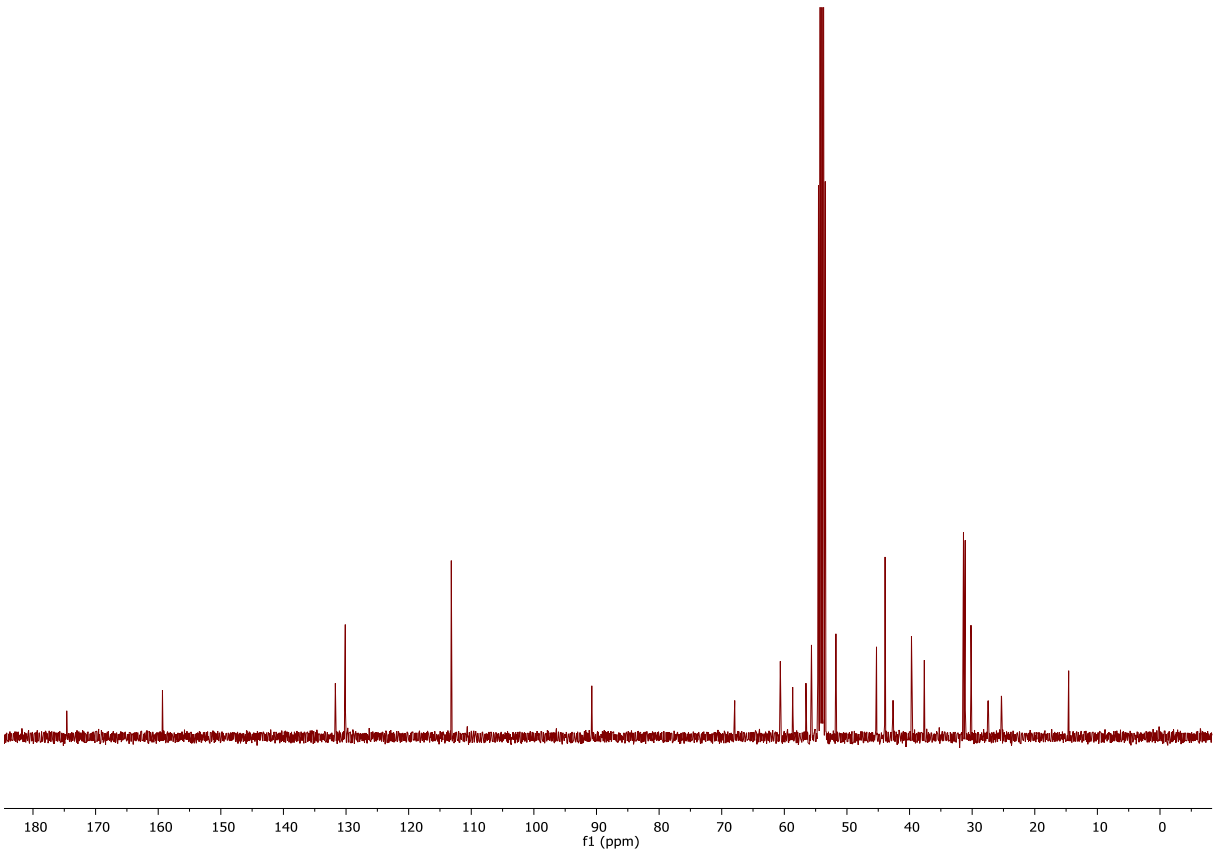

rac-Ethyl 1-{2-[(1_R_)(3-methoxyadamantan-1-yl)(4-methoxyphenyl)methoxy]ethyl}(3_R_)-piperidine-3-carboxylate and _rac_-Ethyl 1-{2-[(1_S_)(3-methoxyadamantan-1-yl)(4-methoxyphenyl)methoxy]ethyl}(3_R_)-piperidine-3-carboxylate ~1:1 (36g)

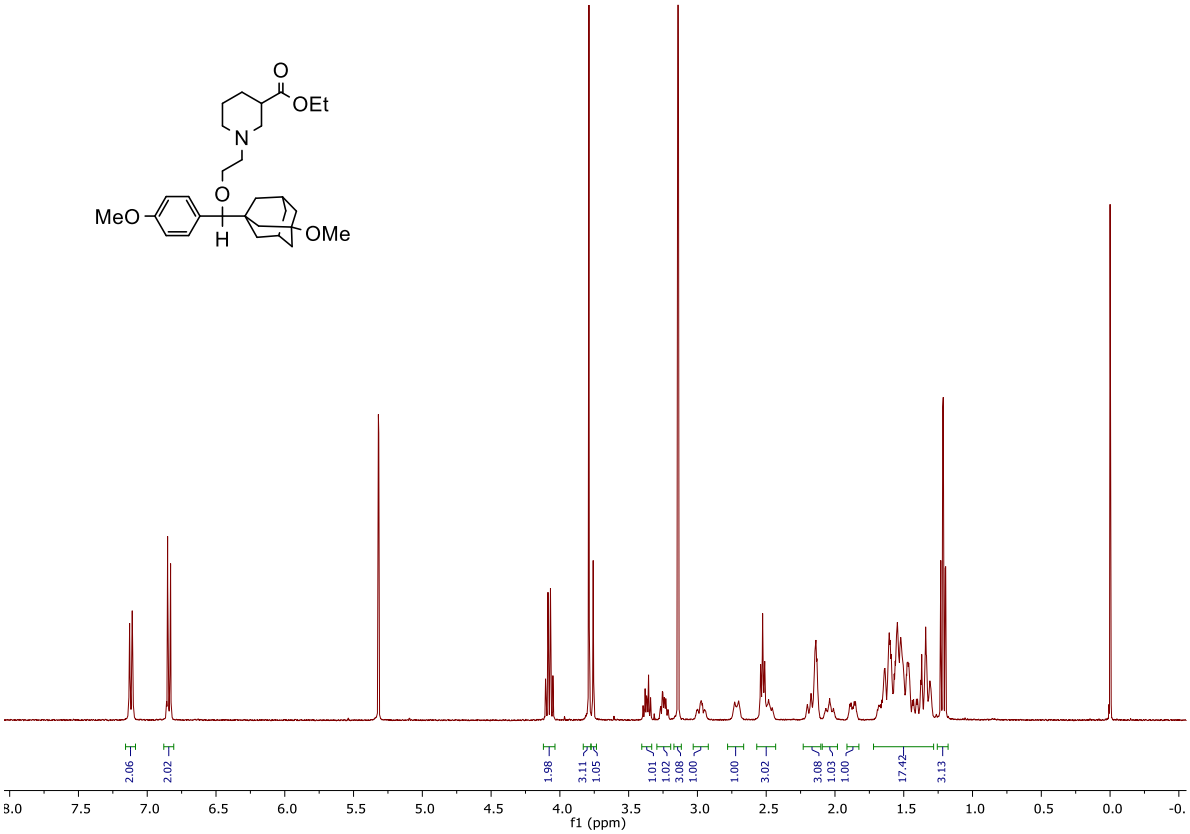

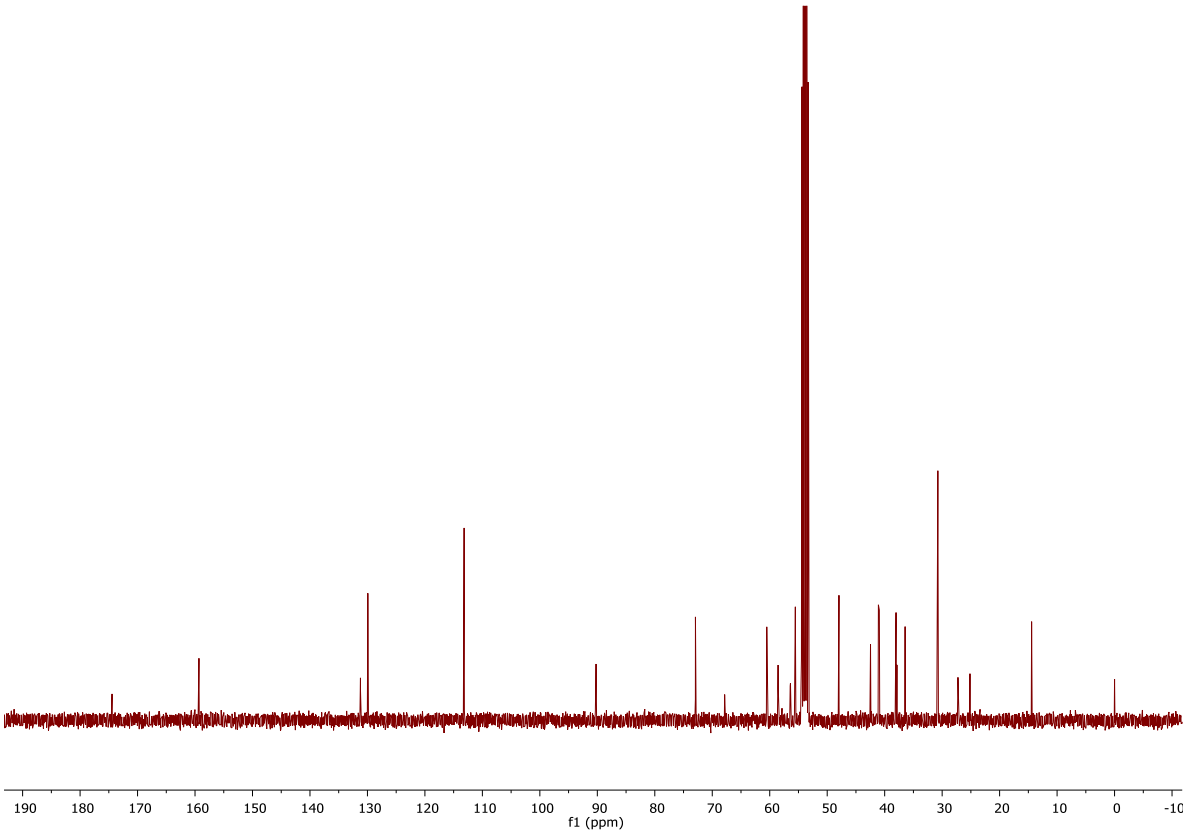

2-(2-Chloroethoxy)-2-(4-methoxyphenyl)adamantane (38)

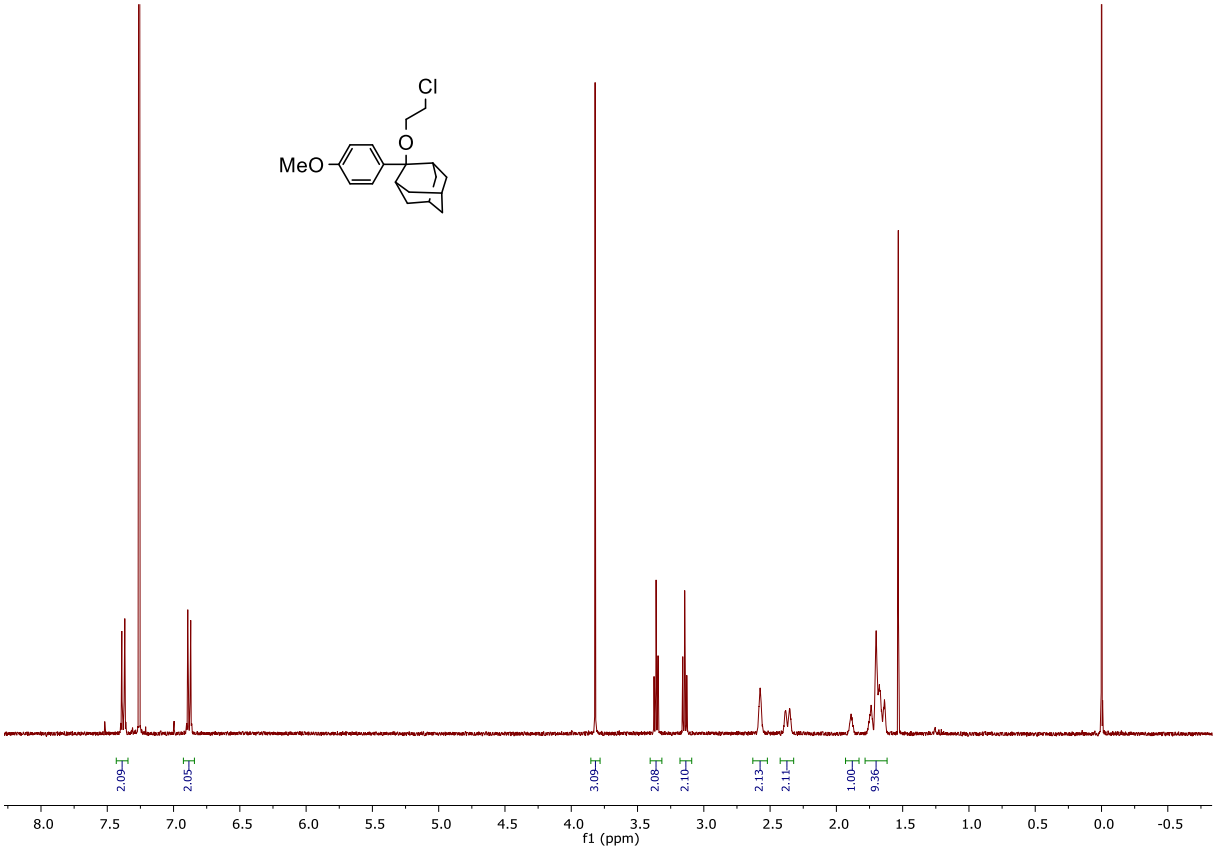

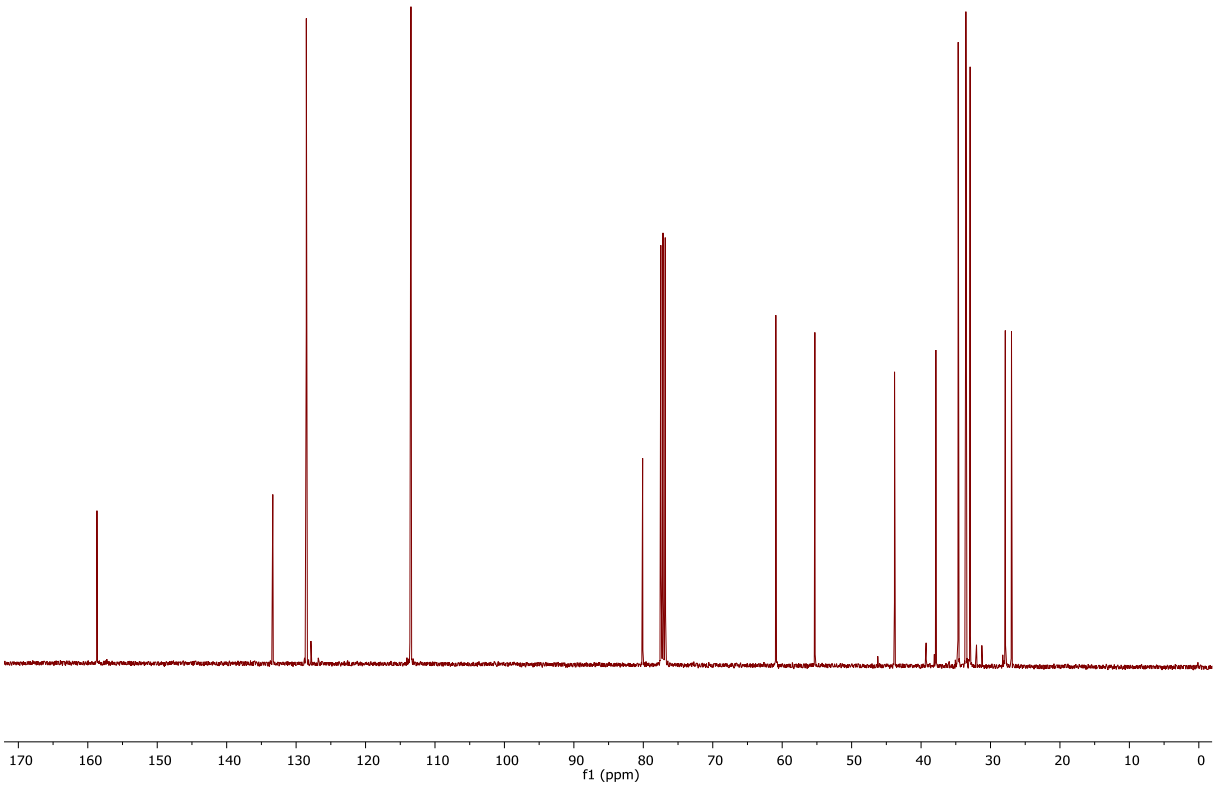

***rac*-Ethyl 1-(2-{[2-(4-methoxyphenyl)adamantan-2-yl]oxy}ethyl)piperidine-3-carboxylate (39)**